

How do lilies open?
The regulation of
flower opening in lilies,
and how to control it
to improve post-
harvest quality

A thesis submitted to Cardiff University for
the degree of Doctor of Philosophy



Rakhee Dhorajiwala

School of Biosciences
Cardiff University
December 2022

Summary

Lilies are a commercial cut-flower crop highly popular in the UK for their large and colourful blooms. However, due to their perishable nature, cold/dark storage is necessary as part of commercial treatment to allow cut flowers to maintain their quality and developmental stage until purchase. Cold/dark storage has been shown to have an impact on the terminal bud's ability to open in some varieties, particularly in stems with a greater number of buds per inflorescence. Understanding the opening process of lilies, and the endogenous and exogenous factors which may impact this process (particularly under commercial conditions) was an overarching aim of this project. Flower opening is driven by differential expansion or division of petal cells in other species, and firstly the mechanism of lily opening was characterised. Factors hypothesised to be affected by commercial treatment such as nutritional status (bud starch and soluble sugar content), time of opening, and secondary metabolism were confirmed to be significantly different between on plant and commercially treated lily buds. Position on stem was identified as a potentially important factor affecting the ability to open, nutritional status and bud metabolism over opening. RNA-sequencing was used to investigate expression patterns in buds which could open comparing to buds which failed to open as a result of commercial treatment-related stress. This differential expression analysis found several putative metabolic pathways associated with flower opening, alongside putative regulatory auxin and stress related elements. The phytohormone auxin was therefore explored as a potential treatment for commercial treatment-related stress due to its accelerating effect on lily opening and the correlated expression of auxin signal transduction components with lily opening. Overall, this work provides new insights into mechanisms of flower opening and indicates possible targets for improving commercially treated cut lily quality.

List of abbreviations

Abbreviation	Full term
ABA	Abscisic acid
ANOVA	Analysis of Variance
ATP	Adenine triphosphate
BLAST	Basic Local Alignment Search Tool
CAP	Canonical Analysis of Principal components
cDNA	Complementary deoxyribonucleic acid
CT	Commercially treated
cv.	Cultivar
DEG	Differentially expressed gene
d.f.	Degrees of freedom
DW	Dry weight
EDTA	Ethylenediaminetetraacetic acid
FC	Fold change
FDR	False discovery rate
FIE-HRMS	Flow infusion electrospray- high resolution mass spectrometry
Fv/Fm	Variable fluorescence/ Maximum fluorescence
FW	Fresh weight
GC-MS	Gas chromatography-mass spectrometry
gDNA	Genomic deoxyribonucleic acid (DNA)
GO	Gene Ontology
HEPES	4-(2-hydroxyethyl)-1-piperazineethanesulfonic acid
IAA	Indole-3-acetic acid
JA	Jasmonic acid
KEGG	Kyoto Encyclopaedia of Genes and Genomes
LA hybrid	Longiflorum-Asiatic hybrid
LFO	Larger Fully Open
MAPK	Mitogen-activated protein kinase
MDA	Malondialdehyde
mRNA	Messenger ribonucleic acid (RNA)
NAA	1-Naphthaleneacetic acid
NADH/NAD⁺	Reduced/oxidised nicotinamide adenine dinucleotide
NCBI	National Centre for Biotechnology Information
NPA	Naphthylphthalamic acid
OD	Optical density
PCR	Polymerase chain reaction
PerMANOVA	Permutational multivariate analysis of variance
PVP	Polyvinylpyrrolidone
qPCR	Quantitative polymerase chain reaction
RHS	Royal Horticultural Society
RNA	Ribonucleic acid
ROS	Reactive oxygen species
SA	Salicylic acid
SDS	Sodium Dodecyl Sulfate
SRC	Small Remained Closed
SSO	Small Semi Open
SSTE	SDS-Sodium chloride-Tris-EDTA
TAE	Tris-Acetate-EDTA
TF	Transcription factor

Table of contents

Summary	i
List of abbreviations	ii
Table of contents	iii
List of figures	x
List of tables	xiv
Acknowledgments	xvi
Chapter 1 – General introduction	1
1.1 – What are lilies.....	1
1.1.1 – Genetic background of current lily varieties	2
1.1.2 – Development and growth of lily plants	9
1.2 – Characterisation of flower anatomy	10
1.3 – Possible regulatory mechanisms for cell expansion and growth	15
1.3.1 – Endogenous regulation of flower development and opening	15
1.3.2 – Exogenous factors affecting flower development and opening	19
1.4 – Lilies in the cut flower industry	21
1.4.1 – Bulb production and propagation	21
1.4.2 – Growing conditions for commercially produced lilies.....	22
1.4.3 – From harvest to consumer: the commercial transport chain	23
1.4.4 – Postharvest issues affecting commercial flowers and current treatments	26
1.5 – Aims of this thesis.....	29
Chapter 2 - General materials and methods	31
2.1 – Plant material, growth and growth room conditions	31
2.1.1 – On plant	31
2.1.1.1 – On plant grown in Cardiff University greenhouse conditions	31
2.1.1.2 – On plant grown in E.M. Cole Farms Ltd. greenhouse conditions	32
2.1.2 – Commercially treated stems	32
2.1.2.1 – E.M. Cole Farms Ltd. Commercial treatment and transport conditions	32
2.1.2.2 – Cardiff University commercial treatment simulation	33
2.1.3 – Cardiff University growth room/vase life conditions	33
2.2 – Stages of lily growth and development.....	34
2.3 – Position on stem nomenclature	35

2.4 – Time of opening assay	36
2.5 – Tepal epidermal pavement cell growth analysis	37
2.6 – Nucleic acid extraction techniques	39
2.6.1 – DNA extraction from lily material using DNeasy Plant Mini Kit (Qiagen)	39
2.6.2 – RNA extraction from lily tepal material.....	39
2.6.3 – RNA extraction using Tri-reagent	40
2.6.4 – RNA extraction using CTAB buffer	40
2.6.5 – Quality assessment of extracted RNA	41
2.7 – DNase treatment for RNA used for RNA-seq and cDNA synthesis	41
2.8 – cDNA synthesis	42
2.9 – Molecular biology techniques for PCR and qPCR.....	42
2.9.1 – Primer design.....	42
2.9.2 – Polymerase chain reaction (PCR) conditions.....	47
2.9.3 – Gel electrophoresis.....	47
2.9.4 – qPCR relative gene expression analysis.....	48
2.10 – Terminal bud opening assay.....	49
Chapter 3 – Characterisation of commercially treated lily flower opening as compared to on plant	51
3.1 – Introduction.....	51
3.1.1 – Time of opening in lilies.....	51
3.1.2 – Endogenous and exogenous factors affecting the physical opening process.....	53
3.1.3 – Global cellular changes causing flower opening in lilies	55
3.1.4 – Aims of investigation	56
3.2 – Materials and methods	57
3.2.1 – Time of opening assay comparing on plant/commercially treated lilies	57
3.2.2 – Assessing impact of cold/dark treatment on time of opening in lilies.....	58
3.2.3 – Preliminary tepal epidermal pavement cell growth assay in commercially treated lilies over opening	58
3.2.4 – Tepal epidermal pavement cell growth assay comparing on plant to commercially treated flowers	59
3.2.5– Assessing effect of competition on ability to open in terminal lily buds	60
3.3 – Results	61
3.3.1 – Variation in flower opening time due to number of buds per stem (competition on stem) and the effect of commercial treatment	61

3.3.2 – Separating the effect of harvest and cold/dark treatment on time of opening ..	64
3.3.3 – Flower opening is driven by differential cell expansion across the tepal	67
3.3.4 – Differential cell expansion for flower opening is not significantly different between on plant and commercially treated flowers.....	73
3.3.5 – Analysing the influence of competition on stem on ability to open of terminal buds	76
3.4 – Discussion	78
3.4.1 – Do lilies maintain the same flower opening time when commercially treated? .	78
3.4.2 – Is harvest or the cold/dark treatment responsible for this delay in flower opening time?.....	80
3.4.3 – Does differential cell expansion cause the change in tepal shape in flower opening?	82
3.4.4 – Is there a significant difference in flower opening regarding cell expansion in commercially treated buds compared to on plant?.....	84
3.4.5 – Does competition on stem outweigh the nutritional benefits of attached vs. detached buds?	85
3.4.6 –Conclusions.....	86
Chapter 4 – Physiological mechanisms and regulation of flower opening in lilies	87
4.1 – Introduction.....	87
4.1.1 – Role of carbohydrates in flower development and opening	87
4.1.2 – Carbohydrate partitioning and competition on stem	88
4.1.3 – Effect of commercial treatment on nutrient availability in flower buds	91
4.1.4 – Effect of position on stem on nutrient availability in flower buds.....	93
4.1.5 – Aims of investigation	93
4.2 – Materials and methods	94
4.2.1 – Qualitative tepal starch stain using Lugol solution comparing on plant and commercially treated flowers	94
4.2.2 – Experimental setup for investigation of sugar and starch metabolism in lilies ..	94
4.2.2.1 – Quantitative starch assay using an enzymatic method	95
4.2.2.2 – Metabolite fingerprinting and quantitative sugar analysis by flow injection electrospray high resolution mass spectrometry (FIE-HRMS) and gas chromatography- time of flight mass spectrometry (GC-tofMS)	97
4.2.3 – Relative expression analysis of cell expansion-related genes across flower opening using qPCR	99
4.3 – Results	101

4.3.1 – Loss of tepal starch and concomitant gain of tepal glucose, fructose and sucrose supports tepal edge vs. midrib differential growth theory of flower opening	101
4.3.2 – Additive effect of commercial treatment and position on stem on starch staining in tepals	103
4.3.3 – Effects of commercial treatment and position on stem on tepal starch content	106
4.3.4 – Effect of commercial treatment and position on stem on tepal glucose, fructose and sucrose content	110
4.3.5 – Commercial treatment and position on stem has a significant impact on tepal metabolism	113
4.3.5.1 – Comparative analysis of metabolomes with regard to treatment and position on stem over development and opening	114
4.3.5.2 – Comparative analysis of the effect of position on stem on metabolome controlling for treatment and location on tepal.....	127
4.3.6 – Relative expression of sugar metabolism, transport, and cell expansion-related genes across flower opening	134
4.4 – Discussion	137
4.4.1 – Is cell expansion in Oriental lily opening driven by carbohydrate mobilisation and metabolism?	137
4.4.2 – Does commercial treatment have a negative impact on bud metabolic physiology over opening?.....	140
4.4.3 – Does position on stem affect bud metabolic physiology over opening?	142
4.4.4 – Conclusions	145
Chapter 5 – Exploring the genetic mechanisms and regulation of lily flower opening to understand its mis-regulation in postharvest bud abortion	147
5.1 – Introduction.....	147
5.1.1 – The regulation of opening in lilies: what is currently known	147
5.1.2 – Mis-regulation of flower opening in postharvest bud abortion	148
5.1.3 – RNA-seq as a tool to compare regulatory gene expression	149
5.1.4 – Aims of investigation	150
5.2 – Materials and methods	151
5.2.1 – Collection of samples.....	151
5.2.2 – RNA extraction and preparation for RNA sequencing.....	152
5.2.3 – RNA sequencing.....	152
5.2.4 – <i>De novo</i> assembly of transcriptome.....	153
5.2.5– Transcript quantification and identification of DEGs	153

5.2.6– Functional analysis of DEGs.....	154
5.2.7– Coexpression analysis of DEGs	155
5.2.8– Identification, network analysis and expression analysis of regulatory genes of interest.....	156
5.2.9– Identification of TF motifs to investigate possible regulation of co-expressed DEGs.....	156
5.2.10– qPCR validation of relative gene expression of genes of interest.....	157
5.3 – Results	158
5.3.1 – Characterisation of DEGs found between all conditions	158
5.3.2 – Characterisation of DEGs between buds which subsequently opened and those which failed to	159
5.3.2.1 –GO term enrichment.....	160
5.3.2.2 –KEGG pathway analysis.....	163
5.3.3 – Separating DEGs into those necessary for opening and those related to differences in size and stage of development.....	169
5.3.4 – Analysis of genes required for flower opening	171
5.3.5 – Analysis of genes relating to magnitude of opening.....	175
5.3.6 – Identifying genes with a degree of opening-dependent effect using K-means clustering.....	179
5.3.7 – Validation of DEG expression using qPCR	183
5.3.8 – Analysis of putative regulatory and hormone-related genes	185
5.3.8.1 – Transcription factor network analysis	192
5.3.8.2 – TF motif analysis in “Required to open” group	195
5.4 – Discussion	200
5.4.1 – Analysis of DEGs significantly involved in ability of the terminal bud to successfully open.....	200
5.4.2 – Analysis of DEGs significantly involved in magnitude of opening.....	203
5.4.3 – Analysis of putative regulatory genes involved in the future opening success of terminal buds.....	204
5.4.4 – A suggested model for the transition from primary to secondary metabolism as part of normal flower bud development	207
5.4.5 – Conclusions.....	209
Chapter 6 – Hormonal regulation of flower opening	210
6.1 – Introduction.....	210
6.1.1 – Regulation of opening by phytohormone signalling	210

6.1.2 – The role of phytohormones in postharvest treatments	213
6.1.3 – Potential new treatments for failure of opening in terminal buds.....	214
6.1.4 – Aims of investigation	215
6.2 – Materials and methods	215
6.2.1 – Effect of exogenous auxin/auxin transport inhibitor application on individual lily bud opening.....	215
6.2.2 – Effect of exogenous auxin application on lily opening on stem	216
6.2.3 – Expression of phytohormone-related genes over flower opening	217
6.2.3.1 – Expression of phytohormone-related genes over flower opening.....	218
6.2.3.2 – Expression of auxin-related and flower opening-related genes on flowers treated with exogenous auxin/auxin transport inhibitor	219
6.2.4 – Effect of exogenous auxin on terminal buds at risk of postharvest bud abortion	219
6.3 – Results	220
6.3.1 – Relative expression of phytohormone-related genes over flower opening	220
6.3.2 – Effect of exogenous auxin on flower opening in individual buds	224
6.3.3 – Effect of exogenous auxin on flower opening in whole stems	226
6.3.4 – Relative expression of auxin- and flower opening-related genes in NAA- and NPA-treated buds	228
6.3.5 – Effect of exogenous auxin on terminal buds at risk of postharvest bud abortion	230
6.4 – Discussion	232
6.4.1 – Do endogenous changes in phytohormones drive flower opening?	232
6.4.2 – Can exogenous auxins be used to support lily opening in postharvest treatments?	234
6.4.3 –Conclusions.....	236
Chapter 7 – General discussion	237
7.1 – The physical and physiological basis of flower opening in lilies	237
7.2 – Regulation of flower opening in lilies on plant	241
7.2.1 – The role of auxin in lily flower opening	243
7.3 – Mis-regulation of flower opening in commercially treated lily stems	245
7.3.1 – Stress and metabolism in commercially treated lilies	247
7.3.2 – Identifying auxin-related targets which may influence postharvest bud abortion.....	248

7.4 – Further work.....	251
7.4.1 – Further work on tepal physiology and metabolism.....	251
7.4.2 – Further work on confirming the hormonal and genetic regulation of flower opening in lilies	253
7.5 – Discussion of potential impact of research	256
7.6 – Final conclusions.....	257
Appendices	259
1 – Preliminary experiment to explore bud length required for flower opening when detached from stem	259
2 – An <i>Agrobacterium tumefaciens</i> driven method for transient expression in <i>Lilium</i>	260
3 – Epidermal pavement cell area growth analysis	261
3.1 – in Oriental lilies	261
3.2 – in <i>L. longiflorum</i> lilies	263
4 – List of DEGs, putative identification and full GO term enrichments	265
4.1 – List of genes, GO term and KEGG pathway enrichment analysis between SRC and SSO/LFO buds.....	265
4.2 – Gene identification and GO term enrichment for ‘Required to open’ group ..	300
4.3 – Gene identification and GO term enrichment for ‘Magnitude of opening’ group	305
4.4 – Gene identification and GO term enrichment for Cluster 3	313
4.5 – Gene identification and GO term enrichment for Cluster 4	317
4.6 – Gene identification and GO term enrichment for Cluster 7	319
4.7 – Gene identification and GO term enrichment for Cluster 8.....	321
5 – Primer design.....	335
6 – Statistical test results	346
7 – Reanalysis of (Shi et al. 2018b) transcriptomic data	374
References	401

List of figures

- 1.1 Crossing polygon showing the hybridisations between species in the genus *Lilium*, p. 7.
- 1.2 Targets for breeding in lilies, including physical aspects (plant or flower phenotype), physiological aspects regarding growth and tolerance to conditions/infection, and regulatory aspects (time of opening), p. 9.
- 1.3 Differences in flower structure between the open and closed lily bud, showing characteristic changes that occur over flower opening in the tepals, anthers, and gynoecium, p. 11.
- 1.4 Diagram showing the genetic regulation of flowering time in *A. thaliana*, describing how long day conditions drive expression of *CONSTANS* (*CO*), which positively regulates the expression of other floral induction genes such as *FLOWERING TIME* (*FT*), p. 16.
- 1.5 Description of the harvest to consumer commercial transport supply chain for Oriental and LA hybrid lilies grown and sold in the UK, p. 25.
- 1.6 Physiological disorders in *Lilium* which have been indicated as occurring postharvest, p.28.
- 2.1 Visual staging of flower development in Oriental and *L. longiflorum* lilies, p.34.
- 2.2 Nomenclature for position on stem, p. 36.
- 2.3 Timelapse photography setup for time of opening experiments and example of photographs taken, p.37.
- 2.4 Schematic of lily tepal prepared for microscopy and example photograph, p. 38.
- 2.5 Experimental setup for collection of material for terminal bud opening assay, p. 50.
- 3.1 The circadian cycle in plants and how light interacts with it, p.53.
- 3.2 Bubble plot showing time of opening in lilies to show the effect of position on stem and commercial treatment on time of opening, pp. 63-64.
- 3.3 Time to open and synchronous opening analysis of Oriental lily buds, comparing commercially harvested stems with cold/dark treatment and harvested only with on plant, pp. 66-67.
- 3.4 Epidermal pavement cell growth in Oriental lily tepals over development and opening, considering different sections of the tepal to identify regions of fastest growth, p. 69.
- 3.5 Epidermal pavement cell growth in *L. longiflorum* lily tepals over development and opening, considering different sections of the tepal to identify regions of fastest growth, p. 72.
- 3.6 Comparison of epidermal pavement cell area change between Stages 1-5 in on plant tepals compared to commercially treated, p. 75.
- 3.7 Frequency of bud opening/failure comparing the influence of competition on stem on terminal buds, p. 78.
- 4.1 Diagram to illustrate the two main phloem loading strategies in plants (symplastic and apoplastic), p. 90.

- 4.2 Sample collection method of tepals for the experiments described in Section 4.2.2.1 and 4.2.2.2, p. 95.
- 4.3 Tepal starch, sucrose and glucose content over flower opening, comparing content in edge vs. midrib sections, p. 102.
- 4.4 Loss in tepal starch over Oriental lily development and opening on plant, p. 103.
- 4.5 Qualitative starch Lugol stain to show the effect of position on stem and commercial treatment on starch content over development for Oriental lily Tisento, Oriental lily Ascot and LA hybrid lily Eyeliner, p. 105.
- 4.6 Tepal starch content over flower development and opening comparing on plant and commercially treated samples, pp. 107-108.
- 4.7 Gas chromatography-mass spectrometry analysis on tepal samples quantifying relative tepal content of glucose isomer 2355, glucose isomer 1695, fructose isomer 235 and sucrose, comparing on plant and commercially treated flowers, p. 112.
- 4.8 Example spectrum from FIE-HRMS, p. 113.
- 4.9 Canonical Analysis of Principal coordinates based on the full metabolomes of all lily tepal samples collected using FIE-HRMS, p. 116.
- 4.10 Random Forest classification based on the full metabolomes of all lily tepal samples collected using FIE-HRMS, p. 118.
- 4.11 Total ion count (TIC) of selected compounds most important in the classification of profiles using Random Forest analysis with respect to stage of development, p. 120.
- 4.12 Total ion count (TIC) of selected compounds most important in the classification of profiles using Random Forest analysis with respect to treatment, p. 122.
- 4.13 Total ion count (TIC) of selected compounds most important in the classification of profiles using Random Forest analysis with respect to location on tepal, p. 124.
- 4.14 Total ion count (TIC) of selected compounds most important in the classification of profiles using Random Forest analysis with respect to position on stem, p. 126.
- 4.15 Canonical Analysis of Principal coordinates based on subsets of lily tepal metabolomes collected using FIE-HRMS, p. 128.
- 4.16 Random Forest classification based on subsets of lily metabolomes collected using FIE-HRMS, p.130.
- 4.17 Random Forest classification based on lily tepal CT Edge metabolomes collected using FIE-HRMS, p. 131.
- 4.18 Total ion count (TIC) of selected compounds most important in the classification of CT edge profiles only using Random Forest analysis with respect to position on stem, p. 133.
- 4.19 Relative expression of putative flower opening-related genes over development and opening by qPCR, p.136.

- 5.1 Photograph of the buds used in the RNA sequencing experiment, p. 152.
- 5.2 GO term enrichment using all DEGs in all comparisons which significantly aligned to an *A. thaliana* orthologue, comparing to a normal *A. thaliana* background using CirGO software, p. 159.
- 5.3 Diagram showing comparisons between SRC and SSO/LFO buds, p. 160.
- 5.4 GO term enrichment analysis of DEGs between SRC and SSO/LFO buds, p. 162.
- 5.5 KEGG pathway enrichment analysis of DEGs between SRC and SSO/LFO buds, p. 163.
- 5.6 KEGG pathway map for photosynthetic components, colour coded to show the log₂FC between SRC and SSO/LFO buds, p. 165.
- 5.7 KEGG pathway map for phenylpropanoid biosynthesis and metabolism, colour coded to show the log₂FC between SRC and SSO/LFO buds, p. 166.
- 5.8 KEGG pathway map for the MAPK signalling pathway, colour coded to show the log₂FC between SRC and SSO/LFO buds, p. 168.
- 5.9 KEGG pathway map for the phytohormone signal transduction pathways, colour coded to show the log₂FC between SRC and SSO/LFO buds, p. 169.
- 5.10 Venn diagram showing the number of DEGs unique to and shared between each comparison, p. 171.
- 5.11 Diagram showing comparisons between SRC and SSO buds only ('Required to open' group), p. 172.
- 5.12 GO term enrichment analysis of DEGs in the 'Required to open' group, p. 173.
- 5.13 STRING analysis of DEGs in the 'Required to open' group, p. 175.
- 5.14 Diagram showing comparisons between SSO and LFO buds only ('Magnitude of opening' group), p. 176.
- 5.15 GO term enrichment analysis of DEGs in the 'Magnitude of opening' group, p. 177.
- 5.16 STRING analysis of DEGs in the 'Magnitude of opening' group, p. 179.
- 5.17 K-means clustering graphs to show the patterns of relative expression (here expressed as log₂FC), and number of DEGs identified in the eight clusters, p. 180.
- 5.18 Relative expression of putative *MYB21*, *EXPA8* and *PSII5* genes compared in flowers which later failed to open (SRC buds) to flowers which opened at a similar length (SSO buds) and flowers which opened at a longer length (LFO buds) measured by qPCR, p. 184.
- 5.19 Analysis of transcription factors (TFs) found in the whole transcriptome, p. 186.
- 5.20 Heatmap of DEGs aligning significantly to *Viridiplantae* transcription factors, pp.188-189.
- 5.21 Heatmaps of DEGs aligning significantly to auxin related genes and cytokinin related genes, p. 189.

- 5.22 Relative expression of putative *YUC3*, *IAA14*, *ARF15* and *SAUR75* genes compared in flowers which later failed to open (SRC buds) to flowers which opened at a similar length (SSO buds) and flowers which opened at a longer length (LFO buds) measured by qPCR, p. 191.
- 5.23 Heatmap of DEGs aligning significantly to stress response signalling components, p. 192.
- 5.24 Network analysis using DEGs more highly expressed in SSO/LFO buds compared to SRC buds, p. 193.
- 5.25 Network analysis using DEGs less highly expressed in SSO buds compared to SRC buds, p. 194.
- 5.26 Network analysis using DEGs more highly expressed in LFO buds compared to SSO buds, p. 195.
- 5.27 Enriched TF motifs in the 'Required to open' group, p. 196.
- 5.28 Putative model showing the expression levels of certain types of genes in precondition of buds going on to open and of buds which fail to, p. 208.
- 6.1 Diagram showing the inputs and outputs of the auxin pathway, integrating environmental and endogenous signals, p. 212.
- 6.2 Relative gene expression of putative auxin-related genes over Stages 1-5 of flower development and opening by qPCR, p. 221.
- 6.3 Relative gene expression of putative cytokinin-related genes over Stages 1-5 of flower development and opening by qPCR, p. 223.
- 6.4 Time taken to open from harvest of individual commercially treated Position A LA hybrid 'Courier' buds, comparing those treated with 10 μ M NAA, 100 μ M NAA, and 100 μ M NPA to controls, p. 224.
- 6.5 Time taken to open from harvest of individual commercially treated Position A Oriental 'Tisento' buds, comparing those treated with 10 μ M NAA and 100 μ M NPA to controls, p. 226.
- 6.6 Time taken to open from harvest of commercially treated Position A Oriental 'Pacific Ocean' stems treated with 10 μ M NAA or without to on plant controls, p. 227.
- 6.7 Relative gene expression of putative auxin-related genes and cell expansion-related genes by qPCR, comparing buds treated with 10 μ M NAA and 100 μ M NPA to controls, p. 229.
- 6.8 Bud length of buds grouped according to terminal bud opening success (failed to open vs. opened) in NAA-treated buds vs. controls, p. 231.
- 6.9 A potential hypothesis for the timing of auxin and cytokinin response in lilies over their development and opening, p. 234.
- 7.1 A model showing the possible physiological methods which may account for cell expansion and global tepal growth over flower development, p. 240.
- 7.2 Diagram showing possible mechanisms for stress-induced auxin signalling inhibition in buds at risk of bud opening failure, p. 250.

List of tables

- 1.1 RHS classification of lily groups and their description, pp. 3-6.
- 2.1 Average bud lengths used to stage different lily varieties at Stage 1 (Position A buds only), p. 35.
- 2.2 List of primers used for PCR and qPCR, annealing temperatures used, and their products, p. 4.2.
- 3.1 Analysis of the influence of competition on stem on the opening ability of terminal buds, p. 77.
- 4.1 Putatively identified genes targeted for qPCR analysis as having a role in tepal cell expansion and flower opening, p. 100.
- 4.2 Statistical comparison (by student's independent T-test or Mann-Whitney-U test) comparing tepal starch content in Position A and C buds at the same stage and treatment in tepal edges only, p. 109.
- 4.3 Statistical comparison (by student's independent T-test or Mann-Whitney-U test) comparing tepal starch content in Position A and C buds at the same stage and treatment in tepal midribs only, p. 110.
- 4.4 Twenty top compounds in the classification of metabolite profiles by Random Forest with regard to stage of development and their putative identification, p. 119.
- 4.5 Twenty top compounds in the classification of metabolite profiles by Random Forest with regard to treatment and their putative identification, p. 121.
- 4.6 Twenty top compounds in the classification of metabolite profiles by Random Forest with regard to location on tepal and their putative identification, p.123.
- 4.7 Twenty top compounds in the classification of metabolite profiles by Random Forest with regard to position on stem and their putative identification, p. 125.
- 4.8 Twenty top compounds in the classification of a subset of metabolite profiles (CT Edge) by Random Forest with regard to position on stem and their putative identification, p. 132.
- 5.1 Genes of interest putatively identified to validate significant DEGs found in the transcriptome by qPCR, pp. 157-158.
- 5.2 Identification of DEGs containing enriched motifs upregulated in the 'Required to open' group, p. 198.
- 5.3 Identification of DEGs containing enriched motifs downregulated in the 'Required to open' group, p. 199.
- 6.1 Putative genes relating to auxin- and other phytohormone-related functions, pp. 217-218.
- 6.2 Analysis of the influence of exogenous auxin treatment on the opening ability of terminal buds, p. 231.

Acknowledgements

Firstly I'd like to thank my wonderful supervisory team for their invaluable help, advice and criticism throughout my project – Hilary Rogers, Walter DeWitte, Paul Devlin (Royal Holloway), and also Tony Stead (Royal Holloway), who offered his expertise throughout. Secondly, I'd like to extend a huge thank you to James and Alex Cole (E.M. Cole Farms Ltd.), who so generously provided many of the lilies used in my experiments, and also for patiently answering my many questions about commercial practices and allowing me to visit and use their greenhouse space. I'd also like to thank Chrysal International for contributing to this project, and in particular Rolf Timmerman and Tracey Thomas, who also helped to enhance my understanding of commercial flower growing and supply chains. I'm so grateful to be a part of the BBSRC SWBio DTP programme who funded my project and allowed me to be part of an excellent cohort of scientists.

I would like to also thank the contributors to the work carried out in this thesis. I'm very grateful to Dr Manfred Beckmann (Aberystwyth) for helping me with the FIE-HRMS and GC-MS work on the tepal material and advising me on the analysis. I would also like to thank Angela Marchbank for her work in the RNA sequencing which I used in this project and Pete Kille for his help in assembling the transcriptome. Sequence data used for primer design in this thesis was kindly sent by Shaochuan Shi (China Agricultural University, Beijing) who I would also like to thank. I'd certainly like to extend a massive thanks to Sarah Christofides and Carsten Müller for going above and beyond in helping and advising me with my Big Data problems. I'm also grateful to the summer students who kindly carried out qPCR experiments and starch assays with me. I also can't forget Lyndon, Richard and Sam, who ensured I had material to work on with their tireless efforts at the greenhouses keeping my lilies alive – I have appreciated it massively!

Thanks to my whole lab and extended fellow PhD student support network for listening to my complaints, offering advice, and supporting my successes over a coffee or beer whenever needed. Special thanks to Ashley, Sven, Toby and Stephe who made working in the lab every day feel like a party and who I will miss working with very much.

Finally, a huge thank you to my partner Brendan and to both of our families and friends for the constant support, hugs, pep talks, and offers to read my thesis. You've all been extremely patient and believed in me at every step.

Chapter 1 - General introduction

Lilies are one of the most popular commercially sold fresh-cut flowers grown in the UK after chrysanthemum and alstroemeria (Hanks 2018), and overall, UK flowers and plants were worth £1.2 billion in 2016 (Brown and Pool 2017). Oriental and Asiatic varieties are popularly used by many growers due to hardiness pre-harvest and large, colourful blooms. However, many cultivars suffer from poor vase life in addition to wastage of up to 50% at the processing stages (Senapati et al. 2016). Commercial growers and sellers rely on experience to harvest stems at the correct maturity to ensure that all blooms on the stem are of the right developmental stage to open (Gill et al. 2006), while also not opening prematurely and limiting their life. This balancing act is difficult to standardise, especially with fluctuating store conditions, and often consumers are disappointed with premature blooming in store or failure of buds to open. A better understanding of the mechanisms and regulation of flower opening in lilies is a vital first step in finding post-harvest treatments that will for example slow opening whilst in store or speed up opening once the consumer brings them home. Additionally, although every effort is taken to ensure that fresh-cut lilies reach the customer in the shortest possible time, it is estimated UK and Europe-grown stems may spend at least 48 hours in transit before reaching the store, and pass through stressful processing treatments which include dehydration, grading, sorting, cooling, and transportation (Balas et al. 2006), some of which are carried out in complete or partial darkness to reduce plant transpiration (RHS (2022)[a]).

1.1 What are lilies?



True lilies fall under the genus *Lilium*, a group of perennial ornamental flowering monocotyledonous plants. They are characterised by large flowers and underground bulbs as a vegetative starch storage organ by which they can perennially grow (Okubo and Sochacki 2013). The genus contains around 110 species which grow in diverse environments in the northern hemisphere across North America, Europe, Middle East and East Asia (Pelkonen and Pirttilä 2012). Several species of lily are specifically endemic to Japan and have contributed to the most popular varieties we use today (Marasek-Ciolakowska et al. 2018).



Lilies have been grown as decorative flowers since the days of ancient Egypt (*L. candidum*) and especially in Europe have been cultivated as garden plants at least since the 16th century (Bos 1993). The introduction of new species and varieties to Europe in particular caused a boom in production of cultivars; however, these were mainly limited to hybridising related species until improvements in breeding techniques overcame the interspecific incompatibility between varieties such as *L. longiflorum* and Asiatics to create LA hybrids (Pelkonen and Pirttilä 2012).





1.1.1 Genetic background of current lily varieties




Today, there are several types of lily sold as cut flowers, with the five main varieties being Asiatics, Orientals, LA hybrids (*L. longiflorum* x Asiatic), OT hybrids (Oriental x Trumpet), and LO hybrids (*L. longiflorum* x Oriental). Asiatic hybrids, *L. longiflorum* and Oriental hybrids are the most popular varieties grown and sold worldwide, with over 740,600 hectares estimated to be used for flower, pot plants and bulb production worldwide (Grassotti and Gimelli 2011). These have variations in features such as flower shape, size, colour, clustering of flowers on the stem, and scent (Gill et al. 2006). Cross breeding and hybridisation have created a huge range of phenotypes which have been classified by the Royal Horticultural Society (RHS, Table 1.1). The commercial hybrids mentioned above (including *L. longiflorum*, which is most commonly grown as a *L. longiflorum* hybrid such as those in Division 5) come mostly from Divisions 7 and 8, being LA and Oriental hybrids (Lim et al. 2008). In 2010, the 25 most grown lily cultivars in the Netherlands in terms of production area included 12 Oriental hybrids, five LA hybrids and four OT hybrids (van Tuyl and Arens 2011).

Table 1.1 - RHS classification of lily groups and their description. Adapted from the RHS International Lily Register and Checklist (Donald 2012). All pictures are taken from <http://rhslilygroup.org/> (Accessed November 2022).

Division	Name	Description	Example
1	Asiatic	<p>Short sturdy plants (height). Small blooms in a wide range of colours. Usually non-scented. Blooming period between April-June. Derived from the following species and interspecific hybrids: <i>amabile</i>, <i>bulbiferum</i>, <i>callosum</i>, <i>cernuum</i>, <i>concolor</i>, <i>dauricum</i>, <i>dauidii</i>, <i>L. × hollandicum</i>, <i>lancifolium</i> (syn. <i>tigrinum</i>), <i>lankongense</i>, <i>leichtlinii</i>, <i>L. × maculatum</i>, <i>pumilum</i>, <i>L. × scottiae</i>, <i>wardii</i> and <i>wilsonii</i>.</p>	 <p>'Grand Cru'</p>
2	Martagon hybrids (Tiger lilies)	<p>Based on the hybrids <i>L. × dalhansonii</i>, <i>hansonii</i>, <i>martagon</i>, <i>medeoloides</i> and <i>tsingtauense</i>. Strongly recurved tepals, blooms face downward. Early flowering.</p>	 <p>'Amelita'</p>

<p>3</p>	<p>Candidum hybrids (Easter lilies)</p>	<p>Trumpet shaped blooms facing downward. Derived from <i>candidum</i>, <i>chalcedonicum</i>, <i>kesselringianum</i>, <i>monadelphum</i>, <i>pomponium</i>, <i>pyrenaicum</i> and <i>L. × testaceum</i></p>	 <p><i>L. candidum</i>/Madonna</p>
<p>4</p>	<p>American hybrids</p>	<p>Taller plants hybridised from <i>bolanderi</i>, <i>L. × burbankii</i>, <i>canadense</i>, <i>horticultural classification 14 columbianum</i>, <i>grayi</i>, <i>humboldtii</i>, <i>kelleyanum</i>, <i>kelloggii</i>, <i>maritimum</i>, <i>michauxii</i>, <i>michiganense</i>, <i>occidentale</i>, <i>L. × pardaboldtii</i>, <i>pardalinum</i>, <i>parryi</i>, <i>parvum</i>, <i>philadelphicum</i>, <i>pitkinense</i>, <i>superbum</i>, <i>vollmeri</i>, <i>washingtonianum</i> and <i>wigginsii</i>. Often referred to as tree lilies. Characterised by rhizomatous root stocks.</p>	 <p>'Peachwood'</p>

5	Longiflorum lilies	Hybrids derived from <i>formosanum</i> , <i>longiflorum</i> , <i>philippinense</i> and <i>wallichianum</i> . Typically all white flowers, strongly scented.	 <p>'White Heaven'</p>
6	Trumpet and Aurelian	Hybrids derived from <i>L. × aurelianense</i> , <i>brownii</i> , <i>L. × centigale</i> , <i>henryi</i> , <i>L. × imperiale</i> , <i>L. × kewense</i> , <i>leucanthum</i> , <i>regale</i> , <i>rosthornii</i> , <i>sargentiae</i> , <i>sulphureum</i> and <i>L. × sulphurgale</i> (except hybrids of <i>henryi</i>). Trumpet shaped flowers.	 <p>'Charlie Kroell'</p>
7	Orientals	Based on hybrids of <i>L. auratum</i> , <i>japonicum</i> , <i>nobilissimum</i> , <i>L. × parkmanii</i> , <i>rubellum</i> and <i>speciosum</i> . Tall plants with large open flowers that tend to face upward. Tend to flower late in the year.	 <p>'Special News'</p>
8	Other hybrids	Any other hybrids that do not fall into the other divisions. Includes all interdivisional hybrids, such as <i>longiflorum</i> /Asiatic (LA) hybrids, <i>longiflorum</i> /Oriental	 <p>LA hybrid 'Toscanini'</p>

		<p>(LO) hybrids, Oriental/Asiatic (OA) hybrids and Oriental/Trumpet hybrids (Oriempets or OT hybrids). Hybrids of <i>henryi</i> with <i>auratum</i>, <i>japonicum</i>, <i>nobilissimum</i>, <i>15 L. × parkmanii</i>, <i>rubellum</i> and <i>speciosum</i>.</p>	
<p>9</p>	<p>Species</p>	<p>All species and subspecies/varieties/cultivars that derive from them.</p>	 <p><i>L. auratum</i></p>  <p><i>L. henryi</i></p>  <p><i>L. martagon</i></p>

Different lily varieties are often bred to bring together desirable characteristics such as flower colour, shape, inflorescence organisation, resistance to disease, and forcing ability (Section 1.2.2). This breeding has been carried out both interspecifically to develop new hybrid varieties such as LA and LO hybrids (Figure 1.1), requiring *in vitro* methods, or intraspecifically within varieties, which can be carried out using classical methods (Lim and van Tuyl 2006; Lim et al. 2008). There are a great number of wild species that have been hybridised over generations to create the commercial varieties we use today (Figure 1.1). This highlights the genetic variation possible between varieties and accounts for the huge variation in physical flower form, physiology and growth. Within each variety are a multitude of cultivars; from 1986-1996 more than 100 new cultivars per year applied for breeders' rights (van Tuyl and van Holsteijn 1996).

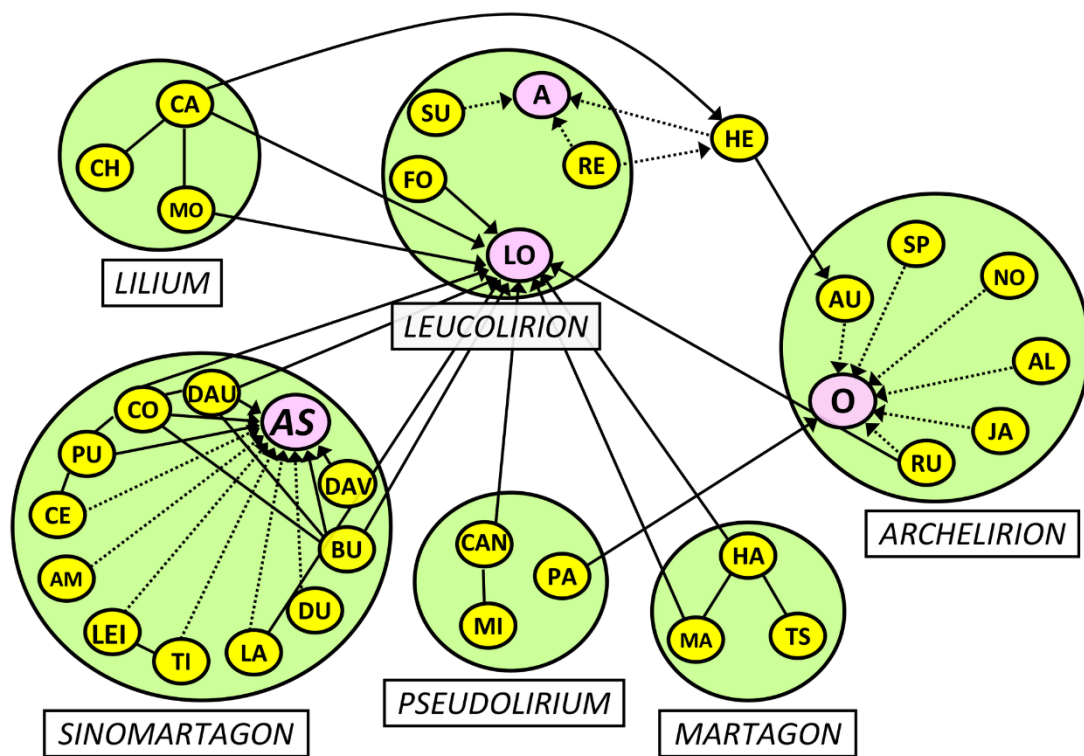


Figure 1.1 – Crossing polygon showing the hybridisations between species in the genus *Lilium* developed at Plant Research International, the Netherlands. The large ellipses indicate hybrid groups, whereas the small ellipses inside indicate the species which hybridise to form them. Arrows show successful crosses between hybrid groups with the relevant species, pointing towards the female parent. Colour coded to show wild species (yellow),

taxonomically classified sections (green) and hybrids of interest (pink). Abbreviations used: A: Aurelian hybrids; AL: *L. alexandrae*; AM: *L. amabile*; AS: Asiatic hybrids; AU: *L. auratum*; BU: *L. bulbiferum*; CA: *L. candidum*; CAN: *L. canadense*; CE: *L. cernuum*; CH: *L. chalcedonicum*; CO: *L. concolor*; DAU: *L. dauricum*; DAV: *L. davidii*; DU: *L. duchartrei*; FO: *L. formosanum*; HA: *L. hansonii*; HE: *L. henryi*; JA: *L. japonicum*; LA: *L. lankongense*; LEI: *L. leichtlinii*; LO: *L. longiflorum*; MA: *L. martagon*; MI: *L. michiganense*; MO: *L. monadelphum*; NO: *L. nobilissimum*; O: Oriental hybrids; PA: *L. pardalinum*; PU: *L. pumilum*; RE: *L. regale*; RU: *L. rubellum*; SP: *L. speciosum*; SU: *L. sulphureum*; TI: *L. tigrinum*; TS: *L. tsingtauense*.
Figure adapted from Lim and Van Tuyl (2006).

Generally, commercial breeders focus on improvements to several areas, in particular relating to the ability of the plant to grow efficiently, even under stress, and the popularity of certain phenotypic traits by consumers and retailers (Figure 1.2). The genus *Lilium* has a large variation in genome size, varying from 40 to over 160 pg in size, and contains some of the largest genomes in the plant kingdom (Du et al. 2017). While most wild lily species are diploid (Du et al. 2017), triploid and tetraploid cultivars are favoured over diploids in commercially grown lily crops due to their faster growth, larger blooms and hardiness (Marasek-Ciolakowska et al. 2018), although progeny are often sterile and this makes varieties very difficult to cross further (Lim et al. 2008). Commercially grown plants can also include cultivars which have been treated with colchicine to make them tetraploid (Jeloudar et al. 2019). Breeding from different taxonomic sections (Figure 1.1) is well known to bring together certain phenotypic characteristics and resistances present in taxonomically distinct hybrid groups; Longiflorum hybrids are known for trumpet shape and scent, Oriental hybrids have excellent resistance to *Botrytis* infection, and Asiatic hybrids flower early in the season and additionally have resistance to *Fusarium* (Figure 1.2, Lim et al. 2008). Breeding lilies also often results in progeny of varied karyotype and is sometimes correlated with the emergence of novel desirable characteristics (Zheng et al. 2010; Anderson et al. 2012).



Figure 1.2 – Targets for breeding in lilies, including physical aspects (plant or flower phenotype), physiological aspects regarding growth and tolerance to conditions/infection, and regulatory aspects (time of opening). Figure created using data from van Tuyl et al. (1986) and van Tuyl and van Holsteijn (1996).

1.1.2 Development and growth of lily plants

Lily plants can grow from seed or bulb; as noted in Section 1.1, the genus *Lilium* produces underground vegetative imbricate bulbs (i.e. non-covered bulbs, unlike tulips, which have an outer protective tunic) which can produce both roots and shoots annually using starch stores (Wu et al. 2021). Growing lilies from seed takes a longer time to produce flowers; on average lily species require two to three years to flower post-sowing (RHS Lily Group 2022), while taking approximately 80 to 100 days to grow fully from bulb depending on variety (personal communication, James Cole, E.M. Cole Farms Ltd.).

Lily plants grow best in temperate climates, with a period of cold temperature usually required for shoot growth. It has been suggested that the evolution of bulbs allowed species such as *Lilium*, *Iris* and *Hyacinthus* to grow in cooler climates earlier in the year due to their nutritional storage and frost tolerance, and also to retain starch in dormancy during dry

weather (Rees 1966). Bulbs are usually planted in the autumn, winter or early spring therefore to ensure an appropriate overwintering period where bulbs can grow a strong root system using the starch stored in the bulb (iBulb and Anthos 2022; RHS 2022b). This overwintering period can be simulated by artificial cooling, after which bulbs can be grown in warmer conditions at any time of year to stimulate growth (known as forcing). During the spring or forcing, with higher ambient temperatures, the bulb is stimulated to produce shoots. Initially plants show vegetative growth of roots and shoots before floral initiation occurs early on in the shoot growth period - in the Oriental hybrids cv. 'Siberia' and 'Sorbonne' this was identified as starting 20 days post planting, with the average shoot length only being 11-13 cm tall - indicating that any preharvest biotic or abiotic stresses from this point onward may have an impact on the quality of the flower eventually produced (Lucidos et al. 2017).

Plant growth, bud development and flower opening are very temperature-dependent. Stem elongation and bud development increased in a linear fashion with average daily temperature increase in *L. longiflorum*, and stem elongation was particularly well correlated with an increase in the difference between day and night temperatures (Erwin and Heins 1990). The whole inflorescence develops in a staggered fashion, with the oldest bud going through the full process of opening and senescence potentially several days prior to the youngest, dependent on the number of buds per stem (Van Meeteren et al. 2001). After the flowers senesce, the remaining photosynthetic material on the stem continues to build starch reserves in the bulb for the winter period and the growth for the next spring (RHS 2022b).

1.2 Characterisation of flower anatomy

Lily flowers are characterised by their double whorl of three large, often brightly coloured tepals (so called due to the similarity in between petals and sepals, and usually called outer and inner tepals) (Okubo and Sochacki 2013). As a bud, these are tightly closed with the outer tepal edges fitting into a groove on the inner tepal midrib, locking the bud in place. As the flower develops, the growing strain of the tepals pulls against the tepal lock until it is overcome by the force, pushing the tepals open (Bialeski et al. 2000a; Liang and Mahadevan

2011). Inside the flower are 6 long filaments with anthers, and a long pistil with a superior ovary (the ovary is located on the receptacle above where above the filament attaches). When fully developed, the anthers can dehisce, allowing the pollen to fully dehydrate and become mature (Clement et al. 1996), while once the pistil has grown to full length, the stigma starts producing a large amount of stigmatic exudate which is highly attractive to pollinators and may also aid in pollen tube growth (Rosen and Thomas 1970, Nepi et al. 2012, Figure 1.3). The development of the anthers and gynoecium is coordinated with the tepals opening in a characteristic change in shape (Figure 1.3), with some varieties reflexing outward more than others (Liang and Mahadevan 2011).

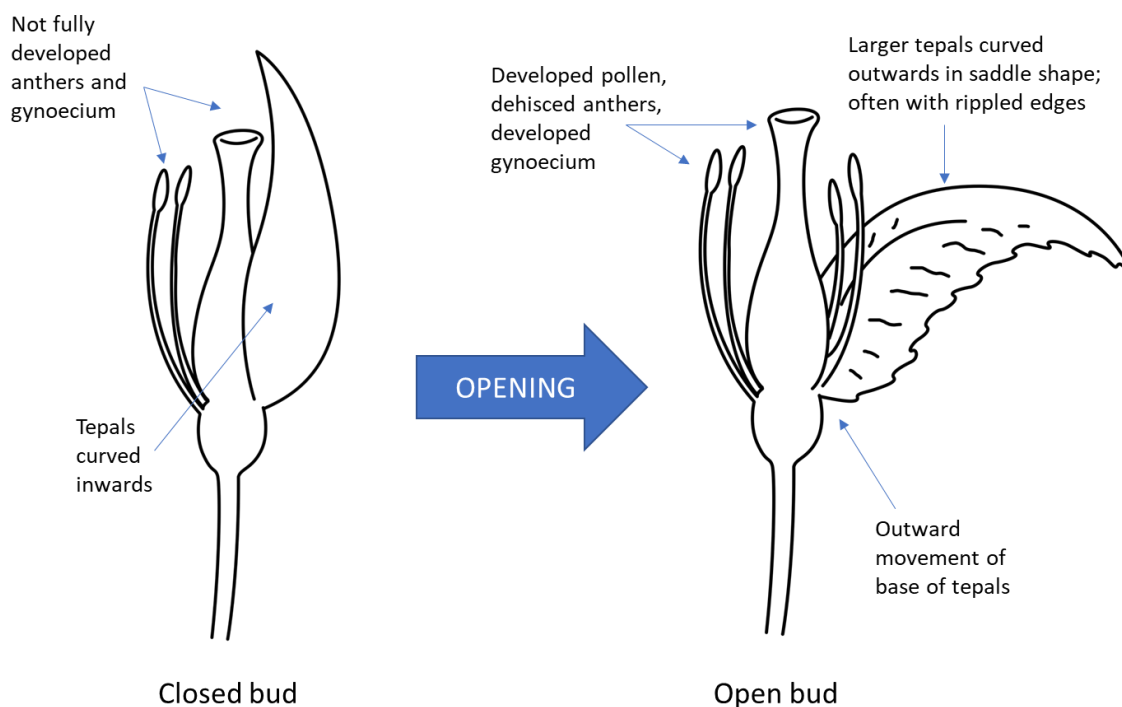


Figure 1.3 – differences in flower structure between the open and closed lily bud, showing characteristic changes that occur over flower opening in the tepals, anthers, and gynoecium. This is accompanied by changes in tepal colour, scent production, and other secondary metabolism related to flower development and maturity.

Despite their high commercial value, the mechanisms behind lily flower opening are still not fully elucidated. This is partly due to the high variation in both opening morphologies and underlying physiology adopted by different plant species, making it extremely difficult to

find common ground between well characterised species such as *Arabidopsis thaliana* and the many lily varieties used today. Physical opening processes are highly dependent on the structure of the flower; for example some flower bud phenotypes such as poppy require breaking the physical barrier of the sepal (Reid and Evans 1985), while other require a change in angle of the petal to the pedicel (Ke et al. 2018). This has also been found to occur reversibly and non-reversibly, and mechanisms for growth are often different depending on this – the non-reversible opening in rose is driven by both cell division and expansion, while flowers which can reversibly open and close such as *E. grandiflorum* have cell expansion strategies (Yamada et al. 2009a; Norikoshi et al. 2016). Physiological mechanisms can also be diverse and involve changes in cell osmotic strength through sucrose uptake, starch breakdown, or uptake of ions, causing the uptake of water and creation of turgor pressure (Eason et al. 1997; Van Doorn and Van Meeteren 2003).

Physical markers of lily development and opening include tepal growth, tepal shape change, changes to the tepal position, and development and maturity of the reproductive anthers and pistil (Van Doorn and Van Meeteren 2003). Being the reproductive organ of the plant, the production of viable pollen and ovules for successful reproduction (viable seed) is of paramount importance. Tepal development in terms of colour, scent, size, and opening, is of significant value to protect pollen from the elements at the closed bud stage, and also to attract pollinators in open flowers, therefore several processes in the flower need to be regulated to ensure coordination of timing of flower opening. This coordination is carried out through endogenous signals such as hormones, which can modulate development of other organs.

Stamens are made up of two parts; the vascular filament, and the anther, which contains both reproductive cells (pollen) and supporting tissues such as the endothecium, middle layer, and tapetum (Goldberg et al. 1993). The tapetum in particular surrounds the developing microspores and is essential for the development into mature pollen (Zhang et al. 2010; Sui et al. 2022). Pollen development occurs in well characterised stages, with a highly intense growth phase, and a slower anther maturation phase. These growth phases involve building up starch reserves in the anther via an increased uptake of soluble sugars, which is also correlated with the uptake of sucrose into and growth of tepals (Clément et al. 1994; Clement et al. 1996). Anther maturation is accompanied by pollen desiccation, which

improves overall viability in many species (Hoekstra and van Roekel 1988) and starts occurring prior to anthesis. Hormones such as abscisic acid (ABA) and jasmonic acid (JA) may be important in this desiccation process (Wang et al. 1998) and start the process of dehiscence. Anther dehiscence is defined as the curling open of the stomium of the anther, caused by swift dehydration of the cells with exposure to the air when the flower opens (Yang et al. 2007; Tong et al. 2013). This was found in Oriental lilies to be probably driven by and regulated by many of the same genes which have been hypothesised to have a role in tepal cell expansion and flower opening, such as genes involved in cell division and expansion, cell wall production (cellulose synthases), and hormone biosynthesis (auxins, gibberellins, ABA and JA) (Sui et al. 2022). Jasmonic acid (JA) is linked to promotion of flower opening in many species such as *Arabidopsis thaliana* and *Eustoma grandiflorum* (Ishiguro et al. 2001; Ochiai et al. 2013), and inhibition of flower opening in others such as iris (van Doorn et al. 2013).

Gynoecium development is not as extensively studied in lilies – the growth of the gynoecium is split into three distinct phases from initiation (Crone and Lord 1991) and may involve auxin and gibberellins, which are found at higher levels in gynoecia in the immature bud stage and drop towards anthesis (Arrom and Munne-Bosch 2012a). In *A. thaliana*, initial cytokinin and auxin signalling is required for establishment of the organ, activating gene regulatory networks which influence cell wall modification in particular (Reyes-Olalde et al. 2013; Zúñiga-Mayo et al. 2019). These same networks have been identified in several species and therefore suggest conservation across angiosperms (Zúñiga-Mayo et al. 2019). Additionally, auxin is required for pedicel and ovary elongation in *Iris* flowers, which is a prerequisite for opening in this species (van Doorn et al. 2013). The early senescence in some species caused by or accelerated by successful pollination of the flower suggests signalling from the pistil, potentially ethylene in some species (Stead 1992). This could also suggest earlier signalling may also modulate the time of flower opening, as well as senescence.

Flower opening in lilies is hypothesised to be influenced by the development of these reproductive organs. The change from a concave to convex shape, wrinkling of the tepal edges, and movement of the tepal base suggest flower opening is driven by differential growth of tepal cells (Liang and Mahadevan 2011). The growth of tepals occurs in the closed

bud until the tension in the bud is great enough for the outer tepals to overcome the attachment to the inner tepal midrib, and the flower can spring open rapidly (Bieleski et al. 2000a; Liang and Mahadevan 2011). This growth has been suggested to be driven by cell expansion due to the speed of flower opening and the lack of cell division observed after very early stages of bud development (Gould and Lord 1989; Bieleski et al. 2000a; Liang and Mahadevan 2011; Watanabe et al. 2022). The correlated rapid starch breakdown and increase in soluble sugars in tepals over flower opening (Bieleski et al. 2000a; Van der Meulen-Muisers et al. 2001) could indicate a fast requirement either for metabolism, cell wall modification and growth, or water turgor pressure related cell expansion (Beauzamy et al. 2014). Other species such as rose have been reported to break down petal starch stores into glucose (Yamada et al. 2009a), active uptake of sucrose or other ions into petals from photosynthetic tissue (Van Doorn and Van Meeteren 2003), or a combination of different approaches to create turgor pressure related cell expansion. Carbohydrates are essential for respiration in plants and are transported via the phloem from photosynthetic tissue in leaves (sources) to flowers, roots and other non-photosynthetic respiring organs (sinks) during organ development. They are transported for the most part as sucrose, and may be converted to starch in sink organs for storage until required (Lemoine et al. 2013). Carbohydrates are also the primary driver in many species for cell expansion. The general principle behind this is that an increase in cellular osmotic potential (either by uptake of sucrose/glucose or breakdown of storage molecules such as starch) can cause water to move into cells and increase their size. This can occur differentially in different regions of petals to cause the specific change in shape needed for opening, such as in petal intermediate cells in waterlily, which reversibly expand and contract in order to cause rhythmic opening and closing (Ke et al. 2018). Different plant species use different cell expansion strategies, such as a high petal insoluble starch content broken down into glucose (rose), a high fructan content broken down to fructose (*Hemerocallis* sp.), an active sucrose uptake into petal cells (gladiolus, freesia), or a combination of strategies (Van Doorn and Van Meeteren 2003).

1.3 Possible regulatory mechanisms for cell expansion and growth

The osmoticum-related cell expansion described in the previous section is driven by the expression of aquaporins and depending on the approach to increase osmotic strength in the cell, various transporters to drive water influx (Ma et al. 2008; Tong et al. 2013). This expression is fundamentally driven by various factors which have been briefly explored in previous sections, such as the endogenous developmental state of the flower, the ambient temperature, the time of day, and the other buds on the inflorescence. Phytohormones are used as chemical messengers to influence global plant activity and development (Biologists 2010). These hormones can influence regulatory mechanisms such as transcription factors, circadian factors and other phytohormones in order to cause changes to the ability and the exact time of development and flower opening.

1.3.1 Endogenous regulation of flower development and opening

The changes in physiology and anatomy which define flower opening are fundamentally caused by changes in gene expression. Development and opening of lily flowers is correlated with a change in the expression of genes involved in several processes such as cell wall loosening, phloem loading and unloading, and water uptake (Tong et al. 2013; Watanabe et al. 2022). The regulation of these processes is paramount to ensure that the timing and the spatial regulation of these processes is correct. The opening process has already been demonstrated to be influenced by many factors such as the time of day, the developmental stage of the bud, the nutritional status of the bud, and the position on stem (Van Doorn and Van Meeteren 2003; van Doorn and Kamdee 2014). Environmental inputs, as well as local input from the other buds on the same stem cause changes to flower opening, mediated by regulatory genes and phytohormones.

In *A. thaliana*, the regulation of flowering time is extensively described as relating to several different environmental and endogenous inputs, which are integrated and coordinated by the three developmental genes *FLOWERING TIME (FT)*, *SUPPRESSOR OF CO 1 (SOC1)*, and *LEAFY (LFY)*. These master transcription factors are able to switch on expression of the floral meristem determining gene *AP1* in response to gibberellins, developmental factors relating to plant age (SPLs) and circadian components (*CONSTANS (CO)* and *FLOWERING LOCUS C (FLC)*). *SOC1* is also involved in restricting expression to the correct time and space, as it is

also later involved in repression of class B and C genes mediating patterning and flower organ development. This can be affected by environmental signals, for example to fine-tune time of flowering in response to environmental temperature (Lee and Lee 2010). *SOC1* in particular integrates these various signals through its activation of *LFY* and subsequent floral organ initiation (Lee and Lee 2010, Figure 1.4). This may be also mediated by gibberellin, which also integrates seasonal signals such as day length and is required in *A. thaliana* for flowering in short-day conditions (Wilson et al. 1992). In monocots such as wheat and rice, this initiation of flowering has been found to be driven by similar genes - although *FLC* is not present in rice, several MADS-box proteins have been indicated to play a similar role in vernalization (Jeon et al. 2000; Trevaskis et al. 2003; Andersen et al. 2004), and therefore may share these pathways also with *Lilium*.

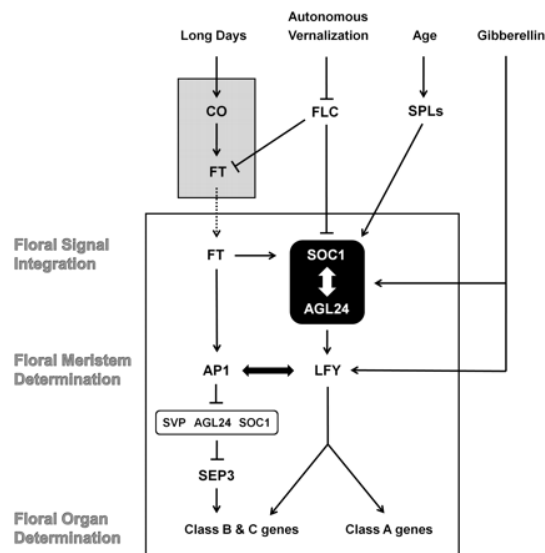


Figure 1.4 - Diagram showing the genetic regulation of flowering time in *A. thaliana*, describing how long day conditions drive expression of *CONSTANS* (*CO*), which positively regulates the expression of other floral induction genes such as *FLOWERING TIME* (*FT*). *SUPPRESSOR OF OVEREXPRESSION OF CO 1* (*SOC1*) integrates endogenous and environmental signals such as plant age, gibberellin signalling, and day length cues. The positive feedback loop between *SOC1* and *AGL24* (black box) drives expression of *LEAFY* (*LFY*) and the positive feedback in class A genes, while repressing expression of class B and C genes via *SEP3* in order to ensure floral organs develop temporally and spatially correct. While the first stages of floral induction occurs in the leaf (grey box) the rest occurs in the shoot apical meristem (white box) (Lee and Lee 2010).

Once the flower organ development has been initiated and the patterning for the developing bud has been laid down, growth occurs in each of the organ primordia by cell division up until a certain point depending on organ type. In *A. thaliana*, this occurs after the first stage of cell proliferation by TCP transcription factors and is also mediated by jasmonic acid (Brioudes et al. 2009; Huang and Irish 2015). This switch from proliferation to expansion has been observed in *L. longiflorum* tepals to stop when the bud is approximately 1/3 of its mature length (Gould and Lord 1989). Unlike the tepals, the reproductive organs such as the anthers and gynoecium require more specialised development and patterning due to their specialised roles and cell types (Reyes-Olalde et al. 2013; Sui et al. 2022). The coordination of flower opening with the reproductive organs being fully developed is important to protect pollen and the gynoecium from the elements and biotic factors. In tomato, this coordination was found to be regulated in the same way by the joint action of jasmonic acid and the MYB transcription factor SIMYB21, which mediate both flower opening and aspects of pollen development (Niwa et al. 2018), and points to coordinated hormonal control of development of several floral organs. Other MYB transcription factors have also been identified in *Lilium* as being responsible for other secondary metabolism-related functions such as anthocyanin production in tepals, sometimes in very discrete sections causing coloured spots (Yamagishi et al. 2014; Fatihah et al. 2019), and scent production (Shi et al. 2018b). In *A. thaliana* MYB transcription factors have been identified as also promoting lignin production (Zhong et al. 2007; Zhou et al. 2009), and therefore can be hypothesised to perhaps also regulate the biosynthesis of lignins in *Lilium* for cell wall production and cell expansion. Gibberellins have been found to be important in flower initiation in many species, as well as pollen development and maturation (Mutasa-Göttgens and Hedden 2009), and may also have a role in petal growth through this repression of DELLA proteins (Cheng et al. 2004). Gibberellin-mediated responses are caused by gibberellin degradation of the DELLA proteins (SLR1/RGA), which are transcriptional repressors of gibberellin-induced genes (Mutasa-Göttgens and Hedden 2009).

Endogenous factors affecting flower development are produced by the plant in response to developmental cues, such as hormonal signals from the anthers or gynoecium, or soluble sugars from the leaves (Van Doorn and Van Meeteren 2003; van Doorn and Kamdee 2014).

These signals work in the same way as for the floral induction and go on to cause a cascade of other effects through modulation of gene expression. It is also important to note that the lily stem is an inflorescence and factors such as time of opening and senescence can also be influenced by the other buds on the stem. The position on stem staggers the opening of buds due to different developmental stages, and therefore each bud is at any time receiving and sending different information about developmental age (Van Meeteren et al. 2001). Removing a lily bud from an inflorescence is well known to have the effect of making the rest of the buds much larger (van der Meulen-Muisers et al. 1995), and additionally, removing an open flower from an inflorescence increases the longevity of the flower compared to on the stem, in both lilies and alstroemeria (van der Meulen-Muisers et al. 1995; van der Meulen-Muisers 2000; Chanasut et al. 2003). The signalling factors involved in this organ-to-organ communication may also be metabolic in nature; sugar signalling is known to affect levels of hormones and circadian genes (Rolland et al. 2006; Bolouri Moghaddam and Van den Ende 2013).

There is evidence to suggest that photoinhibition and degreening is a highly important part of flower development and opening. Breakdown and dismantling of the photosynthetic machinery can be observed through a sharp decrease in the Fv/Fm ratio and tepal carotenoid content over lily flower opening (Muñoz et al. 2018). The dismantling of chloroplasts causes excess production of reactive oxygen species (ROS) which go on to produce lipid peroxidation products malondialdehyde (MDA) and jasmonic acid (JA). These are already well-known signalling molecules involved in the stress response (Weber et al. 2004; Ding et al. 2016), but have also been implicated as being essential to developmental processes too in both *A. thaliana* and lily (Mandaokar et al. 2006; Wasternack et al. 2013; Muñoz et al. 2018). More recently, Zhang et al. (2021) specified this increase in MDA, as well as the concomitant decrease in other tepal nutrients, as being temporally linked with the 'bud cracking' stage, suggesting that the start of opening is a particular turning point in tepal metabolism. The decrease in nutrients post-flower opening may be related to nutrient recycling, often from one flower on the inflorescence to another, which has been observed in several species (Bielecki 1995; Van Meeteren et al. 2001; Chapin and Jones 2007).

1.3.2 Exogenous factors affecting flower development and opening

Exogenous factors affecting opening are defined as the information taken from the plant's environment which may modulate the time of opening slightly. Examples of factors which have been indicated in other species as having a significant impact on flower opening include the ambient temperature, the time of day, and the water availability (van Doorn and Kamdee 2014). The ambient temperature is thought to be the most important factor in affecting time of flower opening. For example, the growth temperature of *L. longiflorum* cv. Nellie White at certain important stages of development (at the last stage of growth prior to harvest when buds were within 1-6 cm long) was found to proportionally influence the day of anthesis when harvested according to commercial guidelines (Healy and Wilkins 1984) and similar results have been found with *L. hansonii* (Lucidos et al. 2013). This may be driven by the circadian gene *PIF4*, which is necessary to induce expression of *FT* in short day conditions for temperature-driven flowering induction (Kumar et al. 2012).

Flower opening in lilies is highly synchronous on plant (defined here as opening of buds of similar developmental stages together at a defined time of day, according to Bielecki et al. (2000b)) in order to protect pollen from the elements until a time of high pollinator activity (Bielecki et al. 2000b). This hypothesised circadian component could feed into the regulation of flower opening to constrain the time of opening set by the developmental stage of the lily bud appropriately. Circadian clock genes in *A. thaliana* such as *PIF4* and *PIF5* peak just prior to dawn and modulate circadian factors such as PhyA by the photoperiod (Seaton et al. 2018). Additionally, the biosynthesis and transport of, or sensitivity to, several hormones such as auxin, gibberellins and jasmonic acid (JA) are found to oscillate in a 24-hour cycle, causing hormone-related signalling when endogenous levels peak in *A. thaliana* (Nozue et al. 2007; Arana et al. 2011; Nozue et al. 2011). In waterlilies, auxin causes circadian-regulated opening and closure of petals through reversible cell expansion and reduction of petal intermediate cells, mediated by auxin synthesis and signalling (Ke et al. 2018).

Stress and development are sometimes closely linked. Ethylene is one of the best known phytohormones due to its common use in ripening of fruit and vegetables (Kader 2002) and has an already characterised role in lily flower senescence and abscission in some varieties (Van Doorn and Han 2011). It is a highly diffusible small compound which regulates a huge number of plant developmental and stress responses (Zhao et al. 2002). This hormone is

known for its varied effects in relation to specific developmental changes such as flower opening and senescence, even within the same species (Reid et al. 1989, Macnish et al. 2010). Ethylene was found to promote flower opening in certain species such as carnation, one of the most ethylene sensitive cut flowers (Jones and Woodson 1997). In species such as *Rosa x hybrida* which has a range of sensitivities dependent on cultivar, exogenous ethylene caused differences in the degree of opening. However, it was also found to have significant senescence-promoting effects on cut flowers, with several cultivars showing petal wilting, abscission and an overall shorter vase life (Macnish et al. 2010). Pollination is found to be a strong driver of local and global ethylene production in many species such as carnation (ten Have and Woltering 1997). Lilies are generally known as ethylene-insensitive, but, like roses, are diverse in their ethylene sensitivity. Some lily cultivars display increased ethylene production over opening (generally Asiatic cultivars), while most do not show any change (generally Oriental cultivars) (Elgar et al. 1999). The Asiatic cultivars 'Prato' and 'Elite' were found to have high endogenous production of ethylene in flowers post-pollination, which was hypothesised to be driving programmed senescence due to completing their function of causing pollinator attraction (Burchi et al. 2005), which may also be linked to the recycling of nutrients and energy balance across the inflorescence.

Finally, water availability is important in flower opening due to the reliance on cell expansion in many species, which requires high turgor pressure in petal cells. Abscisic acid (ABA) has been linked to flower opening and senescence in many species. Petal ABA concentration in citrus flowers rises up until flower opening and *Ipomoea* species have been found to have opening promoted by the addition of exogenous ABA (Kaihara and Takimoto 1983). The importance of water transpiration is observed if the xylem vessels in stems are blocked, for example in roses by bacterial blockage (Nemati et al. 2018; Lear 2020), giving rise to flower wilting and accelerated senescence. Controlling flower opening using water availability and movement is often observed in flowers which repeatedly open and close (Van Doorn and Van Meeteren 2003; Beauzamy et al. 2014), suggesting that this is an effective strategy. ABA is well known for its effect in drought conditions – it drives stomatal closure, limiting water loss (de Ollas and Dodd 2016). ABA may also limit cell expansion under water limitation conditions as has been seen in *Arabidopsis thaliana* leaves (Agehara et al. 2013).

1.4 Lilies in the cut flower industry

Lilies are a highly popular cut flower both in the UK and around the world, being the fourth most produced cut flower worldwide (Miller 2014). Cut flowers are used for multiple reasons, mainly as decorative home items, for weddings and other occasions, and even for worship in some countries (Sazvar et al. 2016). Lilies in particular are either sold individually or as part of mixed bouquets and are often added to larger decorative arrangements due to their sturdiness and showy flowers. Commercially, they are highly regarded due to characteristics such as their resistance to common diseases, their varied colour, flower shapes, and fragrance, sturdiness of stems and tolerance of non-ideal temperatures/light conditions, and ability to tolerate commercial growing and processing practices (Lim and van Tuyl 2006). Certain cultivars are also cultivated for food purposes in areas of China and Japan; their bulbs are edible and also used as medicine due to their reputed anti-inflammatory and antioxidant effects (Luo et al. 2012).

1.4.1 Bulb production and propagation

Although lilies can be propagated sexually through seeds and this is used in breeding new varieties, commercially, vegetative propagation of bulbs is preferred, as lily plants can completely regenerate from very small amounts of bulb material and this clonal propagation ensures maintenance of the genotype (iBulb and Anthos 2022). Commercially, vegetative scaling is used to very rapidly increase the number of plants, and is carried out by manual removal of scales (all bulbs are made up of smaller segments known as leaf bases or scales) and growth in soil over a period of time (commercial size bulbs often take up to three years) to produce bulblets (Panda and Mohanty 2016). Micropropagation is also a recent development aiming to regenerate bulbs efficiently using tissue culture techniques, which can be carried out alongside testing to check for genetic fidelity (Yadav et al. 2013). Bulbs are grown across countries with temperate climates, with the Netherlands, USA and Japan being some of the largest producers (Zhou et al. 2008). Bulb suppliers precool fully grown bulbs in soil at approximately 1-2°C for 6 to 8 weeks for even flowering before freezing for storage until required (Gill et al. 2006), and usually transport them to growers already potted in crates with soil to enable root growth (personal communication, James Cole, E.M. Cole Farms Ltd.). The size of bulb is highly important in determining stem and flower quality

in terms of leaf and flower number (Erwin 2002), and therefore it is important to maximise this size for preharvest lily plant health, growth and yield.

1.4.2 Growing conditions for commercially produced lilies

Growers force lily bulbs at approximately 10-15°C in bright light conditions to simulate end of winter conditions and cause shoot growth of the bulbs to initiate plant development (Miller and Langhans 1989). Commercial flowers are grown usually in greenhouse conditions which are controlled carefully for temperature, air circulation and ventilation, relative humidity and light intensity dependent on the variety. Growers in the UK often grow lilies over the summer/autumn months (approximately April-Nov) to maximise light intensity and temperature without requiring additional heating/light (personal communication, James Cole, E.M. Cole Farms Ltd.). Lilies need high light levels to develop normally and in low-light conditions may abort buds (Runkle 2018). Screening equipment to manipulate light levels can reduce damage in very hot weather (iBulb and Anthos 2022).

Exogenous CO₂ is sometimes used to maximise plant yield and photosynthesis alongside variety-specific fertilising plans, which ensures the micronutrient needs of the plant are met. Nitrogen, phosphorus and potassium are essential plant macronutrients and deficiency in any can cause problems with plant growth, foliage colour, and flower development (Ye et al. 2019; Wang et al. 2021; Jiaying et al. 2022). Different varieties show optimised growth under different NPK ratios and different frequencies of application (Pahare and Mishra 2020). Foliar application is often used commercially for rapid uptake by leaves and stems and is more efficient for micronutrient fertilisation (Fageria et al. 2009). Calcium and boron are extremely important in flower development and deficiency in these micronutrients has been suggested to be responsible for bud abortion, and particularly in conditions of low water transpiration such as high humidity can occur even when there is appropriate amount in the soil (Runkle 2018).

Foliar application of plant growth regulators is also used regularly in commercially grown flowers in order to improve factors such as stem length, number of buds, quality of flowers and shelf life; exogenous gibberellins are well known for their preharvest effect on these parameters and used in other species such as roses (Sajid et al. 2009). Forcing lilies can lead to problems such as overgrowth of stems in *L. longiflorum*, making them less sturdy due to

less cell wall thickening, and other growth regulators such as ancymidol and 2,4-dichlorobenzyl-tributylphosphoniumchloride (CBBP) can reduce these problems (Sanderson and Martin 1975). Foliar application of Promalin™ (a mixture of cytokinin 6-benzyladenine (6-BA) and the gibberellins GA⁴⁺⁷) and 1-MCP (an ethylene signalling inhibitor) carried out just prior to harvest has been found to increase Oriental lily longevity in some cultivars through modulation of plant respiration and energy balance (Wei et al. 2018).

Pesticide regimes and low-level irrigation systems minimise damage by pests and pathogens such as *Botrytis* and *Pythium* (iBulb and Anthos 2022). *Botrytis* can be controlled by pesticides and foliar copper coating spray (Zlesak and Anderson 2003). Pests specific to lilies such as the red lily beetle (*Lilioceris lili*) can decimate crops and also must be controlled during the growing season to ensure minimal damage to leaves and growing buds. A novel chemical-free strategy includes the application of antagonistic bacteria to control *Fusarium* infection in Oriental lily bulbs (Chung et al. 2011).

The commercial growth of lily plants has therefore been shown to be highly optimised in order to produce the best quality product and highest yield through breeding, optimised nutrition and environment, additional growth promoting agents, and pest control. This optimisation is important to protect the quality of flowers postharvest, as starch reserves in closed buds at harvest can predict quality and longevity of the flowers (Van der Meulen-Muisers et al. 2001). Similarly, the lower the ethylene-mediated stress responses in the inflorescence, the less damage observed in flowers post cold storage (Han 2003), suggesting that preharvest stress may have a latent effect in overall postharvest quality.

1.4.3 From harvest to consumer: the commercial transport chain

Commercial lilies undergo highly stressful processing, storage and transport prior to reaching the consumer; the UK imports the majority of the commercial lilies found in shops and therefore cut flowers may spend a significant time in air/sea/road travel before reaching the retailers. These treatments have an as yet uncharacterised effect on factors such as their circadian rhythm, the cold response, and metabolism, which may cause overall changes in flower opening time and longevity.

Harvest of commercial lilies occurs in the early morning when the ambient temperature is lower than 27°C in order to minimise bruising of delicate buds (Gill et al. 2006) and to

prevent desiccation (iBulb and Anthos, 2022 - Figure 1.5). Stems are harvested dependent on the development of buds on the stem to ensure a balance between the stage of development of the oldest bud on the stem and the youngest. This is important so that all blooms remain closed until brought home by the consumer (4-7 days postharvest) but all buds (specifically the youngest buds) are developmentally capable of opening (personal communication, James Cole). Harvesting stems too late when some flowers are already open leads to problems such as tepal bruising, pollen stains, and very rapid maturing of other buds (iBulb and Anthos 2022). Usually, stems are cropped 3-4 inches above the soil so that roots of neighbouring stems are not damaged (often stems from the same crates are gradually cropped over a series of days to ensure all stems are the same developmental stage at harvest) (personal communication, James Cole, E.M. Cole Farms Ltd. – Figure 1.5). Following harvest, stems are further mechanically processed to remove leaves from the bottom third of the stem and tied into bouquet-sized bunches. The ends of flower stems are recut by approximately 3 cm and rehydrated in a flower conditioning solution in water (generally thought to contain a low concentration of sucrose and an antimicrobial agent) to delay opening and minimise vascular occlusion-related problems (van Doorn and de Witte 1991a).

Cold/dark storage is commonly used as a method for slowing metabolism and development in both commercial fresh-cut flowers and potted plants (Ranwala and Miller 1998). When required, stems in the UK are stored at approximately 4°C for up to three days, for example in summer months when the supply of flowers ready to sell is greater than the demand from retailers (personal communication, James Cole, Figure 1.5). This cold storage maintains longevity of flowers especially in hot environmental conditions. Post cold/dark storage, flowers are sleeved and packed dry for transport to retailers. Dry transport is preferable to wet due to the decreased requirement for space, and in cut roses was also found to reduce microbial growth in stems (van Doorn and de Witte 1991b), which outweighs the risk of dehydration. Transportation is often also temperature controlled where possible in order to maintain the drop in metabolism and keep stems as cool as possible before reaching the retailer (Greenway Logistics Ltd. 2019). Retailers recut stems, add the same flower conditioning solution again to rehydrate, and keep bouquets in highly variable conditions in terms of light and temperature for up to 5 days (Figure 1.5). In the UK, consumers are often

supplied with sachets of flower feed, containing a much higher concentration of sucrose and antimicrobial agents in order to stimulate flowering and prevent early senescence from vascular occlusions and microbial overgrowth (van Doorn and de Witte 1991b).

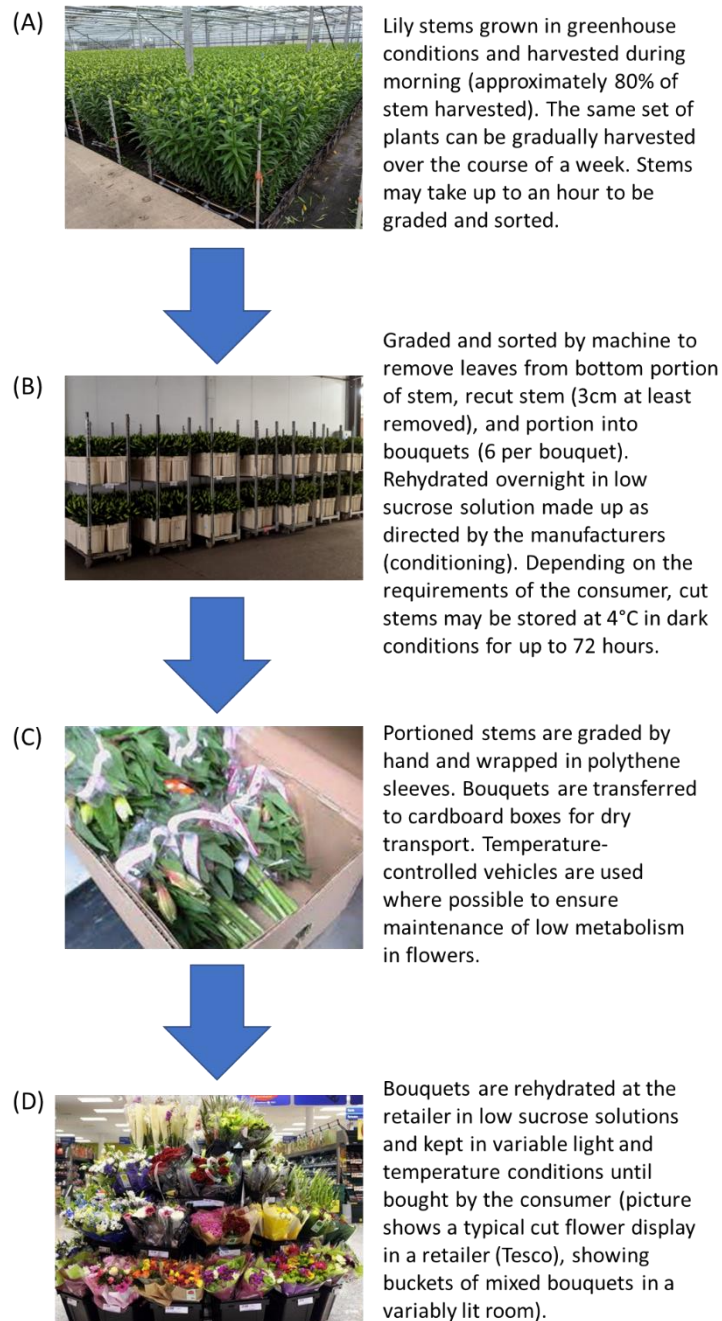


Figure 1.5 – Description of the harvest to consumer commercial transport supply chain for Oriental and LA hybrid lilies grown and sold in the UK, showing (A) the harvest process, (B) the initial grading, sorting and portioning into bouquets, (C) rehydrating and cold/dark treatments, ending in packaging bouquets and dry transport (photograph taken from (Reid

2009)), and (D) showing usual display conditions at retailer (photograph taken from (Yourgiftexpert.com 2022). Information in figure taken from (Bose et al. 1999; iBulb and Anthos 2022).

1.4.4 Postharvest issues affecting commercial flowers and current treatments

The global increase in growth and propagation of lily plants globally has led to increased spreading of diseases and infections affecting lily bulbs and plants, as well as other abiotic physiological conditions, due to the requirements of worldwide transport (Chastagner et al. 2017). While nutrient deficiencies and biotic diseases are a leading cause of waste in the cut flower industry, they are generally identified prior to harvest and not a cause for consumer complaint. However, many physiological issues are either not visible at harvest or caused postharvest, leading to problems later on with flower opening (personal communication, James Cole, E.M. Cole Farms Ltd.).

While in the UK growers have short turnaround times and cut flowers can be at the retailer within two to four days, often when arriving from other countries cut flowers may take much longer. For example, a large proportion of the UK's roses are currently grown in Kenya, and the minimum time taken to move through the supply chain from harvest to consumer is 8 days, although they can take up to 5 weeks when travelling by sea (Harkema et al. 2017). In some cases, lily stems may be stored for one to two weeks (Han 2003), but long-term cold storage is usually responsible for problems such as leaf yellowing (Figure 1.6D) and bud opening failure in cut lily flowers (Chastagner et al. 2017). This was found to have variable effects on flower quality dependent on cultivar: Asiatic varieties such as 'Geneve' and 'Vivaldi' were found to tolerate cold storage before negative effects were noted for up to three days longer than the Oriental cultivars 'Stargazer' and 'Acapulco' (Han 2001). Chemical interventions include treating preharvest plants with Promalin™ to reduce leaf yellowing (Wei et al. 2018).

The condition of flower buds before and at harvest is essential to allow future opening, often several days postharvest. Two of the biggest postharvest issues with commercially treated flowers are flowers opening too early (due to temperature fluctuations or being harvested too late) and flowers failing to open at all (due to being harvested too early,

severe dehydration, and inappropriate storage conditions or time – personal communication, James Cole, E.M. Cole Farms Ltd.). This is generally limited to specific buds on the inflorescence; buds which fail to open are usually terminal buds of inflorescences with more than four buds per stem, which is why most commercial growers prefer a maximum of five buds per stem (personal communication, James Cole, E.M. Cole Farms Ltd.). Commercially grown lilies are harvested whilst taking the developmental stage of both the oldest and youngest bud into account – a balancing act which means the oldest bud does not open before reaching the consumer and decreasing the longevity of the bouquet, whilst allowing the youngest bud to be developmentally capable of opening (Van Meeteren et al. 2001). This opening process can fail under certain circumstances in certain varieties. Bud abortion is defined as arrested bud development prior to anthesis at a very early preharvest stage, whereas bud blast is generally considered to be the arrest of buds just prior to opening (Figure 1.6A and 1.6C, Mason and Miller 1991, Chastagner et al. 2017). To differentiate it from preharvest bud abortion, postharvest bud abortion is defined here as arrested bud development in buds which would generally open 7-10 days postharvest, but that fail to do so, appearing to enter into senescence instead. This has been identified as a significant issue in the cut lily flower industry, and may be partially caused by commercial treatment and in particular the cold/dark treatment (Han 2001). Ethylene exposure, either pre- or postharvest, can also cause bud abortion or premature opening in flowers and may be mediated via an ethylene-driven stress response (Figure 1.6A and B, Chastagner et al. (2017)). Finding pre- or postharvest treatments to prevent postharvest late bud abortion is therefore of great interest to the industry and both causes of bud arrest and possible targets for reducing its incidence will be explored as part of this thesis.

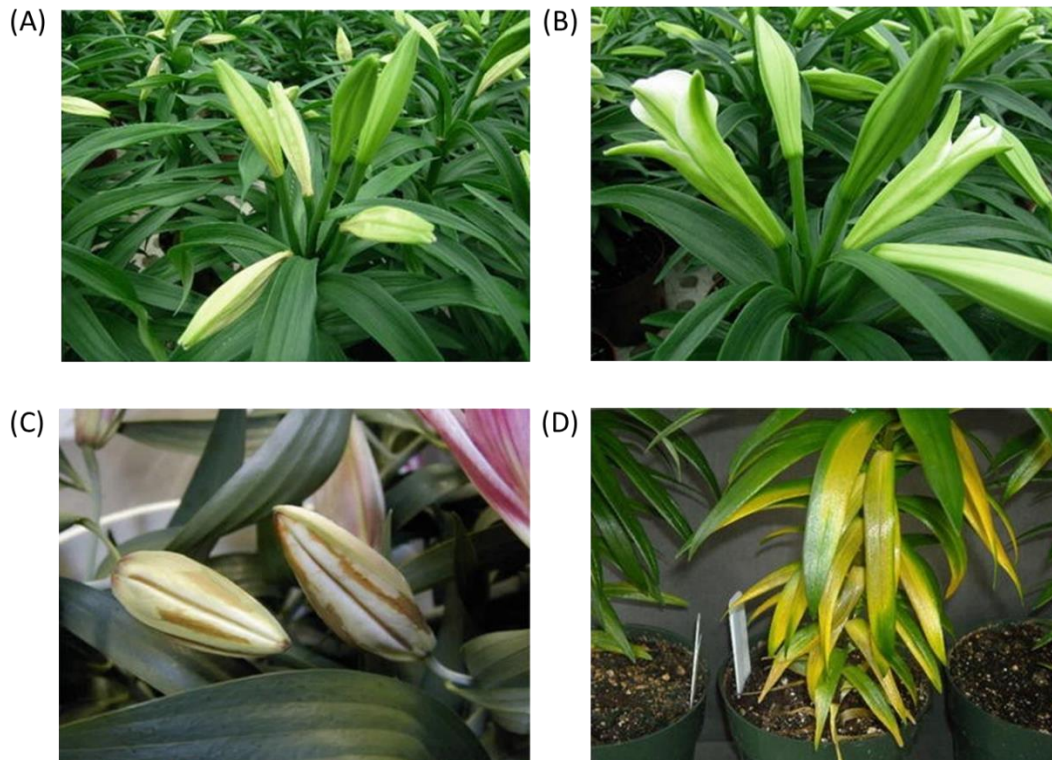


*Figure 1.6 – Physiological disorders in Lilium which have been indicated as occurring postharvest (although they can also be found as preharvest issues under poor growth conditions). This includes (A) flower bud abortion/ bud blast (picture shows *L. longiflorum* buds affected by ethylene exposure, where buds may fail to open), (B) premature opening (*L. longiflorum* buds affected by ethylene can also display very early opening, showing a malformed shape), (C) cold storage related bud chilling injury (Oriental cultivar showing necrosis symptoms during cold storage) and (D) leaf chlorosis, which can be nutrient or cold storage related (shown here on potted plants held in a cooler for two weeks). Photos taken from (Chastagner et al. 2017) by William B. Miller (2016).*

1.5 – Aims of this thesis

The focus of this thesis was to explore the mechanisms of lily flower opening, its regulation by endogenous and exogenous factors, and understand why buds sometimes fail to open in a commercial setting. The specific aims for each chapter are outlined below, alongside the objectives used to address these aims.

1. To understand the physical mechanisms and timing of flower opening in lilies, and establish whether they are affected by harvest and commercial treatment
 - Use microscopy to identify regions of differential cell expansion correlating with flower opening
 - Compare this cell expansion between on plant and commercially treated flowers to establish if it is affected by harvest- or cold/dark storage-related stress
 - Use timelapse photography to investigate the factors affecting time of opening in lilies and if this is affected by commercial treatment
 - Separate the effects of harvest and cold/dark storage on time of opening using timelapse photography
 - Investigate the phenomenon of, and possible risk factors of, postharvest bud abortion in terminal buds
2. To understand the physiological mechanisms and underpinning gene expression driving the physical opening process
 - Use a range of methods to investigate the change in tepal carbohydrate content (starch, glucose, fructose, sucrose) over development and opening
 - Establish if the tepal carbohydrate contents are affected by commercial treatment or position on stem
 - Investigate how changes in tepal metabolome over development and opening are affected by commercial treatment and position on stem
 - Observe changes in expression of genes putatively identified as cell expansion-related
3. To identify potential factors and regulatory targets which may cause commercial harvest-related problems such as postharvest bud abortion

- Use RNAseq to explore the differences in gene expression between flowers which went on to suffer from postharvest bud abortion compared to those which opened normally in order to identify transcriptional pathways related to opening
 - Identify putative transcription factors and hormone-related genes whose expression correlates with the ability of the bud to open
4. To explore the hormonal regulation of flower opening, and the endogenous factors influencing this regulation
- Identify phytohormones likely to be involved in flower opening based on the expression of putative hormone related transcription factors and target genes
 - Explore the effect of adding exogenous auxin (identified as likely to be involved in flower opening) on bud flower opening using timelapse photography, and assess whether the exogenous auxin alters the expression of target genes
 - Investigate the effect of exogenous auxin on terminal buds at risk of postharvest bud abortion

Chapter 2 - General materials and methods

2.1 Plant material, growth and growth room conditions

2.1.1 On plant

Growth of the lily plants to maturity was either carried out at Cardiff University (greenhouse growth conditions in Section 2.1.1.1) or at E.M. Cole Farms Ltd. (greenhouse growth conditions in Section 2.1.1.2). On plant experiments were carried out in E.M. Cole Farms Ltd. greenhouse conditions unless stated otherwise.

2.1.1.1 On plant grown in Cardiff University greenhouse conditions

L. Longiflorum cv. 'White Heaven' and LA hybrid cv. 'Courier' plants were grown under greenhouse conditions at Cardiff University (25°C, additional lighting 12/12h on/off during summer growing period, variable temperature 5-20°C over wintering period) throughout the 2018-2022 growing seasons. Plants were grown in pots (20 cm diameter pots, approximately three bulbs per pot depending on bulb size) and were repotted annually over winter when stems had died back in a 5:3:2 mixture of all purpose compost, potting sand and potting grit to reduce effects of overcrowding.

Whole plants of Oriental lily cv. 'Ascot', Oriental lily cv. 'Tisento', and LA hybrid lily cv. 'Litouwen' were sourced from E.M. Cole Farms Ltd. (West Pinchbeck, Spalding, Lincolnshire) at approximately 80-120 cm height and were from then on grown under Cardiff University greenhouse conditions in crates (approximately 60x40x20 cm, with 12-15 bulbs per crate) until required for experiments. Prior to being moved to Cardiff University, crates were grown and treated under greenhouse conditions at E.M. Cole Farms Ltd. described in Section 2.1.2. These plants were grown annually during the flowering season and discarded once flowered, as standard commercial practice.

All lily plants grown in Cardiff University greenhouse conditions were fed weekly with a standard mixed feed (7% N, 5% P, 19% K) with a biweekly addition of potassium nitrate or calcium nitrate during the growing and flowering period to simulate commercial practice. Lily plants grown at Cardiff University were treated with Movento® insecticide (Bayer CropScience Ltd., Cambridge) made up as directed for indoor plants during vegetative

periods to minimise pest damage by aphids and whitefly. Plants with pest damage to leaves and buds were not used in experiments over that flowering period.

2.1.1.2 On plant grown in E.M. Cole Farms Ltd. greenhouse conditions

Lily stems were grown to maturity (approximately 100 days – personal communication, James Cole, E.M. Cole Farms Ltd.) under greenhouse conditions at E.M. Cole Farms Ltd. (variable temperature average 18-20°C, no additional lighting) in crates (approximately 60x40x20 cm, 12-15 bulbs per crate) prior to harvest for experiments unless otherwise stated. Varieties used included Oriental lily cvs. ‘Ascot’, ‘Tisento’, ‘Pacific Ocean’, and LA hybrid lilies cvs. ‘Litouwen’ and ‘Eyeliner’. These cultivars were chosen for their commercial popularity and long flowering season. Plants were fertilised regularly with a rotating feeding plan of a N-P-K compound fertiliser (14:5:24) with added calcium and micronutrients, and potassium nitrate, calcium nitrate, iron, and a trace elements mixture in a low pH liquid feed. Oriental lilies were supplemented further with EDTPA iron. Plants were also treated with a weekly rotating fungicide/insecticide plan to prevent infection by *Botrytis* and aphids over the growing period with no applications until 14 days after entering the greenhouse and 7-14 days prior to harvest. Additionally, from mid-June/July to early September a thrips programme was combined with the insecticide application (personal communication, James Cole, E.M. Cole Farms Ltd.).

Whole plants were kept in E.M. Cole Farms Ltd. greenhouse conditions for experiments unless otherwise stated. In some cases whole plants or stems/individual buds were harvested and moved to growth room conditions as stated in the experimental methods for individual chapters.

2.1.2 Commercially treated stems

Commercially treated stems were both sourced from E.M. Cole Farms Ltd. (Section 2.1.2.1) and in the case of lily plants grown at Cardiff University, the commercial treatment was mimicked for experiments where necessary (Section 2.1.2.2).

2.1.2.1 E.M. Cole Farms Ltd. commercial treatment and transport conditions

Stems grown in E.M. Cole Farms Ltd. greenhouse conditions (Section 2.1.1.2) were harvested in the morning 07:00-12:00 dependent on the size of the largest bud and the

ambient temperature (personal communication, James Cole, E.M. Cole Farms Ltd.). When harvested and sorted, stems were rehydrated in FloraLife Express Clear ULTRA 200 (1:200 water) with 30 stems per 2 L nutrient solution. Commercial stems were stored in FloraLife solution for up to 72 hours at 4°C in dark room conditions prior to packaging and dry transport to Cardiff University in cardboard boxes (approximately 5 hours). Stems were then cut to remove dry ends by 3-4cm before rehydrating in normal growth room conditions (Section 2.1.3).

2.1.2.2 Cardiff University commercial treatment simulation

Stems grown in Cardiff University greenhouse conditions (Section 2.1.1.1) were subjected to harvest, conditioning, cold/dark treatment and dry transport storage to mimic the commercial situation as closely as possible (personal communication, James Cole, E.M. Cole Farms Ltd.). For simulation of the commercial processing treatment, stems were harvested before 12pm, rehydrated in 2L Chrysal Clear Liliium & Alstroemeria solution in tap water (made up to half strength as directed for conditioning treatment – one sachet per 2 L water (personal communication, James Cole, E.M. Cole Farms Ltd.) for at least four hours, then stored at 4°C in dark conditions for 72 hours. Post cold/dark treatment stems were allowed to return to ambient room temperature before 8 hours at 8°C dry to simulate transport. Stems were then cut by 3-4 cm to remove dry ends before rehydrating in normal growth room conditions (Section 2.1.3).

2.1.3 Cardiff University growth room conditions

Cut lily stems were maintained before and during experiments in growth room conditions (up to 30 stems were rehydrated and stored in 2L Chrysal Clear Liliium & Alstroemeria solution in tap water (made up as directed for conditioning – 1 sachet per 1L tap water - personal communication, James Cole, E.M. Cole Farms Ltd.) at 21°C, 16:8 light/dark) unless otherwise stated. Vase solution was regularly topped up as necessary to prevent containers from drying out.

During experiments lily stems were maintained in containers of various sizes depending on whether the full stem or individual buds were used. All containers were soaked in 100 mM sodium hypochlorite solution for 10 minutes to sterilise and rinsed with tap water

thoroughly before use. All vase solutions used were made up with tap water unless otherwise stated.

2.2 Stages of lily growth and development

Individual lilies were visually staged in terms of developmental stage (Figure 2.1).

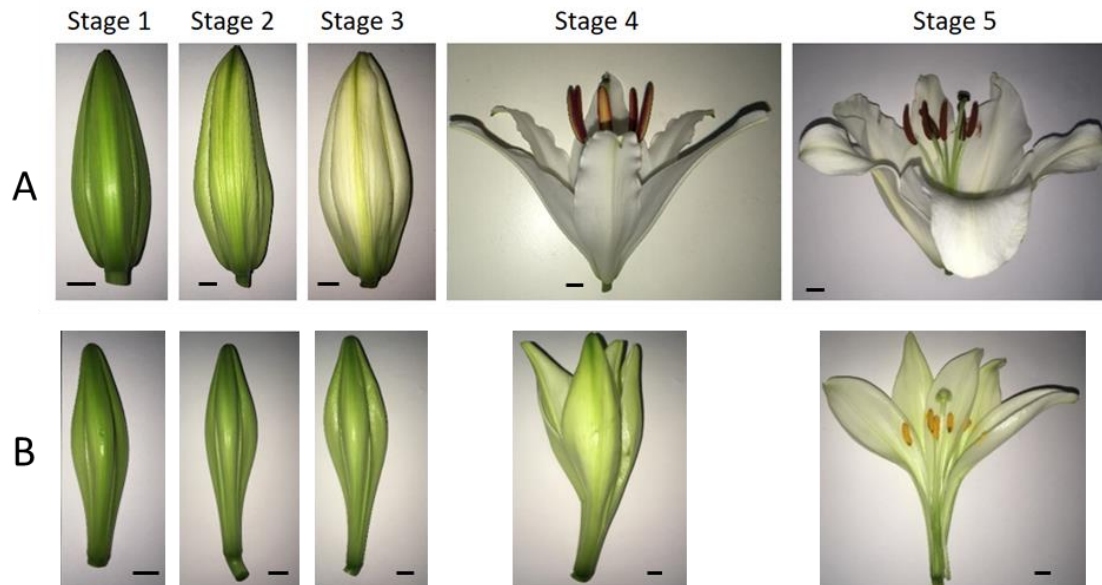


Figure 2.1 - All varieties of lily were visually staged in experiments unless otherwise stated from 1-5 using size, colour and shape as reference. In addition to stage, bud length was used as a measure of development due to varietal differences in size. (A) shows these stages of development for Oriental lily cv. Tisento. (B) shows *L. longiflorum* cv. White Heaven. Scalebar = 1 cm. LA hybrid flowers (not pictured) were staged very similarly to Oriental varieties.

Stage 1 - approximately 3 days prior to opening (small green immature bud)

Stage 2 - approximately 2 days prior to opening (turning colour, larger bud)

Stage 3 - approximately 1 day prior to opening (mature bud, almost fully white)

Stage 4 – half open bud, prior to anther dehiscence.

Stage 5 - fully open mature flower.

Lily cultivars varied significantly in bud length at flower opening. Table 2.1 shows the range of bud lengths that Stage 1 and 3 buds were harvested at/specified as in these experiments (i.e. stems were harvested when the Position A bud was at least within the range for Stage 1 for the variety used, ensuring the other buds on the inflorescence were also of a suitable developmental stage for harvest). This ensured the harvest of stems from plants grown at Cardiff University was in line with standard commercial procedure. Where time of opening experiments were carried out buds as close to each other in size as possible were used unless otherwise stated.

Table 2.1 – Average bud lengths used to stage different lily varieties at Stage 1 and 3 (Position A buds only)

Lily variety	Position A bud length at Stage 1	Position A bud length at Stage 3
Oriental lily cv. Ascot	70-80 mm	100-130 mm
Oriental lily cv. Tisento	80-90 mm	120-150 mm
LA hybrid lily cv. Litouwen	60-70 mm	90-120 mm
LA hybrid lily cv. Eyeliner	70-80 mm	100-130 mm
LA hybrid lily cv. Courier	70-80 mm	100-130 mm
Oriental lily cv. Pacific Ocean	60-70 mm	100-130 mm
<i>Lilium longiflorum</i> cv. White Heaven	90-110 mm	120-150 mm

2.3 Position on stem nomenclature

Labelling the position on stem of specific buds was carried out as described in Figure 2. Commercial lilies depending on cultivar had different average numbers of buds per stem ranging from two to five buds but the most developed bud on the stem was always labelled Bud A. This was more difficult in some LA hybrid varieties due to buds clustering strongly at the top of the stem so bud length was used alongside position on stem in some cases to assign the position, as this decreased sequentially up the stem from most to least developed.

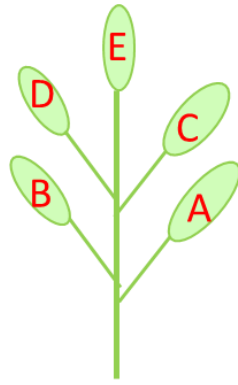


Figure 2.2 – Nomenclature for position on stem. Buds on the same stem were identifiable by their position on stem where the most developed bud at the bottom of the stem was labelled A and the less developed buds (dependent on the number of buds per stem) were labelled B-E sequentially up the stem.

2.4 Time of opening assay

Whole lily plants in crates, cut stems, or individual buds were carefully selected for equal stages of development (bud length) at the start of the experiment. Each bud was labelled with a unique label to identify position on stem and stem identity if appropriate, and bud length was measured using an electronic digital caliper (Precision Gold, Maplin Electronics UK) and recorded. For on-plant samples, stems grown in rectangular crates were tied to an outer scaffold to separate them and easily distinguish them from each other (Figure 2.3A). A black backdrop was sometimes used to make identification of open buds easier. For cut stems, up to 6 stems were arranged in each bucket (containing 2L FloraLife solution made up as directed) to ensure all buds were visible in photographs. For individual buds, up to 6 buds were arranged in sterile plastic boxes filled with tap water or FloraLife solution made up as directed. Plants and flowers were set up facing timelapse cameras (A range of webcams were used: Logitech C270 HD, Wansview 1080p, ToLuLu Pro 1080p). These were programmed with a Raspberry pi using the Python program fswebcam to take photographs hourly or every 30 minutes. A dim green light (Phillips Living Colors 69143/87/PU LED Lamp, ENUOLI green neon light) was used at night to allow continuous 24-hour photography whilst minimising the effect of artificial light on the plants. Although plants are able to perceive green light it has less impact on growth and flowering than red or blue wavelengths (Battle

et al. 2020). Photographs were analysed by hand to identify date and time of opening for each individual bud.

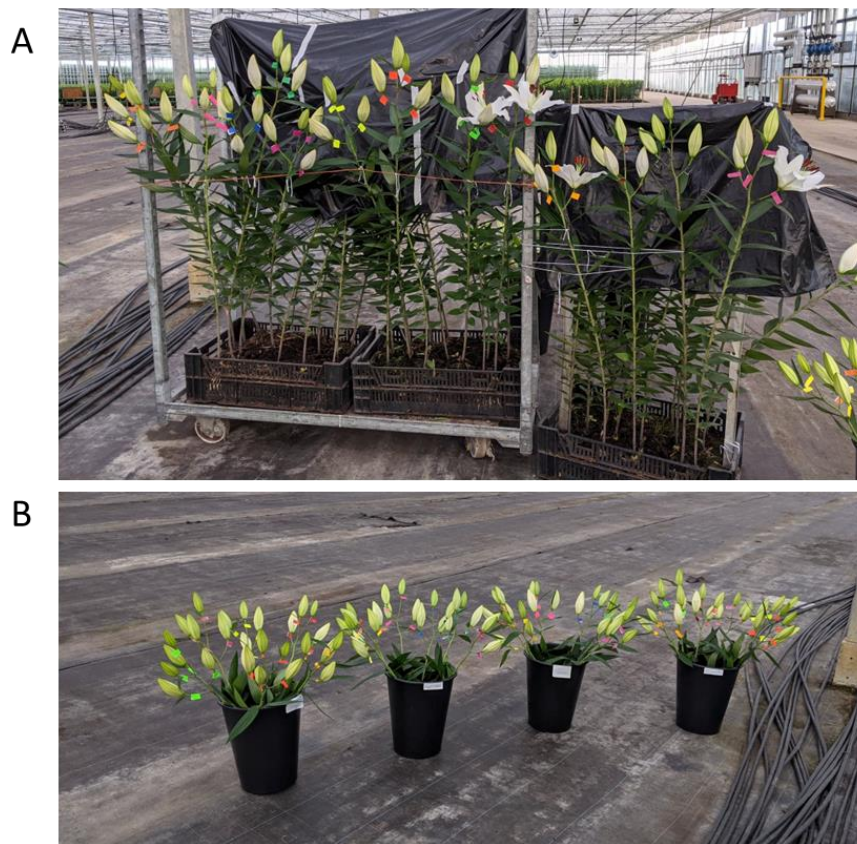


Figure 2.3 – example of photographs taken by timelapse photography of (A) on plant samples and (B) commercially treated samples. Shots were set up in order to allow for good contrast against the buds and all buds were labelled with coloured stickers to identify their stem.

Bud opening time data (number of days/hours from harvest/start of experiment) was statistically analysed using an appropriate statistical test in RStudio (version 1.3.1093) depending on the experiment.

2.5 Tepal epidermal pavement cell growth analysis

Tepal material was prepared for microscopy in 100% ethanol overnight and cut into sections from selected areas of the tepal (Figure 2.4A) and incubated in lactic acid until the tissue

turned clear. Phase contrast light microscopy (Axio Imager M1 (Zeiss) and bScope BS.1153-EPLi (Euromex)) was used to image adaxial epidermal pavement cells (Figure 2.4B, C). Cell area was measured using imageJ Fiji software as described in Figure 2.4. Fold change in epidermal pavement area between Stage 1 and 5 was calculated using the calculation below for each section of the tepal measured:

(Average epidermal pavement cell area at Stage 5 – Average epidermal pavement cell area at Stage 1) / Average epidermal pavement cell area at Stage 1 = Fold change in average epidermal pavement area between Stage 1-5.

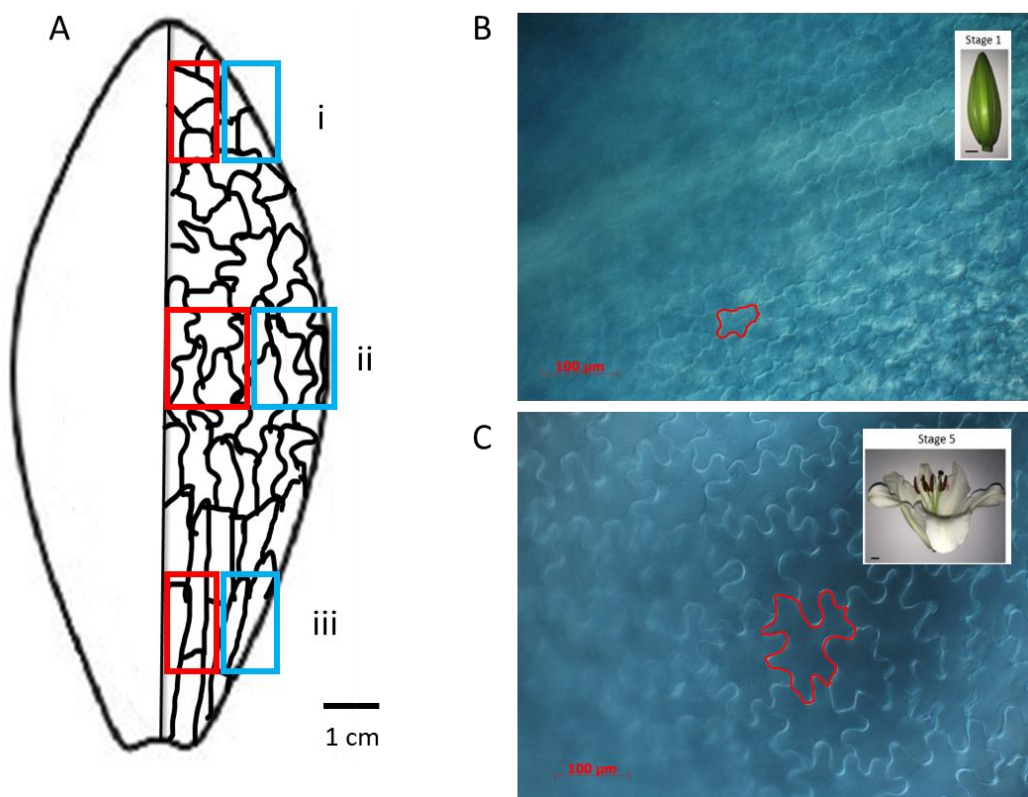


Figure 2.4 - (A) Schematic showing the adaxial face of a lily tepal prepared for microscopy. Top (i), Mid (ii) and Base (iii) sections were taken at equidistant lengths along the tepal with Top and Base sections as close as possible to the edges of the tepal whilst still producing a good image of the epidermal cells. Red sections denote the area Midrib cell measurements were taken from and blue section denote the same for Edge cell measurements. The same was done for both outer and inner tepals. Three photographs were taken for each section. Scalebar is representative of Oriental lily ‘Ascot’ at Stage 1 (Position A) – tepal approximately 8 cm long. The proportional size of sections was maintained regardless of tepal length or

variety. (B + C) Example photograph of Stage 1 (B) and Stage 5 (C) mid adaxial inner tepal edge epidermal pavement cells at 10x magnification (inset photo shows lily material before preparation). Photographs were always taken in the same orientation where the top of the photograph corresponds with the top of the tepal. The red outlines show the cell wall boundary which was used to trace around in imageJ Fiji to measure cell area. Due to high discrepancy between the Stage 1 and Stage 5 epidermal pavement cells, only 6 cells per tepal section were measured in order to allow the same number of cells to be measured using the same magnification accurately. These cells were chosen for good focus and clarity within the photograph.

2.6 Nucleic acid extraction techniques

2.6.1 DNA extraction from lily material using DNeasy Plant Mini Kit (Qiagen)

Genomic DNA (gDNA) was extracted from lily plant leaf tissue. Leaf tissue (20 mg) was weighed in a microcentrifuge tube and flash frozen in liquid nitrogen before homogenising with a sterile microcentrifuge tube pestle pre-cooled in liquid nitrogen. The DNA extraction was then carried out as per the kit's instructions. Buffer AP1 (400 µl) and 4 µl RNase A was added to the tube and the tissue was macerated further using the same pestle. The tube was then vortexed vigorously for 30 seconds and incubated at 65°C for 10 minutes. Buffer P3 (130 µl) was added to the tube and incubated on ice for 5 minutes. The mixture was centrifuged at 20,000 xg for two minutes in a microcentrifuge to remove cellular debris and the lysate was transferred to a QIAshredder spin column. This was again centrifuged at 20,000 xg for two minutes and the flow through was transferred into a new tube. Buffer AW1 (1.5 volumes) was added and mixed well. gDNA was bound onto a DNeasy Mini spin column by centrifuging at 12,000 xg for one minute and discarding the flow-through. The gDNA was washed twice with 500 µl Buffer AW2 (centrifuging at 20,000 xg for two minutes and discarding flow-through each time). The gDNA was eluted with 50 µl sterile dH₂O, which was added to the membrane carefully, left to stand at room temperature for 5 minutes, then centrifuged into a sterile microcentrifuge tube for one minute at 12,000 xg. The eluate was pipetted back onto the membrane and this step was repeated to maximise DNA elution. gDNA was checked for quality by PCR using PUV and AUX1 primers (Table 2).

2.6.2 RNA extraction from lily tepal material

High quality RNA is necessary for downstream analytical techniques such as RNA sequencing and qRT-PCR. However, it is difficult to extract high quality RNA from lily tepal material due to the presence of flavonoids and oligosaccharides which bind to nucleic acids. Several RNA extraction protocols were therefore trialled and used depending on the quality of RNA needed for the procedure. The same extraction method was used for all samples in a standalone experiment. In all cases one biological replicate indicates tepal material from one individual lily flower.

2.6.3 RNA extraction using Tri-reagent

Tepal material was flash frozen in liquid nitrogen and stored at -80°C . RNA was extracted from this material using a method adapted from Chomczynski and Sacchi (1987). Frozen tepal material (200 mg) was ground under liquid nitrogen in a mortar and pestle. Tri-reagent (2 ml, Sigma, St Louis, MO, USA) was added to the mortar and the material ground to a homogenous paste before being transferred to two 1 ml microcentrifuge tubes. The homogenate was centrifuged at $12,000 \text{ xg}$ at 4°C for 10 minutes and supernatant was transferred to a fresh microcentrifuge tube. When large numbers of samples were extracted at once, tubes were stored at -80°C for up to a week. The samples were allowed to stand at room temperature for 5 minutes for dissociation of nucleoprotein complexes. RNA was extracted twice by adding 200 μl chloroform, vortexed vigorously for 30 seconds, left to stand at room temperature for 15 minutes and then centrifuged at $12,000 \text{ xg}$ at 4°C for 15 minutes. Both times the colourless upper phase was carefully transferred to a fresh tube. RNA was then precipitated using 0.5 ml isopropanol and left to stand at room temperature for 10 minutes. The tubes were centrifuged at $12,000 \text{ xg}$ at 4°C for 10 minutes to form an RNA pellet and the supernatant was carefully removed. The RNA pellet was washed twice by adding 1 ml 75% ethanol, vortexing and centrifuging at $7,500 \text{ xg}$ for 5 minutes. Tubes were allowed to air dry fully and then the pellet was resuspended in 30 μl sterile dH_2O . Quality assessment of RNA was carried out (Section 2.6.5). RNA was stored at -80°C to prevent degradation.

2.6.4 RNA extraction using CTAB buffer

RNA was extracted from frozen material ground to a fine powder using a method adapted from Gambino et al. (2008). In summary, 150 mg ground frozen material was added to 900 μ l extraction buffer (2% CTAB, 2% PVP 40, 100 mM Tris-HCl pH 8.0, 25 mM EDTA pH 8.0, 2 M NaCl) with 18 μ l of β -mercaptoethanol and incubated at 65°C for 10 minutes, allowing time for the tube to warm up. Nucleic acids were extracted by adding an equal volume of 24:1 chloroform: isoamyl alcohol, vortexing vigorously for 30 seconds, and centrifuging at 11,000 xg at 4°C for 10 minutes. The upper phase of supernatant was transferred to a fresh tube and this step was repeated. One third volume lithium chloride 9M solution was added to the tube and samples were incubated at -20°C for three hours. The tube was allowed to thaw on ice and centrifuged at 21,000 xg at 4°C for 20 minutes to pellet the RNA, after which the supernatant was removed. The pellets were resuspended in SSTE buffer (1 mM EDTA, 10 mM Tris HCl, 0.5% SDS, 1 M NaCl) and a third extraction was carried out using an equal volume 24:1 chloroform: isoamyl alcohol, vortexed for 30 seconds, and centrifuged at 11,000 xg at 4°C for 10 minutes. RNA was reprecipitated by adding 0.7 volume isopropanol and centrifuged at 21,000 xg at 4°C for 20 minutes to form a pellet. The supernatant was removed from the tube and the RNA pellet was washed twice (1 ml 75% ethanol added, vortexed for 30 seconds, centrifuged at 7,500 xg for 5 minutes. RNA pellets were allowed to air dry fully and resuspended in 30 μ l sterile dH₂O. Quality assessment of RNA was carried out (Section 2.6.5). RNA was stored at -80°C to prevent degradation.

2.6.5 Quality assessment of extracted RNA

RNA was quantified using a Nanodrop (Implen Nanophotometer N60/N50, 1 μ l was used to measure absorbance at 260 nm for quantification and for A₂₆₀/A₂₈₀ ratio to evaluate RNA purity) and by gel electrophoresis (2 μ l was run on a 1% agarose gel with an appropriate DNA ladder as described in Section 2.9.3).

2.7 DNase treatment for RNA used for RNA-sequencing and cDNA synthesis

RNA was DNase treated using the Turbo DNA-free kit (Invitrogen) as per the manufacturer's instructions. RNA (2 μ g) was mixed with 1 μ l Turbo DNase and 1 μ l Turbo 10x buffer and

made up to 12 µl with dH₂O. The solution was incubated at 37°C for 30 minutes in a PCR thermocycler (AB Biosystems Veriti 96 Well Thermal Cycler, Techne Flexigene Thermal Cycler). Inactivation suspension (2 µl) was pipetted into the tubes, flicked well to mix, and left to stand at room temperature for 5 minutes. The tubes were flicked throughout to ensure they were well mixed. PCR tubes were spun in a microcentrifuge at 10,000 xg for 90 seconds to pellet the solid materials and the DNased RNA was pipetted into a fresh tube. The efficacy of the DNase treatment on the RNA (1 µl) was checked by PCR using AUX1 primers (Table 2.1) and gel electrophoresis as detailed in Sections 2.9.2 and 2.9.3.

2.8 cDNA synthesis

cDNA was synthesised from ~2 µg DNased RNA using the GoScript™ Reverse Transcription kit with Oligo-dT (Promega) as indicated in protocol. GoScript Reaction Buffer with Oligo(dT) (4 µl) and 2 µl of GoScript Enzyme Mix was added to 2 µg of DNased RNA and made up to 20 µl with dH₂O. Reactions were incubated in a PCR thermocycler (AB Biosystems Veriti 96 Well Thermal Cycler, Techne Flexigene Thermal Cycler) with the following program: 25°C for 5 minutes, 42°C for 60 minutes, 70°C for 15 minutes. Success of cDNA synthesis was checked for efficacy by PCR using AUX1 primers (Table 2.2) as directed in Sections 2.9.2 and 2.9.3 (1 µl used per sample). cDNA was stored at -80°C for long term storage.

2.9 Molecular biology techniques for PCR and qPCR

2.9.1 Primer design

All primer sequences and associated information are in Table 2.2. Design of primers (if not referenced) are found in Appendix 5.

Table 2.2 – list of primers used for PCR and qPCR, annealing temperatures used, and their products

Putative gene target	Primer name	Sequence	T _a / °C	Product size / nt	Reference (if taken)
----------------------	-------------	----------	---------------------	-------------------	----------------------

					from literature)
Actin-binding gene	ACTB-F	GCAAGGATACAAGCCAA GACG	55	181	(Luo et al. 2014)
	ACTB-R	TTAAACCCGGAAACA CCA	55		
AHP2	AHP2-F	ACCAGCACCAGTCAAATT CAG	58	105	Appendix 5.13
	AHP2-R	TTGACACCATGTTGCAGC TG	58. 5		
Alpha-amylase 2 (AMY2)	AMY2-F	GCCATGCTGACGTAAATC CT	55	163	Appendix 5.5. Sequence data from (Shi et al. 2018b).
	AMY2-R	ATGACAACCCAGGAAGCA GA	55		
ARF6/8	ARF6/8-F	ATGAGCTTGGGCAACTGT TT	60	198	(Lombardi et al. 2015)
	ARF6/8-R	CAACCCCTTCTTTCCCAT T	60		
ARF7/19	ARF7/19-F	GACGGTGATCTAGGGAG CAA	55	208	(Lombardi et al. 2015)
	ARF7/19-R	GCAGACGGTTTTCCAGGT TA	55		
ARF15	ARF15-F	CTCCAGTGTGTCCTTCGTC T	55	127	Appendix 5.7
	ARF15-R	GCATGATCAGAAAGGCC AA	55		
AUX1	AUX1-F	CCAAGTGCTACCAGTGCA AG	55	198	

	AUX1-R	ACCAAACCCAAATTGCAA AC	55		(Lombardi et al. 2015)
Cell wall invertase 4 (CWINV4)	CWINV4-F	GAAAGCCTGGGAAGTTG AGG	60	161	Appendix 5.4. Sequence data from (Shi et al. 2018b)
	CWINV4-R	ATCCAACCCTTCCATCCCA G	60		
Elongation factor 1 (EF1)	EF1-F	ACTGGTGGTTTTGAGGCT GG	55	132	(Luo et al. 2014)
	EF1-R	GGAGTACTTCGGGGTTGT GG	55		
Alpha-expansin 2 (EXPA2)	EXPA2-F	ACGTGATTGGGTGATTGA CA	60	192	(Watanabe et al. 2022)
	EXPA2-R	CATACATGTGACCGCTTG CT	60		
Alpha expansin 8-like (EXPA8L)	EXPA8L-F	CCTCCTCTCCAGCACTTTG A	55	116	Appendix 5.1
	EXPA8L-R	ATCCCTCCTTTCTTCACGC A	55		
Hexose transporter (HXT)	HXT-F	CAGCACTAAGGAAGGCA GATG	60	157	(Gu et al. 2020)
	HXT-R	AGAAGGTCCAGGAGAAG ATGAAT	60		
IAA14	IAA14-F	CGTACGAGGACAAGGAT GGA	55	110	Appendix 5.8
	IAA14-R	TCCAATGGCTTCTGACCCT T	55		

Monosaccharide transporter 6 (MST6)	MST6-F	GGAACACTTGGGCAATGA TGA	60	156	Appendix 5.9. Sequence data from (Lombardi et al. 2015).
	MST6-R	CGAAATTAGGTCTGCTGG CC	60		
MYB21	MYB21-F	GGTGAGGAAAGGACCAT GGA	55	127	Appendix 5.2
	MYB21-R	GCAACTCTCCAGTCCTC T	55		
Oryza Response Regulator 9 (ORR9)	ORR9-F	GTTGGTAGATGATGGCTG CG	55	131	Appendix 5.10. Sequence data from (Lombardi et al. 2015).
	ORR9-R	TGACTCTCTCAGCAGCTC A	55		
Plasma membrane Intrinsic Protein 1 (PIP1)	PIP1-F	GCTCAAGTCATGGTCCTT CTACCGT	60		(Tong et al. 2013)
	PIP1-R	ACAATCTGGTGGTACACA GCAGCA	60		
PSII5	PSII5-F	AGAGCTCCAATATTCCG GG	55	102	Appendix 5.3
	PSII5-R	GGCTTCTGGTTGATGTGA GC	55		
SAUR75	SAUR75L-F	GTACACCATCGACGGAAA GC	55	101	Appendix 5.11. Sequence data from
	SAUR75L-R	GCAACCCGTA CTCTCTTC A	55		

					(Shi et al. 2018b)
Sucrose transporter 2 (SUT2)	SUT5669-F	TTATGGCTCTCTGCTTTGT A	55	182	(Gu et al. 2020)
	SUT5669-R	TGTGCGAGTAGAAATCAT TG	55		
Sucrose transporter 4 (SUT4)	SUT13319-F	TTATGGCTCTCTGCTTTGT A	55	182	(Gu et al. 2020)
	SUT13319-R	TGTGCGAGTAGAAATCAT TG	55		
Sugars Will Eventually be Exported Transporter 7 (SWEET7)	SWEET7-F	GAAGACGGAGATGGGGC TG	60	172	Appendix 5.6. Sequence data from (Shi et al. 2018b)
	SWEET7-R	TCCCATTCAGAACAAGAC CCA	60		
Tonoplast monosaccharide transporter (TMT)	TMT-F	TTGGCTCTGGATCGCTAT CG	60	94	(Gu et al. 2020)
	TMT-R	CTCGCTCTCACTGTCACTC TC	60		
Xyloglucan endotransglycosylase/hydrolase 1 (XTH1)	XTH1-F	ATGCCCAGACTTCAAACG ACA	60	111	(Watanabe et al. 2022)
	XTH1-R	AGTTCCTCTGCACCCATCT TAATC	60		
YUCCA 3 (YUC3)	YUC3-F	CTGGGCCTCTAGAGCTGA AG	55	137	Appendix 5.12
	YUC3-R	GATCAGCTCGACTCTCCC TG	55		

Primers for qPCR were either manually designed from sequence data (referenced in Table 2.2 to show RNAseq experiment of origin) or taken from literature. For those manually

designed, sequences which showed high homology to genes of interest were aligned using the online tool Clustal Omega (EBI-EMBL, found at: <https://www.ebi.ac.uk/Tools/msa/clustalo/>) with several putative orthologs and in the case of genes from large gene families, with putative homologs to ensure they had been correctly identified by BLAST (NCBI BLAST+ 2.13.0, found at <https://blast.ncbi.nlm.nih.gov/Blast.cgi>). The online tools Primer3 (Version 4.1.0, found at: <https://primer3.ut.ee/>) and OligoAnalyser (Integrated DNA Technologies, found at: <https://eu.idtdna.com/calc/analyser>) were then used to design primers from the sequence data and check their suitability for PCR and qPCR. Primers for qPCR normalisation (EF1, Actin-binding) were from Luo et al. (2014) and were selected as the targets showing the best stability of expression over different treatments, tissues and stages in *Lilium brownii* (Luo et al. 2014).

2.9.2 Polymerase chain reaction (PCR) conditions

Polymerase chain reaction (PCR) was used to test primers for suitability on both gDNA and cDNA prior to qPCR, and to check efficacy of DNase treatment and cDNA synthesis. GoTaq® G2 DNA polymerase was used where possible; however, some primers did not amplify using this polymerase and HotStarTaq DNA Polymerase (Qiagen) was used instead. PCR reactions were made up as per manufacturers' instructions for the Taq polymerase used and run on PCR thermocyclers (Applied Biosystems Veriti 96 Well Thermal Cycler, Techne Flexigene Thermal Cycler). The program conditions for reactions using GoTaq® G2 polymerase were: an initial denaturation at 95°C for 4 min, followed by 35 cycles of 95 °C for 30 s, variable annealing temperature for 30 s (See Table 2), 72 °C for 30 s, and finally a final extension at 72 °C for three min. The program conditions for reactions using HotStarTaq DNA Polymerase were the same except for a longer initial denaturation of 95 °C for 15 min.

2.9.3 Gel electrophoresis

Extracted RNA/PCR products/qPCR products were checked for yield and size by gel electrophoresis. Unless otherwise indicated, 12 µl of the product (made up in a 2:2:6 ratio with DNA/RNA/PCR product:NEB 6X Purple Loading Dye (NEB) or 6X loading dye (0.25% bromophenol blue, 0.25% xylene cyanol FF, 30% glycerol in dH₂O) if not already present in PCR buffer:sterile dH₂O) was run on a 1.5% agarose gel made up with Tris-acetate-EDTA (TAE) buffer (made up as 40 mM Tris base, 20 mM glacial acetic acid, 1 mM EDTA in 1X TAE)

with SYBR Safe (Invitrogen) to visualise. Samples were always run alongside 1 µg of a 1 kb or 1 kb Plus Ladder (NEB) depending on the appropriate size of the product. Gels were electrophoresed at 90V for 20-30 min in TAE buffer and visualised using a UV transilluminator (G:BOX Chemi XX6, Syngene, Cambridge or GelDoc-It® 310 Imaging System, UVP, Cambridge). Gel images were recorded using GeneSys software (Syngene, Cambridge) or VisionWorks software (UVP, Cambridge).

2.9.4 qPCR relative gene expression analysis

PCR Biosystems qPCRBIO SyGreen Blue Mix Lo-ROX (PCR Biosystems Ltd., London, UK) as used according to manufacturer's instructions on a LightCycler® 96 instrument (Roche). The 20 µl reaction mixture was prepared with 10 µl PCR Biosystems 2x qPCRBIO SyGreen Blue Mix Lo-ROX master mix, 0.4 µl of each forward and reverse primers (10 mM), and cDNA which had been diluted appropriately to have C_q values within 2 cycles using the EF1 primers for normalisation. The mixture was made up to 20 µl with sterile dH₂O. The reaction mixture was pipetted into the wells of a 96 well plate (Starlab) on ice, film was attached to the top, the plate was gently shaken to remove air bubbles, and was then spun in a centrifuge briefly to spin down the mixture prior to inserting the plate into the LightCycler® 96 instrument. The qPCR program followed the pattern of preincubation at 95°C for five seconds, then 35 cycles at 30 seconds at 95°C, 30 seconds at an annealing temperature depending on primers used, and 30 seconds at 72°C for extension. Fluorescence intensity was measured at the annealing stage. Post cycling, a melting curve was also run on the samples to check primer specificity (95°C for 60 seconds, 55°C for 30 seconds, 95°C for one second. Fluorescence intensity was measured continuously at this final step.).

The LightCycler® 96 reported the Quantification Cycle (C_q) values of each reaction, which is the number of cycles required to raise the total fluorescence of the sample above a threshold (Bustin et al. 2009). The reference gene EF1 was used to normalise cDNA concentrations and calculate the relative expression of other genes of interest. EF1 and Actin-binding primers (Section 2.9.1 and Table 2) were both tested for normalisation and compared to each other to ensure suitability for reference genes. Reference genes were chosen for their constant expression over a variety of tested tissue types and developmental

stages (Luo et al. 2014). Both sets of primers were suitable so EF1 was used to normalise cDNA concentration, where all samples were diluted to produce a C_q value with a range of 2 cycles. Relative gene expression was quantified using the delta-delta C_t ($2^{\Delta\Delta C_t}$) method (Livak and Schmittgen, 2001). Two technical replicates were used to calculate the average and standard deviation (SD) for each biological replicate. To calculate the relative expression the delta- C_t value for the reference gene was subtracted from the delta- C_t value for the gene of interest for each of the independent biological replicates in a randomized way and averaged to calculate the average delta-delta- C_t value. This was also used to calculate the total average variation in $2^{\Delta\Delta C_t}$ between biological samples and used to make standard error values for each condition. Technical replicates were repeated if C_q values were not within 1 cycle.

One way ANOVA and post-hoc Tukey test, or a Kruskal-Wallis statistical test with post-hoc Wilcoxon rank-sum was used to identify statistical differences in relative gene expression between conditions, dependent on if the data was normally distributed or not.

2.10 Terminal bud opening assay

Commercially treated Oriental lily stems (cv. Ascot) were grown as described in Section 2.1.1.1 in Cardiff University greenhouse conditions and commercially harvested as described in Section 2.1.2.2. This cultivar was chosen due to its commercial popularity and greater propensity to have terminal buds which failed to open compared to other Oriental varieties. Stems (where possible stems with the same number of buds per inflorescence were used. The number of stems used depended on the experiment) were maintained in Cardiff University growth room conditions (Section 2.1.3) throughout the experiment to mimic commercial/consumer home conditions. At the start of the experiment the terminal bud (Bud D) was measured using a digital caliper, labelled, and the top third of the inner and outer tepals was cut away carefully as described in Figure 2.5. This material was immediately flash frozen in liquid nitrogen and stored at -80°C . The terminal bud was either separated from the stem and maintained in a clean container full of tap water (individual buds were stored up to 10 per container) or retained on stem, which was maintained in a clean bucket of tap water (stems stored up to 8 per bucket) unless otherwise stated. The

stems/individual buds were monitored for bud opening, here defined as a significant colour development from green to white, opening of tepals at the base and rippling at the edges of tepals, and development of the carpel and anthesis of anthers (Figure 2.5). This is differentiated from loss of tepal locking due to the missing top section of tepals. The length of the buds used in the experiment varied by 1cm. Notably, all buds which failed to open were the smallest of the range. To account for this, a third condition was identified as full opening but with length at harvest closest to the failed to open condition. The conditions identified were named Small Remained Closed (SRC), Small Semi Open (SSO) and Larger Fully Open (LFO). Biological replicates (three individual buds from three individual inflorescences) were collected for each condition (Figure 2.5 shows examples of each condition at the end of the experiment).

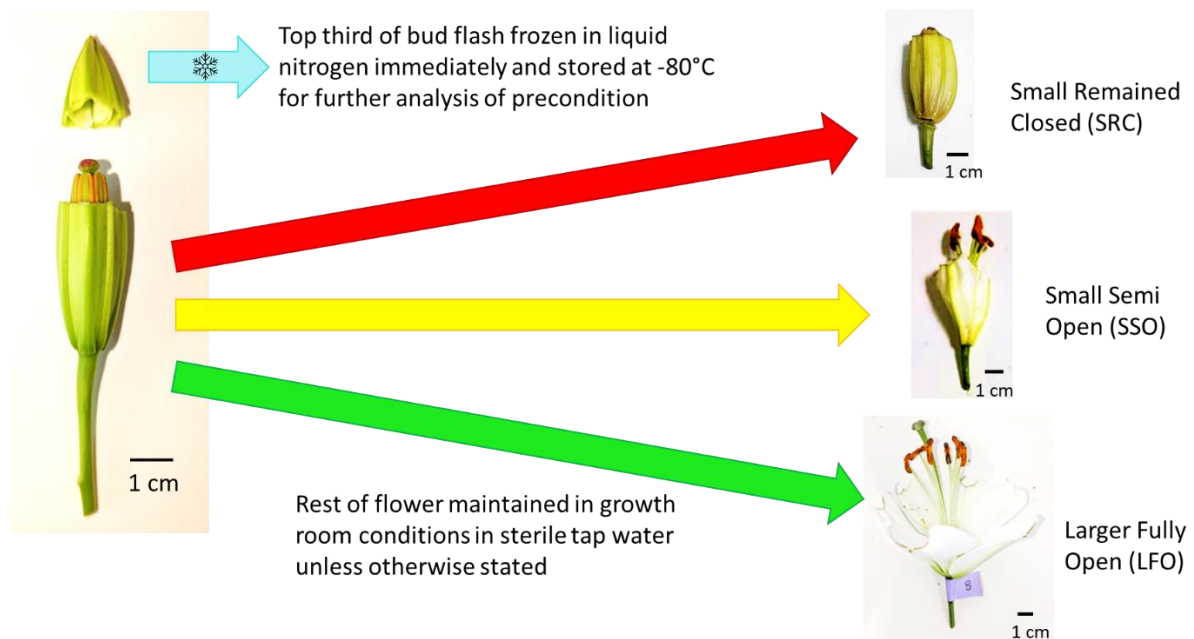


Figure 2.5 – Experimental setup for collection of material for terminal bud opening assay. The image on the left shows the careful removal of the top third section of the tepals (inner and outer) without causing damage to anthers or carpel. This top section was immediately flash frozen in liquid nitrogen and stored at -80°C for further analysis. The rest of the bud was maintained in sterile tap water unless otherwise stated. The buds were grouped according to the degree of opening and development as well as the starting size of the bud. Opening and development were judged according to characteristics such as tepal colour,

growth and the change of tepal angle from the pedicel, as well as development and maturity of the reproductive organs. Small Remained Closed (SRC) buds show complete failure of opening and development; lack of colour change, growth, and change in tepal shape. Small Semi Open (SSO) buds are closest to size of SRC buds at harvest, and some change in opening-related characteristics. Larger Fully Open (LFO) buds are fully open with the greatest change in tepal shape and colour. These buds were larger than SRC or SSO at harvest, implying a greater preharvest development.

Chapter 3 - Characterisation of commercially treated lily flower opening as compared to on plant

3.1 Introduction

This chapter characterises aspects of normal flower opening in lilies including the physical opening process of the tepals and the timing and synchronicity of bud opening. It aims to investigate if these mechanisms are changed by the exogenous stress of commercial processing or endogenous factors such as the other buds on the inflorescence.

3.1.1 Time of opening in lilies

Flowering is an energy costly process, but a successful reproductive cycle is vital to the plant's overall evolutionary success. In lilies, dependent on variety, this can be anywhere from 90-120 days post planting (personal communication, James Cole, E.M. Cole Farms Ltd.). As mentioned in Chapter 1, changes in flower opening time from early bud to mature flower can be explained by differences in temperature (Heins et al. 1982), where Easter lily bud development rate was found to increase proportionally with average daily temperature (Erwin and Heins 1990). While these components influence overall time of opening, circadian signalling fine tunes this further. The circadian clock and light regulates many aspects of plant development, including growth and flowering time (Yakir et al. 2007). It is beneficial to regulate flowering and anthesis in particular, to ensure pollinators will be available to pollinate the flower at the time it is open (Johansson and Staiger 2015).

Lily opening exhibits strong synchronicity, defined by Bieleski et al. (2000b) as being linked to a specific time of day. For example, Asiatic lilies were found to use both the circadian clock and direct light in order to control opening. Lilies placed under a long day (16:8 light/dark) cycle started opening approximately 9h after dusk and reached the fully open stage 2 hours after dawn, taking an average of 4 hours to open completely. Placing them under a short day (8:16 light/dark) cycle held them at a half open stage for an extended time until dawn (Bieleski et al. 2000b). This leads to the suggestion that they have a two-stage opening process, where the first half is clock regulated and the second is light regulated. This opening in time for dawn is proposed to have potential evolutionary benefit: to protect pollen until pollinators such as bees are active (van Doorn and van Meeteren

2003). Another circadian-controlled process relating to pollinator activity is the production of scent; floral volatile compounds are produced differentially across the day, which may act to attract different pollinators active at different times (Shi et al. 2018b).

Circadian mechanisms are regulated by internal and external cues. Plants have a daily circadian rhythm set by the expression of regulatory clock genes throughout 24 hours which negatively regulate each other. This appears to be generally conserved across many monocot and dicot species (Filichkin et al. 2011). The cycle of expression of circadian genes restricts hypocotyl growth to certain periods of the day; maximum hypocotyl growth in *Arabidopsis* occurs just before dawn (Figure 3.1, Nozue et al. 2007). In some species such as waterlily, rhythmic flower opening is strongly tied to changes in auxin levels to allow opening and closing (Ke et al. 2018). Environmental cues such as light can feed into these processes and fine tune this rhythm to allow the plant to sense seasonal changes, mediated by proteins such as phytochromes (Takano et al. 2009). Due to their interaction with phytochrome interacting factors (PIFs), which are also regulated by the clock, processes such as growth can be tightly regulated to certain times of day. Limiting growth to just pre-dawn can be evolutionarily beneficial as at this time of day plants have the most water availability and most available stored energy, which may also be a factor explaining why lilies open at this time. Phytochrome mutants in *Arabidopsis* often have little or no rhythmicity in growth. Clock mutants (e.g. *CCA1ox*, *elf3*) are fully regulated by light; they grow throughout the night and stop at dawn (Nozue et al. 2007). This shows that both a circadian rhythm and direct light are needed for synchronous limited growth. The similarities of the timing of rhythmic growth and the timing of flower opening make flower opening a candidate to be driven by both circadian and phytochrome (direct light) signalling.

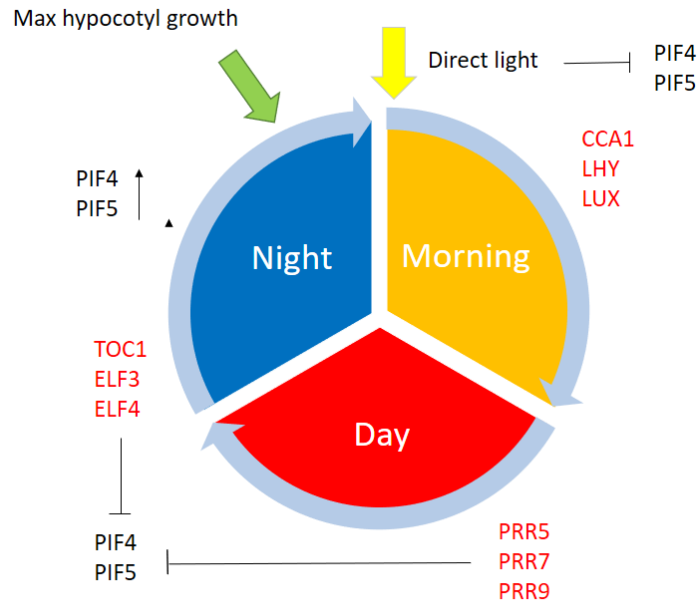


Figure 3.1 – the circadian cycle in plants and how light interacts with it. Clock genes (red) negatively regulate each other in an anticlockwise fashion throughout the day (clockwise). PIF4/5 is the mediator between light and clock, and can be regulated by both to drive hypocotyl/stem growth. Figure adapted from Shim et al. (2017).

3.1.2 Endogenous and exogenous factors affecting the physical opening process

Various factors have been suggested in Section 1.6 as possibly affecting flower development and opening. Some of these are endogenous and relating to the structure of the inflorescence itself, whilst others are exogenous and relate to the conditions of the whole stem.

The position on the inflorescence or stem, strongly relating to the developmental age of the bud, is indicated to be the most important factor affecting the opening process (Section 1.6). The most obvious difference between buds of different ages or positions on stem is of course the time of opening; buds on the same inflorescence open sequentially due to reaching the correct developmental age to open at later times going up the stem. Bud size (length) is related to bud age but may vary dependent on the position on stem – smaller buds higher up the stem never reach the same size as their older counterparts before opening (personal communication, James Cole, E.M. Cole Farms Ltd.).

The most pertinent exogenous factor affecting lily opening is harvest and commercial treatment as part of the cut flower supply chain (the commercial treatment of lilies has been outlined in detail in Section 1.2). Harvesting flowers immediately cuts stems off from receiving water and nutrients from the bulb, and additionally creates a wounding response which may disrupt normal developmental processes and cause stem occlusion problems in several species (van Doorn and Cruz 2000; Williamson et al. 2002; He et al. 2006). Cold/dark postharvest storage of fruits, vegetables and cut flowers, while aiding with overall longevity and quality, has been linked to a range of stress-related issues such as chilling injury (Jackman et al. 1988; Van Doorn and Han 2011; Darras 2020). Cold/dark treatment is designed to retain cut flower quality for a longer period of time by slowing metabolism through reducing transpiration, respiration and ethylene production (Rudnicki et al. 1991). Additional exogenous sucrose is often added to flowers during storage to aid greater degree of opening, longevity and quality (Han 2003; Van Doorn and Han 2011). However, synchronous processes in plants can be disrupted by the breakdown of circadian rhythm associated with long term dark storage. Removal of light cues can lead to breakdown of the circadian rhythm; for example, continuous light or dark conditions caused a slowing in the speed of opening in cut Asiatic lilies compared to those stored in a 12h/12h light/dark cycle (Bielecki et al. 2000b). Additionally, storing cut *Rosa hybrida* L. in red light was shown to delay flower opening and senescence significantly compared to storage in constant darkness (Horibe et al. 2020). Therefore, this raises the question of firstly whether commercially processed cut lilies maintain a circadian rhythm and exhibit synchronous opening, and secondly if this opening is significantly delayed due to the drop in metabolism caused by the cold/dark treatment.

Cold/dark treatment has also been indicated by growers as exacerbating problems relating to position on stem. Inflorescences with a greater number of buds per stem need to be able to share a limited amount of water and nutrients when harvested (Van Meeteren et al. 2001). With a greater number of buds, this can lead to problems with opening of the terminal bud in particular (personal communication, James Cole, E.M. Cole Farms Ltd.). Commercial lilies can have issues with opening caused by age of buds at harvest, where growers try to balance the optimal time of harvest for all buds on the stem to ensure the oldest maintain a good vase life, while the youngest are old enough to continue normal

development off the plant (Reid 2009; Gill et al. (2006). Due to the difficulty of harvesting stems at an appropriate stage of development for both the oldest and youngest bud on the inflorescence, problems such as late bud abortion of terminal buds can arise when there are too many buds per stem (Section 1.3.2). Therefore, it can be hypothesised that harvest and the cold/dark treatment may be responsible for exacerbating the nutrient scarcity already present in stems with multiple buds per inflorescence, leading to problems with flower opening of the smallest bud (postharvest bud abortion, as defined in Section 1.5.4). This chapter will therefore also set out to identify if there are differences in flower opening relating to amount of competition on stem, and if this is affected by removing the competition or not.

3.1.3 Global cellular changes causing flower opening in lilies

Flower opening is a highly dynamic process which, in lilies, involves a large change in tepal shape from being concave facing the reproductive organs of the bud to reflexing in the opposite direction. This also includes movement at the base of the flower to cause the tepals to move apart from each other (Liang and Mahadevan 2011). This change in shape requires differential growth of tissue, either by cell division or expansion. The speed of lily flower opening, which can be as short as four hours from the mature bud to fully open flower (Bieleski et al. 2000b), is consistent with cell expansion, as this is faster than cell division and growth. It has been reported in other species such as rose, carnation and daylily that very little, if any, cell division occurs after a very early stage of flower development, and that flower opening is mainly driven by cell expansion (Kenis et al. 1985; Bieleski 1993; Yamada et al. 2009a). In *L. longiflorum* cell division has been indicated to stop in tepals when they are a third of their mature length (Gould and Lord 1989). More recently, this is partially supported by Watanabe et al. (2022), who also showed only a very small increase in the number of epidermal and parenchymal cells over flower development and opening. There are several theories of how differential cell expansion can cause the change in shape observed by lilies. One suggests that cells expand differentially faster on the adaxial face compared to the abaxial face to effect a global change from a concave to a convex shape. This has been observed in many species such as tulips, crocuses and dandelions (Wood

1953; Tanaka et al. 1987; Van Doorn and Van Meeteren 2003). The second suggests that cells expand faster at tepal edges than the midrib, which could cause the distinctive saddle shape found in lilies, alongside rippled tepal edges (Liang and Mahadevan 2011). One study also found that the number of epidermal pavement cells was initially greater in adaxial compared to abaxial sides of the outer tepal, which suggests that there was asymmetric cell proliferation between the two sides of the tepal prior to harvest, aside from cell expansion itself (Zhang et al. 2021).

More recent work in lilies by Watanabe et al. (2022) has shown that cell expansion occurs in the large irregularly-shaped parenchymal cells making up the inner part of the tepal, and this tissue expansion also creates large air spaces between vascular tissue and the parenchymal cells. A similar increase in air spaces between parenchymal cells has been extensively described in roses (Yamada et al. 2009a). Watanabe et al. (2022) also implicated the involvement of cell wall loosening as part of the flower opening process, showing that genes coding for enzymes essential in this process such as expansins and xyloglucan endotransglucosylase/hydrolases were expressed significantly more in tepal adaxial than abaxial epidermal cells, which correlates with a greater rate of cell expansion in adaxial cells. Zhang et al. (2021) also suggested that the twisting and rolling out of tepal edges is possibly driven by the inner epidermal cells in the outer tepal edges having less cell wall surface area (defined by these authors as fewer wrinkles) and a higher water absorption capacity. Intracellular and cell-wall morphology, composition and structure changes over flower opening. In several species such as carnation and iris, there are increases in cellulose, neutral sugars and uronic acid content up to full flower opening, which decrease immediately post maturity as the flower starts to senesce (O'Donoghue 2006; Watson et al. 2008).

3.1.4 Aims of investigation

1. Elucidating the timing of opening and physical mechanisms of flower opening in lilies
2. Understanding if this timing of opening or growth process is different in commercially treated lilies

3. Understanding and separating the effect of harvest and of cold/dark treatment on time of opening in lilies
4. Exploring the effect of competition on stem on a bud's ability to open, in order to explore the phenomenon of postharvest bud abortion

3.2 Materials and methods

3.2.1 Time of opening assay comparing on plant/commercially treated lilies

Whole lily plants (Oriental lilies 'Ascot' and 'Tisento', LA hybrid 'Eyeliner') in crates or cut stems were grown in E.M. Cole Farms Ltd. greenhouse conditions (Section 2.1.1.2). Half of these were harvested and cut stems were commercially treated as described in Section 2.1.2.1. All stems were carefully selected for similar bud ages and stages of development (bud length) at the start of the experiment. Number of buds per stem was hypothesised to be an important factor in opening time, and therefore where possible an equal number of stems with specific numbers of buds per stem were included in each experimental group. For 'Tisento' and 'Ascot', at least three stems with two, three and four buds per stem were in each experimental group due to stems of these varieties growing with 2-4 buds per stem. For 'Eyeliner' at least three stems with three/four/five buds per stem were used in each group, due to this variety preferentially growing with 3-5 buds per stem. Twelve stems per on plant/cut stem condition were labelled to identify each bud and bud length was measured at the start of the experiment. Cut stems were placed in buckets containing FloraLife conditioning solution made up as directed in Section 2.1.2.1. Plants and flowers were set up facing timelapse cameras programmed to take photographs hourly for 8 days as described in Section 2.4, however, a green light at night to allow night-time photography was not used in this experiment. After six days bud length was measured again. Photographs were analysed manually to identify date of opening for each individual bud. Bud opening time data were analysed statistically using a General Linear Mixed Model (GLMM) in RStudio (version 1.3.1093) to identify if commercial processing affected the overall time taken for each bud to open from the start of the experiment, considering the

different positions of bud on stem, and if a greater number of buds per stem affected this overall opening.

3.2.2 Assessing impact of cold/dark treatment on time of opening in lilies

Oriental lilies cv. Pacific Ocean were used in this experiment. Whole plants were grown in E.M. Cole Farms Ltd. greenhouse conditions (Section 2.1.1.2) for the 'On plant' group (14 stems). Cut stems were either allowed to rehydrate in FloraLife solution overnight at ambient greenhouse temperature for the 'Cut stems no cold/dark treatment' group (12 stems) or treated as usual for commercially treated stems with cold/dark treatment (Section 2.1.2.1) for the 'Cut stems with cold/dark treatment' group (12 stems). Stems were carefully chosen between the groups with and without cold/dark treatment to be similar lengths (all Position A buds (Section 2.3) were within 2 cm bud length). Only stems/plants with four buds per stem were used for each group. Plants/stems were arranged as described in Section 2.4 and timelapse webcams were used to take photographs every 30 minutes for eight days. Photographs were analysed manually to identify approximate hours to start opening from the start of the experiment for each individual bud.

Bud opening time data were analysed statistically using a two-way ANOVA in RStudio (version 1.3.1093) to identify if commercial processing or cold/dark treatment affected the overall time taken for each bud to open from the start of the experiment, considering the different positions of bud on stem.

The circadian synchronous element of flower opening was analysed by counting the frequency of buds opening at discrete times on a 24-hour clock (every 30 minutes). Frequency distributions of on plant and commercially treated stems only were compared using a Watson's U2 test for circular data in RStudio (version 1.3.1093) to determine if they were significantly different.

3.2.3 Preliminary tepal epidermal pavement cell growth assay in commercially treated lilies over opening

Commercially treated Oriental lilies (unknown cultivar) and *L. longiflorum* (unknown cultivar) were bought from a commercial retailer and maintained in growth room conditions in tap water (6 stems per variety) supplemented with Chrysal lily food supplement (made up

as directed). One individual flower at each stage of development 1-5 (outlined in Section 2.2) was prepared for microscopy and imaging was carried out as described in Section 2.5 and Figure 2.4.

For this preliminary experiment, 6 cells were measured from each picture for cell area, perimeter, length and width, and from these measurements the shape factor and length/width ratio was calculated (outlined in Section 2.5). Cell area was averaged for each section of the tepal described in Figure 2.4A for inner and outer tepals across stages of development. This was used to identify the area of the tepal growing fastest and responsible for the change in tepal size and shape. Shape factor and length/width ratio was also compared over the stages of development to identify if the shape of cells changed significantly over flower opening.

A generalised linear mixed model (GLMM) using a negative binomial family was used (R statistical package vers. 3.5.1 software in RStudio version 1.3.1093) to identify significant differences in rate of cell growth over opening between different areas on the tepal, using cell area. The stage of development was investigated as a primary independent variable, but the whorl the tepal came from (inner/outer), the location on the tepal (top/mid/base), the adaxial/abaxial side, and position on the tepal (at midrib/edge) were all also treated as independent variables. Second interactions between stage of development and the other variables were included. The model was refined by deletion of non-significant terms using the Aikake Information Criterion (AIC), which was used as a measure for how well the model fit the data (Bozdogan 1987). Effects were reported using the Wald-Z test.

3.2.4 Tepal epidermal pavement cell growth assay comparing on plant to commercially treated flowers

The rate of growth across the tepal over opening was also compared between on plant and commercially treated flowers. Oriental lilies cv. Ascot were grown in E.M. Cole Farms greenhouse conditions (Section 2.1.1.2) and for on plant samples, continued to develop in the same conditions. Commercially treated 'Ascot' stems were treated with E.M. Cole Farms normal commercial treatment (Section 2.1.2.1). Three individual Position A buds/ flowers (oldest bud on the stem, Section 2.3) at Stages 1, 3 and 5 (Section 2.2) were chosen on basis of similarity of bud/tepal length between biological replicates. As in Section 3.2.1, tepals

were removed and treated as shown in Section 2.5 to carry out microscopy and imaging. Figure 2.4 describes how top, middle and base sections from both inner and outer tepals were used as shown before; however in this analysis only adaxial sections were used. At least 20 cells per field of view were used to measure cell area and perimeter. Cell area was averaged for each section of the tepal described in Figure 2.4A for each biological replicate (for inner and outer tepals separately) across stages of development.

A student's T-test was used to identify if there were significant differences between on plant and commercially treated tepal epidermal pavement cell area at each stage of development for each part of the tepal. A 2-way ANOVA was carried out on the pavement cell area data to identify if there were significant differences between cell area with respect to stage of development or region on tepal (and the interaction with both).

3.2.5 Assessing effect of competition on ability to open in terminal lily buds

Oriental lilies cv. Ascot were grown in Cardiff University greenhouse conditions (Section 2.1.1.1) until inflorescences were approximately one week before standard commercial harvesting stage (Section 2.1.2.2), with a range of terminal bud lengths from 25-60 mm. They were commercially treated as described in Section 2.1.2.2, after which the experiment was carried out under Cardiff University growth room conditions (Section 2.3). The stems were split into groups of four bud stems and five bud stems to reduce the confounding factor of bud number. The bud length was measured at the start of the experiment before the top third of buds was removed for further analysis as described in Section 2.10. The stems were split into a further two groups where one was maintained on stem in vases (approximately 8 buds per vase, tap water only), and the other was removed from the stem using a clean sharp scalpel and placed in a clean container full of tap water (containers treated as described in Section 2.1.3). The stems/individual buds were then monitored for bud opening as shown in Figure 2.10 and labelled as open or failed.

The binary data for each bud length was analysed for minimum bud length required to open and the open:failed ratio for each group. A General Linear Model (GLM) in RStudio (version 1.3.1093) was used to analyse if treatment (on stem vs. individual buds), number of buds per stem (4 bud stems vs. 5 bud stems), or bud length was significantly affecting the ability

of the bud to open (opened vs. failed). Interactions between factors were not added to the model due to very small group sizes, particularly in the 'opened' group.

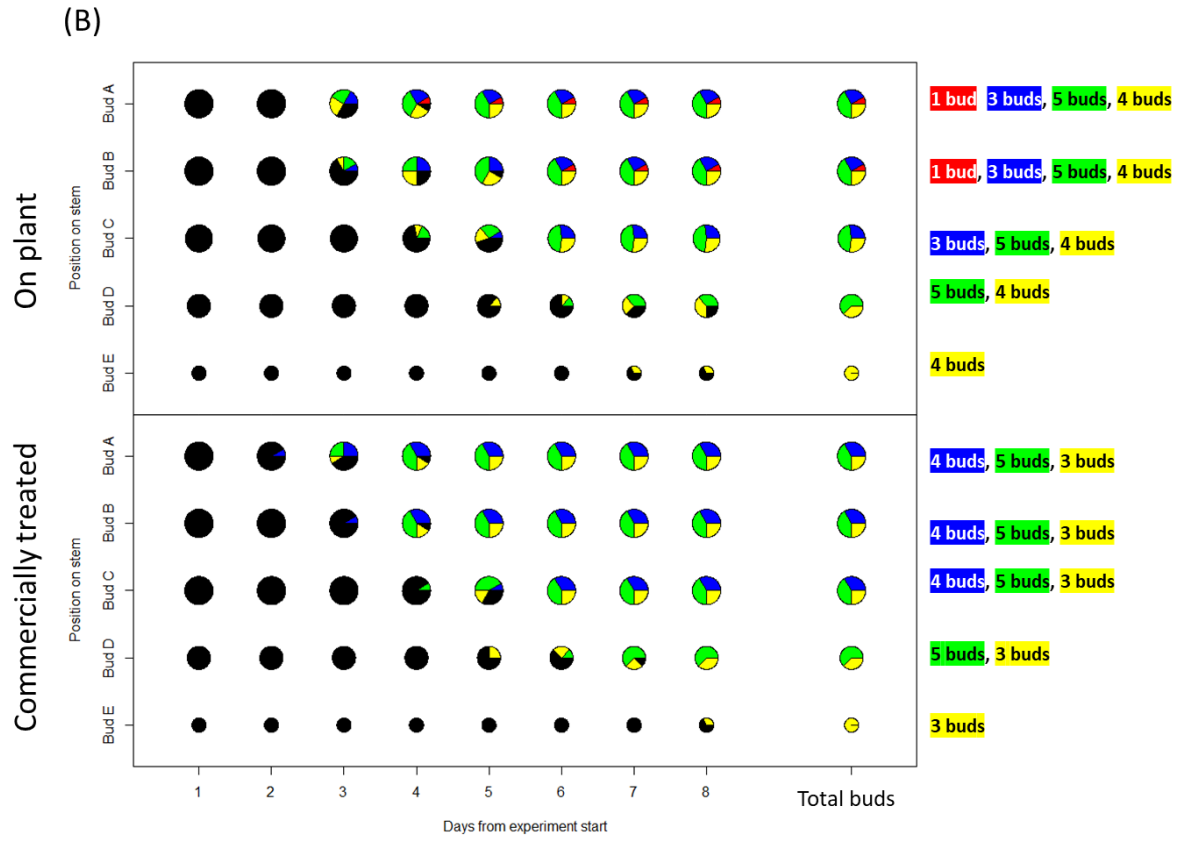
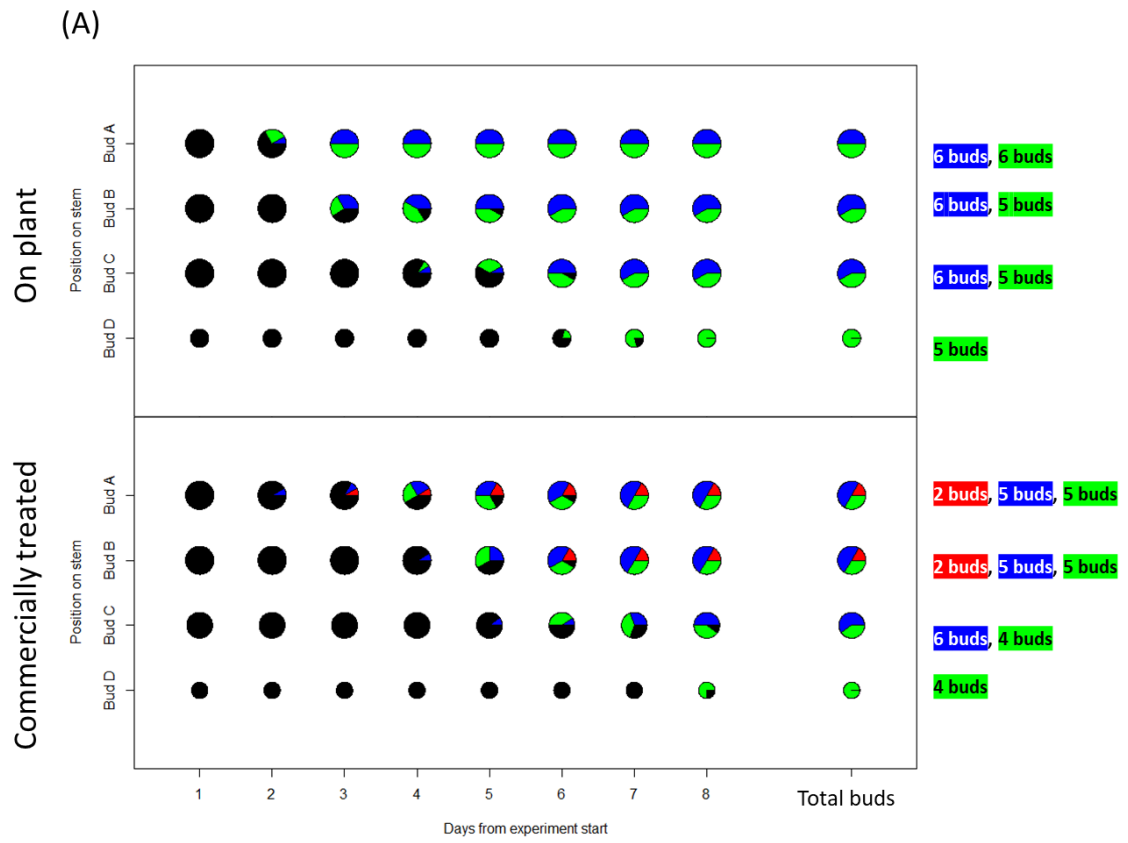
3.3 Results

3.3.1 Variation in flower opening time due to number of buds per stem (competition on stem) and the effect of commercial treatment

Oriental lily cv. 'Tisento' grows as stems containing 2, 3, or 4 buds. On plant (OP) buds showed that all Position A buds (bud A) opened by Day 3 of the experiment and all buds regardless of position opened by Day 8 (Figure 3.2A). Figure 2A shows that for 'Tisento' OP buds, as expected, the position on stem staggers the opening for each bud on the stem; buds at position A started to open on Day 2, whereas buds at position B did not open until day 3, buds at position C on day 4, and buds at position D on day 6. Commercial treatment (CT) was found to delay the date of opening by one day or more for buds at each position on the stem (Figure 3.2A). In fact, CT Position A buds took until Day 7 to all open, compared to Day 3 for OP Position A. Furthermore, buds at positions A and B in all stems opened by the end of the experiment, showing that the developmentally oldest buds were unlikely to fail to open within the experimental timescale because of commercial treatment. However, buds at positions C and D were affected by commercial processing, as some CT buds were still not open by the end of the experiment - whereas all OP buds had opened by Day 8. Time of opening in 'Tisento' did not seem to be affected by the total number of buds on the stem when on plant – an almost equal number of buds opened on Day 2 from stems with 3 buds as from stems with 4 buds (Figure 3.2A). On CT stems, buds from stems with 4 buds opened slightly later than buds from stems with 2 or 3 buds, but this is difficult to confirm due to low sample numbers of stems with two buds per inflorescence. The GLMM showed significant differences between OP and CT groups ($p < 0.05$, Appendix 6.5), which suggests that opening time was significantly faster in OP buds compared to CT. It also showed significant differences between the day of opening of buds at different positions on stem, more unsurprisingly, which showed a significant increase in day of opening with subsequent positions on stem. However, it did not show significant differences between opening time of

buds from stems with different numbers of buds per inflorescence, and between the interaction between treatment and position on stem/number of buds per inflorescence.

The LA hybrid cv. Eyeliner grows as stems of 2, 3, 4 or 5 buds. It showed a similar opening pattern to 'Tisento' for OP buds (Figure 3.2B). While buds at position A did not seem to be affected in time of opening by commercial treatment (Figure 3.2B), there was a similar delay in opening for buds at positions B, C and D (however not by as great a difference as observed in 'Tisento'). Notably, more buds on plant failed to open by Day 8 than in CT buds at position D. CT buds of 'Eyeliner' were similar to OP buds in terms of both being largely unaffected by a greater number of buds per stem. Again, this was not reflected statistically by GLMM (Appendix 6.6), suggesting that while there were unsurprisingly significant differences between bud opening day dependent on the position on stem, there were no significant differences between the opening time between OP and CT conditions, or differences between the number of buds per inflorescence or position on stem in OP or CT conditions.



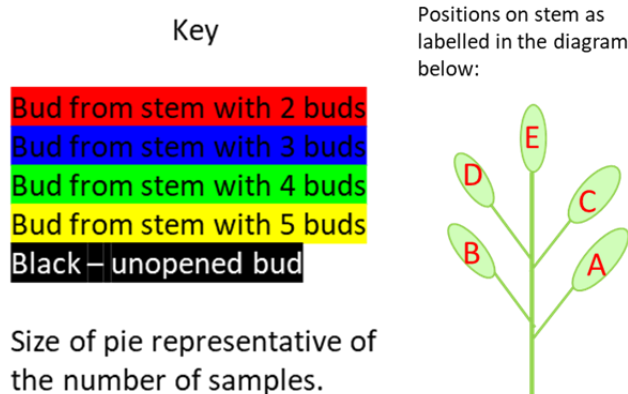


Figure 3.2 - Effect of position on stem and commercial treatment on time of opening. Bubble plot showing time of opening in (A) the Oriental 'Tisento', comparing on plant and commercially treated stems showing when buds from each type of stem (how many buds there are in total on the stem, coloured as shown in key) open at each position on stem. (B) shows the same bubble plot for the LA hybrid lily cv. 'Eyeliner'. The total number of buds of each position on stem used in the experiment is on the far right of the figure to show how many of each type of inflorescence (number of buds per inflorescence) were used. Statistical significance was carried out using a linear mixed model (Appendix 6.5, 6.6).

3.3.2 Separating the effect of harvest and cold/dark treatment on time of opening

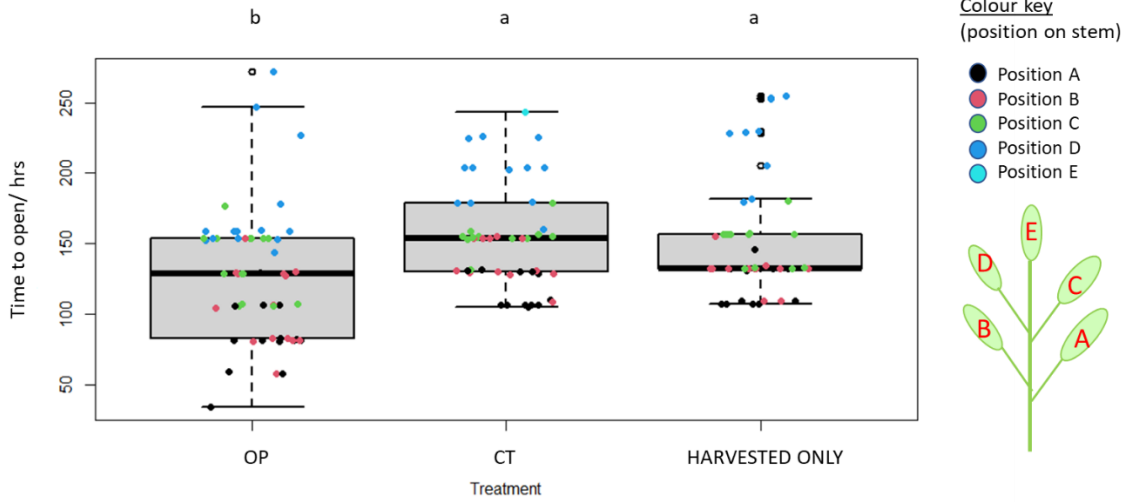
Oriental lilies cv. Pacific Ocean were observed over a different growing season to evaluate the effect of harvest itself on time of opening, as compared to on plant and commercially treated (with a 72 hour cold/dark treatment). Buds showed a variation in opening time depending on the position on stem, which was confirmed by two-way ANOVA as being significant (d.f. 4, $p < 0.05$). The clock plots in Figure 3.3D show the separate bud opening time of day (colour coded for position on stem) showing that they open on average every 24 hours, at around the same time in the morning (between approximately 01:00-04:00 AM), regardless of treatment. The colour coding for position on stem showed that there was also variation in flower opening time within buds at the same position on stem, spreading over a period of around four days. On plant buds showed a significantly faster opening time compared to either commercially treated or harvested only buds, with a similar variation in data. Looking at the spread of data, although this was not statistically significant (Appendix

6.7), the stems which had been harvested only did show a slightly faster opening time, suggesting that the effect of harvest may fall in between these groups with more replication.

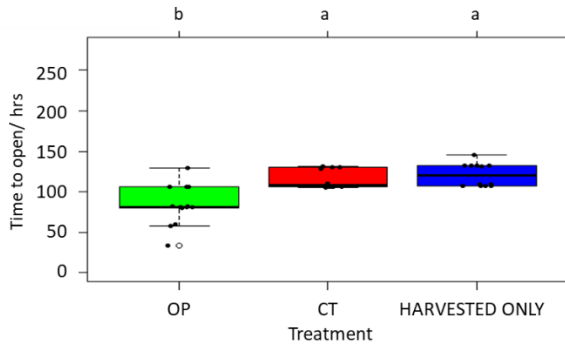
When Position A bud opening time was analysed separately, the same pattern was observed – buds on plant opened significantly faster than both commercially treated and harvested only (Figure 3.3B). However, the spread in opening times was much greater in buds on plant than for those commercially treated/only harvested. When Position D bud opening time was analysed (terminal bud for most stems used in this experiment), buds opened significantly slower in harvested only buds than both on plant and commercially treated buds, which were not significantly different in opening time to each other (Figure 3.3C, Appendix 6.7)).

The circadian element of opening was investigated by counting the frequency of flowers which started to open at a specific time of day in on plant vs commercially treated stems, down to the closest 30 minutes (Figure 3.3D). On plant, buds opened in a highly synchronous fashion, with 18 buds of different positions on stem opening at 02:00 and 49 buds (88%) opening between 01:00 and 04:00 (median opening time 02:00). The remaining 7 buds were Position D buds only. This synchronicity of opening was mostly maintained in commercially treated buds, with 40 out of 46 buds (87%) opening between 01:00 and 04:00. The commercially treated bud opening times were more evenly distributed, with a median opening time of 03:00, and mostly opened between 02:30 and 04:00. Notably, the buds which opened outside the typical range (6 buds) were, unlike on plant buds, not only Position D terminal buds, but a combination of positions on stem. When the distribution of flower opening times for on plant and commercially treated flowers was analysed for statistical differences, a Watson's U2 test showed significant differences between the two treatments ($T=0.7948$, $p<0.05$, Appendix 6.8).

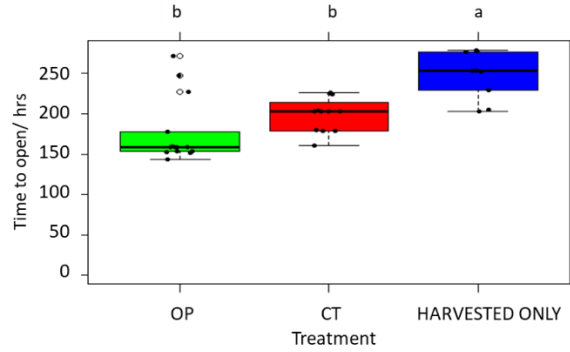
(A) – all buds



(B) – Position A buds



(C) – Position D buds



(D)

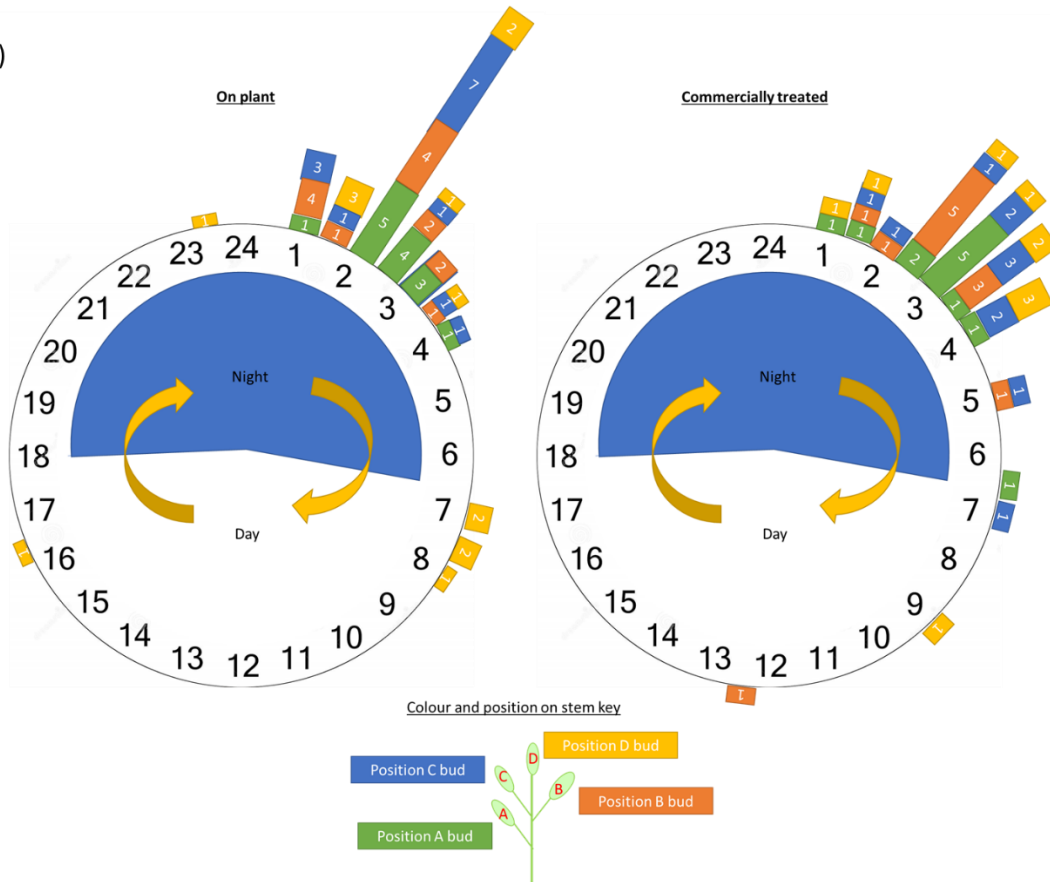


Figure 3.3 – Hours to open from experiment start of (A) all buds , (B) Position A buds only and (C) Position D buds only, comparing commercially harvested stems with cold/dark treatment (CT) and harvested only (HARVESTED ONLY) with on plant (OP). Letters denote significance as found by two-way ANOVA (Appendix 6.7). (D) Frequency of flower opening across a 24-hour clock comparing on plant and commercially treated stems to show distribution of time of opening (start of opening indicated here, defined as tepal tips separating). Clock runs clockwise and indicates time of dawn and dusk during the experiment. Colours on key indicates position on stem and numbers on bars show number of buds from each position on stem open at that time (not necessarily on the same day).

3.3.3 Flower opening is driven by differential cell expansion across the tepal

The epidermal pavement cell area data described here is shown both as a fold change between Stages 1-5 for each section of tepal measured (Figure 3.4A) and as graphs to show the change in mean cell area between each stage of development (Figure 3.4B and C), however the full tables of mean epidermal pavement cell area at each stage of development for each section of tepal are available in Appendix 3.1.

Epidermal pavement cell area in Oriental lily (unknown cultivar) was found to significantly increase sequentially between each stage of development in both outer and inner tepals (Appendix 3.1). The fold change from Stage 1 (green closed bud) to Stage 5 (fully open flower – Section 2.2) in total epidermal pavement cell area was greater in inner tepals than outer tepals (Figure 3.4A). This difference between inner and outer tepal cell size change over development was significant in the mid sections of tepal (indicated to be the greatest expanding tissue in Figure 3.4A (GLMM, Z-value 2.442, $p < 0.05$, Appendix 6.1), therefore inner and outer tepals were treated separately in further statistical analysis. The mean abaxial pavement cell area was larger than their adaxial cell counterparts at Stage 1 (Appendix 3.1), with top abaxial midrib sections showing the largest cell area at Stage 1 in both outer and inner tepals, significantly different to all regions of tepals apart from adaxial midrib top and base sections in outer tepals. In inner tepals the top abaxial midrib section was less significantly different in size to other sections (Appendix 3.1). However, adaxial cells had an overall larger change in size over opening, particularly in mid/base outer tepals

(Figure 3.4A). Differences between adaxial and abaxial sides of the tepal (GLMM, Z-value - 4.642, $p < 0.05$, Figure 8.2C, Appendix 6.1) were indicated to be significantly different overall. On both adaxial and abaxial sides of outer/inner tepals, there was a general trend of the average fold change of tepal epidermal pavement cell size being greater at the edge of the tepal than at the midrib (Figure 3.4A). Edge and midrib sections (GLMM, Z-value 2.635, $p < 0.05$ Figure 8.2D, Appendix 6.1) were observed to be significant according to the GLMM model. The greatest fold changes were observed in the outer adaxial middle tepal edge, outer adaxial base (both midrib and edge) and the inner adaxial middle and base tepal edges (Figure 3.4A). This is supported by the mean outer mid adaxial edge pavement cell area reaching a similar size to mid abaxial midrib at Stage 5 (Appendix 3.1). Similarly, in inner tepals, the base adaxial edge and mid adaxial edge sections had a statistically similar mean pavement cell area to top adaxial midrib sections, which was the largest at Stage 1 and 5 throughout.

Due to the greater growth of tepal edges, the growth of edge epidermal pavement cells only between Stages 1 and 5 were investigated in more detail (Figures 3.4B and C). Different areas of the outer tepal showed a constant increase in cell area from Stages 1 to 3, and a plateau in/ negative pavement cell area change between Stages 3 and 4. The difference in pavement cell area between Stages 4 and 5 reflected a faster growth rate again for certain parts of the tepal, in particular the middle of both abaxial and adaxial sides of the tepal (Figure 3.3B). While this pattern was not as clear in inner tepals, several sections also showed a similar pattern of a plateau in growth between stages - top abaxial and mid adaxial areas showed a plateau between Stages 3 and 4, while top adaxial and base adaxial had an earlier plateau between Stages 2 and 3, before a higher rate of cell expansion in pavement cells between Stages 3 or 4 and 5 (Figure 3.4C). At Stage 5 (fully open flower), the outer mid adaxial edge and outer mid abaxial midrib showed significantly higher mean epidermal pavement cell area than other outer tepal sections, and for inner tepals this was the top abaxial midrib section (Appendix 3.1).

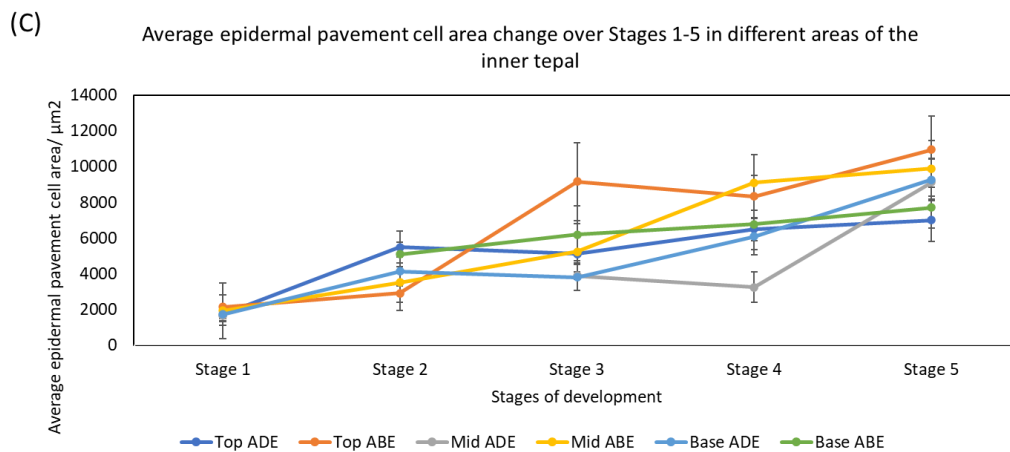
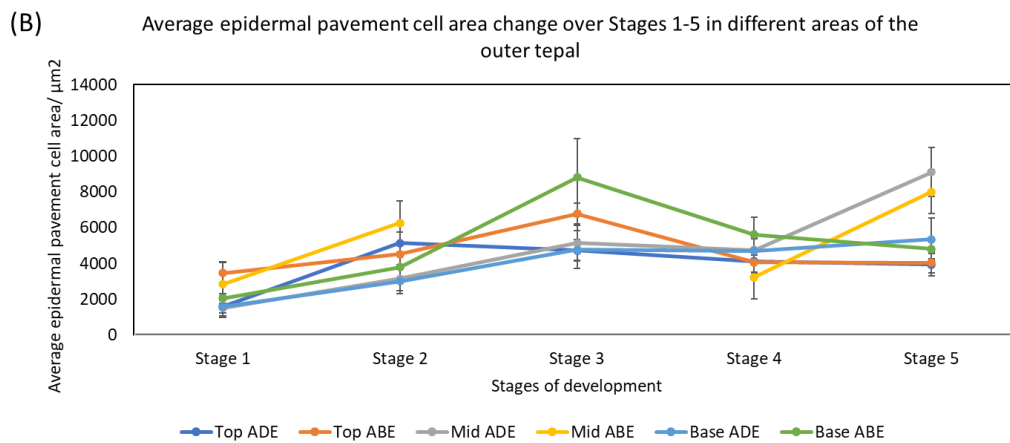
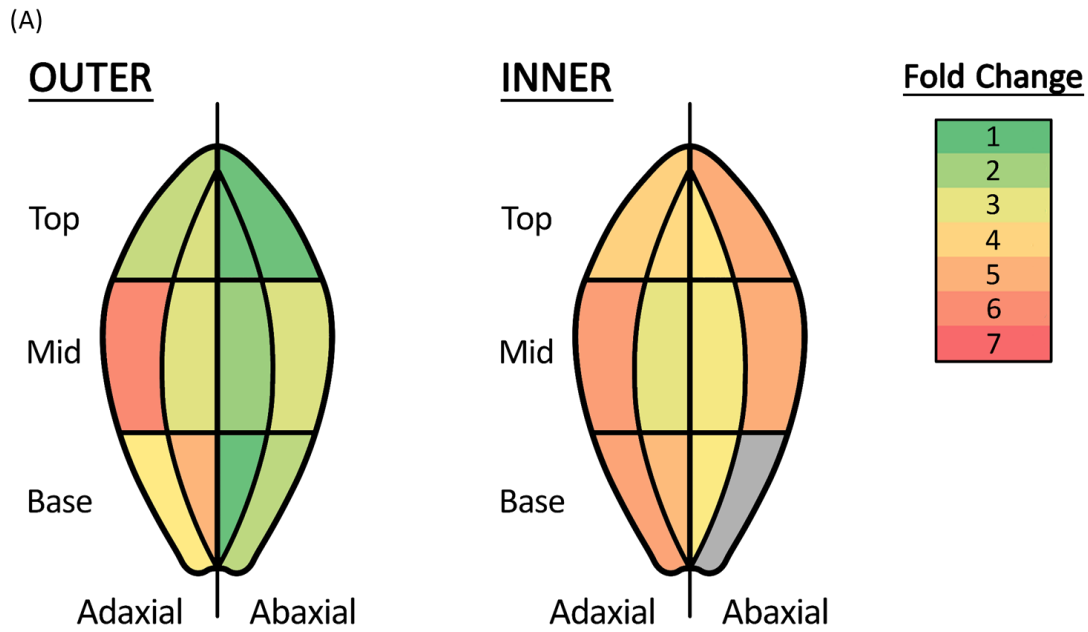


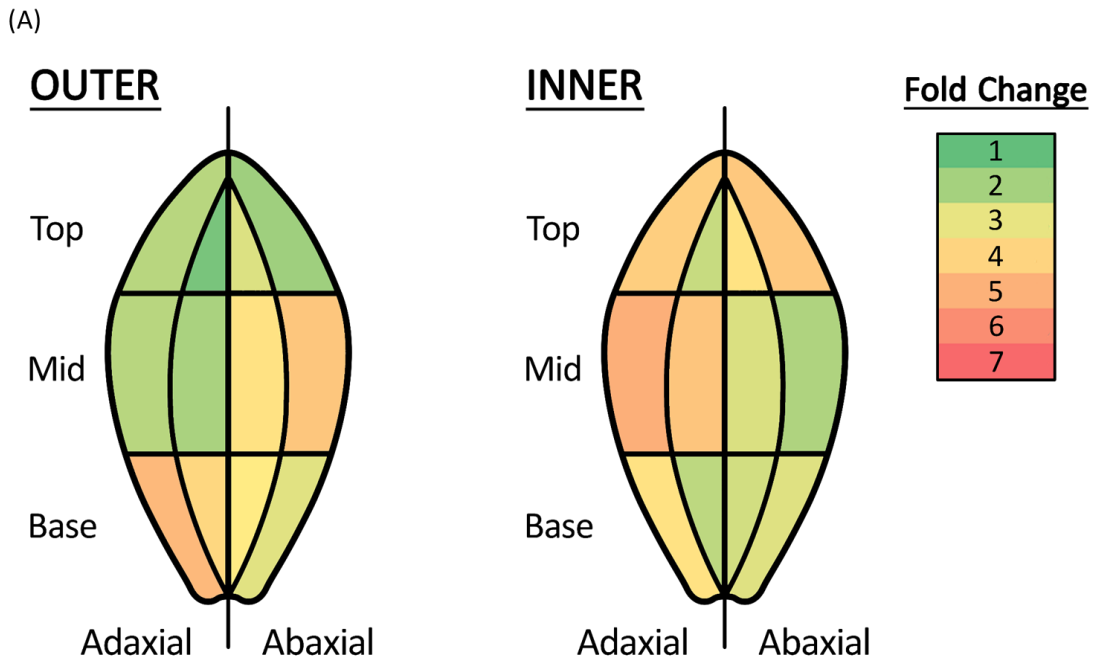
Figure 3.4 – Epidermal pavement cell growth in Oriental lily (unknown cultivar) tepals over development and opening, considering different sections of the tepal to identify regions of

fastest growth. (A) fold change (Stages 1-5) of different regions of the tepal colour coded to reflect magnitude of cell size change. (B) and (C) growth rate for epidermal pavement cells in tepal edge sections in different parts of the (B) outer tepal and (C) inner tepal. Codes for tepal areas: ADE: Adaxial edge, ABE: Abaxial edge. Error bars show standard deviation. Appendix 3.1 contains the data used for these figures, including statistical tests to show differences between mean epidermal pavement cell area at each stage of development on the tepal.

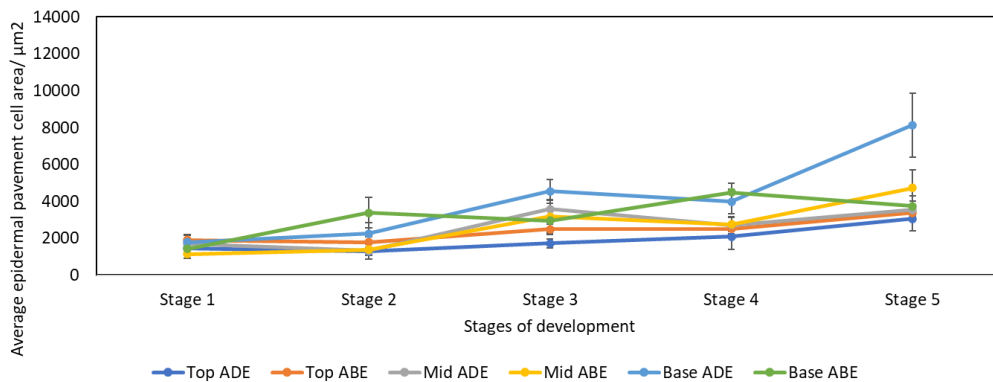
As above, the full tables of mean epidermal pavement cell area at each stage of development for each section of tepal in *L. longiflorum* material are available in Appendix 3.2.

L. longiflorum also showed significant differences by GLMM in epidermal pavement cell area between every stage of development (GLMM, Z-values Z_2 1.919, Z_3 3.882, Z_4 5.48, Z_5 8.761, $p_2 > 0.05$, $p_{3,4,5} < 0.05$, Appendix 6.2). However, this variety showed a much smaller overall fold change of epidermal pavement cell area between Stages 1 and 5 than Oriental tepals. The differences in cell area change over opening were not found to be statistically different with respect to type or region of tepal by GLMM prediction lines (Appendix 6.2, Figure 8.2E-H), which supports the hypothesis of a more uniform change. Like the Oriental lily, *L. longiflorum* also showed a slightly larger fold change in inner tepals compared to outer tepals overall but this was not statistically supported by the GLMM (Figure 3.5A). Outer tepals showed very similar mean epidermal pavement cell area in all regions of the tepal, with no significant differences between any sections, while in inner tepals base adaxial and abaxial midrib sections were the largest (Appendix 3.2). The inner mid adaxial sections in particular showed a high fold change, as well as the outer base adaxial and mid abaxial sections. The GLMM also showed significant differences between edge and midrib sections (GLMM, Z-value 2.854, $p < 0.05$, Appendix 6.2), comparing top sections to mid and base of tepals (GLMM, Z-value -3.067, $p < 0.05$, Appendix 6.2). The outer tepals at Stage 5 showed significantly higher mean pavement cell area in base adaxial midrib and edge sections compared to the top or mid sections, which was very similar to that observed in inner tepals, where base abaxial midrib sections in particular were significantly larger than any top or mid sections (Appendix 3.2).

The pavement cell area in *L. longiflorum* at Stage 1 was smaller than the equivalent in Orientals and also was smaller in the fully open flower, explaining the overall smaller cell area fold change seen in this variety (Figure 3.5B, C). Different parts of the tepal showed high variation in epidermal pavement cell area in Oriental tepals at Stage 1, however in *L. longiflorum*, particularly in outer tepals, there was very little significant difference in cell size of different areas of the tepal (Appendix 3.2). The pavement cell growth of many areas of the tepal also showed a plateau in growth between Stages 2/3 and 4, similarly to Orientals. Outer tepals in particular showed this plateau between Stages 3 and 4 for all base and mid sections, with top sections showing a more constant growth in cell area between Stages 1 and 5 (Figure 3.5B). Inner tepals showed a particularly high rate of pavement cell area change in base adaxial sections, which showed a marked difference from the other section going from Stage 2 through to 4, with base abaxial sections only showing a similar cell area at Stage 5. In the fully open flower (Stage 5), outer adaxial base sections and inner abaxial base sections in particular showed a significantly larger mean epidermal pavement cell area than other areas of the tepal (Appendix 3.2).



(B) Average epidermal pavement cell area change over Stages 1-5 in different areas of the outer tepal



(C) Average epidermal pavement cell area change over Stages 1-5 in different areas of the inner tepal

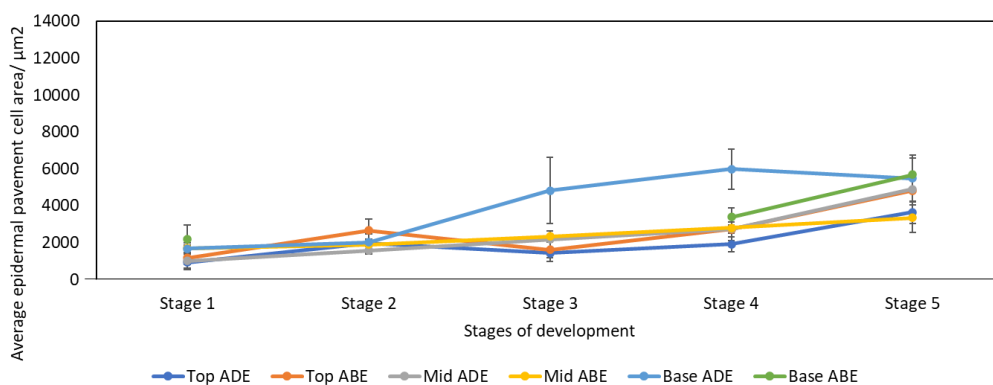


Figure 3.5 – Epidermal pavement cell growth in *L. longiflorum* lily tepals over development and opening, looking at different sections of the tepal to identify regions of fastest growth.

(A) fold change (Stages 1-5) of different regions of the tepal colour coded to reflect magnitude of cell size change. (B) and (C) growth rate for epidermal pavement cells in tepal edge sections in different parts of the (B) outer tepal and (C) inner tepal. Codes for tepal areas: ADE: Adaxial edge, ABE: Abaxial edge. Error bars show standard deviation. Appendix 3.2 contains the data used for these figures, including statistical tests to show differences between mean epidermal pavement cell area at each stage of development on the tepal.

3.3.4 Differential cell expansion for flower opening is not significantly different between on plant and commercially treated flowers

Commercially treated flower cell expansion was compared to on plant to investigate differences in speed or degree of opening. Section 3.3.3 showed there were slight differences between the adaxial and abaxial sections in terms of growth, with the adaxial sections showing significantly more growth overall in Oriental varieties. This experiment focused on adaxial sections only to compare growth of on plant and commercially treated flowers of the same size.

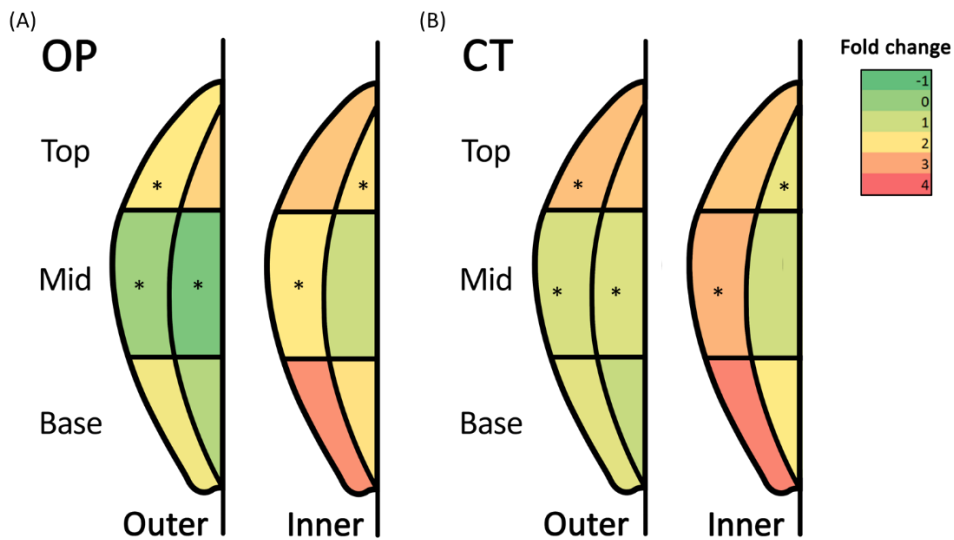
The epidermal tepal pavement cell area change between Stages 1 and 5 in Oriental lily 'Pacific Ocean' was comparable to the previous section when comparing outer and inner tepal growth (as in Section 3.3.3, inner tepal growth was greater than outer tepal growth). Samples on plant did not change as much as was observed in Section 3.3.3, with many sections (outer middle and base sections) not changing at all on average (Figure 3.6A). In both on plant and commercially treated samples, the fold change of pavement cell area between Stages 1 and 5 was greatest in inner base edge sections (Figure 3.6A, B). Due to the natural variation between individual flowers, some average fold change in epidermal tepal pavement cell area also decreased between stages, but not significantly so. There was much less differential growth between midrib and edge sections except at discrete sections such as the inner tepal base edge, in both on plant and commercially treated tepals. Notably, the tepal top sections increased in size more uniformly in 'Pacific Ocean' than the data collected for the unknown Oriental cultivar in Section 3.3.3.

When tepal epidermal pavement cell expansion was compared between on plant and commercially treated flowers, very little difference was observed in the fold change in most

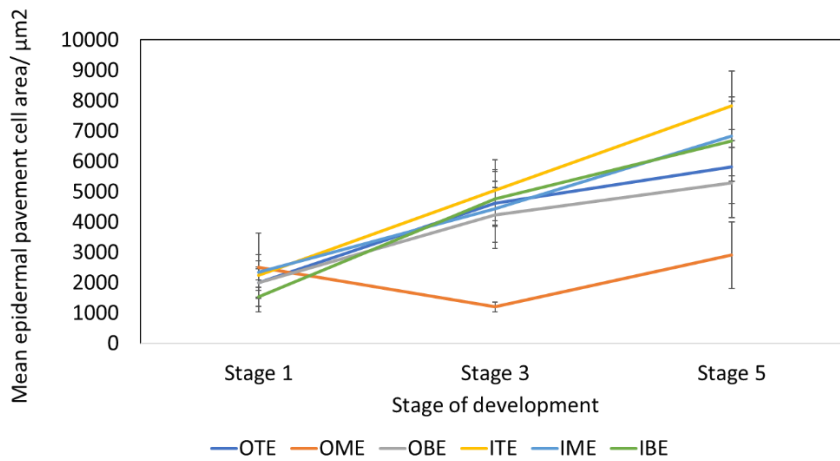
sections (Figure 3.6A, B). Average pavement cell area in OP and CT flowers was comparable at Stage 1 (start of the experiment) and showed no significant differences between groups (independent T-test, $t=-0.629$, $d.f.=69.73$, $p>0.05$, Appendix 6.3). The average cell area was then compared for each group at Stage 3 and 5, and in each case did not show significant differences between groups (Mann-Whitney-Wilcoxon test, $W_{\text{Stage 3}}=733$, $p_{\text{Stage 3}}>0.05$, $W_{\text{Stage 5}}=743$, $p_{\text{Stage 5}}>0.05$, Appendix 6.3), suggesting that cell expansion was overall unaffected by commercial treatment. The fold change of certain tepal sections (outer middle edge and midrib sections, inner middle edge and top midrib sections) showed significant differences between on plant and commercially treated sections. Notably, the outer middle edge and midrib, and inner mid midrib sections showed greater cell area change in commercially treated sections compared to on plant.

The change in pavement cell area between the stages of development, rather than the overall change, was also investigated in tepal edge sections only, having been indicated to be significantly different from midrib sections already in previous sections.

The growth in tepals on plant was significant in terms of stage of development (2-way ANOVA, $F=71.007$, $d.f.=2$, $p<0.05$, Appendix 6.4), region of tepal (2-way ANOVA, $F=11.352$, $d.f.=5$, $p<0.05$), and the interaction between region and stage (2-way ANOVA, $F=4.706$, $d.f.=10$, $p<0.05$ - Figure 3.6C). The average epidermal pavement cell area growth was quite consistent regardless of region of tepal apart from outer middle edge (OME) sections, which were significantly different to all other regions in terms of growth, as well as outer base edges (OBE), which showed differences to top regions (OTE) by post-hoc Tukey. This was comparable to commercially treated tepals (Figure 3.6D), which showed significance in terms of stage of development (2-way ANOVA, $F=86.505$, $d.f.=2$, $p<0.05$), region of tepal (2-way ANOVA, $F=2.911$, $d.f.=5$, $p<0.05$), but not significant in the interaction between region and stage. Again, this seemed to be driven mainly by differences in epidermal pavement cell growth between the OME section compared to the others, although this was not reflected statistically by the post-hoc Tukey test.



(C) Mean epidermal pavement cell area change over development and opening in different regions of the tepal in OP flowers



(D) Mean epidermal pavement cell area change over development and opening in different regions of the tepal in CT flowers

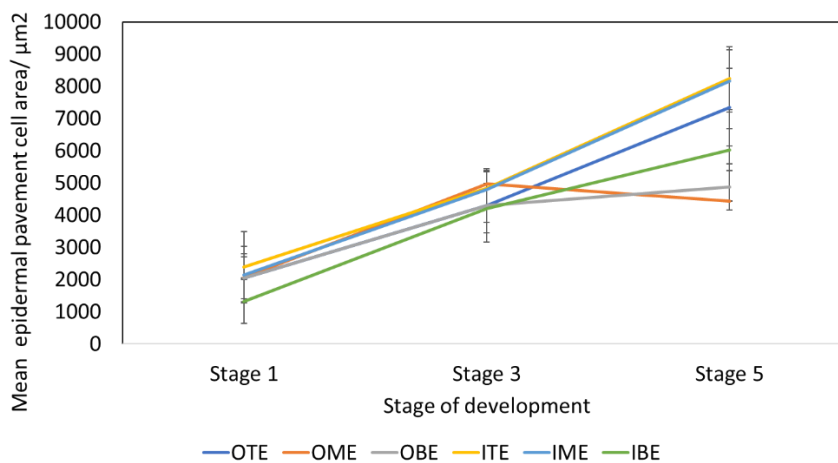


Figure 3.6 – Comparison of epidermal pavement cell area change between Stages 1-5 in on plant Oriental lily ‘Pacific Ocean’ tepals compared to commercially treated. (A) and (B)

shows fold change in cell area in Stage 5 compared to 1 for (A) on plant and (B) commercially treated. Statistical significance between OP and CT tepals in the same tepal regions denoted by asterisks by independent T-test or Mann-Whitney-Wilcoxon test (Appendix 6.3). (C) and (D) epidermal pavement cell area growth change in different parts of the tepal in edge sections only over stages of development and opening. (C) the cell area change in flowers on plant, (D) cell area change in commercially treated flowers. Two-way ANOVA showed significance with regard to stage of development, area of tepal, and the interaction between the two variables (Appendix 6.4) Error bars indicate standard deviation. Cell area codes: OTE (outer top edge), OME (outer mid edge), OBE (outer base edge), ITE (inner top edge), IME (inner mid edge), IBE (inner base edge).

3.3.5 Analysing the influence of competition on stem on ability to open of terminal buds

This experiment was carried out on terminal buds which had been previously identified as being likely to fail to open, particularly when commercially treated on the full inflorescence. A range of bud lengths at harvest was used between 28 and 60 mm. Buds were originally categorised into Small Remained Closed (SRC), Small Semi Open (SSO) and Larger Fully Open (LFO) groups at the end of the experiment, as described in Section 2.10, however due to large differences between and very small group sizes, this was changed to the binary opened vs. not opened.

On stem controls had a much higher opening success rate than individual buds, with 100% in buds from 4 bud stems and 50% in buds from 5 bud stems, while for individual buds the opening success rate was 23 and 25% respectively for 4 and 5 bud stems (Table 3.1). The opening success rate was highly dependent on the bud length at harvest in individual buds; the top bud lengths in each group opened (Figure 3.7B and D). This effect was not observed in buds on stem (5 buds per stem group), where the buds which opened and those which failed were not significantly different in bud length. Moreover, the minimum bud length in on stem controls was 9.1 mm smaller than individual buds from 4 bud stems, and 12.95 mm smaller in individual buds from 5 bud stems.

A GLM was carried out to investigate statistical differences between the number of buds opening with regard to the treatment (on stem vs. individual), number of buds per stem, and bud length (Appendix 6.8). This showed significant differences between bud opening success in on stem controls compared to individual buds (GLM, $T=-3.84$, $p<0.05$) but was not significant with regard to number of buds per stem (4 bud stems vs. 5 bud stems). The factor of bud length at harvest was also shown to be a significant factor (GLM, $T=3.058$, $p<0.05$).

TABLE 3.1 – ANALYSIS OF THE INFLUENCE OF COMPETITION ON STEM ON THE OPENING ABILITY OF TERMINAL BUDS

		4 buds per stem	5 buds per stem
On stem controls	Number of buds	12	8
	Range of bud length	34.8-59.16 mm	28.4-43.7 mm
	Minimum bud length required for opening	38.4 mm	33.8 mm
	Opening success rate	100%	50%
Individual buds	Number of buds	13	12
	Range of bud length	30.4-54.04 mm	32.4-59.79 mm
	Minimum bud length required for opening	47.5 mm	46.75 mm
	Opening success rate	23%	25%

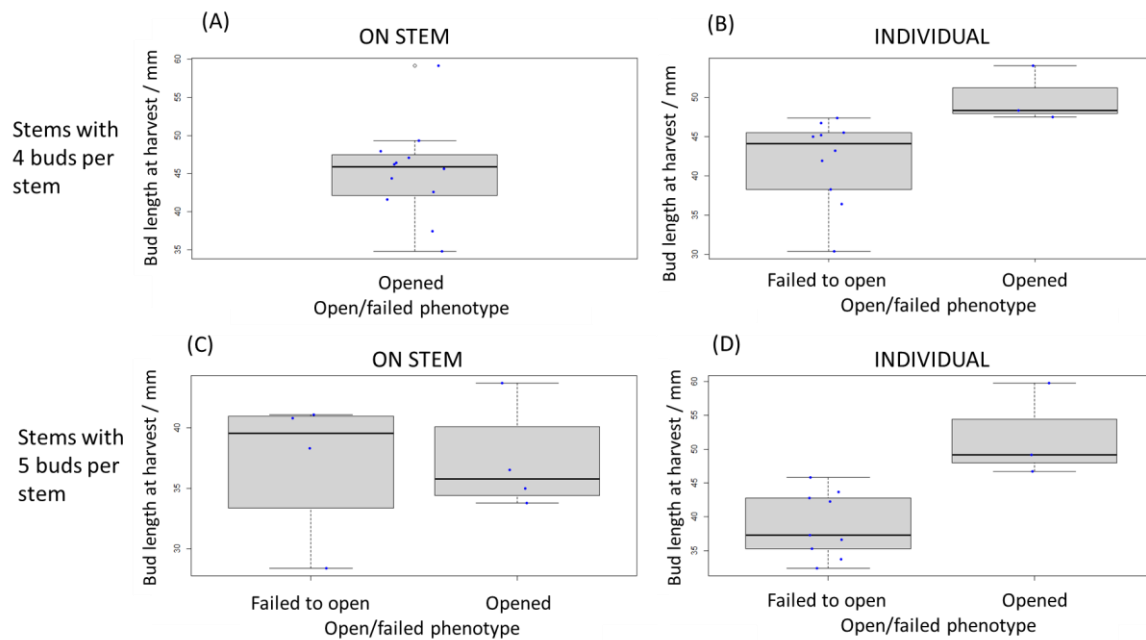


Figure 3.7 – Frequency of bud opening/failure comparing the influence of competition on stem on terminal buds. Buds from stems with 4 buds per stem were either retained on stem (A) or cut off stem and grown in water (B). Buds from stems with 5 buds per stem were also on stem (C) compared to individual buds in water (D). Bud length at harvest is shown as blue points on the boxplots.

3.4 Discussion

3.4.1 Do lilies maintain the same flower opening time when commercially treated?

As commercial treatment has been suggested to have an effect on plant metabolism and therefore perhaps the speed of opening, the global flower opening time was compared in on plant and commercially treated stems. The flower opening time data shown here in Figure 3.2 shows the sequential opening of buds at different positions on stem in the two different varieties Oriental ‘Tisento’ and LA hybrid ‘Eyeliner’. This sequential opening is characteristic of lily flowers and has been observed in many species as a method of temporally and spatially separating the pollen transfer from self- to non self flowers (Brunet and Charlesworth 1995). Some varieties of lily are self-incompatible (Hiratsuka et al. 1983; Lim and van Tuyl 2006) and therefore self-pollination would be inefficient for reproduction. The viability of pollen in many lily varieties has been indicated as having the highest

germination rates 0-1 days post anthesis (He et al. 2017), and therefore this adaptation to reduce rates of self-pollination may explain the general trend observed separating most flowers on the inflorescence by at least one day. Commercially treated flowers also observed this trend, suggesting that the endogenous signals regulating this temporal regulation remain intact postharvest and post-cold storage.

Commercially treated 'Tisento' stems were observed to have a slower opening time than on plant flowers with the same growth conditions and inflorescence 'age', here controlled by picking flowers of a similar bud length at the same positions on stem. This delay in opening was not observed in 'Eyeliner'. In 'Tisento' stems there was over a day's delay in flower opening of most buds at the same position on stem, showing a significant delay in opening for this variety. The cold/dark treatment (72 hours 4-5°C) has been reported to slow metabolism and transpiration in cut flowers and specifically lilies, improving longevity (Van Doorn and Han 2011; Wei et al. 2018), and this was hypothesised to slow the physical age of the whole inflorescence. On the other hand, comparing cell expansion in on plant to commercially treated flowers (Section 3.3.4) shows a slight acceleration in commercially treated buds, particularly for some of the buds on the stem, which supports previous experimental data (Ranwala and Miller 1998). These differing results suggest there may be varietal differences in the response to cold storage between varieties and cultivars. 'Tisento' has particularly large flowers compared to the Oriental varieties 'Stargazer' (used in Ranwala and Miller 1998) and 'Ascot' (also used in this study) and therefore may have a particularly poor response to harvest and cold storage, perhaps due to increased demands on nutrition and water required by larger buds. This could account for the significant delay in flower opening observed in this particular variety.

Abiotic stress has been shown to have several impacts on circadian clock components (Srivastava et al. 2019), making the commercial process a strong candidate for affecting the circadian rhythm of lily stems. However, the data shown here suggests that commercially harvested and treated lilies maintain their synchronous opening time for the most part - while it was not possible to identify the exact time of opening due to low light conditions at night, all flower opening occurred in dark conditions and therefore was likely to have been within the range likely for circadian-regulated flower opening observed previously (Figure 3.6, Bielecki et al. 2000b). Moreover, this was supported by the experiments detailed in

Section 3.3.4, where time of opening was accurate to 30 minutes, and showed that most buds, whether on plant or commercially treated with cold/dark treatment, started to open within the range of 01:00-04:00, which is approximately 3-6 hours before dawn at the time of the experiment. Due to the time to fully open taking up to four hours (Bieleski et al. 2000a), this data supports previous reports of lily flowers opening fully at dawn, as an adaptation to protect pollen from moist pre-dawn conditions (Van Doorn and Van Meeteren 2003). An interesting observation from the bud opening time of day data (Figure 3.7D) was that on plant buds at Position A-C opened within the range of 01:00-04:00 without exception, and the only buds which opened outside this range were terminal Position D buds.

Constant dark storage in particular compared to storage in a light/dark cycle has been linked to accelerated senescence of plant tissue (Liu et al. 2015), but a severe phenotype was only observed after 6 days of storage, suggesting that the maximum three days of cold storage indicated by the grower (personal communication, James Cole) is appropriate to slow metabolism and increase longevity without the possible negative side effects of circadian rhythm loss.

The statistical tests carried out here are valuable as a guide for understanding if the differences between groups are caused by chance or not, but they do not take into account the difference in number of stems with specific numbers of buds per inflorescence due to availability. Groups with unequal sample numbers mean there is an unequal variance and therefore the analysis may be inaccurate in terms of test statistic and p-value. Low replication in this study, as well as very high natural variation, could mean that this unequal variance is significant and therefore places a limitation on the conclusions drawn from this dataset. A greater number of samples with more in each group of number of buds per inflorescence would be better to identify if this factor has a significant effect.

3.4.2 Is harvest or the cold/dark treatment responsible for this delay in flower opening time?

The effects of harvest and cold/dark treatment coincide due to both being required for long distance transport and maintenance of quality in cut flowers (Ranwala and Miller 2005) but were separated here to try to identify specific effects from each treatment. The data did not

suggest that there were any statistically significant differences between flower opening in stems which were harvested only or commercially treated with a 72 hour cold/dark period, but did show significant differences from on plant controls. This suggests that the harvesting itself causes significant slowing to flower opening, rather than being mainly mediated by the slowing of metabolism that occurs in the cold/dark treatment. For commercial growers and retailers, this indicates that the cold/dark treatment has no lasting or worse effects on flower opening than harvesting itself, supporting the use of cold/dark treatment up to 72 hours.

It is interesting to note that 72 hours of cold/dark treatment had no effect on time of flower opening compared to cut flowers which were harvested approximately four days later. Despite significantly changing the age of the cut lilies subjected to the commercial treatment, the developmental age has been completely retained in Position A buds, supporting the use of commercial treatment to slow down development and metabolism (Rudnicki et al. 1991). Notably, there are significant differences between harvested only and commercially treated Position D buds, where harvested only buds are significantly slower to open than either on plant or commercially treated. Differences between harvested only and commercially treated stems could be due to the cold/dark treatment affecting the terminal bud more than Position A buds in terms of slowing their metabolism, but does not account for the differences between Position D bud opening time on plant and cut only stems. The effects of ethylene on development, metabolism and senescence in lilies and other species are well characterised (Van Doorn and Woltering 2008; Hwang et al. 2012; Iqbal et al. 2017; Chen et al. 2022a). The development of both cut and uncut flowers has been found to include a rise in ethylene in multiple species, and often a further increase with the abiotic and biotic stresses of harvest (Scariot et al. 2014). The effects of cold storage on cut flower metabolism and the mechanisms driving these changes are still uncharacterised in lilies, but some of the main findings are a loss of ethylene sensitivity in Asiatic hybrids (Song and Peng 2004). A loss of ethylene sensitivity in the commercially treated flowers, alongside the relatively unstressed condition of the on plant flowers, could therefore account for the delay in opening observed in the susceptible youngest terminal buds of the cut only stems.

3.4.3 Does differential cell expansion cause the change in tepal shape in flower opening?

Differential cell expansion is strongly correlated with flower opening and change in petal shape in other species (Wood 1953; Tanaka et al. 1987; Yamada et al. 2009a) and the data shown here suggests that this is also true for the varieties of lily investigated here. The rate of pavement cell area change between each stage (Figure 3.2B, C, Figure 3.3B, C) showing significant variation across the tepal supports the hypothesis that differential growth is required for flower opening in lilies (Bieleski et al. 2000a; Liang and Mahadevan 2011; Watanabe et al. 2022). Moreover, there is a plateau in growth between stages most involved in opening (Stages 2/3 and 4), implying that there is slowing of total growth as the change in shape requires less total cell expansion. Section 3.3.1 also shows the overall growth across the tepal in Oriental lilies, confirming that the factors hypothesised to show differences (inner/outer tepals, adaxial/abaxial tepal sides, edge/midrib sections) were indeed significantly different to each other. This suggests that flower opening in Oriental lilies is driven both by more growth on the adaxial side compared to abaxial and by more growth at the edges compared to the midrib, supporting previous studies from which these hypotheses were formed (Bieleski et al. 2000a; Liang and Mahadevan 2011; Watanabe et al. 2022). Epidermal pavement cell area growth in inner and outer tepals showed significantly more overall growth in inner compared to outer tepals, which is again consistent with previous reports suggesting that tension in the closed bud from the growth of inner tepals is required to cause the rapid opening observed in lilies (Liang and Mahadevan 2011). Alongside greater growth at the base of tepals, which was also observed here, these phenomena help explain the moving apart of tepals also indicative of opening. While a useful dataset, this experiment could have been improved by biological replication - some of the data was missing (Appendix 3.1, 3.2) due to poor microscopy images, and as there is only one value for fold change at each section of the tepal, it is less robust for assessing statistically significant differences between different sections of tepal.

The difference in bud and flower phenotype between Oriental and *L. longiflorum* may be responsible for the differences in differential cell area growth over development observed here between these varieties. Oriental lilies show a large opening movement at the base of the flower to push the tepals apart from each other, as well as a large change in size of the

bud overall between Stages 1 and 5. The epidermal pavement cell area data shown in Figure 3.4A and 3.5A (Section 3.3.3) shows a highly differential growth in pavement cell area between different parts of the tepal. In particular, the larger fold changes in epidermal pavement cell area at the base compared to the middle or top corroborates the phenotype of moving apart at the base of the flower. The differences between the pavement cell area growth comparing the adaxial and abaxial sides are support work carried out in other species as well as in other similar Oriental lily cultivars (Yamada et al. 2009a; Watanabe et al. 2022), as there was a significantly greater change in pavement cell area in adaxial sections compared to adaxial overall. However, this study also adds that there was also a difference in the pavement cell area change between edge and midrib sections, which experimentally supports mathematical predictions previously made (Liang and Mahadevan 2011). The increased growth in edge sections compared to their midrib counterparts in almost every part of the tepal does also suggest that the change from concave to convex tepal shape may also be driven by both changes in adaxial compared to abaxial cell growth but also by edge compared to midrib cell growth. As described by Liang and Mahadevan (2011), this could also be responsible for certain aspects of tepal development, such as the rippling of tepal edges. This study also indicates that the cell area change across the tepal may be explained by differences in flower and variety phenotype. *L. longiflorum* is commercially harvested at much longer bud lengths and the overall change in size of the bud is much smaller prior to opening. The opening process involves a much smaller change in shape, with the trumpet shaped flowers showing high growth in length, particularly in the outer tepal base, but possibly little outward movement at the base due to small fold changes in inner tepal bases. The greatest increase in cell expansion was observed in the inner tepal midsections and top sections, which could be responsible for the smaller opening movement in *L. longiflorum*. This is supported by the much smaller and more uniform increase in epidermal pavement cell area observed here, with the only sections displaying large differences in growth between midrib and edge sections being the outer tepal adaxial base and inner tepal adaxial base and middle. *L. longiflorum* does not typically show rippling at tepal edges which is also an indicator that a strong edge:midrib pavement cell growth difference may not be necessary to cause opening. This is in agreement with the same principles as the shape change in Oriental lilies; both adaxial:abaxial and edge:midrib growth is likely to be responsible for the change in shape from concave to convex.

3.4.4 Is there a significant difference in flower opening regarding cell expansion in commercially treated buds compared to on plant?

Commercial treatment was hypothesised to have an effect on the speed and in some cases even the degree of opening of flowers due to the stress of wounding, water deprivation, temperature and light causing changes to flower opening (Erwin and Heins 1990; Bielecki et al. 2000b; Williamson et al. 2002). The data in Sections 3.3.1 and 3.3.2 also suggest a delay in flower opening in harvested and commercially treated flowers, which may be driven by a potential stress-related slowing of cell expansion in tepals. However, the data shown here show very few significant differences in the pavement cell area growth of on plant compared to commercially treated flowers. Loss of turgor pressure as part of dehydration is a major factor in reducing cell expansion (Tardieu et al. 2014), but this may be balanced by the reduction in transpiration and metabolism due to the cold/dark treatment. The use of three biological replicates and the greater number of cells measured per section in this experiment (20 cells per tepal section as described in Section 3.2.2 compared to 6 cells in the experiment described in Section 3.2.1) may confound differences between the groups due to the high variation observed between biological replicates, even if certain factors were taken more into consideration, such as the position on stem of the buds (only Position A buds were used in the second experiment).

The significantly greater overall increase (Stage 1-5) in several sections of the tepal in commercially treated samples compared to on plant, even if this is not reflected in overall fold change from Stage 1 to Stage 5, may reflect the difference in age of the flower and may indicate that there is some slight cell expansion occurring in sections of the tepal already indicated to grow at higher rates over flower development and opening than others during the cold storage. There is a lack of data regarding whether cut flowers grow significantly during cold storage; some varieties (Oriental cv. Stargazer) show a reduced time for the terminal bud on the inflorescence to open compared to non-cold stored controls, thought to be due to the more advanced age of the stem (Ranwala and Miller 1998).

The rate of epidermal pavement cell expansion was similar in buds on plant and commercially treated apart from in the outer middle edge (OME) tepal region, which showed a significantly lower rate of growth in both treatments. While this reduced growth was over Stages 1-5 in on plant samples, it was only observed between commercially

treated flowers at Stage 3 and 5. This observation may point to this particular tepal region being particularly unchanging in cell size, as a similar drop in cell area was not observed in other tepal regions, as would be expected if the differences were due to biological variation in pavement cell size (all regions of the tepal for one particular tepal at a stage of development were observed for each biological replicate). Section 3.3.3 also shows a very low overall change in this particular tepal region for *L. longiflorum* flowers but notably, not for the unknown Oriental cultivar used, which showed a very high fold change and a particularly fast rate of expansion in this tepal region. Varietal differences may account for the differences observed here; as it has been pointed out in Section 3.4.1, there are distinct differences between Oriental and *L. longiflorum* phenotype. This comparison experiment however was also carried out on an Oriental cultivar very similar to the one used in Section 3.3.3, suggesting that perhaps the small number of cells measured in experiments in Section 3.3.3 (only 6 cells per stage of development and tepal region), which makes the data collected in Section 3.3.4 likely to be more accurate (20 cells were measured for each tepal region). Ideally, repeating the experiment (Section 3.3.4) to include more stages of development observed would help establish if this is a real variation phenomenon or due to the experimental setup.

3.4.5 Does competition on stem outweigh the nutritional benefits of attached vs. detached buds?

The effect of competition on stem was explored here comparing both number of buds per stem (4 or 5 buds per stem), and in a more extreme example, comparing on stem controls to individual flowers. Preliminary experiments in non cold-stored flowers suggested that individual terminal buds would open at lengths much smaller than expected from the same sized buds on stem, which suggested that the competition on stem was responsible for terminal postharvest bud abortion, rather than a developmental immaturity at harvest (Appendix 1). This could either be driven by endogenous signals from other buds on the inflorescence to prevent premature opening of other buds on the stem (negative temporal regulation) or by limited nutrition shared between buds on the same stem. When repeated here with cold-stored buds however, the difference between opening ability of buds attached on stem and individual flowers was significant in the opposite direction to expected. This experiment showed that having a nutritional source from the leaves/ other

buds on the inflorescence did significantly increase the ability of the terminal bud to open, which does support the hypothesis that there may be a nutritional deficiency, as well as a developmental deficiency, partially responsible for the failure to open observed in these terminal buds. The significant difference in opening success of buds from 4 bud stems and 5 bud stems (100% opening vs 50% opening, respectively), even when the range of bud lengths is consistent, also suggests that there is a nutritional basis for postharvest bud abortion, related to competition on stem. However, the lack of statistical power to make these conclusions about the factors significantly affecting the ability of buds to open must be noted, and the results of this experiment need to be interpreted with caution. The size of this study is a limiting factor and in particular the group sizes of buds which did open, which even when SSO and LFO buds were added together was still only three buds altogether. The conclusions made here could be made more confidently by repeating this experiment with a larger sample size.

3.4.6 Conclusions

Harvest and commercial treatments have been found in this study to have little effect on the physical mechanisms of flower opening and a minor impact on the time of opening, which validates the commercial growing, harvesting and transport process in many ways as suitable for the supply chain. While the effects are small due to small group sizes, competition on stem has been identified as a possible factor in the ability to open and therefore may have an impact on other physiological and regulatory elements of flower opening, making it an important factor to be considered and is explored in later chapters.

Chapter 4 - Physiological mechanisms and regulation of flower opening in lilies

4.1 Introduction

Understanding the physiological mechanisms driving flower opening is important in order to recognise differences in these same mechanisms when lily stems are under stressful and nutrient-deprived conditions, such as postharvest commercially treated stems. This chapter will focus on the effect of carbohydrate mobilisation and metabolism as part of the physiology of flower opening.

4.1.1 Role of carbohydrates in flower development and opening

Being a highly energetic biological process, flower opening is well regulated to ensure the least wastage of energy and the greatest chance of pollination (van Doorn and Kamdee 2014). The regulation of sucrose uptake and starch breakdown, and in particular in relation to competition between flowers on the stem, is therefore a promising area of study and may lead to strategies to improve flower opening and quality. Sugar uptake from photosynthetic tissue in the leaves or, in a commercial setting, from the vase medium, has been shown to have a role in opening and longevity of lily flowers, potentially by repressing senescence-associated changes in tepals such as expression of starch and protein breakdown-related genes (Doorn 2004). There is a positive correlation between lily bud development (length) and tepal sucrose content, with the opening flower containing the most sugars. Glucose, fructose and sucrose make up the majority of these sugars (Van der Meulen-Muisers et al. 2001). Supplementing LA hybrid lilies (cv. Courier) with additional 1% sucrose accelerated flower opening by 2.4 days on average and delayed senescence by 1 day (Arrom and Munné-Bosch 2012), while addition of 2% sucrose in the vase solution of Oriental lilies (cv. Stargazer) was found to slightly improve opening of flowers compared to controls in 0% sucrose (some controls could not complete full opening and remained partially closed - (Han 2003). However, the timing of opening was not changed in Oriental lilies, which suggests that different varieties may have different responses to exogenous sucrose.

Oriental lily tepals show an initial high starch content in immature buds, which is gradually lost throughout development and flower opening. Fully open cut Asiatic lily flowers have no discernible starch based on Lugol staining, implying that starch breakdown is highly important for opening, and additionally, treatment of excised Asiatic tepal segments with the starch breakdown inhibitors phosphoglyceric acid (PGA) and α -amylase inhibitor protein (AIP) caused a reduction in growth of the tepal segments compared to controls (Bieleski et al. 2000a). The relative activities of α -amylase and starch synthases (carrying out the antagonistic function to amylases) may therefore have an important role in flower opening. The production and breakdown of starch has been shown in *A. thaliana* to move transiently from state to state within sink organs such as flowers as required by the use of different tissue types during their development (Hedhly et al. 2016). Therefore, regulation of starch production and turnover in petal cells may similarly be essential in lilies to maintain a nutritional store for respiration and a suitable cellular osmotic strength depending on the developmental stage. Starch metabolism needs to be coordinated with sucrose uptake, respiration, and secondary metabolism to ensure homeostasis of sugars in the cell. This coordination has also been observed in the increased expression of genes relating to sucrose, hexose phosphate and starch metabolism in *A. thaliana* flowers during pollen development (Hedhly et al. 2016), implying levels of sucrose or glucose may act as a signal or feedback mechanism to favour catabolism or anabolism of starch levels.

4.1.2 Carbohydrate partitioning and competition on stem

It is important to note that in both on-plant and commercially treated lily flowers, the changes in sucrose and starch content of the bud over development and opening do not exist in a vacuum – i.e. they are highly influenced by the other buds on the same stem. This dynamic movement of carbohydrates from bud to bud helps to maintain an energy balance and share nutrients in an appropriate way between buds at different stages of development. The development of pollen in *Lilium* flowers for example requires high levels of photoassimilates during the anther growth phase but during the anther maturation stage this requirement is much lower (Clément et al. 1994; Clement et al. 1996).

Phloem loading and unloading is an important regulatory step which can influence the sucrose and starch content throughout development of flower buds. There are three main

mechanisms for phloem loading in plants, which are used differentially by species depending on their physiology and sucrose needs, and may be interchanged flexibly depending on the environment (Figure 4.1). Apoplastic phloem loading involves active uptake of sucrose from the apoplast by active transport, while symplastic loading is driven by creating a high sucrose gradient from mesophyll to phloem. Symplastic loading is further split into two types: with and without polymer trapping. Polymer trapping is a process when specialised cells that are part of the phloem convert sucrose to larger oligosaccharides, trapping them in the phloem (Rennie and Turgeon 2009). Sink organs compete for photoassimilates generated by the source organs, and take photoassimilates from the phloem as a function of their sink strength. This can be defined as an ability to produce a strong photoassimilate gradient at sink organs, either due to rapid cellular uptake or breakdown of compounds (Lemoine et al. 2013). Developing lily buds are strong sinks for sugars and those under 60mm in length can exert a pull on sugars and metabolites from larger buds on the stem, limiting their growth and often causing earlier senescence (Van der Meulen-Muisers et al. 2001). This is supported by the fact that many growers often remove some buds from a stem in order to make the remainder larger (Van Meeteren et al. 2001). Differences in loading strategies may be caused by plasticity in the type of loading used by different buds over development, depending on their sink strengths. Phloem loading and unloading is therefore an essential regulatory point for establishing priority of specific sink organs over others (Lemoine et al. 2013). Models for phloem loading suggest there is a complex interaction between the maintenance metabolic need of the organ, and its proportional sink strength, which determines the access the flower has to sucrose uptake (Van Meeteren et al. 2001). This is also strongly impacted by environmental factors such as drought, mineral deficiency, light levels, temperature and pathogens (Lemoine et al. 2013). Expression of sucrose mobilisation- and metabolism-related genes will therefore have a large impact on the type of phloem loading and the modulation of sucrose uptake by plant organs (Figure 4.1). SWEET transporters are highly expressed in *Arabidopsis thaliana* as a vital part of phloem unloading, and act to move sucrose from phloem cells into companion cells and the apoplast, ready to be taken up by sink cells as needed (Durand et al. 2018). Invertases may also have an important role in this sugar uptake from the phloem. Cell wall invertases (CWINVs) have a role in breakdown of sucrose from the phloem in the

extracellular matrix, which can be taken up into cells by hexose transporters (HXTs) and monosaccharide transporters (MSTs). Vacuolar and cytoplasmic invertases (VINVs, CINVs) have also been implicated as having a role in cell expansion for many species such as potato, carrot, and maize, through changing the osmotic pressure of root and ovary cells, changing cell wall flexibility, and through the effect of glucose on auxin-mediated signalling (Ruan et al. 2010). In *A. thaliana*, genes coding for sucrose synthases (that catalyse the breakdown of sucrose to UDP-glucose and fructose), β -glucosidases (that degrade cellulose to glucose often as a signalling molecule) are both essential for starch and cellulose biosynthesis, and importantly, remove/add intracellular sucrose from/to the cytosolic pool as required to adjust the rate of sucrose uptake by the cell. Additionally, sucrose phosphate synthases (SPSs) catalyse the production of sucrose and are the counterpart to sucrose synthases (SUSs) in source leaves, but in sink tissues it has been proposed they ensure a negative feedback loop of sucrose synthesis/breakdown and therefore an easily modulated homeostasis of cell sucrose levels (Argüello-astorga et al. 2017).

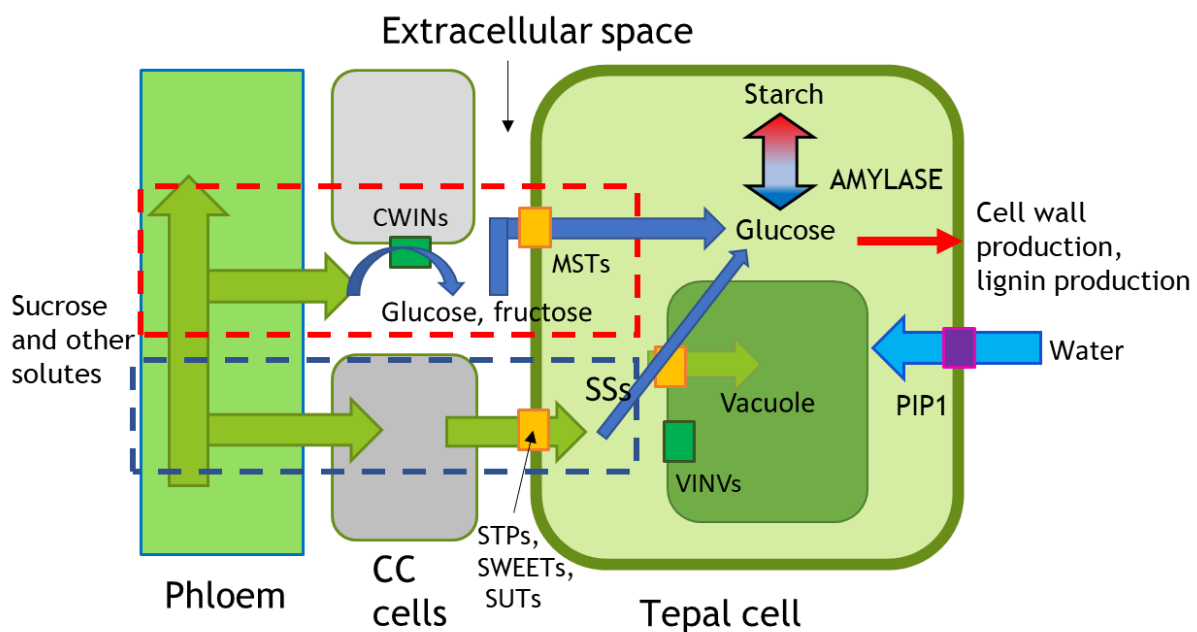


Figure 4.1 – diagram to illustrate the two main phloem loading strategies (symplastic and apoplastic). Symplastic strategies (outlined in blue dashed line) show the movement of sucrose from the phloem into companion cells (CC) and then into tepal cells via sucrose transporter proteins (STPs/ SUTs) and Sugars Will Eventually be Exported transporters (SWEETs), entering the cell as sucrose. This can go on to be broken down into

monosaccharides by the action of enzymes such as sucrose synthases (SSs) or taken up into the vacuole and broken down there by vacuolar invertases (VINVs). Apoplastic strategies (outlined in red dashed line) are the conversion of sucrose into monosaccharides in the extracellular space by cell wall invertases (CWINVs) and uptake into tepal cells by hexose/monosaccharide transporters (HXTs/ MSTs). Monosaccharides produced by both of these strategies can cause cell expansion by increasing osmotic pressure in the cell or be used in lignin and cell wall production. Diagram produced using information from (Ruan et al. 2010; Lemoine et al. 2013; Ruan 2014; Durand et al. 2018).

4.1.3 Effect of commercial treatment on nutrient availability in flower buds

Commercial treatment has been shown to cause problems with flower opening - growers and consumers reference the failure of the youngest buds on the stem to bloom (especially on varieties with more than four blooms per stem) only when commercially treated, leading to customer dissatisfaction (personal communication, James Cole). This failure to bloom has been strongly linked to nutrient competition between buds on the stem exacerbated by insufficient nutrition (Van Doorn and Van Meeteren 2003) and low-light conditions during transport, storage and after being sold. Low light conditions can be responsible for severely restricting photosynthesis of buds, presumably at least partially responsible for minimal growth in terms of tepal length and 'absolute growth' once harvested (Van der Meulen-Muisers et al. 2001). Moreover, cut lilies have a naturally shorter lifespan than on plant (7.7 days on average), which may be due to an accelerated senescence due to limited nutrition (Arrom and Munné-Bosch 2012) and microbial overgrowth causing xylem occlusion and concomitant water relation issues (Nemati et al. 2014). Commercial stems are often supplemented with sucrose to aid in opening of all buds on the stem and improve longevity of the bouquet (Van Meeteren et al. 2001, Han 2003), however this has been shown in some studies to be insufficient. Certain varieties respond well to exogenous sucrose supplementation – in Oriental lily cv. Rialto additional nutrition in the form of Chrysal Professional or Floralife 200 improved longevity and reduced leaf chlorosis slightly compared to controls (Rabiza-Świder et al. 2015), however, in Oriental lily cv. Stargazer, Han (2003) reported additional 2% sucrose in vase water as having a negligible effect on

opening, longevity, or bud size, rather citing improvements in tepal colour. Sucrose pulsing alongside STS was found to improve flower longevity by two to three days in lilies, potentially by improving bud water uptake (Bích and Nhung 2020).

Therefore, supplementation with sucrose may be limited in its effectiveness dependent on variety and specific treatment. Additionally, too much sucrose may cause microbial overgrowth of the vase water stems are maintained in. Physical microbial blockage and enzymatic damage to the xylem vessels supplying the buds with water can lead to failure to open or early senescence (Vehniwal and Abbey 2019). Supplementing with sugars may have other negative effects, for example to the hormone balance (Arrom and Munné-Bosch 2012). High sucrose concentrations in vase solutions have been reported to cause leaf chlorosis and in extreme examples, leaf blackening, which is thought to occur from sucrose's osmotic effects on leaf tissue (Han 2003). This suggests that even in cases where it may be beneficial to the flower buds, sucrose may have a concomitant negative impact on the foliage, another important aspect of overall stem quality.

Cold/dark treatment is very commonly used in commercial treatment of fresh-cut fruit, vegetables and flowers to slow metabolism, lower respiration rate, and therefore retain product quality for longer periods of time (Galati et al. 2020). This treatment is also partially continued during transport where stems are transported dry in boxes, largely minimising light. Dry transport therefore also causes additional dehydration of the buds, which has been shown to exacerbate cold stress effects and reduce the longevity of cut flowers (Rudnicki et al. 1991; Wagstaff et al. 2010). Cold/dark treatment may also have its drawbacks, especially when carried out for long periods; potted Oriental lilies were found to have accelerated leaf chlorosis and abscission when stored at ~1°C in darkness for 2 weeks (Ranwala and Miller 2005). Cold and dehydration stress was found to upregulate the expression of genes related to stress and senescence coding for metallothioneins and remobilisation/proteolytic enzymes in cut *Alstroemeria* flowers (Wagstaff et al. 2010). Therefore, treatments to ameliorate the side effects of cold/dark treatment and transport are of great interest to the commercial cut flower industry.

4.1.4 Effect of position on stem on nutrient availability in flower buds

Competition on stem has been hypothesised to exert a significant effect on nutrient partitioning and therefore flower opening. The effect of position on stem should also be considered, particularly in a commercial context. On a single stem, every bud may be at a different stage of development from Stage 1 at the top of the stem to between Stage 2 to Stage 5 at the bottom (Section 2.2). The effects of nutrient deprivation when harvested will therefore affect buds on a stem differentially dependent on their respective stages of development, which may cause differences in phloem loading and sink strength of the organ. Additionally, bud length at harvest is often proportional to flower longevity in Asiatic cultivars. Asiatic lilies also maintained higher levels of sucrose, glucose and fructose in their tepals for longer when detached from the stem compared to on the inflorescence. This was hypothesised to be part of the recycling process to ensure energy redistribution within the stem (Van der Meulen-Muisers et al. 2001). Competition between buds on the same cut stem may also exert pressure on the starch reserves in the same way as for sucrose. This is supported by a study showing that lily stems grown in low light conditions (another form of nutrient limitation) had increased dry mass of remaining buds when some were removed (Van Meeteren et al. 2001).

The regulation of phloem loading or unloading will be explored here, looking at physiological effects of competition on endogenous and exogenous sucrose uptake, as well as looking at the changes in gene expression relating to sucrose mobilisation/metabolism during development and opening.

4.1.5 Aims of investigation

1. Elucidating the changes in tepal carbohydrate content within the tepal over development and flower opening
2. Understanding the effect of commercial treatment on the changes in tepal carbohydrate content over development and flower opening
3. Understanding the physiological effects of position on stem on tepal carbohydrate content
4. Elucidating the genetic mechanisms behind sucrose uptake and starch breakdown

4.2 Materials and methods

4.2.1 Qualitative tepal starch stain using Lugol solution comparing on plant and commercially treated flowers

In a preliminary experiment, Oriental lily cv. 'Tisento' was grown in Cardiff University greenhouse conditions as described in Section 2.1.1.1 and harvest and commercial treatment was simulated as described in Section 2.1.2.2. Samples were taken at each stage of development (Stages 1-5 - Section 2.2), photographed, and then stained for starch as described below.

Oriental varieties cv. Ascot and Tisento and LA hybrid cv. Eyeliner were grown in E.M. Cole Farms Ltd. greenhouse conditions as described in Section 2.1.1.2. 'On plant' samples were harvested at Stages 1, 3, and 5 as described in Section 1.2. Commercially treated samples were also treated as described in Section 2.1.2.1. Flowers from Position A on stem were harvested at Stages 1, 3 and 5 for both groups. For 'Tisento', flowers from Position C/D were also harvested in the same way as a comparison.

For all varieties, three individual flowers were taken from each stage for three biological replicates. One inner and one outer tepal from each flower were immediately submerged in hot 80% ethanol and incubated at 80°C for 30 minutes. Tepals were rinsed in dH₂O and incubated in Lugol solution (Sigma-Aldrich, London) at room temperature for 15 minutes. Tepals were rinsed in dH₂O again and photographed.

4.2.2 Experimental setup for investigation of sugar and starch metabolism in lilies

Oriental lily cv. Ascot was grown in commercial greenhouse conditions as described in Section 2.6. On plant (OP) and commercially treated (CT) samples were also treated as described in Section 2.6. Flowers from position A and C on stem were harvested at Stages 1, 3 and 5 for both groups (Figure 4.2A+B). Tepals from each flower were split into midrib and edge sections (Figure 4.2C) and flash frozen in liquid nitrogen before being stored at -80°C. Frozen material was fragmented by pestle and mortar under liquid nitrogen prior to use.

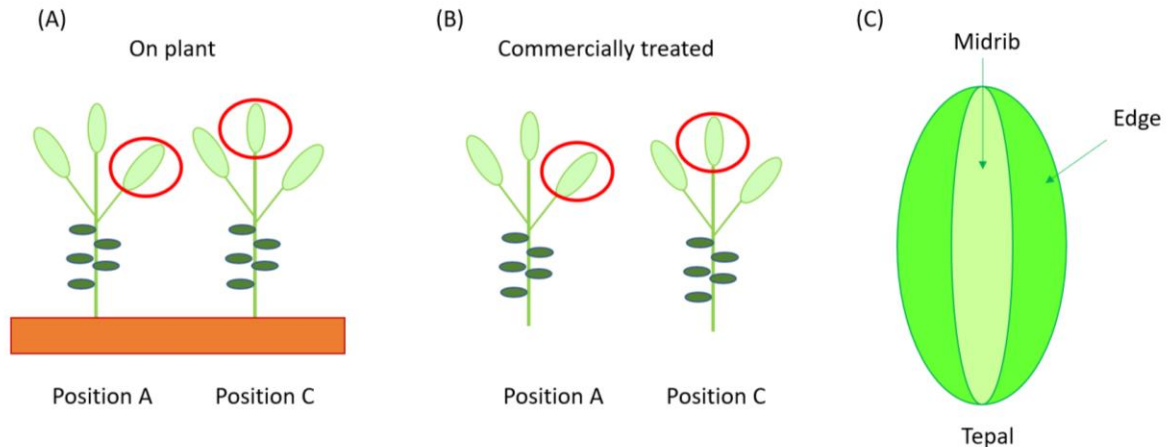


Figure 4.2 – sample collection method of tepals for the experiments described in Section 4.2.2.1 and 4.2.2.2. Buds were collected from either (A) whole plants grown in soil or (B) commercially treated stems, with Position A and Position C buds sampled from each treatment group (three biological replicates). All tepals were split into (C) Midrib and edge sections with a clean scalpel and immediately flash frozen in liquid nitrogen.

4.2.2.1 Quantitative starch assay using an enzymatic method

A protocol to extract starch from plant material was adapted from Smith and Zeeman (2012). Fragmented frozen material (150 mg) was weighed into 15 ml Falcon™ tubes. Soluble sugars were extracted from the material three times - 80% ethanol (5 ml) was added to the tubes, material was incubated in a 100°C waterbath for three minutes, and then centrifuged at 8000 g for five minutes before the supernatant was removed by pouring off. The insoluble pellet was allowed to fully air dry before it was thoroughly ground by pestle and mortar with 5 ml dH₂O. The suspension was mixed well by pipetting and 0.5 ml of each sample was pipetted into four tightly closing tubes (1.5 ml screw top microcentrifuge tubes, Starlab). These tubes were incubated for 30 minutes in a 100°C waterbath and then autoclaved to gelatinize starch particles. Breakdown of starch granules was confirmed with 20 µl of one sample per extraction by adding Lugol solution (Sigma-Aldrich, London) to stain for starch and visually identifying breakdown of granules by light microscopy (bScope BS.1153-EPLi (Euromex)). Post gelatinization, 0.5 ml of 200 mM sodium acetate (pH 4.8) was added to each tube. Amylase (0.5 units, Sigma-Aldrich) and 3 units of amyloglucosidase

(Sigma-Aldrich) were added to two tubes (positive samples), and to another two tubes an equal volume of dH₂O was added instead (control samples). Samples were incubated for four hours at 37°C and stored at -80°C until required. Samples were thawed and centrifuged at 13,000 g for 5 minutes to pellet insoluble material and the supernatant was used in further assays.

An enzymatic assay for the released glucose was then carried out on the samples. Within 24 hours of the assay, 100 mM 4-(2-hydroxyethyl)-1-piperazineethanesulfonic acid (HEPES) buffer with 5 mM MgCl₂ (pH 7.5) was prepared and used to dilute the enzymatic reagents. Adenosine 5'-triphosphate (ATP, 100 mM) and β-Nicotinamide adenine dinucleotide (NAD, 40 mM) were also prepared using the HEPES buffer as solute. Hexokinase (1500 U/ml) and glucose-6-phosphate dehydrogenase (G-6-PDH, 1000 U/ml) were diluted 1:30 and 1:20 respectively in HEPES buffer. The following was pipetted into each well of a 96 well plate: 200 μl HEPES buffer, 10 μl NAD, 10 μl ATP, 10 μl G-6-PDH diluted 1:20, 10 μl starch extract sample. Optical density (OD) was first measured at 340 nm without hexokinase using a spectrophotometer (Clariostar) and taken as the pre-hexokinase value for each well. Hexokinase diluted 1:30 in HEPES (10 μl) was pipetted into each well and mixed by pipetting up and down several times. The OD was measured again at 340 nm over 15 minutes and the OD at the earliest time where no further change in values occurred was taken as the post-hexokinase value.

The glucose content per cuvette was calculated by taking the change in OD from pre- to post-hexokinase addition divided by the millimolar extinction coefficient of NADH at 340 nm in a 1 cm width cuvette (6.22). The average value for glucose content in control samples (those without addition of amylase and amyloglucosidase) was subtracted from the average glucose content of positive samples (with enzymes added) for the change in glucose content arising purely from starch breakdown per cuvette. Mmol glucose equivalents g⁻¹ fresh weight (FW) were calculated by dividing the change in glucose content per cuvette by the volume of incubation assayed (10 μl), multiplying by two, and multiplying by (5 ml/0.2 g). The starch content (expressed here as mg starch g⁻¹ FW) was calculated by multiplying the mmol glucose equivalents g⁻¹ FW by the mass of anhydroglucose (162).

Statistical analysis was performed to evaluate differences between:

1. Tepal midrib and edge tepal starch content across Stages 1, 3 and 5
2. OP and CT tepal starch content across Stages 1, 3 and 5
3. Position A and Position C tepal starch content across Stages 1, 3 and 5

These differences were evaluated using one way ANOVA and post hoc Tukey test for the first two comparisons and using an independent T-test/ Mann-Whitney U test for the last comparison. All statistical analyses were carried out in RStudio (version 1.3.1093).

4.2.2.2 Metabolite fingerprinting and quantitative sugar analysis by flow injection electrospray high resolution mass spectrometry (FIE-HRMS) and gas chromatography- time of flight mass spectrometry (GC-tofMS)

The following section was carried out by Dr Manfred Beckmann (Aberystwyth University), unless stated otherwise. The same lily tepal material from the previous sections (Section 4.2.2) was used in this experiment. Fragmented material was weighed into 2ml microcentrifuge tubes (50 mg) and delivered to Aberystwyth University, where metabolites were extracted using chloroform/methanol/water (1:3:1). Supernatant from the extraction was used in further analysis.

Flow injection electrospray high resolution mass spectroscopy (FIE-HRMS) was carried out on an Exactive HCD mass analyser linked to an Accela UHPLC system (Thermo-Scientific) which produced metabolite fingerprints in positive and negative ionisation mode in a single run. Supernatant extract (60 μ l) was directly injected to a flow of 100 μ l min⁻¹ methanol: water (70: 30, v/v). Ion intensities were measured between 50 and 1000 m/z for at a resolution setting of 100,000 (at m/z 200) – resulting in 3 (\pm) ppm mass accuracy for 3.5 mins. ESI source parameters were set according to the manufacturer's recommendations. Raw files were exported as CDF-files, mass aligned and centroided in MATLAB (V8.2.0, The MathWorks). Mass spectra around the apex of the infusion peak were combined in a single intensity matrix for each ion mode. Data from the intensity matrix was log-transformed before further statistical analysis. Data mining and feature selection was performed using Random Forest in R package FIEms-pro as reported previously (Enot et al. 2008).

This following section was completed by myself (Rakhee Dhorajiwala). Data analysis of full profiles from FIE-HRMS was carried out using PerMANOVA, Canonical Analysis of Principal component (CAP) analysis, and Random Forest in RStudio (randomForest, vegan packages,

RStudio version 1.3.1093 (Liaw and Wiener 2002; Oksanen et al. 2022) to identify significant differences between whole metabolic profiles (Breiman 2001; Anderson and Willis 2003). Compounds which were most important in the classifications for each of the Random Forest analyses were putatively identified using the DIMEdb database (<https://dimedb.ibers.aber.ac.uk/search/mass>) using the m/z ratio and ionisation type, as well as the ion type information if available for each compound (O'Shea et al. 2018). The compounds suggested by the database were screened for accuracy to the measured m/z ratio and for reasonable presence in plant tissue, and the most likely candidate was taken as the 'putatively identified compound'. As this was an imprecise method, the chemical class(es) of the suggested compounds was more generally noted rather than specific compounds.

Gas chromatography- time of flight mass spectrometry (GC-tofMS) was also carried out by Dr Manfred Beckmann using the same material to identify glucose, fructose and sucrose content, alongside other selected compounds. Supernatant extract (5 μ l) and 5, 20 and 30 μ l of the carbohydrate standards were used. An internal standard (25 μ l L-threo-tert-butylserine) was added and carbonyl moieties of metabolites were protected by methoximation using 10 μ l 20 mg ml⁻¹ solution of methoxyamine hydrochloride (Fluka) at 30°C for 90 mins. Acidic protons were then derivatised with 20 μ l N-methyl-N-trimethylsilyltrifluoride (MSTFA, M and N) at 37°C for 30 mins. Derivatised material (1 μ l) was injected split-less into a Leco Pegasus III GC-tofMS (St. Joseph, USA) – comprising a Focus autosampler (Anatune), Agilent 6890N gas chromatograph equipped with DB5-MS column (20 m x 0.25 mm ID x 0.25 μ m film). An injector temperature of 250°C was used, transferline of 260°C and ion source temperature of 230°C. The helium flow rate was 1.4 ml min⁻¹. After 1 min at 80°C, oven temperature was increased by 30°C min⁻¹ to 330°C, held at 330°C for 3 min and cooled to 80°C. Automated deconvolution and peak finding was performed using ChromaTof software (Leco, St. Joseph, USA) and peak alignment was carried out in MATLAB (V7.5.0, The MathWorks).

This following section was completed by myself (Rakhee Dhorajiwala). Data analysis of full profiles was carried out using Permanova, Canonical Analysis of Principal component (CAP) analysis, and Random Forest in RStudio (version 1.3.1093). Statistical analysis of differences in individual tepal sugar content (glucose (two anomers), fructose (two anomers), sucrose

(one isomer)) was carried out using the area under the peak measurements from GC-MS data, using the peaks at retention times confirmed by internal standards of fructose, glucose and sucrose.

Statistical analysis was performed to evaluate differences between:

1. Tepal midrib and edge glucose, fructose and sucrose content across Stages 1, 3 and 5
2. OP and CT tepal glucose, fructose and sucrose content across Stages 1, 3 and 5
3. Position A and Position C tepal glucose, fructose and sucrose content across Stages 1, 3 and 5

These differences were evaluated using one way ANOVA and post hoc Tukey test in RStudio (version 1.3.1093). If necessary datasets were \log^{10} transformed to ensure they met the conditions of the statistical test.

4.2.3 Relative expression analysis of cell expansion-related genes across flower opening using qPCR

Oriental lily cv. Tisento was grown by E.M. Cole Farms Ltd. in E.M. Cole Farms Ltd. greenhouse conditions (Section 2.1.1.2) and harvested with commercial treatment as described in Section 2.1.2.1. Stems were maintained in Cardiff University growth room conditions (Section 2.1.3) until required. Tepal material from one individual flower per biological replicate, with three biological replicates for each stage of development (Stages 1-5, described in Section 2.2), were flash frozen in liquid nitrogen and stored at -80°C . RNA was extracted from this material as described in Section 2.6.3. The quality of extracted RNA was assessed as described in Section 2.6.5. DNase treatment was carried out using the Turbo DNA-free kit (Invitrogen) and checked for efficacy by PCR as described in Section 2.7. cDNA was synthesised from DNased RNA using the GoScript™ Reverse Transcription kit with Oligo-dT (Promega) and checked for efficacy by PCR as described in Section 2.8.

qPCR was used (as described in Section 2.9.4) to measure the relative expression of the putatively identified genes related to flower opening listed below in Table 4.1. Primers designed for qPCR of these genes can be found in Table 2.2.

Table 4.1 – putatively identified genes targeted for qPCR analysis as having a role in tepal cell expansion and flower opening

Putative gene name	ENCODES	FUNCTION
AMY2	A-amylase	Enzyme which hydrolyses alpha bonds between monomers of starch in plants, producing glucose, dextrans, and maltose (Beck and Ziegler 1989).
CWINV4	Cell wall invertase 4	Cell wall-localising protein with hydrolytic activity breaks down sucrose into glucose and fructose in the extracellular matrix. Important for carbohydrate partitioning by removing sucrose from the phloem (Sherson et al. 2003).
EXPA2	A-expansin 2	Extracellular protein causing disruption of non-covalent bonds between cellulose microfibrils and matrix glucans in cell walls, allowing cell growth and expansion (Marowa et al. 2016).
MST6	Monosaccharide transporter 6	Plasma membrane monosaccharide transporter (Wang et al. 2008).
PIP1	Plasma membrane Intrinsic Protein 1	Plasma membrane aquaporin (Tong et al. 2013).
SUT2	Sucrose transporter 2	Plasma membrane sucrose/H ⁺ symporter (Hu et al. 2021).
SUT4	Sucrose transporter 4	Vacuolar sucrose/H ⁺ antiporter (Hu et al. 2021).
SWEET7	Sugars Will Eventually be Exported Transporter 7	Membrane bidirectional sucrose transporter (Ji et al. 2022).
XTH2	Xyloglucan endotransglycosylase/hydrolase 2	Enzyme catalysing endohydrolysis or endotransglycosylation of xyloglucans in the extracellular matrix to facilitate cell growth (Eklöf and Brumer 2010).

Relative expression of these genes was measured at Stages 1-5 in commercially treated 'Tisento' tepals as described in Section 2.9.4. A one-way ANOVA or Kruskal-Wallis statistical test was used as appropriate to identify significant differences in relative gene expression between conditions.

4.3 Results

4.3.1 Loss of tepal starch and concomitant gain of tepal glucose, fructose and sucrose supports tepal edge vs. midrib differential growth theory of flower opening in Oriental lilies

Total tepal starch content in Oriental lily cv. Ascot was significantly higher in edge than in midrib samples at Stages 1 and 3 (before opening), before significantly decreasing between Stages 3 and 5 for both edge and midrib samples (Figure 4.2A, Appendix 6.10).

In comparison, 'Ascot' tepal sucrose and glucose (only one isomer was shown here as it is representative of both) increased significantly over time between Stages 3 and 5.

Sucrose content was significantly higher in midrib sections than edge at Stage 5 (Figure 4.2B), whereas glucose content for both isomers showed no significant differences between edge and midrib sections (Figure 4.2C). However, at Stage 5 glucose content was slightly but not significantly higher in edge compared to midrib samples, showing differences in the types of sugar found in different areas of the tepal. Due to significant differences between midrib and edge starch and sucrose content (Figure 4.2A, B), tepal edge and midrib samples were compared separately in the following sections 4.3.3, 4.3.4 and 4.3.5.

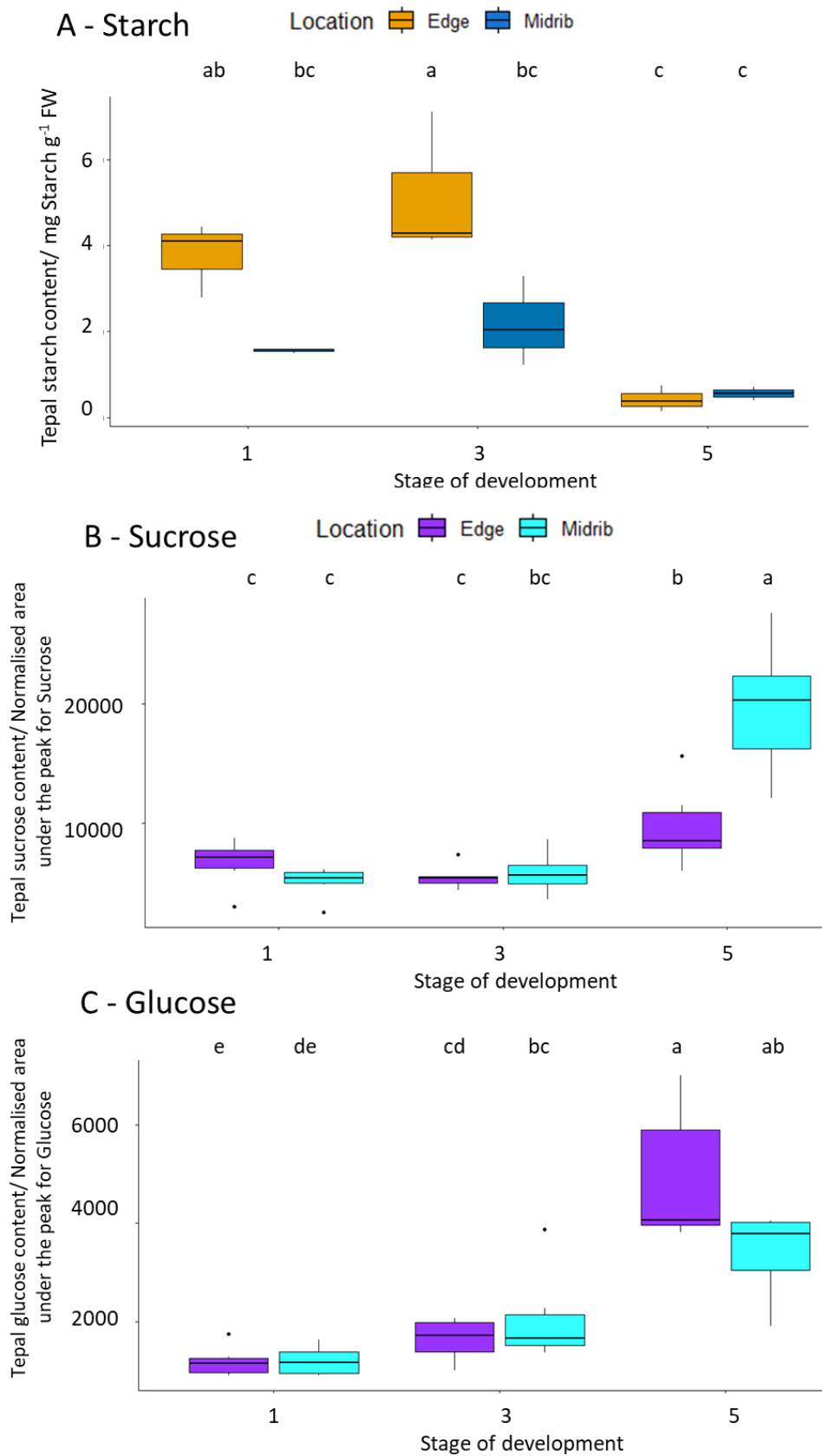


Figure 4.3 – Tepal (A) starch, (B) sucrose and (C) glucose content over flower opening, comparing content in edge vs. midrib sections. Starch was assayed using an enzymatic

assay. Glucose and Fructose were measured using gas chromatography-mass spectrometry analysis as normalised area integrations for relative content comparison. Letters indicate results of the two way ANOVA with Post-hoc Tukey carried out.

4.3.2 Additive effect of commercial treatment and position on stem on starch staining in tepals

Staining for starch was carried out in a preliminary experiment on Oriental lily cv. 'Tisento' over development and opening grown on plant at Cardiff University. Qualitative starch staining was strong between Stages 1 and 3, and then visibly decreased in tepals between Stages 3 and 4. Stage 5 tepals showed the least starch staining, indicating very little starch in open flowers compared to closed buds.

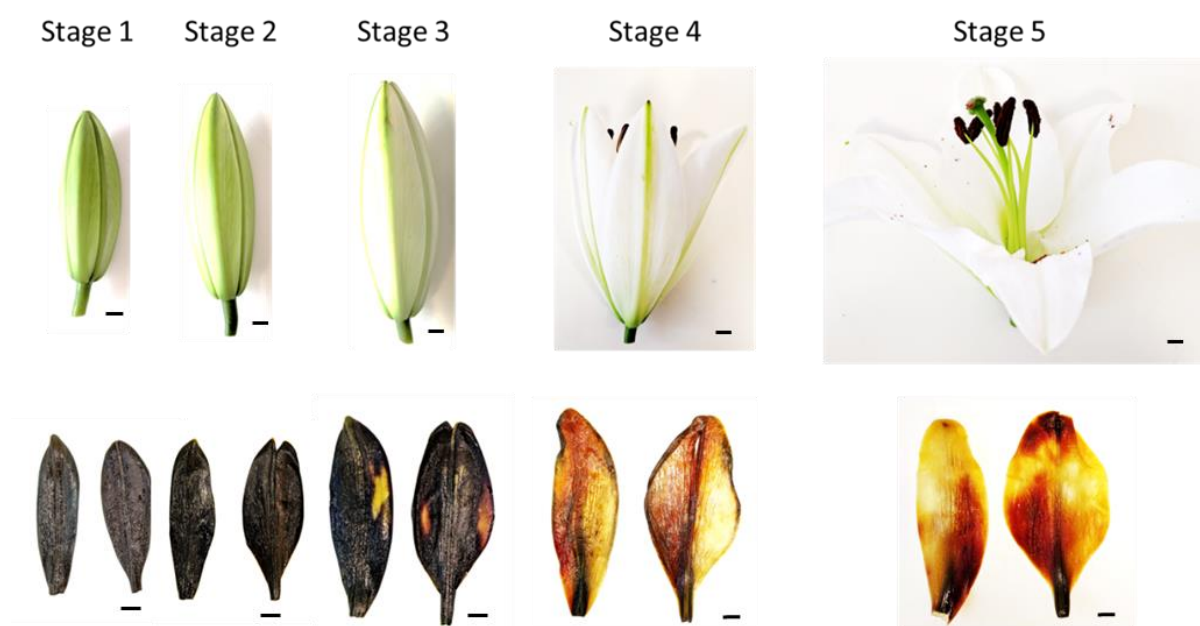


Figure 4.4 – Loss in tepal starch over Oriental lily (cv. 'Tisento') development and opening on plant. Tepals from flowers at the stages of development indicated (Stages 1-5, described in detail in Section 2.2) were stained for starch using Lugol solution (method described in Section 4.2.1). Scalebars represent 1 cm.

The Lugol staining in tepals indicating presence of starch was lost over development between Stages 3 and 5 for all three varieties ('Tisento', 'Ascot' and 'Eyeliner') regardless

of treatment or position on stem. Tepals from 'Tisento' (Figure 4.5A) and 'Eyeliner' (Figure 4.5C) on plant at Position A still showed some reduced staining at Stage 5, particularly retained around the edge of the tepals, while 'Ascot' (Figure 4.5B) showed negligible staining at Stage 5 but was otherwise similar to the other two varieties. Commercially treated Position A tepals from all varieties showed slightly less staining at Stage 3 compared to on plant flowers and a complete absence of staining in Stage 5 tepals.

Tepals from 'Tisento' on plant at Position C/D however showed a similar appearance to 'Tisento' on plant tepals at Position A at Stages 1 and 3; however at Stage 5 the staining was completely absent in Position C/D tepals (Figure 4.5A). Tepals from 'Tisento' which were both commercially treated and from flowers at Position C/D displayed an additive effect on the staining - tepals at Stage 1 and 3 had visibly less staining than any of the other groups at Stage 1 and 3 respectively, and also had no visible staining in Stage 5. While on plant samples were missing from Position C/D buds in 'Ascot' and 'Eyeliner' due to lack of material, the Stage 1 tepals were shown here to illustrate that they had the same visible staining at Stage 1 as Stage 1 commercially treated tepals from the same position on stem. Commercially treated Position C buds for both 'Ascot' and 'Eyeliner' show much less staining at Stage 1 and 3 than Position A buds at the same stages of development, which is a similar pattern to 'Tisento'.

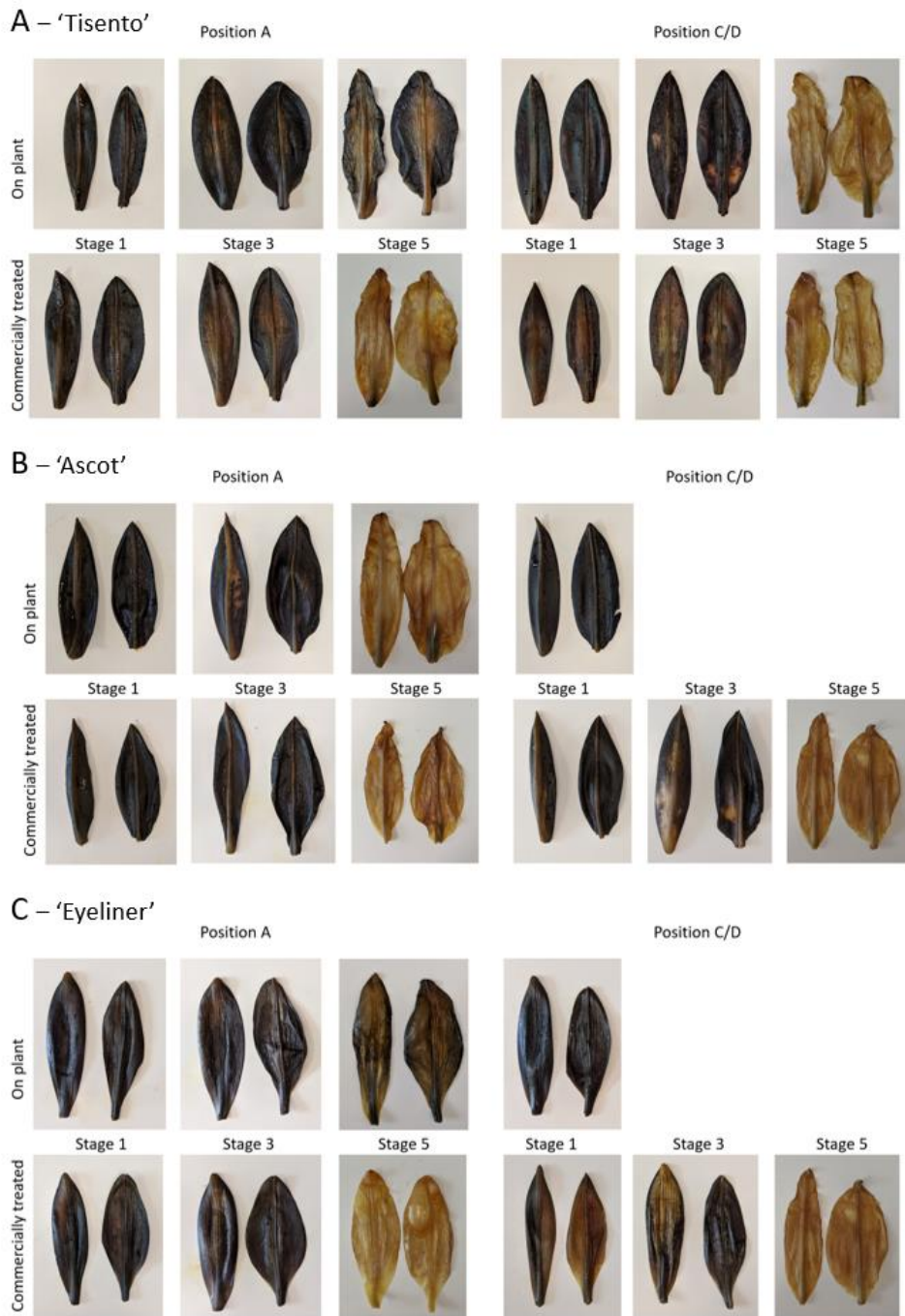


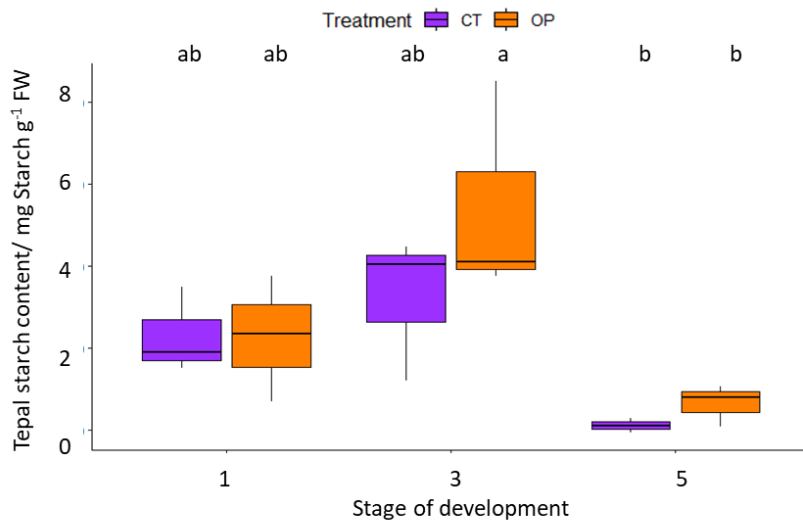
Figure 4.5 – Qualitative starch Lugol stain to show the effect of position on stem and commercial treatment on starch content over development for (A) Oriental lily Tisento (B) Oriental lily Ascot and (C) LA hybrid lily Eyeliner.

4.3.3 Effects of commercial treatment and position on stem on tepal starch content

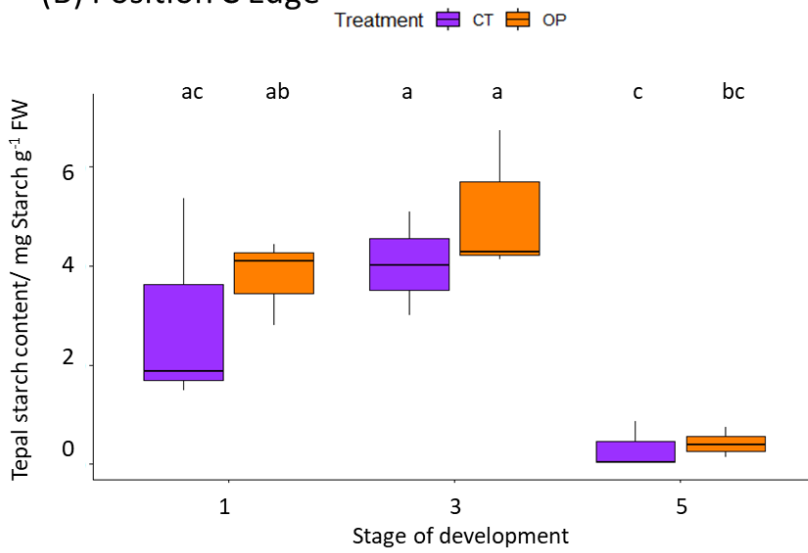
Oriental 'Ascot' tepal starch content was maintained from Stage 1 to Stage 3 and then decreased to below the amount in Stage 1 from Stage 3 to 5 regardless of location on tepal, position on stem or commercial treatment (Figure 4.6). While there are significant differences between stages of development (Appendix 6.11), particularly between Stages 3 and 5, there is only a significant difference between OP and CT tepal starch content at Stage 3 in Position A Midrib samples (Figure 4.6C), where OP starch content is significantly higher.

Comparing position on stem showed no significant differences between Position A and C tepal starch content in tepal Edge samples (Table 4.2). However, Midrib samples showed significant differences at Stage 1 in OP tepals, showing significantly more starch in Position C tepals than Position A tepals (Table 4.3). CT tepal midribs showed a similar pattern, with slightly more starch in Position C tepals at Stage 1 and significantly more starch in Position C tepals at Stage 3 than their Position A counterparts (Figure 4.7D). This suggests commercial treatment may affect starch content and metabolism in tepal midribs in terms of partitioning between different buds on the same stem.

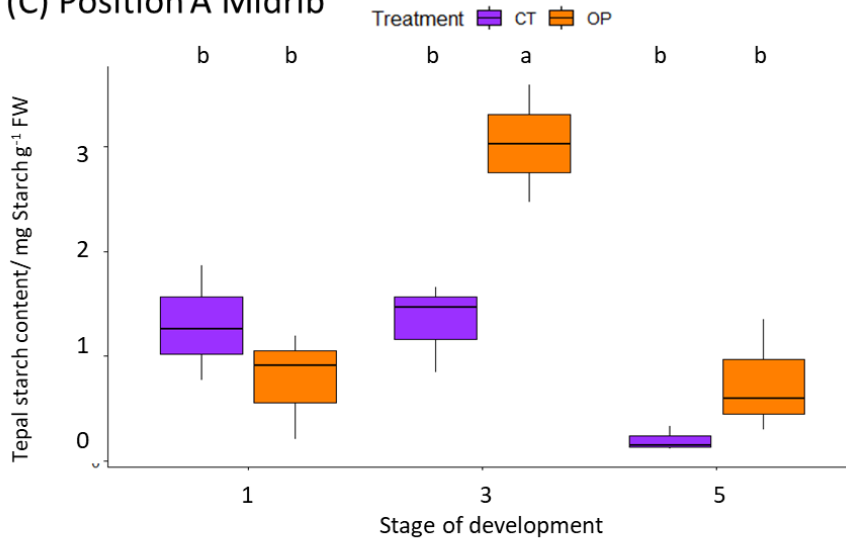
(A) Position A Edge



(B) Position C Edge



(C) Position A Midrib



(D) Position C Midrib

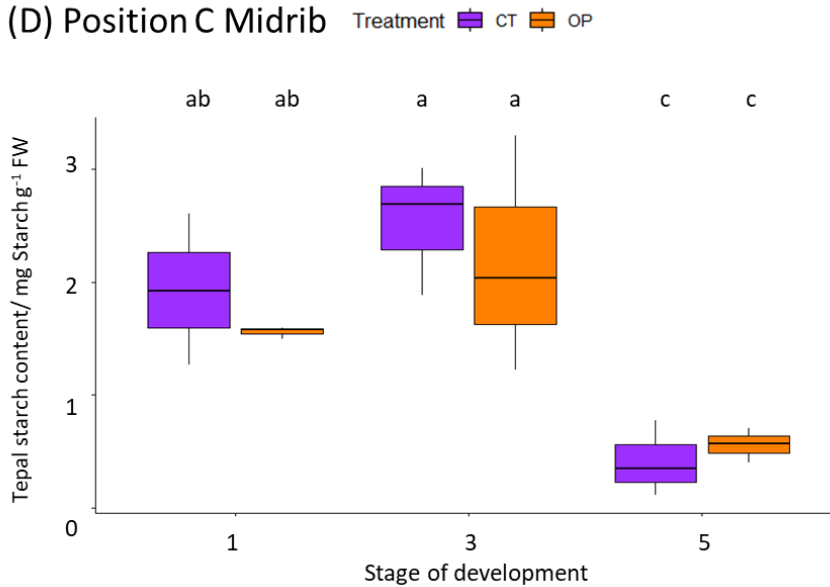


Figure 4.6 – Tepal starch content over flower development and opening comparing on plant (OP) and commercially treated (CT) samples in (A) Position A Edge, (B) Position C Edge, (C) Position A Midrib and (D) Position C Midrib. Letters denote results of two-way ANOVA with post-hoc Tukey carried out to check for significant differences between stages of development and treatment.

Table 4.2 - Statistical comparison (by student's independent T-test or Mann-Whitney-U test) comparing tepal starch content in Position A (A) and C buds (B) at the same stage and treatment in tepal edges only

Sample	Position A	Position C	Test statistic	P-value
CT Stage 1	2.298 ±1.055	2.911 ±2.129	W=5	>0.05
OP Stage 1	2.273 ± 1.533	3.777 ±0.864	T=-1.48 D.f.=3.15	>0.05
CT Stage 3	3.245 ±1.768	4.034 ±1.048	T=-0.67 D.f.=3.25	>0.05
OP Stage 3	5.455 ±2.645	5.174 ±1.675	W=3	>0.05
CT Stage 5	0.111 ±0.179	0.316 ±0.482	W=4	>0.05
OP Stage 5	0.651 ±0.515	0.423 ±0.308	T=0.65 D.f.=3.27	>0.05

Table 4.3 - Statistical comparison (by student's independent T-test or Mann-Whitney-U test) comparing tepal starch content in Position A (D) and C buds (E) at the same stage and treatment in tepal midribs only

Sample	Position A	Position C	Test statistic	P-value
CT Stage 1	1.301 ±0.548	1.930 ±0.672	T=-1.25 D.f.=3.84	>0.05
OP Stage 1	0.770 ±0.507	1.556 ±0.053	T=-2.67 D.f.=2.04	>0.05
CT Stage 3	1.325 ±0.423	2.525 ±0.579	T=-2.89 D.f.=3.66	<0.05
OP Stage 3	2.468 ±1.117	2.182 ±1.046	T=0.32 D.f.=3.98	>0.05
CT Stage 5	0.201 ±0.118	0.408 ±0.337	T=-1.01 D.f.=2.49	>0.05
OP Stage 5	0.657 ±0.391	0.556 ±0.155	T=0.42 D.f.=2.61	>0.05

4.3.4 Effect of commercial treatment and position on stem on tepal glucose, fructose and sucrose content

Tepal glucose content of both isomers identified by GC-MS increased significantly between Stages 3 and 5. At Stages 1 and 3 tepal glucose content was equal or very similar between OP and CT samples in Glucose isomer 1695 (Figure 4.7A) but significantly higher in OP samples than CT samples at Stage 5 (2 way ANOVA, df=5, p>0.05). Tepal glucose isomer 3255 content (Figure 4.7B) was significantly higher in OP

samples at Stage 3 as well as Stage 5, suggesting that there was a larger increase in glucose content over flower opening in OP buds.

Tepal fructose content showed a very similar pattern to both glucose isomers, showing a significant increase in content between Stages 3 and 5 (Figure 4.7C). Fructose content at Stages 3 and 5 were also significantly higher in OP compared to CT samples.

Sucrose content remained constant over stages of development but at each stage OP samples showed significantly higher levels than their CT counterparts (Figure 4.7D).

The tepal edge in commercially treated flowers only was then investigated for the same soluble sugars. As this is the fastest growing region of the tepals, it was therefore hypothesised to perhaps be impacted the most by commercial treatment.

Tepal edge glucose content showed no significant differences between Position A and Position C samples at any stages of development for either isomer identified here (Figure 4.7E, F). At Stage 1 and 3, both isomers showed very slightly (but not significantly) higher glucose content in Position C compared to A. Tepal fructose content showed a very similar pattern to both glucose isomers (Figure 4.7G). There was a slightly higher tepal sucrose content in Position C than Position A at Stages 1 and 3 (Figure 4.7H), however this was not reflected statistically. At Stage 5, sucrose content in Position A and Position C tepals were very similar.

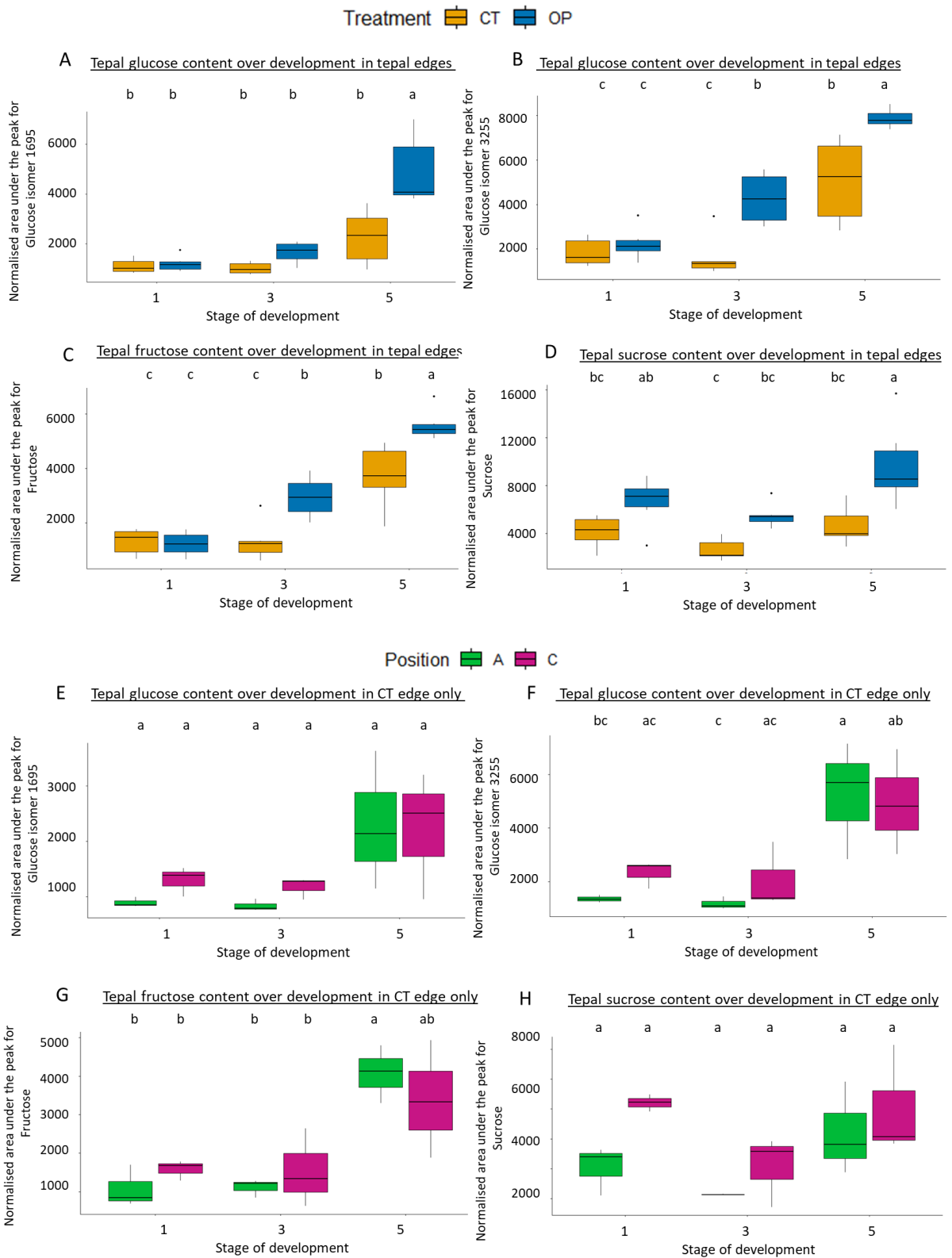


Figure 4.7 - Gas chromatography-mass spectrometry analysis on tepal samples quantifying relative tepal content of (A) glucose isomer 3255 (B) glucose isomer 1695 (C) fructose isomer 235 and (D) sucrose, comparing On plant (OP) and Commercially treated (CT) flowers. The same analysis was also used to compare position A and position C tepal

(E) glucose isomer 3255, (F) glucose isomer 1695, (G) fructose isomer 235 and (H) sucrose content in CT edge tepals only. Letters show significance from two way ANOVA with Post-hoc Tukey carried out to identify significant differences between groups (Appendix 6.12, 6.13).

4.3.5 Commercial treatment and position on stem has a significant impact on tepal metabolism

Flow infusion electrospray- high resolution mass spectrometry (FIE-HRMS) was used as a measure of tepal metabolism due to its suitability for untargeted fingerprinting of large metabolome datasets (Enot et al. 2008). A total of 6611 individual compounds were found across negative and positive ionisation modes. Internal standards run alongside identified major peaks as glucose, fructose, sucrose, and myo-inositol (Figure 4.8). These profiles were treated as the total secondary metabolite 'metabolome' of a particular tissue at a particular stage of development.

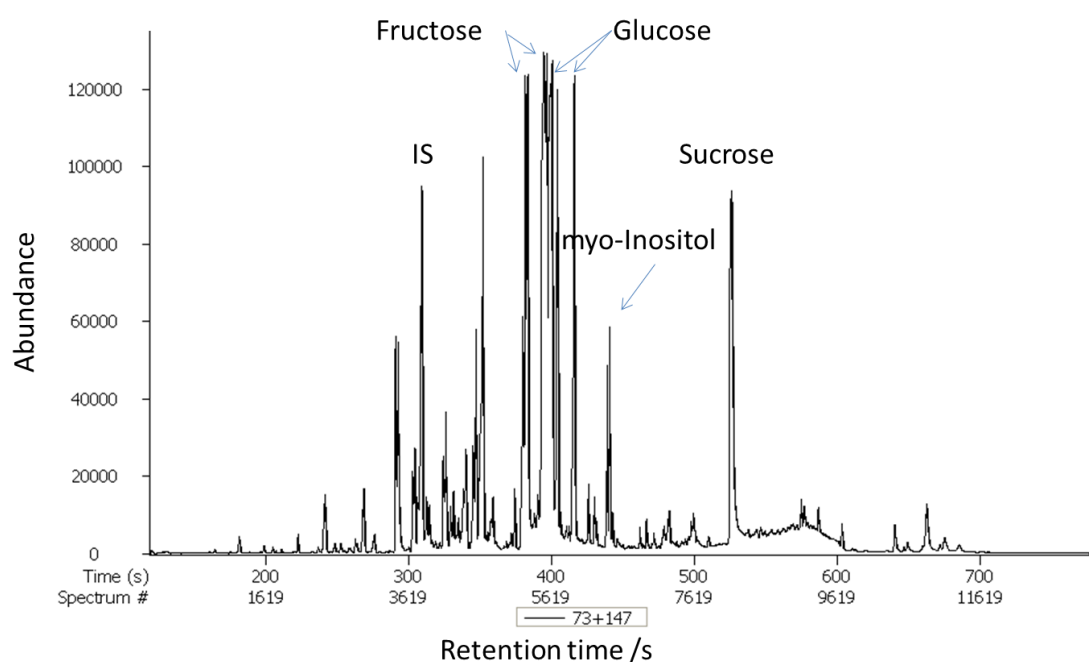


Figure 4.8 – Example spectrum from FIE-HRMS. A mixture of all samples was injected (60µl of the supernatant extract). Major peaks were identified from previous data (Manfred Beckmann, Aberystwyth University).

4.3.5.1 Comparative analysis of metabolomes with regard to treatment and position on stem over development and opening

Canonical Analysis of Principal components (CAP) with respect to sample (the independent variables of treatment (OP vs. CT), stages of development (Stages 1, 3 and 5), and position on stem (Position A vs. Position C)) showed 85.9% overall correct classification. There were significant differences in the metabolome (shown by separation between the 95% confidence interval ellipses) between Stage 1 and the other stages of development for both OP and CT samples, and in all cases OP and CT samples were well discriminated too (Figure 4.9A). However, samples from Position A and Position C at the same stage of development and treatment did not show separation, indicating that the metabolome between buds at Position A is similar to buds at Position C when at the same stage of development and treatment. PerMANOVA showed significant differences between the metabolomes with respect to all factors (treatment (R^2 0.078, $p < 0.05$), stage of development (R^2 0.287, $p < 0.05$), position on stem (R^2 0.0329, $p < 0.05$), and location on tepal (R^2 0.160, $p < 0.05$), with the interaction between treatment and stage of development also showing significant differences (R^2 0.0446, $p < 0.05$). A post-hoc test for stage of development showed significant differences between metabolomes at all stages.

Random Forest analysis was also carried out on the dataset to investigate the accuracy of classification of the profiles according to the same variables as for CAP. Random Forest with regard to sample (5000 trees, 50 variables per split) corroborated the strong separation between Stage 1 and the other stages of development seen in CAP, but however, did not separate metabolomes on basis of treatment (OP vs. CT) as well as CAP did (Figure 4.10A). The estimate of error was 25.35%, suggesting that there may be confounding variables controlling certain factors may help with the overall separation of metabolomic profiles.

CAP was also carried out with respect to each of the independent variables individually to ascertain if there were general differences between these factors with a greater number of data points per factor for more statistical power. With respect to treatment, CAP showed a very strong separation between all OP and all CT samples regardless of stage of development, position on stem or location on tepal (Figure 4.9B - 100% correct

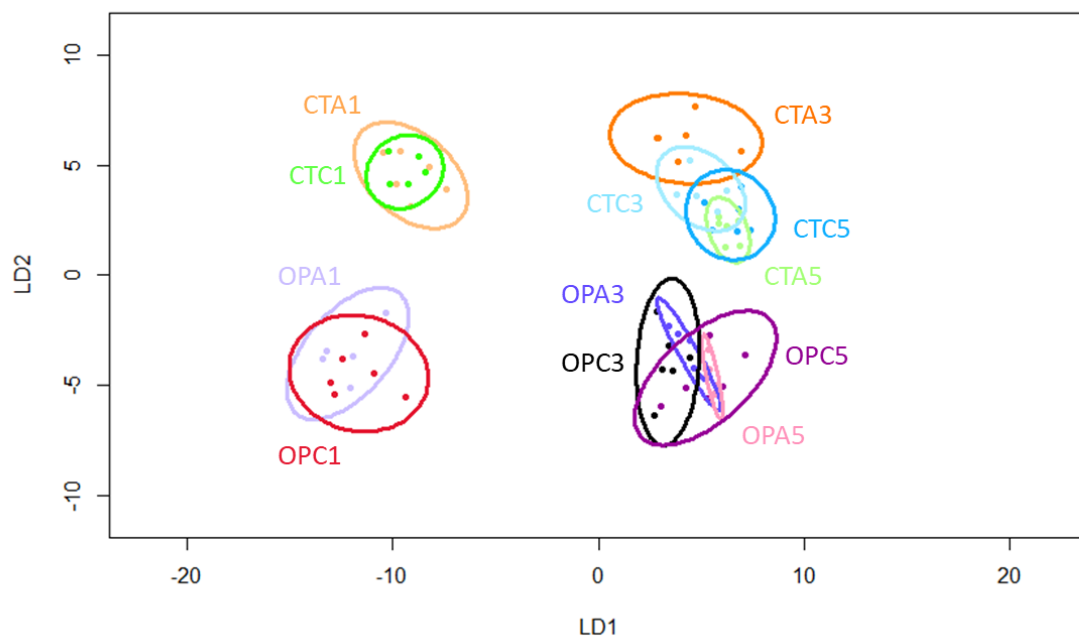
classification ($m=6$). Random Forest analysis (5000 trees, 50 variables per split) confirmed this strong significant difference with excellent discrimination between data points and 95% confidence interval ellipses (Figure 4.10B).

While CAP showed separation between Stage 1, 3 and 5 when it was carried out with respect to sample (Figure 4.9A), Stages 3 and 5 were not separated on the plot when only stage of development was considered (Figure 4.9C). Random Forest (5000 trees, 50 variables per split) also lost this discrimination between Stages 3 and 5 and additionally showed far greater spread of data, particularly in Stage 3, where the 95% confidence ellipse is much larger than the other stages of development (Figure 4.10C).

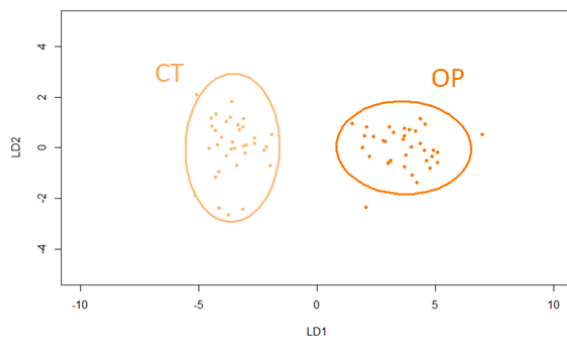
CAP with respect to location on tepal was carried out on the full dataset to identify if there were significant differences between tepal edge and midrib metabolomes (Figure 4.9D). As was found for Treatment, this showed a 100% correct classification and a very strong separation of metabolomes, suggesting that further analysis should be separated by location on tepal in order to show differences between other factors. Random Forest analysis (5000 trees, 50 variables per split) also showed significant differences between edge and midrib samples with an error rate of 1.42% (Figure 4.10D).

CAP according to position on stem was carried out on the full dataset to identify if there were general differences between profiles (Figure 4.9E). The percentage of correct classifications was 91.5%, showing strong differences between profiles which may have been masked by the stronger effects of treatment, stage of development and location on tepal. Random Forest (5000 trees, 50 variables per split) showed a similar effect with some similarities between metabolomes from position A and C buds, but a good error rate of only 5.62% (Figure 4.10E).

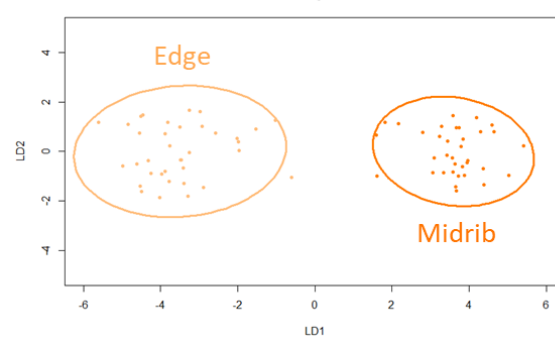
(A) - Sample



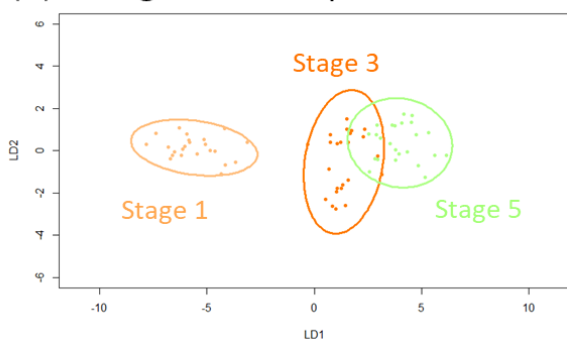
(B) - Treatment



(D) – Location on tepal



(C) – Stage of development



(E) – Position on stem

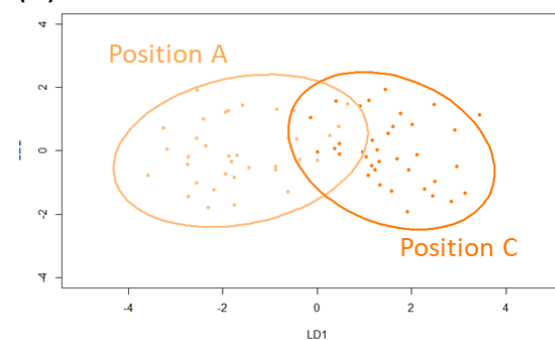


Figure 4.9 – Canonical Analysis of Principal coordinates was based on the full metabolomes of all lily tepal samples collected using FIE-HRMS. A CAP model was generated for tepal metabolomes with respect to (A) sample, which separated samples by treatment, stage of development and position on stem, (B) treatment only, (C) stage of development only, (D) location on tepal, and (E) position on stem. The models are

plotted using the first two linear discriminants and each ellipse represents 95% confidence interval. Percentage of correct classifications was for (A) 85.9% ($p < 0.05$, $n=6$ (for OPA1 $n=5$)), (B) 100% ($p < 0.05$, $n_{OP}=35$, $n_{CT}=36$), (C) 93% ($p < 0.05$, $n_1=23$, $n_{2,3}=24$), (D) 100% ($p < 0.01$, $n_{Edge}=36$, $n_{Midrib}=35$), (E) 91.5% ($p < 0.05$, $n_A=35$, $n_C=36$).

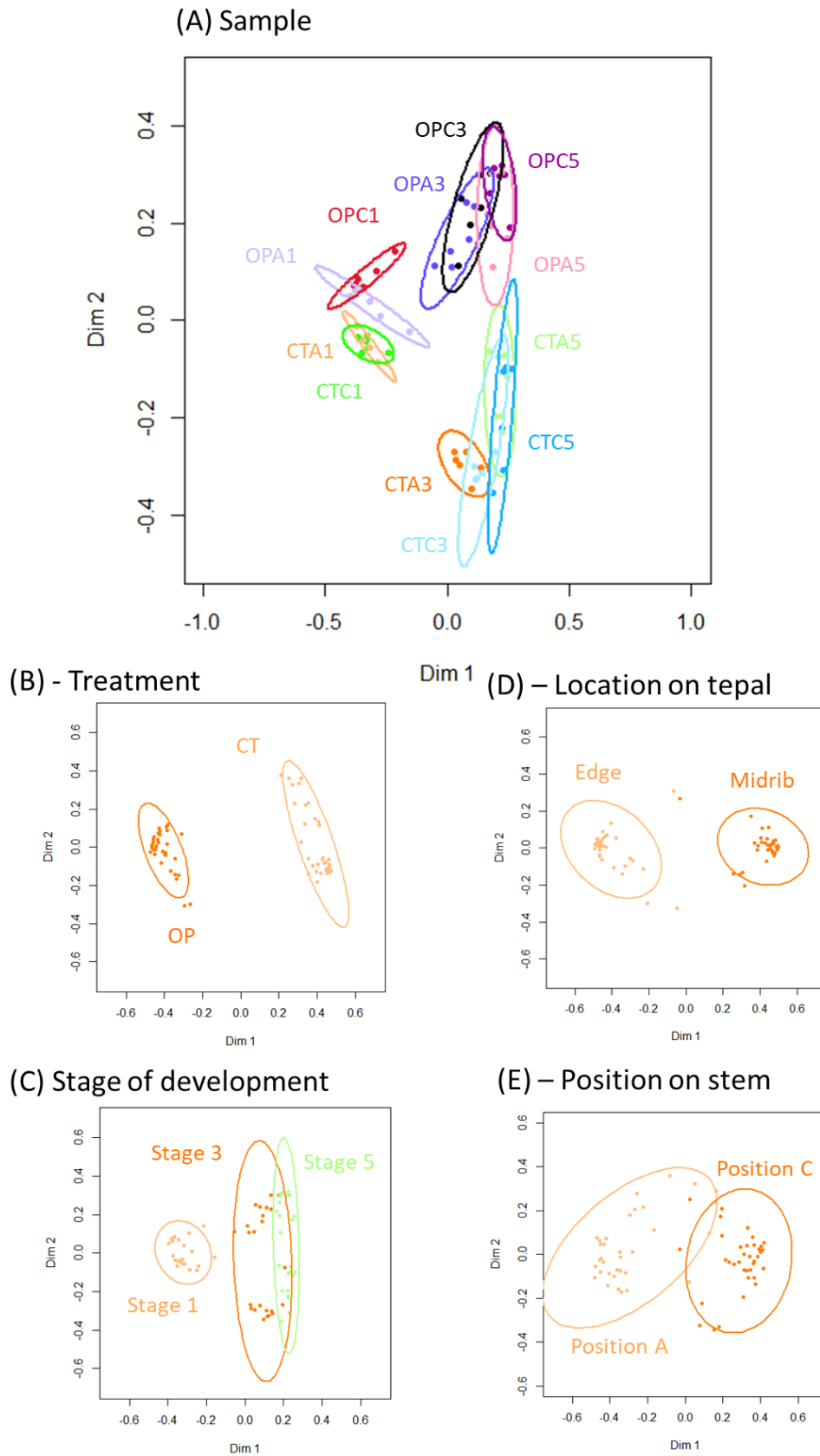


Figure 4.10 – Random Forest classification was based on the full metabolomes of all lily tepal samples collected using FIE-HRMS. Random Forest classification was carried out

(5000 trees, 50 variables) and a plot was generated for tepal metabolomes with respect to (A) sample, which separated samples by treatment, stage of development and position on stem, (B) treatment only, (C) stage of development only, (D) location on tepal, and (E) position on stem. Each ellipse represents 95% confidence interval. The OOB estimate of error rate was (A) 23.95%, (B) 0%, (C) 4.23%, (D) 1.41%, and (E) 8.45%.

Random Forest analysis was also carried out with regard to stage of development, treatment, and position on stem to putatively identify compounds which were most important in the classification of profiles according to each of those variables separately. With regard to stage of development, the top 20 compounds involved in the classification comprised putative flavonoids (coumarins, glycosides), phenolic compounds (oxyresveratrol, ferulic acid glycosides, lignans) and quinones (dicafeoylquininate, fusaroskyrin) (Table 4.4). A selection of compounds which could be putatively identified were investigated for relative abundance over the stages of development (Figure 4.11) and apart from X1380, a putative coumarin glycoside, all increased over the stages of development significantly, in particular between Stages 3 and 5.

Table 4.4 – showing the 20 top compounds in the classification of all metabolite profiles by Random Forest analysis with regard to stage of development, and their putative identification by m/z ratio, ionisation mode and adduct (where known) using the DIME-DB online database.

Compound ID	M/z ratio	Ionisation	Adduct	Putative chemical class	Putatively identified compound
X5313	561.17383 p			Polyphenol glycoside/lignan	Isolariciresinol 9-O-beta-D-glucoside
X1641	509.15302 n			Hydroxycinnamic acid	6-Feruloylglucose 2,3,4-trihydroxy-3-methylbutylglycoside
X4856	445.09 p		[M+K]1+	Stilbene glycoside	(E)-Oxyresveratrol 3'-O-b-D-glucoside
X4738	426.16113 p		[M+H]1+	Coumarin	4'-Nitro-2-(triphenylphosphoranylidene)acetophenone
X5450	599.138 p		[M+H]1+	Quinone	Fusaroskyrin
X4735	425.15689 p		[M+H]1+	Flavonoid	(S)-3',4',5,7-Tetrahydroxy-5',8-diprenylflavanone
X6319	88.04747 p		[M+H]1+	Chlorobenzyl organic compound	3-Isoxazolidinone
X1380	443.00061 n			Furanocoumarin glycoside	Xanthotoxol glucoside
X1969	595.05084 n			Oligosaccharide	b-D-Glucuronopyranosyl-(1->3)-a-D-galacturonopyranosyl-(1->2)-L-rhamnose
X4805	438.0882 p			Glucosinolate	6-Heptenyl glucosinolate
X5280	554.27979 p		[M+H]1+	Cyclopeptide	Vignatic acid A
X5723	683.24762 p			Diarylheptanoid	Myricanol 5-laminaribioside
X4780	433.63531 p				n/a
X1194	388.93143 n		[M+Cl]1-	Diselenide	Selenohomocystine
X1336	429.1778 n		[M-H]1-	Glycoside	Phenethyl rutinoside
X6300	87.0442 p		[M+H]1+	Phytol	Gamma-Butyrolactone
X530	171.00652 n		[M+Cl37]1-	Sugar acid	Threonine acid
X5462	600.14038 p		[M+H]1+		n/a
X5249	545.15613 p			Hydroxycinnamic quinone	Methyl 3,4-dicafeoylquininate
X2323	767.24133 n		[2M-H]1-	Coumarin	Licofuranocoumarin

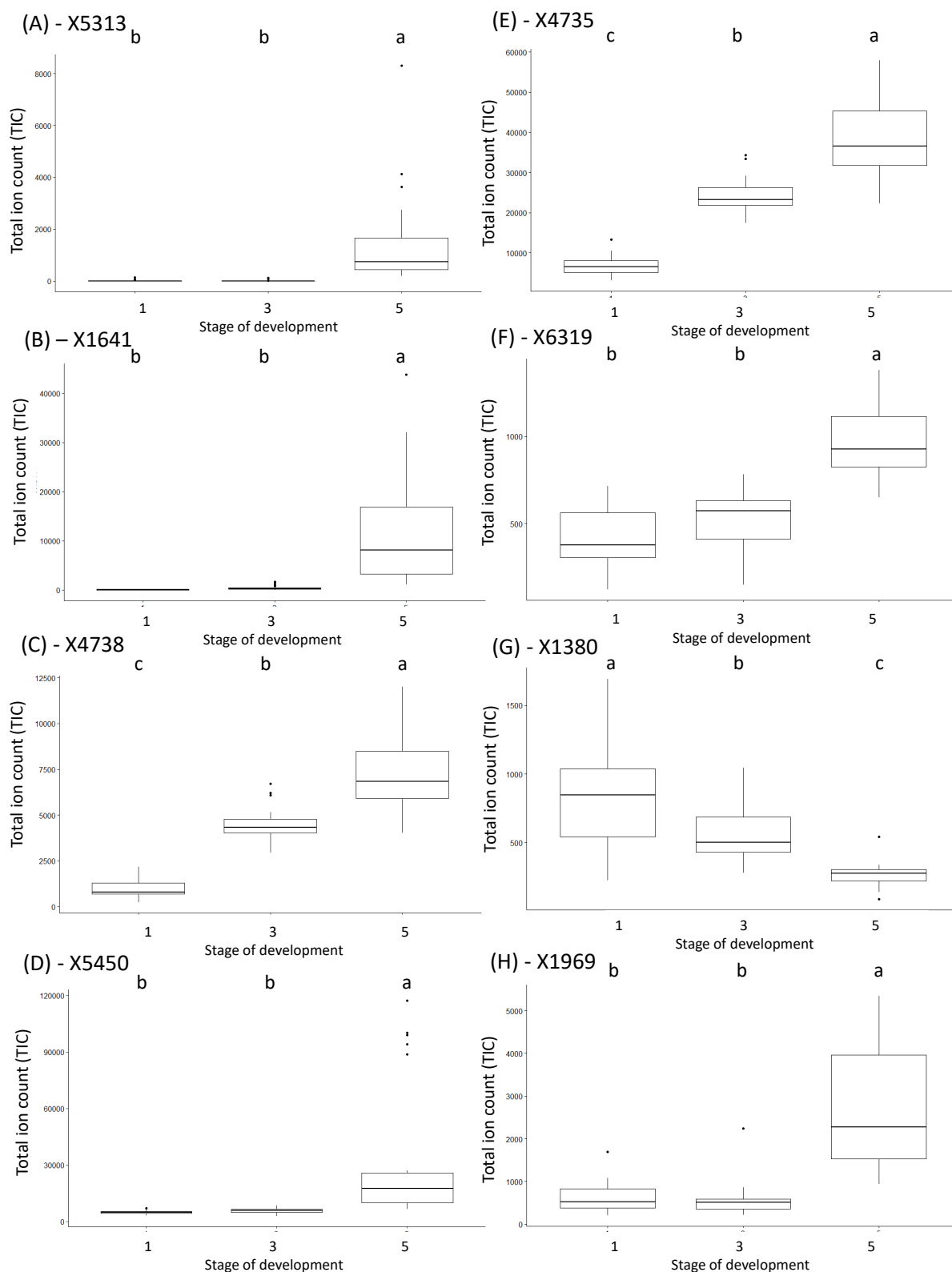


Figure 4.11 – Total ion count (TIC) of selected compounds most important in the classification of profiles using Random Forest analysis with respect to stage of development (Table 4.2) across stages of development. Letters indicate significance by

one-way ANOVA with post-hoc Tukey test or Kruskal Wallis with post-hoc Dunn test (Appendix 6.25).

The compounds important in the classification of profiles by treatment (Table 4.5) was very similar to the compounds important in the Random Forest classification according to stage of development, and contained putatively identified hydroxycinnamic acids, phenylpropanoid glycosides and coumarins. These compounds were all indicated to show significantly higher abundance in CT samples than OP samples at the same stage of development (Figure 4.12) apart from X3732 (a putative aglycone, genipin), which showed significantly higher abundances in OP samples.

Table 4.5 – showing the 20 top compounds in the classification of all metabolite profiles by Random Forest analysis with regard to treatment, and their putative identification by m/z ratio, ionisation mode and adduct (where known) using the DIME-DB online database.

Compound ID	M/z ratio	Ionisation	Adduct	Putative chemical class	Putatively identified compound
X2343	78.91866	n		Organosulfur	Methanedithiol
X4159	321.13004	p	[M+K]1+		n/a
X1055	355.07782	n	[M-H]1-	Hydroxycinnamic acid	Caffeic acid 3-O-glucuronide
X5113	497.23572	p	[M+2H]2+		n/a
X4768	430.99997	p		Organic compound	6-Hydroxy-5-[(4-sulfophenyl)azo]-2-naphthalenesulfonic acid
X4217	335.11005	p		Phenylpropanoid glycoside	3-Hydroxychavicol 1-glucoside
X3938	278.10748	p	[M+K]1+		n/a
X4359	365.15607	p	[M+K]1+		2-Dodecylbenzenesulfonic acid
X3728	226.13388	p	[M+H]1+	Organic compound	4-(Dimethylamino)azobenzene
X5235	542.26544	p		Phospholipid	LysoPE(20:3(8Z,11Z,14Z)/0:0)
X4889	453.20963	p	[M+K]1+	Fatty acid ester	Ascorbyl palmitate
X4162	322.13416	p	[M+K]1+	Amino acid	Lysyl-Histidine
X4377	367.15503	p	[M+K41]1+	Coumarin	5-Geranyloxy-7-methoxycoumarin
X4339	363.06879	p	[M+H]1+	Glucuronic acid derivative	2-O-Galloylgalactaric acid
X4071	305.15704	p	[M+Na]1+	Organic compound	(-)-(E)-1-(4-Hydroxyphenyl)-7-phenyl-6-hepten-3-ol
X4369	366.16046	p	[M+K]1+		n/a
X2361	80.91684	n			Sulfurous acid
X4894	454.21292	p	[M+K]1+		Triethanolamine lauryl sulfate
X3732	227.13704	p	[M+H]1+	Aglycone	Genipin
X4170	323.12875	p	[M+K41]1+	Sesquiterpene	Alpha-dihydroartemisinin

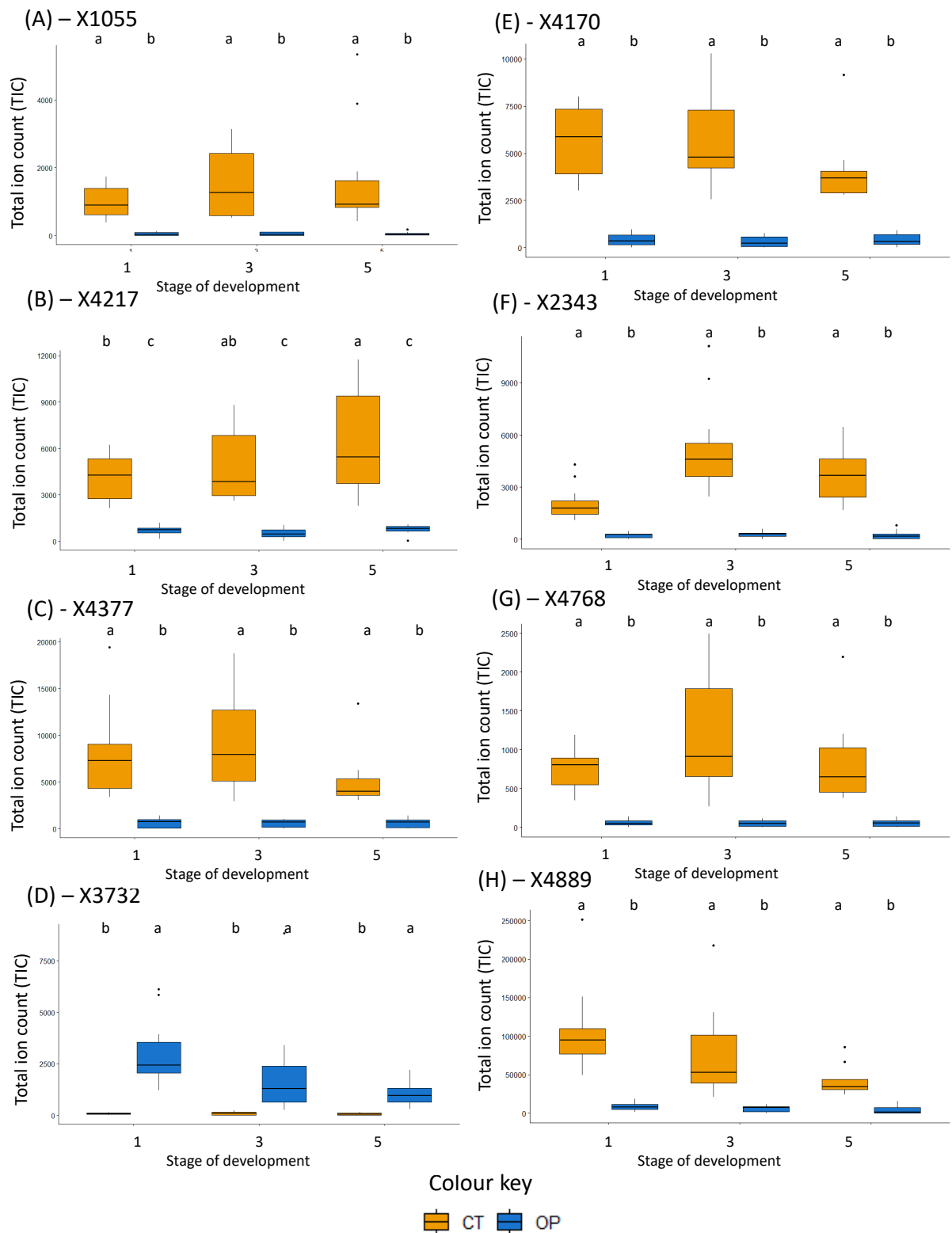


Figure 4.12 – Total ion count (TIC) of selected compounds most important in the classification of profiles using Random Forest analysis with respect to treatment (Table 4.3) across stages of development comparing OP and CT samples. Letters indicate

significance by one-way ANOVA with post-hoc Tukey test or Kruskal Wallis with post-hoc Dunn test (Appendix 6.22).

The compounds identified by Random Forest analysis according to location on tepal (Table 4.6) also included several types of putative organic compound, flavonoids and hydroxycinnamic acids/lignans. Compounds putatively identified as organic compounds and flavones (X1921, X5075, X5137) were found significantly more abundantly in tepal edges compared to midrib samples, while compounds putatively identified as lignin precursors (X2432, X939, X1178) were found more abundantly in tepal midribs. Additionally, the putatively identified cytokinin precursor molecule (X4681 - 6-methylthiopurine 5'-monophosphate ribonucleotide) was found significantly more abundantly in tepal midribs.

Table 4.6 – showing the 20 top compounds in the classification of all metabolite profiles by Random Forest analysis with regard to location on tepal, and their putative identification by m/z ratio, ionisation mode and adduct (where known) using the DIME-DB online database.

Compound ID	M/z ratio	Ionisation	Adduct	Putative chemical class	Putatively identified compound
X1921	58.03049	n		Organic compound	N-Methylformamide
X2432	855.25824	n	[M-H]1-	Lignan	Sesaminol glucosyl-(1->2)-[glucosyl-(1->6)]-glucoside
X5080	490.23312	p	[M+Na]1+		n/a
X6356	895.22662	p	[M+H]1+		n/a
X4681	417.00238	p	[M+K]1+	Cytokinin precursor	6-Methylthiopurine 5'-monophosphate ribonucleotide
X1948	588.23114	n	[M-H]1-		n/a
X5368	577.16815	p		Flavonoid	Citrusin A
X939	339.02057	n		Hydroxycinnamic acid	Sinapinic acid-O-sulphate
X601	232.14569	p			n/a
X1261	406.13635	n	[M-H]1-	Benzophenanthridine alkaloid	8-Carboxymethylidihydrochelerythrine
X2434	856.26044	n	[M-H]1-		n/a
X660	277.12988	n		Organic disulfide	Pantetheine
X1178	382.96091	n		Hydroxycinnamic acid	Sinapinic acid-O-sulphate
X1144	376.06607	n	[M+K-2H]1-	Betaxanthin	Vulgaxanthin I
X1213	392.96353	n	[M+K-2H]1-	Organic compound	Grevilline D
X5075	489.22968	p	[M+H]1+	Flavone	Rubraflavone D
X5137	505.20633	p	[M+K]1+	Organic compound	Carbiphene hydrochloride
X604	233.12228	n	[M-H]1-	Polyprenol compound	Geranyl Phosphate
X1325	424.14569	n	[M-H]1-		n/a
X606	234.12384	n	[M-H]1-	Purine	2',3'-Dideoxyadenosine

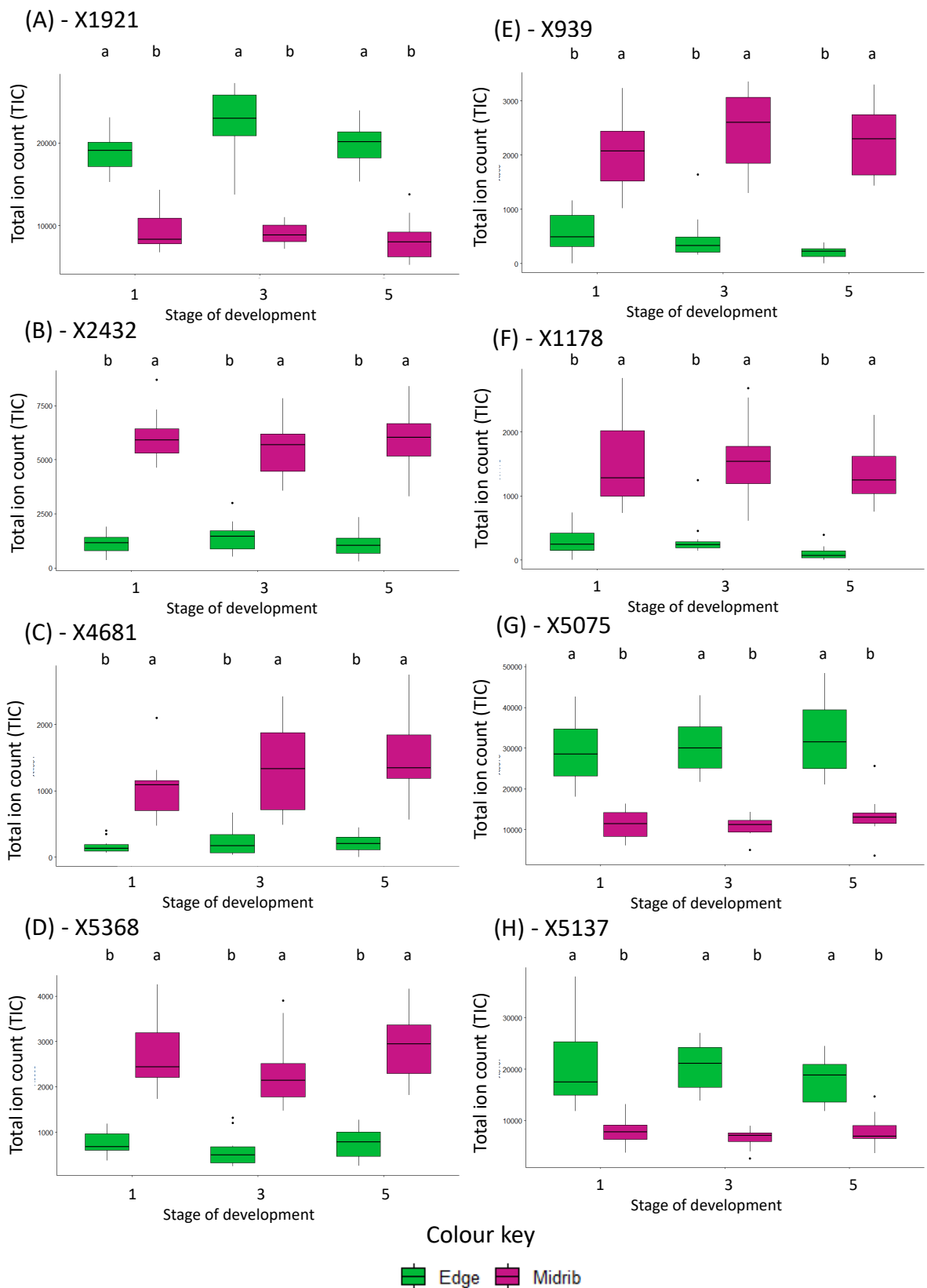


Figure 4.13 – Total ion count (TIC) of selected compounds most important in the classification of profiles using Random Forest analysis with respect to location on tepal

(Table 4.4) across stages of development comparing tepal midrib and tepal edge samples. Letters indicate significance by one-way ANOVA with post-hoc Tukey test or Kruskal Wallis with post-hoc Dunn test (Appendix 6.23).

The top 20 compounds important in the classification with regard to position on stem (Table 4.7) were very different to the compounds which have been identified by Random Forest as important for classification by stage of development, treatment or location on tepal, and was mainly made up of putative phospholipids (phosphatidic acids, phosphatidylethanolamines), glycerides (mono- and diglycerol), and long chain fatty acids (oleic acid). When the individual compounds were analysed, these compounds were significantly more abundant in Position A compared to C for all eight compounds analysed (Figure 4.14).

Table 4.7 – showing the 20 top compounds in the classification of all metabolite profiles by Random Forest analysis with regard to position on stem, and their putative identification by m/z ratio					
Compound ID	M/z ratio	Ionisation	Adduct	Putative chemical class	Putatively identified compound
X2110	671.46722n		[M-H]1-	Phospholipid	PA(16:0/18:2(9Z,12Z))
X2102	669.45026n			Diglyceride	DG(14:0/0:0/20:3n6)
X2111	672.47101n		[M-H]1-	Phospholipid	PE(P-18:1(11Z)/14:0)
X2164	695.46838n		[M-H]1-	Phospholipid	1,2-Di-(9Z,12Z-octadecadienoyl)-sn-glycero-3-phosphate
X2159	693.45135n			Diglyceride	DG(16:1(9Z)/20:4(5Z,8Z,11Z,14Z)/0:0)
X2172	698.48712n		[M-H]1-	Phospholipid	PE(15:0/18:3(9Z,12Z,15Z))
X2166	696.47198n		[M-H]1-	Phospholipid	PE(18:4(6Z,9Z,12Z,15Z)/15:0)
X2170	697.48376n		[M-H]1-		n/a
X5498	61.08431p		[M+H]1+	Organic compound	1,2-Ethanediamine
X5969	773.39209p			Terpenoid	Mubenin B
X2766	104.10709p		[M+H]1+	Organic compound	Ethyl 2-aminoacetate
X2176	699.49988n		[M-H]1-	Phospholipid	PA(18:1(9Z)/18:1(11Z))
X2112	673.48108n		[2M-H]1-	Monoglyceride	N-octadeca-9,12-dienoylglycine
X2289	744.49225n		[M-H]1-		n/a
X2781	105.11021p		[M+H]1+	Organic compound	2-(2-Aminoethylamino)ethanol
X2178	700.50262n		[M-H]1-	Phospholipid	PE(18:2(9Z,12Z)/15:0)
X680	281.24893n		[M-H]1-	Long chain fatty acid	Oleic acid
X5458	60.08107p		[M+H]1+	Organic compound	N-Ethylmethylamine
X4386	369.24002p			Monoglyceride	MG(i-16:0/0:0/0:0)
X2105	670.45532n			Phospholipid	PE(14:0/14:0)

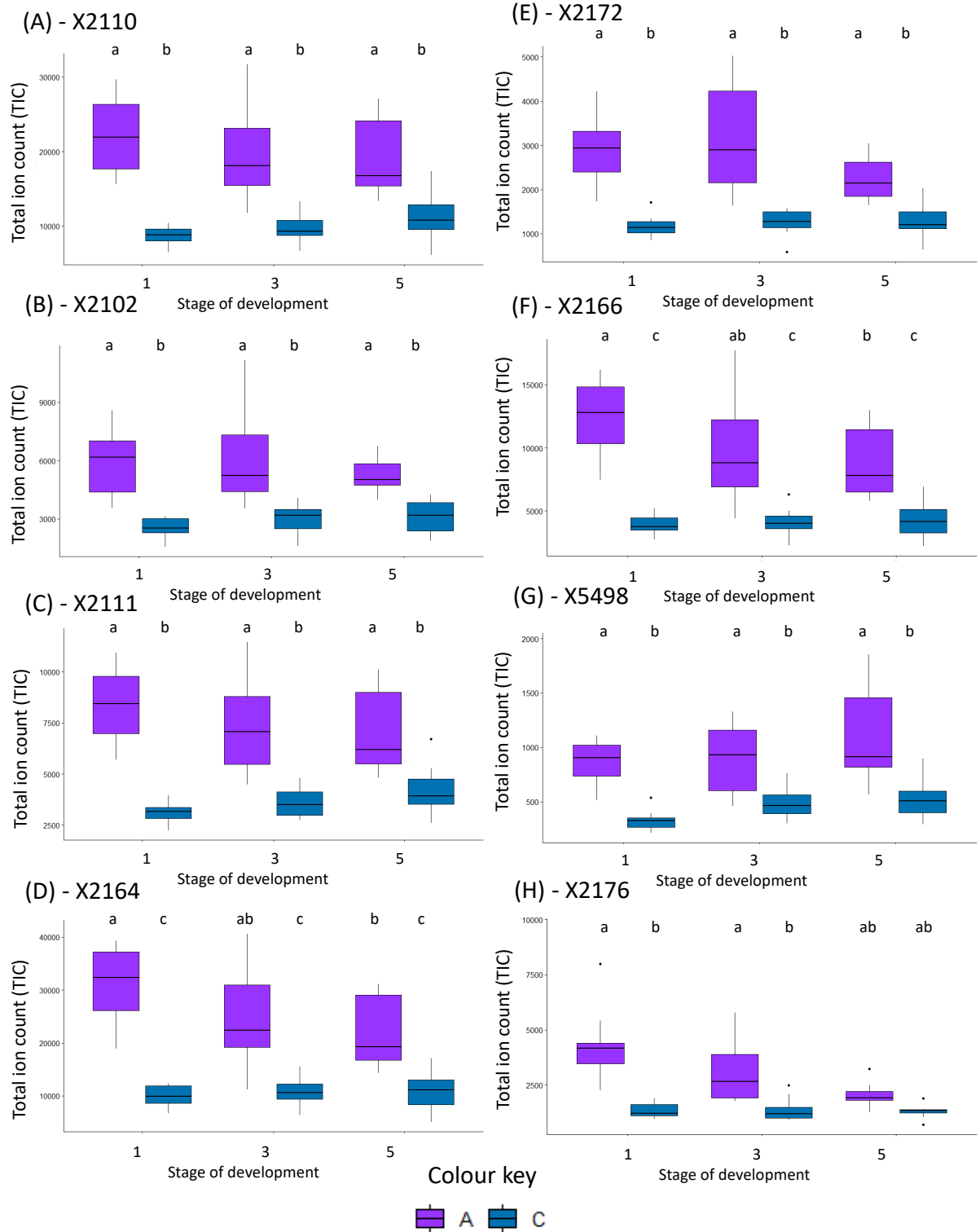


Figure 4.14 – Total ion count (TIC) of selected compounds most important in the classification of profiles using Random Forest analysis with respect to position on stem (Table 4.5) across stages of development comparing Position A and Position C samples.

Letters indicate significance by one-way ANOVA with post-hoc Tukey test or Kruskal Wallis with post-hoc Dunn test (Appendix 6.24).

4.3.5.2 Comparative analysis of the effect of position on stem on metabolome controlling for treatment and location on tepal

The effect of position on stem was further explored using a subset of profiles where treatment and location on tepal were controlled (i.e. profiles for OP edge tepals only were used separately to OP midrib/CT edge/CT midrib profiles). CAP analysis on OP edge profiles with regard to sample (stage of development and position on stem) showed excellent discrimination between all samples (Percentage of correct classifications 94.4%) showing significant differences between metabolite profiles in samples commercially treated and on plant at each stage of development (Figure 4.15A). OP midrib tepal metabolomes show poorer discrimination (88.24%) and more variation between biological samples for Stage 1 and Stage 3 samples, shown by the larger ellipses (Figure 4.15B). Metabolomes show separation between Stage 1 and the other stages of development but a lack of discrimination between Position A and C and Stage 3 and 5. CT edge metabolomes showed equally good discrimination on basis of sample (Correct classifications 94.4%) to OP edge metabolomes (Figure 4.15C), except that CTA5 and CTC5 samples are much more similar to each other than in on plant samples and were not discriminated, suggesting that the commercial treatment makes profiles more similar between position A and C at Stage 5 specifically. CT midrib metabolomes similarly showed less separation than CT edge profiles (83.33% correct classifications), like OP samples (Figure 4.15D). However, midrib CTA1 and CTC1 profiles showed separation by 95% confidence intervals unlike the same profiles on plant. CTC3 also separated from the other clustered profiles for CTA3, CTA5, and CTC5, showing some slight differences in commercial treatment in the tepal midrib.

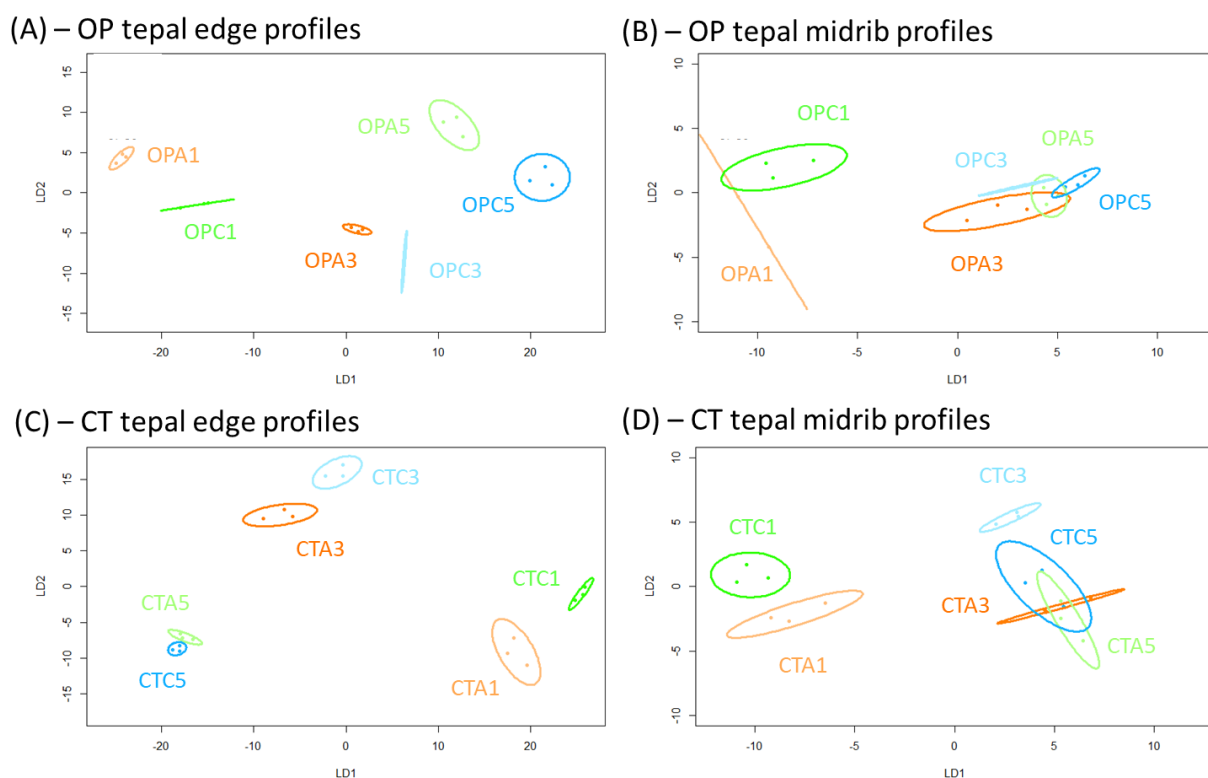


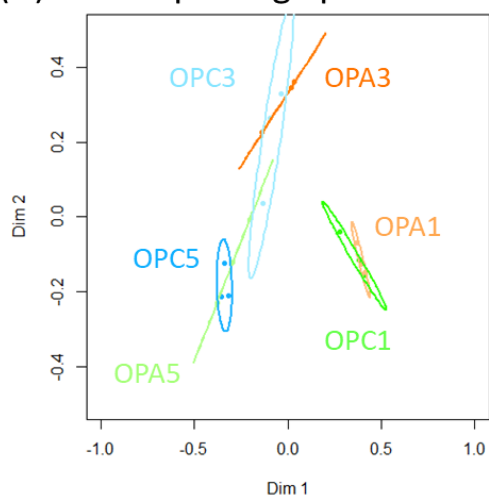
Figure 4.15 - Canonical Analysis of Principal coordinates was based on lily tepal midrib and edge metabolomes collected using FIE-HRMS. A CAP model was generated for tepal metabolomes with respect to sample, which separated samples by treatment, stage of development and position on stem in (A) OP edge profiles, (B) OP midrib profiles, (C) CT edge profiles and (D) CT midrib profiles. The models are plotted using the first two linear discriminants and each ellipse represents 95% confidence interval. Percentage of correct classifications was for (A) 94.4% ($p < 0.05$, $n = 3$), (B) 94.4% ($p < 0.05$, $n = 3$), (C) 88.2% ($p < 0.05$, $n = 3$), and (D) 83.3% ($p < 0.05$, $n = 3$).

Random Forest analysis with respect to sample showed some notable differences between treatment and location on tepal. OP edge profiles (Figure 4.16A) had an estimate of error of 66.7%; they showed significant separation between some stages of development but not position on stem – OPA1 and OPC1 profiles could be discriminated from OPA3/OPC3 and OPA5/OPC5 profiles, but OPA and OPC metabolomes for each stage of development had overlapping 95% confidence intervals, suggesting similar metabolomes. OP midrib profiles showed similar patterns and a similar estimate of error

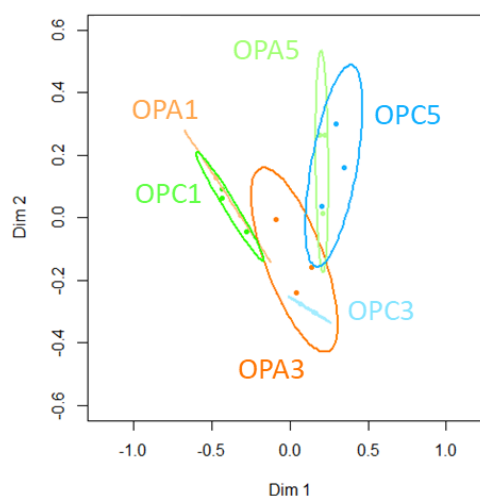
(64.7%); samples were more similar to each other and there was less discrimination between 95% confidence intervals (Figure 4.16B).

Analysed by Random Forest, CT edge profiles had a poorer estimate of error than OP edge profiles (50%) but showed a very similar pattern (Figure 4.16C) and showed the same separation of Stage 1 profiles to Stage 3 and 5 but no separation between Position A and C profiles. A lack of overlap of 95% confidence intervals suggests that CTA3 and CTA5 are less similar to each other than CTC3 and CTC5, where the confidence intervals do overlap. CT midrib profiles (Figure 4.16D), had a large estimate of error by Random Forest analysis (83.3%) and like OP midrib profiles, had a high variation indicated by the larger 95% confidence interval ellipses. However, they still show the same pattern of Stage 1 separated from the other stages.

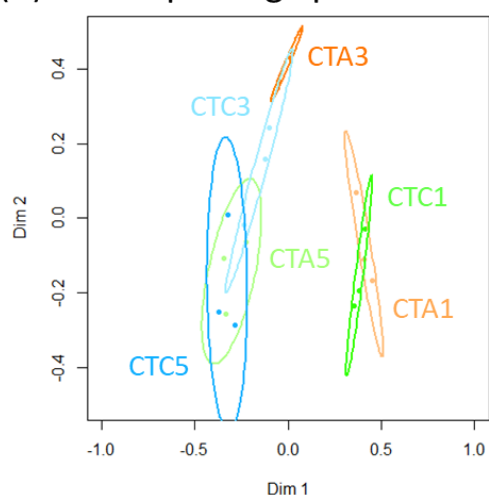
(A) – OP tepal edge profiles



(B) – OP tepal midrib profiles



(C) – CT tepal edge profiles



(D) – CT tepal midrib profiles

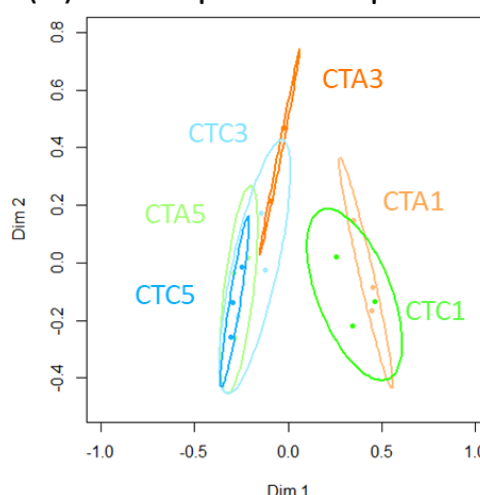


Figure 4.16 - Random Forest classification was based on lily tepal midrib and edge metabolomes collected using FIE-HRMS. Random Forest classification was carried out (5000 trees, 50 variables) and a plot was generated for tepal metabolomes with respect to sample, which separated samples by stage of development and position on stem in (A) OP Edge profiles, (B) OP Midrib profiles, (C) CT Edge profiles and (D) CT Midrib profiles. Each ellipse represents 95% confidence interval. The OOB estimate of error rate was (A) 55.6%, (B) 64.7%, (C) 50% and (D) 88.9%.

Random Forest analysis was finally also carried out with regard to position on stem to putatively identify compounds which were most important in the classification of profiles according to position on stem only. Only CT Edge samples were used for this

analysis as they were assumed to be the most metabolically active tissue involved in opening and most likely to be responsible for problems with flower opening when commercially treated and at a terminal position on stem. The Random Forest analysis with respect to position on stem in this subset of profiles showed an OOB estimate of error of only 22.2% (5000 trees, 50 variables per split), suggesting there was a good ability to discriminate despite the slight overlap of 95% confidence interval ellipses (Figure 4.17). The 20 top compounds which were important in this classification comprised a combination of putative flavonoids (genistein, ponasteroside, proanthocyanidin A2, chamameloside) and phospholipids/glycerides (Table 4.8).

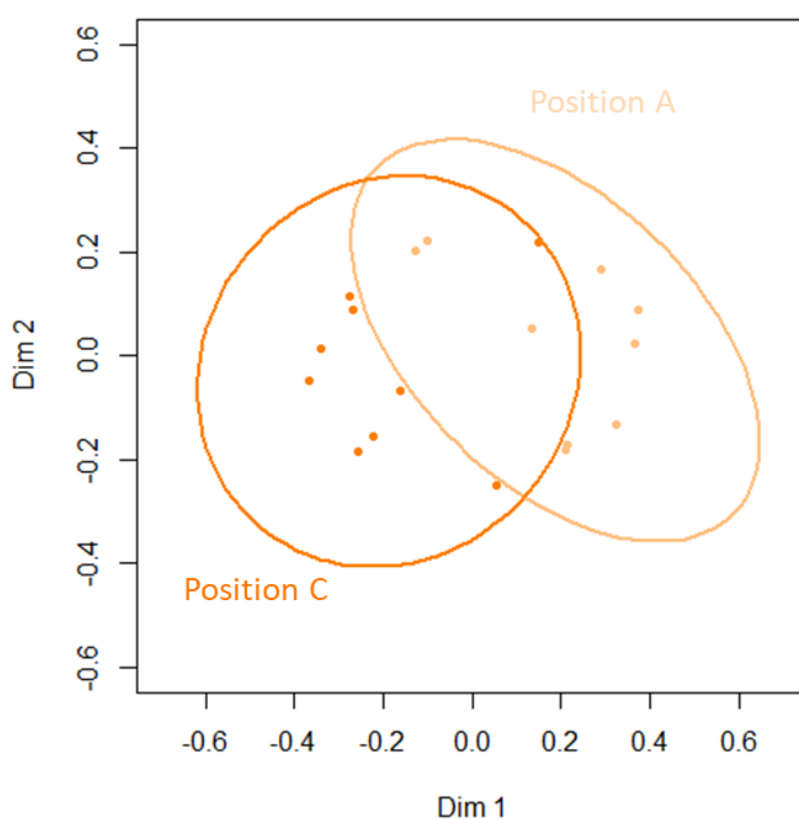


Figure 4.17 - Random Forest classification was based on lily tepal CT Edge metabolomes collected using FIE-HRMS. Random Forest classification was carried out (5000 trees, 50 variables) and a plot was generated for tepal metabolomes with respect to Position on stem. Each ellipse represents the 95% confidence interval. The OOB estimate of error rate was 22.2%.

Table 4.8 – showing the 20 top compounds in the classification of a subset of metabolite profiles (Commercially treated tepal edge profiles only) by Random Forest analysis with regard to position on stem, and their putative identification by m/z ratio, ionisation mode and adduct (where known) using the DIME-DB online database

Compound ID	M/z ratio	Ionisation	Adduct	Putative chemical class	Putatively identified compound
X4899	455.05206 p		[M+K]1+	Isoflavone	Genistein 4'-rhamnoside
X2421	843.5979 n			Diglyceride	DG(a-25:0/i-21:0/0:0)
X2170	697.48376 n		[M-H]1-		n/a
X5737	689.21735 p		[M+H]1+	Phenylpiperazine	CHLORCYCLIZINE PAMOATE
X5675	665.29065 p			Glycoside	Ponasteroside A
X2159	693.45135 n			Diglyceride	DG(16:1(9Z)/20:4(5Z,8Z,11Z,14Z)/0:0)
X1275	409.23627 n			Monoglyceride	MG(0:0/16:0/0:0)
X2102	669.45026 n			Phospholipid	PHOSPHATIDIC ACID, DIPALMITOYL
X2164	695.46838 n		[M-H]1-	Phospholipid	1,2-Di-(9Z,12Z-octadecadienoyl)-sn-glycero-3-phosphate
X3883	272.09784 p		[M+K]1+	Amino acid	AsparaginyI-Threonine
X3880	272.06522 p		[M+K]1+	Amino acid	AsparaginyI-Threonine
X3912	274.08719 p		[M+K41]1+	Organic compound	3,5-Diisopropylphenyl methylcarbamate
X5515	615.12372 p			Flavonoid	Proanthocyanidin A2
X3628	205.09698 p			Flavonoid	Chamaemeloside
X951	340.33047 n		[M-H]1-	Fatty acid ester	N-Palmitoyl GABA
X2353	79.01125 n				2-chloroethanol
X5612	641.06976 p		[M+K]1+	Flavonoid glycoside	Eriodictyol 7-(6-galloyl)glucoside)
X5284	555.19159 p			Phenolic glycoside	Nomilinic acid
X2781	105.11021 p		[M+H]1+	Organic compound	2-(2-Aminoethylamino)ethanol
X1289	415.06192 n		[M+Cl37]1-	Glycoside	4-Methoxybenzyl O-(2-sulfoglucoside)

Selected individual top compounds identified as important in the classification of the subset of CT edge metabolomic profiles (Table 4.8) were investigated for abundance, comparing Position A to Position C samples over stages of development (Figure 4.18). The compounds putatively identified as flavonoids (X4899, X5737, X5515, X3628) were all significantly more abundant in Position C buds compared to Position A, but the compounds putatively identified as phospholipids or fatty acids (X2421, X2159, X1275, X2102) showed the opposite trend, with significantly greater abundance in Position A buds.

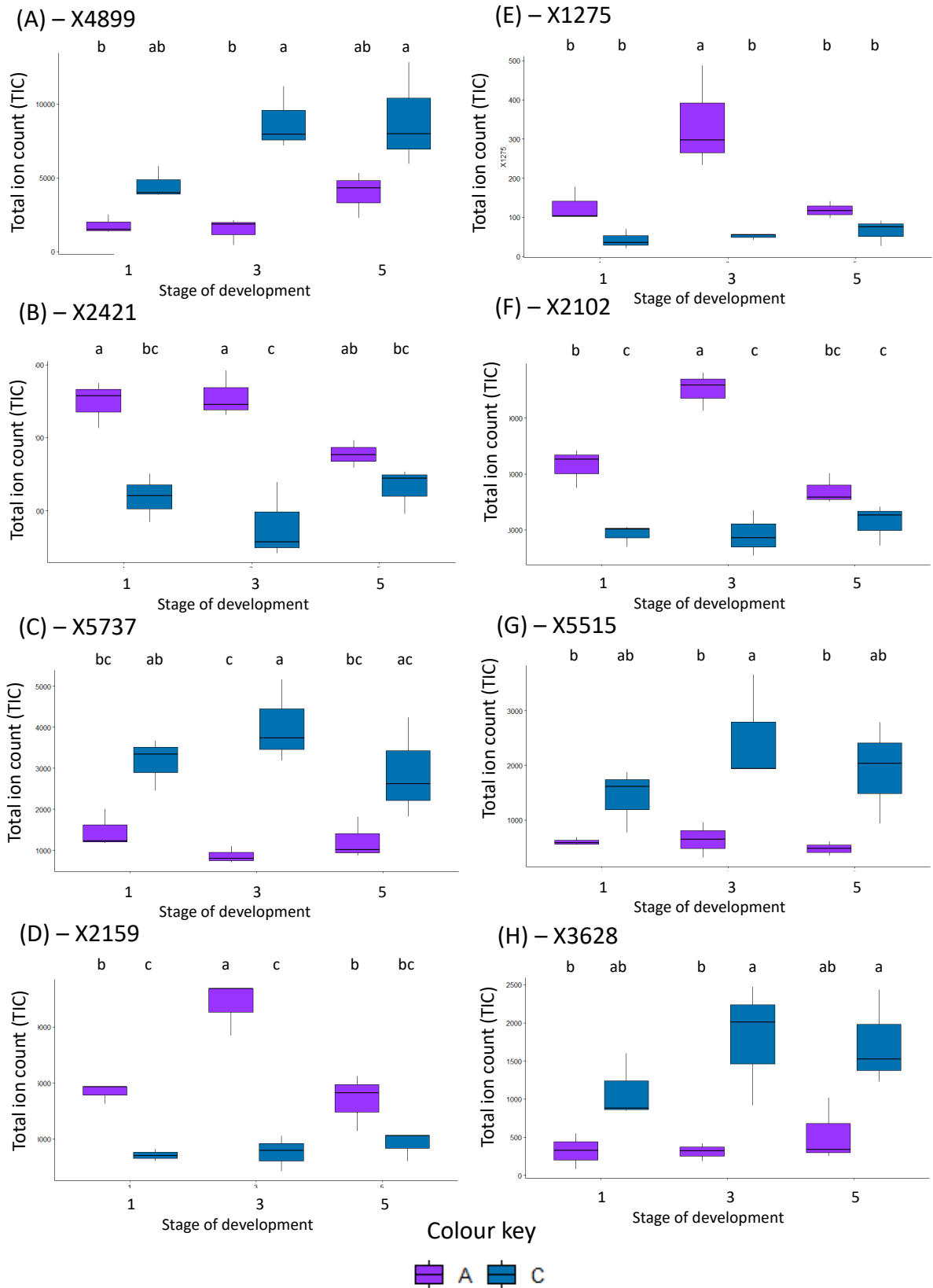


Figure 4.18 – Total ion count (TIC) of selected compounds most important in the classification of the subset of CT edge metabolomic profiles using Random Forest

analysis with respect to position on stem (Table 4.6) across stages of development comparing Position A and Position C samples. Letters indicate significance by one-way ANOVA with post-hoc Tukey test (Appendix 6.26).

Statistical analyses (CAP and Random Forest) were repeated (not shown here) on the GC-tofMS datasets where similar classifications of sample groups were observed, which maintains confidence in the data shown above.

4.3.6 Relative expression of sugar metabolism, transport, and cell expansion-related genes across flower opening

The *EXPA1* gene putatively coding for an α -expansin showed non-significant but notable increases in relative expression at Stages 2 and 3 compared to Stage 1 before dropping to Stage 1 levels at Stages 4 and 5 (Figure 4.19A). Relative expression of the *XTH1* gene coding for a xyloglucan transferase-hydrolase showed a very slight increase in Stages 1 and 3 compared to the other stages of development, but this was very variable and was not reflected statistically (Figure 4.19B).

The putative *PIP1* gene coding for Plasma membrane Intrinsic Protein 1 (PIP1) was found to increase significantly in relative expression from Stage 1 to Stage 3, peaking at an average of 4.82-fold higher than Stage 1 (Figure 4.19C). In Stages 4 and 5 relative expression of *PIP1* significantly decreased again until relative expression in Stage 5 was very similar to Stage 1.

Relative expression of the putative *AMY2* gene coding for the α -amylase enzyme was also found to increase over development and opening, peaking at Stage 5 with 2.46-fold higher relative expression compared to Stage 1 (Figure 4.19D).

Sucrose transporter genes were also found to be increased in relative gene expression over Stages 1-5. The putative gene *SWEET7* coding for a Sugars Will Eventually be Exported Transporter protein (*SWEET7* – Figure 4.19E) and the putative gene *MST6* coding for Monosaccharide Transporter 6 protein (*MST6* – Figure 4.19F) showed very similar patterns in relative expression over Stages 1-5 showing a significant increase

between Stage 4 and Stage 5 for *SWEET7*, and a non-significant rise for *MST6*. However genes coding for other sucrose transporters such as Sucrose Transporter 2 (*SUT2*) and Sucrose Transporter 4 (*SUT4*) did not show significant changes in gene expression over development and opening at all (Figures 4.19G, H). The putative gene coding for a cell wall invertase 4 (*CWINV4*) also showed no significant change in relative expression over Stages 1-5, possibly due to high variability in relative expression since there was a general trend in increase in mean expression from Stage 2 to 5 (Figure 4.19I).

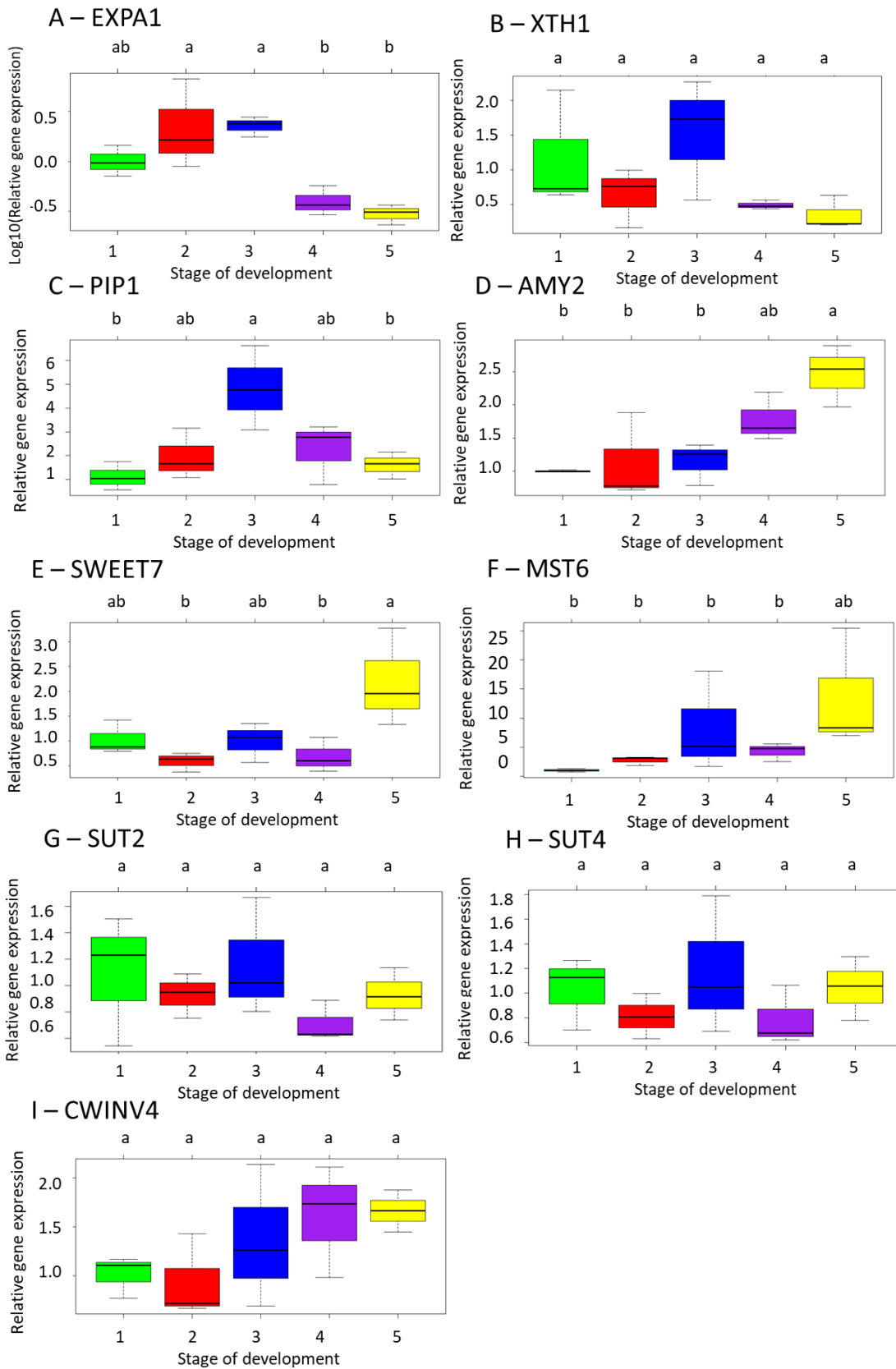


Figure 4.19 – Relative expression of putative flower opening-related genes over development and opening by real time qPCR. The values represent the medians of 3 biological replicates \pm

SD. Letters indicate statistical significance by one-way ANOVA with post-hoc Tukey or Kruskal-Wallis test with post-hoc Dunn. (A) relative expression of putative EXPA1 (Appendix 6.14A), (B) relative expression of putative XTH1 (Appendix 6.14B), (C) relative expression of putative PIP1 (Appendix 6.14C), (D) relative expression of putative AMY2 (Appendix 6.14D), (E) relative expression of putative SWEET7 (Appendix 6.14E), (F) relative expression of putative MST6 (Appendix 6.14F), (G) relative expression of putative SUT2 (Appendix 6.14G), (H) relative expression of putative SUT4 (Appendix 6.14H), (I) relative expression of CWINV4 (Appendix 6.14I).

4.4 Discussion

4.4.1 Is cell expansion in Oriental lily opening driven by carbohydrate mobilisation and metabolism?

Cell expansion was hypothesised to be driven in lilies through an osmotic pressure-driven change in soluble sugar content (related to starch breakdown, sucrose uptake from phloem unloading, or both). The starch breakdown was initially hypothesised as being highly important due to the work of Bielecki et al. (2000), who indicated cell expansion in lily tepals was related to amylase activity. That was supported in this study with correlative starch staining and starch assays showing that there was a gradual loss of tepal starch to a negligible amount between Stages 3 and 5 in several varieties. Mean starch content in Oriental lily ‘Sorbonne’ tepals on plant was also found to peak at mature bud stage at around $3.5 \text{ mg g}^{-1} \text{ FW}$ and then drop to less than $0.5 \text{ mg g}^{-1} \text{ FW}$ in the fully open flower (Watanabe et al. 2022), and under $3 \text{ mg g}^{-1} \text{ FW}$ in commercially treated Asiatic hybrid lily ‘Enchantment’ tepals (Clement et al. 1996) throughout development and opening (between closed bud to open flower). The data collected in this study supports the already published work relating to absolute starch content and the pattern over development, showing a drop in starch content with flower opening. However, the data in this study additionally compared differences in tepal starch content in different locations on the tepal (between tepal midribs and edges). Tepal edge sections showed significantly higher tepal starch content in Stages 1 and 3

compared to midrib sections and therefore suggests that tepal edges may retain a greater starch store and higher metabolism during flower opening.

The increased opening ability and acceleration in opening speed in cut lily flowers with added sucrose in the vase solution (Han 2003) suggested that the starch content in tepals may be insufficient in some cases and that a higher tepal soluble sugar content is required for opening. The tepal glucose, fructose and sucrose content was measured here as the major soluble sugars in lily flowers (Clement et al. 1996; Watanabe et al. 2022). The absolute content was difficult to compare due to differences in the method, but the pattern in changes in tepal glucose and fructose was very similar, showing a similar significant rise between the mature closed bud and open flower. The tepal sucrose content in this study showed no significant change over the stages of development, whereas Watanabe et al. (2022) showed a decrease in sucrose content between the mature bud and open flower. This may point to varietal differences as both experiments used flowers on plant. Higher concentrations of soluble sugars (glucose, sucrose, fructose) in tepal edge sections compared to tepal midrib sections again suggest that tepal edges are a much more metabolically active tissue than the midrib and also that they have a greater osmotic strength. This suggests that the cell expansion may be related to the correlated decrease in tepal starch content and increase in soluble sugar content.

The relative expression of several putative carbohydrate mobilisation or metabolism related genes was also investigated here to explore correlations between the expression pattern of these genes and other genes coding for more well-known proteins that have been indicated to have a direct impact on tepal cell expansion (aquaporin PIP1, expansin EXPA1 - Watanabe et al. (2022)). The genes putatively coding for PIP1 and EXPA1 showed a strong increase in relative expression between Stages 1 and 3, suggesting that these genes are involved very directly in flower opening, as they are expressed prior to opening and peak in the mature bud (Stage 3). A PIP aquaporin (PIP2) has been functionally characterized and identified as responsible for cell expansion in rose (Ma et al. 2008) and expansin expression strongly correlates with flower opening in rose (Yamada et al. 2009b) and lily (Watanabe et al. 2022). The expression of these genes therefore supports the already published literature, showing that PIP1 and EXPA1 are

transcriptionally upregulated just prior to flower opening and therefore may be important in opening.

The data for relative expression of putatively identified sucrose mobilisation/metabolism-related genes (*AMY2*, *MST6*, *SWEET7*, *SUT2/4*, *CWINV4*, *XTH1*) show late upregulation or no significant change at all over development and opening (Figure 4.14). Expression of these putative genes is not similar to the relative expression of putative *EXPA1* or *PIP1*. The significant increases in tepal soluble sugar contents and significant decreases in starch content during flower opening suggest that even if these particular putative genes are not involved, other members of the large gene families may be mediating this change in tepal metabolism during flower development and opening. Many processes are also not controlled transcriptionally but by post-transcriptional modification or protein localisation/modification. Xu et al. (2018) suggested that phloem loading is highly modifiable by external stimuli, but likely to be downregulated by transcriptional regulation of *SUT* genes; upregulation is more likely to be caused by post-transcriptional regulation. The tepal material used for qPCR was also from a range of positions on stem and therefore may show variability because of this inconsistency.

The increase in relative expression at Stage 5 compared to 1 may also suggest that these putative genes code for proteins involved in the recycling of nutrients around the stem rather than the opening process. Lilies and other species such as petunia remobilise nutrients such as sucrose from senescing flowers to buds at an earlier stage of development further up the stem due to changes in the sink strength of different flower organs (Van Meeteren et al. 2001; Chapin and Jones 2007). Therefore late expression post-anthesis could be linked to phloem loading out from the flower rather than an uptake, as once the cells have expanded and flowers are open there is no need for the cells to maintain their turgor and many species including lily show a decrease in turgor pressure in senescence, which is thought to be driven by ethylene (Eze et al. 1986; O'Donoghue 2006; Zhang et al. 2021).

4.4.2 Does commercial treatment have a negative impact on bud metabolic physiology over opening?

Commercial treatment (in particular harvest itself and cold/dark treatment) has been reported to affect opening, overall quality and longevity in multiple flower species. These problems were hypothesised to be related to starch and sugar content of tepals as a driver of cell expansion. Commercial treatment has been found here to significantly affect several factors which were hypothesised to be important in flower opening, such as tepal glucose, fructose, and sucrose content. In particular, tepal sucrose content was significantly lower in CT samples compared to OP at every stage of development, which suggests that commercially treated buds may be limited nutritionally. However, as most buds still open, the effects of nutritional constraint may affect longevity of the flower more than the flower opening itself.

Remarkably, considering the effect of commercial treatment on tepal soluble sugar contents, commercial treatment did not seem to have a significant impact on tepal edge starch content compared to on plant (Section 4.3.3). However, the starch staining experiments in Section 4.3.2 did not reflect this, as they suggested commercial treatment did have an impact on the quantity of starch stored in the tepal/ on how quickly that starch was broken down over development and opening. This could have occurred because of varietal differences between 'Tisento' and 'Ascot', as although they are both Oriental varieties, the increased size of 'Tisento' buds may lead to an increased energy requirement and a faster/more pronounced starch breakdown.

Metabolomic profiling also suggested that commercial treatment has a significant impact on the metabolome of flowers regardless of stage of development. The metabolome consists of all secondary metabolites produced by a particular tissue at a particular time. Untargeted techniques similar to this can therefore potentially provide information about chemicals related to colour or scent, secondary messengers, cell membrane and wall contents, and metabolically active compounds (Baptista et al. 2018; Antonio et al. 2021). However, it must be noted that untargeted analysis is unlikely to produce identification of individual metabolites (O'Shea et al. 2018), and the DIMEdb database used in this study was limited, particularly for plant compounds, so many of the compounds identified as important by Random Forest in this study could not be

specifically identified. CAP and Random Forest were therefore used as methods for comparing whole metabolome 'fingerprints' without requiring identification of compounds. These two powerful methods can identify differences between large datasets using both supervised (CAP) and unsupervised (Random Forest) approaches. Supervised (or constrained) approaches such as CAP require initial knowledge of groups and therefore are often better at classification, but require most of the factors which may affect the classification to be already known. Unsupervised/ unconstrained approaches such as Random Forest classify data without an *a priori* hypothesis or knowledge of sample groups (here individual metabolomic profiles), and therefore whilst less able to classify precisely, may be more accurate overall (Breiman 2001; Anderson and Willis 2003). Additionally, Random Forest can identify compounds important in the classification of profiles which can be partially identified as compound types/ classes using the DIMEdb database. Therefore differences identified by Random Forest in particular can be stated with more confidence, although if there is a good classification by CAP these differences are also of interest and could be investigated more thoroughly using a subset of compounds as has been done in this study.

When Random Forest analysis was carried out on all profiles with regard to treatment, putative flavonoids, coumarins and phenolic acids were identified as being most important in the classification according to this variable, which was similar to the classes of compound also putatively identified as being important in the classification according to stage of development. This suggests these two variables are similar in their effects, i.e. commercial treatment has the same effect on secondary metabolic activity relating specifically to these compounds. This has been observed previously in metabolic activity specifically relating to respiration (Ranwala and Miller 2005), but not to secondary metabolism as a whole. Phenolics, flavonoids, terpenoids and fatty-acid derivatives are important in many aspects of flower development such as colour and scent - in species such as *Rosa x hybrida* phenolics and flavonoids have been shown to correlate strongly with opening and colour change (Schmitzer et al. 2009) and in Oriental lily terpenoids, flavonoids and fatty acid derivatives were also highly linked to scent production (Vainstein et al. 2001; Shi et al. 2018b). Putative coumarins and stilbenes were important in the classification by Random Forest with regard to stage of development

and many of these compounds increased over development and opening, which may relate to plant chemical defence against herbivory (Matos et al. 2015), as well as being intermediates in anthocyanin and flavonoid production (Paul et al. 2022). Similar compounds were also important in the classification according to location on tepal, which suggests that the tepal edges are different to midribs on basis of different amounts or types of putative flavonoids and phenolic compounds being synthesised in different areas of the tepal. Metabolomes also showed many putative phenolic compounds, hydroxycinnamic acids and terpenes as being important in the ability to discriminate between on plant and commercially treated profiles using Random Forest. This may suggest that commercial treatment either delays/ physically reduces, or increases, certain aspects of metabolism such as scent, colour and cell wall production. When individual compounds were investigated in this study, the majority of the compounds in this chemical family showed significant increases in abundance in CT samples compared to OP at the same stage of development. In many species anthocyanin and flavonoid content have been observed to increase, often alongside a decrease in volatile scent compounds over cold/dark storage (*A. houstonianum* Mill., *T. lemmonii* A. Gray, *S. dorisiana* Standl., and *P. odoratissimum* (L.) L'Her "Lemon") stored at 4°C for six days (Marchioni et al. 2020). Gerberas, which also have highly pigmented petals in a large variety of colours, show increased anthocyanin and flavonoid content when stored at 6°C compared to 22°C, as well as increased expression of flavonoid metabolism genes (Naing et al. 2018b), which may explain differences in putative flavonoid and anthocyanin content between commercially treated and on plant buds. It should be noted that none of these studies compared the content to on plant controls. However, comparisons of flavonoid content in baby spinach leaves at harvest and after six and nine days of cold/dark storage (2°C) showed increases in many types of flavonoids (Bergquist et al. 2007), again suggesting that these compounds may increase in content with cold storage.

4.4.3 Does position on stem affect bud metabolic physiology over opening?

Position on stem was investigated here to understand if there was a nutritional deficiency in certain commercially treated stems with more buds per stem, disproportionately affecting the terminal bud's ability to open. It was hypothesised that

this deficiency was affecting the amount of nutrition taken up by each of the sink organs (the buds) on the stem, which take up differing amounts of sucrose in particular due to differences in sink strength of each organ (Van Meeteren et al. 2001). The sink strength is thought to be greater in less developed buds and would imply that terminal buds had access to more sucrose. However, due to the terminal bud being at the youngest developmental stage at harvest, these terminal buds presumably require the most nutrition to open, and in a nutrient-limited environment may be the most affected (Han 2003). However, the data presented here suggests there are no significant differences between Position A and C in tepal soluble sugar or starch content, which may indicate that Position C is not significantly different to Position A in terms of nutrition. This may partially explain why stems with three buds per stem do not have problems with opening, especially in Oriental cultivars (personal communication, James Cole, E.M. Cole Farms Ltd.) and furthermore suggests that in this particular environment there is no difference in the distribution of nutrition between buds, rather than a position on stem-dependent difference in overall nutrient content.

However, both CAP and Random Forest analysis comparing Position A and Position C tepal metabolomic profiles showed some subtle differences. In OP tepal edges and CT tepal midribs, CAP according to position on stem did show good separation between Position A and Position C tepals, suggesting that there are significant differences between the metabolic activity in specific regions of tepals from different positions on stem, and there is also very little overlap in the CAP plots for OP Midrib and CT Edge tepal metabolomes. Random Forest analysis, whilst not showing as much of a difference in the plots, was able to successfully classify Position A and C metabolomes with an estimate of error rate of below 25%. Compounds identified by Random Forest as being important in the classification of both all profiles (Table 4.7) and the subset of CT Edge profiles (Table 4.8) with regards to position on stem were mostly putative phospholipids, glycerides, and fatty acids. Phospholipids are the major component of cell membranes and alongside structural roles, some are essential as secondary messengers to regulate growth, development, senescence, and the stress response (Xue et al. 2007). Phosphatidic acid for example has been shown to be highly important as a secondary messenger in *Arabidopsis thaliana* and petunia flowers for development and other

uncharacterised processes (Yunus et al. 2015). Differences in phospholipid and fatty acid content can also be related to temperature stress; phospholipid composition is known to change in fruit such as peaches, with an increase in desaturated FAs such as linolenic acid and in particular N-acylphosphatidylethanolamines (NAPEs) after storage at 0°C (Zhang and Tian 2010). This may perhaps indicate differences in the tolerance or response of buds at different positions on stem to cold temperature. The individual compounds analysed here showed significantly higher abundances in Position A buds compared to Position C. The decreased levels of phospholipid and fatty acids observed in Position C buds could be due to a lower chilling tolerance in these buds; chilling injury often presents as membrane deterioration (Aghdam et al. 2016; Mohammadi et al. 2021), which may suggest that Position A buds have lower membrane deterioration or alternatively, that these particular compounds protect against chilling injury due to unsaturation or structure (Fobel et al. 1987; Parkin et al. 1989).

When the compounds indicated to be important in separating the subset of profiles (CT Edge profiles) by position on stem were analysed however, some compounds were significantly higher in Position A and some were higher in Position C tepals. Notably, the compounds which were putatively identified as fatty acids (X2421, X2159, X1275) or phospholipids (X2102) were found to be significantly higher in abundance in Position A tepals, whereas the compounds putatively identified as flavonoids (X4899, X5515, X3628) were significantly more abundant in Position C tepals. The increased abundance of flavonoids in Position C buds could indicate commercial treatment has an increased impact on the secondary metabolism of these buds as compared to Position A – as discussed in the previous section, commercial treatment has a significant impact on the flavonoid and anthocyanin content in several species (Naing et al. 2018b; Marchioni et al. 2020) and supported now in Oriental lily. The decreased fatty acid/phospholipid content in Position C buds could also be due to this same increased impact of commercial treatment on these buds in terms of greater chilling injury-related membrane deterioration, as mentioned above.

The lack of conclusive data to establish whether position on stem does have an impact on the physiology of lily buds shown here could be because commercially treated stems with three or even usually four buds do not usually show problems with opening,

especially for Oriental cultivars. As mentioned above, a higher position on stem did not show significant differences, either between the soluble sugar and starch content or the whole metabolomic profile in a position-dependent manner. According to the data, the differences between positions on stem are negligible or very subtle, suggesting that the carbon partitioning between buds at positions on stem, perhaps up to a certain point, is equal. This supports work showing that limiting carbohydrate supply to lily inflorescences did not cause differences between the weight of individual buds on the stem at each position, and it was concluded that it was unlikely that carbohydrates completely fulfilled a bud's requirement sequentially up the stem, leaving the terminal buds only lacking in nutrition, and it was more likely to be distributed more equally according to the bud's sink strength (Van Meeteren et al. 2001). There were also problems inherent in studying the effects of position on stem because of the non-comparable relationship between bud size and developmental stage between Position A and Position C/terminal buds. Position A buds were larger at the same stages of development by approximately at least 1 cm (depending on variety) in length and therefore may have had differences in the number of cells per bud and density of the tissue at each stage of development, although this was not measured in this study. This would have an impact on the measurable tepal starch and soluble sugar content per gram of fresh weight and may account for some of the slight observed differences between Position A and Position C buds.

4.4.4 Conclusions

The physiological mechanisms underlying flower opening in lilies have been investigated in this study. A significantly different sucrose, glucose, fructose and starch content in tepal edges compared to midribs correlates with the very different metabolomes observed in each. These differences indicates that tepal edges have a distinct physiology compared to midribs and that the greater cell expansion observed in tepal edges could be due to divergent development in each area, allowing for flower opening. While the genetic mechanisms behind cell expansion are still unclear, aquaporin- and expansin-coding gene expression correlates well with opening and their expression pattern provides a good comparison for other putatively important genes.

Commercial treatment has been shown here to have measurable, significant impact on the nutritional and metabolic status of tepals over development and opening. The lower levels of tepal sucrose, glucose and fructose content points to limited nutrient availability in commercially treated buds compared to on plant, which is corroborated by significantly different metabolomes comparing treatment. The lower tepal sucrose and glucose content justifies the current use of additional sugars in vase water to improve opening and longevity. Position on stem was hypothesised here to have significant impact on physiology and in particular nutrient availability, but thus far data suggests there may be very little nutritional difference between Position A and terminal bud content. Metabolomic differences point to subtle differences in cell membrane content, which may be exploitable if this effect is due to a greater propensity of higher position buds to commercial treatment-related chilling injury.

Chapter 5 - Exploring the genetic mechanisms and regulation of lily flower opening to understand its mis-regulation in postharvest bud abortion

5.1 Introduction

This chapter introduces some of the possible genetic mechanisms and regulation mediating the physical and physiological effects explored in Chapters 3 and 4. Understanding the difference in the precondition of postharvest terminal buds leading to successful versus unsuccessful opening can identify the regulators of flower opening in lilies, and may eventually lead to producing better pre- and postharvest treatments for commercially treated cut lilies.

5.1.1 The regulation of opening in lilies: what is currently known

Section 1.3 and 1.4 set out in detail the current knowledge around regulation of flower initiation, development, and opening, both in model species and in lilies. In short, several endogenous and exogenous factors, comprising information about the age of the plant, the other buds on the inflorescence, the nutritional status of the bud, the season (via light and temperature), and the time of day (Heins et al. 1982; Erwin and Heins 1990; Bielecki et al. 2000b; Van der Meulen-Muisers et al. 2001) have been shown to have an impact on the time or ability of bud opening. These factors can effect development and growth or mediate stress responses in plant species through phytohormonal and other subsequent forms of regulation (Kou et al. 2021; Mazzoni-Putman et al. 2021; Wahab et al. 2022).

Phytohormone signal transduction often leads to cascades of transcription factor expression and later, expression of target genes in large developmental changes such as flowering in *A. thaliana* (Izawa 2021). Understanding which target genes and which transcription factors and phytohormone related genes are co-expressed over flower opening can be a powerful method of identifying large scale changes in development in terms of gene expression and characterisation of groups of genes with identified functions (Rao and Dixon 2019). For example, genes which are thought to have a role in flower opening in lilies (coding for expansins, XTHs, aquaporins - Chapter 4) have been strongly implied to be auxin-promoted in other species such as waterlily (Ke et al. 2018). The co-expression of auxin response genes and regulatory genes (transcription factors, phytohormone biosynthesis and transduction

components) can be very useful to make accurate predictions of the role of different phytohormones and other pathways potentially feeding into flower development (van Dam et al. 2018).

5.1.2 Mis-regulation of flower opening in postharvest bud abortion

As described fully in Chapter 1, postharvest bud abortion or failure is a problem arising from too early harvest of lily inflorescences, specifically affecting terminal buds in stems which have a larger number of buds per stem than commercially ideal (Section 1.5.4). The arrested development in these terminal buds is the cause of consumer complaints and as mentioned before, is a latent issue generally not picked up by growers or retailers (personal communication, James Cole, E.M. Cole Farms Ltd.).

While nutrient insufficiency may have a role in some varieties in causing opening failure, generally it has not been found to be the primary reason preharvest (i.e. reduced irradiance only has not been found to increase risk of bud abortion). Miller and Langhans (1989) also suggested that other environmental stressors such as calcium levels, temperature, and moisture levels could be responsible, mediated by the ethylene response. As shown in Section 1.5.4, ethylene can be a preharvest cause of this arrested development and therefore will also be investigated in this study as a response to the hypothesised stress of commercial processing. Postharvest cold/dark treatment seems to have an additional negative effect on this failure to open of the terminal bud, with this phenotype being more pronounced in certain lily varieties - warmer storage temperatures were found to aid with opening of smaller or terminal buds in Oriental lilies, whilst having a senescing effect on larger ones (Miller 2014). Preliminary studies (Appendix 1) suggested very discrete bud lengths at harvest, depending on cultivar, at which buds which had the ability to open, and below which range all smaller buds failed to open. This suggests a tightly regulated opening process which is activated or arrested at a specific stage of development depending on the stress status of the stem and the bud, either due to nutritional or water insufficiency, temperature, or other developmental issues.

Harvesting stems at an earlier stage of development without the risk of problems like postharvest bud abortion is highly sought after by the commercial cut flower industry for the increased efficiency and throughput of lily crops. Understanding the endogenous

regulation of further bud development and opening at this early stage in lilies may therefore lead to targets for prevention.

5.1.3 RNA-seq as a tool to compare regulatory gene expression

RNA sequencing is a powerful tool to characterize the transcriptome in a snapshot of a certain context or condition compared to controls. Previously microarrays have been the major technique to compare expression of genes either over a time series (Van Doorn et al. 2003) or comparing the effects of different treatments on gene expression (Meir et al. 2010; Wagstaff et al. 2010) and work on the basis of comparing hybridisation of extracted mRNA in treatment and control samples to designed fluorescent probes (Galbraith and Edwards 2010). While much less initial sequence data is required for oligonucleotide microarrays, a certain amount is required to design microarrays and ensure accuracy of the probe hybridisations and resulting signals (Rao et al. 2019). However, newer technologies such as next generation sequencing (NGS) have revolutionised transcriptomic studies in non-model species such as lily due to no prior requirement for sequence information using a shotgun approach. This can sequence millions of reads from extracted mRNA converted to a cDNA library, which can either be mapped onto a reference genome, or *de novo* assembly of NGS reads allows contigs to be assembled without the requirement of a reference genome to align reads to (Hornett and Wheat 2012), which is often necessary in non-model species such as lily. RNA-seq is attractive for several reasons, including the ability to differentiate spliced gene variant expression (Trapnell et al. 2010) and having a large dynamic range, which can pick up transcripts expressed at low levels, such as transcription factors (Rao et al. 2019). Additionally, the large genome size of most commercial lily species make RNA sequencing a more attractive option since it limits sequencing to coding regions only (Strickler et al. 2012). Several studies have used *de novo* RNA sequencing methods to great effect in lily such as Shi et al. (2018), who used Illumina paired end sequencing with Trinity software to build a transcriptome and identify genes which may be related to a particular function by comparing gene expression in Oriental lilies in different conditions, and Zhang et al. (2015), who used a similar platform to find regulatory genes and pathways involved in flavonoid biosynthesis in relation to tepal colour.

Differentially expressed genes (DEGs) can be identified using a range of tools, which quantify and compare normalised count data for each assembled gene/gene fragment in pairwise statistical comparisons. Use of these methods is dependent on the experimental conditions and species used (Soneson and Delorenzi 2013; Stupnikov et al. 2021). Log² fold change (Log₂FC) values are commonly used as a measure of change in expression between conditions for a particular gene/gene fragment. The datasets can then be further analysed for enrichment of particular gene functions and pathways using databases such as Gene Ontology (GO) and the Kyoto Encyclopaedia of Genes and Genomes (KEGG - Kanehisa and Goto 2000). Regulatory networks can in this way be identified through analysis of groups of coexpressed genes, as well as databases of known interactions using model organisms such as *Arabidopsis thaliana*. Although lilies are a monocotyledonous plant, the organ of interest in this case (flowers) have a very different structure to the floral architecture of the closest well-annotated relative, rice (Yoshida and Nagato 2011), and therefore it may be more useful to find genes of interest by comparing to *A. thaliana*.

These analytical tools can therefore be a robust method to find transcription factors, hormone response genes and other early developmental factors such as circadian-related genes whose expression is assumed to be a necessary prerequisite to opening.

5.1.4 Aims of investigation

1. Identifying genes and pathways which may have a role in the physical flower opening process in Oriental lilies.
2. Identifying regulatory genes/pathways which may regulate the expression or activity of the genes identified in Aim 1.
3. Understanding how mis-regulation of these developmental processes may cause postharvest bud abortion.

5.2 Materials and methods

5.2.1 Collection of samples

Commercially treated Oriental lily stems (cv. Ascot) were grown under Cardiff University greenhouse conditions as described in Section 2.1.1.1. This cultivar was chosen due to its commercial popularity and greater propensity to have terminal buds which failed to open compared to other Oriental varieties. 15 stems (all stems had 4 buds per inflorescence) were harvested and commercially treated as described in Section 2.1.2.2. They were maintained in Cardiff University growth room conditions (Section 2.1.3) prior to and during the experiment to mimic commercial/consumer home conditions. At the start of the experiment the terminal bud (Bud D) for each stem was removed from the inflorescence and length was measured using a digital caliper. The top third of the inner and outer tepals was cut away carefully as described in Section 2.10. This top tepal material was immediately flash frozen in liquid nitrogen and stored at -80°C. The buds were maintained in a clean container full of sterile tap water (Section 2.1.3) and monitored for bud opening (identified as Small Remained Closed (SRC), Small Semi Open (SSO), or Larger Fully Open (LFO)) as indicated in Figure 2.5.

The length of the buds used in the experiment varied by 1 cm in order to keep the stage of development at the start of the experiment as similar as possible for all buds used. Notably, all buds which failed to open were the smallest of the range. Biological replicates (three individual buds from three individual inflorescences) were collected for each condition (Figure 5.1 shows the individual buds used in the experiment).

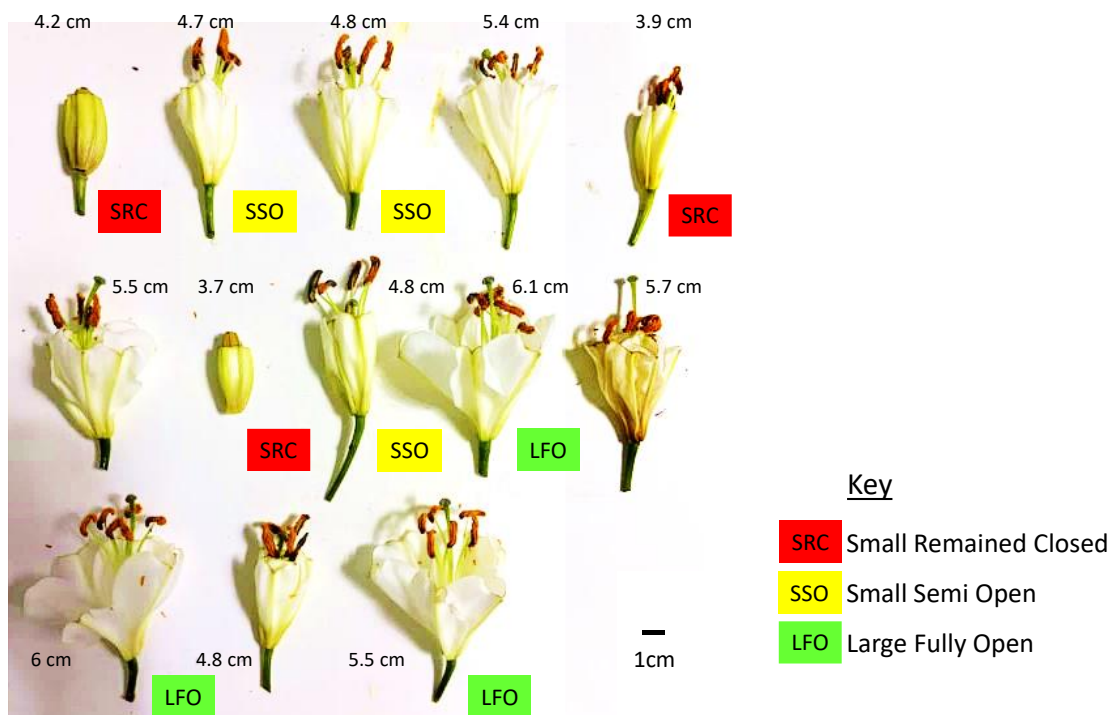


Figure 5.1 - the buds used at the end of this experiment. They were grouped according to the degree and magnitude of opening as described in Section 2.10. Three biological replicates were taken for each condition (Section 2.10) and are colour coded as described in the key to show the specific buds used in the experiment. The length of each bud at harvest is indicated.

5.2.2 RNA extraction and preparation for RNA sequencing

RNA was extracted from frozen material ground to a fine powder using a method adapted from Gambino et al. (2008), as described in Section 2.6.4. All buffers were made up fresh one day prior to RNA extraction. The RNA was checked for quality as described in Section 2.6.5. The extracted RNA (2 μ g) was treated with DNase (Invitrogen Turbo DNA-free kit) as described in Section 2.7 to remove genomic DNA. Treated RNA quantity and quality was assessed as described in Section 2.9.2 and 2.9.3.

5.2.3 RNA sequencing

RNA samples were assessed for quality using Qubit assay (Qubit RNA HS Assay Kit, Invitrogen) and then run on RNA ScreenTape (Agilent Technologies) on a TapeStation 2200 (Agilent Technologies). cDNA libraries were prepared using Illumina RNA Prep with

Enrichment (Illumina) and assessed for quality using D1000 ScreenTape (Agilent Technologies) on a TapeStation 2200 (Agilent Technologies) prior to sequencing. Paired-end sequencing was carried out on an Illumina NovaSeq 5000 for each sample. Quality of reads and sequence was assessed using FastQC (Babraham Bioinformatics). The quality assessment, library preparation and sequencing was carried out by Angela Marchbank at the Genomics Research Hub, Cardiff University School of Biosciences.

5.2.4 De novo assembly of transcriptome

A *de novo* transcriptome assembly and quantitative gene analysis was carried out using a Cardiff University based computer cluster (IAGO) accessed using MobaXterm Personal Edition (version 21.2). Unix scripts were adapted from those written by Professor Pete Kille of Cardiff University. Sequence files were uploaded to the cluster from Nextcloud. Adapter sequences and poor quality bases/sequence was removed from the reads using FastP software (version 0.23.1), using default settings.

The Trinity software package (v2.6.6) was used to assemble all reads into a reference transcriptome. The Trinity pipeline was used due to its indicated efficacy in constructing *de novo* transcriptome assemblies in complex and large non-model species (Haas et al. 2013; Madritsch et al. 2021). Post assembly, EviGene software (version 2019.10, v4) was used to annotate the reference transcriptome and BUSCO (v4.0.6) was used to compare orthologs (in this case, across all *Viridiplantae* genomes) and assess the completeness of the transcriptome.

5.2.5 Transcript quantification and identification of DEGs

Transcript quantification was carried out using RSEM (v1.3.3, Li and Dewey 2011) and Bowtie2 (v2.4.1) to estimate gene/isoform expression in each sample separately. The R package edgeR (Chen et al. 2014) was used to analyse count data and test for differential expression pairwise between SRC and SSO buds, SSO and LFO buds, and SRC and LFO buds.

NCBI BLAST+ (v.2.7.1) was used to identify genes/isoforms in the samples using default settings and an e-value cut-off of $1E^{-5}$. The sequences were queried against the *Arabidopsis thaliana*, *Oryza sativa* and *Viridiplantae* databases to compare the genes aligned with a well-annotated flowering plant (*A. thaliana*) and a monocotyledonous plant phylogenetically

closer but with less similar flower morphology (*O. sativa*), alongside a perhaps closer match from a more distantly related *Viridiplantae* orthologue. Due to small numbers of putatively identified genes in some groups, online blastP (protein-protein BLAST) was used to find the closest *Arabidopsis thaliana* orthologue. Again, blastP was run using default settings and an e-value cut-off of $1E^{-5}$. If an appropriate orthologue was not found using any of these methods, the DEG was not used in further GO term enrichment, KEGG pathway analysis or STRING protein functional network analysis.

The *A. thaliana* gene identifiers were used for further GO term enrichment, KEGG pathway analysis and STRING protein functional network analysis, but transcripts of interest from these analyses were cross referenced with the putative *O. sativa*/*Viridiplantae* gene to evaluate identification of these genes where possible.

5.2.6 Functional analysis of DEGs

A cut-off of <0.05 adjusted p-value (FDR) per DEG was used for subsequent analyses. No cut-off was applied for log₂FC value due to little variation in most transcript log₂FC values across conditions. DEGs were separated into lists of upregulated and downregulated genes for each comparison (SSO/SRC, LFO/SSO, LFO/SRC). Accession codes were assigned to transcripts using the Trinity unique identifiers to identify genes in each list.

The online tool Venny (v2.0) was used to create a Venn diagram of the DEGs in each comparison to identify common genes between each group. This was used to identify 3 distinct groups – those which were involved directly as a prerequisite of flower opening, those which are specifically to do with size of bud at harvest and therefore involved in the degree of flower opening only, and those which could be involved in either.

Gene ontology (GO) enrichment analysis was carried out using singular enrichment analysis (SEA) to identify enriched biological processes, molecular functions and cellular components in a dataset by comparing to the expected presence in a background. The online GO term/KEGG pathway enrichment tool ShinyGO (Ge et al. 2020) was used for GO term enrichment. In the case of some of the analyses with very small numbers of identified genes (Section 6.3.5), GO term enrichment was also carried out with PlantRegMap due to small numbers of enriched GO terms (Tian et al. 2020). In each case, the background was changed to all of the putative genes identified in the whole transcriptome assembly which aligned significantly to

an *Arabidopsis thaliana* gene. GO terms for each group with an P_{adj} value > 0.05 were also filtered out.

Several tools were used to create meaningful visual summaries of GO term enrichment analyses. Lists of GO terms enriched in various lists of DEGs alongside their respective p-values created by the online tool g:Profiler (Raudvere et al. 2019) were condensed using the online tool REVIGO (Supek et al. 2011). CirGO (Kuznetsova et al. 2019) was used to create circular diagrams using the condensed GO term lists and associated data. The online GO term/ KEGG pathway enrichment tool ShinyGO (Ge et al. 2020) was also used to create diagrams of the most enriched GO terms/ KEGG pathways for each list/group.

KEGG pathway analysis was carried out online using the KEGG Mapper tool (Kanehisa and Goto 2000). Due to lack of DEGs which aligned significantly to an *A. thaliana* gene, KEGG was only used to compare both SSO and LFO to SRC buds, as a comparison of preconditions of buds which opened to those which failed to. The pathway diagrams were colour coded to reflect the $\log_2\text{FC}$ between the conditions. Where more than one value was available (if the same read was found as a DEG in more than one comparison), the SSO/SRC comparison $\log_2\text{FC}$ value was taken.

STRING analysis was carried out using the online tool (Szklarczyk et al. 2015) to identify predicted gene coexpression and protein-protein interactions between the *A. thaliana* genes aligning significantly to DEGs in the 'Required to open' and 'Magnitude of opening' groups. These were also colour coded to reflect the $\log_2\text{FC}$ in the SSO/SRC comparison.

Selected DEGs of interest which were significantly highly different in $\log_2\text{FC}$ between SRC and SSO or LFO buds were validated by qPCR. Primers were designed from the read sequences of the DEGs of interest and are available in Table 2.2.

5.2.7 Coexpression analysis of DEGs

The package Genelines was also used in parallel in RStudio (v. 1.3.1093) to carry out K-means clustering on the count data quantified by RSEM and Bowtie2. This algorithm is used to identify clusters of DEGs which have similar expression patterns (from all the DEGs available) and therefore may be regulated together. Clusters showing meaningful patterns

were identified, and the *A. thaliana* genes aligning significantly to each cluster of interest was analysed for GO term enrichment analysis as described above (Section 5.2.6).

5.2.8 Identification, network analysis and expression analysis of regulatory genes of interest

The online tool PlantTFDB was used to identify transcription factors using the *A. thaliana* accession codes for each list of upregulated/downregulated genes. The PlantTFDB PlantRegMap was also used to identify functional interactions using *A. thaliana* accession codes between transcription factors and other genes in:

1. All DEGs identified in all comparisons
2. Each list of upregulated or downregulated genes for each comparison.

Additionally, the NCBI BLASTx online tool was used to manually identify other auxin-, cytokinin- and gibberellin-related genes, as well as MAPK pathway component-coding genes. Heatmaps of these identified TFs, hormone related genes and MAPK signalling-related genes were made using Genesis software (Sturn and Quackenbush 2002). Certain DEGs were selected on the basis of high raw count numbers and significant differences in log₂FC between SRC and SSO/LFO buds to validate by qPCR. Primers were designed from the read sequences of the DEGs of interest (Table 5.1, Section 5.2.10) and are available in Table 2.2.

5.2.9 Identification of TF motifs to investigate possible regulation of coexpressed DEGs

The online tool Simple Enrichment Analysis (SEA) (Bailey and Grant 2021), available on <https://meme-suite.org>, was used to identify enriched specific transcription factor motifs (background and database used here was *Arabidopsis thaliana* TF motifs from DNA affinity purification sequencing (DAP-seq) (O'Malley et al. 2016)) within query nucleotide sequences of a group of coregulated genes of interest. The query sequences used here were those up- or downregulated in the 'Required for opening' group only. Only motif alignments with E-values ≤ 10 were used – E value was here defined as the expected no. of motifs that would be as enriched in the background. The list of motifs identified from the nucleotide sequences was analysed for abundance of common plant TF motifs.

The online tool Find Individual Motif Occurrences (FIMO), available on <https://meme-suite.org>, was then used to identify which putative *A. thaliana* genes containing the three top labelled motifs most closely homologous to the DEGs in the ‘Required to open’ group, both upregulated and downregulated. The STRING database was used to annotate the TAIR gene identifiers.

5.2.10 qPCR validation of relative gene expression of genes of interest

Putative genes of interest identified to validate the transcriptomic data and their putative functions are shown in Table 5.1. Primers suitable for qRT-PCR were designed for the genes of interest (Table 2.1) using the online software Primer3. These genes of interest were chosen both on basis of $FDR < 0.05$ and an appropriate change in \log_2FC , indicating a significantly large fold change between SRC and SSO/LFO buds. The raw read count was also checked to ensure an appropriate expression level comparable to the reference gene. Relative expression analysis using qPCR was carried out as described in Section 2.9.4.

Table 5.1 – Genes of interest putatively identified to validate significant DEGs found in the transcriptome by qPCR

Putative gene name	Encodes	Function	Log ₂ FC SSO/SRC	Log ₂ FC LFO/SSO
ARF15	Auxin Response Factor 15	Part of the auxin transduction pathway	0.904	1.134
EXPA8	Alpha-expansin protein	Loosening cell walls – involved in cell expansion and growth (Marowa et al. 2016)	1.835	6.235
PSII5/PSBT	Photosystem II 5kDa protein, chloroplastic	Part of the Photosystem II reaction centre complex	-1.181	-2.698
R2R3MYB	MYB transcription factor	Part of a large family of transcription factors involved in secondary metabolism (e.g. biosynthesis and	1.441	3.204

		metabolism of phenylpropanoids, anthocyanins, lignins)		
SAUR75	Small Auxin Upregulated Response protein 75	Part of the auxin transduction pathway. Transcription occurs in response to auxin (Wang et al. 2020).	0.995	1.687
YUCCA 3 (YUC3)	Flavin monooxygenase-like enzyme	Enzyme catalysing a rate limiting step in auxin synthesis (Yamamoto et al. 2007).	0.379	1.234

5.3 Results

5.3.1 Characterisation of DEGs found between all conditions

Differential expression analysis using edgeR found 843 DEGs that were significantly differentially expressed in all three comparisons ($FDR/P_{adj} < 0.05$). Of these DEGs, 536 were used in subsequent analyses where an *Arabidopsis thaliana* orthologue could be identified using the cut offs stated in Section 5.2.5. The largest group of DEGs was identified as GO 1 (Response to wounding) which contained terms related to light intensity, abiotic stimulus, stress, and signal transduction (Figure 5.2). The second largest group, GO 2, contained varied terms related to photosynthesis, wounding, energy and metabolism, and signalling. DEGs relating to positive regulation of biological processes, protein modification and transmembrane transport were also found as more minor terms. This shows some very broad patterns which were explored further in subsequent analyses.

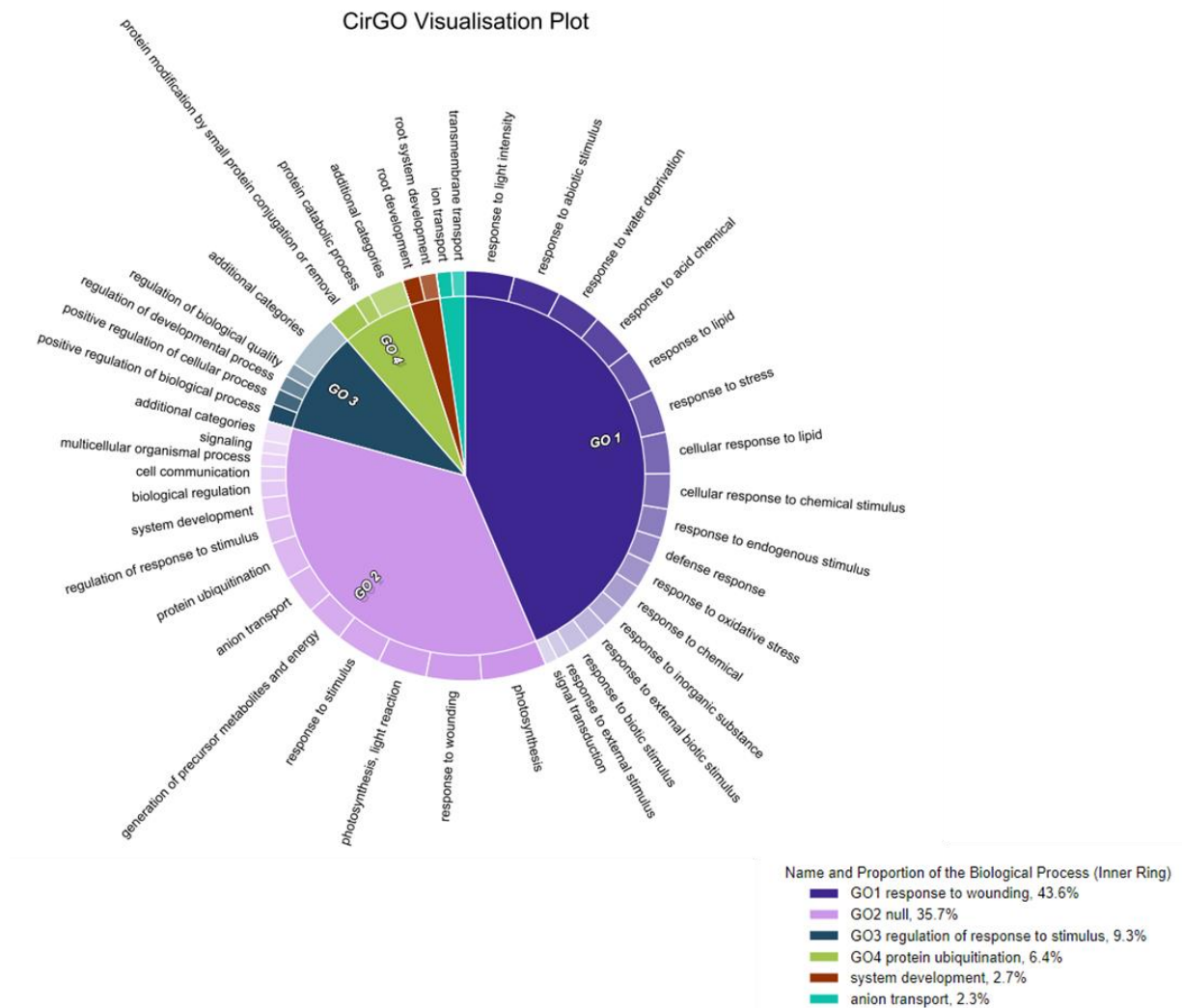


Figure 5.2 – Gene Ontology (GO) term enrichment using all DEGs in all comparisons which significantly aligned to an *A. thaliana* orthologue, comparing to a normal *A. thaliana* background using CirGO software (Kuznetsova et al. 2019).

5.3.2 Characterisation of DEGs between buds which subsequently opened and those which failed to

The comparison of DEGs between buds which failed to open (SRC) and all buds which showed opening ability (SSO and LFO buds) were first carried out as a general comparison between the transcriptome of normal opening buds and those which went on to suffer from postharvest bud abortion (Figure 5.3).

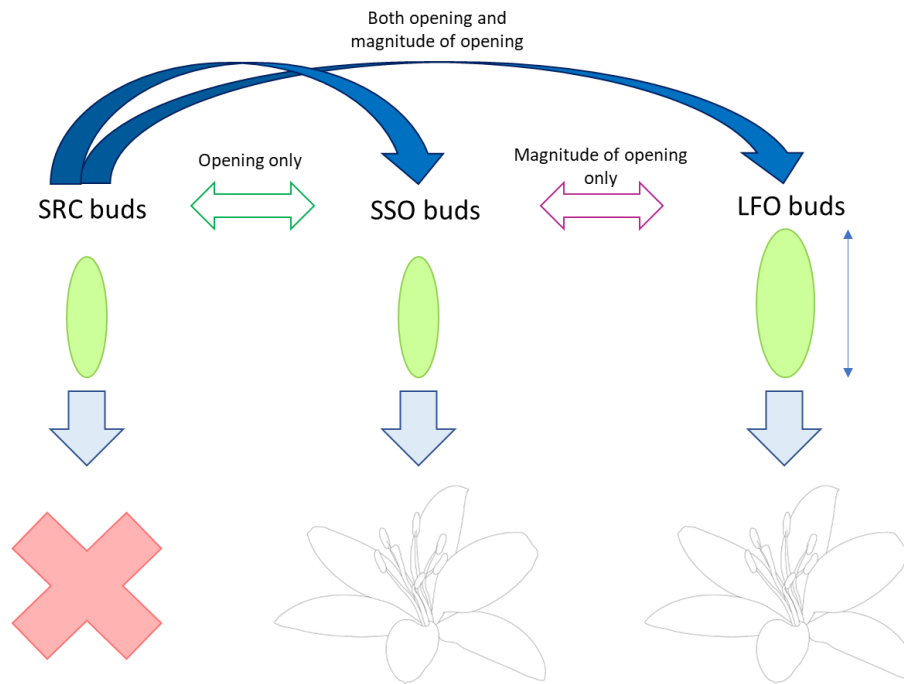


Figure 5.3 – filled in arrows indicate the comparisons used in the analysis in this section.

Comparisons between SRC and SSO/LFO were used here to show differences in gene expression between buds which went on to suffer from postharvest bud abortion (SRC buds) and those which developed normally (SSO/LFO buds).

5.3.2.1 GO term enrichment

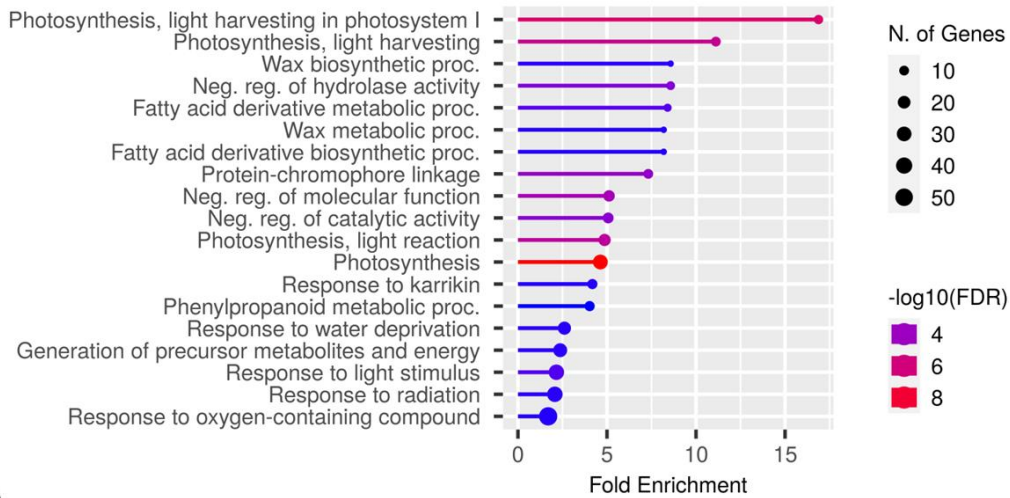
GO term enrichment was repeated using the list of DEGs which were significantly different in the SSO/SRC and LFO/SRC comparisons, as a general comparison between buds which went on to open and those which failed to. These analyses were carried out in a background of all the putative genes identified in the transcriptome, given the genotypic and phenotypic differences between *Lilium* species and *A. thaliana*. When these analyses were compared to the same analyses in an *A. thaliana* background there were also differences in the enrichment of certain terms. Biological process GO term analysis (Figure 5.4A) indicated a highly enriched process was photosynthesis (31 out of 275 genes), and in particular light harvesting in Photosystem I (9 out of 23 genes), indicating a greater expression of photosynthesis-related genes in SRC buds. Fatty acid derivative metabolic process (7 out of 39 genes), phenylpropanoid metabolism (11 out of 147 genes), and wax biosynthetic process (6 out of 29 genes) were also highly enriched in DEGs found between SRC and

SSO/LFO buds. Additionally, negative regulation of molecular function (15 out of 272 genes) and of catalytic activity (13 out of 259 genes) was also identified as being significantly overrepresented (Figure 5.4A, Appendix 4.1A). Finally, response to water deprivation (22 out of 404 genes) and response to light (35 out of 746 genes) were also significantly enriched.

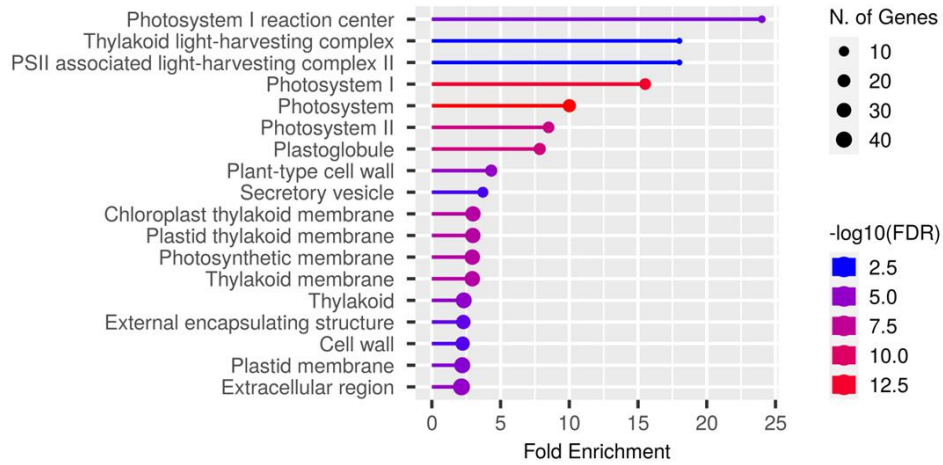
Cellular compartment GO term analysis (Figure 5.4B, Appendix 4.1A) showed strong enrichment of Photosystem I and II (Figure 5.5B), specifically Photosystem I reaction centre (4 out of 8 genes), and PSII associated light harvesting complex II (3 out of 6 genes), supporting this overrepresentation of putative photosynthesis-related DEGs. Also of interest was the enrichment of the plant-type cell wall (17 out of 237 genes) and extracellular region (47 out of 1923 genes).

Molecular function GO term analysis (Figure 5.4C) contained several significantly enriched (FDR<0.05) GO terms (Appendix 4.1A). DEGs with hydroxycinnamoyltransferase activity (2 out of 3 genes) were found to be over 30-fold enriched, and serine-type endopeptidase inhibitor activity compared to the transcriptome background was also 15 fold enriched (3 out of 28 genes). DEGs putatively containing chlorophyll binding functions were also found overrepresented (9 out of 34 genes), as well as those putatively containing abscisic acid binding activity (4 out of 19 genes).

(A)



(B)



(C)

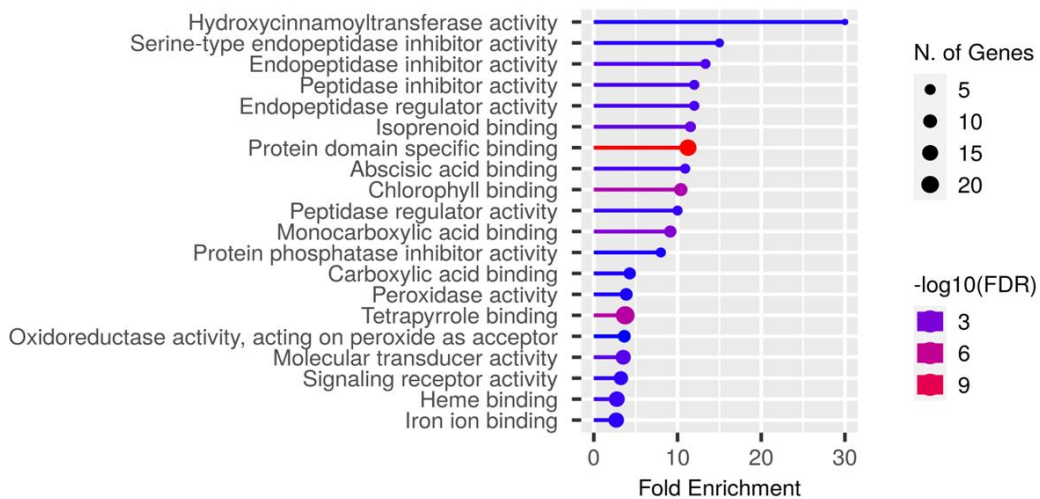


Figure 5.4 – Gene Ontology (GO) term enrichment showing the most significant GO terms, number of genes and adjusted p-value (FDR) overrepresented in the DEGs which significantly aligned to an *A. thaliana* orthologue between buds which opened (SSO and LFO buds) compared to those which failed to open (SRC). This was compared to a background

containing all putative genes identified in the transcriptome also aligning to an *A. thaliana* orthologue. GO term enrichment is shown for (A) biological process, (B) cellular compartment, and (C) molecular function. Graphs created using the online ShinyGO tool (Ge et al. 2020). A full list of significantly enriched GO terms and the associated *A. thaliana* genes can be found in Appendix 4.1A.

5.3.2.2 KEGG pathway analysis

The list of DEGs statistically significantly different in the comparisons between SRC and SSO/LFO buds (FDR<0.05) was used for KEGG pathway analysis due to the number of DEGs required to see change in whole pathways. This was carried out in a background of all putative genes identified in the transcriptome. Differences in photosynthetic pathways were the most overrepresented, with the phenylpropanoid pathway alongside general secondary metabolism, and the hormone and MAPK signalling pathways also significantly overrepresented (Figure 5.5, Appendix 4.1B). The specific genes involved in this enrichment were further investigated to identify which parts of the pathways these genes were involved in and which conditions they were more or less expressed in.

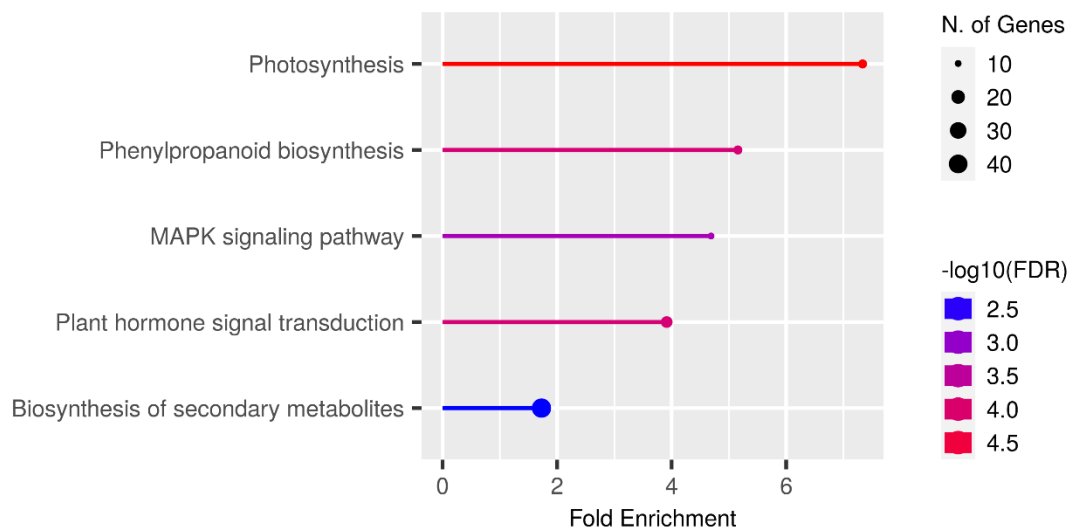


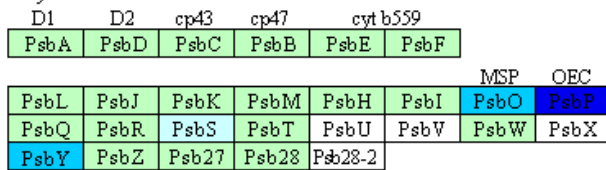
Figure 5.5 – KEGG pathway analysis of all DEGs between SRC and SSO/LFO buds, carried out using a background of all putative genes found in the transcriptome, showing all significant pathways enriched. Size of the circle represents number of genes found, whilst colour represents FDR. Photosynthesis (ko00196, 11 out of 76 genes) was found as most enriched

(7.34 fold), with phenylpropanoid biosynthesis (ko00940, 11 out of 174 genes), MAPK signalling pathway (ko04010, 10 out of 136 genes), plant hormone signal transduction (ko04075, 15 out of 286 genes), and biosynthesis of secondary metabolites (ko01110, 43 out of 1243 genes). A full list of significantly enriched KEGG pathway terms and the associated A. thaliana genes can be found in Appendix 4.1B.

In-depth KEGG pathway analysis was carried out on the same subset of putative genes significantly differentially expressed between SSO/LFO and SRC buds using the KEGG Mapper tool (Kanehisa and Goto 2000, Figures 5.6, 5.7, 5.8, 5.9). KEGG pathway analysis showed enrichment of photosynthesis-related pathways very strongly (11 out of 76 genes, FDR= 1.2E-05). Indeed, all of the putative genes involved in photosynthesis were significantly less expressed in buds which later could open compared to those which failed to open (Figure 5.6). In particular, DEGs aligning significantly with individual components in Photosystem I (6) and the light harvesting chlorophyll protein complex (7) were expressed considerably less in SSO/LFO compared to SRC buds, showing log₂FC values under -2.1.

PHOTOSYNTHESIS

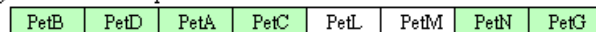
Photosystem II



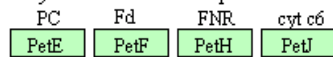
Photosystem I



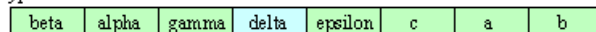
Cytochrome b6/f complex



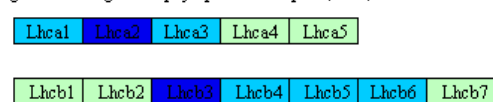
Photosynthetic electron transport



F-type ATPase



Light-harvesting chlorophyll protein complex (LHC)



Key (log₂FC)

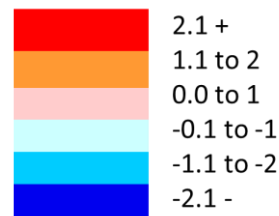


Figure 5.6 – KEGG pathway map for photosynthetic components, colour coded to show the log₂FC value for the SSO/SRC and LFO/SRC comparisons (red indicates positive log₂FC and blue indicates negative). The log₂FC for the SSO/SRC comparison was used if the component was a DEG in both SSO/SRC and LFO/SRC comparisons.

The phenylpropanoid synthesis and metabolism pathway was also indicated by ShinyGO to be highly overrepresented. The DEGs aligning significantly with components of these pathways show large differences in log₂FC between SRC and SSO/LFO buds (Figure 5.7). Some components such as the putative genes coding for an O-methyltransferase (2.1.1.68) and cinnamyl-alcohol dehydrogenase (1.1.1.195) showed higher expression in SSO and LFO buds compared to SRC (pathway components coloured red/orange, Figure 5.7). Putative ferulic acid 5-hydroxylase (F5H) a lysophospholipase (3.1.1.-), and a peroxidase (1.11.1.7) on the other hand show higher expression in SRC compared to SSO or LFO buds (pathway components coloured blue, Figure 5.7). It is therefore unclear if phenylpropanoid synthesis

and metabolism as a whole is upregulated or downregulated between SRC and SSO/LFO buds, suggesting a possible shift in the type of metabolites being synthesised.

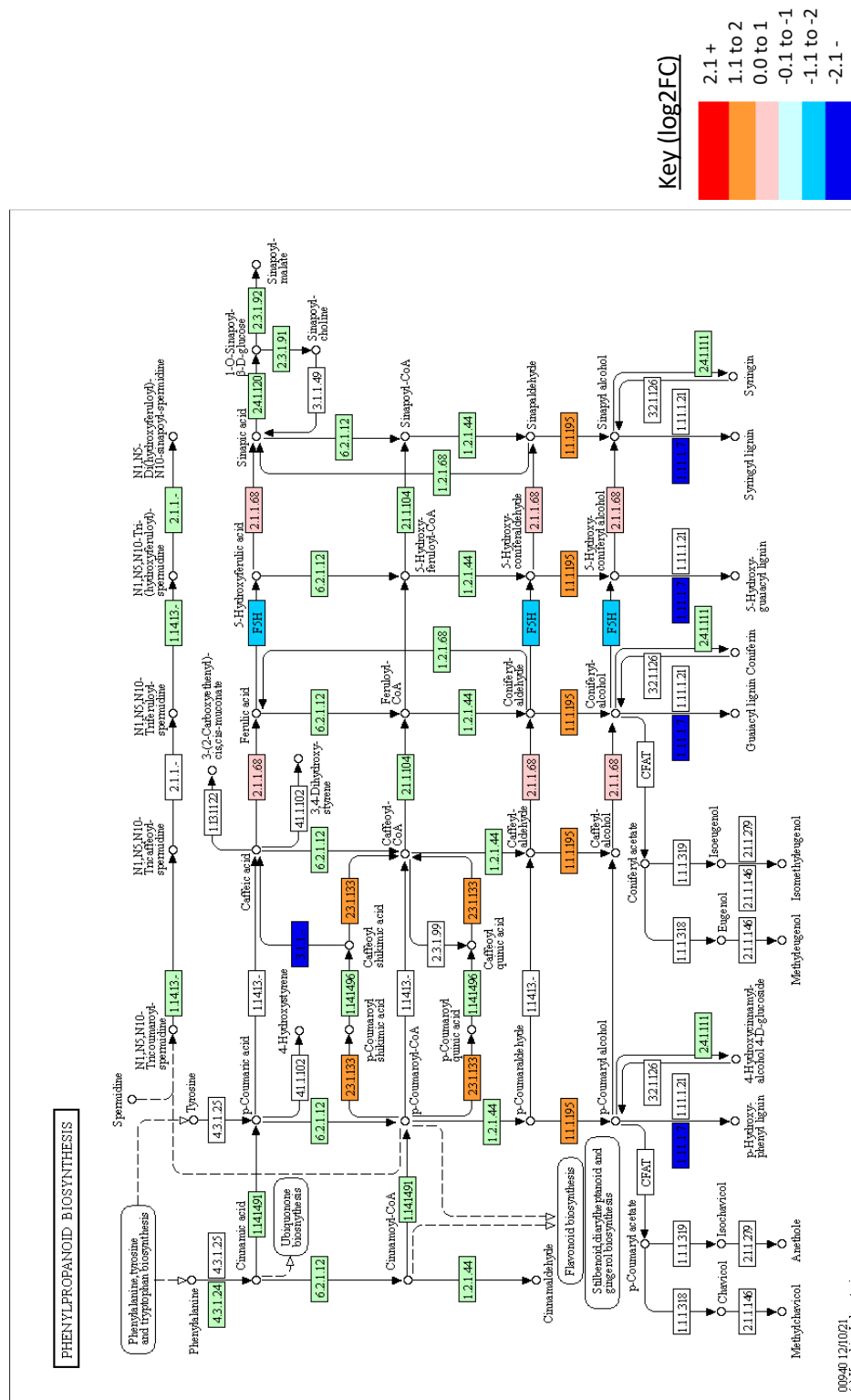


Figure 5.7 – KEGG pathway map for the phenylpropanoid biosynthesis and metabolism pathway, colour coded to show the log₂FC for the SSO/SRC and LFO/SRC comparisons (red

indicates positive \log_2FC and blue indicates negative). The \log_2FC for the SSO/SRC comparison was used if the component was a DEG in both SSO/SRC and LFO/SRC comparisons.

The MAPK signalling pathway (10 out of 136 genes, FDR=0.0006) and plant hormone signal transduction pathways (15 out of 286 genes, FDR= 0.0001) were also both found to be over 4-fold enriched. Both pathways have a great deal of overlap in terms of components and were looked at together. Putative *ERF1*, part of the ethylene response, was found to be expressed less highly in buds which went on to open (SSO/LFO) compared to those which failed (SRC), as well as other DEGs significantly aligning to ethylene-, ABA- and jasmonic acid-involved genes such as *RANI*, *PYL* genes and *MYC2* (Figure 5.8). Putative *MKK4/5*, a key part of the MAPK cascade was also found to be expressed more in buds which would fail to open (SRC) compared to buds which could open (SSO/LFO). The auxin, cytokinin and gibberellin signal transduction pathways also showed several putative components downregulated in buds which eventually opened compared to those which failed to do so (Figure 5.9). For auxin or cytokinin, these seem to be part of the negative regulation of these pathways, such as Aux/IAAs or A-type ARRs. In the gibberellin transduction pathway, *GID2*, an inhibitor of the DELLA proteins appears to be expressed more highly in buds which fail to open compared to those which go on to open. The DEG aligning significantly to a gene coding for a PYL receptor, which directly negatively regulates the ABA response, was expressed less in buds which opened, suggesting there may be a slight upregulation of the ABA-mediated drought response in SSO/LFO buds compared to SRC buds.

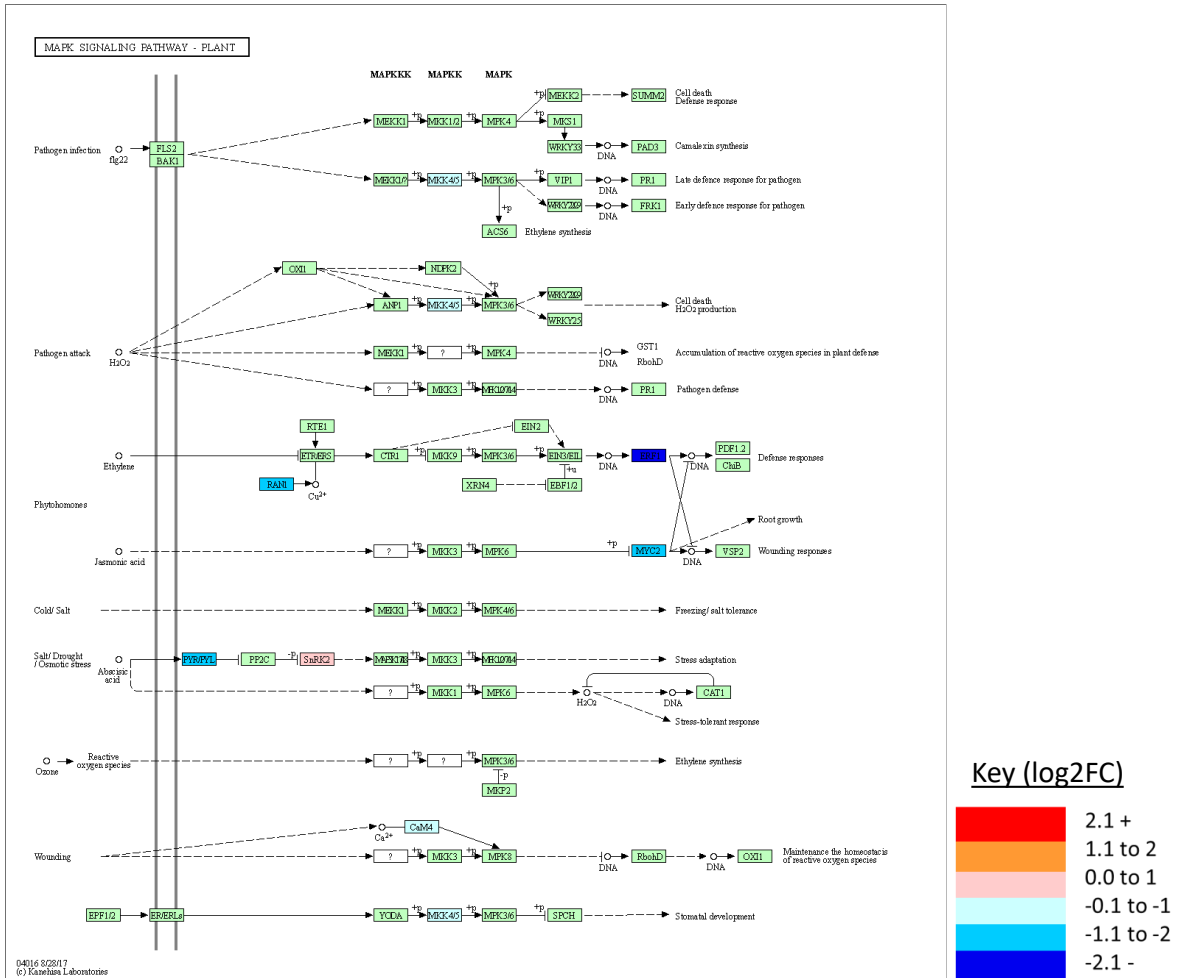


Figure 5.8 – KEGG pathway map for the MAPK signalling pathway, colour coded to show the log2FC for the SSO/SRC and LFO/SRC comparisons (red indicates positive log2FC and blue indicates negative). The log2FC for the SSO/SRC comparison was used if the component was a DEG in both SSO/SRC and LFO/SRC comparisons.

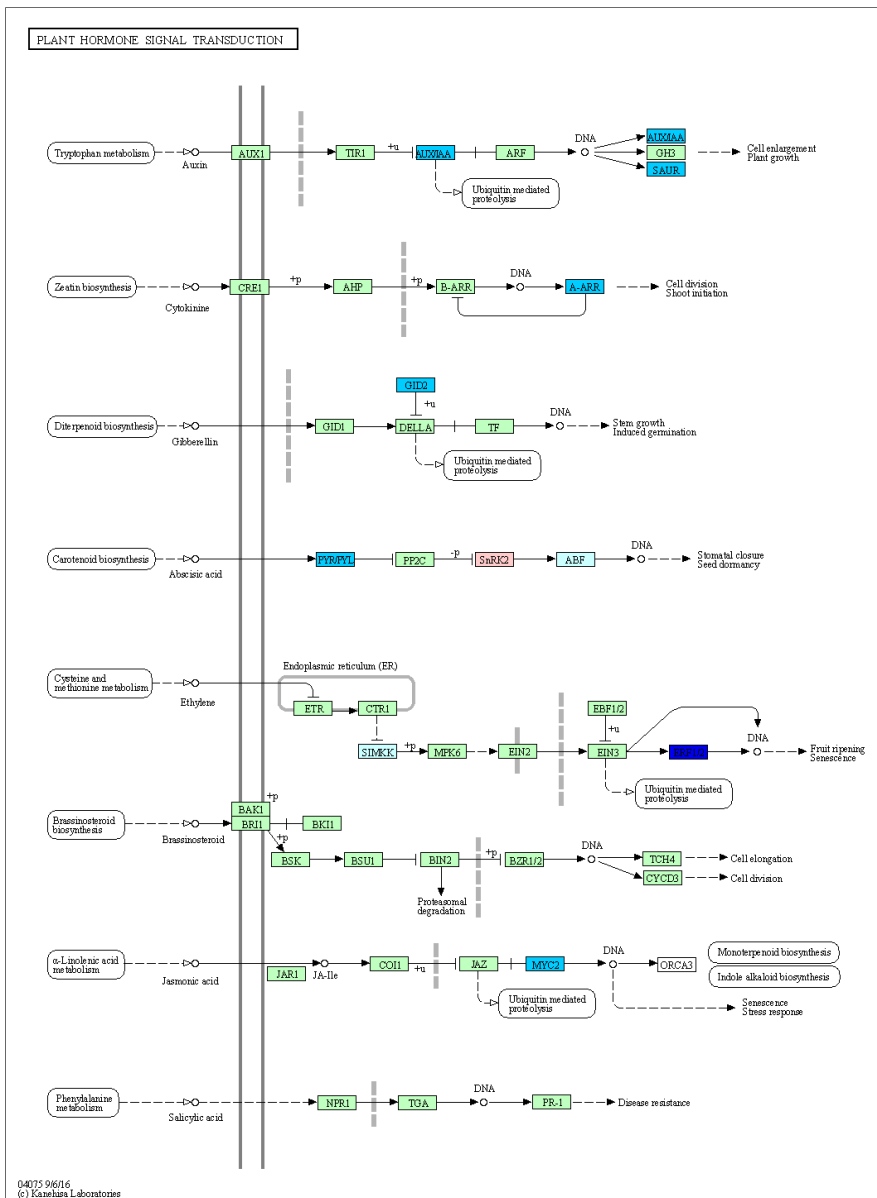


Figure 5.9 – KEGG pathway map for the plant hormone signal transduction pathway, colour coded to show the log₂FC for the SSO/SRC and LFO/SRC comparisons (red indicates positive log₂FC and blue indicates negative). The log₂FC for the SSO/SRC comparison was used if the component was a DEG in both SSO/SRC and LFO/SRC comparisons.

5.3.3 Separating DEGs into those necessary for opening and those related to differences in size and stage of development

Analysis of common DEGs between each comparison (Figure 5.10) showed the most DEGs in the LFO/SRC only group with 382 unique transcripts. SSO/SRC and LFO/SSO only groups had

a similar number of unique transcripts with 151 and 143 unique transcripts respectively (Figure 5.10). The smallest groups were those shared with all three comparisons (4 DEGs), and DEGs shared between SSO/SRC and LFO/SSO comparisons (10 DEGs). DEGs were split into three groups for further analysis. The 'Required to open' group was identified as DEGs purely required to open controlling for size (SSO/SRC only consisted of 151 DEGs and the 77 DEGs overlapping between the SSO/SRC and LFO/SRC groups because they are specifically found differentially expressed between buds which open and those which cannot, even at the same size). The 'Magnitude of opening' group was specifically involved in the degree of opening only, rather than the opening process (LFO/SSO only: 143 DEGs). The last group comprised the rest of the DEGs from all other sections of the Venn diagram, which may have been involved in both opening and degree of opening (472 DEGs).

The 'Required to open' group comprised 134 DEGs out of 228 more highly expressed in SSO compared to SRC buds (more highly expressed in flowers which opened compared to those which failed), while 126 were significantly less expressed in SSO compared to SRC buds (less expressed in flowers which opened). The 'Magnitude of opening' group contained 83 DEGs significantly more expressed in SSO (smaller buds which opened partially) compared to LFO buds (larger buds which opened fully) while only having 20 DEGs which were less highly expressed in SSO buds compared to LFO buds. This suggests that the degree of opening is driven more by genes being upregulated than downregulated, whereas the genes involved as a prerequisite to opening are more equally split between up- and downregulated.

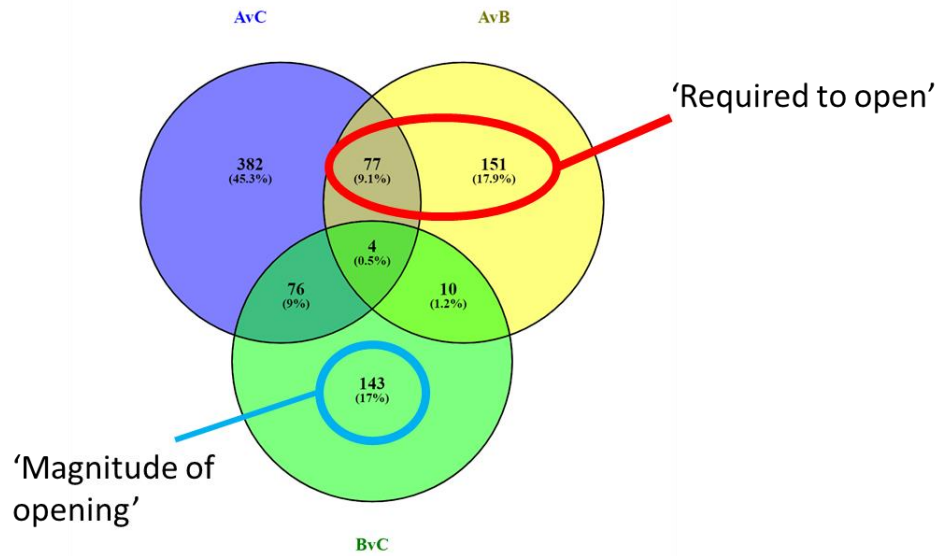


Figure 5.10 – Venn diagram showing the number of DEGs unique to and shared between each comparison, with groups identified as having a role purely in flower opening ('Required to open' group) and having a role in the degree of opening only, relating to size at harvest of the bud ('Magnitude of opening' group).

5.3.4 Analysis of genes required for flower opening

This section analyses the DEGs hypothesised to be purely involved in flower opening (Figure 5.11). GO term analysis using ShinyGO showed 44 significantly enriched GO terms in the 'Required to open' group of genes. As shown in Figure 5.12A, a large proportion of these were related to regulation or negative regulation of various protein activities (12 out of 272 genes, FDR=1.22E-07). Some of the other enriched terms of note were response to water deprivation (10 out of 402 genes, FDR=0.013) and response to wounding (7 out of 222 genes, FDR=0.012), suggesting that there are differences in stress levels between SRC buds and SSO buds. The putative genes associated with these stress-related terms were found to be upregulated in SRC compared to SSO buds. Photosynthesis and response to light intensity were not significantly overrepresented in the group of DEGs significantly changed between SRC and SSO buds but the photosystem was indicated to be overrepresented as a cellular compartment (6 out of 95 genes, FDR=0.009 - Figure 5.12B), supporting the possible small differences in photosynthesis between SRC and SSO buds. Arsenate ion transmembrane

transport was highly enriched, with 2 out of 3 genes putatively identified (Figure 5.12A,C) aligning significantly with two *A. thaliana* phosphate transporter genes *PHT1.1* and *PHT1.7*.

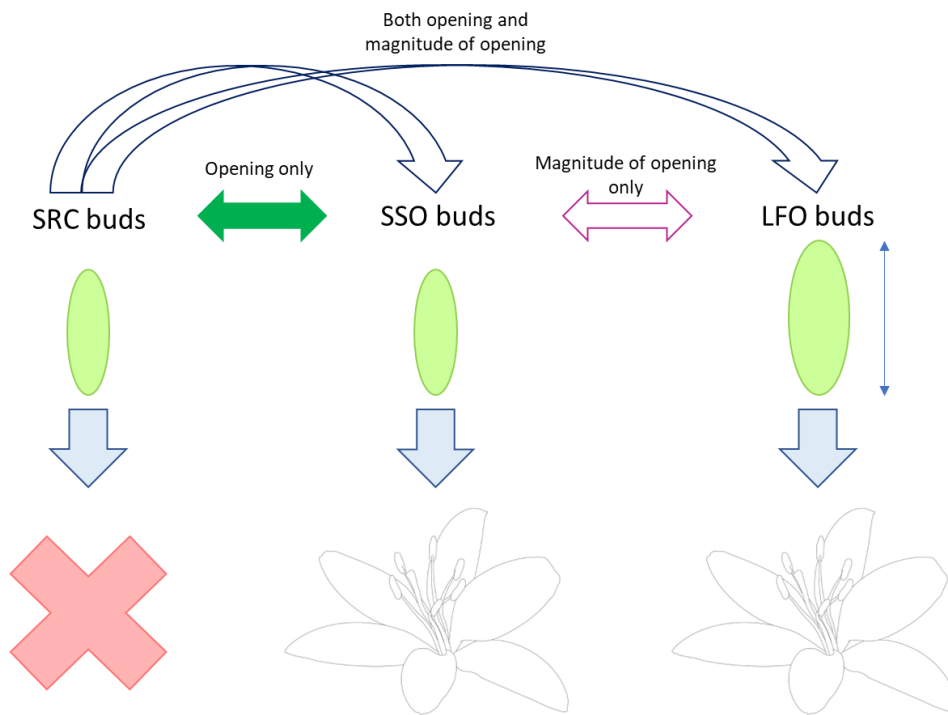


Figure 5.11 – filled in arrows indicate the comparisons used in the analysis in this section. Comparisons between SRC and SSO buds only were used here to show differences in gene expression specifically between precondition of the same sized buds at harvest which failed to open and those which were able to.

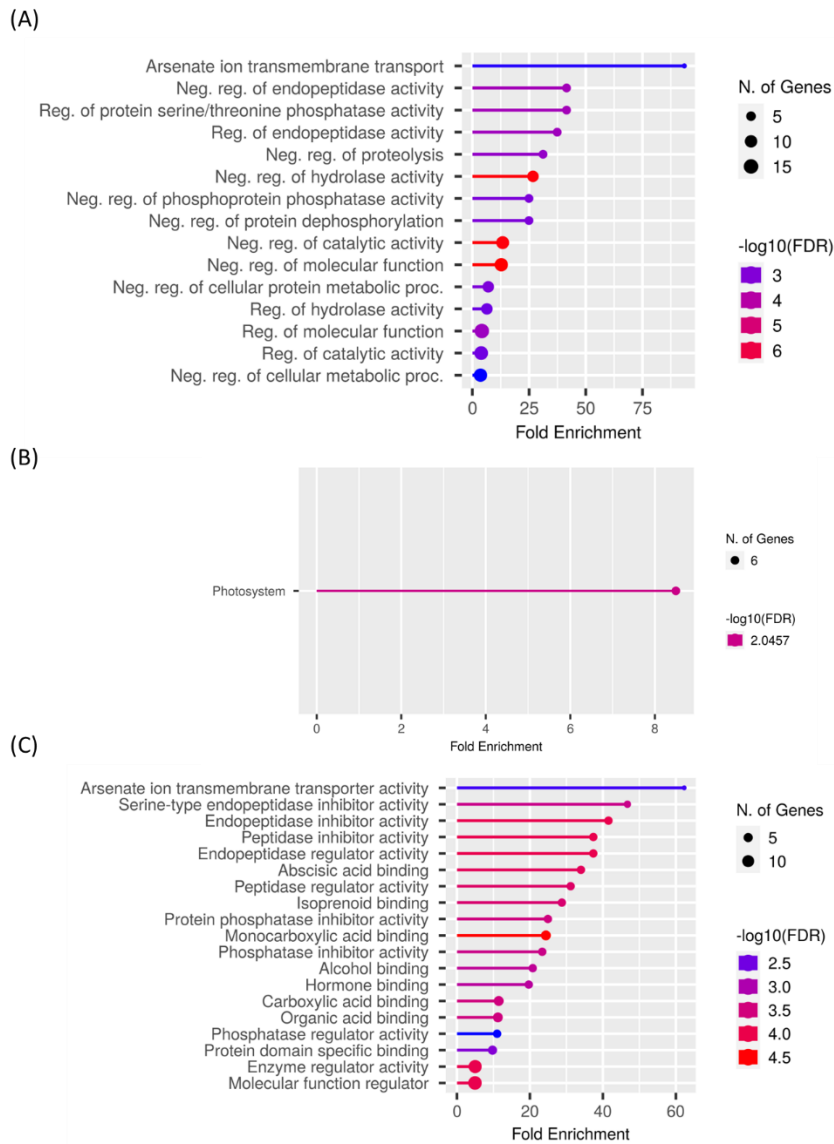


Figure 5.12 – Gene Ontology (GO) term enrichment showing the most significant GO terms, number of genes and adjusted p-value (FDR) overrepresented in the DEGs between similar sized buds which opened (SSO) compared to those which failed to open (SRC), including only DEGs which significantly aligned to an *A. thaliana* orthologue. This was compared to a background containing all putative genes identified in the transcriptome also aligning to an *A. thaliana* orthologue. GO term enrichment is shown for (A) biological process, (B) cellular compartment, and (C) molecular function. Graphs created using the online ShinyGO tool (Ge et al. 2020). A full list of significantly enriched GO terms and the associated *A. thaliana* genes can be found in Appendix 4.2.

STRING analysis showed some possible networks of known interactions which may be important in the flower opening process (Figure 5.13). The largest network showed links between several photosynthesis-related genes, namely *LHCA1*, *PSAK*, *PSBY*, *PSBX*, *AT1G51400* (coding for PSII 5kD protein), and *PSAD-2*. These were all both found coexpressed in *A. thaliana* and also were shown to have protein-protein interactions in literature. The generally similar expression between this group of genes which showed greater expression in SRC buds compared to SSO buds supports the same coexpression observed in this study. *LHCA1*, *PSAK* and *PSAD-2* were additionally found to have known protein-protein interactions which had been experimentally determined and from curated databases. *PSAD-2* was also found to interact with the product of *AT1G03220*, putatively coding for an aspartyl protease. This in turn was also found to have links with a gene product putatively coding for an anthocyanidin 3-O-glucosyltransferase, which was found to be highly upregulated in SSO buds compared to SRC buds.

Another network found by STRING centres around putative *MYC2*, which was suggested to have interactions with six other DEGs in the 'Required to open' group. *PHOT1*, coding for a phototropin, and putative *ABCG22* (coding for an ABC transporter) were found significantly more expressed in SSO compared to SRC buds. *PHOT1* protein was experimentally shown by yeast-2-hybrid to have interactions with *MYC2*. Other proteins also suggested to have an interaction with *MYC2* were the putative ABA receptor *PYL6*, a putative uncharacterised WRKY transcription factor, putative *SLY1* (a regulator of gibberellin signalling via interactions with DELLA proteins), and a putative fatty acid hydroxylase (*CYP94C1*) involved in negative feedback of the jasmonate pathway. The genes coding for these proteins were all upregulated in SRC compared to SSO buds, as was *MYC2*.

Another network which shows strong links between each other is the network of putative *FAR4*, *LACS1* and *CER1*, all of which show similar coexpression (upregulated in SSO compared to A). These putative genes all encode fatty acid metabolism-related proteins - *FAR4* being a fatty acid reductase, *LACS1* a fatty acid synthase, and *CER1* is a hydroxylase. This suggests that fatty acid synthesis is upregulated in buds which open compared to those which fail to open.

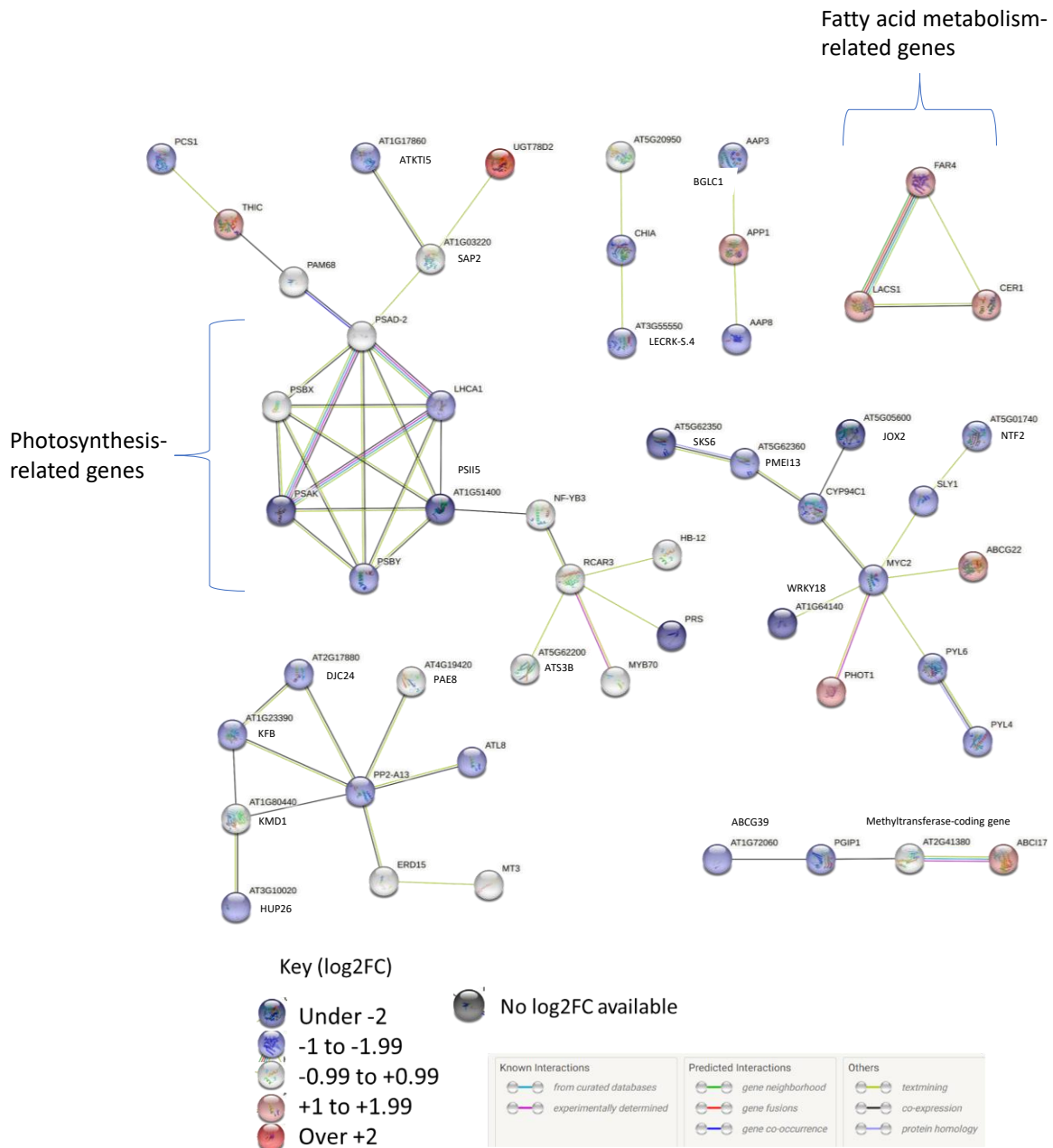


Figure 5.13 – STRING analysis to show protein-protein interactions between the DEGs in the ‘Required to open’ group, showing expression (log₂FC) as colour of the bubbles (log₂FC as expressed in the SSO/SRC comparison) and interaction type as line colour (Szklarczyk et al. 2015).

5.3.5 Analysis of genes relating to magnitude of opening

This section analysed the genes specifically differentially expressed between buds which opened at a smaller and larger length at harvest, displaying a difference in the magnitude of

opening (Figure 5.14). GO term enrichment analysis using ShinyGO identified several significantly enriched terms in an *A. thaliana* expression background in the list of DEGs between SSO and LFO buds (Figure 5.15). The following analyses were also carried out in a background of all the putative genes identified in the transcriptome significantly aligning to an *A. thaliana* gene. Significantly enriched terms in both analyses included various mannosidase activities as well as fructose-1,6-bisphosphate phosphatase activity (Figure 5.15B), and were highly enriched in lipid droplets, the apoplast/extracellular region, and the stromule (Figure 5.15A). The genes associated with these terms were more highly expressed in LFO compared to SSO buds, suggesting these activities and cellular regions were more active in buds harvested at a larger size. Additionally, although significantly overrepresented GO terms for biological process were not found using the transcriptome as a background, they were identified in an *A. thaliana* background; the terms for the dark reactions of photosynthesis, carbon fixation, and the pentose-phosphate cycle were significantly overrepresented, as well as the pigment metabolic process, all of which were also associated with DEGs upregulated in LFO compared to SSO buds (Appendix 4.3).

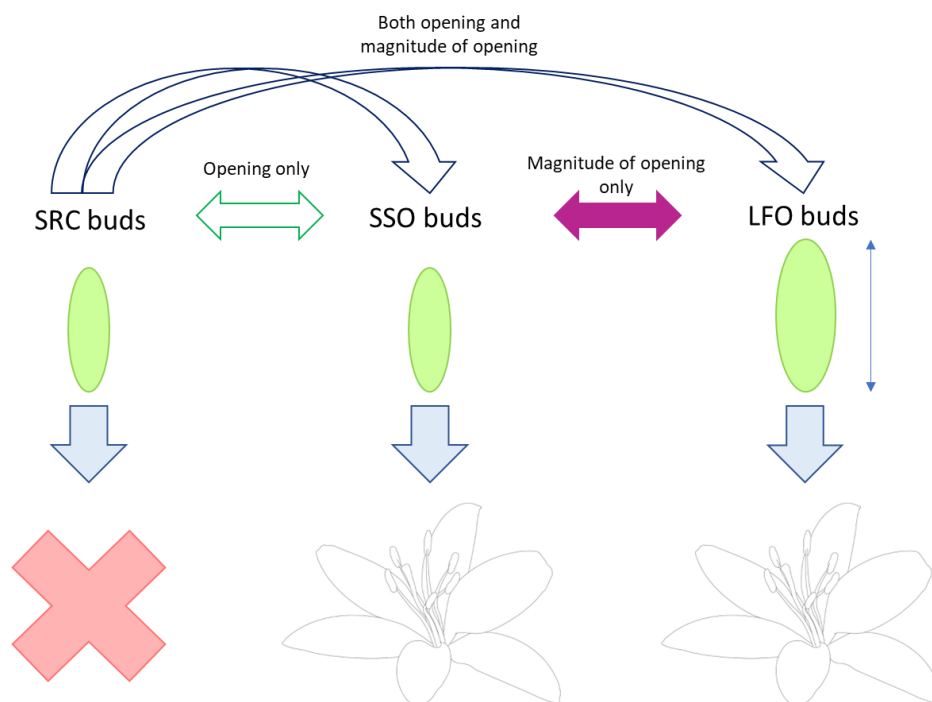
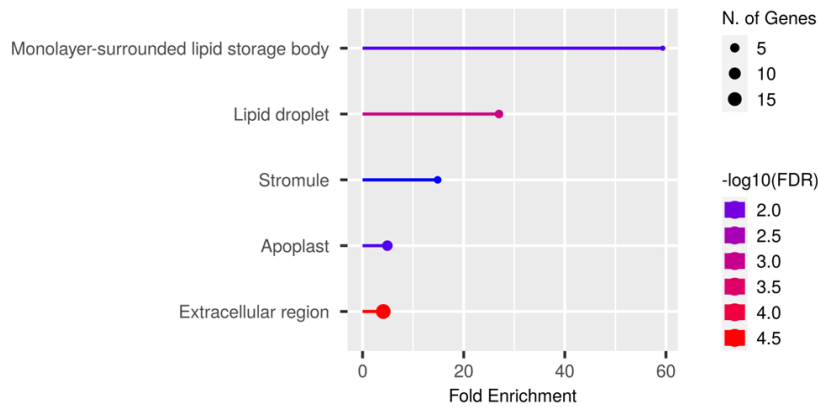


Figure 5.14 – filled in arrows indicate the comparisons used in the analysis in this section. Comparisons between SSO and LFO buds only were used here to show differences in gene

expression between precondition of buds which both showed an opening phenotype but differed in their size at harvest and in the magnitude of their opening.

(A)



(B)

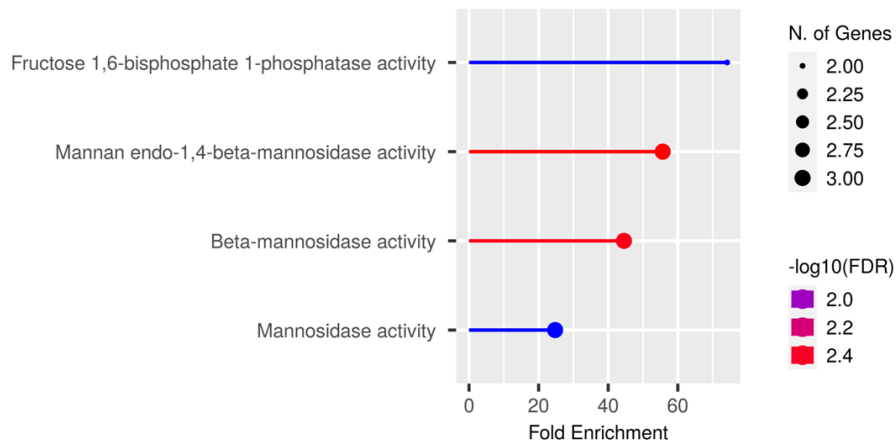


Figure 5.15 – Gene Ontology (GO) term enrichment showing the most significant GO terms, number of genes and adjusted p-value (FDR) overrepresented in the DEGs between smaller buds which opened (SSO) compared to larger buds which opened fully (LFO), and which significantly aligned to an *A. thaliana* orthologue. This was compared to a background containing all putative genes identified in the transcriptome also aligning to an *A. thaliana* orthologue. GO term enrichment is shown for (A) cellular compartment, and (B) molecular function. GO term enrichment for biological process did not show any significant terms. Graphs created using the online ShinyGO tool (Ge et al. 2020). A full list of significantly enriched GO terms and the associated *A. thaliana* genes can be found in Appendix 4.3.

STRING analysis of the 'Magnitude of opening' comparison group showed two main suggested networks, one showing a highly coexpressed group of genes more highly expressed in LFO compared to SSO buds (Figure 5.16). Putative *HCEF1* and *SBPASE* code for enzymes in the Calvin cycle relating to carbon fixation, while *CRB* is involved in chloroplast rRNA metabolism and translation. Alongside these the putative ferredoxin-coding *FD3* and ferredoxin reductase *FNR1* were also identified. An upregulated gene putatively coding for a serine/ threonine kinase (*F4HYK7*) was also found to have links with *FNR1* as found by several affinity coimmunoprecipitation assays in orthologs from other species. *NYE1*, coding for a protein involved in chlorophyll catabolism and chloroplast breakdown was found to be more highly expressed in LFO compared to SSO, and interacted with putative genes coding for reductases involved in chlorophyll biosynthesis (*HEMA1*) and a chloroplastic developmental gene (*CLA1*) which did not show much change in expression (log₂FC) between the two conditions. Also part of this network was *AT4G36770*, a gene encoding a glycosyltransferase showing responses to ABA and drought which was highly downregulated in LFO compared to SSO buds. This was linked to the putative *DFR* (coding for a dihydroflavonol reductase), which is involved in anthocyanin biosynthesis and was also unchanged in expression between conditions.

The other network showed significantly more expression in SSO than LFO and included DEGs putatively coding for a phospholipid binding protein PEBP (*AT5G01300*), oleosin1 (*OLEO1*), calcium binding Caleosin 3 (*RD20*), and a serine/threonine-protein kinase (*SIP4*). Interactions between *RD20* and *SIP4* not only showed coexpression in the literature but had also been experimentally determined by yeast-2- hybrid assay. *RD20* also showed possible interactions with *AT3G05500* (LD-associated protein 3) which was more highly expressed in LFO compared to SSO buds, and is involved in developmental cell growth.

Two putative flower opening-related genes which also showed higher expression in LFO compared to SSO buds were *XTH7*, coding for a xyloglucan endotransglycosylase/hydrolase, and *AT3G26130*, coding for a cellulase. The similarity of their expression reflects their similar function and suggests they may be regulated in the same way.

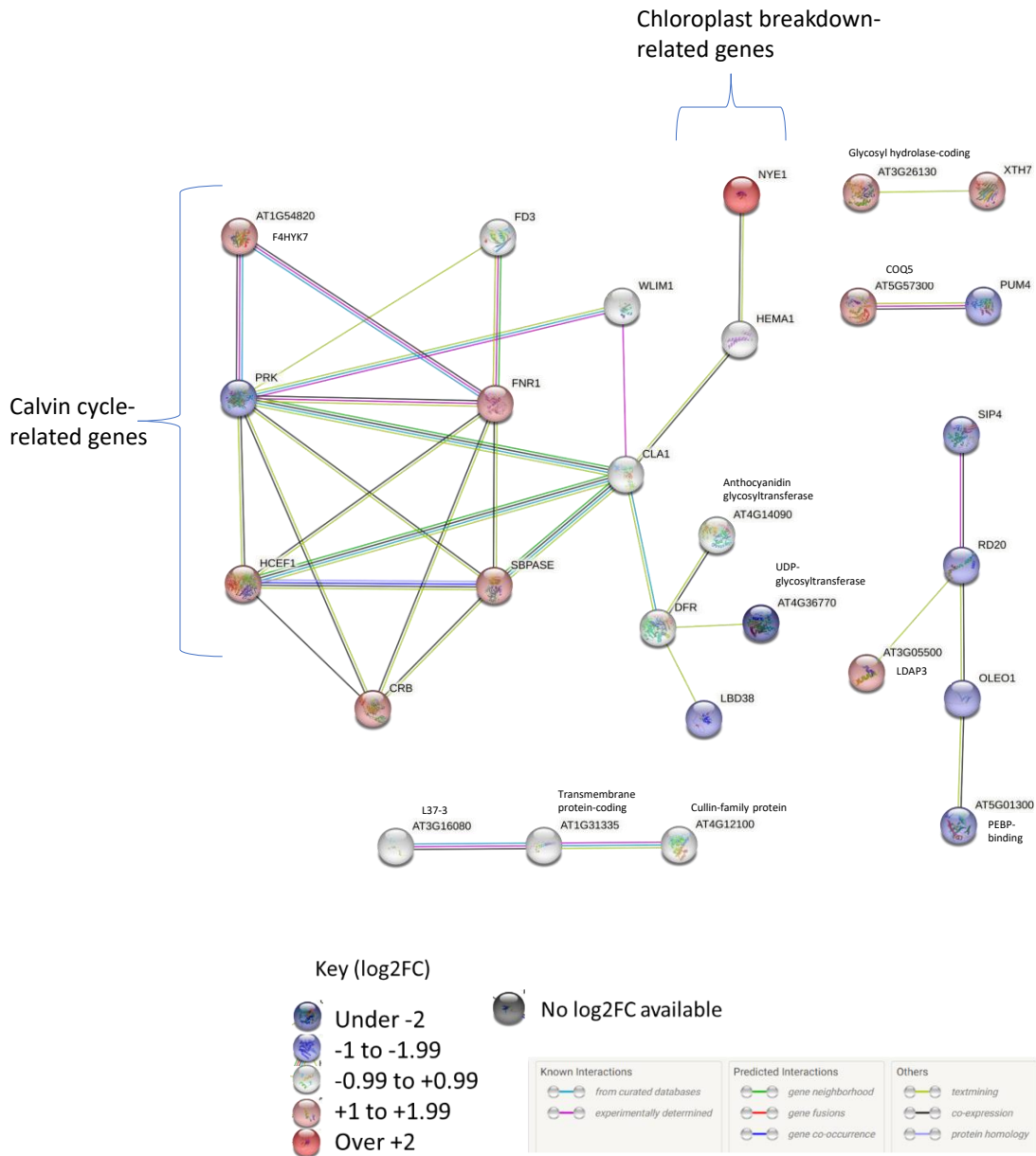


Figure 5.16 – STRING analysis to show protein-protein interactions between the DEGs in the ‘Magnitude of opening’ group, showing expression (log₂FC - as expressed in the LFO/SSO comparison) (Szklarczyk et al. 2015).

5.3.6 Identifying genes with a degree of opening-dependent effect using K-means clustering

K-means clustering was used here to identify genes which had a degree of opening-dependent effect, i.e. genes which had a significant upregulation in SSO compared to SRC buds but also had a significant upregulation in LFO compared to SSO buds, for example. This

analysis identified 8 distinct expression patterns across SRC-SSO-LFO buds (Figure 5.17) which were individually analysed for the possible function, cellular location and identity of putative DEGs they contained. GO term enrichment was carried out for each cluster of interest (Clusters 3, 4, 7, 8) using PlantRegMap (Appendix 4.4, 4.5, 4.6, 4.7).

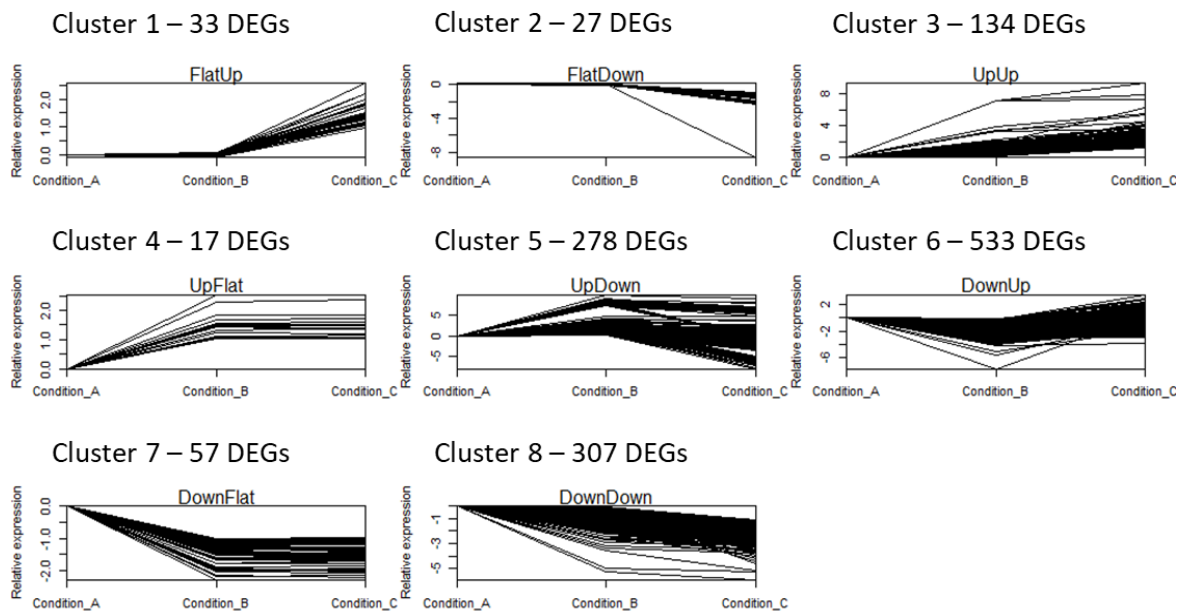


Figure 5.17 - K-means clustering graphs to show the patterns of relative expression (here expressed as log₂FC), and number of DEGs identified in the eight clusters. Clusters 3 and 4 were further analysed as being significantly more highly expressed in the buds which were able to open compared to those which failed to, while Clusters 7 and 8 were further analysed as being significantly less expressed in the same comparison.

DEGs in Clusters 3 and 4 were investigated as upregulated in SSO or LFO buds compared to SRC buds. Cluster 3 had 134 DEGs while Cluster 4 had 17 (a total of 151 DEGs upregulated in SSO/LFO vs. SRC buds).

Cluster 3 comprised more highly expressed DEGs related to both opening and the degree of opening. As expected, the GO terms for reproduction (GO:0000003, 6 genes), stamen development (GO:0048443, 3 genes), floral whorl and organ development (GO:0048438, GO:0048437, 4 genes) were enriched significantly. GO term enrichment also found the cell wall (GO:0005618), the phenylpropanoid metabolic and biosynthetic process (GO:0009698

(6 genes), GO:0009699 (5 genes)) to be significantly overrepresented in the group, as well as the lignin biosynthetic process (GO:0009809, 3 genes). DEGs were putatively identified to code for proteins involved in cell expansion such as expansins EXPA1 and EXPA8 (AT1G69530, AT2G40610), the hydroxycinnamoyltransferase HCT (AT5G48930), cinnamoyl-CoA reductase (AT2G33590), UDP-glucosyl transferases (AT2G15480, AT5G17050), sucrose transporter SWEET17 (AT4G15920), Beta-galactosidase 16 (AT1G77410), aquaporin Δ -TIP (AT3G16240), glycoside hydrolases BXL2 (AT1G02640), Leucine-rich repeat (LRR) family protein (AT3G20820), and pectin lyase-like (AT1G48100). The response to hormones such as gibberellin (GO:0009739, 4 genes), salicylic acid (GO:0009751, 4 genes), and JA (GO:0009753, 4 genes) were also found to be significantly enriched. Putative hormone-related genes such as the gibberellin positive regulator SLY1 (AT4G24210) was found in this cluster. Several transcription factors were putatively identified as Mini zinc finger 1 MIF1 (AT1G74660), MYB24 (AT5G40350), MYB21 (AT3G27810), MYB4 (AT4G38620), homeobox-leucine zipper protein-40 (AT4G36740) and PLATZ transcription factor (AT1G32700). A full list of genes and GO term enrichments for Cluster 3 can be found in Appendix 4.4.

DEGs in Cluster 4 were identified as upregulated genes related to purely opening rather than the degree of opening. GO terms relating to transcription and RNA binding (GO:0006366 (2 genes), GO:0003723 (2 genes)) were overrepresented, as well as general cellular metabolism and biosynthesis (GO:0046483, GO:0009058, 4 genes). Two DEGs were putatively identified as the bHLH transcription factors bHLH111 (AT1G31050) and unknown bHLH protein (AT1G31050). Putative MYC6 (AT5G41370) was also found in this group. DEGs putatively coding for cell-wall remodelling proteins such as alpha-l-arabinofuranosidase 1 (AT3G10740) and lipid metabolic processes such as triglyceride lipase (AT4G13550), triacylglycerol lipase-like 1 (AT1G45201). Several DEGs were putatively identified as having DNA repair or cell-cycle functions such as the Regulator of chromosome condensation (RCC1) family protein (AT5G48330), Regulator of chromosome condensation-like RUG2 (AT5G48330), XPB1 (AT5G41370), and Maturase K (ATCG00040), reflecting the enrichment of DNA metabolism-related GO terms (GO:0006259, 2 genes). A full list of genes and GO term enrichments for Cluster 4 can be found in Appendix 4.5.

DEGs in Clusters 7 and 8 were investigated as downregulated in SSO or LFO buds compared to SRC buds. Cluster 7 comprised 57 DEGs while Cluster 8 had 307, therefore in total a 364 out of a total 19898 DEGs in these groups.

Cluster 8 was analysed here as putative genes downregulated in SSO/LFO buds compared to SRC buds (i.e. related to both opening and the degree of opening). The response to abiotic (GO:0009628, 29 genes) and biotic (GO:0043207, 14 genes) stimuli were enriched in this group. GO terms relating to photosynthesis (GO:0015979, 21 genes), and specifically light harvesting in photosystem I (GO:0009768, 9 genes) were highly overrepresented, as well as response to light (GO:0009637, GO:0010218, GO:0010114, 6 genes). Many DEGs significantly aligning with *A. thaliana* genes were found to code for photosynthesis-related proteins, transcription factors, and stress-related proteins. Many of the photosynthesis-related DEGs were identified as several members of the same family – for example DEGs putatively coding for light-harvesting complex I chlorophyll a/b binding proteins (LHCA) were identified in this cluster, with LHCA1 (AT3G54890), LHCA2 (AT3G61470), LHCA3 (AT1G61520) and LHCA4 (AT3G47470) all being found. DEGs coding for light-harvesting complex II chlorophyll b binding proteins (LHCB) were also putatively identified as LHCB2.3 (AT3G27690), LHCB3 (AT5G54270), LHCB4.1 (AT5G01530) and LHCB5 (AT4G10340). Several stress and hormone-related GO terms for response to herbivory or wounding (GO:0080027 (3 genes), GO:0009611 (7 genes)), response to JA (GO:0009753, 7 genes), response to ethylene (GO:0009723, 6 genes), and stress (GO:0006950, 37 genes) were significantly enriched in this group. ERF1 and 2 (AT3G23240, AT5G47220) are ethylene- and stress-related genes significantly aligning with the DEGs found in this cluster, and a putatively identified WRKY transcription factor WRKY40 (AT1G80840). Jasmonate-related DEGs were also putatively identified as Jasmonate-zim-domain protein JAZ8 (AT1G30135). A full list of genes and GO term enrichments for Cluster 8 can be found in Appendix 4.7.

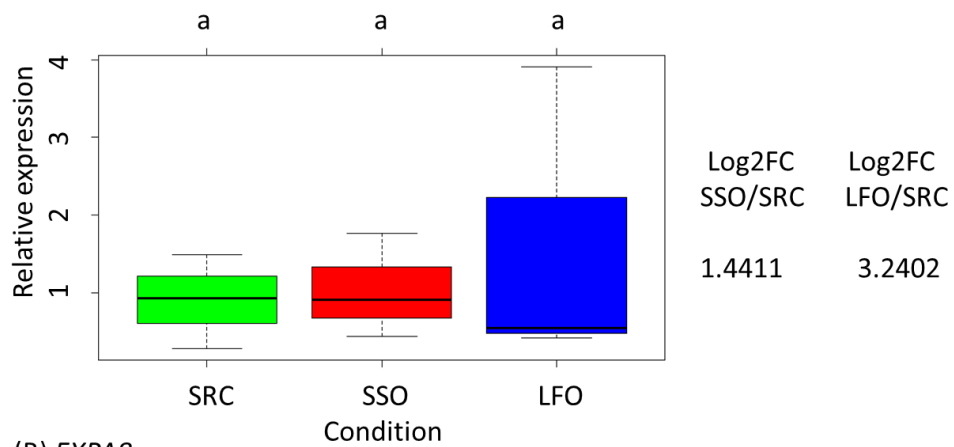
Looking at DEGs in Cluster 7 separately as downregulated genes perhaps more related to purely bud opening rather than the degree of opening, showed GO terms relating to secondary metabolism (GO:0019748, 4 genes) negative regulation of catalytic activity (GO:0043086, 2 genes), molecular function (GO:0044092, 2 genes), and metabolic process (GO:0009892, 3 genes) as significantly enriched. The ABA response pathway was also identified as overrepresented (GO:0009738, GO:0071215, 2 genes). Within this group,

hormone related genes coding for SAUR-like proteins (AT2G21220, AT5G53590), Gibberellin 2-beta-dioxygenase 2 (AT1G30040), Abscisic acid receptor PYL12 (AT5G45870), Ethylene-responsive transcription factor 11 (AT1G28370) were identified as significantly aligning to the identified DEGs. Some putative transcription factor genes were also expressed more greatly in SRC buds compared to SSO/LFO buds, putatively coding for the PLATZ transcription factor family protein (AT1G32700), AP2/ERF and B3 domain-containing transcription repressor RAV2 (AT1G68840), bHLH protein MYC4 (AT4G17880). Notably, GO terms for sugar transporter activity (GO:0005351, GO:0005402, GO:0051119, 2 genes) and phosphate transporter activity (GO:0005315, GO:1901677, GO:0015295, 2 genes) were enriched. Many of the related genes aligning to the DEGs were identified as physical drivers of cell expansion and metabolism, including alpha-amylase-like 2 (AT1G76130), Sugar transport protein STP11 (AT5G23270), ABC transporter ABCI17 (AT1G67940), and inorganic phosphate transporters 1-1 (AT5G43350), 1-3 (AT5G43360) and 1-7 (AT3G54700). A full list of genes and GO term enrichments for Cluster 7 can be found in Appendix 4.6.

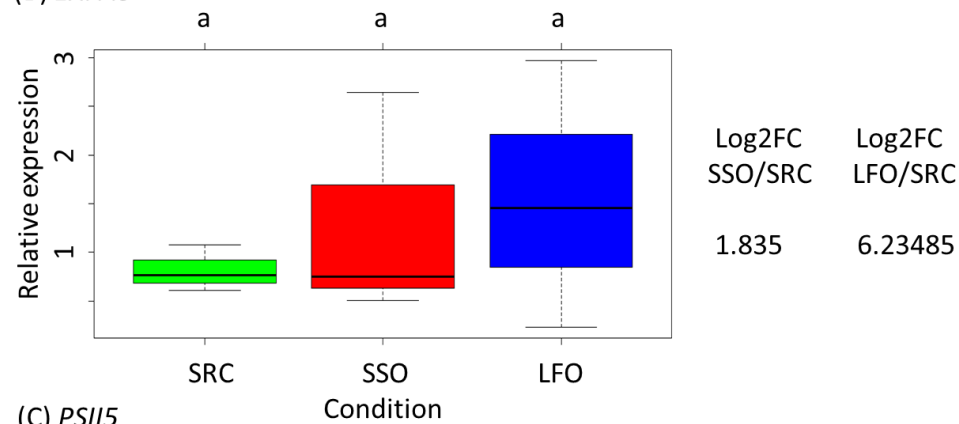
5.3.7 Validation of DEG expression using qPCR

Some of the DEGs aligning significantly to *A. thaliana* genes which were identified in the previous analyses as significantly differentially expressed between buds which failed to open (SRC) and buds which eventually did open (SSO and LFO buds) were validated by qPCR. A DEG which showed the greatest alignment with the *A. thaliana* MYB21 gene showed an increased expression in LFO buds compared to SRC or SSO buds, however this was not found to be statistically significant (Figure 5.18A). Similarly, a DEG aligning significantly with the expansin-encoding EXPA8 gene was also found to show an increased expression in SSO buds and again in LFO buds compared to SRC buds, but this was not reflected statistically by one-way ANOVA (Figure 5.18B). A DEG aligning most significantly with the photosystem II gene PSII5 was used as an example of a DEG significantly more expressed in buds which did not open (SRC) to buds which did open (SSO and LFO buds) and showed an only slightly higher but very variable expression in SRC compared to SSO and LFO buds (Figure 5.18C).

(A) MYB21



(B) EXPA8



(C) PSII5

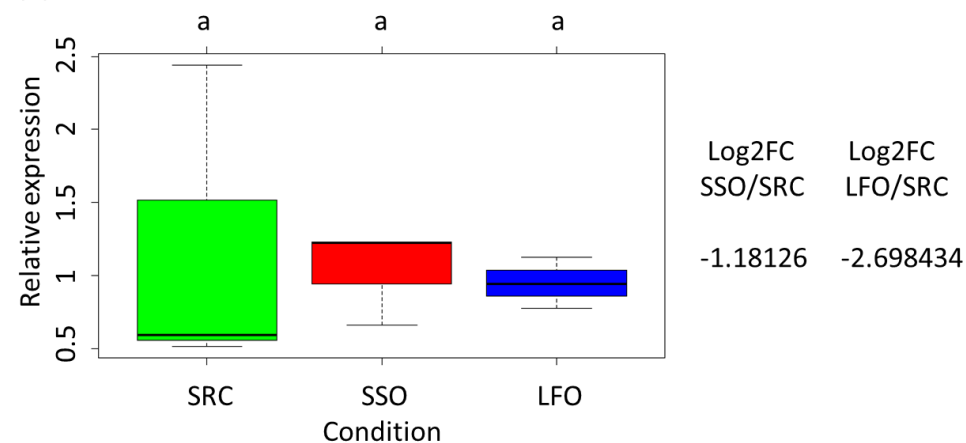
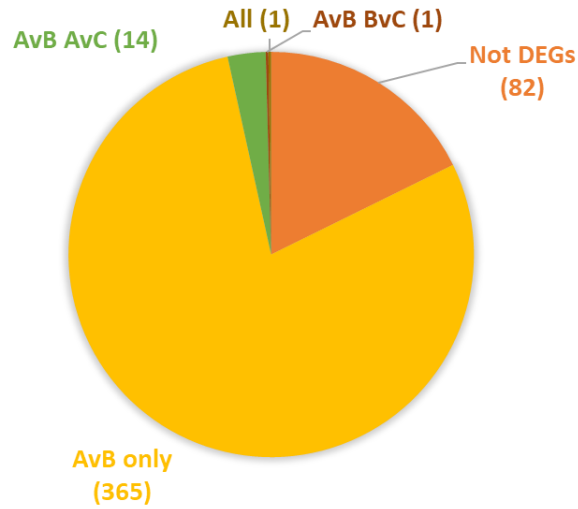


Figure 5.18 - Relative expression of putative (A) MYB21 (B) EXPA8 and (C) PSII5 genes compared in flowers which later failed to open (SRC) to flowers which opened at a similar length (SSO) and flowers which opened at a longer length (LFO) measured by qPCR. The values represent the medians of 3 biological replicates \pm SD. Letters indicate significance by one-way ANOVA and post-hoc Tukey test (Appendix 6.20). Log2FC values for the reads used to design qPCR primers for the genes indicated in the SSO/SRC and LFO/SRC comparisons are on the right.

5.3.8 Analysis of putative regulatory and hormone-related genes

Transcription factors and regulatory genes (i.e. involved in signal transduction of phytohormones) were identified from the transcriptome by PlantTFDB to investigate patterns in log₂FC between the SRC vs. SSO/LFO buds in different transcription factor families/types (Figure 5.19A). The majority of transcription factors (TFs) identified here were DEGs in the SSO/SRC comparison only (365 DEGs). A significant proportion was also found in both SSO/SRC and LFO/SRC comparisons (14 DEGs) or not identified as DEGs (82 DEGs). There were no TFs only found as DEGs in the LFO/SSO comparison and only one TF in both the SSO/SRC and LFO/SSO comparison, suggesting that differences between SSO and LFO buds may not be transcriptionally regulated. TFs were identified as coming from several different families, with MYB, ERF, bHLH and NAC families the major types (Figure 5.19B).

(A) Number of TFs in each group



(B) Types of TF (by family) found in the full transcriptome

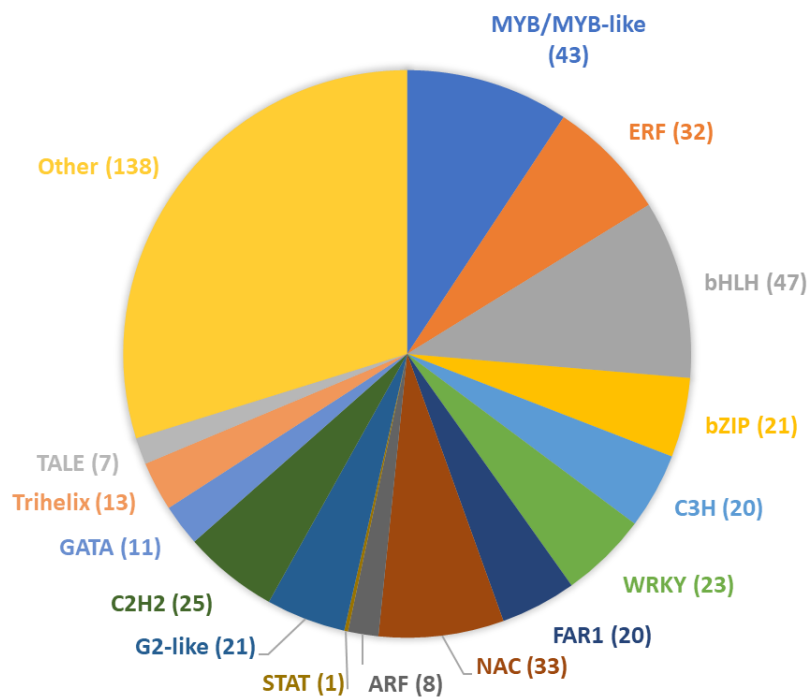


Figure 5.19 – Analysis of transcription factors (TFs) found in the whole transcriptome, in terms of (A) number of TFs found in each group, and (B) types of TF by family. Number of TFs identified in each group can be found in brackets next to the name.

TFs identified using PlantTFDB and manually identified phytohormone-related genes were further analysed to show differences in expression between the three conditions (Figures 5.20, 5.21). The majority of transcription factor expression was lower in SSO and LFO buds

compared to SRC buds, showing particularly high downregulation in smaller buds which opened (SSO) in TF families such as the putative genes coding for NAC- and zinc-finger TFs (Figure 5.20). Several WRKY transcription factors also showed downregulation in SSO and LFO buds compared to SRC buds. The few TFs upregulated in buds which went on to open (SSO and LFO buds) included two putative circadian-related genes REVEILLE1 and 8, which showed a strong magnitude of change related to opening. REVEILLE 8 was found differentially expressed in all conditions, increasing in expression in SSO buds compared to SRC buds and further in LFO buds compared to SSO buds (showing increased expression with magnitude of opening). Other TFs found here which had phytochrome-responsive expression such as the FAR1 family also showed slight upregulation in SSO buds compared to SRC buds.

Putative auxin transport-related genes coding for auxin transporters such as AUX and PIN-like (PILS) did not show any difference in expression (Figure 5.21A). However, there were significantly higher levels of expression of the putative auxin synthesis YUCCA genes, several Auxin Response Factors (ARFs), and Small Auxin Upregulated Response genes (SAURs) in both sets of buds which later were able to open (SSO and LFO buds) compared to SRC (Figure 5.21A). Other hormone-related genes relating to cytokinin for example did not show large changes in expression (\log_2FC) between conditions (Figure 5.21B).

Figure 5.20 – DEGs aligning significantly to *Viridiplantae* transcription factors and their expression change (\log_2FC) between preconditions which fail to open (SRC) and those which open (SSO and LFO).

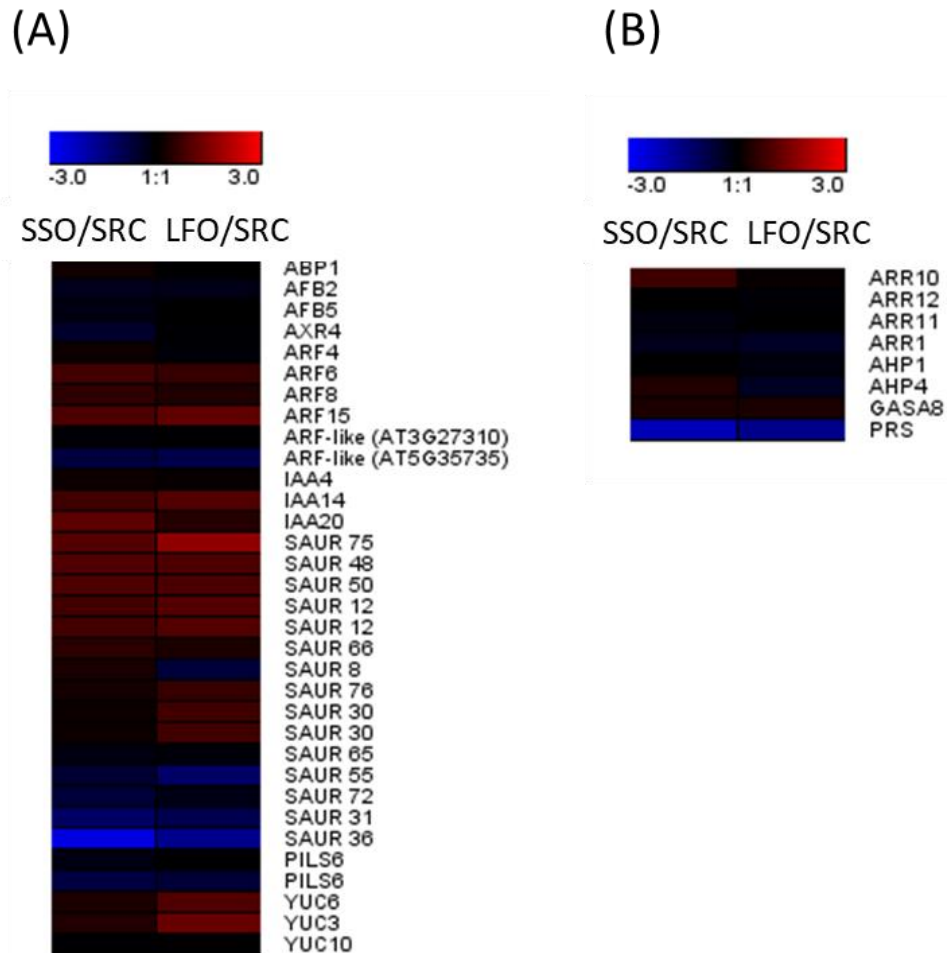


Figure 5.21 - DEGs aligning significantly to *A. thaliana* (A) auxin related genes and (B) cytokinin related genes and their expression change (\log_2FC) between preconditions which fail to open (SRC) and those which open (SSO and LFO).

The expression of some auxin related genes selected for significantly higher expression in flowers which opened compared to flowers which could not (*YUC3*, *IAA14*, *ARF15*, *SAUR75*) was validated using qPCR (Figure 5.22). Although the expression of these putatively identified genes followed the same general trend of slightly higher expression in SSO and/or

LFO buds compared to SRC (log₂FC values for SSO/SRC and LFO/SRC comparisons also given in Figure 5.22), the differences in relative expression as measured by qPCR was not statistically significant in any of the putative genes investigated due to extremely high variation between biological replicates.

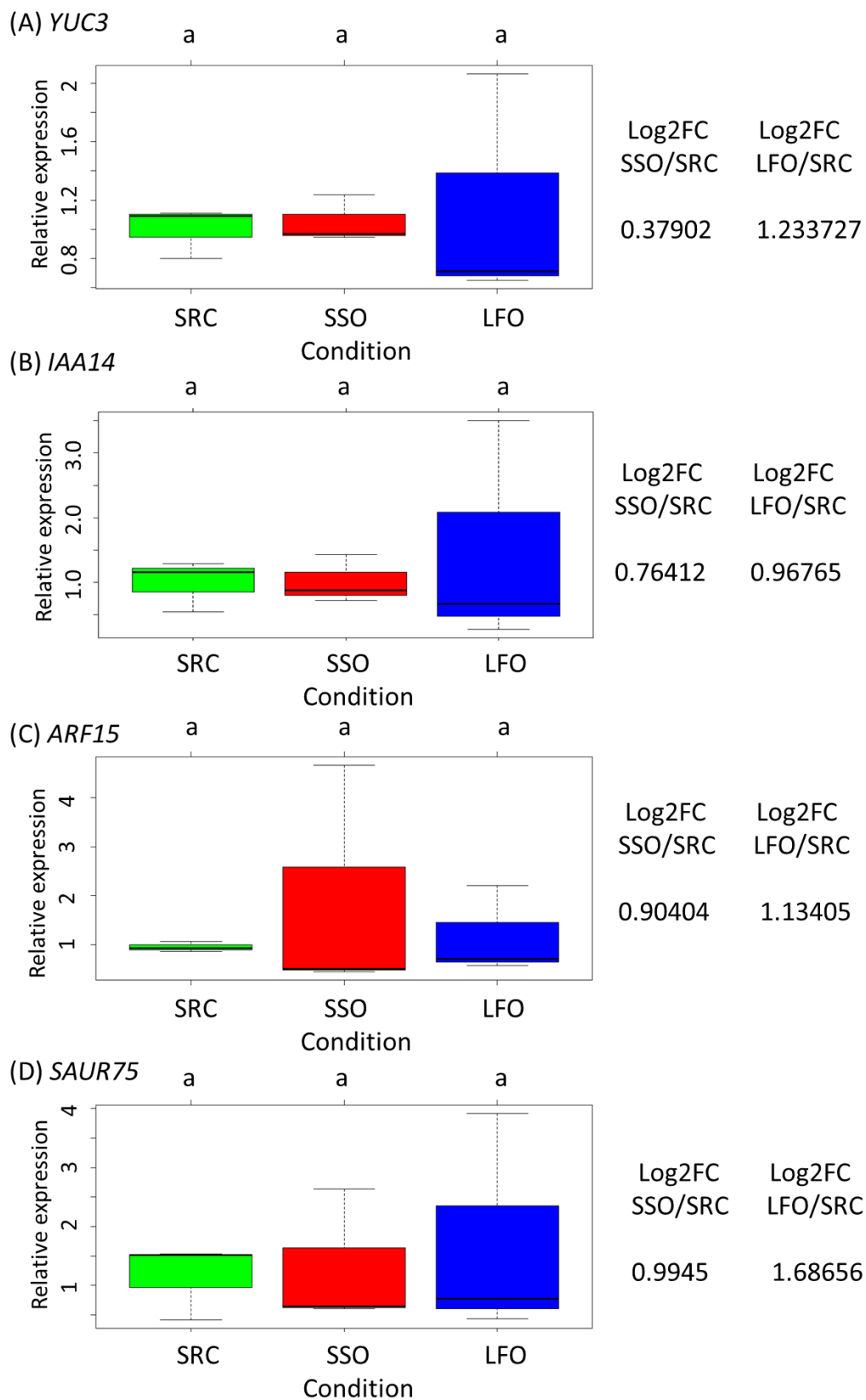


Figure 5.22 – Relative expression of (A) *YUC3* (B) *IAA14* (C) *ARF15* and (D) *SAUR75* auxin-related genes compared in flowers which later failed to open (SRC) to flowers which opened

at a similar length (SSO) and flowers which opened at a longer length (LFO) measured by qPCR. The values represent the medians of 3 biological replicates \pm SD. Letters indicate significance by one-way ANOVA and post-hoc Tukey test (Appendix 6.21). Log₂FC values for the reads used to design qPCR primers for the genes indicated in the SSO/SRC and LFO/SRC comparisons are on the right.

Putative regulatory genes relating to the stress response were also investigated in these buds to compare expression in buds which eventually opened and those which failed to do so (Figure 5.23). Significant DEGs were putatively identified through KEGG pathway analysis and showed links to the MAPK pathway (*MKK5*), with DEGs putatively identified as part of the ethylene response (*ERF1*, *PAA1*), the JA response (*MYC2*), the drought response (*OST1*, *PYL4*, *PYL6*, *PYL12*), and the wounding response (*RCAR3*). All DEGs apart from putative *OST1* showed a higher expression in SRC buds compared to SSO/LFO buds.

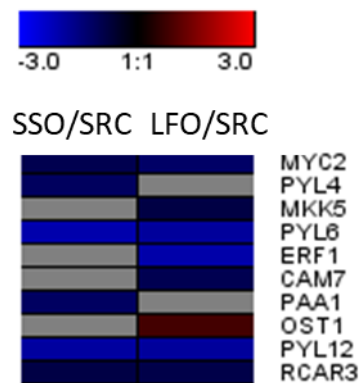


Figure 5.23 – Heatmap showing DEGs aligning significantly to genes relating to the stress response (MAPK pathway, ethylene, drought and wounding response) and their expression change (log₂FC) between bud conditions which fail to open (SRC) and those which open (SSO and LFO).

5.3.8.1 Transcription factor network analysis

Network analysis showed several links between DEGs putatively coding for transcription factors identified by PlantRegMap (Tian et al. 2020). Putative interactions between the most

differentially expressed transcription factors between conditions were investigated to explore some of the possible regulatory networks which might have been mis-regulated in buds which would fail to open (SRC buds). The putative circadian-related factors Reveille-1 and Reveille-8 were found to be expressed more highly in SSO/LFO compared to SRC buds (Figure 5.24) and were therefore hypothesised to have a positive regulatory effect on flower opening. Reveille-1 was found to interact with pyrimidine synthesis proteins as well as putative tetratricopeptide repeat (TPR)-like superfamily proteins, while both Reveille-1 and -8 were found to have direct interactions with an unknown PLATZ transcription factor family protein which was also more highly expressed in buds which opened than those which failed to open.

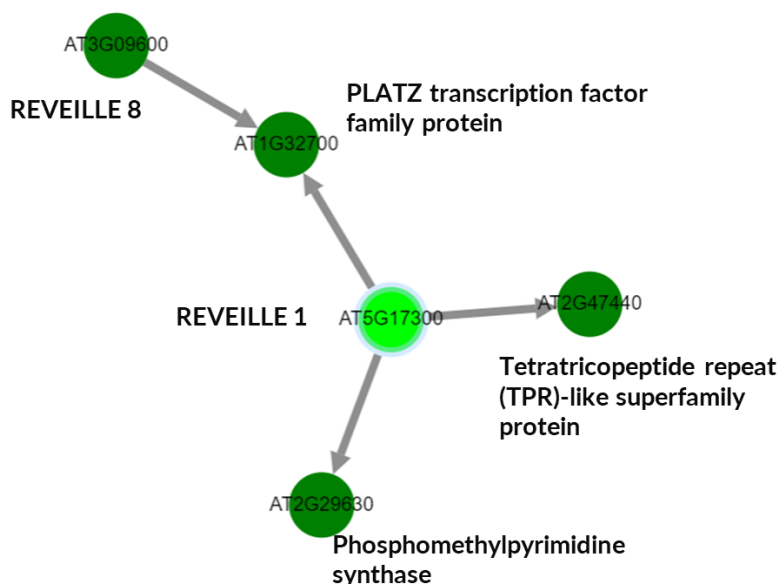


Figure 5.24 – Network analysis using DEGs upregulated in SSO/LFO compared to A to identify putative interactions between coexpressed DEGs. Figure created using PlantRegMap (Tian et al. 2020).

A putative MYC2 transcription factor was also investigated as it was found to be more highly expressed in SRC buds compared to SSO or LFO buds (Figure 5.25) and therefore was hypothesised to perhaps acting as a negative regulator of flower opening. This was found to have interactions with a histone methyltransferase (H3 K4 specific methyltransferases are linked to transcription) and a putative WRKY transcription factor. This in turn is also shown to interact with the putative ethylene-responsive RAP2-10, which also has links to several

other putative regulatory proteins found in this group, such as phosphoenolpyruvate carboxylase, which may have a role in photosynthesis (Iglesias et al. 1987).

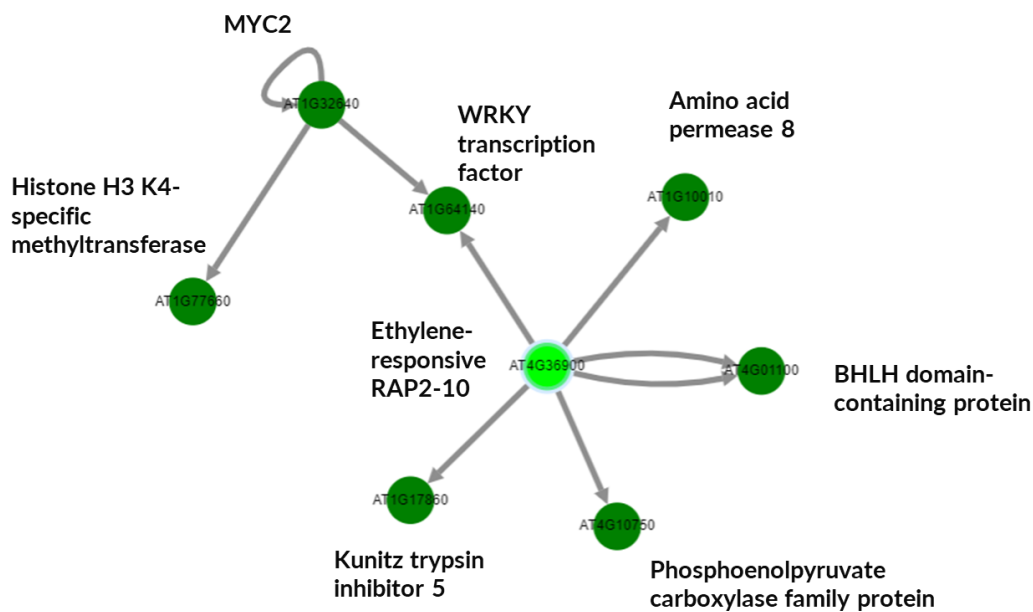


Figure 5.25 – Network analysis using DEGs downregulated in SSO compared to SRC buds to identify putative interactions between coexpressed DEGs. Figure created using PlantRegMap (Tian et al. 2020).

A putative MADS-box protein (SOC1) was found more highly expressed in LFO buds compared to SSO buds and was identified as interacting with 12 other DEGs in the list (Figure 5.26). This included photosynthesis-related genes such as putative chlorophyll a-b binding protein 3, photosystem I subunit 0, sedoheptulose-1,7-bisphosphatase, and protochlorophyllide reductase C. It also includes possible terpenoid synthesis related genes coding for enzymes such as geranylgeranyl diphosphate reductase.

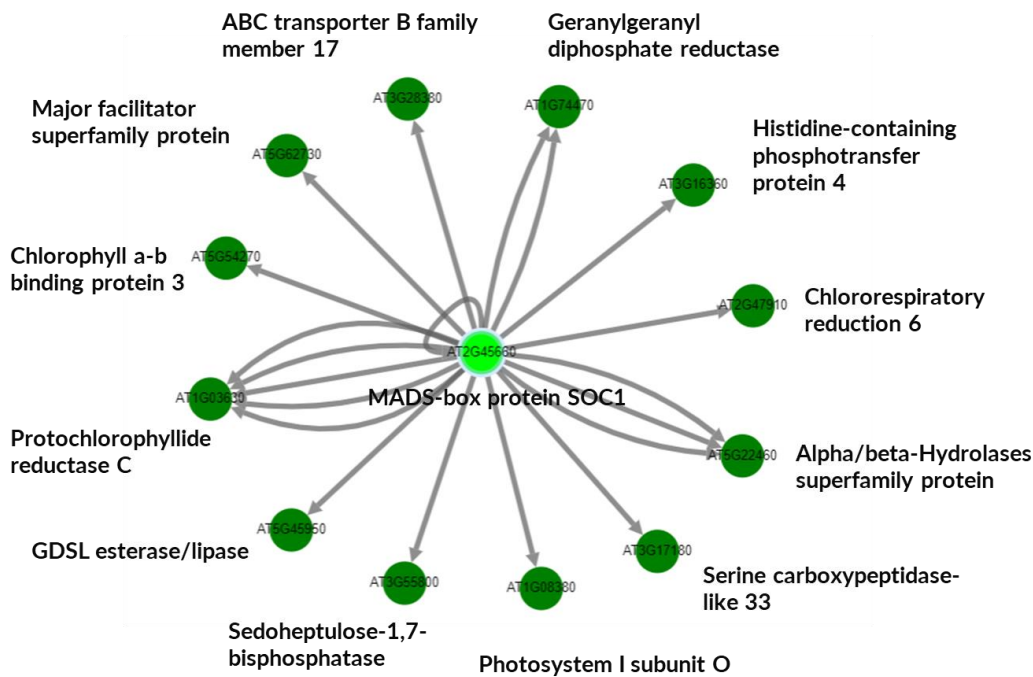


Figure 5.26 – Network analysis using DEGs upregulated in LFO compared to SSO buds to identify putative interactions between coexpressed DEGs. Figure created using PlantRegMap (Tian et al. 2020).

5.3.8.2 TF motif analysis in “Required to open” group

TF motif analysis was carried out to identify enriched transcription factor motifs in the list of DEGs in the ‘Required to open’ group (higher expression in SSO than SRC) significantly aligning to an *A. thaliana* orthologue. Although there are significant differences in motif occurrence and sequence between monocot and dicot species (Filichkin et al. 2011; Cserhati 2015), these enriched motifs were identified to compare with the presence of DEGs aligning significantly to corresponding *A. thaliana* TF classes which are also expressed more highly in SSO compared to SRC to explore coexpression of putatively regulated genes.

There were 205 enriched TF motifs identified in total in the closest *A. thaliana* match of all DEGs in the ‘Required to open’ group (Figure 5.27A). The vast majority were AP2/ERF motifs (59%) with C2C2, Trihelix and MYB-binding motifs also identified. There was a large disparity between the number of DEGs which were expressed more highly in this comparison (12 DEGs) and those which were expressed less (139 DEGs). However, proportionally, in the DEG

group expressed more highly in SSO there were more bZIP and MYB motifs (Figure 5.27B), whereas in the group expressed more highly in SRC there were more AP2/ERF, C2C2, MYB and Trihelix motifs (Figure 5.27C). This suggests many of DEGs important in flower opening may be regulated (either positively or negatively) by AP2 or ERF transcription factors.

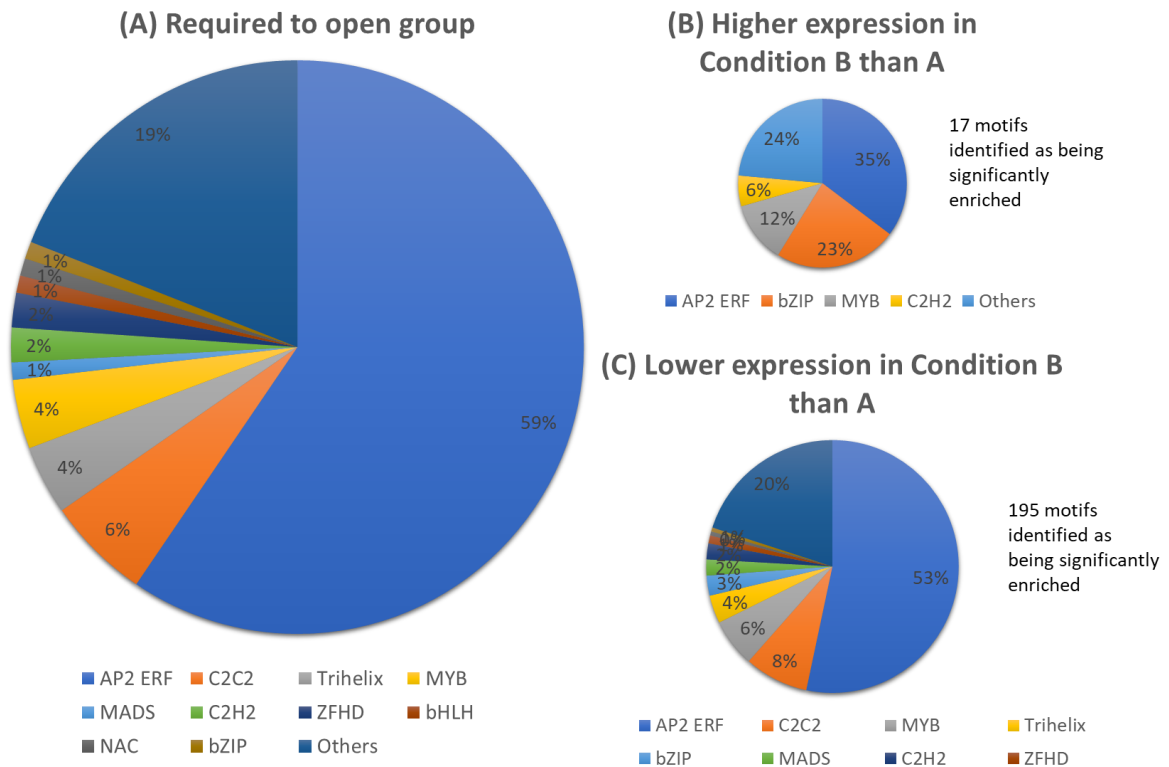


Figure 5.27 – Enriched TF motifs in (A) the whole ‘Required to open’ group, (B) DEGs expressed significantly more highly in SSO than SRC buds, and (C) DEGs expressed significantly less in SSO than SRC buds.

The three top motifs enriched in the groups of upregulated and downregulated DEGs in the ‘Required to open’ group were analysed to understand which groups of genes might be coregulated by specific transcription factors (Table 5.2). The upregulated list of DEGs in the ‘Required to open’ group were particularly enriched in bZIP- and TGA-binding motifs, as well as the AP2/ERF RAP2-1-binding motif. The DEGs containing bZIP and TGA motifs were varied but many of the putative fatty acid metabolism genes such as CER1, LACS1 and FAR4 were identified as having one or both motifs. Other putative genes included the cell wall remodelling glycosyl hydrolases and pectinacetylsterases. The coexpression of the PLATZ transcription factor here makes it a strong candidate for going on to regulate the expression of other flower opening-related genes. The RAP2-1 binding genes in contrast were more

related to carbohydrate metabolism and respiration (putatively coding for phosphoenolpyruvate carboxylase, 2-oxoglutarate (2OG) and Fe(II)-dependent oxygenase).

The three top motifs in the downregulated DEGs in the 'Required to open' group were the FRS9-binding motif and AP2-ERF-binding motifs (Table 5.3). The putative FRS9 motif-containing LOG8 is a cytokinin activator and NAC074 has been linked to positive regulation of programmed cell death, suggesting that these may be coregulated. The two AP2/ERF motifs, being similar to the RAP2-1 motif in the upregulated group, was found in several of the same DEGs, but notably, some photosynthesis-related putative genes coding for Photosystem II 5kDa protein and plastid movement impaired 2 contained motifs for ERF9. Several putative stress-related chaperone proteins (DNAJ-domain superfamily protein, HSP20-like) were also found to contain similar AP2/ERF motifs.

TABLE 5.2 - IDENTIFICATION OF DEGS CONTAINING ENRICHED MOTIFS UPREGULATED IN 'REQUIRED TO OPEN' GROUP

Motif binding	Sequence	Putative <i>A. thaliana</i> gene	Codes for
bZIP	GAGGCTGAGGTCTCT	AT1G32700	PLATZ transcription factor family protein
bZIP	GAAGCTGTCGTTATC	AT1G33470	RNA-binding (RRM/RBD/RNP motifs) family protein
bZIP	GATGTCGGCGTCACC	AT1G51090	Heavy metal transport/detoxification superfamily protein
bZIP	TGTGATGACTTCAAC	AT1G77660	Histone H3 K4-specific methyltransferase SET7/9 family protein
bZIP	ATAGATGACGCCATG	AT2G44310	Calcium-binding EF-hand family protein
bZIP	GTTGTTGAGTTCACC	AT3G49830	P-loop containing nucleoside triphosphate hydrolases superfamily protein
bZIP	GTTGATGACGTGGCG	AT5G18850	Low-density receptor-like protein; Unknown protein
bZIP	AATGGTGGCGCCATA	AT5G20950	Glycosyl hydrolase family protein
bZIP	GATGATGACGGCATA	AT5G25280	Serine-rich protein-related
bZIP	TTTCGTGGCGTCACT	AT5G37840	BEST Arabidopsis thaliana protein match is: plastid movement impaired 2
bZIP	ATTGCTGACTTAATT	AT5G57123	Uncharacterized protein At5g57123; Unknown protein
bZIP	AATGCTTACCTCACA	CER1	Fatty acid hydroxylase superfamily
bZIP	AATTATGATGCATA	LACS1	Alcohol-forming fatty acyl-coa reductase; Probable fatty acyl-CoA reductase 4
bZIP	GATGATAACGTGATT	FAR4	Fatty acid reductase
bZIP	GTTTCTGAAGACACC	PHOT1	Nonphototropic hypocotyl 1; Phototropin-1
TGA	TGGCGCCACCA	AT5G20950	Glycosyl hydrolase family protein
TGA	TGCCGTATCA	AT5G25280	Serine-rich protein-related
TGA	CCACGTATCA	AT5G18850	Low-density receptor-like protein; Unknown protein
TGA	AGACGTAAGCA	AT5G01740	Nuclear transport factor 2 (NTF2) family protein
TGA	TGACCTCGGCA	AT4G19420	Pectinacetylesterase family protein
TGA	GGACTTATCA	AT3G49830	P-loop containing nucleoside triphosphate hydrolases superfamily protein
TGA	TGGCGTATCT	AT2G44310	Calcium-binding EF-hand family protein
TGA	TGAAGTATCA	AT1G77660	Histone H3 K4-specific methyltransferase SET7/9 family protein
TGA	AATGCTTACCTCACA	CER1	Fatty acid hydroxylase superfamily
TGA	AATTATGATGCATA	LACS1	Alcohol-forming fatty acyl-coa reductase; Probable fatty acyl-CoA reductase 4
RAP21	GTGTTGATGGTGT	AT1G32700	PLATZ transcription factor family protein
RAP21	GGGTGGGTGCCGG	AT1G60010	Uncharacterized protein At1g60010/T2K10_6
RAP21	ACGGCGGTGGTGA	AT1G77660	Histone H3 K4-specific methyltransferase SET7/9 family protein
RAP21	GTGACGGTGGTGA	AT2G17880	Chaperone DnaJ-domain superfamily protein
RAP21	CAGTCGGTGAAGA	AT2G44310	Calcium-binding EF-hand family protein
RAP21	GTCACGGCGCGG	AT4G10750	Phosphoenolpyruvate carboxylase family protein
RAP21	ATGGTGGTGGAGG	AT5G05600	2-oxoglutarate (2OG) and Fe(II)-dependent oxygenase superfamily protein
RAP21	ATTTCGGTTGCCGG	AT5G10770	Eukaryotic aspartyl protease family protein
RAP21	TTGTCGGTGACGA	AT5G18850	Low-density receptor-like protein; Unknown protein
RAP21	TTGTTGGTGGAAA	AT5G20950	Glycosyl hydrolase family protein
RAP21	ATTTCGTTGGTGG	AT5G62350	Plant invertase/pectin methylesterase inhibitor superfamily protein

TABLE 5.3 - IDENTIFICATION OF DEGS CONTAINING ENRICHED MOTIFS DOWNREGULATED IN 'REQUIRED TO OPEN' GROUP

Motif binding	Sequence	Putative <i>A. thaliana</i> gene	Codes for
FRS9	CTTCTCTCTCTCTCTCTC	AT1G32700	PLATZ transcription factor family protein
FRS9	CTCTCTCTTTCTCGATCTC	AT1G77660	Histone H3 K4-specific methyltransferase SET7/9 family protein
FRS9	GACTCTCTCTCTCTCTCTC	AT5G62350	Plant invertase/pectin methylesterase inhibitor superfamily protein
FRS9	ATCTACTTCTCTCACTCTCTC	PRS5	Homeodomain-like superfamily protein
FRS9	CTCGTTTGCTCTCTATCTCTC	LOG8	Cytokinin riboside 5'-monophosphate phosphoribohydrolase – cytokinin activating enzyme
FRS9	CTCCCTCTCCCTCTCCCTCTC	NAC074	NAC transcription factor positively regulating programmed cell death
AP2ERF	CCGCCTCAACCCAGCCTCAA	AT1G51090	Heavy metal transport/detoxification superfamily protein
AP2ERF	GTGGGTGCCGGCACGGAGAT	AT1G60010	Uncharacterized protein At1g60010/T2K10_6
AP2ERF	GCGGTTGCGGGTCGGCGTGAA	AT1G72060	Serine-type endopeptidase inhibitors
AP2ERF	CTCCGACGATTCGATCGTCGA	AT1G77660	Histone H3 K4-specific methyltransferase SET7/9 family protein
AP2ERF	CGCGAGCAACGTCGTCGGGAA	AT1G80440	Galactose oxidase/kelch repeat superfamily protein
AP2ERF	GCAGGTGTAGGACGCGGTGGT	AT2G17880	Chaperone DnaJ-domain superfamily protein
AP2ERF	CCCCGCCCGGTGACCGTCAC	AT4G10750	Phosphoenolpyruvate carboxylase family protein
AP2ERF	GGCCACCATTGTGGTCACCGT	AT5G01740	Nuclear transport factor 2 (NTF2) family protein
AP2ERF	CGACCGGAGCTGGCTTTGGT	AT5G05600	2-oxoglutarate (2OG) and Fe(II)-dependent oxygenase superfamily protein
AP2ERF	GTCGCGGACTTCTCGGTCTT	AT5G10770	Eukaryotic aspartyl protease family protein
AP2ERF	CTCCGGCGAAGCCAACGCCAA	AT5G17540	HXXXD-type acyl-transferase family protein
AP2ERF	CTCCATCATCGTCACCGACAA	AT5G18850	Low-density receptor-like protein; Unknown protein
AP2ERF	AGGGATCCCAAGCGGGTCTGA	AT5G20950	Glycosyl hydrolase family protein
AP2ERF	CACCGCATTGCCATTGCCAT	AT5G20970	HSP20-like chaperones superfamily protein
AP2ERF	CGTCATCATCTCCGTCGTCGT	AT5G25280	Serine-rich protein-related
AP2ERF	GGCTGCGGTGGCCGCCGTGAG	AT5G62350	Plant invertase/pectin methylesterase inhibitor superfamily protein
ERF9	AAGCATTGGTAGCGGAGGAGG	AT1G05870	Protein of unknown function (DUF1685)
ERF9	TGGAGGAGATTCGAGAGAAGA	AT1G23390	Kelch repeat-containing F-box family protein
ERF9	CTGGGGCTGGGGCTGGGGCAG	AT1G51090	Heavy metal transport/detoxification superfamily protein
ERF9	CTGCAGCTGCAGCTGTGAAGA	AT1G51400	Uncharacterized protein F5D21.10; Photosystem II 5 kD protein
ERF9	CGGTTGATGCGGCTGCGTTGG	AT1G60010	Uncharacterized protein At1g60010/T2K10_6
ERF9	CGGCGCAGGTGTAGGACGCGG	AT2G17880	Chaperone DnaJ-domain superfamily protein
ERF9	CGAGGGTTACTCCGGCGGCTT	AT3G49830	P-loop containing nucleoside triphosphate hydrolases superfamily protein
ERF9	TGACGGTCACGGCGGGGGGA	AT4G10750	Phosphoenolpyruvate carboxylase family protein
ERF9	TTGCGGTACTGCGACTGCGA	AT4G19420	Pectinacetylesterase family protein
ERF9	CGGCGTTTATTTCGGTTGCGG	AT5G10770	Eukaryotic aspartyl protease family protein
ERF9	TGGCGTTGGCTTCGCCGGAGA	AT5G17540	HXXXD-type acyl-transferase family protein
ERF9	TGTCGGTGACGATGATGGAGA	AT5G18850	Low-density receptor-like protein; Unknown protein
ERF9	CGACGGAGATGATGACGGCAT	AT5G25280	Serine-rich protein-related
ERF9	CTCCGGTGACGGCGAGTGACG	AT5G37840	BEST Arabidopsis thaliana protein match is: plastid movement impaired 2
ERF9	AGGCTGCGGTGGCCGCCGTGA	AT5G62350	Plant invertase/pectin methylesterase inhibitor superfamily protein

5.4 Discussion

5.4.1 Analysis of DEGs significantly involved in ability of the terminal bud to successfully open

A large proportion of DEGs more highly expressed in SRC in the SSO/SRC and LFO/SRC comparisons aligned significantly with genes involved in photosynthesis in *Arabidopsis thaliana* or other species. Young flower buds in many species such as tobacco are still a photosynthetic tissue (Müller et al. 2010), but have been suggested to gradually lose this ability as they develop and open (Brazel and Ó'Maoiléidigh 2019). This is linked in carnation to the active breakdown of chloroplasts, degradation of chlorophyll, and concomitant increase in the expression of tepal colour-related compounds, such as flavonoids, anthocyanins and carotenoids, depending on the petal colour, and their uptake by the chromoplast (Ohmiya 2013; Iijima et al. 2020). This programmed downregulation of photosynthesis has been extensively described in leaf senescence (Biswal and Biswal 1999; Thakur et al. 2016) and also in tomato fruit ripening (Barsan et al. 2012), but is not as well characterised in petal tissues. In carnations, greater expression of chlorophyll catabolic genes compared to biosynthesis genes in petals prevents chlorophyll accumulation and therefore causes the reduction in green colour observed over flower development (Ohmiya et al. 2014). In lilies, flower opening causes changes in the cell wall, cell membrane and vacuolar membrane as tepals develop as shown by the increase in compounds such as malondialdehyde (MDA) (Zhang et al. 2021). The rise in MDA is an indicator that ROS from photosynthesis is not being appropriately processed, and correlates with downregulation in photosynthetic capability, changes in the chloroplast membrane and a breakdown of the photosynthetic apparatus, as characterised in *Pistacia lentiscus* leaves during senescence (Munné-Bosch and Peñuelas 2003). The observed downregulation of photosynthesis in flowers which go on to open is supported by the KEGG pathway analysis of DEGs between all buds which go on to open (SSO and LFO buds) compared to those which fail to open (SRC buds). These DEGs showed lower expression of many components of the photosynthetic machinery in flowers which went on to open. SSO and LFO buds also showed higher expression of a gene putatively encoding trehalase (enzyme catalysing trehalose to D-glucose). Trehalose-6-phosphate has been strongly linked to regulation of primary and secondary metabolism (Delatte et al. 2011; Lastdrager et al. 2014; Oszvald et al. 2018;

Nardozza et al. 2020). Higher levels were shown to promote higher photosynthetic rates, while lower levels caused upregulation of lipid-related metabolism and other development relating to flower maturity in *Zea mays* (Oszvald et al. 2018). Trehalose is also important in salt and osmotic stress, and higher trehalose levels also imply higher levels of cellular stress (Bae et al. 2005). These pieces of evidence suggest the balance between chloroplast development and breakdown is swinging more towards breakdown in buds which open (SSO and LFO) compared to those which failed to open (SRC).

DEGs upregulated in the 'Required to open' group (i.e. those important in opening but probably not related to bud size at harvest) showed a significant enrichment in many putative cell-wall remodelling genes, as well as wax- and flavonoid biosynthesis genes. This indicates that buds which were able to open successfully may have a greater expression of genes involved in cell expansion, cuticular wax production and scent production at this early stage of development compared to SRC buds which failed to open. Wax biosynthesis was found to be upregulated in flowers which went on to open (SSO and LFO) compared to SRC, with several putative genes in the pathway found during KEGG analysis of DEGs expressed more highly in SSO/LFO buds than in SRC buds. Cuticular wax production is important in flower development for water retention in open flowers and may lead to a longer shelf-life (Cheng et al. 2021), suggesting that the buds which went on to fail to open (SRC) may have less wax production due to their earlier developmental stage at harvest than flowers which could open (SSO/LFO), possibly leading to issues with dehydration later on. KEGG pathway analysis also indicated differences in phenylpropanoid biosynthesis between buds which did and did not open. Phenylpropanoids encompass a large proportion of the secondary metabolites produced in plants. They are produced for several different purposes, such as cell wall structure (lignins), scent and colour, UV protection (flavonoids), biotic protection (coumarins), antioxidant activity (phenolic acids) and general protective activity (stilbenes) (Deng and Lu 2017). The complexity and shared pathways for all of these different compounds explains the mixed higher and lower expression of genes encoding pathway enzymes observed between buds which do go on to open compared to those which fail to. While expression of genes putatively encoding putative cinnamyl-alcohol dehydrogenase (CAD, KEGG 1.1.1.195) was found to be expressed more highly in SSO/LFO compared to A, several other putative enzymes such as peroxidase (KEGG 1.11.1.7), carboxylesterase (KEGG

3.1.1.-), and ferulate-5-hydroxylase (F5H) were found to be expressed less in SSO/LFO compared to SRC buds. CAD is an enzyme catalysing the conversion of cinnamic acid derivatives to monolignols but also the precursors for scent compounds such as eugenol, for example (Vogt 2010; Bao et al. 2020). F5H catalyses the rate-limiting step for lignin biosynthesis, converting G-monolignol to S-monolignol (Jiang et al. 2020). These lignin precursors can then be converted to polymers by peroxidation in the final step (Sakamoto et al. 2020). The difference in phenylpropanoid metabolism-related gene expression between flowers which went on to open (SSO and LFO buds) compared to those which failed (SRC) may therefore reflect differences in both the levels of other developmental secondary metabolites (flavonoids, stilbenes, coumarins, and waxes such as cutin and suberin), and also differences in the kind of lignins produced.

The significantly lower expression of putative photosynthetic genes in flowers which go on to successfully open compared to those which fail in this study, even in those which are similar in size and therefore developmental stage, may point to a reduced breakdown of chloroplasts in tepals which will fail to open in the future. Alongside an increased expression in sets of genes coding putatively for 'flower opening' related genes in flowers which can successfully open, this data is consistent with the hypothesis that the precondition of flowers which fail to open involves a partial arrest of normal flower opening genes. When validation of the gene expression of some of these putatively identified DEGs (Figures 5.18, 5.22) was attempted using qPCR, the log₂FC between conditions showed a similar pattern to the qPCR data for all three genes investigated, although there were no statistically significant differences between the relative expression in SRC and SSO or LFO buds. This was likely due to the high variation observed across biological replicates, where often only one replicate showed a visibly higher expression than the other two. This variation could be due to natural variation in expression or due to the method used. The primers used in qPCR were designed from short sequences aligning significantly to these genes of interest and therefore putatively identified as *MYB21*, *EXPA8* and *PSII5*. Every effort was made to ensure these primers were specific to these sequences only, however this could be compromised due to lack of good quality lengths of sequence data, large gene families of the genes involved in the case of *EXP* and *MYB* genes (Stracke et al. 2001; Cosgrove et al. 2002), and observed high ploidy in *Lilium*, possibly meaning duplication and diversification of very

similar genes (Moghe and Shiu 2014). Thus, the primers may have amplified multiple products and may explain why the qPCR data do not accurately reflect the expression of the DEGs of interest.

5.4.2 Analysis of DEGs significantly involved in magnitude of opening

Magnitude of opening was found to be related to the length of the bud at harvest, and so the DEGs likely to be only involved in this process are those which are expressed significantly differently in tepal tissue in response to having more time on plant (LFO) rather than less (SSO). Some of the genes identified in the 'Magnitude of opening' group were again cell-wall remodelling-related, such as the putative XTH7 and cellulase. This was strongly supported by the K-means clustering, where Cluster 3 contained putative expansins and XTHs, alongside other putative cell expansion-related DEGs aligning closely to aquaporins and sucrose transporters. Expression of cell-wall remodelling enzyme-coding genes is strongly correlated to areas in the lily tepal with higher levels of cell expansion (Watanabe et al. 2022), and may indicate that higher expression is correlated with more cell expansion and a greater global tepal opening phenotype. Similarly, overexpression of *SWEET* transporter-encoding genes in *A. thaliana* was found to promote early flowering (Andrés et al. 2020) and silencing of a petal-specific aquaporin in rose was found to reduce petal cell volume and overall petal size (Ma et al. 2008).

Notably, several of the DEGs more highly expressed in buds with a very strong opening phenotype (LFO) compared to buds with a less strong opening phenotype (SSO) aligned significantly to photosynthesis-related *A. thaliana* genes. *CRB*, *SBPASE* and *HCEF1* are all chloroplastic genes which are involved in the Calvin cycle and chloroplastic transcription. This is surprising given the strong downregulation of several other photosynthetic genes observed in SRC compared to SSO buds. While the downregulation of photosynthesis and disassembly of chloroplasts is well described in the conversion of green to red leaves during leaf senescence, it is not so extensive in flower petals. In leaves, while there is a strong downregulation of photosystem I and II components in leaf senescence, KEGG pathway analysis indicated little to no change to sugar metabolism in many components (Vangelisti et al. 2020), which may explain the slight upregulation of certain sucrose synthesising parts of the Calvin cycle. Additionally, some species such as tobacco do not show a drop in

photosynthesis at anthesis in the corolla, even with a reduction in green petal colour, and this may suggest that there is still a limited amount of photosynthesis occurring (Müller et al. 2010).

Water-related stress may be a significant factor in the opening success of buds at risk of late bud abortion. *RD20* encodes a strongly drought stress-responsive caleosin activated via ABA (Aubert et al. 2010), which was putatively identified here as being more highly expressed in SSO compared to A. This is suggestive that smaller buds may have greater ABA signalling and may be more affected by the dehydration of dry transport or less able to take up water. This could perhaps be due to differences in the function of or a less developed pedicel. Putative genes involved in the ABA response showed a potential overall increase in ABA signalling in SRC buds compared to SSO or LFO buds, supporting this hypothesis.

5.4.3 Analysis of putative regulatory genes involved in the future opening success of terminal buds

KEGG pathway analysis showed that the MAPK signalling pathway (ath04016) and plant hormone signal transduction (ath04075) were enriched in the full list of DEGs in all comparisons, suggesting that several transduction pathways were significantly different between buds which later showed opening and failure to open phenotypes. The TF analysis using PlantTFDB showed the vast majority of these putative TFs were more highly expressed in SRC compared to SSO buds (Figure 5.19), showing families such as the NAC, ERF, and WRKY all showing higher expression in flowers which fail to open (SRC) compared to those which go on to open (SSO). These groups of TFs are all implicated in the plant stress response, and have been found to be upregulated in several biotic or abiotic stress conditions (Nakashima et al. 2012; Bakshi and Oelmüller 2014; Müller and Munné-Bosch 2015; Erpen et al. 2018). Conversely, many DEGs putatively coding for MYB transcription factors were found more highly expressed in SSO and LFO buds compared to SRC buds, which supports their known roles in positively regulating secondary metabolism related to flower development (Cao et al. 2020).

TFDB analysis identified several putative transcription factors which were found significantly differentially expressed in the 'Required to open' group, signifying TFs which were likely to be negatively or positively regulating the opening process, rather than related to bud

size/developmental stage. These included genes putatively coding for *MYB70* and *AP2-10* (both expressed less in SSO compared to A) were both identified. *MYB70* has been shown to integrate several phytohormone pathways; it was found to promote auxin conjugation through positive regulation of *GH3* expression in *A. thaliana*, leading to inhibited seed germination and root growth (Wan et al. 2021). *RAP2-10* encodes an APETALA2 family protein (APETALA 2/ethylene-responsive element binding factor 10) which has been hypothesised to be involved in vegetative growth throughout *Arabidopsis* development (Okamoto et al. 1997). The greater expression of these TFs in SRC buds supports the hypothesis that buds in this condition have higher levels of vegetative growth and less of the hormone-driven differentiation needed to cause bud development and opening. However, the *A. thaliana* homologs of the DEGs found may be similar in sequence to other proteins in the same family, especially in large gene families, and so the identification of genes here may not be completely accurate and should be considered when making conclusions about putative genes and pathways involved in flower opening.

AP2/ERF mediated gene expression may be important in flower opening, as the high incidence of AP2/ERF motifs in DEGs found uniquely between flowers which opened vs. failed to open correlates with the higher expression of several ERF transcription factors in SSO and LFO buds compared to SRC buds. AP2/ERF factors are a large group of plant-specific TFs. They have important roles in plant development, particularly flower differentiation and development (Kunst et al. 1989; Feng et al. 2020). The AP2/ERF domain in these proteins can bind to target promoter DNA sequences, activating transcription of genes involved in a huge range of functions such as abscission, ripening, and floral identity specification (Nakano et al. 2014). However, the putative DEGs which were identified in the 'Required to open' group as containing these AP2/ERF motifs aligned to *A. thaliana* orthologues which did not show any significant enrichment of GO terms or KEGG pathways in either analysis, suggesting there are no specific shared functions, processes or cellular compartment significantly in common with these putative DEGs. As with identification of transcription factors, the *A. thaliana* AP2/ERF motifs identified here may be different to the motifs in monocots such as lily (Licausi et al. 2010), and so the conclusions which can be drawn from this analysis are limited. However, the coexpression of genes significantly aligning to *A. thaliana* ERF TFs with genes significantly aligning to *A. thaliana* genes containing AP2/ERF

motifs does suggest that the data shown here may be at least partially accurate and supports the hypothesis that ERF transcription factors may also be involved in flower opening.

Plant abiotic stress responses are the result of environmental stressors on the plant, for example temperature, light levels, nutrient deficiency, salinity or water imbalances (either drought or flooding) and depending on the severity of the stressor, can lead to altered growth and yield, either positively or negatively (Chen et al. 2022a). This diversity of responses can make it difficult to predict the effect stress will have on the plant. Cut lilies undergo stressful commercial practices before reaching the consumer in terms of nutrient deficiency, cold and dark, and water loss, which can be hypothesised to affect some flowers more than others depending on the growth and development they were able to attain on the plant preharvest. The terminal bud on the stem is the most affected in many cases due to its small size at harvest, meaning that they often have the smallest starch content. The DEGs putatively identified as genes relating to the stress response showed a much higher expression in buds which went on to suffer from postharvest bud abortion than those which opened normally. These putative genes were linked to the MAPK pathway, and the JA, ABA and ethylene response, which have a well-known upregulation in stress conditions (Colcombet and Hirt 2008; de Ollas and Dodd 2016; Chen et al. 2022a).

The phytohormone ethylene is essential for many developmental processes but is most well-known for its role in the abiotic stress response (Müller and Munné-Bosch 2015). The ethylene response, which is mediated through ERF proteins (transcribed in direct response to presence of ethylene) was found to be more highly expressed in SRC buds compared to SSO buds here. This suggests that at the very early developmental stage sampled, a subpopulation of terminal buds were already showing increased stress responses, which went on to suffer from late bud abortion. However, ethylene has also been observed to have other effects on flower development and transition in many species, both positive and negative, suggesting that it also may be important in flower development (Iqbal et al. 2017; Dubois et al. 2018; Chen et al. 2022a). Dubois et al. (2018) in particular stressed the temporal separation of ethylene as a stress regulator in mature leaves while a positive developmental regulator in young leaves, possibly regulated by different ERF proteins expressed at different developmental stages which have opposing responses to ethylene.

5.4.4 A suggested model for the transition from primary to secondary metabolism as part of normal flower bud development

Auxin is a strong effector of plant growth via cell elongation and expansion. Many of the components of the auxin signal transduction pathway were found in the 'Required to open' group of DEGs. Expression of putative *Aux/IAA* genes was found to have higher expression in SRC compared to SSO buds. *Aux/IAAs* are a type of early auxin response protein which inhibit the expression of target auxin-responsive genes by binding to and causing the degradation of ARFs by ubiquitylation and eventual degradation by the 26S proteasome (Luo et al. 2018). The higher expression of putative *Aux/IAA* genes in buds that fail to open shown here may be indicative of an overall decreased auxin signalling in buds which are at risk of postharvest bud abortion. *SAUR* genes are likewise a very large family of auxin-related proteins with varied roles. Overexpression of some *SAURs* was found to produce an early senescence phenotype (Kant et al., 2009; Hou et al., 2013; Bemer et al., 2017b) rather than an expected effect on cell elongation (Spartz et al. 2014), suggesting that some *SAURs* may have an antagonistic effect on plant growth and development. This may also have an effect on the auxin transport to the tissue - overexpression of the growth-inhibiting *SAUR* genes *OsSAUR39* and *OsSAUR45* was found to inhibit auxin transport (Kant et al., 2009; Xu et al., 2017). This could point to a greater inhibition of auxin signalling in SRC buds, which show a slightly higher expression of *SAUR* genes compared to SSO buds (Figure 5.28). The repression of the normal cell expansion-related auxin transduction pathway observed here in buds which fail to open with may therefore be responsible for the observed phenotype.

Auxin has been shown to be a mediator for flower opening in other species such as waterlily (Ke et al. 2018) and tomato (Niwa et al. 2018), and therefore it can be hypothesised that some of the same transcription factors and hormone pathways may also be active here. JA is a fatty acid-derived plant growth regulator; *A. thaliana* mutants with reduced ability to synthesise JA show signs of defective flower development and delayed opening (Ishiguro et al. 2001). In tomato flowers, the presence of both jasmonic acid and auxin coordinate the expression of MYB transcription factors, which are essential in the opening process (Niwa et al. 2018). In rice, the JA conjugation gene *OsJAR1* is important to coordinate the opening of rice flowers with anther dehiscence and can be promoted by ARFs (Xiao et al. 2014). In turn, JA is a strong positive regulator of auxin synthesis through the *YUCCA* genes (Hentrich et al.

2013). The upregulation of fatty acid synthesis and metabolism observed here in buds which opened compared to those which did not, may perhaps indicate upregulation of JA synthesis, although genes specifically relating to synthesis were not found in this dataset.

Again, auxin-related genes of interest (*YUC3*, *ARF15*, and *SAUR75*) were not found to show significantly different relative expression between conditions, even when the log₂FC for the DEGs used to design primers showed high differential change, due to high variation within biological replicates as mentioned before. However, these genes did show the same general trend in being expressed slightly more in buds which did open (SSO and LFO buds) compared to buds which did not (SRC), which still supports the hypothesis that the auxin transduction pathway is upregulated in buds which can open, and in particular that the response to auxin is upregulated (SAUR genes being a transcriptional readout for auxin transduction success).

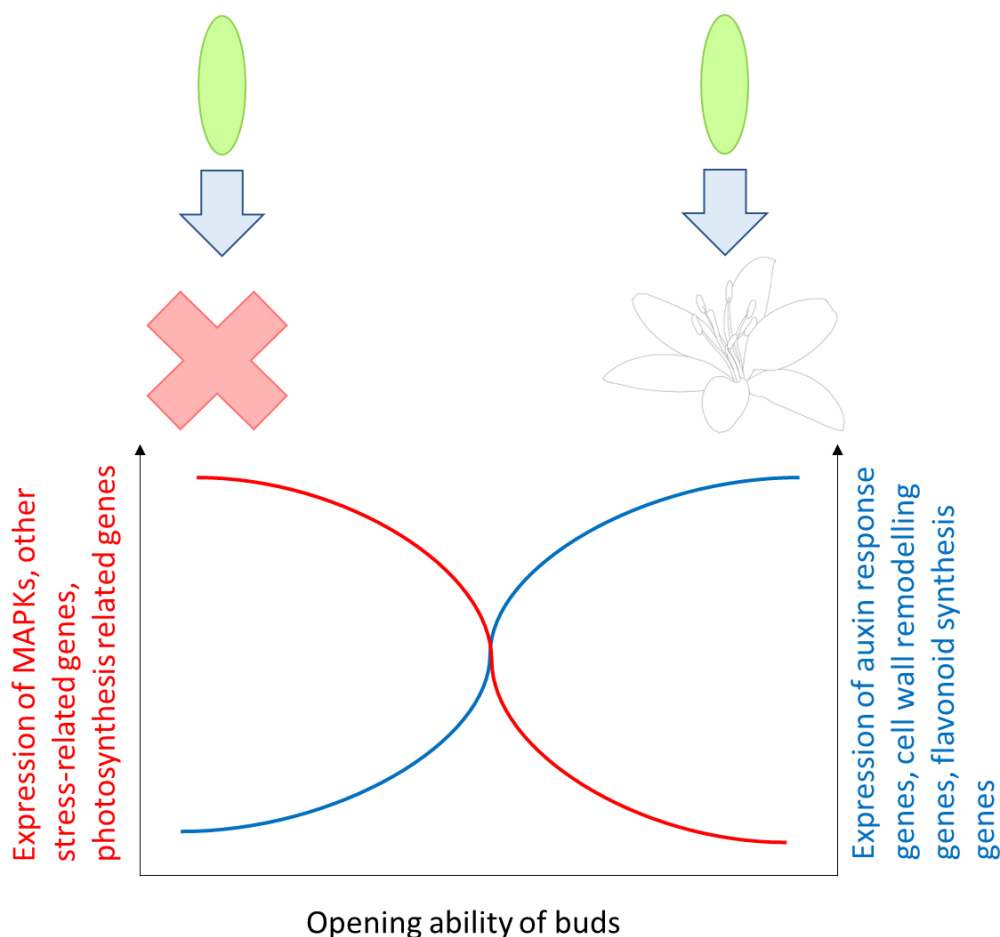


Figure 5.28 – putative model showing the observed expression levels of certain types of genes in precondition of buds going on to open (SSO, LFO) and of buds which fail to (SRC).

The lower expression of putative stress-related genes is correlated with the lower expression of putative photosynthesis related genes, alongside the higher expression of positive auxin response genes and secondary metabolism/ flower opening related genes in terminal buds which go on to open compared to those which fail.

5.4.5 Conclusions

Bud size and developmental stage have a complex relationship which has been shown to not be completely linear (Section 4.4.3). Despite this, a group of putative photosynthesis-related genes have been identified here as expressed at significantly lower levels in the group of buds which go on to open, while several putative groups of genes relating to bud development and maturity are expressed more highly in these same successfully opening buds. This ability to open is also correlated with the positive regulation of the auxin transduction pathway and may indicate a major role for auxin in the early development of lily flower buds. This is suggested to be auxin-mediated with input from several other stress (ethylene), light, and nutrition factors. More work is certainly required to confirm that the presence of auxin/ the auxin response is a requirement for opening.

Chapter 6 - Hormonal regulation of flower opening

6.1 Introduction

As the auxin transduction pathway was indicated in Chapter 5 to be significantly different between buds which can open and those which fail to, it will be studied further in this chapter to elucidate the mechanisms driving lily development and opening. Auxin will be investigated here as a potential treatment for buds at risk of postharvest bud abortion.

6.1.1 Regulation of opening by phytohormone signalling

Phytohormones are well known for their varied roles in plant development and growth and often work in complex feedback systems. Similarly to the variation in physical mechanisms across species, species use different hormonal strategies to drive flower opening. Adaptations for a well-regulated flower life cycle directs pollinators to virgin flowers (Shykoff et al. 1996) and in species with several blooms per inflorescence allows for the largest number of pollinated flowers per stem and therefore maximises viable seed production (Bell 1985). Phytohormones do not exist in a vacuum – they work together in complex networks which fine-tune and integrate environmental and developmental signals (Altmann et al. 2020). There are many examples of hormone crosstalk in flower opening specifically (Chandler 2011; Sun et al. 2021) but often examples are species-specific. In rose, gibberellins and ethylene regulate flower opening acting antagonistically, where ethylene was found to repress gibberellin synthesis and responses, decreasing petal cell expansion (Chen et al. 2020). Auxin and cytokinin often act antagonistically in other tissues to maintain meristematic growth in a very restricted area (Moubayidin et al. 2009) and may in the same way regulate the very specific differential growth observed in lily tepals over opening. Although Chapter 1 described in detail the role of several other hormones which may influence each other and have a role in flower opening, either already indicated in lilies or hypothesised from other species, this chapter will focus on the role of auxin and cytokinins as two important growth regulators found in plants (Moubayidin et al. 2009). Appendix 7 outlines the reanalysis of published transcriptomic data (Shi et al. 2018b), showing many expressed auxin and cytokinin related genes can be identified. The data showed that auxin related genes are found in general to be more highly expressed in early stages prior to flower opening, whereas cytokinin related genes showed the opposite trend and were

expressed more highly post opening and into senescence. These two hormones therefore are hypothesised to oppose each other's functions in terms of flower opening in lilies and will be studied to confirm these roles.

Auxin is a key regulator of nearly every developmental process in plants due to its important role in cell elongation, division and differentiation, which has been well characterised in the model species *Arabidopsis thaliana* (Aloni et al. 2006; Tromas and Perrot-Rechenmann 2010). Therefore, it would not be surprising if this group of hormones was involved in lily flower opening, which has been shown in Chapter 3 to be mainly due to differential cell expansion. Auxin may have been identified as a major driver of flower opening in lilies due to the identification and differential expression of auxin biosynthesis and transduction components between buds which can open and those which fail to in Chapter 5, and will be investigated in this chapter to assess the hypothesised importance of the auxin response in flower opening. The processes involved in auxin biosynthesis, transport and transduction appear to be well conserved across monocotyledonous and dicotyledonous plants (McSteen 2010) and therefore data on *A. thaliana* and other species may be relevant in this study to develop hypotheses about auxin's function in lilies.

Auxin is transported in a polar fashion known as polar auxin transport (PAT) around the plant. Polar auxin transport using the AUX1/LAX importer proteins and PIN1 exporter proteins is required to maintain an auxin gradient and specify/develop flower primordia at the ends of inflorescences (Cheng and Zhao 2007). Measurements of IAA using high performance liquid chromatography-mass spectrometry (HPLC-MS) in outer and inner tepals of the LA hybrid (cv. Courier) showed a rise in IAA from the immature green bud stage to flower opening in outer tepals and a strong peak in IAA levels at mature bud stage in inner tepals (Arrom and Munne-Bosch 2012). The correlation between IAA levels and time of flower opening may point to a role for auxin in flower opening. In *A. thaliana*, auxin is thought to mediate its effects directly by binding to Aux/IAA receptors (IAA), and also transcriptionally through auxin response factors (ARFs) and their targets, Small Auxin Upregulated Response factors (SAURs) (Gan et al. 2020). Aux/IAA receptors coregulate auxin recognition with the TIR1/AFB F-box protein receptors (Luo et al. 2018). When auxin is present, these proteins bind to each other, causing the ubiquitinylation and degradation of Aux/IAA. This in turn causes the derepression of ARF transcription. ARFs have a wide range

of transcriptional targets dependent on the tissue and developmental stage. SAUR genes are often very sensitive to regulation, sometimes being induced within 5 minutes of exogenous auxin application (Wang et al. 2020). These genes go on to regulate expression of genes coding for cell wall remodelling enzymes such as expansins, xyloglucan endotransglycosylase/ transferases (XTHs), pectin related genes and peroxidases, which may be also activated by other factors such as nutritional status, stress, and light (Figure 6.1, Majda and Robert 2018).

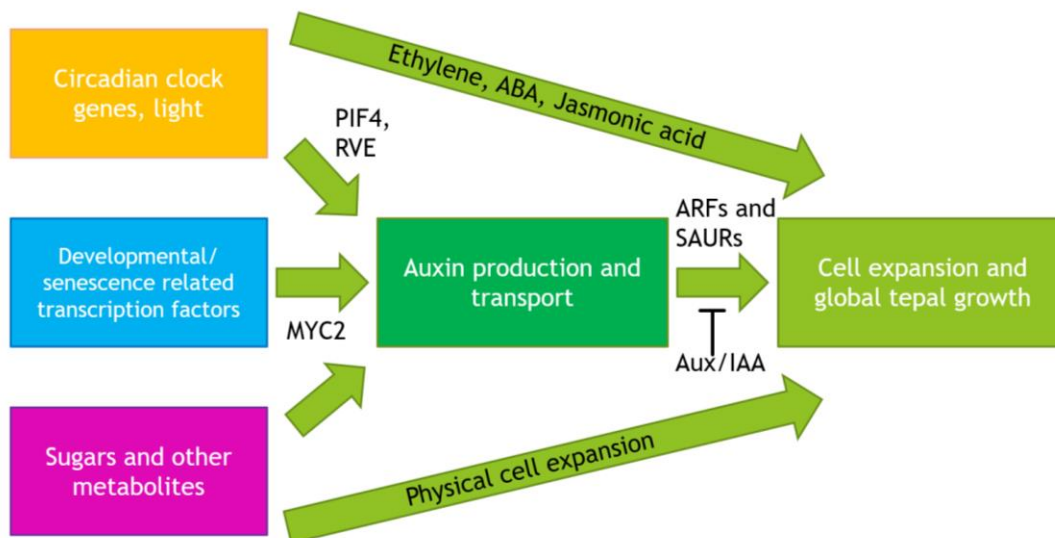


Figure 6.1 – diagram showing the inputs and outputs of the auxin pathway, integrating environmental and endogenous signals. The REVEILLE and PIF clock genes can regulate auxin synthesis to certain times of day in *A. thaliana* (Rawat et al. 2009). Other local environmental factors which may affect auxin production or transport are developmental transcription factors such as MYC2, which is activated by jasmonic acid to promote auxin synthesis (Pérez-Alonso et al. 2021), and presence of glucose and other sugars, which can also induce expression of auxin-producing YUC genes (Mroue et al. 2017). The production of auxin within or transport into specific tissues can cause the activation of Auxin Response Factors (ARFs) and the transcription of genes such as Small Auxin Upregulated Response (SAURs) alongside other genes involved in cell expansion and growth. Other hormones such as ethylene, ABA and JA can also be involved in this growth through auxin independent or dependent pathways and are also induced in response to developmental signals, the circadian rhythm and stress.

Cytokinins are also tightly involved in many areas of plant development and regulate a wide range of developmental and physiological processes, including cell expansion and growth in *A. thaliana* (Maximino Leite et al. 2003; Werner et al. 2021). Studies in rice, a monocot, have shown strong similarities in components and functions of cytokinin signalling to *A. thaliana* (Jain et al. 2006; Worthen et al. 2019). Cytokinins mediate their effects through the two-component pathway; they bind to a histidine kinase receptor (HK). This HK causes the phosphorylation of response regulators (RRs) through the activation and nuclear translocation of a histidine phosphotransfer protein. RR are a diverse family of proteins found both in the cytoplasm and nucleus. Type A RRs are involved in negative feedback of cytokinin signalling, whereas Type B RRs contain a DNA-binding domain to effect transcription of target genes related to regulation of growth and development (Müller and Sheen 2007). The cytokinins zeatin and zeatin riboside have been found to increase in inner tepals prior to flower opening – zeatin increased three-fold from 20-60 ng/g DW from immature bud to open flower, and zeatin riboside increased over two-fold from immature bud to mature bud stage (Arrom and Munne-Bosch 2012a), suggesting they may be involved in the opening process.

6.1.2 The role of phytohormones in postharvest treatments

Manipulating phytohormone levels in plants is commonly used in pre- and postharvest treatments for many crop types due to their global, varied and long-lasting physiological effects (Kumari et al. 2018; Wei et al. 2018; Miceli et al. 2019; García-Pastor et al. 2020). Application of phytohormones is generally compound- and effect-specific, i.e. dependent on the type of compound and on the length of application, for example. Foliar spraying and soil drench is often used in preharvest treatments due to ease of application in a commercial setting and effectiveness. Compounds which can pass through cell membranes and the waxy layer on leaves are preferable here such as 1-MCP (Wei et al. 2018). Postharvest treatments are incredibly varied depending on the species, length of time applied, the concentration, and the method of application (Redman et al. 2002). Pulsing treatments offer a dose of concentrated compound over a relatively short period of time (e.g. 24 hours) and may offer a good option if long term dosage is suboptimal. Sucrose pulsing in particular has been used

for many cut flower crops to extend vase life (Ichimura 1998; Van Doorn and Han 2011; Bích and Nhung 2020) and offers a stage to simultaneously add other treatments to cut flowers prior to storage or transport.

Commercially, the cytokinin 6-benzyladenine (6-BA) and gibberellins GA₄₊₇ are used in the formulation Promalin® to delay flower opening, improve longevity of the stem, and reduce leaf chlorosis in cut flowers. Promalin® has been found to have detrimental effects on lilies in vase solution but effective as a foliar spray of 25 mg L⁻¹ (Han 2001). Ethylene inhibitors such as silver thiosulfate (STS) and 1-Methylcyclopropene (1-MCP) have been used for a long time in many cut flower species (Serek et al. 1995; Redman et al. 2002). 1-MCP was shown to delay senescence in cut cold-stored Oriental lily cv. 'Sorbonne', hypothesised to be due to manipulation of respiratory metabolism (Wei et al. 2018), suggesting that in some cultivars ethylene may be a driver of senescence and inhibiting it can improve longevity, whereas in others treatment with STS or 1-MCP was found to have no effect (Elgar et al. 1999), perhaps linked to the ethylene sensitivity of the cultivar. 1-MCP is used widely for its anti-ethylene effects but is transient and temperature-sensitive (Reid and Jiang 2012) and therefore may also be inefficient as a commercial treatment. In Iris, pulsing with gibberellins (GA₃) before storing dry improved flower opening by reducing the effects of water stress and is a promising treatment (Celikel and van Doorn 1995).

6.1.3 Potential new treatments for failure of opening in terminal buds

As of yet, apart from exogenous sucrose pulsing (Pattaravayo et al. 2013), there are not many commercial treatments which promote flower opening in flowers. As discussed in previous chapters, terminal buds on inflorescences with a larger number of buds are more likely to fail to open in certain lily varieties (personal communication, James Cole, E.M. Cole Farms Ltd.). This may be due to insufficient nutrition, stress, or a combination of factors, and can be partially improved with hormone treatments (Vonk and Ribôt 1982; Mason 1989; Ohno 1994). The drivers of this process are not fully understood but bud abortion (a similar phenomenon in preharvest lilies where buds arrest in development very early) was found to be promoted by ethephon treatment (ethylene) and reduced by silver thiosulfate (STS) treatment (ethylene inhibitor) in Easter lilies, which suggests ethylene may be involved in this response (Mason and Miller 1991). Furthermore, reducing their light levels for two

weeks during growth was also found to significantly increase rates of bud abortion in terminal buds (Mason and Miller 1991), suggesting that in some lily varieties, a low-light stress response, perhaps mediated by ethylene, may be at least partially responsible.

Exogenous auxin is not used commonly as a postharvest treatment for cut flowers but has been used in postharvest fruit and vegetables to delay fruit softening and overripening (Castro et al. 2021), promoting colour development in citrus fruits (Kato 2022), and preventing calyx abscission (Sdiri et al. 2013). Although not used as a commercial treatment, exogenous auxins were found to promote pedicel and ovary elongation in iris flowers, whilst application of inhibitors of auxin transport and signalling was found to do the opposite (van Doorn et al. 2013). Due to auxins' effects on cell expansion, growth and development detailed here, it was considered in this study as a potential flower opening treatment.

6.1.4 Aims

1. Understanding and supporting what is currently known about endogenous hormonal control of flower opening in lilies.
2. Exploring the effect of exogenous auxin post-harvest treatments on bud opening failure in terminal buds.

6.2 Materials and methods

6.2.1 Effect of exogenous auxin/auxin transport inhibitor application on individual lily bud opening

1-Naphthaleneacetic acid (NAA) was used here as a synthetic auxin to assess the effect of exogenous auxin on flower opening in lilies. LA hybrid lilies (cv. Courier) were grown in Cardiff University greenhouse conditions (Section 2.1), harvested at Stage 1 (for 'Courier' at bud length 7.5–8 cm, buds were from Position A on stem only) and immediately put in either dH₂O (n=9), 100µM NAA in dH₂O (Sigma-Aldrich, n=8) or 10µM NAA in dH₂O (n=9) constantly under vase life conditions (Section 2.1) to assess the minimum concentration of NAA required to have an effect. Timelapse photography was used to measure time from harvest to start of opening and time taken to fully open from start of opening. When it was observed that 100µM NAA had toxic effects on individual flower buds, only 10µM NAA in dH₂O was used in further experiments. A control for each day of harvest was taken due to

variation in developmental stage:bud length caused by temperature fluctuations in the greenhouse. The effect of naphthylphthalamic acid (NPA) was also assessed as an auxin transport inhibitor. Position A buds from LA hybrid cv. Courier which had been treated in the same way were also split into two groups (n=11) and either maintained in dH₂O or 100µM NPA in dH₂O (Sigma-Aldrich). For both experiments, the time from harvest to when the movement of tepals fully stopped in full reflexed opening (fully opened) was measured. Differences between control and the treatment groups (10µM NAA, 100µM NAA) was assessed for statistical significance by one-way ANOVA and post-hoc Tukey or Kruskal-Wallis with post-hoc Dunn test dependent on normality of the dataset. Statistical significance between control and NPA-treated bud opening time was assessed using a student's T-test in RStudio (version 1.3.1093).

This experiment was repeated with Oriental lilies (cv. Tisento). 'Tisento' plants were grown in greenhouse conditions until Position A buds were approximately Stage 2 (between 11.5-12cm long) and harvested individually. At least 9 buds were used per group (control, 10 µM NAA, 100µM NPA), which was set up in the same way as for 'Courier' and in the same conditions. The data was analysed by measuring the time from harvest to the start of opening (from Stage 2 to 'kissing tips' (between Stage 3 and 4 when the lily tepals start to separate at the tip of the bud)) and the time from the start of opening to full opening (from 'kissing tips' to when the movement of tepals fully stopped in full reflexed opening – Stage 5). These two times were measured separately to assess if NAA and NPA selectively impacted the time to start opening or the opening process itself. These two times were added together for the total opening time. The time taken for total opening, harvest to start of opening and start of opening to fully open was compared between groups using ANOVA and post-hoc Tukey test in RStudio (version 1.3.1093).

6.2.2 Effect of exogenous auxin application on lily opening on stem

Oriental lilies cv. Pacific Ocean were grown in E.M. Cole Ltd greenhouse conditions until maturity, and were harvested and commercially treated as described in Section 2.1.2. Stems with four or five buds per stem were selected for this experiment. Stems were trimmed by approximately 3 cm and either added to FloraLife Express Clear ULTRA 200 (1:200 water) made up with tap water or a solution of 10µM NAA made up in FloraLife. All stems were

grown in 2L solution per four stems. A time of opening assay was set up as described in Section 2.4 (Figure 3B shows an example of the timelapse photographs used for analysis) to take timelapse photographs every 30 minutes for 8 days. A dim green light (ENUOLI green neon light) was used at night to allow continuous 24-hour photography.

Bud opening time data (hours to open from start of the experiment) for each position on stem (Position A-E) was analysed statistically for differences between stems grown in FloraLife and 10 μ M NAA using a Kruskal-Wallis test and post-hoc Dunn test in RStudio (version 1.3.1093) due to non-normality of the residuals from the dataset. Bud opening time for Position A and Position D buds was also divided into subsets and analysed statistically in the same way as for all buds. Position E bud opening time was not analysed separately due to lack of biological samples.

6.2.3 Expression of phytohormone-related genes over flower opening

Relative expression of the putative genes ARF6/8, ARF7/19, ARF15, IAA14, ORR9, SAUR75 and YUC3 (primer sequences and design can be found in Section 2.9.1 Table 2.2. Origin of sequences can be found in Appendix 5) was measured using qPCR as described in Section 2.9.4 using tepal material (Sections 6.2.2.1, 6.2.2.2).

Table 6.1 – Putative genes relating to auxin- and other phytohormone-related functions

Putative gene name	Encodes	Function
AHP	<i>Arabidopsis thaliana</i> histidine phosphotransfer protein	Part of the two-component cytokinin signalling pathway. Cytokinin receptors such as CRE1 activate AHP to phosphorylate response regulator target proteins (Müller and Sheen 2007).
ARF6/8	Auxin response factor 6/8	Part of signal transduction pathway for auxin response. In <i>A. thaliana</i> found to regulate jasmonic acid biosynthesis and flower organ development (Tabata et al. 2010).

ARF7/19	Auxin response factor 7/19	Part of signal transduction pathway for auxin response. Found to be relevant in inhibiting lily tepal abscission (Lombardi et al. 2015).
ARF15	Auxin response factor 15	Part of signal transduction pathway for auxin response (Shen et al. 2010).
AUX1	Auxin influx carrier	Aux1/LAX carriers found upregulated in rose petals over opening, suggesting a role for auxin transport in flower petal cell expansion (Han et al. 2019).
IAA14	Aux/IAA receptor 14	Auxin co-receptor (Luo et al. 2018).
ORR9	Oryza Response Regulator 9	Part of the two-component cytokinin signalling pathway. B-type ARRs/ORRs cause direct transcription of target genes (Müller and Sheen 2007).
SAUR75	Small Auxin Upregulated Response factor 75	Part of signal transduction pathway for auxin response (Wang et al. 2020).
YUC3	YUCCA 3	Encodes an enzyme essential for auxin biosynthesis (Yamamoto et al. 2007).

6.2.3.1 Endogenous expression of phytohormone-related genes over flower opening

cDNA from lily tepal material (Oriental lily cv. Tisento) over flower opening (Stages 1-5) was used to quantify relative expression of the phytohormone genes in Table 6.1 over flower opening using qPCR as described in Section 2.9.4. Primers for these genes are detailed in Table 2.1. Some of the primers used were designed from sequences from the RNAseq experiment in Chapter 5.

6.2.3.2 Expression of auxin-related and flower opening-related genes on flowers treated with exogenous auxin/auxin transport inhibitor

LA hybrid Position A buds (cv. Courier) grown in Cardiff University greenhouse conditions were harvested at Stage 2 (bud length 9.5-10 cm) and placed under vase room conditions in either dH₂O, 10 µM NAA in dH₂O (Sigma-Aldrich) or 100 µM NPA in dH₂O (Sigma-Aldrich) as described in Section 6.2.1. When buds reached Stage 5 (fully open flower) outer tepals were removed from the flower, the top 2/3 of the tepal was cut with a clean scalpel and discarded, and the remaining bottom third of the tepal was flash frozen in liquid nitrogen in order to use the part of the tepal closest to the pedicel and most likely to have taken up NAA/NPA. Biological samples (from one individual flower) were collected in triplicate for buds grown in either dH₂O, 10 µM NAA or 100 µM NPA. Material was stored at -80°C until required.

RNA was extracted from the frozen tepal material as described in Section 2.6.3 using the Tri-reagent extraction protocol. Quality of RNA was assessed as described in Section 2.6.5. Section 2.7 and 2.8 also describe the DNase treatment and cDNA synthesis methods used to produce cDNA. This cDNA was used to quantify relative expression of the phytohormone-related genes described in Table 6.1. Primers for these genes can be found in Section 2.9.1 Table 2.

6.2.4 Effect of exogenous auxin on terminal buds at risk of postharvest bud abortion

Oriental lilies cv. Ascot were grown under Cardiff University greenhouse conditions (Section 2.1.1.1) and a terminal bud opening ability assay was carried out using individual terminal buds as described in Section 2.10. In short, stems with 4 or 5 buds per stem which had a range of bud lengths of the terminal bud from 2.5-4 cm (lengths at which it was potentially likely to fail to open on stem with commercial treatment) were harvested and commercially treated (Section 2.1.2.2). Terminal buds were individually labelled, cut off the stem, length was measured, and the top third of the inner and outer tepals was cut away carefully (Figure 2.5). This section was immediately flash frozen in liquid nitrogen, and stored at -80°C. The remainder of the bud was either maintained in tap water or 10 µM NAA in tap water in a clean container in Cardiff University growth room conditions (Section 2.1.3) and monitored for opening. The number of buds which opened when stored in 10 µM NAA

solution and tap water was compared separately for stems with 4 and 5 buds per stem originally. Statistical significance was measured using a Chi-squared test.

6.3 Results

6.3.1 Relative expression of phytohormone-related genes over flower opening

Auxin related genes showed either stable expression or an increase in relative expression over flower opening from Stages 1-5. Putative *YUC3* (coding for the auxin synthesis enzyme YUCCA 3) showed no significant changes in relative gene expression over Stages 1-5, however showed a small decrease in expression from Stage 1, 2, and 3 to Stage 4 and 5, which may have been significant with more biological replicates (Figure 6.2A). The auxin transporter gene *AUX1* also showed no change in relative expression over Stages 1-5, suggesting a constant expression regardless of stage of development (Figure 6.2B). Putative *IAA14* (coding for the Aux/IAA 14 protein) showed an initial fast increase in relative expression from Stages 1 to 3 (Figure 6.2C). The relative expression of *IAA14* was then maintained from Stages 3-5 with an average expression of around 3.5-fold compared to Stage 1. Putative *ARF6/8* (coding for Auxin Response Factor 6/8) showed a consistent increase in relative expression over Stages 1-5, peaking at Stage 5 with a 4-fold relative expression compared to Stage 1 (Figure 6.2D). However, *ARF7/19* (coding for Auxin Response Factor 7/19) did not show the same trend, with no significant differences observed over Stages 1-5 (Figure 6.2E), although a downward trend may have been observed with less sample variability. Putative *SAUR75* (coding for Small Auxin Upregulated Response factor 75) showed a constant relative expression over Stages 1-3, and then showed a small significant increase in Stages 4 and 5, peaking in Stage 5 with a 10-fold increase in expression compared to Stage 1 (Figure 6.2F).

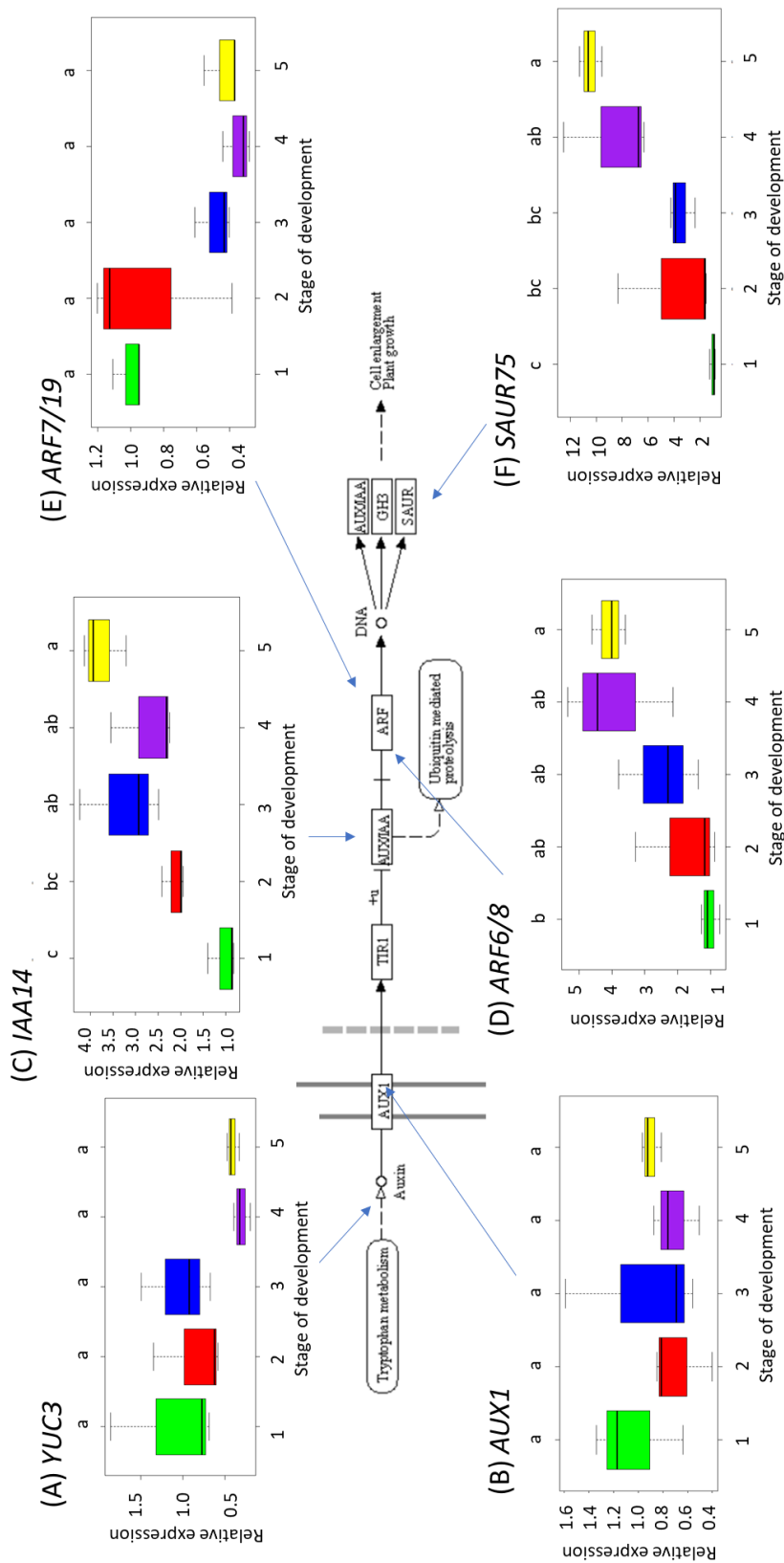


Figure 6.2 – Relative gene expression of putative auxin-related genes over Stages 1-5 of flower development and opening by qPCR. Significance denoted by letters using the

statistical tests (A) One-way ANOVA ($F=2.48$, $d.f.=4$, $p>0.05$) and post-hoc Tukey, (B) One-way ANOVA ($F=0.66$, $d.f.=4$, $p>0.05$) and post-hoc Tukey, (C) One-way ANOVA ($F=9.35$, $d.f.=4$, $p<0.05$) and post-hoc Tukey, (D) One-way ANOVA ($F=4.28$, $d.f.=4$, $p<0.05$) and post-hoc Tukey, (E) Kruskal-Wallis ($\chi^2=7.97$, $d.f.=4$, $p>0.05$) and post-hoc Dunn, and (F) One-way ANOVA ($F=7.86$, $d.f.=4$, $p<0.05$) and post-hoc Tukey (Appendix 6.15). Diagram of auxin signal transduction pathway taken from Kyoto Encyclopedia of Genes and Genomes (KEGG) database.

Cytokinin-related genes also showed an increase in relative expression late into flower opening. Putative *AHP* showed stable relative expression in Stages 1-4, and a significant rise at Stage 5, reaching a mean relative expression of 2.4-fold higher than at Stage 1 (Figure 6.3A). This was not as dramatic an increase as the similar pattern observed in putative *ORR9* expression, which increased over 1000-fold by Stage 5 significantly compared to Stage 1, but showed very minimal expression in Stages 1-3 (Figure 6.3B).

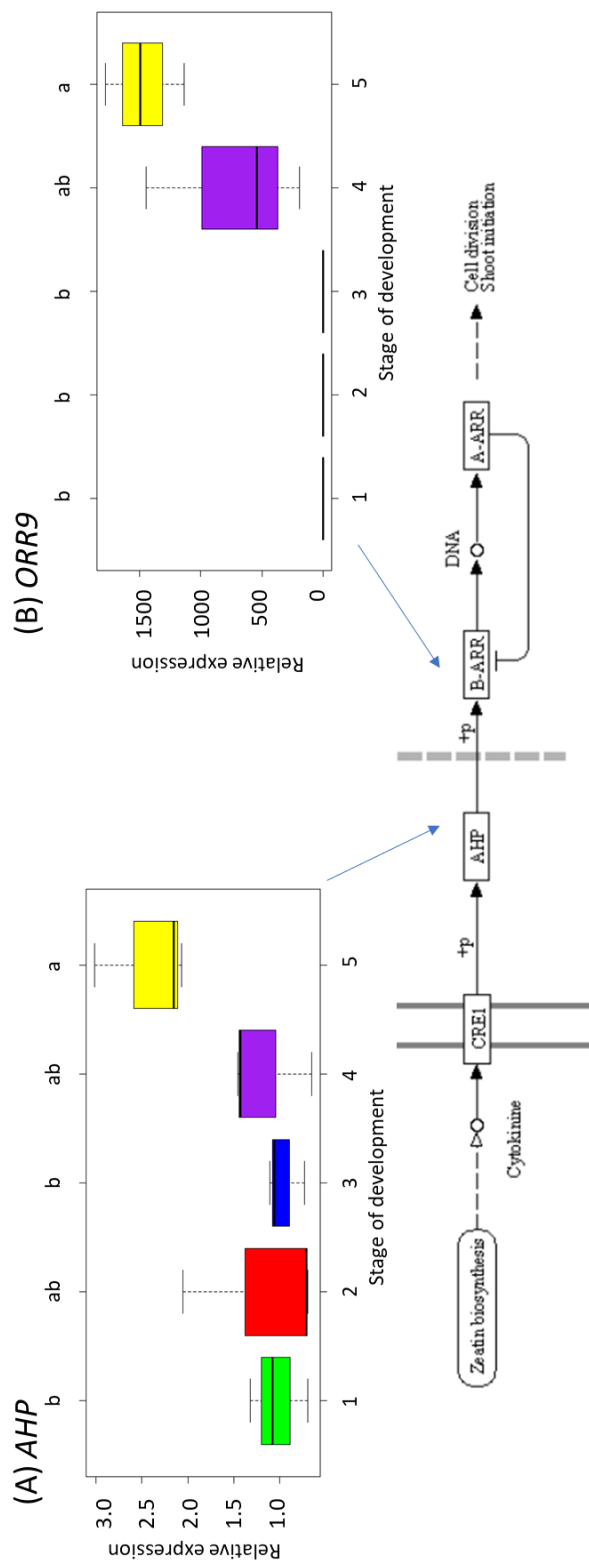


Figure 6.3 - Relative gene expression of putative cytokinin-related genes over Stages 1-5 of flower development and opening by qPCR. Significance denoted by letters using the statistical tests (A) One-way ANOVA ($F=4.39$, $d.f.=4$, $p<0.05$) with post-hoc Tukey and (B)

Kruskal-Wallis ($\chi^2 = 12.289$, $d.f.=4$, $p < 0.05$) and post-hoc Dunn test (Appendix 6.16). Diagram of cytokinin signal transduction pathway taken from Kyoto Encyclopedia of Genes and Genomes (KEGG) database.

6.3.2 Effect of exogenous auxin on flower opening in individual buds

To ensure NAA treatment was not causing toxic side effects at an inappropriate dose, the effect of 10 μM NAA and 100 μM NAA were compared to control. ‘Courier’ control Position A buds showed a variation in opening time from between 76 and 127.5 hours (Figure 6.4A). The 10 μM NAA treatment caused a significant reduction in the time taken for buds to open (One-way ANOVA, $F=5.598$, $d.f.=2$, $p < 0.05$), and caused a drop in variation in opening times (56-96.5 hours). The 100 μM NAA treatment caused a slight reduction in opening time compared to control, but not significantly different to either control or 10 μM NAA treatment. This also showed a similar range of opening time to control flowers (59-106 hours). Additionally, 100 μM NAA treatment caused discolouration of the tepals and stem and was not used in further experiments due to potential toxicity.

NPA treatment showed a significant increase in ‘Courier’ flower opening time compared to controls (Figure 6.4B). Notably, the set of controls in this experiment were observed to have a much shorter opening time and smaller variation (8.5-28 hours). Comparatively, buds treated with NPA showed a range of opening time between 19 and 44.5 hours.

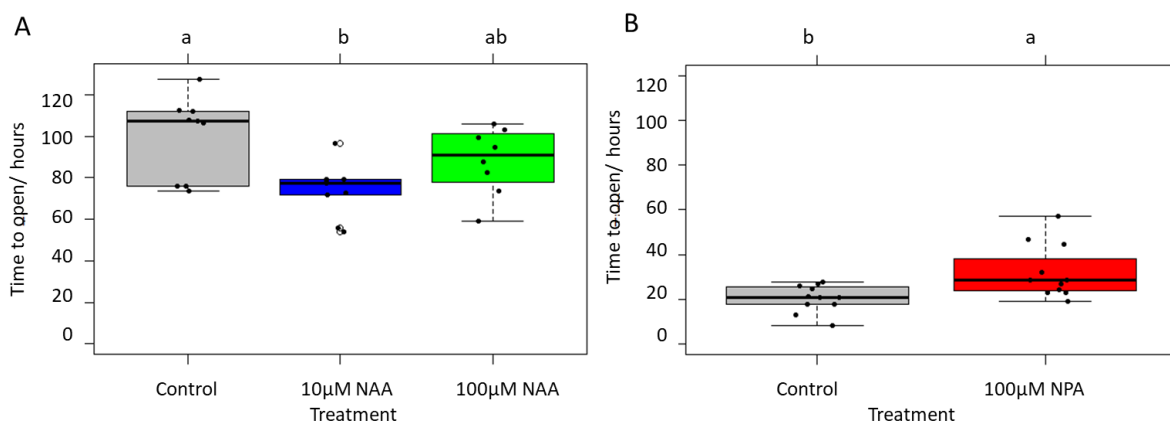


Figure 6.4 – Time taken to fully open (Stage 5) from harvest (harvested at Stage 1) of individual commercially treated Position A LA hybrid ‘Courier’ buds, comparing those treated

*with (A) 10 μ M NAA, 100 μ M NAA, and (B) 100 μ M NPA to controls. Letters show significance as shown by (A) One-way ANOVA ($F=5.598$, $d.f.=2$, $p<0.05$) and post-hoc Tukey and (B) 2-sample student's *T*-test ($t=-2.85$, $d.f.=14.7$, $p<0.05$) (Appendix 6.17).*

The effect of 10 μ M NAA and 100 μ M NPA was also investigated in Oriental lilies cv. Tisento. 'Tisento' Position A buds showed a range of total opening time from 33.5-60.5 hours. Buds treated with 10 μ M NAA showed a significant acceleration in total flower opening time compared to controls (Figure 6.5A; Kruskal Wallis chi squared=15.574, $d.f.=2$, $p<0.05$). 'Tisento' buds treated with NPA showed no significant differences to the total time of flower opening (Figure 6.5A) compared to controls. These buds also showed much more variability in the time of opening compared to control buds, from 32-77.5 hours.

When split into the time taken from harvest to start of opening (Figure 6.5B), there were significant differences between 'Tisento' control buds and NPA-treated buds (Kruskal-Wallis chi squared=8.52, $d.f.=2$, $p<0.05$). NPA-treated buds showed a huge amount of variation, taking between 14.5 and 57 hours to reach this start of opening from harvest. NAA-treated buds did not show significant differences to control buds, indicating that NAA treatment has little effect on this first phase of flower opening.

In the later phase of opening, going from start of opening to fully open (Figure 6.5C), 'Tisento' control buds show much more variation than the treatment groups (9.5-37.5 hours), whereas NAA-treated buds opened within 11 hours of each other (12-23 hours) and NPA-treated buds had a very similar range (15-21.5 hours). There were no significant differences in this later stage of opening between control and NAA/NPA-treated buds.

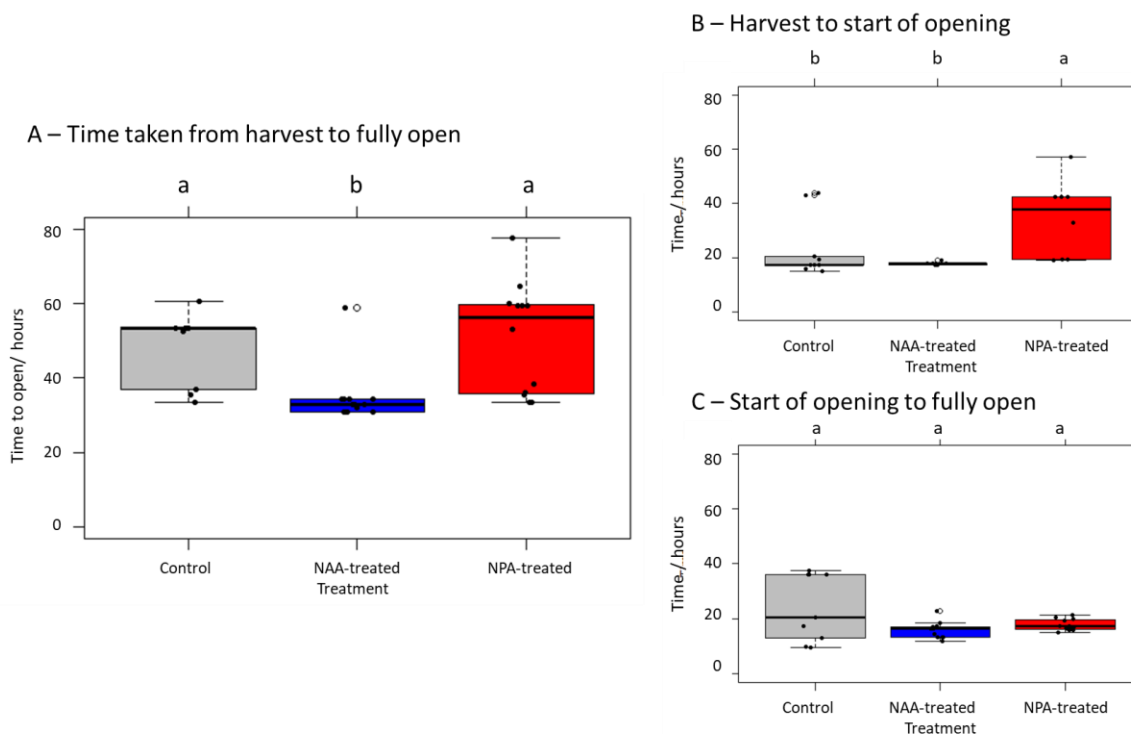


Figure 6.5 – (A) Total time taken to open from harvest (approximately Stage 2) of individual commercially treated Position A Oriental ‘Tisento’ buds, (B) Time taken from harvest (approximately Stage 2) to start of opening (defined ‘kissing tips’ as the first movement of tepal tips), and (C) Time taken from start of opening to fully open (Stage 5). Letters denote significance as shown by Kruskal-Wallis and post-hoc Dunn test (Appendix 6.17).

6.3.3 Effect of exogenous auxin on flower opening in whole stems

Oriental ‘Pacific Ocean’ buds which were on plant had a significantly shorter opening time compared to both commercially treated buds and commercially treated buds with added 10 μ M NAA (Kruskal-Wallis chi-squared: 16.68, d.f.:2, $p < 0.05$, Figure 5.6). The box plot in Figure 6.6A shows the variation in opening time as segregated by position on stem for each treatment, as also described in Section 3.3.2. The variation in opening time is also larger for buds on plant than commercially treated or NAA commercially treated, with two outliers from Position D on plant which showed a similar opening time for Position E buds to buds in the other two treatment groups.

When Position A bud opening time was analysed separately, Position A buds on plant (Figure 6.6B) also showed a significantly different opening time to the two commercially treated groups, regardless of NAA treatment (Kruskal-Wallis chi squared: 16.1, d.f.:2, $p < 0.05$). The opening time was much more variable for buds on plant, with a range of between 34 and 129.5 hours. In comparison, commercially treated Position A buds had a range of between 105-131.5 hours and NAA-treated Position A buds were between 104-135.5 hours, with in NAA-treated nearly all buds opening between 104 and 105.5 hours, at the very upper end of the range for on plant buds.

Position D buds (Figure 6.6C) showed a slightly but non-significantly shorter opening time for buds on plant compared to commercially treated or NAA-treated (Kruskal-Wallis chi squared: 8.33, d.f.:2, $p > 0.05$). Again, the range for bud opening on plant was greater than opening time for commercially treated and NAA-treated, and only slightly shorter on average for buds on plant than commercially treated and NAA-treated buds.

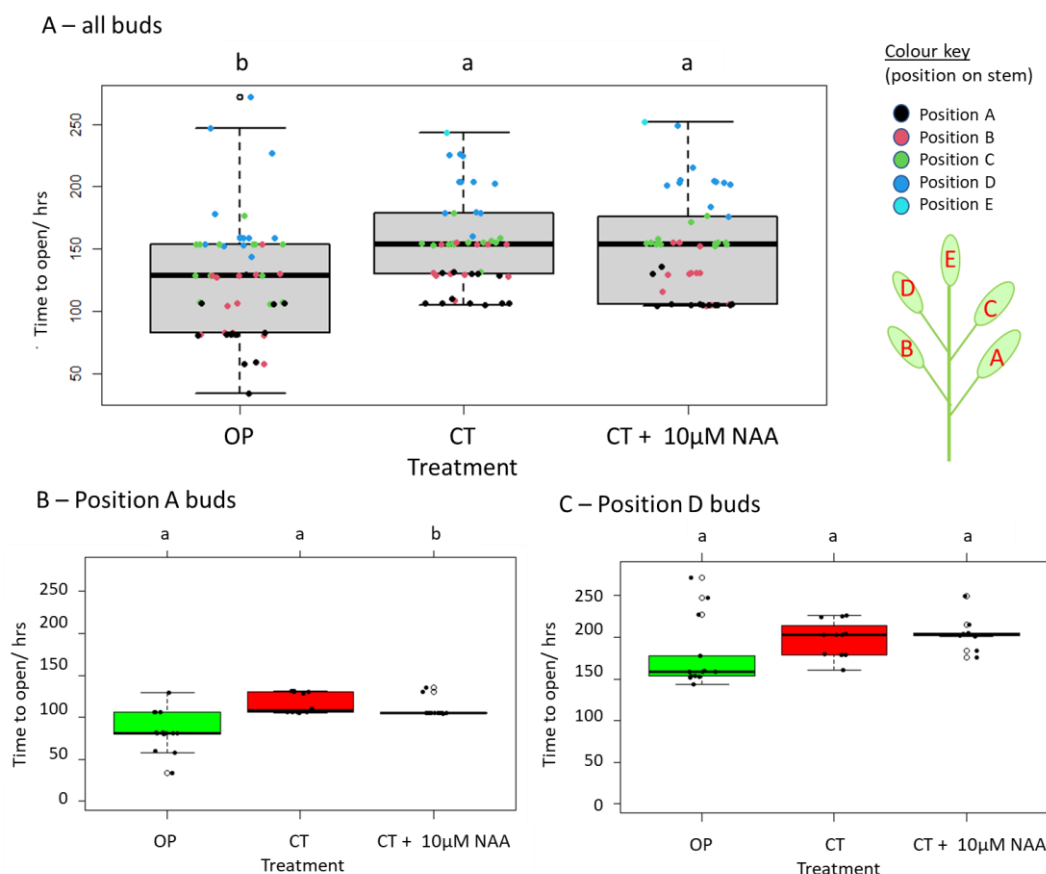


Figure 6.6 – Time of opening in Oriental ‘Pacific Ocean’ for (A) all buds on stem, (B) Position A buds only, and (C) Position D buds only in commercially treated Oriental ‘Pacific Ocean’

whole stems treated with and without 10 μ M NAA, compared to time of opening of buds on plant. Letters denote significance as shown by Kruskal-Wallis with post-hoc Dunn test (Appendix 6.17).

6.3.4 Relative expression of auxin- and flower opening-related genes in NAA- and NPA-treated buds

When the relative expression of the putatively identified auxin-related genes *IAA14*, *ARF6/8*, and *SAUR75* was measured, there were no significant differences between control buds or NAA-/NPA-treated buds and very little variation in relative expression (Figures 6.7A, 6.7B, 6.7C). Relative expression of putative *SAUR75* in NAA-treated buds showed the most variability; although not significant, one biological replicate showed a mean 5.19x fold greater relative expression compared to controls (Figure 6.7C).

Similarly to the auxin related genes, there were no significant differences in relative expression of *PIP1*, *EXPA1* and *XTH1*, flower opening related genes (Figures 6.7D, 6.7E, 6.7F) between controls or the NAA-/NPA-treated flowers.

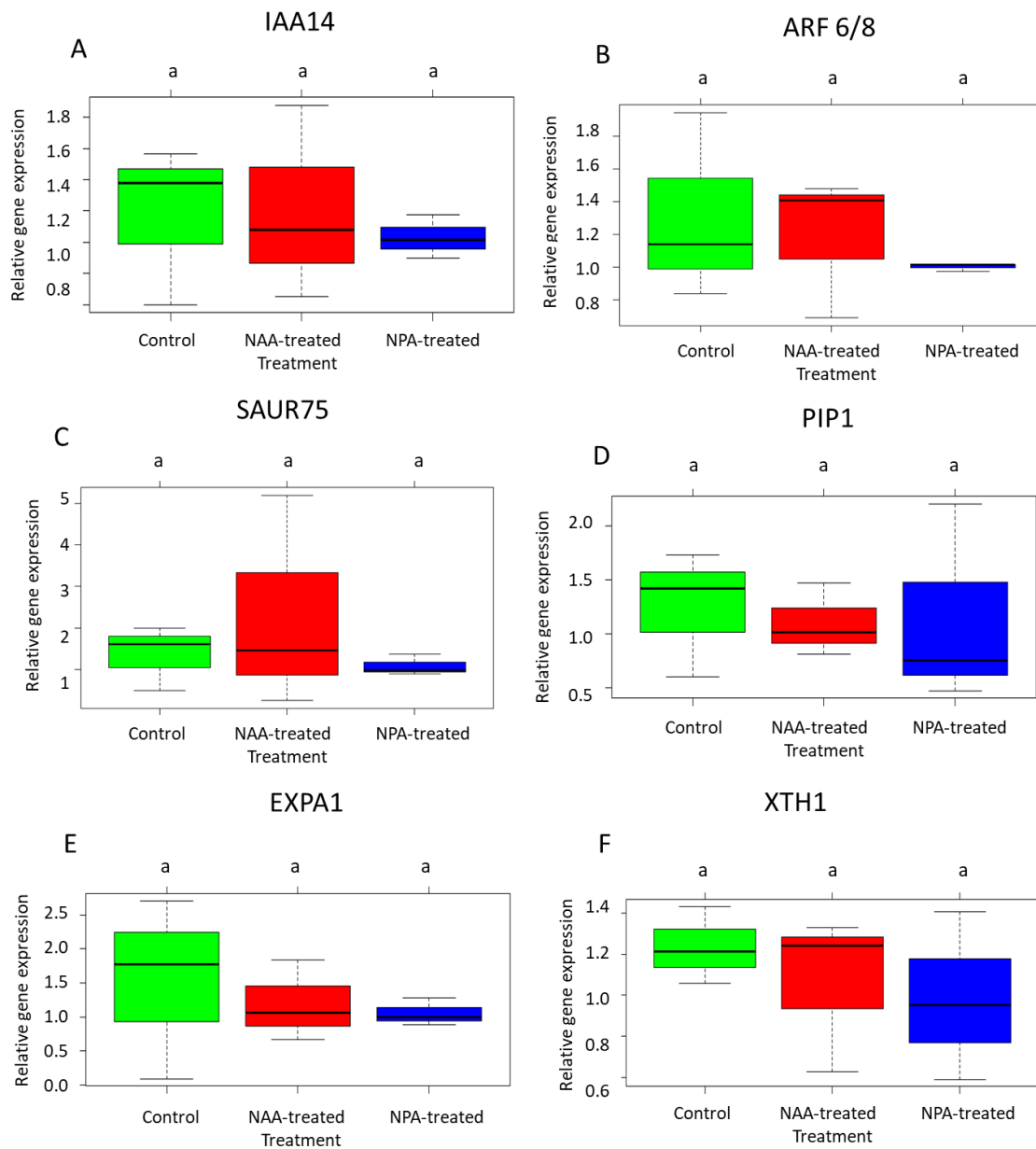


Figure 6.7 - Relative gene expression of putative auxin-related genes and cell expansion-related genes in Oriental lily 'Pacific Ocean' by qPCR, comparing buds treated with 10 μ M NAA and 100 μ M NPA to controls. Significance denoted by letters showing significance from One-way ANOVA and post-hoc Tukey test, which did not show any significant differences between groups in any of the putative genes investigated here (Appendix 6.18).

6.3.5 Effect of exogenous auxin on terminal buds at risk of postharvest bud abortion

Individual terminal commercially treated buds (Oriental 'Ascot') which had been identified as at risk of postharvest bud abortion were treated with 10 μ M NAA and observed for ability to open, similarly to the experiment carried out in Section 3.3.5, categorising them as Small Remained Closed (SRC), Small Semi Open (SSO) and Larger Fully Open (LFO) . The bud lengths at harvest were of an equal range for each group (from 30.4- 59.79 mm for individually harvested control buds in water and 31.70- 59.05 mm for NAA-treated buds - Table 6.2). The minimum bud length for opening required for opening in this experiment was comparable regardless of number of buds per inflorescence in water controls and while it was slightly higher in NAA-treated buds from 4 bud stems, it was slightly lower in NAA-treated buds from 5 bud stems and suggested in general, terminal buds from 5 bud stems opened at a smaller size. The % opening success for buds in water was similar whether from stems with 4 buds or 5 buds per stem and therefore due to low replication the datasets from both groups for each treatment (water vs. NAA treated) were added together for greater statistical power. Buds labelled as SSO and LFO were added together due to very small sample sizes for these groups.

The majority of buds in both treatment groups (Water controls + NAA-treated) failed to open, but were not significantly different to each other in terms of opening success or in terms of bud length distribution. Amongst the buds which did have the ability to open, there were also no significant differences between water controls and NAA-treated buds (Figure 6.8), either in number of buds able to open or their length at harvest. However, a GLM showed significant differences between treatments (individual buds in water vs. NAA treated - $t=3.082$, $p<0.05$) and differences between ability to open relating to bud length (GLM, $t=4.716$, $p<0.05$).

TABLE 6.2 - ANALYSIS OF THE INFLUENCE OF EXOGENOUS AUXIN TREATMENT ON THE OPENING ABILITY OF TERMINAL BUDS			
		4 buds per stem	5 buds per stem
Individual buds in water	Number of buds	13	12
	Range of bud length	30.4-54.04 mm	32.4-59.79 mm
	Minimum bud length required for opening	47.5 mm	46.75 mm
	Opening success rate	23%	25%
Individual buds + 10 μ M NAA	Number of buds	13	9
	Range of bud length	37.5-59.05 mm	31.7-57.43 mm
	Minimum bud length required for opening	59.05 mm	53.66 mm
	Opening success rate	8%	22%

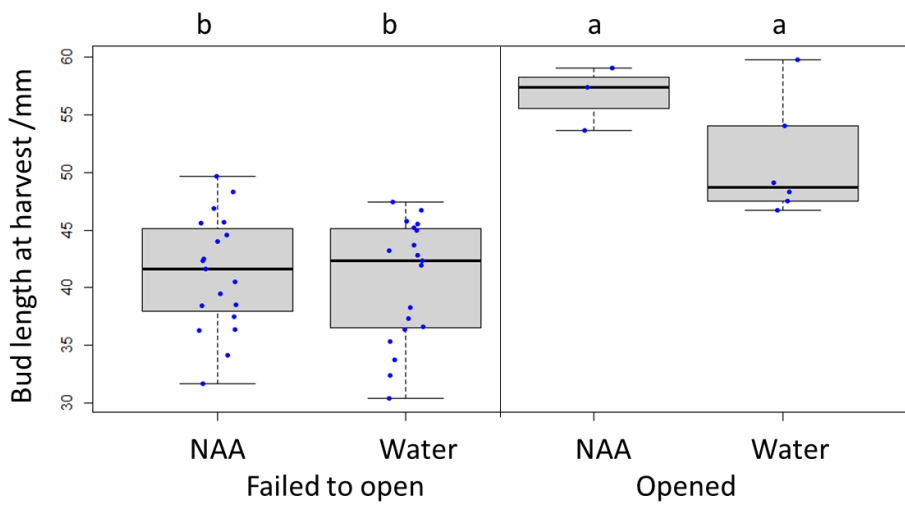


Figure 6.8 – Length of terminal bud grouped according to opening success (failed to open vs. opened) in NAA-treated buds vs. controls. Individual samples (blue) plotted on chart according to their length at harvest. Letters indicate significance by GLM and ANOVA between treatments (GLM, $t=3.082$, $p<0.05$). Bud length was also found to be a significant factor (GLM, $t=4.716$, $p<0.05$) (Appendix 6.19).

6.4 Discussion

6.4.1 Do endogenous changes in phytohormones drive flower opening?

Auxin is important in flower opening of several species such as waterlily by promoting cell wall growth and flexibility during cell expansion (Ke et al. 2018). However, the *AUX1* gene (auxin influx carrier) is expressed here at a constant level over all stages of development, and may suggest that a large, transcriptionally controlled uptake of auxin into tepal cells is not involved in opening. Ke et al. (2018) found that in waterlilies five isoforms of *AUX1* were upregulated over the flower closing stages, showing clear transcriptional control regulating flower opening/closing. Similarly, putative *YUC3*, was found in this study to have no significant change in relative expression over development and opening. *YUC3* encodes a YUCCA flavin monooxygenase protein involved in local auxin synthesis. Inhibition of YUCCA proteins caused a reduction in flower petal width in *Malus domestica* (Song et al. 2020), suggesting that they have an important role in cell expansion; however, this may not be transcriptionally regulated.

However, certain auxin-related genes were found to be significantly upregulated over lily flower opening and support the hypothesis that auxin is a partial driver of flower opening. Relative expression of putative *IAA14*, coding for an Aux/IAA protein, increased significantly between Stages 1 and 3, peaking at almost 4-fold expression at Stage 5 compared to at Stage 1. This early expression that was maintained from Stage 3 to 5 supports its early role in the auxin response pathway (Luo et al. 2018). Aux/IAA proteins act as repressors of ARF proteins until auxin signalling causes their ubiquitinylation and eventual degradation, allowing ARFs to cause transcription of target genes (Luo et al. 2018). Early transcriptional upregulation could therefore point to high auxin levels causing negative feedback through production of more IAA proteins. In many species such as rice, *Aux/IAA* gene transcription was strongly correlated to auxin application and also light- and circadian signals (Thakur et al. 2001). Putative *ARF6/8* was found to increase in relative expression significantly 5-fold comparing Stage 1 to Stage 5. Knocking out *ARF6* and *ARF8* in *A. thaliana* was found to cause reduced jasmonate production and flower opening failure (Nagpal et al. 2005) and therefore this rise in expression may be indicative of auxin signalling upstream and

jasmonate signalling downstream. Putative *SAUR75* was shown to increase in relative expression by almost 12-fold in Stage 5 compared to Stage 1, indicating an upstream auxin response. In *Malus domestica*, *SAUR* genes were found to be upregulated in response to auxin application by 20- to 40-fold (Wang et al. 2020), which supports the upregulation observed in this study. In *A. thaliana*, *SAUR75* transcription was also found to be induced by phytohormones such as brassinosteroids (Ren and Gray 2015), suggesting that other factors could have caused this observed upregulation too.

A tentative model can therefore be created showing the timing of expression of these phytohormone-related genes and how they change sequentially throughout development and opening (Figure 6.9). This may explain for example the early auxin response gene coding for *IAA14* peaking at Stage 3, whereas the later response genes coding for *ARF6/8* and *SAUR75* not significantly upregulated until Stage 4/5. This suggests that auxin may be produced or transported to lily tepals at Stage 3, causing a response which continues until the flower is fully open. The few cytokinin-related genes investigated here (putative *AHP*, *ORR9*) are only significantly upregulated at Stage 5, suggesting that the cytokinin response comes later after the auxin response. Cytokinin and auxin have been known to have antagonistic functions in many plant tissues; while auxin is known to have cell expansion and growth function, cytokinins may play a role in differentiation and (Schaller et al. 2015). This is in agreement with Arrom et al. (2012), who carried out some assays for endogenous phytohormones in lily tepals over flower opening. Tepal IAA concentration peaked at the mature bud stage (here Stage 3) and then a later peak in zeatin and zeatin riboside concentration at the fully open flower (here Stage 5), is in agreement with the data shown here. Alongside the data showing the accelerating effect of exogenous NAA on flower opening, this makes a strong case implicating auxins as a driver of cell expansion in lily tepals.

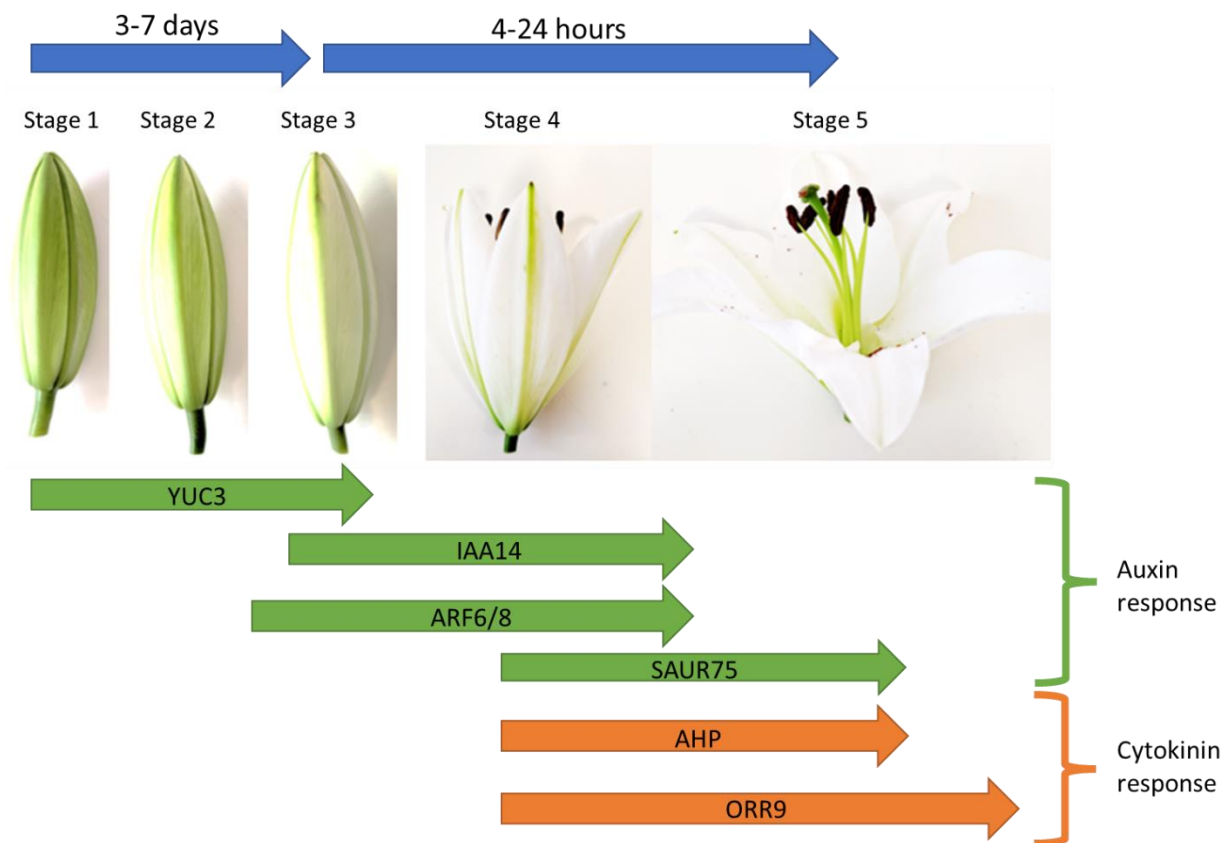


Figure 6.9 – A potential hypothesis for the timing of auxin and cytokinin response in lilies over their development and opening, showing the stages of development that expression of hormone-related/response genes were indicated to be high in this study.

6.4.2 Can exogenous auxins be used to support lily opening in postharvest treatments?

The results from the studies carried out here are very mixed about the effects of exogenous auxin and auxin inhibitors on flower opening. While exogenous NAA (10 μ M) was shown to have a significant accelerating impact on the time taken to open in individual buds, this effect was not observed in whole stems, where flower opening time was not significantly different between commercially treated stems and those treated with 10 μ M NAA. A similar experiment on *Eustoma grandiflorum* stems showed 5 μ M NAA was sufficient in a pulse treatment to cause changes in the longevity of the inflorescence (Shimizu-Yumoto and Ichimura 2010), making it surprising that there was no effect here. The effect of auxin in an inflorescence compared to an individual bud is likely to be different due to the complexity of

the system. A large inflorescence like a lily stem has a large energy requirement, requiring regulation of timing of opening for the individual buds so that there is sufficient nutrition to develop the reproductive pollen and carpel of as many flowers as possible. Evidence to support this is the increased longevity of lily buds taken off the inflorescence, suggesting that there could be a recycling of nutrients from older bud to younger bud (Van der Meulen-Muisers et al. 2001). It is unclear if auxin is taken up by the stem in the same way as in an individual bud or if it is preferentially being taken up by another organ such as leaves, for example. Understanding if it is a problem with uptake or there are other mechanisms affecting it could be investigated again by applying auxin locally with lanolin to individual buds on the inflorescence (Reinhardt et al. 2000).

The bud opening promoting effects of exogenous NAA were hypothesised to have a rescuing effect on the terminal buds which showed postharvest bud abortion phenotypes when commercially treated and in particular when removed from the stem. Removal from the stem was shown in Section 3.3.5 to significantly impact bud opening ability, where terminal buds on stem were significantly more capable of opening compared to individual buds in a highly nutrient deprived condition. However, adding 10 μM NAA to these buds was not shown to here have any significant impact on bud opening ability. This could be due to the auxin requirement of these particularly deprived buds being greater than normal buds; either because there is significantly less auxin in these terminal buds compared to Position A buds which do not show problems with opening normally (personal communication, James Cole, E.M. Cole Farms Ltd.), or potentially because the auxin transport or transduction in these terminal buds is inhibited. This inhibition could perhaps occur because of stress - PIN2 trafficking was found to be reduced by cold stress (8-12h at 4°C) in *A. thaliana* roots (Shibasaki et al. 2009), and auxin biosynthesis, transport and transduction were significantly affected by osmotic stress (Naser and Shani 2016).

NPA (100 μM) was found to elicit no significant differences in the overall time of flower opening compared to controls in the Oriental lily 'Tisento' but when this time of opening was split into the two phases before flower opening and length of the physical opening, some significant differences were observed. 'Tisento' buds showed a difference in flower opening time from harvest to the start of flower opening, with no significant difference in the actual time for the flower to open (start of opening to fully open). NPA is a polar auxin

transport inhibitor which works by targeting machinery in the auxin transport chain in a way still not fully understood (Teale and Palme 2018) and therefore may only cause differences in the amount of auxin in certain cell types/organs rather than the overall levels of auxins, which may account for the lack of consistency in results. Carrying out auxin assays in tepal material treated with NPA in the same way as this study would be able to identify if the variation in flower opening time was because of local increases in auxin content. The data shown here suggests that the opening process itself (the differential growth causing the shape change of tepals) is not affected but the vegetative growth phase (time taken to get to that point from harvest) may be affected by differences in auxin transport.

A factor that may have accounted for NAA and NPA not having a significant impact on auxin-related gene expression (Section 6.3.4) is the experimental design used in this study. Here, samples were frozen at the fully open stage, which may have taken longer or shorter depending on the treatment and biological sample. Therefore each sample may have been exposed to the treatment for different times, explaining some of the variation observed in the data. The auxin response has been shown to have transcriptional effects on *SAUR* genes in as little as 10 minutes (Ren and Gray 2015), suggesting that this may be short lived and subject to negative feedback after a relatively short period. Furthermore, the genes important for flower opening such as *PIP1*, *EXPA1* and *XTH1* have been shown (Figure 4.16, Section 4.3.6) to have relatively low expression at Stage 5 and peak earlier prior to flower opening at Stage 2 or 3. An improvement to this study would therefore have been to measure relative gene expression much sooner, for example measuring the change in relative expression of these genes in a time course starting from 10 minutes to 24 hours post treatment of Stage 2-3 buds, comparing to controls in each case.

6.4.3 Conclusions

The data shown here suggests that auxin signal transduction may have an important role in flower opening in lilies, due to the correlation of expression of genes encoding auxin signal transduction components prior to flower opening and the accelerating effect of exogenous auxin on flower opening time. While a promising target, the lack of effect of NAA on whole stems and terminal buds points to some inconsistencies in the role and effect of auxins in lilies to be explored further.

Chapter 7 - General discussion

The aims of this project as set out in the introduction (Section 1.6) revolved around understanding the physical and physiological mechanisms underpinning flower opening in lilies, as well as the regulation of these processes by endogenous factors (bud size at harvest, competition, position on stem) and exogenous factors (time of day, harvest, commercial treatment). These aims were investigated using a series of objectives related to understanding the cell expansion in tepals by microscopy, how this expansion occurs physiologically by starch breakdown/sucrose transport (using methods such as assays for starch and metabolomic analysis by FIE-HRMS and GC-MS, and if this is different in commercially treated stems/buds compared to on plant, as well as in buds more likely to suffer from the effects of commercial treatment (terminal buds/buds from larger inflorescences). Additionally, the effect of commercial treatment on flower opening was assessed for synchronicity and opening time. The regulation of these processes was investigated using molecular biology techniques such as RNA-sequencing and RT-qPCR to look at the expression of regulatory genes (transcription factors, hormonal signalling genes) and to look at differences between the overall transcriptional profile between buds which go on to open and those which fail to open. The further aim is for this understanding to help shed light on commercial harvest related issues such as postharvest bud abortion, which is responsible for profit loss and consumer dissatisfaction in the cut flower industry.

7.1 - The physical and physiological basis of flower opening in lilies

Flower opening has been shown in Chapter 3 to be associated with differential growth across the tepal, especially between Stages 3 and 5, and likely mainly driven by more growth in the adaxial edge epidermal pavement cell area than in other parts of the tepal for Oriental cultivars. This supports previous work carried out in other similar Oriental cultivars (Liang and Mahadevan 2011; Watanabe et al. 2022). It has been shown here that less differential growth was observed for some varieties: for example, *L. longiflorum* has much less differential growth occurring across the tepal associated with flower opening. This likely reflects the differences in flower organ phenotype between the varieties. Cell expansion related to flower opening has been already been shown to be at least partially driven by the breakdown of tepal starch stores in tepals (Bieleski et al. 2000a). Watanabe et al. (2022)

then also showed that tepal glucose and fructose content rose significantly over flower opening, with a slightly higher level in epidermal adaxial cells compared to abaxial, while sucrose levels remained similar over development and opening. The data shown in Chapter 3 and 4 complements this experiment and more specifically points to the tepal edges, which were identified as growing more than the midribs, as also containing significantly more starch just prior to opening (Stage 3) and slightly more glucose in the open flower (Stage 5). Tepal sucrose also significantly increased in tepals in Stage 5 compared to Stages 1 and 3, but the increased content in tepal midribs compared to edges suggests it may be broken down into glucose and fructose in midrib or vascular tissue before reaching tepal edges. This supports a possible apoplastic phloem unloading strategy of releasing sucrose into the apoplasm, where it is broken down before being taken up by monosaccharide transporters into tepal edge cells. This is supported by work carried out by Bielecki (1995), who showed that labelled sucrose was restricted to vascular tissue in daylily petals and therefore sucrose was unlikely to be used directly in cell expansion or metabolism. Moreover, the expression of genes putatively coding for some sucrose and monosaccharide transporter proteins (*SUT2*, *SUT4*, *CWINV4*) did not show any significant differences over flower opening, and others (*MST6*, *SWEET7*) only showed a significantly higher expression at Stage 5 in the open flower. As mentioned in Chapter 4, these soluble sugar transporter genes may not be transcriptionally regulated and are part of large gene families. The difficulty of designing primers to limited sequence information, especially in *Lilium* was also discussed in Chapter 6 and may also be responsible for some of the problems observed in validating the mechanisms of opening using biomolecular methods at present.

The metabolome of tepal tissue, comprising the reactants, intermediates and products of the combined primary and secondary metabolism in the tepals, is highly specific to the stage of development. This is presumably due to the differences in tepal cell architecture and content throughout development and opening. As already discussed, there were changes in tepal soluble sugar and starch content over development, which could go on to cause changes in the flux of metabolites through pathways which use these as substrates. For example, increased expression of a gene putatively coding for α -amylase correlates with the loss of starch over the opening process between Stages 3 and 5 (Section 4.3.7, Figure 7.1), and with increased tepal glucose content (Section 4.3.1), which is the product of starch

breakdown (Zeeman et al. 2010). This change in primary metabolite content, alongside the transcription of genes coding for pathway components and changes in activity of enzymes can rapidly and radically change secondary metabolism throughout development (Davies and Schwinn 2003). Compounds putatively related to hydroxycinnamic acids, coumarins, and flavonoids were found to be important in separating metabolic profiles on the basis of stage of development (Table 4.4) for example, and therefore suggests that these particular compound classes may change significantly in amount and content over development. The increase in these compounds was suggested in Chapter 4 to perhaps be linked to developmental changes associated with scent and colour production (Vainstein et al. 2001; Shi et al. 2018b) as well as lignin biosynthesis (Flourat et al. 2021). These metabolite changes correlate with the increased expression of genes putatively related to lignin biosynthesis and the phenylpropanoid metabolic pathway (putatively coding for CAD, F5H, hydroxylases) observed in buds which went on to open normally compared to those which failed to open in Chapter 5, which suggests that these pathways are important in flower development and opening. Lignin production is necessary for primary cell wall growth and overall tissue growth in many plant cell types (Liu et al. 2018) and may therefore also be linked to cell expansion, however it should be noted that the phenylpropanoid metabolic pathway is diverse and lignin deposition does not always correlate with increased expression of the genes coding for components of this pathway (Wang et al. 2013). The increased expression of genes coding for aquaporins and cell wall remodelling enzymes such as PIPs, expansins, and XTHs over bud development prior to flower opening fits with this hypothesised cell expansion strategy (Figure 7.1). Indeed, expansins and XTHs are expressed specifically in parts of the tepal with the greatest cell expansion (Watanabe et al. 2022)). Thus these data overall build a coordinated picture of osmotic cell expansion via these mechanisms (Figure 7.1).

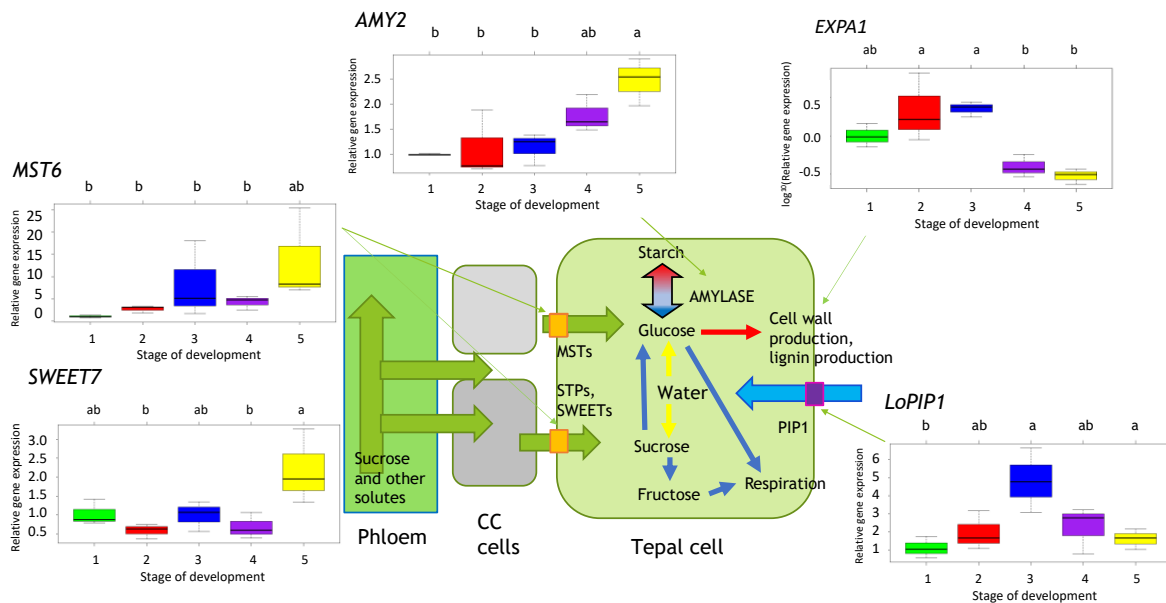


Figure 7.1 – model building on Figure 4.1 showing the possible physiological methods which may account for cell expansion and global tepal growth over flower development. Depending on the flower's sink strength, sucrose is removed from the phloem, and through the companion cells (CC) to tepal cells (currently unknown if this occurs symplastically, apoplastically or a mixture of strategies) throughout development. This can be taken up by sucrose transporter proteins (STPs) or monosaccharide transporter proteins (MSTs). The expression of genes putatively coding for MST6 (an MST) and SWEET7 (an STP) were found to be only significantly upregulated at very late stages of development, making it uncertain if these proteins are transcriptionally regulated during the opening process itself. Sucrose can be broken down into glucose and fructose, which can go on to be used for respiration, cell wall production and starch biosynthesis. Cell wall production is suggested by the increased expression of a gene putatively coding for an expansin EXPA1 in Stages 1-3 compared to 4 and 5. The biosynthesis and catabolism of starch is balanced until flower opening starts, when it is rapidly broken down into glucose - expression of a gene putatively coding for an amylase is significantly higher in Stages 4 and 5. This would create a large glucose pool in the cell, supported by evidence that glucose is significantly higher at Stage 5 compared to 1 or 3. Expression of aquaporins such as PIP1 peak in expression just prior to opening (Stage 3) and may be involved in osmotic strength related cell expansion. Blue arrows indicate catabolic pathways, red arrows indicate anabolic pathways and yellow arrows indicate

association by osmotic pressure. The biosynthesis/breakdown of starch is dependent on the developmental stage.

7.2 – Regulation of flower opening in lilies on plant

Flower opening has been shown to be regulated by several factors (bud size/age related, position on stem, circadian rhythm, light and temperature, nutritional status, etc) based on data from this study and the literature (Heins et al. 1982; Healy and Wilkins 1984; Van Meeteren et al. 2001; Kumar et al. 2012). These factors have been investigated to understand the specific elements driving this observed regulation. It was also shown in these studies (Heins et al. 1982; Healy and Wilkins 1984; Van Meeteren et al. 2001; Kumar et al. 2012) that a network of hormones present in flowers, both synthesised there and transported from other organs, mediate the regulation of flower opening in response to the multiple factors mentioned above.

Bud age (length) has been hypothesised to be a highly important factor in flower opening, due to the observation that lily flowers open sequentially on the stem according to their age and developmental stage (Section 3.3.3). The flower bud needs some internal sensing of age in order to coordinate opening with the maturity of the reproductive organs, and the other buds on the inflorescence. This assumes that there are endogenous signals coming from the anthers and gynoecium to signal when the bud is ready to open (Cheng et al. 2004; Nagpal et al. 2005). This stage of development in lilies can also be potentially sensed by the plant via sugar signalling and in particular glucose, a potent signalling molecule (Ruan 2014). An increase in glucose in grape plantlets was shown to have upregulating effects on the auxin and JA signalling pathways, and in the case of developing plants, an upregulation in photosynthesis and the TCA cycle (Mao et al. 2018). This is partially analogous to the rise in tepal glucose content observed between Stage 1 and 3 and in particular 5 in lily tepals (Section 4.3.4). This rise in glucose, particularly at earlier stages, could be responsible for the observed increase in auxin content (Arrom and Munne-Bosch 2012b) and signalling (Section 5.3.1).

Another factor which was found to regulate the time of opening included the time of day, which in Section 3.3.2 was shown to strongly correlate with frequency of opening in on

plant controls and supported previous data showing the synchronicity of flower opening to be coordinated with the time of dawn (Bialeski et al. 2000b). The peak in auxin levels and sensitivity at night shown in *A. thaliana* (Covington and Harmer 2007) could link the circadian element of flower opening with the observed increased auxin signalling observed over flower development and opening to fine tune this process to the most appropriate time of day.

Bud competition was not shown here to affect the ability of the buds to open on plant, but did affect the bud opening when stems were commercially treated. A higher position on stem was not found to affect tepal starch or soluble sugar content significantly (Sections 4.3.3, 4.3.5) but the overall number of buds per stem was shown to affect the ability of the terminal bud to open (Section 3.3.5). This suggests that perhaps this inability to open was nutrition-related, and indeed was only observed in stems with over four buds per stem. This inability to open is not observed in flowers on plant (Section 3.3.1, personal communication, James Cole, E.M. Cole Farms Ltd.) and could potentially be due to lower stress levels compared to harvested flowers (Burchi et al. 1999) and higher tepal content of nutrients such as soluble sugars (Section 4.3.4). This suggests that these factors negatively regulate lily flower opening in stress conditions, which can potentially be observed on plant perhaps only in very high stress conditions such as light or water deprivation (Mason and Miller 1991; Su et al. 2013), or pest damage/infection (Lawson and Hsu 1996) unlikely to be found in a commercial setting.

While commercially treated flowers may be subject to more stress and therefore may be in a different state to the on plant condition, the RNAseq experiment in Chapter 5 showed some DEGs putatively coding for regulatory genes which may be important for flower opening whether on plant or commercially treated. This was identified as a group of DEGs which showed a highly positive log₂FC comparing SSO/LFO (buds which did open at differing sizes) to SRC (buds which failed to open), with high levels of expression in buds which showed a strong opening phenotype. Several DEGs putatively coding for MYB transcription factors were highly expressed in SSO only or both SSO and LFO buds compared to SRC buds (*MYB4*, *MYB24*, *MYB70*), which suggests this family of TFs may be important in regulating flower opening. There was also a high incidence of AP2-ERF, bZIP and MYB motifs in promoters of the *Arabidopsis* genes most significantly aligning with DEGs that were more

highly expressed in flowers which went on to open. MYB TFs in particular are linked to processes potentially involved in cell wall growth such as phenylpropanoid metabolism (Tamagnone et al. 1998). This also suggests that these classes of TF are important for flower opening in lilies, beyond their general known involvement in other aspects of flower maturation and senescence (Kunst et al. 1989; Nakano et al. 2014; Yamagishi et al. 2014; Fatihah et al. 2019), which was discussed in Section 5.4 in detail.

The similarity of flower opening, in particular petal/tepal development, to early leaf senescence has been suggested due to the common evolutionary origin of leaves and flowers (Friedman et al. 2004) and some of the similar processes that occur, for example the disassembly of the photosynthetic apparatus, catabolism of chlorophyll, and the production of carotenoids in chromoplasts (Rodoni et al. 1997; Morelli et al. 2022). These two processes are also regulated similarly by environmental and endogenous inputs about the leaf age, temperature and light information (Guo and Gan 2005). These inputs are mediated by hormones such as ethylene, JA, SA and ABA, and negatively regulated by auxin, gibberellins and cytokinins (Gan and Amasino 1995; Gan and Amasino 1997; Lim et al. 2007; Miao and Zentgraf 2007; Li et al. 2013; Zhang et al. 2013), again showing similar hormonal effects as observed in flower development and senescence. Late stage leaf senescence and flower senescence are also thought to involve similar processes such as nutrient remobilisation (Van Meeteren et al. 2001; Lim et al. 2007). This similarity suggests that aspects of leaf senescence not measured in this study may also be applicable in flower opening in *Lilium* and may provide a useful starting point for identifying regulatory genes or pathways.

7.2.1 The role of auxin in flower opening

Previous research on lilies has indicated the correlation between a rise in tepal auxin and SA levels just prior to opening (Arrom and Munne-Bosch 2012a), which suggests that these hormones may be involved in the opening process. In contrast, cytokinin and gibberellin levels peaked after opening, which suggests they may be more involved in senescence. Presence of a hormone in a tissue does not always correlate with their signal transduction due to sequestration, conjugation and inhibition strategies (Kleczkowski et al. 1995). However, the qPCR data in Chapter 6 suggested that the temporal expression of genes related to the auxin/cytokinin transduction pathways (putative *YUCCA* genes, *ARFs*, and

SAURs for auxin, *AHP2* and *ORR9* for cytokinin) correlate with the levels of each hormone observed in LA hybrid tepals (Arrom and Munne-Bosch 2012a), suggesting that in healthy flower opening the auxin transduction pathway may be activated. This is supported by the evidence that exogenous auxin (NAA) significantly accelerated flower opening in harvested buds (Section 5.3.2). The RNAseq experiment also showed higher expression of DEGs putatively identified as *YUC*, *ARF* and *SAUR* genes in buds which went on to open compared to those which failed to open (Section 6.3.6). This further supports the hypothesis that auxin production and signalling is not only increased over, but is required for flower opening.

Auxin signalling is known to have input from many endogenous and exogenous signals and as such could coordinate signals in the opening process in the on plant condition. As discussed in Chapter 6, auxin production in *A. thaliana* is regulated by several factors such as the time of day, endogenous signals from the bud, and the soluble sugar content (Rawat et al. 2009; Mroue et al. 2017; Pérez-Alonso et al. 2021). This modulates the magnitude of auxin signal transduction through changing the amount of free auxin available. These factors affecting auxin production in *A. thaliana* have also been shown here to be correlated with development in lily, indicating that they may also be mediated via auxin signalling in lily flower opening.

Cytokinin and auxin have been well characterised as having an antagonistic relationship in *A. thaliana* in root meristem maintenance and organogenesis (Dello Ioio et al. 2008; Pernisová et al. 2009) and in the gynoecium cytokinin has been shown to cause specific spatiotemporal control of auxin biosynthesis and signalling for organ patterning (Müller et al. 2017). These examples demonstrate that this auxin-cytokinin crosstalk is highly important for tissue and organ growth. In LA hybrid lily, Arrom and Munne-Bosch (2012a) showed tepal cytokinin content (zeatin and zeatin riboside) only rose significantly after flower opening, which correlated with a drop in auxin levels post-anthesis. The data here supports this late cytokinin signalling, with genes putatively coding for AHP and B-type ORRs showing a rise very late in flower development, at Stages 4 and 5, when the flower is already open, compared to auxin transduction related genes such as those putatively coding for ARF6/8, which peaked at Stage 3. While the effect of exogenous cytokinin was not measured in this study, it is known to have a delaying effect on lily flower opening (Wang 1996; Muñoz et al. 2018; Wei et al. 2018), particularly in combination with gibberellins in

the commercial formulation Promalin[®], which is the opposite effect on lily flower opening to that shown in Section 5.3.2 with exogenous auxin. The temporal separation of auxin and cytokinin responses alongside their known effects on flower opening therefore suggests there may be an antagonistic relationship between these phytohormones in lily flower organs.

7.3 – Mis-regulation of flower opening in commercially treated lily stems

Commercial processing, and in particular the effect of the cold/dark treatment, was hypothesised to have a significant impact on flower opening due to the possible changes to the plant's metabolism, physiology and circadian rhythm (Van Doorn and Han 2011). Results presented in Chapter 3 indicated that commercial processing caused a slight delay in flower opening compared to flowers on plant, especially in certain varieties (Oriental 'Tisento' was more sensitive compared to LA hybrid 'Eyeliner'). However, while flowers were developmentally delayed by cold/dark treatment compared to on plant, buds of the same size (the assumption being that the bud size was equivalent to developmental age) did not show significant differences in opening time between freshly harvested and rehydrated to those which had been cold/dark treated for 72 hours, although both groups were significantly delayed compared to on plant controls. This suggests that the commercial cold/dark treatment is successful at maintaining the developmental stage and age of the stems. However, commercial treatment was found in Section 3.3.2 to have a significant impact on the distribution of the time of day flowers opened, which suggests that while there were no significant differences between the average time of opening of on plant vs. commercially treated flowers, there may still be effects of cold/dark treatment on the circadian rhythm of lilies, which may be worse for certain varieties. Asiatic lilies lost synchronicity of opening following continuous dark treatment for 3-4 and this treatment also delayed opening in several cultivars consistently (Bieleski et al. 2000b), suggesting that the dark storage used in commercial treatment may have a negative impact on both synchronicity and time of opening.

Although commercial treatment was not found to affect some aspects of flower physiology negatively such as the total amount of cell expansion (Section 3.3.4) and tepal starch content over Stages 1-5 compared to on plant (Section 4.3.3), it did affect other

physiological and metabolic aspects of bud development. Tepal glucose, fructose and sucrose content was found to be significantly higher in on plant tepals than in tepals from commercially treated stems (Section 4.3.4), especially in the fully open flower (Stage 5). Sucrose content did not significantly increase over development, however at each stage of development on plant samples had a significantly higher tepal sucrose content, suggesting that the commercially treated flowers are limited nutritionally despite the addition of sucrose to the vase water. Commercially, adding sucrose to rehydration and conditioning solutions is limited prior to selling to the consumer to delay flower opening (van Doorn and de Witte 1991a), and this experiment suggests that the greater sucrose concentrations in commercial vase sachets (used in the experiments in this study using cut stems unless stated otherwise) do not counterbalance the deficit from the commercial practices. This was further developed in Chapter 3 showing that in an extreme nutrient deprived environment (individual buds removed from stem) only the largest buds showed an ability to open. Van der Meulen-Muisers et al. (2001) showed that tepal length at harvest is directly proportional to the tepal carbohydrate content in the Asiatic lily 'Orlito', suggesting that the carbohydrate content of these buds may be responsible for the differences in opening, as starch breakdown has been shown to drive tepal cell expansion directly (Bieleski et al. 2000a). Competition on stem has also been indicated to be an important factor in the ability of the terminal bud to open (Section 3.3.5); terminal buds on four bud stems were found to have significantly greater opening ability than similarly sized terminal buds on five bud stems, suggesting that perhaps a nutritional deficiency is responsible for the differences in opening.

The metabolomic profile in tepals showed some possible differences in secondary metabolism between on plant and commercially treated flowers. The differences in putative flavonoids, coumarins and phenolic acids could mean potential differences in scent, colour and cell wall-related compounds between on plant and commercially treated flowers, with commercially treated flowers being indicated to have significantly more putative colour-related compounds in particular (Section 4.3.6.1). This was further developed in Chapter 5, where there was differential expression of some putative cell wall remodelling, tepal colour, scent and wax biosynthesis-related genes with flowers which went on to show a strong opening phenotype and those which did not, showing that these processes can start

occurring early on in flower bud development. As indicated in Section 4.4.2, the levels of certain colour compounds such as anthocyanins and flavonoids may also be increased in commercially treated flowers and plants (Bergquist et al. 2007; Naing et al. 2018b; Marchioni et al. 2020) and can account for the importance of these compounds in separating OP and CT metabolomic profiles using Random Forest. This is supported by the observed differences in expression between genes in the phenylpropanoid metabolism pathways between buds which could open (SSO/LFO) compared to those which could not (SRC), which suggested a difference in the flux through parts of the pathway rather than decreased expression of all pathway components (Section 5.3.2.2). Increased flavonoid and anthocyanin production in the flowers and fruit of several species has been linked to several factors such as cold, drought and biotic stress (Chalker-Scott 1999; Naing et al. 2018a; Chen et al. 2022b) and can perhaps account for the increased levels of these putative compounds in CT samples. The lower expression levels of flavonoid and anthocyanin production-related genes in SRC buds in contrast suggests that these stress-induced pathways may not be as active in buds which show problems with opening.

7.3.1 – Stress and metabolism in commercially treated lilies

One of the main findings in the RNA-seq experiment comparing buds showing late bud abortion phenotypes compared to those showing normal opening was that putative stress-related genes were more highly expressed in flowers which went on to fail to open compared to those which did open (Chapter 5). Genes putatively coding for several NAC, ERF and WRKY-family transcription factors were found to be more highly expressed in SRC than SSO and LFO buds, suggesting that stress-related pathways are being activated more in buds which cannot open compared to those which can (Section 5.3.6). NAC TFs are a huge family of transcription factors which can integrate stress responses from different abiotic factors such as dehydration, wounding, light and temperature (Nakashima et al. 2012). They are transcriptionally regulated by stress related hormones such as ABA, JA and SA (Nakashima et al. 2012). Similarly, *ERFs* and *WRKY* genes can be induced by ABA, ethylene and presence of ROS (Bakshi and Oelmüller 2014; Müller and Munné-Bosch 2015). The overexpression of some of these TFs can cause increased resistance to abiotic stresses in multiple species (Erpen et al. 2018). This suggests that their endogenous production may be in response to the stresses imposed by commercial treatment: dehydration, cold, and

wounding stress. These stresses may cause the observed differences in metabolism between on plant and commercially treated tepals such as changes in the cell wall composition (Section 4.3.6.1), which has been shown to change under abiotic stress and in particular ROS presence (Tenhaken 2015).

The coexpression of these stress-related TFs with the increased photosynthetic genes could also indicate that these are linked. There is evidence to suggest that the change in primary metabolism during the stress response is mediated by sensing molecules such as trehalose-6-phosphate. As already discussed in Section 4.4, a higher trehalose level has been shown to be correlated with reduced photosynthesis, indicating a possible role in sugar sensing and feedback (Paul et al. 2001). This has also been observed in rice (*O. indica*), and is also linked to a better tolerance against several abiotic stresses (Garg et al. 2002). A gene putatively coding for the enzyme trehalase was found to have significantly more expression in buds which could open compared to those which failed to open (Chapter 6), and may indicate that there is more breakdown of trehalose into glucose in the normal phenotype, whereas in the postharvest bud abortion phenotype there may be less. The *A. thaliana* gene coding for the enzyme involved in trehalose-6-phosphate synthesis (*TPS1*) is highly expressed in flower tissue and its knockout produces a late flowering phenotype with severely reduced root and leaf growth (Van Dijken et al. 2004), suggesting it is important in cell expansion and growth. The expression of trehalase is strongly induced in response to trehalose-6-phosphate levels (Brodmann et al. 2002). This suggests that flowers with the ability to open may have greater trehalose-6-phosphate levels, and perhaps their ability to open could at least be in part mediated by the effect of trehalose on photosynthesis and stress tolerance.

7.3.2 – Identifying auxin-related targets which may influence postharvest bud abortion

The qPCR data investigating expression of certain putative auxin related genes showed an increase in their expression over normal flower development and opening (Section 6.3.1). The effect of exogenous auxin on individual Stage 1 LA hybrid and Oriental buds (Section 6.3.2) suggested that there was a significant accelerating effect on flower opening through raising the auxin levels in the bud. This suggested that this could be a potential treatment for buds at risk of postharvest bud abortion. However, this was not corroborated by experiments on whole stems (Section 6.3.3). A role for auxin was also supported by the

RNA-seq experiment (Chapter 5), which showed significantly higher expression of genes putatively coding for components of auxin transduction pathway in buds which opened compared to buds which failed to open.

Auxin transduction is modulated by MAPK signalling as shown by Kovtun et al. (1998), who showed that a plant MAPKKK (NPK-1) could negatively regulate the auxin transduction pathway, and may be the mechanism behind the defective embryogenesis observed in NPK-1 overexpressing tobacco. The significantly greater expression of DEGs putatively coding for MAP kinases such as MKK4/5 in buds which failed to open could indicate the mechanism by which auxin signalling is inhibited in buds which later fail to open. This has been shown by other studies which show that some Aux/IAA proteins may be stabilised by MPKs, reducing the sensitivity of plants to auxin (Lv et al. 2019). This mechanism could also explain why adding exogenous auxin to buds at risk of failing to open does not have the same accelerating effect on flower opening that adding auxin to buds which are not at risk does. Buds that are able to open may not have the same desensitisation to auxin via increased MAPK signalling and therefore a higher level of Aux/IAA proteins (Figure 7.2). While expression of *IAA* genes was shown in this study to be significantly higher in buds which opened compared to those which failed to, the ratio of Aux/IAA proteins: ARF proteins is important in modulating the strength of the auxin response (Liscum and Reed 2002). Additionally, specificity in the pairs of Aux/IAA proteins and ARFs has been indicated to cause specific context-dependent responses (Weijers et al. 2005) and therefore further work to confirm the identity of the specific components is important to confirm the mechanism described in Figure 7.2. MAPK signalling is upregulated in both biotic and abiotic stress conditions through recognition of bacterial PAMPs and presence of H₂O₂ (Colcombet and Hirt 2008). H₂O₂ levels may be higher in these small terminal buds due to the observed greater expression of photosynthesis-related genes, implying a greater rate of photosynthesis. Plant cells produce reactive oxygen species such as H₂O₂ as part of photosynthesis, and cellular H₂O₂ levels act as a signalling molecule to communicate the overall stress level of the tissue (Ślesak et al. 2007), although it must be noted there are several other sources of H₂O₂ including the mitochondria and peroxisomes (a major source), particularly under stress conditions (Saxena et al. 2016). Thus the greater expression of both putative photosynthesis and stress-related genes in buds which later fail to open compared

to those which can open may be involved in negative regulation of flower opening via modulation of auxin sensitivity or perturbation in the Aux/IAA:ARF ratio. This auxin insensitivity correlating with risk of postharvest bud abortion could therefore be a useful floral marker and a possible target for modulation in order to reduce this risk in flowers.

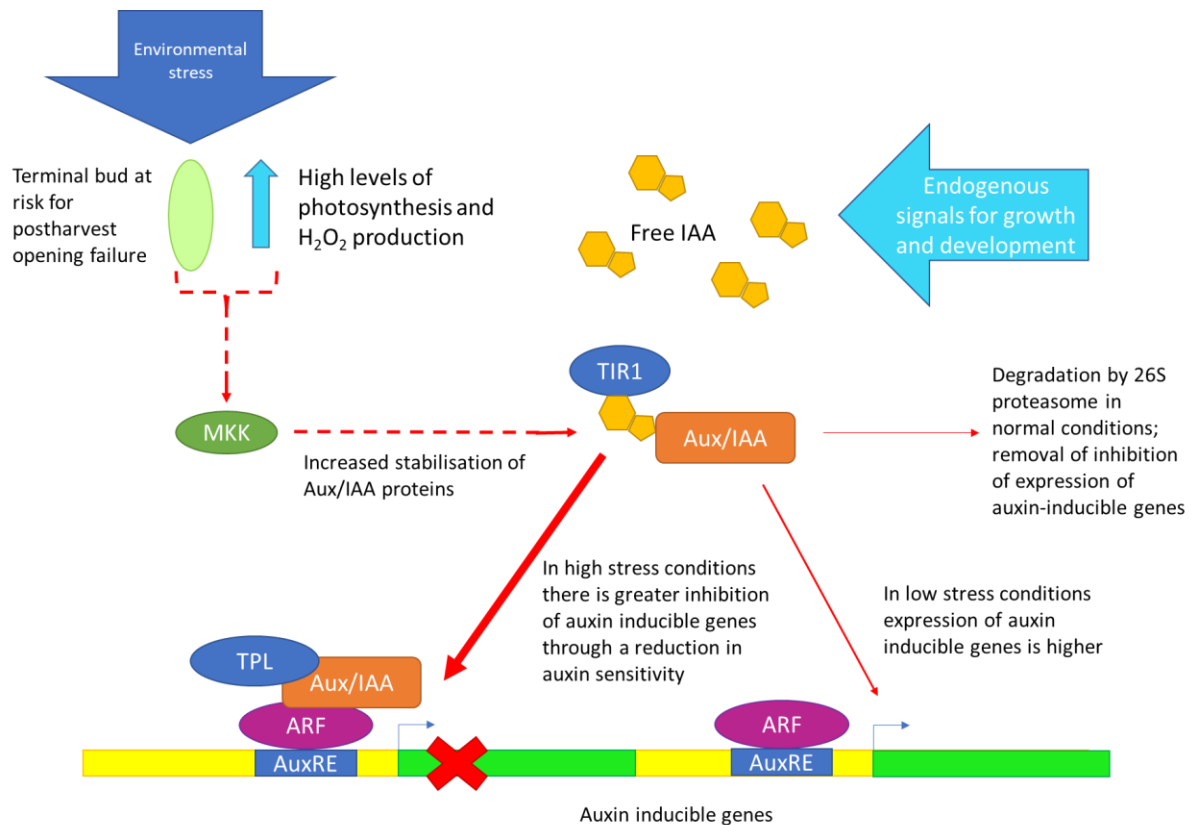


Figure 7.2 – diagram showing the possible mechanism for stress-induced auxin signalling inhibition in buds at risk of bud opening failure. In a normal system, endogenous signals for growth and development (circadian clock genes, bud age and development factors, nutritional status) cause production of IAA. IAA causes the derepression of auxin inducible genes through binding to the TIR1 receptor and free Aux/IAA inhibitors, and causes degradation of the whole complex. ARF proteins, when no longer bound to the Aux/IAA proteins, can cause transcription of inducible genes such as SAURs and other cell growth-related genes. In high stress conditions, such as the postharvest and post-cold storage terminal bud in a highly nutrient-limited environment, the higher levels of H_2O_2 perhaps through continued photosynthesis could be responsible for upregulation of the MAPK pathway (MKK4/5). MKKs may be able to stabilise Aux/IAA proteins and reduce their degradation, making the system less sensitive to presence of auxin and preventing auxin-

related growth and development. This could cause the arrested flower opening phenotype associated with these particular buds. Red arrows indicate experimentally determined and confirmed pathways, and red dashed arrows indicate hypothesised input from this study. Diagram adapted from Kuhn et al. (2019).

7.4 Further work

This study has offered several broad approaches to developing our understanding of flower opening and leaves many avenues for study open to confirm necessary parts of the flower opening pathway and targets for late bud abortion.

7.4.1 Further work on tepal physiology and metabolism

The mobilisation and metabolism of soluble sugars has been suggested in this thesis as being important for flower opening, however certain gaps in knowledge are present, particularly relating to the specific genes and proteins which drive the hypothesised phloem unloading into tepal cells to confirm if they are required for opening. The requirement of putative certain genes of interest coding for sucrose or monosaccharide transporters would be supported by correlatory molecular biology techniques such as qPCR. This is better confirmed by genetic manipulation methods (knockout or knock-down of genes of interest), but is made difficult by the lack of sequence data and large gene families of the genes of interest. As mentioned in Section 4.4.1, these particular proteins may be more likely to be post-transcriptionally regulated in any case (Xu et al. 2018) and therefore studying the activity of these transporters and the transport of sugars itself may be more advantageous, as discussed below.

The position on stem was hypothesised throughout this thesis to be an important additive factor to commercial treatment in causing problems with flower opening. The data showed some very slight differences in terms of physiology (soluble sugar content, metabolome) between Position A and C, but this was not statistically significant. Considering the data in Section 3.3.5 showed there were no problems with the terminal bud's ability to open until stems with five buds per stem were used, the use of Position C could have been insufficient to show differences in physiology from Position A. Repeating this experiment comparing

Position A and E buds would be a better way to show if there are differences in soluble sugar content and metabolome between these positions on stem during opening.

Investigating the relative expression of putative genes related to soluble sugar metabolism and mobilisation (*SUT*, *MST*, *SWEET*, *CWINV* genes) in Position A vs terminal buds may also shed some light on if differential phloem unloading drives these hypothesised differences.

There are also other methods to investigate both the use of sucrose in vase solution by opening buds and carbon partitioning across the inflorescence. For example, we do not know if the sucrose in the vase solution is translocated directly to buds and enters tepal cells in order to cause cell expansion, or if it is preferentially used by other tissues such as anthers and the pistil, both of which have high soluble sugar demands during parts of their development (Clement et al. 1996). Confirming the carbon partitioning between different positions on stem and if this changes with different number of buds per inflorescence and the commercial treatment would also be important to establish if these factors affect the soluble sugar uptake from the vase. A simple method to measure carbon translocation in *Brassica juncea* was found, using the uptake of labelled ^{14}C sucrose in a hydroponics medium by a stem to mimic source-to-sink transport (Srivastava et al. 2008). The sink organs were then extracted in acetone and filtrate was used for scintillation counting. This method could be easily adapted for use with lily stems due to the similarity of the system. Analysing material from the inner tepal base or mid tepal edge, which have been shown to have the greatest change in cell size over opening, and comparing this in cold/dark treated vs. non cold/dark treated flowers would be useful data to help understand if translocation is disrupted in high stress (nutrient deficient) conditions, in particular to the terminal buds on the inflorescence. Other methods to measure sucrose translocation are using high-performance anion exchange chromatography (Chuang and Chang 2013) or using fluorescent phloem mobile probes such as esculin. The benefits of using esculin are that the transport, at least in barley, is highly specific to the sucrose transporter SUC2 (Knoblauch et al. 2015), which would immediately indicate if this particular transporter is active during flower opening in tepals.

The significant differences in photosynthesis-related genes between buds which were capable of opening and those which were not suggested that there may be differences in the photosynthetic capability of these physiological states. Measuring photosynthetic ability

can be carried out relatively easily on leaves using devices such as a pulse-amplitude modulated photosynthesis yield analyzer (PAM), which measure the photosynthesis yield and are available as small portable meters suitable for use in a greenhouse, but may need to be adapted to use with a flower bud. The maximum quantum efficiency of photosystem II (Fv/Fm), a ratio of variable chlorophyll fluorescence to maximum chlorophyll fluorescence in dark adapted tissue, can be used as a measure of photosynthetic rate and has also been used as an indication of plant stress or photoinhibition (Maxwell and Johnson 2000). This can therefore be a useful readout of the developmental stage of buds, if photosynthetic efficiency is consistently lost over development and opening. It could also possibly indicate stem stress levels by showing the differences between on plant and commercially treated flowers, as well as differences between positions on stem related to differential stress levels between groups. This could be developed as a simple measure for growers to ensure developmental stages had been met on all buds on an inflorescence prior to harvest in new varieties. Alternatively, it could also be used postharvest to assess the most effective cold/dark storage time of specific varieties, so that buds are less likely to suffer from postharvest bud abortion.

7.4.2 Further work on confirming the hormonal and genetic regulation of flower opening in lilies

Confirming the requirement of endogenous positive auxin signalling for flower opening in lilies is important to be able to create potential solutions for late bud abortion. Firstly, while there is data to show the levels of auxins in tepals and other floral organs over development and opening (Arron and Munne-Bosch 2012a), it is not known how this compares to flowers which are unable to open. Measuring tepal auxin content in buds which can open compared to buds which cannot open would show if the differences observed in RNA-seq data on the expression levels of components of the auxin signal transduction pathway are correlated with a greater/lesser auxin content. Using a sensitive method such as high-performance liquid chromatography (HPLC) or LC-MS would be most appropriate and would also give information on levels of auxin conjugation (Stuepp et al. 2017), which may be important to assess how the observed increased auxin pathway inhibition in aborted buds occurs. Similarly, the high incidence of AP2-ERF transcription factors and motifs significantly upregulated in the precondition of buds which failed to open compared to those which did

open may suggest that there is a higher level of ethylene signalling in these buds at risk for late bud abortion, which can be confirmed using sensitive ethylene detecting methods such as GC, GC-MS or electrochemical sensors (Cristescu et al. 2013). It may also be useful to measure levels of other hormones: ABA and JA have been linked to having a role in flower opening or have signal transduction pathway elements differentially expressed between preconditions of flowers which opened vs. didn't open. This would provide an understanding of the whole hormonal profile between these two sets of buds.

Understanding the auxin inhibition or lack of sensitivity in buds which failed to open in Chapter 5 was hypothesised to perhaps be driven by Aux/IAA stabilisation, although many of the genes coding for these proteins were not found to be differentially expressed between these conditions by qPCR. This may not necessarily reflect the amount of protein present in tepal tissue – carrying out a Western blot (Lv et al. 2019) to show differences between Aux/IAA content in SRC buds compared to SSO and LFO buds, or more importantly, the ratio of Aux/IAA to ARF content, would be helpful to support the data collected in this study.

Secondly, being able to make changes to the levels of phytohormones is important to identify if the changes in hormone levels and transduction are really linked to changes in the phenotype and opening process. While this was explored in this study by adding hormones exogenously (auxin and auxin transport inhibitors), similar experiments could be carried out by adding ABA and JA as these hormones are also thought to be important due to increases in tepals prior to opening (Arrom and Munne-Bosch 2012a). The limitations of adding hormones exogenously are that this is a huge global change for the plant, even within the flower, and the effects may be different due to differences in the endogenous sites/types of hormone production, transport, cell localisation, and responses (Medford et al. 1989). These limitations could be partially overcome by using methods to apply NAA locally, for example by adding it to lanolin paste and administering it to small sections of tepal similarly to previous experiments (Reinhardt et al. 2000). This is particularly important for auxin as exogenous auxin added to stems did not cause any change in the time of flower opening, suggesting that adding auxin via the stem was not effective (Section 6.3.3), and this would allow auxin to be added to buds on stem and on plant easily. The cell expansion (carried out using epidermal pavement cell area measurements as carried out in Section 3.2.3/3.2.4)

could then be compared between auxin-treated and untreated areas on the same tepal, removing much of the possible biological variation between cell size of different flowers, and problems with auxin uptake by the phloem/xylem, or non-target effects in leaves/stem tissue.

Changing the levels of hormones in vivo using the same cellular machinery also circumvents the limitations of exogenous application and has been shown to work to great effect in model species such as *A. thaliana* and *O. sativa* (Medford et al. 1989; Yamamoto et al. 2007). This is however difficult to do via genetic methods such as creating stable transgenics in *Lilium* due to the large genome size and lack of sequence data available, making it extremely unamenable to genetic manipulation (Zhang et al. 2015; Du et al. 2017). The genetic diversity in the genus *Lilium* and breeding hybridisations which created the commercial varieties we use today also mean the understanding of genetic regulation in one variety may not be applicable to others. However, as there appears to be conservation in the most important regulatory pathways between varieties, creating transgenic plants with a changed endogenous levels of hormones may be useful for assessing the requirement of the specific hormone for opening. An *Agrobacterium tumefaciens* driven method for confirming the role of these putative transcription factors/regulatory genes was developed (Appendix 2) to assess the importance of these candidate genes in driving cell expansion and flower opening. Overexpression or silencing of putative genes related to auxin/ethylene production or signal transduction (such as the *YUCCA*, *ACS* or *ACO* genes for changes in amount of hormone, or the *IAA* or *ARF* genes to disrupt the ratio of Aux/IAA:ARF protein in cells) should in theory change the cell expansion of epidermal pavement cells, which can then be measured using methods such as timelapse photography to measure time of opening (Section 3.2.1), or microscopy to measure the growth of epidermal pavement cells (Section 2.5). The specific mechanisms driving this growth and opening could indicate mis-regulated mechanisms in conditions where the opening process is malfunctioning, such as the late bud abortion phenotype which has been identified in this study.

Another easier way of functionally analysing if DEGs identified in the RNA-seq experiment (Chapter 5) are required for flower opening is using heterologous expression of these genes of interest in a model species (*A. thaliana* or *N. tabacum*), due to the simpler, more easily manipulated system and greater sequence knowledge of the genome (Page and

Grossniklaus 2002). The expression can either be tested in wild type lines, which would show the effect of overexpression of the gene of interest (Hwang et al. 2011), particularly if constitutively expressed under a 35S promoter or similar (Ping et al. 2019), or in a mutant line if available, which may rescue the phenotype (Min et al. 2014). The large numbers of mutants available for various aspects of plant development and physiology mean that testing genes of interest for well characterised systems like auxin transduction or the MAPK signalling pathway would be possible in *A. thaliana*. This method has already been used using *MYB* genes cloned from several Asiatic hybrid lily cultivars and both transiently and stably expressed in tobacco and petunia to investigate the regulation of anthocyanin production in tepals (Sakai et al. 2019). Using a transient expression method in lily alongside heterologous stable expression in a species more amenable to genetic manipulation is perhaps the best approach due to possible differences in pathways of interest between species. Wu et al. (2018) showed that overexpressing the same gene (*L. longiflorum heat-stress transcription factor A3*) using these two methods showed contrasting results in proline accumulation, perhaps showing differences in the specific pathways in lily compared to *A. thaliana*. Overexpressing components of the MAPK signalling pathway transiently in lilies using an agroinfiltration method should indicate if this has an effect on the stability of Aux/IAA proteins compared to controls (measured by Western blot), as well as changes in the ability of the bud to open (measured by time of opening or cell expansion studies).

7.5 Discussion of potential impact of research

The research carried out in this study could have an impact on the cut-flower industry relating to current commercial lily pre- and postharvest processing conditions, as well as directions in breeding of new commercial varieties. As discussed in Chapter 1, problems relating to flower opening such as postharvest bud abortion are generally caused by inappropriately early harvest of stems, particularly relating to the terminal bud in stems with more buds per stem than suitable for the variety. This was supported by the terminal bud studies in Chapter 3 (Section 3.3.5), which showed that in Oriental lilies this problem was not observed in stems with four buds per stem but was observed in stems with five buds per stem, suggesting that the opening success of all buds on the inflorescence was not compromised in this variety until this limit (which may vary between varieties) was reached. This could indicate that breeding varieties which produce under a certain number of buds

per inflorescence unlikely to cause problems with postharvest bud abortion may be an important breeding goal. In specific cases where lilies with more buds per stem are required for consumer preference, reducing cold/dark storage to a minimum (for example by preferentially growing these varieties in the UK due to the smaller requirement for cold/dark storage and transport) may be advisable to reduce the risk of postharvest bud abortion.

The difficulty of harvesting stems at the correct time to avoid developmental problems is a common problem cited by growers (personal communication, James Cole, E.M. Cole Farms Ltd.), and lengthening the time period suitable to harvest flowers would therefore be beneficial, ideally being able to harvest at much earlier developmental stages to current guidelines. The data collected and examined in this study has shown that adding exogenous auxin itself is insufficient to cause development and opening in terminal buds at risk of postharvest bud abortion, and additionally has not been shown to cause effects in whole stems when added to vase water. Therefore it is unclear if auxin-related postharvest treatments independently would rescue these phenotypes, but if the role of ethylene, stress and MAPKs in postharvest bud abortion and the potential auxin insensitivity of these buds was verified, designing treatments towards these targets may be able to overcome the developmental arrest of specific buds in the future.

7.6 Final conclusions

In conclusion, this study has shown that flower opening in lilies is most likely driven by differential cell expansion which is correlated with changes in levels of soluble sugars and starch in parts of the tepal expanding the most. This could be driven by the expression of genes putatively coding for aquaporins and cell wall-remodelling enzymes. The regulation of flower opening appears to be caused by several endogenous factors which were hypothesised to have an effect, namely, bud length, competition on stem, and the circadian rhythm, which use hormonal signals to cause the creation of specific transcriptional landscapes in tepals critical to allow flower opening. Commercial processing has been shown to cause differences in physiology and temporal regulation of flower opening in lilies. The associated stress is particularly high in small terminal buds and suggests that postharvest bud abortion may be linked to a reduction of auxin sensitivity through high

levels of auxin signal transduction inhibitors in this particular high stress, low nutrition condition. This study has therefore identified several potential key pathways for modulation in further study to improve flower opening and quality of postharvest cut lily flowers.

Appendices

Appendix 1 – Preliminary experiment to explore bud length required for flower opening when detached from stem

A preliminary experiment was developed to identify minimum bud lengths required for flower opening in detached buds from stem, which aimed to mimic the effect of “extreme competition in a nutrient deficient condition”, where water was taken up but no sucrose. Oriental lily cv. ‘Debonair’ and LA hybrid ‘Ercolano’ were grown under Cardiff University growth conditions and terminal buds were harvested at different bud lengths (grouped under the bud length groups in Table 8.1, with number of samples per group in brackets). Buds were grown in tap water as described in Section 2.x and observed for % of successfully opening buds (Table 8.1).

Personal communication from James Cole (EM Cole Farms Ltd.) indicated that terminal ‘Debonair’ buds below 4.5 cm and ‘Ercolano’ buds below 4 cm from stems with 5 buds per stem was unlikely to open. However, the results showed that 80% of ‘Debonair’ buds 4.1-4.5 cm at harvest opened normally with no postharvest nutrition and 100% of ‘Ercolano’ buds 3.6-4 cm and 64% of buds 3.1-3.5 cm at harvest opened. This suggested that competition on stem has a specific non-nutritional effect inhibiting the opening of small terminal buds, which is removed from the buds when they are individually grown in water, even in the absence of any soluble sugar-based nutrition.

This particular experiment was limited due to the buds not being subjected to 72 hours of cold/dark storage prior to the experiment. The unexpected opening success of the buds could have been caused by lower stress from the absence of cold/dark storage. This experiment could have been improved by repeating both with and without cold/dark storage to fully understand the effect of the storage itself.

Table 8.1 – Effect of bud length at harvest on percentage of buds which opened in Oriental lily cv. ‘Debonair’ and LA hybrid lily cv. ‘Ercolano’

Size of bud at harvest	Oriental lily cv. ‘Debonair’	LA hybrid lily cv. ‘Ercolano’
<2.5 cm	ND	0% (n=5)
2.6 cm-3 cm	ND	0% (n=11)
3.1 cm-3.5 cm	0% (n=9)	64% (n=11)
3.6 cm-4 cm	0% (n=10)	100% (n=10)
4.1 cm-4.5 cm	80% (n=10)	100% (n=10)
4.6 cm-5 cm	100% (n=10)	100% (n=10)
5.1 cm-5.5 cm	100% (n=10)	ND
ND= not determined		

Appendix 2 - An *Agrobacterium tumefaciens* driven method for transient expression in *Lilium*

A method was developed to test if it was possible to transiently express genes in lily tepals using an *Agrobacterium tumefaciens* agroinfiltration driven approach. This method was optimised and adapted from Fatihah et al. (2019). A Golden Gate cloning method was used to create a construct containing the β -glucuronidase (GUS) and mCherry reporter genes (pL2B-Kan-pLjUBI-GUS-tNOS-p35S-mCherry-t35S), which was transformed into competent *Agrobacterium tumefaciens* strain EHA105 and confirmed by growth on selective media. A single colony of *A. tumefaciens* containing the construct was inoculated and grown overnight at 30 °C in Luria-Bertani (LB) liquid medium with the appropriate antibiotics (~15-17 hours). The cells were pelleted by centrifugation, supernatant was removed, and the cells were resuspended in a lily-specific infection buffer (20 g/L sucrose, 5 g/L MS salts (no vitamins), 1.95 g/L MES, 100 μ M acetosyringone – buffer contents taken from (Fatihah et al. 2019)) and shaken gently at room temperature for approximately two hours. A 1 ml syringe with needle was used to inject 1 ml of the buffer mixture slowly into the outer tepal midribs of all flowers on a stem, with approximately 0.3 ml being injected into each tepal midrib. The stems were kept in Cardiff University growth room conditions for between three and 6 days to assess the time required to see GUS staining in tepals. One tepal was removed from each flower on stem at 3, 5 and 6 days post injection for GUS staining.

GUS staining was carried out using a method adapted from (ref). Tepals were incubated in ice-cold 90% acetone for 5 minutes on ice, before rinsing with dH₂O and incubating in GUS staining buffer (0.5 mg/ml X-GlucA, 100 mM sodium phosphate pH7, 0.8 mM potassium ferricyanide, 0.8 mM potassium ferrocyanide, 0.1 mg/ml chloroamphenicol and 0.1% Triton X-100). Samples were vacuum infiltrated for 5 minutes and then incubated at 37 °C overnight in a rotary shaker to ensure full coverage of tepals. The staining solution was replaced with 70% ethanol the next day and the samples were incubated at 37 °C overnight before taking photos/ samples for microscopy to assess quality of GUS staining. The GUS staining appeared best after 6 days of incubation post injection and therefore this was carried out for all samples. LA hybrid lilies (cv. Courier) also worked best with this method, while other Oriental cultivars such as 'Tisento' and 'Ascot' failed to show any GUS staining. Staining appeared in tepals in a similar variable fashion (Figure 8.1A) across the tepal to Fatihah et al. (2019), which led to the conclusion that this method could be used to show differences between cell size/phenotype within the same tepal in order to reduce biological variation between individual flowers, which has been found to be highly variable in this study.

Samples showing strong GUS staining were then added to 10% formalin and incubated at 4°C overnight to fix. Samples were embedded in wax and transverse sections were produced by Marc Isaacs of the Cardiff University Bioimaging Hub to analyse cellular location of stain. I (Rakhee Dhorajiwala) then imaged the sections produced using light microscopy (Figure 8.1B - bScope BS.1153-EPLi (Euromex)). Parenchymal cells were shown to have severe shrinkage due to the rapid dehydration of the tissue and so more optimisation of this protocol is required before it can be used to compare parenchymal cell area in GUS stained vs. non GUS stained tepal sections.

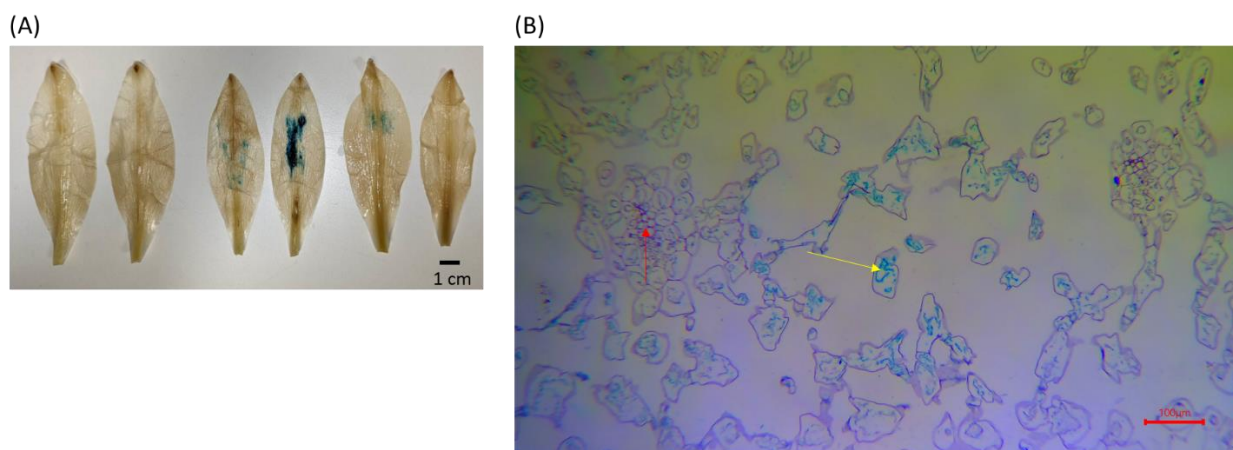


Figure 8.1 – (A) GUS staining observed in two outer tepals each from flowers injected with competent *Agrobacterium tumefaciens* strain EHA105 transformed with pL2B-Kan-pLjUBI-GUS-tNOS-p35S-mCherry-t35S as described above, showing variable staining in different flowers. Transverse sections were imaged (B) showing the vascular tissue (red arrow) and parenchymal cells containing GUS stain (yellow arrow), confirming intracellular location of stain.

Appendix 3- Epidermal pavement cell area growth analysis

Appendix 3.1 – Epidermal pavement cell area growth analysis in Oriental lilies

Mean cell area change in Oriental lily epidermal pavement cells over development with standard deviation. Letters indicate significance by ANOVA. One-way ANOVA carried out to show significance between cell area at the same stage of development of all locations on the tepal (outer and inner tepals treated separately).

Tepal	Stage of development	Degrees of freedom	F-value	P-value
Outer	Stage 1	11	27.3	<0.05
	Stage 2	11	12.73	<0.05
	Stage 3	10	4.815	<0.05
	Stage 4	11	8.483	<0.05
	Stage 5	11	14.84	<0.05
Inner	Stage 1	10	6.722	<0.05
	Stage 2	9	11.59	<0.05
	Stage 3	10	14.63	<0.05
	Stage 4	11	18.33	<0.05
	Stage 5	11	3.753	<0.05

Appendix 3.2 – Epidermal pavement cell area growth analysis in *L. longiflorum* lilies

Mean cell area change in *L. longiflorum* lily epidermal pavement cells over development with standard deviation. Letters indicate significance by ANOVA. One-way ANOVA carried out to show significance between cell area at the same stage of development of all locations on the tepal (outer and inner tepals treated separately).

Tepal	Stage of development	Degrees of freedom	F-value	P-value
Outer	Stage 1	11	2.374	<0.05
	Stage 2	11	17.45	<0.05
	Stage 3	11	14.38	<0.05
	Stage 4	11	11.27	<0.05
	Stage 5	11	11.41	<0.05
Inner	Stage 1	11	11.74	<0.05
	Stage 2	10	6.578	<0.05
	Stage 3	10	14.94	<0.05
	Stage 4	11	13.85	<0.05
	Stage 5	11	7.614	<0.05

	Table - Epidermal pavement cell area (μm^2) over development and opening in different regions of the tepal in <i>L. longiflorum</i> liliaceae. Standard deviation and significance by one-way ANOVA.																			
	Stage 1				Stage 2				Stage 3				Stage 4				Stage 5			
	Cell area / μm^2	Standard deviation	Significance		Cell area / μm^2	Standard deviation	Significance		Cell area / μm^2	Standard deviation	Significance		Cell area / μm^2	Standard deviation	Significance		Cell area / μm^2	Standard deviation	Significance	
Top ADM	2020.678333	+422.136071920734	a	1403.018333	+514.7768956612718	d		2242.926667	+734.359217840062	ef		3524.575	+814.8039666012684	bde		2602.478333	+793.9978765002617	e		
Top ADE	1461.97	+330.614586187603	ab	1291.198333	+193.7251267561	d		1728.061667	+243.214911748164	f		2090.853333	+697.200808280274	f		3054.05	+648.086569587733	de		
Top ABM	1685.795	+657.675333913785	ab	1998.525	+578.912879758258	cd		2354.526667	+665.748574062811	def		3414.546667	+663.862299115307	bde		4294.205	+948.459376415246	bcd		
Top ABE	1906.316667	+662.160999022644	ab	1784.006667	+261.819144729077	cd		2504.475	+446.637129972418	def		2519.568333	+424.020856299154	ef		3379.86	+602.904789100234	ce		
Mid ADM	2092.25	+511.568592272827	a	1870.4	+430.693433569632	cd		5287.413333	+1406.27317782381	ab		4972.49	+818.361469180947	ab		3986.956667	+818.31274186992	ce		
Mid ADE	1697.583333	+381.5609351423	ab	1324.94	+307.767356878535	d		3586.646667	+519.631637438162	bcd		2718.945	+640.96416725898	df		3538.281667	+716.2991170011179	ce		
Mid ABM	1598.5	+300.795606483871	ab	2507.643333	+336.711608393908	bc		4408.64	+1424.91934929665	ac		4175.788333	+661.232846519207	abc		5256.088333	+870.966639393644	ce		
Mid ABE	1140.571667	+235.379476795804	a	1384.693333	+134.110989358317	d		3173.708333	+930.30697764591	ce		2752.555	+379.580568720262	cdf		4725.638333	+991.694802435036	bcd		
Base ADM	1853.321667	+522.649681504416	ab	2654.99	+523.306825027154	ac		4181.685	+991.187431129957	ac		4056.088333	+984.41447001589	ad		6715.988333	+2134.915305666828	ab		
Base ADE	1793.025	+413.54145063101	ab	2256.863333	+578.08981269926	bc		4549.19	+649.694556818819	ac		3996.478333	+679.465548013045	ad		8126.96	+1718.85548889952	ab		
Base ABM	1550.151667	+242.006887705013	ab	4038.993333	+836.506761494891	a		5824.758333	+986.60736920858	a		5911.671667	+1911.59944888848	a		4620.298333	+1430.34742659984	bcd		
Base ABE	1435.861667	+216.131764848822	ab	3388.863333	+835.054254181526	ab		2959.596667	+622.667920422278	ce		4488.853333	+488.819571484885	ab		3747.76	+532.282522350677	ce		
Top ADM	1513.338333	+437.494981704551	bce	n/a	n/a	n/a		2432.943333	+354.090629170932	bc		3282.955	+220.26751396881	bc		3451.226667	+723.946424306842	d		
Top ADE	939.1516667	+322.081762129845	e	1954.516667	+524.231030697982	bc		1429.365	+254.328609617556	d		1909.318333	+408.512034653408	d		3642.158333	+1101.13340869155	cd		
Top ABM	1449.168333	+327.724705899123	bce	1958.56	+340.56166460716	bc		2129.24	+471.927831389505	bd		3692.598333	+844.14258505105	bc		4705.52	+692.932671130461	bd		
Top ABE	1179.933333	+400.893326991941	ce	1194.713333	+269.479797979566	cd		1610.676667	+596.417398058329	cd		2734.938333	+510.387997680849	cd		4826.441667	+456.223541936041	bd		
Mid ADM	1315.878333	+468.637687576092	bce	2659.426667	+808.936517130155	a		3387.758333	+953.03806661469	ab		3721.466667	+788.534908464217	bc		5499.876667	+1550.05214239608	abc		
Mid ADE	1010.31	+188.572110663269	de	1387.19	+194.077314903109	bd		2182.931667	+459.869001234771	bd		2751.031667	+218.636224209683	c		4904.643333	+850.37494000392	bd		
Mid ABM	1805.558333	+454.171905710455	ac	1577.543333	+313.483018338579	bd		3214.313333	+478.959242552713	ab		4634.706667	+978.618260910078	ab		4547.255	+995.0979798726335	bd		
Mid ABE	1704.895	+343.296148929754	bcd	1147.405	+317.709246623386	d		2342.52	+280.902450469909	bc		2814.89	+266.132784526822	c		3354.566667	+572.436737383847	d		
Base ADM	2946.833333	+434.67750314766	a	1892.973333	+252.863907560306	bc		2777.843333	+449.638651437647	b		3327.348333	+704.503961476916	bc		6327.935	+1856.45755905972	ab		
Base ADE	1669.931667	+216.861833379382	bcd	1462.761667	+451.176341286493	bd		4827.753333	+1794.67290515756	a		5979.39	+1104.8383903721	a		5493.1	+1232.01751628781	abc		
Base ABM	3125.308333	+996.084205826329	a	2016.105	+474.849026944353	bc		4177.468333	+1629.19466965021	a		4393.09	+941.643651133484	ab		7547.83	+1422.08051029356	a		
Inner: Base ABE	2205.153333	+745.483220459499	ab	1849.18	+226.769574502401	abc		n/a	n/a	n/a		3380.12	+493.081562380909	bc		5679.935	+915.631452119247	ab		

Appendix 4 – List of DEGs, putative identification and full GO term enrichments

Appendix 4.1 – List of DEGs, GO term enrichment and KEGG pathway enrichment for all DEGs between buds which open and those which fail to

Read identifier	TAIR ID	Viridiplantae gene	Log2FC SSO/SRC	Log2FC LFO/SRC
TRINITY_DN2268_c0_g1	#N/A	XP_026446801.1	#N/A	-2.0793158
TRINITY_DN13791_c0_g1	AT5G62360	#N/A	#N/A	-1.696571103
TRINITY_DN4968_c1_g1	#N/A	XP_008229808.1	#N/A	-8.662651304
TRINITY_DN271_c0_g3	#N/A	SIK19391.1	#N/A	-3.800459742
TRINITY_DN26761_c0_g3	#N/A	#N/A	#N/A	-8.179389161
TRINITY_DN5145_c0_g1	AT3G47600	XP_024169373.1	#N/A	-1.470072724
TRINITY_DN39998_c0_g1	AT1G63310	#N/A	#N/A	-3.274655011
TRINITY_DN6920_c0_g1	#N/A	#N/A	#N/A	-2.319739599
TRINITY_DN11476_c0_g2	#N/A	#N/A	#N/A	-8.31124889
TRINITY_DN7245_c0_g1	AT2G46410	QGH84099.1	#N/A	-1.434920679
TRINITY_DN36709_c0_g1	AT2G46170	#N/A	#N/A	-2.981024105
TRINITY_DN46539_c0_g1	#N/A	#N/A	#N/A	-8.54200734
TRINITY_DN31416_c0_g1	#N/A	#N/A	#N/A	-7.583419941
TRINITY_DN2611_c0_g1	AT3G51470	XP_010940247.1	#N/A	-1.163964544
TRINITY_DN14225_c0_g2	#N/A	#N/A	#N/A	-7.823720621
TRINITY_DN51313_c0_g1	#N/A	#N/A	#N/A	-2.362038142
TRINITY_DN15038_c0_g1	AT1G29520	#N/A	#N/A	-2.76168187
TRINITY_DN12012_c0_g1	#N/A	#N/A	#N/A	-2.933950757
TRINITY_DN14882_c0_g1	#N/A	#N/A	#N/A	-2.926077402
TRINITY_DN7461_c0_g1	#N/A	QUV77621.1	#N/A	-2.874332171
TRINITY_DN37855_c0_g1	#N/A	#N/A	#N/A	-7.572570976
TRINITY_DN1927_c0_g4	#N/A	#N/A	#N/A	-2.001454283
TRINITY_DN41740_c0_g1	#N/A	#N/A	#N/A	-7.551035394
TRINITY_DN14262_c0_g2	#N/A	#N/A	#N/A	-4.39486611
TRINITY_DN22821_c0_g1	#N/A	#N/A	#N/A	-2.575269249
TRINITY_DN3486_c0_g1	#N/A	#N/A	#N/A	-1.606361577
TRINITY_DN51959_c0_g1	#N/A	#N/A	#N/A	-2.438013833
TRINITY_DN12689_c0_g1	AT2G39420	XP_010922433.1	#N/A	-2.979783169
TRINITY_DN13956_c0_g2	#N/A	#N/A	#N/A	-1.044796824
TRINITY_DN10333_c0_g1	#N/A	KAG8637463.1	#N/A	-2.87127434
TRINITY_DN42282_c0_g1	#N/A	#N/A	#N/A	-2.329057154
TRINITY_DN2754_c0_g1	AT5G52300	#N/A	#N/A	-1.617776229
TRINITY_DN4914_c1_g1	#N/A	XP_020690032.1	#N/A	-2.075128946
TRINITY_DN129_c0_g1	#N/A	#N/A	#N/A	-1.730574297
TRINITY_DN816_c0_g1	#N/A	#N/A	#N/A	-1.428182921
TRINITY_DN4909_c0_g2	#N/A	XP_020264240.1	#N/A	-2.497785155
TRINITY_DN12936_c2_g2	AT3G55470	KAH7656953.1	#N/A	-0.979439363

TRINITY_DN3925_c0_g1	#N/A	XP_010905284.1	#N/A	-0.939357627
TRINITY_DN8958_c0_g2	#N/A	#N/A	#N/A	-1.592625072
TRINITY_DN1878_c0_g1	AT4G03140	XP_010921846.1	#N/A	-1.100294736
TRINITY_DN17788_c0_g1	AT3G20570	#N/A	#N/A	-2.335011839
TRINITY_DN5453_c0_g2	AT5G53160	XP_020576858.1	#N/A	-0.873808249
TRINITY_DN48463_c0_g1	#N/A	#N/A	#N/A	-3.931656379
TRINITY_DN756_c0_g1	AT5G38280	KAG1326436.1	#N/A	-1.348617194
TRINITY_DN1473_c0_g1	AT1G31330	XP_029120880.1	#N/A	-1.704912617
TRINITY_DN2268_c0_g2	#N/A	XP_009416779.1	#N/A	-0.905303561
TRINITY_DN20362_c0_g1	#N/A	#N/A	#N/A	-2.398235602
TRINITY_DN14680_c0_g1	AT5G22870	#N/A	#N/A	-2.796744834
TRINITY_DN16932_c0_g1	#N/A	#N/A	#N/A	-2.810423438
TRINITY_DN11370_c0_g1	#N/A	KAF5197858.1	#N/A	-2.046875776
TRINITY_DN12401_c1_g1	AT1G13920	THU45620.1	#N/A	-2.869148563
TRINITY_DN6216_c0_g1	AT4G12800	XP_020111553.1	#N/A	-2.225971795
TRINITY_DN296_c1_g2	#N/A	XP_008779130.1	#N/A	-2.008282512
TRINITY_DN12884_c0_g1	#N/A	CAG1854707.1	#N/A	-1.948942864
TRINITY_DN52274_c0_g1	#N/A	#N/A	#N/A	-4.028911833
TRINITY_DN36786_c0_g1	#N/A	#N/A	#N/A	-2.368982923
TRINITY_DN9748_c0_g1	#N/A	XP_010930890.2	#N/A	-1.693441416
TRINITY_DN6215_c0_g1	#N/A	XP_009384890.1	#N/A	-1.574423219
TRINITY_DN9958_c0_g2	#N/A	RWR93378.1	#N/A	-2.304049985
TRINITY_DN4395_c0_g1	AT3G61470	XP_009405484.1	#N/A	-2.092329236
TRINITY_DN4420_c0_g1	AT1G30320	XP_010923709.1	#N/A	-1.871003711
TRINITY_DN3678_c0_g1	AT3G52070	DAD29701.1	#N/A	-1.027437403
TRINITY_DN21143_c0_g2	#N/A	#N/A	#N/A	-4.841179897
TRINITY_DN3063_c0_g1	AT3G49200	XP_039119934.1	#N/A	-1.167712935
TRINITY_DN9564_c0_g1	AT3G23240	XP_021649290.1	#N/A	-2.008467955
TRINITY_DN7941_c0_g1	AT5G39210	XP_010906148.1	#N/A	-1.444286911
TRINITY_DN12486_c0_g3	#N/A	#N/A	#N/A	-7.381702291
TRINITY_DN3933_c0_g1	AT1G61520	RWR95748.1	#N/A	-1.466236364
TRINITY_DN356_c0_g1	AT1G62770	XP_008779098.1	#N/A	-1.277094596
TRINITY_DN1953_c0_g1	#N/A	ONK69953.1	#N/A	-1.888980501
TRINITY_DN42562_c0_g1	AT1G48130	#N/A	#N/A	-2.171412851
TRINITY_DN44351_c0_g1	#N/A	#N/A	#N/A	-2.481921531
TRINITY_DN10214_c0_g1	AT1G06680	KAF3445023.1	#N/A	-2.03998268
TRINITY_DN5574_c0_g1	AT1G15820	XP_010939618.1	#N/A	-1.611635403
TRINITY_DN4075_c0_g1	AT3G30180	XP_008786029.2	#N/A	-1.226676778
TRINITY_DN8098_c0_g3	#N/A	#N/A	#N/A	-0.976353573
TRINITY_DN5671_c0_g1	AT5G67210	XP_008644968.1	#N/A	-1.225227472
TRINITY_DN3967_c0_g1	AT5G08380	XP_038972842.1	#N/A	-1.203109685
TRINITY_DN7488_c0_g1	#N/A	KAG1354946.1	#N/A	-1.864469487
TRINITY_DN49967_c0_g1	#N/A	#N/A	#N/A	-6.309431476
TRINITY_DN2284_c0_g1	AT4G10340	XP_010930383.1	#N/A	-1.894796293
TRINITY_DN556_c0_g1	AT2G36840	XP_020261029.1	#N/A	-0.962626086
TRINITY_DN2184_c0_g1	#N/A	XP_038977452.1	#N/A	-0.913972422

TRINITY_DN15164_c1_g1	#N/A	#N/A	#N/A	-2.257734792
TRINITY_DN12185_c0_g1	AT3G22400	XP_010934565.1	#N/A	-2.324717697
TRINITY_DN6736_c0_g3	#N/A	XP_002285709.1	#N/A	-1.677127091
TRINITY_DN14499_c0_g1	#N/A	#N/A	#N/A	-3.287683342
TRINITY_DN6708_c0_g1	#N/A	XP_018684714.1	#N/A	-0.873889438
TRINITY_DN10658_c0_g2	#N/A	KAH0458273.1	#N/A	-2.598585641
TRINITY_DN9307_c0_g1	#N/A	XP_010272016.1	#N/A	-1.96879437
TRINITY_DN2977_c0_g1	#N/A	MQL91171.1	#N/A	-1.212699207
TRINITY_DN10448_c0_g1	AT2G20260	ACJ84185.1	#N/A	-1.496361377
TRINITY_DN12122_c0_g1	#N/A	#N/A	#N/A	-1.577109862
TRINITY_DN11880_c0_g3	AT4G39730	XP_020154970.1	#N/A	-1.29816418
TRINITY_DN49676_c0_g1	AT5G56840	#N/A	#N/A	-2.187552085
TRINITY_DN13154_c0_g1	#N/A	#N/A	#N/A	-2.859500682
TRINITY_DN12101_c0_g1	AT2G26640	CDO99138.1	#N/A	-2.153921104
TRINITY_DN12713_c0_g1	AT5G46240	XP_020105265.1	#N/A	-3.331883759
TRINITY_DN10210_c0_g2	AT3G10910	KAG1354522.1	#N/A	-2.470274847
TRINITY_DN11005_c0_g1	#N/A	EHA8587619.1	#N/A	-1.767770922
TRINITY_DN8742_c0_g2	#N/A	EHA8589301.1	#N/A	-1.295591103
TRINITY_DN849_c0_g2	#N/A	XP_009388934.1	#N/A	-0.811059631
TRINITY_DN16972_c0_g1	AT4G06536	#N/A	#N/A	-1.632083308
TRINITY_DN48449_c0_g1	#N/A	#N/A	#N/A	-7.458698935
TRINITY_DN19242_c0_g1	#N/A	#N/A	#N/A	-2.45986251
TRINITY_DN6296_c0_g1	#N/A	XP_010908657.1	#N/A	-1.075458502
TRINITY_DN10376_c0_g1	AT1G55370	XP_010932681.1	#N/A	-1.798432107
TRINITY_DN45412_c0_g2	#N/A	#N/A	#N/A	-1.09848711
TRINITY_DN10267_c0_g1	AT1G80870	KAG1327562.1	#N/A	-1.159127497
TRINITY_DN10468_c0_g1	AT2G20870	ABI48859.1	#N/A	-2.04512684
TRINITY_DN3025_c0_g1	AT2G35370	XP_008799361.1	#N/A	-1.546031208
TRINITY_DN51997_c0_g1	#N/A	#N/A	#N/A	-3.088597511
TRINITY_DN13501_c0_g1	#N/A	#N/A	#N/A	-2.35093605
TRINITY_DN12847_c0_g1	#N/A	OVA18710.1	#N/A	-1.476134029
TRINITY_DN4157_c1_g1	#N/A	XP_009415186.1	#N/A	-1.145385717
TRINITY_DN14780_c0_g1	AT3G43810	#N/A	#N/A	-0.967686811
TRINITY_DN18817_c0_g1	#N/A	#N/A	#N/A	-0.757071229
TRINITY_DN6558_c0_g1	AT4G23060	XP_010933871.1	#N/A	-0.693855107
TRINITY_DN13921_c0_g1	AT4G15680	#N/A	#N/A	-1.521410659
TRINITY_DN34731_c0_g1	AT4G18250	#N/A	#N/A	-3.062462013
TRINITY_DN48380_c0_g1	#N/A	#N/A	#N/A	-1.374881734
TRINITY_DN1852_c0_g1	#N/A	XP_008785647.2	#N/A	-1.118889139
TRINITY_DN16271_c0_g1	#N/A	#N/A	#N/A	-2.863975472
TRINITY_DN673_c0_g2	AT4G37320	XP_038971683.1	#N/A	-0.933252302
TRINITY_DN11827_c0_g1	AT1G78830	XP_010916746.2	#N/A	-3.463590758
TRINITY_DN9746_c0_g1	#N/A	#N/A	#N/A	-0.739913002
TRINITY_DN13641_c0_g1	AT5G18970	#N/A	#N/A	-2.671914904
TRINITY_DN16888_c0_g1	#N/A	#N/A	#N/A	-1.341145647
TRINITY_DN49392_c0_g1	#N/A	#N/A	#N/A	-1.712878148

TRINITY_DN12404_c0_g1	#N/A	#N/A	#N/A	-2.23863377
TRINITY_DN42304_c0_g1	#N/A	#N/A	#N/A	-0.963056141
TRINITY_DN28596_c0_g1	#N/A	#N/A	#N/A	-4.176147258
TRINITY_DN3220_c0_g1	#N/A	XP_008781323.3	#N/A	-2.445440334
TRINITY_DN18456_c0_g1	AT3G57040	#N/A	#N/A	-4.285654721
TRINITY_DN8262_c0_g1	AT3G11600	RRT36732.1	#N/A	-2.179207821
TRINITY_DN18972_c0_g1	#N/A	#N/A	#N/A	-1.135560237
TRINITY_DN11317_c0_g2	#N/A	#N/A	#N/A	-1.29876395
TRINITY_DN13310_c0_g1	#N/A	XP_010932423.2	#N/A	-3.165090546
TRINITY_DN13365_c0_g1	#N/A	AHG94647.1	#N/A	-2.272903677
TRINITY_DN3356_c0_g1	#N/A	#N/A	#N/A	-0.950967131
TRINITY_DN15573_c0_g1	#N/A	#N/A	#N/A	-2.08802715
TRINITY_DN24459_c0_g1	AT2G41200	#N/A	#N/A	-2.481532202
TRINITY_DN52287_c0_g1	#N/A	#N/A	#N/A	-4.567257662
TRINITY_DN16035_c0_g1	#N/A	#N/A	#N/A	-0.8819967
TRINITY_DN3709_c0_g1	#N/A	CAD1837432.1	#N/A	-0.75289123
TRINITY_DN3420_c0_g1	AT5G25930	XP_008794105.2	#N/A	-1.468183971
TRINITY_DN48425_c0_g1	AT4G35170	#N/A	#N/A	-2.112582069
TRINITY_DN2101_c0_g1	#N/A	#N/A	#N/A	-1.255212578
TRINITY_DN5963_c0_g2	#N/A	ADW08475.1	#N/A	-1.872988887
TRINITY_DN16724_c0_g1	#N/A	#N/A	#N/A	-3.068878719
TRINITY_DN132_c1_g2	AT3G03910	KAF3325150.1	#N/A	-0.942477567
TRINITY_DN40081_c0_g1	#N/A	#N/A	#N/A	-1.945012639
TRINITY_DN8128_c0_g1	AT4G30320	XP_020089643.1	#N/A	-1.702918213
TRINITY_DN3354_c1_g1	#N/A	AAL61539.1	#N/A	-2.020785748
TRINITY_DN5149_c0_g3	#N/A	#N/A	#N/A	-3.471711167
TRINITY_DN6206_c0_g1	AT3G50820	O49079.1	#N/A	-1.117088855
TRINITY_DN11222_c0_g1	#N/A	XP_038989333.1	#N/A	-1.022640376
TRINITY_DN17539_c0_g1	#N/A	#N/A	#N/A	-1.574076193
TRINITY_DN18109_c0_g1	#N/A	#N/A	#N/A	-2.963432983
TRINITY_DN5234_c0_g1	AT4G02530	XP_038974535.1	#N/A	-0.775535487
TRINITY_DN18155_c0_g1	#N/A	#N/A	#N/A	-1.401577792
TRINITY_DN12282_c0_g1	AT3G11810	KAG1368615.1	#N/A	-0.77290114
TRINITY_DN42374_c0_g1	AT1G51950	#N/A	#N/A	-1.486286104
TRINITY_DN2151_c0_g1	#N/A	#N/A	#N/A	-0.884715845
TRINITY_DN5943_c1_g2	#N/A	#N/A	#N/A	-2.731190725
TRINITY_DN7199_c0_g1	#N/A	RWR89859.1	#N/A	-0.813961483
TRINITY_DN2537_c0_g1	AT4G23180	KAH9688432.1	#N/A	-0.82311635
TRINITY_DN3297_c0_g1	AT2G02850	P60496.1	#N/A	-1.595973801
TRINITY_DN11858_c0_g1	AT3G46530	XP_020244414.1	#N/A	-1.00625243
TRINITY_DN7007_c0_g1	#N/A	KAH7654286.1	#N/A	-1.471146475
TRINITY_DN3609_c0_g1	#N/A	EHA8587029.1	#N/A	-0.650387977
TRINITY_DN1629_c0_g2	#N/A	APU50922.1	#N/A	-1.426517686
TRINITY_DN5893_c0_g1	#N/A	THU64384.1	#N/A	-1.724931421
TRINITY_DN692_c0_g1	#N/A	XP_017698759.2	#N/A	-1.598672498
TRINITY_DN52008_c0_g1	#N/A	#N/A	#N/A	-1.411999756

TRINITY_DN4960_c0_g1	AT1G21680	XP_038989131.1	#N/A	-0.959226013
TRINITY_DN14670_c0_g1	#N/A	#N/A	#N/A	-1.52347326
TRINITY_DN40087_c0_g1	#N/A	#N/A	#N/A	-1.641667138
TRINITY_DN5454_c0_g1	AT5G65720	XP_010943368.1	#N/A	-0.631176302
TRINITY_DN8580_c1_g1	AT5G44230	KAH7661785.1	#N/A	-1.16249067
TRINITY_DN1525_c1_g1	#N/A	#N/A	#N/A	-1.849256922
TRINITY_DN4639_c0_g1	#N/A	KAF8391110.1	#N/A	-1.380608901
TRINITY_DN6787_c0_g1	#N/A	APU50913.1	#N/A	-1.305295049
TRINITY_DN6707_c0_g2	#N/A	#N/A	#N/A	-5.418412465
TRINITY_DN9559_c0_g1	#N/A	RWR85764.1	#N/A	-3.67091839
TRINITY_DN10251_c0_g1	#N/A	XP_010923372.2	#N/A	-0.862656246
TRINITY_DN45104_c0_g1	#N/A	#N/A	#N/A	-1.504027298
TRINITY_DN3074_c0_g2	AT5G07290	CBI31752.3	#N/A	-0.694025446
TRINITY_DN10270_c1_g1	AT1G69560	CAA7389119.1	#N/A	-2.47299753
TRINITY_DN3705_c0_g1	AT1G42550	KAG1361107.1	#N/A	-1.117984512
TRINITY_DN9974_c0_g1	#N/A	XP_031102147.1	#N/A	-0.944461231
TRINITY_DN1733_c0_g1	#N/A	QGH84091.1	#N/A	-1.08620329
TRINITY_DN10648_c0_g1	AT1G75540	RLM75104.1	#N/A	-1.051756127
TRINITY_DN9581_c0_g1	#N/A	AMT81306.1	#N/A	-2.677627296
TRINITY_DN15215_c0_g2	#N/A	#N/A	#N/A	-2.35758945
TRINITY_DN15211_c0_g1	AT3G01680	#N/A	#N/A	-2.002927764
TRINITY_DN14143_c0_g1	#N/A	#N/A	#N/A	-1.44445066
TRINITY_DN9620_c0_g1	#N/A	RWR84246.1	#N/A	-1.30722785
TRINITY_DN40482_c0_g1	AT4G24700	#N/A	#N/A	-1.669684637
TRINITY_DN14977_c0_g1	AT1G73370	#N/A	#N/A	-2.013753336
TRINITY_DN28445_c0_g2	#N/A	#N/A	#N/A	-3.57174145
TRINITY_DN5826_c0_g1	#N/A	#N/A	#N/A	-1.610811147
TRINITY_DN48785_c0_g1	#N/A	#N/A	#N/A	-2.186808821
TRINITY_DN2633_c0_g1	#N/A	XP_008783924.2	#N/A	-0.668750651
TRINITY_DN1209_c0_g1	AT4G22190	XP_017701695.2	#N/A	-0.766976309
TRINITY_DN12340_c0_g1	#N/A	EER2174132.1	#N/A	-3.69255863
TRINITY_DN9115_c0_g1	#N/A	QQY00481.1	#N/A	-1.419618379
TRINITY_DN21792_c0_g1	#N/A	#N/A	#N/A	-2.302875554
TRINITY_DN45639_c0_g1	AT5G43290	#N/A	#N/A	-2.769235702
TRINITY_DN11851_c0_g1	#N/A	#N/A	#N/A	-3.121421986
TRINITY_DN2248_c0_g1	AT3G21220	KAG0468622.1	#N/A	-0.82077617
TRINITY_DN6527_c0_g1	AT1G75460	XP_009397187.1	#N/A	-0.697868102
TRINITY_DN8502_c0_g1	AT5G01530	OUZ99077.1	#N/A	-1.890120793
TRINITY_DN18193_c0_g1	AT3G48100	#N/A	#N/A	-1.358779899
TRINITY_DN7307_c0_g3	AT5G07980	XP_010939426.1	#N/A	-1.131032581
TRINITY_DN1913_c0_g1	AT5G47390	XP_010941064.1	#N/A	-0.680360648
TRINITY_DN10313_c0_g1	AT2G44940	XP_010919644.3	#N/A	-1.294208385
TRINITY_DN10712_c0_g1	AT5G20630	ABV03161.1	#N/A	-2.092682389
TRINITY_DN49072_c0_g1	#N/A	#N/A	#N/A	-3.493874945
TRINITY_DN13397_c0_g1	AT3G26330	XP_010909080.1	#N/A	-2.401093181
TRINITY_DN13835_c0_g2	#N/A	#N/A	#N/A	-1.439510207

TRINITY_DN14746_c0_g1	#N/A	#N/A	#N/A	-1.159998073
TRINITY_DN1128_c0_g1	AT3G04720	APG55503.1	#N/A	-2.312713424
TRINITY_DN16920_c0_g1	AT5G41040	#N/A	#N/A	-1.410381309
TRINITY_DN3829_c0_g1	AT1G15030	KAF7820302.1	#N/A	-0.753772384
TRINITY_DN833_c0_g1	AT3G19700	KAG1348101.1	#N/A	-0.689561947
TRINITY_DN6217_c0_g1	#N/A	AYU71104.1	#N/A	-0.947441904
TRINITY_DN2192_c0_g1	#N/A	#N/A	#N/A	-1.11320103
TRINITY_DN30040_c0_g3	#N/A	#N/A	#N/A	-3.227747336
TRINITY_DN3317_c0_g3	AT3G49550	RRT56083.1	#N/A	-0.737734246
TRINITY_DN9647_c0_g1	#N/A	#N/A	#N/A	-2.057333148
TRINITY_DN14885_c0_g1	#N/A	#N/A	#N/A	-2.252259478
TRINITY_DN9351_c0_g1	AT3G52910	XP_008780035.2	#N/A	-1.301549717
TRINITY_DN51601_c0_g1	#N/A	#N/A	#N/A	-3.27359131
TRINITY_DN991_c0_g1	AT2G02070	EHA8590263.1	#N/A	-0.984388381
TRINITY_DN20054_c1_g1	#N/A	#N/A	#N/A	-2.193751983
TRINITY_DN6297_c0_g1	#N/A	#N/A	#N/A	-1.466122517
TRINITY_DN14674_c2_g1	#N/A	#N/A	#N/A	-3.997005561
TRINITY_DN51584_c0_g1	#N/A	#N/A	#N/A	-6.718558541
TRINITY_DN52861_c0_g1	#N/A	#N/A	#N/A	-3.7993897
TRINITY_DN4592_c0_g1	#N/A	#N/A	#N/A	-2.610978314
TRINITY_DN18879_c0_g1	AT5G27420	#N/A	#N/A	-1.908477369
TRINITY_DN3924_c0_g1	#N/A	AIF76294.1	#N/A	1.613216627
TRINITY_DN53844_c0_g1	#N/A	#N/A	#N/A	8.660825153
TRINITY_DN16909_c0_g1	#N/A	#N/A	#N/A	9.464272122
TRINITY_DN30449_c0_g1	#N/A	#N/A	#N/A	7.875782412
TRINITY_DN5158_c1_g1	#N/A	KAG1328113.1	#N/A	1.240218635
TRINITY_DN15875_c0_g2	#N/A	#N/A	#N/A	10.84468111
TRINITY_DN3741_c0_g3	#N/A	XP_010921105.1	#N/A	1.362944073
TRINITY_DN29108_c0_g1	#N/A	#N/A	#N/A	7.81628063
TRINITY_DN9952_c0_g2	#N/A	#N/A	#N/A	7.996852304
TRINITY_DN13406_c0_g2	#N/A	#N/A	#N/A	8.224359201
TRINITY_DN46507_c0_g1	#N/A	#N/A	#N/A	8.119739085
TRINITY_DN13241_c0_g1	AT1G13680	RWR77191.1	#N/A	1.071626883
TRINITY_DN52903_c0_g1	#N/A	#N/A	#N/A	7.75762286
TRINITY_DN6300_c0_g1	#N/A	XP_010929210.1	#N/A	1.026541744
TRINITY_DN2153_c1_g1	#N/A	#N/A	#N/A	8.260388608
TRINITY_DN17428_c0_g1	#N/A	#N/A	#N/A	7.448885191
TRINITY_DN12585_c0_g1	#N/A	#N/A	#N/A	1.232990857
TRINITY_DN26573_c1_g1	#N/A	#N/A	#N/A	2.283365884
TRINITY_DN14278_c0_g1	#N/A	#N/A	#N/A	1.316418021
TRINITY_DN6998_c0_g2	#N/A	XP_020577573.1	#N/A	1.329382705
TRINITY_DN583_c0_g1	AT4G32940	AXQ06494.1	#N/A	2.164418427
TRINITY_DN1006_c0_g1	AT5G53880	#N/A	#N/A	0.991042675
TRINITY_DN11247_c0_g1	#N/A	#N/A	#N/A	1.941438331
TRINITY_DN1255_c0_g1	AT4G33420	KAG1328230.1	#N/A	1.053166085
TRINITY_DN2131_c0_g1	#N/A	XP_010913679.1	#N/A	1.323806734

TRINITY_DN1997_c0_g1	#N/A	XP_020255626.1	#N/A	0.784773981
TRINITY_DN4624_c0_g1	#N/A	XP_020271182.1	#N/A	1.00649371
TRINITY_DN5496_c0_g1	AT1G48480	XP_022994241.1	#N/A	1.109741372
TRINITY_DN2950_c0_g1	#N/A	#N/A	#N/A	1.695277961
TRINITY_DN4792_c0_g2	AT3G07810	THU53196.1	#N/A	0.967434359
TRINITY_DN9067_c0_g1	#N/A	#N/A	#N/A	2.725176928
TRINITY_DN714_c0_g2	#N/A	XP_010917185.1	#N/A	1.209655214
TRINITY_DN13265_c0_g1	AT3G09280	XP_020081805.1	#N/A	2.80315008
TRINITY_DN12678_c0_g1	AT5G17300	THU54927.1	#N/A	1.606115797
TRINITY_DN15478_c0_g1	AT1G27500	#N/A	#N/A	1.698549081
TRINITY_DN5512_c0_g1	#N/A	KAG1360653.1	#N/A	2.15362678
TRINITY_DN5340_c0_g1	AT1G22530	MQM16770.1	#N/A	1.09152819
TRINITY_DN4450_c0_g1	#N/A	XP_020273450.1	#N/A	0.748032212
TRINITY_DN16396_c0_g1	AT5G11420	#N/A	#N/A	5.710469919
TRINITY_DN15123_c0_g1	AT2G02500	#N/A	#N/A	1.083408309
TRINITY_DN12070_c0_g1	AT3G51000	XP_008775616.2	#N/A	4.477523702
TRINITY_DN15060_c0_g1	AT4G13830	#N/A	#N/A	5.34769118
TRINITY_DN2153_c0_g1	#N/A	XP_038974717.1	#N/A	1.335606962
TRINITY_DN10603_c0_g1	#N/A	#N/A	#N/A	2.194117146
TRINITY_DN11733_c0_g1	AT2G42900	CAG1841029.1	#N/A	1.652014411
TRINITY_DN6500_c0_g1	#N/A	KAG1347111.1	#N/A	1.745211527
TRINITY_DN9402_c0_g1	#N/A	XP_039140383.1	#N/A	1.29395222
TRINITY_DN13336_c0_g1	#N/A	XP_010922298.1	#N/A	1.955374477
TRINITY_DN529_c0_g1	#N/A	KAG1360878.1	#N/A	0.738824227
TRINITY_DN2960_c0_g1	AT1G22050	XP_038973152.1	#N/A	0.90669247
TRINITY_DN6942_c0_g1	#N/A	XP_010933881.1	#N/A	1.253953433
TRINITY_DN7672_c0_g1	#N/A	#N/A	#N/A	2.379158351
TRINITY_DN17748_c0_g1	AT2G22950	#N/A	#N/A	4.955808111
TRINITY_DN400_c0_g1	AT3G13730	KAG1335422.1	#N/A	0.991669887
TRINITY_DN15554_c0_g1	AT3G01930	#N/A	#N/A	2.111783624
TRINITY_DN47_c0_g1	AT3G01510	XP_010925641.1	#N/A	0.985778741
TRINITY_DN8932_c0_g1	#N/A	XP_009414681.1	#N/A	1.80777651
TRINITY_DN12440_c0_g1	#N/A	XP_023773198.1	#N/A	2.249642726
TRINITY_DN2082_c0_g1	#N/A	XP_038973817.1	#N/A	1.171747582
TRINITY_DN7519_c0_g2	#N/A	XP_039117444.1	#N/A	1.32138171
TRINITY_DN2830_c5_g2	#N/A	#N/A	#N/A	2.64072139
TRINITY_DN7551_c0_g1	AT5G52920	XP_020265108.1	#N/A	1.00538998
TRINITY_DN15429_c0_g1	AT4G24040	#N/A	#N/A	1.59915938
TRINITY_DN6381_c0_g1	AT3G50920	XP_008784928.2	#N/A	0.906473291
TRINITY_DN14733_c0_g1	AT1G13130	#N/A	#N/A	1.047956939
TRINITY_DN14293_c0_g1	AT3G14280	#N/A	#N/A	2.007635197
TRINITY_DN16264_c0_g1	#N/A	#N/A	#N/A	4.953790381
TRINITY_DN13925_c0_g1	#N/A	#N/A	#N/A	4.392718995
TRINITY_DN6733_c0_g1	#N/A	XP_010929549.1	#N/A	1.415080877
TRINITY_DN9702_c0_g1	#N/A	#N/A	#N/A	3.198187095
TRINITY_DN2664_c3_g1	AT5G57700	XP_029122021.1	#N/A	0.944065769

TRINITY_DN6363_c0_g1	#N/A	BBE08044.1	#N/A	1.886562672
TRINITY_DN2074_c0_g1	#N/A	#N/A	#N/A	1.933430089
TRINITY_DN9603_c0_g1	#N/A	XP_010919962.1	#N/A	1.546413757
TRINITY_DN11409_c0_g1	AT3G06860	EEE56720.1	#N/A	0.828784995
TRINITY_DN10871_c1_g1	AT2G47440	XP_010921523.1	#N/A	2.128454764
TRINITY_DN9785_c0_g1	AT5G27730	XP_008789968.3	#N/A	1.200260594
TRINITY_DN12840_c1_g1	#N/A	#N/A	#N/A	1.876890817
TRINITY_DN11506_c0_g1	#N/A	XP_008791574.1	#N/A	4.073564481
TRINITY_DN13690_c0_g1	AT1G02640	#N/A	#N/A	1.867548797
TRINITY_DN51949_c0_g1	#N/A	#N/A	#N/A	1.907970296
TRINITY_DN15837_c0_g1	#N/A	#N/A	#N/A	1.993270629
TRINITY_DN7996_c0_g1	#N/A	XP_010917201.1	#N/A	0.936265517
TRINITY_DN12473_c0_g1	AT2G45120	XP_008787063.2	#N/A	2.396501286
TRINITY_DN31_c2_g2	AT4G35630	XP_020690673.1	#N/A	0.707254695
TRINITY_DN886_c0_g1	#N/A	AJG44463.1	#N/A	1.239008548
TRINITY_DN3823_c0_g1	#N/A	KAA8550439.1	#N/A	1.965505585
TRINITY_DN39281_c0_g1	#N/A	#N/A	#N/A	2.907535573
TRINITY_DN36356_c0_g1	#N/A	#N/A	#N/A	5.041495825
TRINITY_DN10641_c0_g3	#N/A	CAD1839397.1	#N/A	3.334835182
TRINITY_DN10131_c0_g1	AT2G24762	#N/A	#N/A	1.676158605
TRINITY_DN3809_c0_g1	#N/A	QYS25849.1	#N/A	0.83696101
TRINITY_DN10641_c0_g2	AT3G07700	XP_010929058.1	#N/A	2.581851737
TRINITY_DN4007_c0_g1	AT4G16155	XP_010914552.1	#N/A	0.743868915
TRINITY_DN8141_c0_g1	AT5G10220	XP_008786903.2	#N/A	1.063074127
TRINITY_DN15749_c0_g3	#N/A	#N/A	#N/A	1.719452949
TRINITY_DN10530_c0_g1	AT5G26830	XP_010913364.1	#N/A	1.887373608
TRINITY_DN1791_c0_g1	AT1G55910	PKA49713.1	#N/A	0.840717033
TRINITY_DN7030_c0_g1	#N/A	XP_010923090.1	#N/A	1.342420848
TRINITY_DN10131_c0_g3	#N/A	#N/A	#N/A	2.17234077
TRINITY_DN2131_c0_g3	#N/A	CAD1840263.1	#N/A	1.893631843
TRINITY_DN3118_c0_g1	AT2G21890	KAH7656019.1	#N/A	1.027408037
TRINITY_DN2710_c0_g1	#N/A	CAD1826492.1	#N/A	1.198964066
TRINITY_DN30324_c0_g3	#N/A	#N/A	#N/A	6.006565545
TRINITY_DN892_c0_g3	#N/A	XP_004296457.1	#N/A	1.212873535
TRINITY_DN5686_c0_g1	#N/A	XP_026660939.1	#N/A	1.136747156
TRINITY_DN16423_c0_g1	#N/A	#N/A	#N/A	1.452466903
TRINITY_DN1815_c0_g1	AT1G67750	XP_009406385.1	#N/A	0.723885259
TRINITY_DN5329_c0_g1	AT1G01610	XP_039116416.1	#N/A	1.179258938
TRINITY_DN40078_c0_g1	AT4G15920	#N/A	#N/A	1.284097272
TRINITY_DN12601_c0_g1	#N/A	XP_038981334.1	#N/A	1.249641089
TRINITY_DN3123_c0_g1	#N/A	KAH7656428.1	#N/A	0.742423664
TRINITY_DN10659_c0_g1	AT2G01170	XP_010924660.1	#N/A	1.176343849
TRINITY_DN1351_c0_g1	AT4G16800	XP_038708112.1	#N/A	0.822840212
TRINITY_DN6643_c0_g1	AT2G45510	XP_010907146.1	#N/A	0.7337908
TRINITY_DN7077_c0_g1	#N/A	KAG9452539.1	#N/A	0.789314524
TRINITY_DN2198_c0_g1	#N/A	XP_010911620.1	#N/A	0.70567257

TRINITY_DN7917_c0_g1	AT5G17220	QEE82349.1	#N/A	1.668194081
TRINITY_DN8666_c0_g1	AT2G25530	XP_010250073.1	#N/A	0.939450724
TRINITY_DN4753_c0_g3	#N/A	OAY81337.1	#N/A	0.823789296
TRINITY_DN15068_c0_g1	AT4G00430	#N/A	#N/A	0.928353602
TRINITY_DN8045_c0_g1	#N/A	XP_008783229.2	#N/A	1.322815099
TRINITY_DN5080_c0_g1	AT5G03650	AJG44456.1	#N/A	1.093244512
TRINITY_DN39414_c0_g1	#N/A	#N/A	#N/A	0.792086744
TRINITY_DN4467_c0_g1	#N/A	XP_009383524.1	#N/A	3.603893446
TRINITY_DN16943_c0_g1	AT1G32450	#N/A	#N/A	3.658699932
TRINITY_DN16893_c0_g1	#N/A	#N/A	#N/A	0.753099134
TRINITY_DN3257_c2_g1	#N/A	#N/A	#N/A	1.341892521
TRINITY_DN5390_c0_g1	#N/A	THU63617.1	#N/A	1.554927877
TRINITY_DN10323_c0_g1	#N/A	XP_010905672.1	#N/A	1.521977988
TRINITY_DN10664_c0_g1	#N/A	#N/A	#N/A	2.100391104
TRINITY_DN13634_c0_g1	AT1G21890	#N/A	#N/A	1.019793174
TRINITY_DN6829_c0_g1	#N/A	XP_010912262.1	#N/A	1.117982665
TRINITY_DN9631_c0_g1	#N/A	RRT62196.1	#N/A	2.26248271
TRINITY_DN10060_c0_g1	AT1G76690	XP_020111995.1	#N/A	0.712196339
TRINITY_DN5425_c0_g1	#N/A	KAG1334902.1	#N/A	1.063214658
TRINITY_DN15788_c0_g1	AT3G57030	#N/A	#N/A	0.820623821
TRINITY_DN9720_c0_g1	#N/A	XP_038971650.1	#N/A	0.959298858
TRINITY_DN11797_c0_g1	AT1G78170	KAG1334577.1	#N/A	1.151647331
TRINITY_DN36652_c0_g1	#N/A	#N/A	#N/A	1.968550555
TRINITY_DN8988_c0_g1	#N/A	KAG1331458.1	-1.390920677	#N/A
TRINITY_DN11814_c0_g2	AT4G28530	AXU39984.1	-7.773352806	-7.773352806
TRINITY_DN38736_c0_g1	#N/A	#N/A	-7.724380507	#N/A
TRINITY_DN216_c0_g1	#N/A	#N/A	-1.352862933	#N/A
TRINITY_DN28207_c0_g1	#N/A	#N/A	-7.686745497	#N/A
TRINITY_DN46436_c0_g1	#N/A	#N/A	-7.611276651	#N/A
TRINITY_DN12534_c0_g1	#N/A	AHG94647.1	-1.575922636	#N/A
TRINITY_DN9141_c0_g1	#N/A	EHA8588615.1	-1.185963278	#N/A
TRINITY_DN13367_c0_g2	#N/A	#N/A	-2.17544882	#N/A
TRINITY_DN2253_c0_g1	#N/A	#N/A	-0.974376406	#N/A
TRINITY_DN3495_c0_g1	#N/A	RWW49383.1	-1.33561807	#N/A
TRINITY_DN3495_c6_g2	#N/A	#N/A	-1.340052737	#N/A
TRINITY_DN1525_c0_g1	AT3G13227	KAF5200381.1	-1.628820932	-1.628820932
TRINITY_DN24124_c0_g1	#N/A	#N/A	-8.131945996	#N/A
TRINITY_DN20492_c0_g1	#N/A	#N/A	-1.520924974	#N/A
TRINITY_DN13304_c0_g1	#N/A	#N/A	-2.049375242	#N/A
TRINITY_DN4725_c0_g2	#N/A	#N/A	-0.812489487	#N/A
TRINITY_DN2643_c0_g2	#N/A	XP_031392979.1	-2.672067742	#N/A
TRINITY_DN17614_c1_g1	#N/A	#N/A	-1.627988024	#N/A
TRINITY_DN44196_c0_g1	#N/A	#N/A	-2.94593619	#N/A
TRINITY_DN10949_c2_g1	AT1G64140	XP_039115949.1	-2.205521386	-2.205521386
TRINITY_DN10717_c0_g1	AT4G00880	KAF3320619.1	-1.188575785	-1.188575785
TRINITY_DN21339_c0_g1	AT5G26330	#N/A	-1.250360966	-1.250360966

TRINITY_DN3427_c0_g1	#N/A	XP_008788382.1	-1.199397391	#N/A
TRINITY_DN5152_c1_g1	#N/A	XP_022868103.1	-1.234499205	#N/A
TRINITY_DN150_c1_g1	#N/A	#N/A	-1.913933428	#N/A
TRINITY_DN9814_c0_g1	AT1G53035	XP_039133657.1	-0.763122652	-0.763122652
TRINITY_DN48511_c0_g1	AT3G10020	#N/A	-1.092858053	-1.092858053
TRINITY_DN2196_c0_g1	#N/A	XP_019704430.1	-0.865995116	#N/A
TRINITY_DN9807_c0_g1	#N/A	XP_001728955.1	-3.058026347	#N/A
TRINITY_DN12444_c0_g1	#N/A	XP_020260298.1	-1.467311413	#N/A
TRINITY_DN17123_c0_g1	AT2G04520	#N/A	-0.761697176	-0.761697176
TRINITY_DN51443_c0_g1	AT2G06520	#N/A	-0.715294493	-0.715294493
TRINITY_DN18894_c0_g1	#N/A	#N/A	-1.829516815	#N/A
TRINITY_DN19594_c0_g1	AT1G67940	#N/A	-1.015055365	-1.015055365
TRINITY_DN11829_c0_g1	#N/A	#N/A	-1.421432955	#N/A
TRINITY_DN9821_c0_g1	AT1G03130	XP_004134141.1	-0.760012095	-0.760012095
TRINITY_DN13087_c0_g1	#N/A	KRX85841.1	-5.746413904	#N/A
TRINITY_DN5962_c0_g2	AT5G53750	KAG1361248.1	-1.332985169	-1.332985169
TRINITY_DN3427_c1_g1	#N/A	XP_010920182.1	-1.223944349	#N/A
TRINITY_DN1180_c0_g1	#N/A	XP_010936409.1	-0.910560029	#N/A
TRINITY_DN1947_c0_g1	#N/A	ERN09395.1	-1.367664226	#N/A
TRINITY_DN1609_c0_g2	AT4G36900	RWW25567.1	-1.549247348	-1.549247348
TRINITY_DN23873_c0_g1	#N/A	#N/A	-3.437181899	#N/A
TRINITY_DN4861_c0_g1	AT1G76410	XP_008812592.1	-1.105393562	-1.105393562
TRINITY_DN1544_c0_g2	AT5G16520	#N/A	-1.556452444	-1.556452444
TRINITY_DN4901_c0_g1	#N/A	#N/A	-1.172448253	#N/A
TRINITY_DN2299_c0_g1	AT5G13330	QGT40631.1	-0.78665751	-0.78665751
TRINITY_DN7919_c0_g1	AT5G24930	AWU68238.1	-0.672562038	-0.672562038
TRINITY_DN5745_c0_g1	AT2G17120	KAG1361052.1	-1.062200369	-1.062200369
TRINITY_DN3739_c0_g1	AT1G22340	XP_008785471.1	-0.775698623	-0.775698623
TRINITY_DN9114_c0_g1	AT1G47200	XP_016568815.1	-0.627766053	-0.627766053
TRINITY_DN5038_c0_g1	AT3G61890	XP_008791625.2	-0.72248837	-0.72248837
TRINITY_DN2929_c1_g1	#N/A	KAF3330450.1	-0.718707882	#N/A
TRINITY_DN23367_c0_g3	AT3G61980	#N/A	-0.799818008	-0.799818008
TRINITY_DN9646_c1_g1	#N/A	XP_027339502.1	-1.998459155	#N/A
TRINITY_DN4060_c0_g2	AT2G22870	#N/A	-2.348501343	-2.348501343
TRINITY_DN1355_c0_g2	#N/A	#N/A	-1.124376112	#N/A
TRINITY_DN2941_c0_g1	#N/A	XP_020250858.1	-0.64768623	#N/A
TRINITY_DN2176_c0_g1	#N/A	KAG1360811.1	-1.335004093	#N/A
TRINITY_DN25043_c0_g1	#N/A	#N/A	-2.558406251	#N/A
TRINITY_DN9141_c0_g2	#N/A	XP_038984919.1	-1.692667825	#N/A
TRINITY_DN1909_c0_g1	AT2G42760	KAH7657748.1	-1.037065194	-1.037065194
TRINITY_DN12992_c0_g1	AT5G56550	KAH0469580.1	-0.823817832	-0.823817832
TRINITY_DN10335_c0_g1	AT2G23290	THU73863.1	-0.992796556	-0.992796556
TRINITY_DN10393_c0_g2	#N/A	XP_029123682.1	-0.684484236	#N/A
TRINITY_DN10835_c0_g1	#N/A	XP_010259038.1	-1.893792147	#N/A
TRINITY_DN9337_c0_g1	#N/A	XP_025373624.1	-3.207591256	#N/A
TRINITY_DN444_c0_g2	#N/A	XP_020703020.2	-2.197752157	#N/A

TRINITY_DN2843_c0_g1	#N/A	XP_044949984.1	-1.475869106	#N/A
TRINITY_DN7854_c0_g1	AT2G22425	CAA2630461.1	-0.62536931	-0.62536931
TRINITY_DN23381_c0_g1	AT4G35750	#N/A	-0.701907763	-0.701907763
TRINITY_DN7925_c1_g1	#N/A	#N/A	-1.868528449	#N/A
TRINITY_DN6743_c0_g1	#N/A	XP_009385637.1	-1.152962495	#N/A
TRINITY_DN9934_c0_g1	#N/A	#N/A	-1.172275892	#N/A
TRINITY_DN7471_c0_g2	AT3G16080	XP_027085236.1	-0.730934535	-0.730934535
TRINITY_DN6304_c0_g1	#N/A	MQM02084.1	-1.144212895	#N/A
TRINITY_DN1531_c0_g1	#N/A	#N/A	-1.957399176	#N/A
TRINITY_DN3186_c0_g1	AT5G24090	KAG1367719.1	-1.536365349	-1.536365349
TRINITY_DN18190_c0_g1	#N/A	#N/A	-1.388562648	#N/A
TRINITY_DN2039_c0_g1	AT3G15353	AAB95221.1	-0.883408865	-0.883408865
TRINITY_DN15165_c0_g1	AT3G06890	#N/A	-0.877920763	-0.877920763
TRINITY_DN43355_c0_g1	AT2G35910	#N/A	-3.132113258	-3.132113258
TRINITY_DN1103_c0_g1	AT2G31980	TKY59925.1	-1.365089058	-1.365089058
TRINITY_DN7343_c0_g2	#N/A	XP_038985274.1	-0.862338573	#N/A
TRINITY_DN17060_c0_g1	#N/A	#N/A	-1.706533113	#N/A
TRINITY_DN5149_c0_g1	#N/A	#N/A	-0.990265627	#N/A
TRINITY_DN1301_c0_g2	AT5G20950	XP_039052548.1	-1.384715894	-1.384715894
TRINITY_DN1546_c0_g1	#N/A	ALO77720.1	-1.123958892	#N/A
TRINITY_DN5700_c0_g1	AT1G03220	XP_010938774.1	-0.923032338	-0.923032338
TRINITY_DN12566_c0_g1	#N/A	XP_008802491.2	-0.77559159	#N/A
TRINITY_DN10233_c0_g1	AT1G70250	KAG1362448.1	-1.275052323	-1.275052323
TRINITY_DN34118_c0_g1	#N/A	#N/A	-2.013685741	#N/A
TRINITY_DN18896_c1_g1	#N/A	#N/A	-1.915434358	#N/A
TRINITY_DN4055_c0_g1	#N/A	XP_010931537.1	-1.643239373	#N/A
TRINITY_DN13251_c0_g1	AT3G52740	KAG1369690.1	-1.355092822	-1.355092822
TRINITY_DN1024_c0_g2	#N/A	#N/A	-2.926303765	#N/A
TRINITY_DN9121_c1_g3	#N/A	XP_042450825.1	-1.088757683	#N/A
TRINITY_DN40559_c0_g1	#N/A	#N/A	-2.73155588	#N/A
TRINITY_DN43290_c0_g1	#N/A	#N/A	-2.185008943	#N/A
TRINITY_DN15416_c0_g1	#N/A	#N/A	-0.917427577	#N/A
TRINITY_DN3427_c0_g2	#N/A	XP_008788382.1	-1.515530344	#N/A
TRINITY_DN19912_c0_g1	#N/A	#N/A	-2.89602992	#N/A
TRINITY_DN8492_c0_g1	AT3G57950	XP_008782877.2	-1.01478216	-1.01478216
TRINITY_DN5121_c0_g1	#N/A	XP_020581044.1	-0.962888873	#N/A
TRINITY_DN21083_c0_g1	AT2G28610	#N/A	-2.150581141	-2.150581141
TRINITY_DN9591_c0_g1	AT1G63850	XP_008807229.2	-0.98273523	-0.98273523
TRINITY_DN10312_c2_g1	AT2G17880	MQM05311.1	-1.003001476	-1.003001476
TRINITY_DN7085_c0_g1	#N/A	RZS22009.1	-2.147326636	#N/A
TRINITY_DN43167_c0_g1	#N/A	#N/A	-1.97309041	#N/A
TRINITY_DN7349_c0_g1	#N/A	#N/A	-1.243430449	#N/A
TRINITY_DN4663_c0_g1	#N/A	XP_039127861.1	-0.782110592	#N/A
TRINITY_DN16588_c0_g1	#N/A	#N/A	-2.720844277	#N/A
TRINITY_DN17882_c1_g1	#N/A	#N/A	-3.387773972	#N/A
TRINITY_DN1380_c0_g1	AT3G54700	CAG1848942.1	-1.145108453	-1.145108453

TRINITY_DN2228_c0_g1	AT5G51550	XP_010934660.1	-1.095235341	-1.095235341
TRINITY_DN982_c0_g1	#N/A	RWW14545.1	-1.040645738	#N/A
TRINITY_DN6783_c1_g1	AT2G41380	XP_010938137.1	-0.683235774	-0.683235774
TRINITY_DN14393_c0_g2	#N/A	#N/A	-1.224107474	#N/A
TRINITY_DN35798_c0_g1	#N/A	#N/A	-2.393356528	#N/A
TRINITY_DN698_c0_g1	#N/A	#N/A	-1.473492698	#N/A
TRINITY_DN7922_c0_g3	AT4G36220	ASV46327.1	-1.197115986	-1.197115986
TRINITY_DN7587_c0_g1	#N/A	XP_010941428.2	-1.02358632	#N/A
TRINITY_DN1965_c0_g1	AT1G71691	XP_020247647.1	-1.526201649	-1.526201649
TRINITY_DN9016_c0_g1	#N/A	XP_039115610.1	-1.420930332	#N/A
TRINITY_DN4000_c0_g1	#N/A	#N/A	-0.877725504	#N/A
TRINITY_DN6130_c0_g1	#N/A	XP_043636005.1	-0.719456283	#N/A
TRINITY_DN143_c0_g1	AT5G62200	KAH7681642.1	-0.618280169	-0.618280169
TRINITY_DN4562_c0_g1	#N/A	XP_010917660.1	-1.539822016	#N/A
TRINITY_DN6591_c0_g1	#N/A	EOS28076.1	-1.819019419	#N/A
TRINITY_DN39729_c0_g1	#N/A	#N/A	-1.589054521	#N/A
TRINITY_DN8171_c0_g1	#N/A	XP_008811805.1	-1.44134016	#N/A
TRINITY_DN16127_c0_g1	AT4G02780	#N/A	-2.939207856	-2.939207856
TRINITY_DN19898_c1_g1	#N/A	#N/A	-4.177520101	#N/A
TRINITY_DN4485_c0_g1	#N/A	XP_019702654.1	-0.684962026	#N/A
TRINITY_DN20923_c0_g2	#N/A	#N/A	-2.271744438	#N/A
TRINITY_DN12532_c0_g1	#N/A	RWR94019.1	-1.729061399	#N/A
TRINITY_DN13169_c0_g1	#N/A	#N/A	-1.338740811	#N/A
TRINITY_DN21494_c0_g1	#N/A	#N/A	-2.898528394	#N/A
TRINITY_DN13884_c1_g1	#N/A	#N/A	8.954579399	#N/A
TRINITY_DN12539_c1_g6	#N/A	#N/A	7.585518119	#N/A
TRINITY_DN42602_c0_g1	#N/A	#N/A	7.738819814	#N/A
TRINITY_DN1771_c0_g1	#N/A	KAH7684777.1	1.133888987	#N/A
TRINITY_DN5721_c0_g2	#N/A	#N/A	1.553480521	#N/A
TRINITY_DN52040_c0_g1	#N/A	#N/A	1.970640145	#N/A
TRINITY_DN352_c0_g2	#N/A	XP_038989947.1	0.822438707	#N/A
TRINITY_DN14988_c1_g1	#N/A	#N/A	1.735034165	#N/A
TRINITY_DN20233_c0_g1	#N/A	#N/A	0.65952093	#N/A
TRINITY_DN22573_c0_g1	#N/A	#N/A	3.961186245	#N/A
TRINITY_DN10106_c0_g1	#N/A	XP_038980310.1	0.778724178	#N/A
TRINITY_DN6596_c0_g1	#N/A	#N/A	0.853450829	#N/A
TRINITY_DN10463_c0_g1	AT4G33650	#N/A	-4.986638154	-5.269619269
TRINITY_DN6118_c0_g1	#N/A	OIF70527.1	-0.939881559	-1.942111103
TRINITY_DN7665_c0_g1	#N/A	#N/A	-0.734103929	-1.372865214
TRINITY_DN7483_c0_g1	#N/A	XP_028555417.1	-1.467876877	-3.085417955
TRINITY_DN356_c0_g2	#N/A	XP_008784634.1	-1.320310509	-2.02467588
TRINITY_DN10511_c0_g1	AT1G60010	XP_010928565.1	-0.893633991	-1.203645504
TRINITY_DN1840_c0_g1	#N/A	XP_008776339.1	-2.078622046	-2.567701074
TRINITY_DN9958_c0_g1	#N/A	PKA50908.1	-1.381334035	-2.326261595
TRINITY_DN52856_c0_g1	#N/A	#N/A	-7.589727288	-7.551035394
TRINITY_DN2028_c0_g1	AT5G45870	AHG94648.1	-1.88870438	-1.845373077

TRINITY_DN16113_c0_g1	#N/A	#N/A	-1.211635174	-1.507984987
TRINITY_DN985_c0_g2	#N/A	THU46822.1	-1.180293456	-1.394447326
TRINITY_DN8927_c0_g1	#N/A	#N/A	-0.909650474	-1.195584574
TRINITY_DN669_c0_g1	#N/A	XP_039135834.1	-1.105752849	-1.086181341
TRINITY_DN11550_c0_g1	#N/A	ANH58193.1	-1.381620694	-2.47001152
TRINITY_DN13257_c0_g2	AT1G10586	XP_008782439.2	-2.199759191	-3.276283645
TRINITY_DN2633_c0_g2	#N/A	XP_008783924.2	-0.695653939	-0.856732071
TRINITY_DN7241_c0_g1	AT3G61060	KAH0448712.1	-0.875613102	-1.100727283
TRINITY_DN1462_c0_g1	#N/A	XP_039131304.1	-1.111248838	-1.397478546
TRINITY_DN4952_c0_g1	AT3G54890	RWR96686.1	-0.756378746	-1.930278877
TRINITY_DN1278_c0_g3	AT4G40060	XP_010942613.1	-1.03033016	-1.137760104
TRINITY_DN14038_c0_g1	AT5G43350	#N/A	-1.967661235	-2.324388077
TRINITY_DN190_c0_g1	#N/A	ASV46331.1	-2.460974949	-4.01011399
TRINITY_DN953_c0_g1	#N/A	XP_010907146.1	-1.11516194	-1.856799884
TRINITY_DN20030_c0_g1	#N/A	#N/A	-1.483775714	-1.953678386
TRINITY_DN3670_c0_g1	#N/A	ART33469.1	-0.948921696	-1.215789402
TRINITY_DN14219_c0_g1	#N/A	#N/A	-1.224878628	-2.535222268
TRINITY_DN4199_c0_g1	AT1G67740	XP_008796872.2	-0.655358672	-1.818168684
TRINITY_DN7179_c0_g1	AT2G42620	XP_010925635.1	-0.784170267	-0.990566227
TRINITY_DN3069_c2_g2	AT4G15800	EHA8591026.1	-1.007860183	-0.843715375
TRINITY_DN8427_c0_g2	#N/A	XP_008797486.2	-0.929198125	-1.159993426
TRINITY_DN13325_c1_g1	#N/A	#N/A	-3.151567663	-3.488588659
TRINITY_DN8956_c0_g1	#N/A	KAG0483062.1	-1.40827832	-1.601323286
TRINITY_DN9961_c0_g1	#N/A	OMO50028.1	-0.828921286	-0.871576284
TRINITY_DN9045_c0_g1	#N/A	XP_020247063.1	-1.539755521	-1.875962655
TRINITY_DN11055_c0_g1	AT4G10750	XP_042391501.1	-0.915731497	-0.948096806
TRINITY_DN12371_c0_g1	AT2G28105	XP_010918616.1	-0.853968957	-0.947401252
TRINITY_DN51615_c0_g1	#N/A	#N/A	-0.604113953	-0.901443739
TRINITY_DN2288_c0_g1	#N/A	#N/A	-1.127830628	-1.408779458
TRINITY_DN3362_c0_g1	AT1G12060	XP_010928141.1	-1.00032409	-1.204963708
TRINITY_DN724_c0_g1	AT1G24620	PKA61755.1	-1.222626927	-1.058795405
TRINITY_DN5555_c0_g1	AT1G51400	KHN45088.1	-1.181260061	-2.698433561
TRINITY_DN1108_c1_g1	AT5G13180	AXU39994.1	-0.810292349	-1.289524191
TRINITY_DN1659_c0_g2	#N/A	THU58070.1	-1.533964614	-1.820445272
TRINITY_DN27402_c0_g1	#N/A	#N/A	-3.257514473	-4.52534623
TRINITY_DN749_c0_g1	#N/A	#N/A	-1.494768186	-2.204807176
TRINITY_DN13411_c0_g1	AT5G18850	XP_008458516.1	-1.107166745	-1.3209134
TRINITY_DN6925_c0_g1	AT1G30380	XP_009406707.1	-0.77379511	-2.409956978
TRINITY_DN5257_c0_g1	#N/A	XP_008792869.2	-0.576086406	-0.649689273
TRINITY_DN9387_c0_g1	AT3G03990	XP_009405896.1	-1.368702126	-0.984964001
TRINITY_DN5401_c0_g1	#N/A	KAG1339283.1	-1.580269775	-1.642152815
TRINITY_DN20041_c0_g1	#N/A	#N/A	-2.100987658	-2.411927298
TRINITY_DN5532_c0_g1	#N/A	KAG1362360.1	-1.038694343	-1.64376395
TRINITY_DN5233_c0_g2	#N/A	XP_008802804.2	-3.381859407	-3.800144325
TRINITY_DN3240_c0_g1	AT2G40330	KAG0481158.1	-2.043364319	-1.838776521
TRINITY_DN3045_c0_g1	#N/A	AAL61539.1	-0.716330927	-0.977347415

TRINITY_DN9750_c0_g1	AT5G05600	XP_008789107.2	-1.602242001	-2.165782151
TRINITY_DN884_c0_g1	AT5G02190	RRT55245.1	-1.671469712	-1.619827699
TRINITY_DN15207_c0_g2	AT2G44310	#N/A	-0.86613167	-0.675668592
TRINITY_DN547_c0_g1	AT3G55550	XP_039129668.1	-1.226636962	-1.169075739
TRINITY_DN3238_c0_g1	#N/A	XP_010928441.1	-1.051472471	-1.480309878
TRINITY_DN6825_c0_g1	#N/A	EHA8589342.1	-1.266099902	-1.339648974
TRINITY_DN6469_c0_g1	AT5G17050	THU57562.1	1.607382556	2.220993287
TRINITY_DN16067_c0_g1	#N/A	#N/A	1.026195878	1.496452531
TRINITY_DN12209_c0_g1	AT3G54720	XP_010908058.1	3.877311414	5.503549049
TRINITY_DN4775_c0_g1	#N/A	KAH7651119.1	0.980950168	1.203891814
TRINITY_DN2583_c0_g1	AT4G36760	XP_010943163.1	0.80410103	1.250769376
TRINITY_DN5476_c0_g1	AT1G02205	EHA8587100.1	1.263610128	1.600794929
TRINITY_DN3968_c0_g1	AT3G06850	XP_010938375.1	0.80252701	1.089354652
TRINITY_DN19508_c0_g2	#N/A	#N/A	1.413127868	1.226170784
TRINITY_DN6590_c0_g1	#N/A	XP_008801227.1	1.120938912	1.629972794
TRINITY_DN7721_c0_g1	AT3G45780	AML76307.1	1.073520908	1.350315084
TRINITY_DN9447_c0_g2	#N/A	BAD13764.1	0.699189695	0.890719296
TRINITY_DN10196_c0_g1	#N/A	#N/A	1.69444295	1.747473828
TRINITY_DN2170_c0_g1	#N/A	XP_038976343.1	0.871046271	0.907499109
TRINITY_DN7572_c0_g1	AT2G29630	XP_042510165.1	1.039098926	1.078508786
TRINITY_DN4333_c0_g1	#N/A	XP_019703623.1	1.162413669	1.019922948
TRINITY_DN3440_c0_g1	AT4G09600	AEX55233.1	-1.232236176	0.134976892
TRINITY_DN16799_c0_g1	#N/A	#N/A	-2.486821458	-0.942067171
TRINITY_DN5908_c0_g1	AT1G72170	XP_008802880.1	-0.707346024	0.162765578
TRINITY_DN17453_c0_g1	#N/A	#N/A	-2.760441194	-0.246766282
TRINITY_DN6771_c0_g1	#N/A	#N/A	-1.859880126	0.045552543
TRINITY_DN373_c0_g2	#N/A	#N/A	-1.914378565	0.40515817
TRINITY_DN3944_c0_g1	#N/A	CDB46314.1	-1.460171722	0.703553673
TRINITY_DN48749_c0_g1	#N/A	#N/A	7.923661665	#N/A
TRINITY_DN33880_c1_g1	#N/A	#N/A	7.814050146	#N/A
TRINITY_DN38749_c0_g1	#N/A	#N/A	7.639181149	#N/A
TRINITY_DN3658_c0_g1	#N/A	#N/A	#N/A	-1.819745077
TRINITY_DN14241_c0_g1	AT5G62730	#N/A	#N/A	-8.468814144
TRINITY_DN5124_c1_g1	#N/A	#N/A	#N/A	-3.904130078
TRINITY_DN5855_c0_g1	#N/A	KAF5180224.1	#N/A	-1.853405197
TRINITY_DN3658_c0_g2	#N/A	#N/A	#N/A	-2.396917386
TRINITY_DN8239_c0_g1	AT1G60000	XP_008789424.1	#N/A	-1.49287615
TRINITY_DN5503_c0_g1	#N/A	RZR71021.1	#N/A	-2.171646281
TRINITY_DN25662_c0_g1	#N/A	#N/A	#N/A	-1.474468287
TRINITY_DN9678_c0_g1	AT1G74470	XP_031105696.1	#N/A	-1.181803605
TRINITY_DN2371_c0_g1	AT1G49740	XP_020111392.1	#N/A	-1.773732387
TRINITY_DN14370_c0_g1	AT1G03630	#N/A	#N/A	-1.904568981
TRINITY_DN12139_c0_g1	#N/A	#N/A	#N/A	-2.664294568
TRINITY_DN1492_c0_g1	AT5G13630	XP_010938532.1	#N/A	-1.563836858
TRINITY_DN2647_c0_g1	#N/A	KAG1354805.1	#N/A	-2.598290716
TRINITY_DN3470_c0_g1	AT2G05790	XP_010928243.1	#N/A	-1.131865167

TRINITY_DN13043_c0_g1	#N/A	XP_008783427.2	#N/A	-0.83150896
TRINITY_DN5575_c2_g1	#N/A	O49080.1	#N/A	-0.853432725
TRINITY_DN9383_c1_g1	AT2G40435	XP_010921091.1	#N/A	-2.283730695
TRINITY_DN4272_c0_g1	AT3G46780	XP_010920513.1	#N/A	-0.913636523
TRINITY_DN7571_c0_g1	AT1G76450	XP_026659702.2	#N/A	-1.22899036
TRINITY_DN10386_c0_g2	#N/A	#N/A	#N/A	9.834882642
TRINITY_DN22014_c1_g1	#N/A	#N/A	#N/A	1.262725401
TRINITY_DN17590_c0_g2	#N/A	#N/A	#N/A	4.08335382
TRINITY_DN1966_c0_g1	#N/A	#N/A	#N/A	2.182893231
TRINITY_DN13132_c1_g2	AT3G29430	KAG1359306.1	#N/A	1.11322946
TRINITY_DN12890_c0_g1	#N/A	KAH7685886.1	#N/A	1.936949898
TRINITY_DN12121_c0_g1	AT5G50260	CCW72556.1	#N/A	2.350455455
TRINITY_DN17226_c0_g1	#N/A	#N/A	#N/A	7.744483131
TRINITY_DN4487_c0_g1	#N/A	XP_020269965.1	#N/A	1.699225444
TRINITY_DN9429_c1_g1	AT1G03870	XP_010916030.1	#N/A	3.912043493
TRINITY_DN5799_c0_g1	#N/A	XP_010912100.1	#N/A	1.069304954
TRINITY_DN11270_c0_g1	AT5G42180	XP_008806161.2	#N/A	4.481403239
TRINITY_DN596_c0_g1	#N/A	XP_020265424.1	#N/A	3.107697098
TRINITY_DN8496_c0_g1	#N/A	UIP35220.1	#N/A	1.49560525
TRINITY_DN15660_c0_g1	AT1G32700	#N/A	#N/A	2.548325118
TRINITY_DN4637_c0_g1	AT3G45010	KDO35820.1	#N/A	2.42265957
TRINITY_DN8529_c0_g2	#N/A	ONK73772.1	#N/A	1.178869278
TRINITY_DN386_c0_g1	AT1G48300	XP_010908889.1	#N/A	1.248300643
TRINITY_DN2152_c0_g1	AT3G09600	XP_020274936.1	#N/A	4.435515353
TRINITY_DN4499_c0_g1	#N/A	KAF3333718.1	#N/A	2.247218391
TRINITY_DN290_c0_g1	#N/A	XP_010935733.1	#N/A	1.156492129
TRINITY_DN11407_c0_g1	#N/A	#N/A	#N/A	9.048045233
TRINITY_DN6702_c0_g1	#N/A	XP_009384464.1	#N/A	1.707958042
TRINITY_DN52584_c0_g1	#N/A	#N/A	#N/A	3.543312697
TRINITY_DN922_c0_g1	#N/A	XP_010935251.1	#N/A	1.039049298
TRINITY_DN210_c0_g1	#N/A	#N/A	#N/A	0.911887476
TRINITY_DN3193_c1_g2	#N/A	XP_023741127.2	#N/A	0.941971311
TRINITY_DN5872_c0_g1	#N/A	PKA60416.1	#N/A	0.922060387
TRINITY_DN11906_c0_g1	AT1G33730	XP_020260547.1	#N/A	0.795243236
TRINITY_DN3006_c0_g1	#N/A	XP_039143725.1	#N/A	0.895679513
TRINITY_DN3823_c0_g2	#N/A	KAH7677790.1	#N/A	6.234851291
TRINITY_DN7609_c0_g1	#N/A	#N/A	#N/A	1.04411234
TRINITY_DN443_c0_g1	#N/A	#N/A	#N/A	1.262476768
TRINITY_DN12121_c0_g2	#N/A	CCW72556.1	#N/A	2.658395378
TRINITY_DN9105_c0_g2	#N/A	XP_042450825.1	#N/A	2.405538774
TRINITY_DN2046_c0_g2	#N/A	#N/A	#N/A	3.352767978
TRINITY_DN15198_c0_g1	AT5G02890	#N/A	#N/A	2.094961003
TRINITY_DN2514_c0_g1	#N/A	KAG1364087.1	#N/A	0.920315269
TRINITY_DN13552_c0_g1	AT3G16330	#N/A	#N/A	2.561918173
TRINITY_DN977_c0_g1	#N/A	XP_008783343.2	#N/A	2.701052735
TRINITY_DN22640_c0_g1	AT5G67400	#N/A	#N/A	3.097352814

TRINITY_DN14340_c0_g1	AT5G20885	#N/A	#N/A	2.545826298
TRINITY_DN30449_c0_g2	#N/A	#N/A	#N/A	1.761597218
TRINITY_DN18077_c1_g2	#N/A	#N/A	#N/A	3.196914112
TRINITY_DN14462_c0_g1	AT5G66460	#N/A	#N/A	5.008413459
TRINITY_DN9975_c0_g1	#N/A	#N/A	#N/A	3.813026077
TRINITY_DN1297_c0_g1	AT3G48340	CCW72556.1	#N/A	1.792926831
TRINITY_DN3893_c0_g1	#N/A	XP_010912092.1	#N/A	2.759092742
TRINITY_DN2281_c0_g2	AT3G08640	KAH0454886.1	#N/A	0.866219178
TRINITY_DN6446_c0_g1	#N/A	XP_010938322.2	#N/A	1.457271493
TRINITY_DN45664_c0_g1	#N/A	#N/A	#N/A	6.012764994
TRINITY_DN51888_c0_g1	#N/A	#N/A	#N/A	6.059314914
TRINITY_DN12964_c0_g1	AT5G54570	XP_010910029.1	#N/A	1.687357257
TRINITY_DN14557_c0_g2	#N/A	#N/A	#N/A	4.194821899
TRINITY_DN7855_c0_g1	AT4G38620	BAU68654.1	#N/A	1.707636233
TRINITY_DN3118_c0_g2	#N/A	#N/A	#N/A	2.379668241
TRINITY_DN3742_c0_g1	#N/A	KAG1361207.1	-1.417632866	-2.975415112
TRINITY_DN10833_c0_g1	AT5G54270	XP_010905042.1	-0.848915657	-2.627254284
TRINITY_DN4065_c0_g1	AT1G08380	XP_020253235.1	-0.776451771	-2.455975808
TRINITY_DN977_c0_g2	AT1G77410	ONK73113.1	2.013156981	3.998962744

GO term enrichment of DEGs significantly identified between LFO/SRC and SSO/SRC comparisons

GO aspect	GO term	Pathway	Enrichment FDR	nGenes	Pathway Genes	Fold Enrichment	Genes
BP	GO:0009768	Photosynthesis, light harvesting in photosystem I	2.95E-07	9	23	16.96092	AT1G08380 AT1G15820 AT1G29930 AT1G61520 AT3G54890 AT3G61470 AT4G10340 AT5G01530 AT5G54270
BP	GO:0009765	Photosynthesis, light harvesting	3.49E-06	10	36	11.16768	AT1G08380 AT1G15820 AT1G29930 AT1G61520 AT3G54890 AT3G61470 AT4G02530 AT4G10340 AT5G01530 AT5G54270
BP	GO:0051346	Neg. reg. of hydrolase activity	0.000422	8	73	8.61507	AT1G17860 AT1G72060 AT2G31980 AT2G38310 AT2G40330

							AT3G61980 AT5G45870 AT5G53160
BP	GO:0010025	Wax biosynthetic proc.	0.004326	6	29	8.61507	AT1G02205 AT1G68530 AT2G47240 AT3G47600 AT5G02890 AT5G57800
BP	GO:1901568	Fatty acid derivative metabolic proc.	0.0019	7	39	8.442768	AT1G02205 AT1G68530 AT2G47240 AT3G44540 AT3G47600 AT5G02890 AT5G57800
BP	GO:0010025	Wax metabolic proc.	0.004565	6	30	8.223476	AT1G02205 AT1G68530 AT2G47240 AT3G47600 AT5G02890 AT5G57800
BP	GO:1901570	Fatty acid derivative biosynthetic proc.	0.004565	6	31	8.223476	AT1G02205 AT1G68530 AT2G47240 AT3G47600 AT5G02890 AT5G57800
BP	GO:0017003	Protein-chromophore linkage	0.000153	10	58	7.354328	AT1G15820 AT1G29930 AT1G61520 AT3G45780 AT3G54890 AT3G61470 AT4G10340 AT5G01530 AT5G24850 AT5G54270
BP	GO:0044092	Neg. reg. of molecular function	4.96E-05	15	272	5.139672	AT1G17860 AT1G28280 AT1G62770 AT1G72060 AT2G31980 AT2G38310 AT2G40330 AT3G45780 AT3G61980 AT5G06860 AT5G45870 AT5G47390 AT5G53160

							AT5G62350 AT5G62360
BP	GO:0043086	Neg. reg. of catalytic activity	0.000264	13	259	5.090723	AT1G17860 AT1G62770 AT1G72060 AT2G31980 AT2G38310 AT2G40330 AT3G61980 AT5G06860 AT5G45870 AT5G47390 AT5G53160 AT5G62350 AT5G62360
BP	GO:0019684	Photosynthesis, light reaction	8.14E-06	18	144	4.889634	AT1G06680 AT1G08380 AT1G15820 AT1G29930 AT1G54500 AT1G55370 AT1G61520 AT1G67740 AT3G50820 AT3G54890 AT3G61470 AT4G02530 AT4G09650 AT4G10340 AT4G19100 AT4G33520 AT5G01530 AT5G54270
BP	GO:0015979	Photosynthesis	9.92E-10	31	275	4.650423	AT1G03130 AT1G03630 AT1G06680 AT1G08380 AT1G15820 AT1G29930 AT1G30380 AT1G31330 AT1G44575 AT1G54500 AT1G55370 AT1G61520 AT1G67740 AT1G74470 AT1G75540 AT1G76450 AT2G06520 AT2G20260

							AT3G50820 AT3G54890 AT3G61470 AT4G02530 AT4G09650 AT4G10340 AT4G12800 AT4G19100 AT4G33520 AT5G01530 AT5G13630 AT5G54270 AT5G64040
BP	GO:0080 167	Response to karrikin	0.00456 5	11	127	4.19848 3	AT1G44575 AT2G23910 AT2G46170 AT2G47730 AT3G11600 AT3G47600 AT3G52740 AT5G05600 AT5G17050 AT5G25460 AT5G51550
BP	GO:0009 698	Phenylpropanoid metabolic proc.	0.00547 1	11	147	4.04488	AT1G80440 AT2G21890 AT3G44540 AT4G36220 AT4G38620 AT4G39230 AT5G05340 AT5G17050 AT5G41040 AT5G48930 AT5G54160
BP	GO:0009 414	Response to water deprivation	0.00418 4	22	402	2.62197 8	AT1G02205 AT1G30270 AT1G32640 AT1G45249 AT1G48130 AT1G52690 AT2G18960 AT2G21660 AT2G33590 AT2G41230 AT2G41430 AT2G42620 AT3G47600 AT3G61890 AT4G00430 AT4G33950

							AT4G39730 AT5G06530 AT5G10220 AT5G13330 AT5G24090 AT5G52300
BP	GO:0006091	Generation of precursor metabolites and energy	0.004184	26	517	2.382892	AT1G06680 AT1G08380 AT1G15820 AT1G29930 AT1G54500 AT1G55370 AT1G61520 AT1G67740 AT2G01140 AT2G02850 AT3G10020 AT3G20570 AT3G50820 AT3G54890 AT3G61470 AT4G01100 AT4G02530 AT4G09650 AT4G10340 AT4G19100 AT4G33520 AT5G01530 AT5G03650 AT5G26330 AT5G52920 AT5G54270
BP	GO:0009416	Response to light stimulus	0.002006	35	746	2.167035	AT1G15820 AT1G29930 AT1G42550 AT1G44575 AT1G51400 AT1G61520 AT1G67740 AT1G68530 AT1G75540 AT2G26640 AT2G41430 AT2G42620 AT3G06850 AT3G08640 AT3G09600 AT3G43810 AT3G45780 AT3G48100 AT3G50820

							AT3G52740 AT3G54720 AT3G54890 AT3G61470 AT4G10340 AT4G15920 AT4G33950 AT4G36220 AT4G38620 AT4G40060 AT5G01530 AT5G03650 AT5G10220 AT5G24090 AT5G47390 AT5G54270
BP	GO:0009314	Response to radiation	0.004184	35	770	2.08155	AT1G15820 AT1G29930 AT1G42550 AT1G44575 AT1G51400 AT1G61520 AT1G67740 AT1G68530 AT1G75540 AT2G26640 AT2G41430 AT2G42620 AT3G06850 AT3G08640 AT3G09600 AT3G43810 AT3G45780 AT3G48100 AT3G50820 AT3G52740 AT3G54720 AT3G54890 AT3G61470 AT4G10340 AT4G15920 AT4G33950 AT4G36220 AT4G38620 AT4G40060 AT5G01530 AT5G03650 AT5G10220 AT5G24090 AT5G47390 AT5G54270

BP	GO:1901700	Response to oxygen-containing compound	0.004565	56	1692	1.703889	AT1G02205 AT1G30270 AT1G32450 AT1G32540 AT1G32640 AT1G42550 AT1G45249 AT1G48130 AT1G51400 AT1G52690 AT1G61120 AT1G71960 AT2G18960 AT2G21660 AT2G29630 AT2G33590 AT2G38310 AT2G40330 AT2G41230 AT2G41430 AT2G42620 AT3G03990 AT3G04290 AT3G06850 AT3G07700 AT3G08640 AT3G13960 AT3G15730 AT3G21220 AT3G23240 AT3G47600 AT3G61460 AT3G61890 AT4G00430 AT4G02780 AT4G09600 AT4G15920 AT4G23060 AT4G24210 AT4G32940 AT4G33950 AT4G39730 AT5G03650 AT5G05600 AT5G06530 AT5G10220 AT5G13180 AT5G13330 AT5G24090 AT5G27420 AT5G42650
----	------------	--	----------	----	------	----------	---

							AT5G45870 AT5G47390 AT5G52300 AT5G53160 AT5G54270
CC	GO:0009538	Photosystem I reaction center	7.63E-05	4	8	24.1222	AT1G03130 AT1G31330 AT2G20260 AT4G12800
CC	GO:0009503	Thylakoid light-harvesting complex	0.003233	3	6	18.09165	AT1G44575 AT4G10340 AT5G54270
CC	GO:0009517	PSII associated light-harvesting complex II	0.003233	3	6	18.09165	AT1G44575 AT4G10340 AT5G54270
CC	GO:0009522	Photosystem I	2.52E-13	15	43	15.59625	AT1G03130 AT1G08380 AT1G15820 AT1G29930 AT1G30380 AT1G31330 AT1G61520 AT2G20260 AT3G54890 AT3G61470 AT4G10340 AT4G12800 AT5G01530 AT5G54270 AT5G64040
CC	GO:0009521	Photosystem	1.55E-14	22	95	10.05091	AT1G03130 AT1G06680 AT1G08380 AT1G15820 AT1G29930 AT1G30380 AT1G31330 AT1G44575 AT1G61520 AT1G67740 AT1G76450 AT2G06520 AT2G20260 AT3G50820 AT3G54890 AT3G61470 AT4G10340 AT4G12800 AT4G19100 AT5G01530

							AT5G54270 AT5G64040
CC	GO:0009523	Photosystem II	4.89E-09	15	76	8.533796	AT1G06680 AT1G15820 AT1G29930 AT1G44575 AT1G61520 AT1G67740 AT1G76450 AT2G06520 AT3G50820 AT3G54890 AT3G61470 AT4G10340 AT4G19100 AT5G01530 AT5G54270
CC	GO:0010287	Plastoglobule	1.46E-09	17	78	7.886102	AT1G15820 AT1G29930 AT1G31330 AT1G61520 AT2G01140 AT2G20260 AT3G07700 AT3G50820 AT3G54890 AT4G09650 AT4G10340 AT4G12800 AT4G39730 AT5G01530 AT5G17230 AT5G42650 AT5G54270
CC	GO:0009505	Plant-type cell wall	7.26E-06	17	237	4.344039	AT1G02640 AT1G78830 AT3G57030 AT4G15800 AT4G19420 AT4G33420 AT5G05340 AT5G06860 AT5G08380 AT5G11420 AT5G20950 AT5G23870 AT5G25460 AT5G42180 AT5G50260 AT5G51550 AT5G64260

CC	GO:0099503	Secretory vesicle	0.000921	12	173	3.730236	AT1G03220 AT1G03870 AT1G17860 AT1G21680 AT1G76160 AT1G78830 AT2G02850 AT3G04720 AT4G39730 AT5G06860 AT5G08380 AT5G20630
CC	GO:0009535	Chloroplast thylakoid membrane	1.52E-07	35	445	3.006684	AT1G03130 AT1G03630 AT1G06680 AT1G08380 AT1G15820 AT1G29930 AT1G30380 AT1G31330 AT1G44575 AT1G51400 AT1G54500 AT1G55370 AT1G60000 AT1G61520 AT1G67740 AT1G74470 AT1G76450 AT2G06520 AT2G20260 AT3G07700 AT3G46780 AT3G50820 AT3G54890 AT3G61470 AT4G02530 AT4G09650 AT4G10340 AT4G12800 AT4G19100 AT4G25080 AT4G39730 AT5G01530 AT5G42650 AT5G54270 AT5G64040
CC	GO:0055035	Plastid thylakoid membrane	1.52E-07	35	446	2.998142	AT1G03130 AT1G03630 AT1G06680 AT1G08380

							AT1G15820 AT1G29930 AT1G30380 AT1G31330 AT1G44575 AT1G51400 AT1G54500 AT1G55370 AT1G60000 AT1G61520 AT1G67740 AT1G74470 AT1G76450 AT2G06520 AT2G20260 AT3G07700 AT3G46780 AT3G50820 AT3G54890 AT3G61470 AT4G02530 AT4G09650 AT4G10340 AT4G12800 AT4G19100 AT4G25080 AT4G39730 AT5G01530 AT5G42650 AT5G54270 AT5G64040
CC	GO:0034357	Photosynthetic membrane	1.52E-07	36	466	2.957762	AT1G03130 AT1G03630 AT1G06680 AT1G08380 AT1G15820 AT1G29930 AT1G30380 AT1G31330 AT1G44575 AT1G51400 AT1G54500 AT1G55370 AT1G60000 AT1G61520 AT1G67740 AT1G74470 AT1G76450 AT2G06520 AT2G20260 AT2G41430

							AT3G07700 AT3G46780 AT3G50820 AT3G54890 AT3G61470 AT4G02530 AT4G09650 AT4G10340 AT4G12800 AT4G19100 AT4G25080 AT4G39730 AT5G01530 AT5G42650 AT5G54270 AT5G64040
CC	GO:0042651	Thylakoid membrane	1.52E-07	36	466	2.957762	AT1G03130 AT1G03630 AT1G06680 AT1G08380 AT1G15820 AT1G29930 AT1G30380 AT1G31330 AT1G44575 AT1G51400 AT1G54500 AT1G55370 AT1G60000 AT1G61520 AT1G67740 AT1G74470 AT1G76450 AT2G06520 AT2G20260 AT2G41430 AT3G07700 AT3G46780 AT3G50820 AT3G54890 AT3G61470 AT4G02530 AT4G09650 AT4G10340 AT4G12800 AT4G19100 AT4G25080 AT4G39730 AT5G01530 AT5G42650

							AT5G54270 AT5G64040
CC	GO:0009579	Thylakoid	1.11E-05	39	622	2.333248	AT1G03130 AT1G03630 AT1G06680 AT1G08380 AT1G15820 AT1G29930 AT1G30380 AT1G31330 AT1G44575 AT1G51400 AT1G54500 AT1G55370 AT1G60000 AT1G61520 AT1G67740 AT1G74470 AT1G76450 AT2G01140 AT2G06520 AT2G20260 AT2G35370 AT2G41430 AT2G47730 AT3G07700 AT3G46780 AT3G50820 AT3G54890 AT3G61470 AT4G02530 AT4G09650 AT4G10340 AT4G12800 AT4G19100 AT4G25080 AT4G39730 AT5G01530 AT5G42650 AT5G54270 AT5G64040
CC	GO:0030312	External encapsulating structure	0.000323	29	813	2.301131	AT1G02460 AT1G02640 AT1G03220 AT1G17860 AT1G73370 AT1G76160 AT1G77410 AT1G78830 AT2G02850 AT2G20870

							AT2G40610 AT3G06860 AT3G57030 AT4G15800 AT4G19420 AT4G33420 AT5G05340 AT5G06860 AT5G08380 AT5G11420 AT5G20630 AT5G20950 AT5G23870 AT5G25460 AT5G26830 AT5G42180 AT5G50260 AT5G51550 AT5G64260
CC	GO:0005618	Cell wall	0.000617	28	793	2.251405	AT1G02460 AT1G02640 AT1G03220 AT1G17860 AT1G73370 AT1G76160 AT1G77410 AT1G78830 AT2G20870 AT2G40610 AT3G06860 AT3G57030 AT4G15800 AT4G19420 AT4G33420 AT5G05340 AT5G06860 AT5G08380 AT5G11420 AT5G20630 AT5G20950 AT5G23870 AT5G25460 AT5G26830 AT5G42180 AT5G50260 AT5G51550 AT5G64260
CC	GO:0042170	Plastid membrane	2.56E-05	40	701	2.221197	AT1G03130 AT1G03630 AT1G06680 AT1G08380

							AT1G15820 AT1G29930 AT1G30380 AT1G31330 AT1G44575 AT1G51400 AT1G54500 AT1G55370 AT1G60000 AT1G61520 AT1G67740 AT1G74470 AT1G76450 AT2G06520 AT2G20260 AT3G07700 AT3G08640 AT3G46780 AT3G50820 AT3G50920 AT3G54890 AT3G61470 AT4G02530 AT4G09650 AT4G10340 AT4G12800 AT4G19100 AT4G25080 AT4G33520 AT4G39730 AT5G01530 AT5G13630 AT5G17230 AT5G42650 AT5G54270 AT5G64040
CC	GO:0005576	Extracellular region	8.29E-06	47	1923	2.16694	AT1G02640 AT1G03130 AT1G03220 AT1G03630 AT1G03870 AT1G06680 AT1G08380 AT1G13020 AT1G13130 AT1G15000 AT1G17860 AT1G62770 AT1G71691 AT1G73370 AT1G76160

							AT1G77410 AT1G78830 AT2G02850 AT2G20870 AT2G27360 AT2G31980 AT2G40610 AT2G42840 AT3G04290 AT3G24100 AT3G45010 AT3G48340 AT4G09600 AT4G15800 AT4G19420 AT4G30320 AT4G33420 AT5G05340 AT5G06860 AT5G08380 AT5G20630 AT5G20950 AT5G23870 AT5G24090 AT5G42180 AT5G45650 AT5G50260 AT5G51550 AT5G62200 AT5G64260 AT5G66460 AT5G67400
MF	GO:0050734	Hydroxycinnamoyltransferase activity	0.030177	2	3	30.15274	AT5G41040 AT5G48930
MF	GO:0004867	Serine-type endopeptidase inhibitor activity	0.023767	3	28	15.07637	AT1G17860 AT1G72060 AT3G61980
MF	GO:0004866	Endopeptidase inhibitor activity	0.009307	4	42	13.40122	AT1G17860 AT1G72060 AT2G31980 AT3G61980
MF	GO:0030414	Peptidase inhibitor activity	0.011749	4	43	12.0611	AT1G17860 AT1G72060 AT2G31980 AT3G61980
MF	GO:0061135	Endopeptidase regulator activity	0.011749	4	43	12.0611	AT1G17860 AT1G72060 AT2G31980 AT3G61980
MF	GO:0019840	Isoprenoid binding	0.004004	5	23	11.59721	AT1G44575 AT2G38310

							AT2G40330 AT5G45870 AT5G53160
MF	GO:0019904	Protein domain specific binding	2.38E-12	18	69	11.30728	AT1G03130 AT1G06680 AT1G15820 AT1G29930 AT1G31330 AT1G44575 AT1G51400 AT1G61520 AT2G06520 AT2G20260 AT2G29630 AT3G54890 AT3G61470 AT4G10340 AT4G12800 AT5G01530 AT5G54270 AT5G64040
MF	GO:0010427	Abscisic acid binding	0.016183	4	19	10.96463	AT2G38310 AT2G40330 AT5G45870 AT5G53160
MF	GO:0016168	Chlorophyll binding	1.39E-05	9	34	10.43749	AT1G15820 AT1G29930 AT1G44575 AT1G61520 AT3G54890 AT3G61470 AT4G10340 AT5G01530 AT5G54270
MF	GO:0061134	Peptidase regulator activity	0.019701	4	45	10.05091	AT1G17860 AT1G72060 AT2G31980 AT3G61980
MF	GO:0033293	Monocarboxylic acid binding	0.000803	7	44	9.176922	AT2G26310 AT2G38310 AT2G40330 AT3G06850 AT4G36760 AT5G45870 AT5G53160
MF	GO:0004864	Protein phosphatase inhibitor activity	0.031702	4	23	8.040732	AT2G38310 AT2G40330 AT5G45870 AT5G53160
MF	GO:0031406	Carboxylic acid binding	0.030177	7	86	4.307535	AT2G26310 AT2G38310

							AT2G40330 AT3G06850 AT4G36760 AT5G45870 AT5G53160
MF	GO:0004601	Peroxidase activity	0.029808	8	145	3.890677	AT1G48130 AT1G65820 AT2G47730 AT4G33420 AT4G39730 AT5G05340 AT5G42180 AT5G67400
MF	GO:0046906	Tetrapyrrole binding	5.39E-06	24	432	3.769093	AT1G15820 AT1G29930 AT1G33730 AT1G44575 AT1G61520 AT2G27690 AT2G45510 AT2G46950 AT3G13730 AT3G26330 AT3G30180 AT3G54890 AT3G61470 AT4G10340 AT4G33420 AT4G36220 AT4G37320 AT4G39730 AT5G01530 AT5G05340 AT5G42180 AT5G42650 AT5G54270 AT5G67400
MF	GO:0016684	Oxidoreductase activity, acting on peroxide as acceptor	0.036106	8	151	3.654878	AT1G48130 AT1G65820 AT2G47730 AT4G33420 AT4G39730 AT5G05340 AT5G42180 AT5G67400
MF	GO:0060089	Molecular transducer activity	0.006308	13	236	3.531403	AT1G09970 AT2G38310 AT2G40330 AT2G41820 AT3G21220 AT3G45780

							AT3G48100 AT3G55550 AT3G57040 AT5G24850 AT5G38280 AT5G45870 AT5G53160
MF	GO:0038023	Signaling receptor activity	0.021083	11	207	3.251767	AT1G09970 AT2G38310 AT2G40330 AT2G41820 AT3G21220 AT3G45780 AT3G55550 AT5G24850 AT5G38280 AT5G45870 AT5G53160
MF	GO:0020037	Heme binding	0.016408	15	396	2.757873	AT1G33730 AT2G27690 AT2G45510 AT2G46950 AT3G13730 AT3G26330 AT3G30180 AT4G33420 AT4G36220 AT4G37320 AT4G39730 AT5G05340 AT5G42180 AT5G42650 AT5G67400
MF	GO:0005506	Iron ion binding	0.024133	14	355	2.68878	AT1G02205 AT1G33730 AT1G54500 AT2G27690 AT2G34770 AT2G45510 AT2G46950 AT3G13730 AT3G26330 AT3G30180 AT4G36220 AT4G37320 AT5G42650 AT5G57800

KEGG pathway analysis of DEGs significantly identified between LFO/SRC and SSO/SRC comparisons

KO pathway	Pathway	Enrichment FDR	nGenes	Pathway Genes	Fold Enrichment	Genes
ko00196	Photosynthesis	1.13E-05	11	76	7.370671	AT1G06680 AT1G08380 AT1G30380 AT1G31330 AT1G44575 AT1G67740 AT2G20260 AT3G50820 AT4G09650 AT4G12800 AT5G64040
ko00940	Phenylpropanoid biosynthesis	0.000118	11	174	5.182503	AT1G48130 AT2G21890 AT2G39420 AT4G33420 AT4G36220 AT5G05340 AT5G20950 AT5G42180 AT5G48930 AT5G54160 AT5G54570
ko04010	MAPK signaling pathway	0.000582	10	136	4.711366	AT1G32640 AT2G38310 AT2G40330 AT3G21220 AT3G23240 AT3G43810 AT4G33520 AT4G33950 AT5G45870 AT5G53160
ko04075	Plant hormone signal transduction	0.000118	15	286	3.932967	AT1G32640 AT1G45249 AT1G51950 AT1G56150 AT2G38310 AT2G40330 AT3G21220 AT3G23240 AT3G48100 AT3G57040 AT4G00880 AT4G24210 AT4G33950 AT5G45870 AT5G53160
ko01110	Biosynthesis of secondary metabolites	0.003128	43	1243	1.7357	AT1G01610 AT1G02205 AT1G03630 AT1G22340 AT1G48130 AT1G61120 AT1G68530 AT1G73370 AT1G74470 AT1G76690 AT2G01140 AT2G02500 AT2G21890 AT2G26640 AT2G35370 AT2G39420 AT3G06850 AT3G06860 AT3G13730 AT3G15730 AT3G29430 AT3G30180 AT3G61440 AT4G02780 AT4G16155 AT4G24040 AT4G25080 AT4G33420 AT4G35630 AT4G36220 AT5G03650 AT5G05340 AT5G13630 AT5G17050 AT5G17230 AT5G20950 AT5G42180 AT5G42650 AT5G48930 AT5G52920 AT5G54160 AT5G54570 AT5G67400

Appendix 4.2 – ‘Required to open’ group

Read	A. thaliana gene	Viridiplantae gene	Gene description	Log2FC (SSO/SRC)
TRINITY_DN13884_c1_g1	#N/A	#N/A		8.954579
TRINITY_DN42602_c0_g1	#N/A	#N/A		7.73882
TRINITY_DN12539_c1_g6	#N/A	#N/A		7.585518
TRINITY_DN22573_c0_g1	#N/A	#N/A		3.961186
TRINITY_DN52040_c0_g1	#N/A	#N/A		1.97064
TRINITY_DN14988_c1_g1	#N/A	#N/A		1.735034
TRINITY_DN5721_c0_g2	#N/A	#N/A		1.553481
TRINITY_DN1771_c0_g1	AT2G41230	KAH7684777.1	ORGAN SIZE-like protein	1.133889
TRINITY_DN6596_c0_g1	#N/A	#N/A		0.853451
TRINITY_DN352_c0_g2	AT1G33470	XP_038989947.1	RNA-binding (RRM/RBD/RNP motifs) family protein	0.822439
TRINITY_DN10106_c0_g1	AT2G47240	XP_038980310.1	AMP-dependent synthetase and ligase family protein (LACS1)	0.778724
TRINITY_DN20233_c0_g1	#N/A	#N/A		0.659521
TRINITY_DN143_c0_g1	AT5G62200	KAH7681642.1	Embryo-specific protein 3, (ATS3)	-0.61828
TRINITY_DN7854_c0_g1	AT2G22425	CAA2630461.1	Microsomal signal peptidase 12 kDa subunit (SPC12)	-0.62537
TRINITY_DN9114_c0_g1	AT1G47200	XP_016568815.1	WPP domain protein 2	-0.62777
TRINITY_DN2941_c0_g1	AT1G14870	XP_020250858.1	PLANT CADMIUM RESISTANCE 2	-0.64769
TRINITY_DN7919_c0_g1	AT5G24930	AWU68238.1	zinc finger CONSTANS-like protein	-0.67256
TRINITY_DN6783_c1_g1	AT2G41380	XP_010938137.1	S-adenosyl-L-methionine-dependent methyltransferases superfamily protein	-0.68324
TRINITY_DN10393_c0_g2	AT4G14540	XP_029123682.1	nuclear factor Y, subunit B3	-0.68448
TRINITY_DN4485_c0_g1	AT5G25280	XP_019702654.1	serine-rich protein-like protein	-0.68496
TRINITY_DN23381_c0_g1	AT4G35750	#N/A	SEC14 cytosolic factor family protein / phosphoglyceride transfer family protein	-0.70191
TRINITY_DN51443_c0_g1	AT2G06520	#N/A	PSBX photosystem II subunit X	-0.71529
TRINITY_DN2929_c1_g1	AT2G41430	KAF3330450.1	dehydration-induced protein (ERD15)	-0.71871

TRINITY_DN6130_c0_g1	AT1G05870	XP_043636005.1	hypothetical protein (DUF1685)	-0.71946
TRINITY_DN5038_c0_g1	AT3G61890	XP_008791625.2	homeobox 12	-0.72249
TRINITY_DN7471_c0_g2	AT3G16080	XP_027085236.1	Zinc-binding ribosomal protein family protein	-0.73093
TRINITY_DN9821_c0_g1	AT1G03130	XP_004134141.1	PSAD-2 (AT1G03130) photosystem I subunit D-2	-0.76001
TRINITY_DN17123_c0_g1	AT2G04520	#N/A	Nucleic acid-binding, OB-fold-like protein	-0.7617
TRINITY_DN9814_c0_g1	AT1G53035	XP_039133657.1	uncharacterized protein	-0.76312
TRINITY_DN12566_c0_g1	AT4G19100	XP_008802491.2	PAM68-like protein (DUF3464)	-0.77559
TRINITY_DN3739_c0_g1	AT1G22340	XP_008785471.1	UDP-glucosyl transferase 85A7	-0.7757
TRINITY_DN4663_c0_g1	AT1G77660	XP_039127861.1	Histone H3 K4-specific methyltransferase SET7/9 family protein	-0.78211
TRINITY_DN2299_c0_g1	AT5G13330	QGT40631.1	Rap2.6L	-0.78666
TRINITY_DN23367_c0_g3	AT3G61980	#N/A	serine protease inhibitor, Kazal-type family protein	-0.79982
TRINITY_DN4725_c0_g2	#N/A	#N/A		-0.81249
TRINITY_DN12992_c0_g1	AT5G56550	KAH0469580.1	oxidative stress 3	-0.82382
TRINITY_DN7343_c0_g2	AT5G37840	XP_038985274.1	plastid movement impaired protein	-0.86234
TRINITY_DN2196_c0_g1	AT1G80440	XP_019704430.1	Galactose oxidase/kelch repeat superfamily protein	-0.866
TRINITY_DN4000_c0_g1	#N/A	#N/A		-0.87773
TRINITY_DN15165_c0_g1	AT3G06890	#N/A		-0.87792
TRINITY_DN2039_c0_g1	AT3G15353	AAB95221.1	metallothionein 3	-0.88341
TRINITY_DN1180_c0_g1	AT1G51090	XP_010936409.1	Heavy metal transport/detoxification superfamily protein	-0.91056
TRINITY_DN15416_c0_g1	#N/A	#N/A		-0.91743
TRINITY_DN5700_c0_g1	AT1G03220	XP_010938774.1	Eukaryotic aspartyl protease family protein	-0.92303
TRINITY_DN5121_c0_g1	AT3G61440	XP_020581044.1	cysteine synthase C1	-0.96289
TRINITY_DN2253_c0_g1	#N/A	#N/A		-0.97438
TRINITY_DN9591_c0_g1	AT1G63850	XP_008807229.2	BTB/POZ domain-containing protein	-0.98274
TRINITY_DN5149_c0_g1	#N/A	#N/A		-0.99027
TRINITY_DN10335_c0_g1	AT2G23290	THU73863.1	myb domain protein 70	-0.9928

TRINITY_DN10312_c2_g1	AT2G17880	MQM05311.1	Chaperone DnaJ-domain superfamily protein	-1.003
TRINITY_DN8492_c0_g1	AT3G57950	XP_008782877.2	cotton fiber protein	-1.01478
TRINITY_DN19594_c0_g1	AT1G67940	#N/A	non-intrinsic ABC protein 3	-1.01506
TRINITY_DN7587_c0_g1	AT5G17540	XP_010941428.2	HXXXD-type acyl-transferase family protein	-1.02359
TRINITY_DN1909_c0_g1	AT2G42760	KAH7657748.1	DUF1685 family protein	-1.03707
TRINITY_DN982_c0_g1	AT1G32700	RWW14545.1	PLATZ transcription factor family protein	-1.04065
TRINITY_DN5745_c0_g1	AT2G17120	KAG1361052.1	LYM2 lysm domain GPI-anchored protein 2 precursor	-1.0622
TRINITY_DN9121_c1_g3	AT4G24210	XP_042450825.1	F-box family protein (SLY1)	-1.08876
TRINITY_DN48511_c0_g1	AT3G10020	#N/A	uncharacterized protein	-1.09286
TRINITY_DN2228_c0_g1	AT5G51550	XP_010934660.1	EXORDIUM like 3	-1.09524
TRINITY_DN4861_c0_g1	AT1G76410	XP_008812592.1	RING/U-box superfamily protein	-1.10539
TRINITY_DN1546_c0_g1	AT2G38310	ALO77720.1	PYR1-like 4 (PYL4)	-1.12396
TRINITY_DN1355_c0_g2	#N/A	#N/A		-1.12438
TRINITY_DN6304_c0_g1	#N/A	MQM02084.1		-1.14421
TRINITY_DN1380_c0_g1	AT3G54700	CAG1848942.1	phosphate transporter 1;7	-1.14511
TRINITY_DN6743_c0_g1	AT4G33520	XP_009385637.1	P-type ATP-ase 1	-1.15296
TRINITY_DN9934_c0_g1	#N/A	#N/A		-1.17228
TRINITY_DN4901_c0_g1	#N/A	#N/A		-1.17245
TRINITY_DN9141_c0_g1	AT1G72060	EHA8588615.1	serine-type endopeptidase inhibitor	-1.18596
TRINITY_DN10717_c0_g1	AT4G00880	KAF3320619.1	SAUR-like auxin-responsive protein family	-1.18858
TRINITY_DN7922_c0_g3	AT4G36220	ASV46327.1	ferulic acid 5-hydroxylase 1	-1.19712
TRINITY_DN3427_c0_g1	AT2G13210	XP_008788382.1	retroelement pol polyprotein -related	-1.1994
TRINITY_DN3427_c1_g1	AT2G17880	XP_010920182.1	Chaperone DnaJ-domain superfamily protein	-1.22394
TRINITY_DN14393_c0_g2	#N/A	#N/A		-1.22411
TRINITY_DN5152_c1_g1	AT3G05890	XP_022868103.1	Low temperature and salt responsive protein family	-1.2345
TRINITY_DN7349_c0_g1	#N/A	#N/A		-1.24343
TRINITY_DN21339_c0_g1	AT5G26330	#N/A	Cupredoxin superfamily protein	-1.25036

TRINITY_DN10233_c0_g1	AT1G7025 0	KAG1362448.1	receptor serine/threonine kinase	-1.27505
TRINITY_DN5962_c0_g2	AT5G5375 0	KAG1361248.1	CBS domain-containing protein	-1.33299
TRINITY_DN2176_c0_g1	AT5G4761 0	KAG1360811.1	RING/U-box superfamily protein	-1.335
TRINITY_DN3495_c0_g1	AT1G1786 0	RWW49383.1	Kunitz family trypsin and protease inhibitor protein	-1.33562
TRINITY_DN13169_c0_g1	#N/A	#N/A		-1.33874
TRINITY_DN3495_c6_g2	#N/A	#N/A		-1.34005
TRINITY_DN216_c0_g1	#N/A	#N/A		-1.35286
TRINITY_DN13251_c0_g1	AT3G5274 0	KAG1369690.1	uncharacterized protein	-1.35509
TRINITY_DN1103_c0_g1	AT2G3198 0	TKY59925.1	PHYTOCYSTATIN 2	-1.36509
TRINITY_DN1947_c0_g1	#N/A	ERN09395.1		-1.36766
TRINITY_DN1301_c0_g2	AT5G2095 0	XP_039052548. 1	Glycosyl hydrolase family protein	-1.38472
TRINITY_DN18190_c0_g1	#N/A	#N/A		-1.38856
TRINITY_DN8988_c0_g1	AT5G4125 0	KAG1331458.1	Exostosin family protein	-1.39092
TRINITY_DN9016_c0_g1	AT5G2409 0	XP_039115610. 1	chitinase A	-1.42093
TRINITY_DN11829_c0_g1	#N/A	#N/A		-1.42143
TRINITY_DN8171_c0_g1	AT3G3311 0	XP_008811805. 1		-1.44134
TRINITY_DN12444_c0_g1	AT1G0803 0	XP_020260298. 1	TPST tyrosylprotein sulfotransferase	-1.46731
TRINITY_DN698_c0_g1	#N/A	#N/A		-1.47349
TRINITY_DN2843_c0_g1	#N/A	XP_044949984. 1		-1.47587
TRINITY_DN3427_c0_g2	AT2G1321 0	XP_008788382. 1	retroelement pol polyprotein -related	-1.51553
TRINITY_DN20492_c0_g1	#N/A	#N/A		-1.52092
TRINITY_DN1965_c0_g1	AT1G7169 1	XP_020247647. 1	GDSL-like Lipase/Acylhydrolase superfamily protein	-1.5262
TRINITY_DN3186_c0_g1	AT5G2409 0	KAG1367719.1	chitinase A	-1.53637
TRINITY_DN4562_c0_g1	AT5G5655 0	XP_010917660. 1	oxidative stress 3	-1.53982
TRINITY_DN1609_c0_g2	AT4G3690 0	RWW25567.1	RAP2.10	-1.54925
TRINITY_DN1544_c0_g2	AT5G1652 0	#N/A		-1.55645
TRINITY_DN12534_c0_g1	#N/A	AHG94647.1	pathogenesis-related protein 10 [<i>Lilium regale</i>]	-1.57592
TRINITY_DN39729_c0_g1	#N/A	#N/A		-1.58905
TRINITY_DN17614_c1_g1	#N/A	#N/A		-1.62799

TRINITY_DN1525_c0_g1	AT3G13227	KAF5200381.1	serine-rich protein-like protein	-1.62882
TRINITY_DN4055_c0_g1	AT2G30140	XP_010931537.1	UDP-Glycosyltransferase superfamily protein	-1.64324
TRINITY_DN9141_c0_g2	AT1G72060	XP_038984919.1	serine-type endopeptidase inhibitor	-1.69267
TRINITY_DN17060_c0_g1	#N/A	#N/A		-1.70653
TRINITY_DN12532_c0_g1	At1g23390	RWR94019.1	Kelch repeat-containing F-box family protein	-1.72906
TRINITY_DN6591_c0_g1	#N/A	EOS28076.1		-1.81902
TRINITY_DN18894_c0_g1	#N/A	#N/A		-1.82952
TRINITY_DN7925_c1_g1	#N/A	#N/A		-1.86853
TRINITY_DN10835_c0_g1	AT5G62360	XP_010259038.1	Plant invertase/pectin methylesterase inhibitor superfamily protein	-1.89379
TRINITY_DN150_c1_g1	#N/A	#N/A		-1.91393
TRINITY_DN18896_c1_g1	#N/A	#N/A		-1.91543
TRINITY_DN1531_c0_g1	#N/A	#N/A		-1.9574
TRINITY_DN43167_c0_g1	#N/A	#N/A		-1.97309
TRINITY_DN9646_c1_g1	AT5G57123	XP_027339502.1	uncharacterized protein	-1.99846
TRINITY_DN34118_c0_g1	#N/A	#N/A		-2.01369
TRINITY_DN13304_c0_g1	#N/A	#N/A		-2.04938
TRINITY_DN7085_c0_g1	AT5G64260	RZS22009.1	EXORDIUM like 2	-2.14733
TRINITY_DN21083_c0_g1	AT2G28610	#N/A	PRS Homeodomain-like superfamily protein	-2.15058
TRINITY_DN13367_c0_g2	#N/A	#N/A		-2.17545
TRINITY_DN43290_c0_g1	#N/A	#N/A		-2.18501
TRINITY_DN444_c0_g2	#N/A	XP_020703020.2		-2.19775
TRINITY_DN10949_c2_g1	AT1G64140	XP_039115949.1	WRKY transcription factor	-2.20552
TRINITY_DN20923_c0_g2	#N/A	#N/A		-2.27174
TRINITY_DN4060_c0_g2	AT2G22870	#N/A	P-loop containing nucleoside triphosphate hydrolases superfamily protein	-2.3485
TRINITY_DN35798_c0_g1	#N/A	#N/A		-2.39336
TRINITY_DN25043_c0_g1	#N/A	#N/A		-2.55841
TRINITY_DN2643_c0_g2	AT1G72060	XP_031392979.1	proteinase inhibitor PSI-1.2 [Punica granatum]	-2.67207
TRINITY_DN16588_c0_g1	#N/A	#N/A		-2.72084
TRINITY_DN40559_c0_g1	#N/A	#N/A		-2.73156
TRINITY_DN19912_c0_g1	#N/A	#N/A		-2.89603
TRINITY_DN21494_c0_g1	#N/A	#N/A		-2.89853
TRINITY_DN1024_c0_g2	#N/A	#N/A		-2.9263
TRINITY_DN16127_c0_g1	AT4G02780	#N/A	GA1 Terpenoid cyclases/Protein	-2.93921

			prenyltransferases superfamily protein	
TRINITY_DN44196_c0_g1	#N/A	#N/A		-2.94594
TRINITY_DN9807_c0_g1	#N/A	XP_001728955.1		-3.05803
TRINITY_DN43355_c0_g1	AT2G35910	#N/A	RING/U-box superfamily protein	-3.13211
TRINITY_DN9337_c0_g1	#N/A	XP_025373624.1		-3.20759
TRINITY_DN17882_c1_g1	#N/A	#N/A		-3.38777
TRINITY_DN23873_c0_g1	#N/A	#N/A		-3.43718
TRINITY_DN19898_c1_g1	#N/A	#N/A		-4.17752
TRINITY_DN13087_c0_g1	#N/A	KRX85841.1		-5.74641
TRINITY_DN46436_c0_g1	#N/A	#N/A		-7.61128
TRINITY_DN28207_c0_g1	#N/A	#N/A		-7.68675
TRINITY_DN38736_c0_g1	#N/A	#N/A		-7.72438
TRINITY_DN11814_c0_g2	AT4G28530	AXU39984.1	NAC074	-7.77335
TRINITY_DN24124_c0_g1	#N/A	#N/A		-8.13195

Appendix 4.3 – ‘Magnitude of opening’ group

Read	A. thaliana gene	Viridiplantae gene	Gene description	Log2FC (LFO/SSO)
TRINITY_DN23906_c0_g1	#N/A	#N/A	#N/A	8.227593511
TRINITY_DN50930_c0_g1		#N/A	#N/A	8.204534908
TRINITY_DN43285_c0_g1	#N/A	#N/A	#N/A	8.105195284
TRINITY_DN9509_c2_g1	#N/A	#N/A	#N/A	8.060024297
TRINITY_DN20873_c0_g1	AT3G28380	#N/A	ABC transporter B family member 17	8.043032885
TRINITY_DN33908_c0_g1	#N/A	#N/A	#N/A	8.009356178
TRINITY_DN17055_c0_g1	#N/A	#N/A	#N/A	7.825079112
TRINITY_DN18672_c0_g1	#N/A	#N/A	#N/A	7.748398608
TRINITY_DN26273_c0_g1	AT3G12270	#N/A	Arabidopsis thaliana protein arginine methyltransferase 3	7.641595427
TRINITY_DN19302_c0_g2	#N/A	#N/A	#N/A	7.274073243
TRINITY_DN16536_c0_g1	#N/A	#N/A	#N/A	1.984512899

TRINITY_DN19714_c0_g1	#N/A	#N/A	#N/A	1.806653539
TRINITY_DN10374_c0_g1	AT5G45950	XP_008784445.2	GDSL-like Lipase/Acylhydrolase superfamily protein	1.660476504
TRINITY_DN17802_c0_g1	#N/A	#N/A	#N/A	1.575756689
TRINITY_DN1541_c0_g1	#N/A	#N/A	#N/A	1.31426509
TRINITY_DN3338_c0_g1	AT1G32060	XP_042504145.1	Phosphoribulokinase, chloroplastic	1.286266368
TRINITY_DN4687_c0_g1	AT4G37800	XP_010915332.1	Probable xyloglucan endotransglucosylase/hydrolyase protein 7	1.239620515
TRINITY_DN1738_c0_g1	#N/A	#N/A	#N/A	1.233067909
TRINITY_DN6777_c0_g1	AT3G57880	KAG1361458.1	Calcium-dependent lipid-binding (CaLB domain) plant phosphoribosyltransferase family protein	1.203456008
TRINITY_DN5889_c0_g1	AT3G55800	XP_020272960.1	Sedoheptulose-1,7-bisphosphatase, chloroplastic	1.188887797
TRINITY_DN21132_c0_g3	AT1G54820	#N/A	Protein kinase superfamily protein	1.157530259
TRINITY_DN2908_c0_g1	AT1G30440	XP_020586553.1	BTB/POZ domain-containing protein At1g30440	1.138067475
TRINITY_DN5460_c0_g1	AT3G54050	THU54394.1	Fructose-1,6-bisphosphatase 1, chloroplastic	1.058609072
TRINITY_DN128_c0_g1	AT1G09340	XP_008777573.2	Chloroplast stem-loop binding protein of 41 kDa b, chloroplastic	1.051005898
TRINITY_DN3989_c0_g1	#N/A	#N/A	#N/A	1.013689499
TRINITY_DN3619_c0_g1	AT5G66190	ASV46328.1	Ferredoxin--NADP reductase, leaf isozyme 1, chloroplastic	1.009454143
TRINITY_DN17435_c0_g1	AT2G47910	#N/A	Protein chlororespiratory reduction 6, chloroplastic	0.955609104
TRINITY_DN11352_c0_g1	AT2G45660	AQR58148.1	MADS-box protein SOC1	0.906941198
TRINITY_DN12380_c0_g1	AT1G14790	XP_024964345.1	RNA-dependent RNA polymerase 1	0.891586682
TRINITY_DN4548_c0_g1	AT3G17180	KAG1326147.1	Serine carboxypeptidase-like clade ii	0.876676863
TRINITY_DN50240_c0_g1	#N/A	#N/A	#N/A	0.84785083
TRINITY_DN6154_c0_g1	AT3G16360	XP_010915447.1	Encodes AHP4, a histidine-containing phosphotransmitter	0.845322272

TRINITY_DN4205_c0_g1	AT1G58290	XP_039139549.1	Glutamyl-trna reductase 1, chloroplastic	0.800596386
TRINITY_DN276_c0_g1	AT3G16360	XP_020264894.1	Encodes AHP4, a histidine-containing phosphotransmitter	0.784552452
TRINITY_DN8449_c0_g1	AT5G41650	XP_038970587.1	Lactoylglutathione lyase / glyoxalase I family protein	0.764516023
TRINITY_DN1356_c0_g1	AT5G22460	XP_020260342.1	alpha/beta-Hydrolases superfamily protein	0.591158924
TRINITY_DN15991_c0_g1	AT4G23500	#N/A	Pectin lyase-like superfamily protein	-0.648374251
TRINITY_DN2219_c0_g1	AT2G27510	RVW86929.1	Ferredoxin-3, chloroplastic	-0.65882741
TRINITY_DN6552_c0_g1	AT5G48820	KAH0451702.1	Inhibitor/interactor with cyclin-dependent kinase	-0.662350009
TRINITY_DN10113_c0_g1	AT1G08450	KAF3784727.1	Ems-mutagenized bri1 suppressor 2	-0.679469993
TRINITY_DN6484_c0_g1	AT4G12100	XP_020684168.1	Cullin family protein	-0.682100595
TRINITY_DN2763_c0_g1	AT5G64850	XP_016551588.1	Uncharacterized protein At5g64850	-0.689289743
TRINITY_DN7471_c0_g3	AT3G16080	KAG6501549.1	Zinc-binding ribosomal protein family protein	-0.694872391
TRINITY_DN477_c1_g2	AT1G72930	EHA8590132.1	Toll/interleukin-1 receptor-like protein	-0.717134723
TRINITY_DN6408_c0_g1	AT5G48020	XP_010928464.1	2-oxoglutarate (2OG) and Fe(II)-dependent oxygenase superfamily protein	-0.719555641
TRINITY_DN6561_c0_g1		XP_008786716.1	#N/A	-0.7218368
TRINITY_DN1639_c0_g1	AT2G47780	PSS06225.1	Rubber elongation factor protein (REF)	-0.732445848
TRINITY_DN20051_c0_g1	#N/A	#N/A	#N/A	-0.740584679
TRINITY_DN7903_c0_g1	AT1G15400	KAH7686661.1	Uncharacterized protein At1g15400	-0.745926489
TRINITY_DN1802_c0_g1	AT5G51340	KAG1331560.1	Tetratricopeptide repeat (tpr)-like superfamily protein	-0.75381766

TRINITY_DN8265_c0_g1	#N/A	#N/A	#N/A	- 0.7705579 94
TRINITY_DN5181_c0_g1	AT4G1556 0	AVI24632.1	1-deoxy-D-xylulose-5-phosphate synthase, chloroplastic	- 0.7821639 5
TRINITY_DN3689_c0_g1	AT1G5658 0	KAH0449511.1	Plant/protein (protein of unknown function, duf538)	- 0.8180389 57
TRINITY_DN15367_c0_g1		#N/A	#N/A	- 0.8211587 68
TRINITY_DN7510_c0_g1	AT2G2094 0	XP_020092685 .1	Transmembrane protein, putative (DUF1279)	- 0.8302432 08
TRINITY_DN1696_c0_g1	AT5G5932 0	AFD32272.1	Non-specific lipid-transfer protein 3	- 0.8535635 61
TRINITY_DN319_c0_g1	AT3G1357 0	KAF3796823.1	Fus-interacting serine-arginine-rich protein 1	- 0.8548744 03
TRINITY_DN9946_c0_g1	AT1G3133 5	XP_008787343 .2	Unknown protein	- 0.8562293 12
TRINITY_DN5560_c0_g1	AT4G2727 0	XP_010928688 .1	Nad(p)h dehydrogenase (quinone)	- 0.8666205 05
TRINITY_DN13358_c0_g2	AT4G1409 0	KAG1335490.1	UDP-Glycosyltransferase superfamily protein	- 0.8688035 87
TRINITY_DN3374_c0_g1	AT2G2369 0	OVA18620.1	HTH-type transcriptional regulator	- 0.8745101 72
TRINITY_DN892_c0_g1	AT2G2017 0	KAH7671728.1	NEP-interacting protein, putative (DUF239)	- 0.8788550 97
TRINITY_DN4948_c0_g2	#N/A	#N/A	#N/A	- 0.9039396 1
TRINITY_DN9122_c0_g1	AT1G1020 0	XP_010928557 .1	Gata type zinc finger transcription factor family protein	- 0.9116847 34
TRINITY_DN346_c0_g1	AT2G3598 0	RWW01042.1	Late embryogenesis abundant (LEA) hydroxyproline-rich glycoprotein family	- 0.9329334 76
TRINITY_DN8481_c0_g1	AT3G1019 0	XP_010922185 .1	Calcium-binding EF-hand family protein	- 0.9348453 44

TRINITY_DN17647_c1_g2	#N/A	#N/A	#N/A	- 0.93976827
TRINITY_DN6152_c0_g1	AT1G10370	XP_008778822.1	Glutathione S-transferase family protein	- 0.954425321
TRINITY_DN9719_c0_g1	#N/A	#N/A	#N/A	- 0.967771475
TRINITY_DN274_c0_g1	AT4G23920	XP_020274359.1	UDP-D-glucose/UDP-D-galactose 4-epimerase 2	- 0.973165316
TRINITY_DN1582_c0_g1	AT2G21620	KAG1342800.1	Adenine nucleotide alpha hydrolases-like superfamily protein	- 0.983794124
TRINITY_DN11486_c0_g1	AT3G49940	KAG0485455.1	LOB domain-containing protein 38 (LBD38)	- 1.032242352
TRINITY_DN9758_c0_g1	AT2G31090	#N/A	mRNA, clone: RAFL21-78-F02	- 1.084365946
TRINITY_DN14544_c0_g2	#N/A	#N/A	#N/A	- 1.090095334
TRINITY_DN7848_c1_g1	AT1G47240	XP_010936565.1	Natural resistance-associated macrophage protein 2	- 1.090584457
TRINITY_DN1105_c0_g1	AT1G10650	KAH7653739.1	E3 ubiquitin-protein ligase BOI and related proteins	- 1.117700713
TRINITY_DN7416_c0_g1	#N/A	#N/A	#N/A	- 1.137884745
TRINITY_DN16590_c0_g1	#N/A	#N/A	#N/A	- 1.138919181
TRINITY_DN11769_c0_g1	#N/A	#N/A	#N/A	- 1.151690109
TRINITY_DN12801_c0_g1	#N/A	#N/A	#N/A	- 1.182953456
TRINITY_DN2066_c0_g1	AT5G48900	KAG0497755.1	Pectin lyase-like superfamily protein	- 1.186554479
TRINITY_DN6969_c0_g1	AT1G11910	XP_008797519.2	Aspartic proteinase A1	- 1.189289132
TRINITY_DN12503_c0_g1	#N/A	#N/A	#N/A	- 1.232138628

TRINITY_DN5123_c0_g1	AT5G01300	XP_010922582.1	PEBP (phosphatidylethanolamine-binding protein) family protein	- 1.246601986
TRINITY_DN41022_c0_g1	AT5G01960	#N/A	Uncharacterized protein At5g01960	- 1.273474667
TRINITY_DN2619_c0_g1	AT2G18670	XP_010913606.1	RING/U-box superfamily protein	- 1.284173105
TRINITY_DN3278_c0_g1	#N/A	#N/A	#N/A	- 1.291288361
TRINITY_DN21841_c0_g1	AT3G60190	#N/A	Enhanced disease resistance 3	- 1.292168898
TRINITY_DN5260_c0_g1	#N/A	#N/A	#N/A	- 1.298696494
TRINITY_DN2928_c0_g1	AT2G33380	A8B479.1	Arabidopsis thaliana caleosin 3	- 1.322366586
TRINITY_DN4048_c0_g4	AT2G30360	RWR79019.1	CBL-interacting serine/threonine-protein kinase 11	- 1.41770954
TRINITY_DN18086_c0_g1	AT3G06720	#N/A	Importin subunit alpha-6/7	- 1.421873186
TRINITY_DN48804_c0_g1	#N/A	#N/A	#N/A	- 1.433299736
TRINITY_DN36548_c0_g1	#N/A	#N/A	#N/A	- 1.446583167
TRINITY_DN9587_c0_g1	AT1G54550	XP_010943076.1	F-box and associated interaction domains-containing protein	- 1.460003297
TRINITY_DN620_c0_g2	#N/A	#N/A	#N/A	- 1.501672691
TRINITY_DN9783_c0_g1	AT5G60930	XP_019702665.1	P-loop containing nucleoside triphosphate hydrolases superfamily protein	- 1.535394473
TRINITY_DN13556_c0_g1	AT3G10360	#N/A	Pumilio rna-binding family	- 1.537267637
TRINITY_DN13359_c0_g1	AT5G18150	ONK65369.1	Uncharacterized protein At5g18150/MRG7_11	- 1.537934658

TRINITY_DN23981_c0_g1	#N/A	#N/A	#N/A	- 1.5592569 86
TRINITY_DN6347_c0_g1	#N/A	#N/A	#N/A	- 1.5840587 79
TRINITY_DN17859_c0_g1	#N/A	#N/A	#N/A	- 1.6314270 1
TRINITY_DN271_c0_g1	AT2G07777	CDM84611.1	ATP synthase 9 mitochondrial	- 1.6405189 17
TRINITY_DN8643_c0_g1	AT5G62510	XP_010927806.1	F-box family protein	- 1.7522417 53
TRINITY_DN46088_c0_g1	AT4G25140	#N/A	Oleosin 18.5 kDa	- 1.7986025 71
TRINITY_DN16529_c0_g1	#N/A	#N/A	#N/A	- 1.8002548 32
TRINITY_DN9653_c0_g2	#N/A	#N/A	#N/A	- 1.8022848 68
TRINITY_DN620_c0_g1	#N/A	#N/A	#N/A	- 1.8235251 61
TRINITY_DN738_c0_g1	AT2G18420	AHK24891.1	Gibberellin-regulated family protein	- 1.8306548 32
TRINITY_DN3085_c0_g1	AT3G05500	KAH9680063.1	Rubber elongation factor protein (REF)	- 1.8324591 91
TRINITY_DN7753_c0_g1	#N/A	AEV23220.1	#N/A	- 1.8641158 59
TRINITY_DN3161_c0_g1	AT1G13130	KAH7681532.1	Cellulase (glycosyl hydrolase family 5) protein	- 1.8955086 66
TRINITY_DN142_c1_g1	AT3G10410	XP_010918615.1	Serine carboxypeptidase-like clade iv	- 1.9116675 01
TRINITY_DN10795_c0_g1	AT1G11190	QGT40635.1	Encodes a bifunctional nuclease that acts on both RNA and DNA	- 1.9167343 3
TRINITY_DN11651_c0_g1	AT5G57300	KAG1326583.1	S-adenosyl-L-methionine-dependent methyltransferases superfamily protein	- 1.9198978 14

TRINITY_DN2235_c0_g1	AT3G26130	XP_039124145.1	Cellulase (glycosyl hydrolase family 5) protein	- 1.9456117 26
TRINITY_DN10208_c0_g1	#N/A	#N/A	#N/A	- 1.9495061 85
TRINITY_DN14136_c0_g1	#N/A	#N/A	#N/A	- 2.0163997 17
TRINITY_DN1566_c0_g1	AT3G26140	RWW03470.1	Cellulase (glycosyl hydrolase family 5) protein	- 2.0658934 26
TRINITY_DN10083_c0_g1	AT1G10140	XP_008796991.1	Uncharacterised conserved protein UCP031279	- 2.1066666 21
TRINITY_DN3161_c0_g2	AT1G13130	KAH7681532.1	Cellulase (glycosyl hydrolase family 5) protein	- 2.1187185 58
TRINITY_DN3116_c0_g1	AT4G36770	XP_008794220.4	UDP-Glycosyltransferase superfamily protein	- 2.1420935 19
TRINITY_DN7416_c0_g2	AT5G24660	#N/A	Response to low sulfur 2	- 2.2609659 98
TRINITY_DN9590_c0_g1	#N/A	#N/A	#N/A	- 2.3425978 34
TRINITY_DN19576_c0_g1	#N/A	#N/A	#N/A	- 2.4171672 89
TRINITY_DN16784_c0_g1	#N/A	#N/A	#N/A	- 2.4294458 64
TRINITY_DN7404_c0_g1	AT5G10430	XP_010928894.1	Classical arabinogalactan protein 4	- 2.4903278 75
TRINITY_DN8665_c0_g1	AT1G74660	XP_043697939.1	Mini zinc finger 1	- 2.5130221 58
TRINITY_DN19924_c0_g1	#N/A	#N/A	#N/A	- 2.9958747 77
TRINITY_DN18856_c0_g1	#N/A	#N/A	#N/A	- 3.1937813 53
TRINITY_DN14284_c0_g1	AT5G46060	#N/A	Protein of unknown function, DUF599	- 3.2205861 26
TRINITY_DN3453_c0_g1	AT2G14095	THU64240.1	Unknown protein	- 3.2646388 4

TRINITY_DN9254_c0_g1	#N/A	#N/A	#N/A	- 3.4940645 85
TRINITY_DN10457_c0_g1	AT5G4280 0	BAE79202.1	Bifunctional dihydroflavonol 4-reductase/flavanone 4- reductase	- 3.6687912 65
TRINITY_DN9780_c0_g1	AT4G2292 0	XP_009386177 .1	Magnesium dechelataase	- 4.1674756 82
TRINITY_DN49594_c0_g1	#N/A	#N/A	#N/A	- 4.3091846 48
TRINITY_DN14392_c0_g1	#N/A	#N/A	#N/A	- 4.8077031 11
TRINITY_DN17446_c0_g1	#N/A	#N/A	#N/A	- 7.4218946 93
TRINITY_DN53554_c0_g1	#N/A	#N/A	#N/A	- 7.4801717 76
TRINITY_DN383_c1_g1	#N/A	#N/A	#N/A	- 7.9141640 41
TRINITY_DN17604_c0_g2	#N/A	#N/A	#N/A	- 8.1810725 39
TRINITY_DN43946_c0_g1	#N/A	#N/A	#N/A	- 8.2258789 1
TRINITY_DN14087_c0_g2	#N/A	#N/A	#N/A	- 8.4939631 39

Appendix 4.4 – Cluster 3 ‘UpUp’ group

TAIR ID	Gene name	Gene annotation	Log2FC SSO/SRC	Log2FC LFO/SSO	Log2FC LFO/SRC
AT3G54720	AMP1	N-acetylated-alpha-linked acidic dipeptidase	3.877311 4	#N/A	5.503549
AT4G13830	J20	Chaperone protein dnaJ 20, chloroplastic	3.278263 1	#N/A	5.347691 2
AT3G16310	AT3G16310	Mitotic phosphoprotein N' end (MPPN) family protein	3.278139	#N/A	#N/A
AT1G03870	FLA9	Fasciclin-like arabinogalactan protein 9	2.299274 1	1.605183	3.912043 5
AT1G77410	BGAL16	Beta-galactosidase 16 (BGAL16)	2.013157	1.976556 5	3.998962 7

AT1G48100	AT1G48100	Pectin lyase-like superfamily protein	1.725353 7	#N/A	#N/A
AT2G33600	CRL2	NAD(P)-binding Rossmann-fold superfamily protein	1.712475 2	#N/A	#N/A
AT3G07700	AT3G07700	Protein kinase superfamily protein	1.687234	#N/A	3.334835 2
AT5G17050	UGT78D2	UDP-glucosyl transferase 78D2	1.607382 6	#N/A	2.220993 3
AT1G74660	MIF1	Mini zinc finger 1	1.594783 5	2.513022 2	#N/A
AT3G47380	AT3G47380	Plant invertase/pectin methylesterase inhibitor superfamily protein	1.533452 3	#N/A	#N/A
AT3G54800	AT3G54800	Pleckstrin homology (PH) and lipid-binding START domains-containing protein	1.505395 4	#N/A	#N/A
AT4G30190	HA2	ATPase 2, plasma membrane-type	1.479855 1	#N/A	1.893631 8
AT3G27810	MYB21	Arabidopsis thaliana myb domain protein 3	1.441100 9	#N/A	3.20402
AT3G01930	AT3G01930	Major facilitator superfamily protein	1.409242	#N/A	2.111783 6
AT2G33590	CRL1	NAD(P)-binding Rossmann-fold superfamily protein	1.400461 3	1.698351	3.107697 1
AT5G38500	AT5G38500	B3 domain-containing protein At5g38500	1.363117 1	#N/A	1.807776 5
AT4G22990	AT4G22990	Major Facilitator Superfamily with SPX (SYG1/Pho81/XPR1) domain-containing protein	1.328881 5	#N/A	#N/A
AT1G19250	FMO1	Dimethylaniline monooxygenase (n-oxide forming)	1.297163 7	#N/A	#N/A
AT1G60780	HAP13	Clathrin adaptor complexes medium subunit family protein	1.285276 4	#N/A	2.153626 8
AT1G02205	CER1	Fatty acid hydroxylase superfamily	1.263610 1	#N/A	1.600794 9
AT5G48900	AT5G48900	Pectin lyase-like superfamily protein	1.260031 9	1.186554 5	#N/A
AT3G08560	VHA-E2	V-type h ⁺ -transporting atpase subunit e	1.177933 3	#N/A	#N/A
AT1G28060	AT1G28060	U4/U6 small nuclear ribonucleoprotein PRP3	1.126129	#N/A	1.239008 5
AT3G44540	FAR4	Alcohol-forming fatty acyl-coa reductase	1.120938 9	#N/A	1.629972 8
AT3G09600	RVE8	Homeodomain-like superfamily protein	1.117847 8	3.300534 7	4.435515 4
AT4G15920	SWEET17	Solute carrier family 50 (sugar transporter)	1.080483 2	#N/A	1.284097 3
AT3G45780	PHOT1	Nonphototropic hypocotyl 1	1.073520 9	#N/A	1.350315 1

AT5G42630	ATS	Homeodomain-like superfamily protein	1.0539115	#N/A	#N/A
AT1G71980	AT1G71980	Protease-associated (pa) ring/u-box zinc finger family protein	1.0180854	1.6717844	2.7010527
AT1G71000	AT1G71000	Chaperone DnaJ-domain superfamily protein	1.0007179	#N/A	#N/A
AT2G45120	AT2G45120	C2H2-like zinc finger protein	0.9512666	#N/A	2.3965013
AT3G09280	AT3G09280	Unknown protein	0.9480387	#N/A	2.8031501
AT5G02890	AT5G02890	HXXXD-type acyl-transferase family protein	0.9272578	1.1587648	2.094961
AT3G61460	BRH1	Brassinosteroid-responsive RING-H2	0.8814376	#N/A	2.2496427
AT4G32940	GAMMA-VPE	Vacuolar-processing enzyme gamma-isozyme	0.7811222	#N/A	2.1644184
AT2G38640	AT2G38640	Lurp-one-like protein (duf567)	0.7369186	#N/A	#N/A
AT5G49130	AT5G49130	MATE efflux family protein	0.7363634	#N/A	#N/A
AT2G33670	MLO5	homologs of the barley mildew resistance locus o (MLO) protein of closely-related AtMLO genes	0.6799146	#N/A	#N/A
AT3G49940	LBD38	LOB domain-containing protein 38 (LBD38)	0.6773848	1.0322424	#N/A
AT2G42900	AT2G42900	Plant basic secretory protein (BSP) family protein	0.6089177	#N/A	1.6520144
AT3G20820	AT3G20820	Leucine-rich repeat (LRR) family protein	0.5791173	#N/A	#N/A
AT1G32700	AT1G32700	PLATZ transcription factor family protein	0.56705	1.9711821	2.5483251
AT4G38620	MYB4	Transcription factor myb, plant	0.5485113	1.1488721	1.7076362
AT3G51990	AT3G51990	Serine/threonine-protein kinase-like protein At3g51990	0.5224573	#N/A	#N/A
AT4G36740	HB40	Homeobox-leucine zipper protein athb-40	0.453223	#N/A	#N/A
AT5G50260	CEP1	Cysteine proteinases superfamily protein	0.3789071	1.9623863	2.3504555
AT1G02640	BXL2	Probable beta-D-xylosidase 2	0.3648567	#N/A	1.8675488
AT3G14280	AT3G14280	LL-diaminopimelate aminotransferase	0.3635262	#N/A	2.0076352
AT2G47440	AT2G47440	Tetratricopeptide repeat (TPR)-like superfamily protein	0.3540903	#N/A	2.1284548
AT4G17340	TIP2;2	Tonoplast intrinsic protein 2	0.3535485	#N/A	#N/A

AT1G75280	AT1G75280	NmrA-like negative transcriptional regulator family protein	0.3429027	1.3459499	1.6992254
AT1G08720	EDR1	Serine/threonine-protein kinase EDR1	0.3310825	#N/A	#N/A
AT2G40610	EXPA8	Expansin-A8	0.3174337	#N/A	1.9655056
AT1G10650	AT1G10650	E3 ubiquitin-protein ligase BOI and related proteins	0.2718225	1.1177007	#N/A
AT4G24210	SLY1	F-box family protein	0.2651377	2.1325491	2.4055388
AT1G10290	ADL6	Dynamin-like protein 6	0.2454857	#N/A	#N/A
AT4G25140	OLEO1	Oleosin 18.5 kDa	0.2284516	1.7986026	#N/A
AT5G48930	HCT	Hydroxycinnamoyl-coa shikimate/quinic acid hydroxycinnamoyl transferase	0.1922999	1.2942388	1.4956053
AT4G10770	OPT7	Oligopeptide transporter 7	0.1572322	#N/A	#N/A
AT3G59140	ABCC10	Multidrug resistance-associated protein 14	0.1526519	#N/A	#N/A
AT5G20885	AT5G20885	Uncharacterized protein At5g20885/At5g20880	0.1240965	2.412401	2.5458263
AT1G28590	AT1G28590	GDSL-like Lipase/Acylhydrolase superfamily protein	0.1195009	#N/A	#N/A
AT3G14067	AT3G14067	Subtilisin-like protease SBT1.4	0.1095489	#N/A	#N/A
AT1G10140	AT1G10140	Uncharacterised conserved protein UCP031279	0.1056267	2.1066666	#N/A

GO term enrichment for Cluster 3, carried out using ShinyGO (Ge et al. 2020).

Aspect	GO term	Enrichment FDR	Pathway Genes	nGenes	Fold Enrichment	Pathway	Genes
CC	GO:0000322	0.033170477	23	2	27.71428571	Storage vacuole	AT1G71980 AT4G32940
CC	GO:0000326	0.033170477	23	2	27.71428571	Protein storage vacuole	AT1G71980 AT4G32940
CC	GO:0030136	0.025134772	67	3	13.85714286	Clathrin-coated vesicle	AT1G08720 AT1G10290 AT1G60780

CC	GO:0000325	0.00016886	187	7	12.34545455	Plant-type vacuole	AT1G71980 AT3G59140 AT4G15920 AT4G17340 AT4G22990 AT4G32940 AT5G50260
CC	GO:0009705	0.016772885	137	4	9.82278481	Plant-type vacuole membrane	AT1G71980 AT4G15920 AT4G17340 AT4G22990
CC	GO:0005774	0.009274189	661	9	4.088992974	Vacuolar membrane	AT1G10290 AT1G71980 AT3G08560 AT3G14067 AT3G59140 AT4G15920 AT4G17340 AT4G22990 AT4G30190
CC	GO:0005576	0.001301455	1923	13	3.874039939	Extracellular region	AT1G02640 AT1G03870 AT1G10290 AT1G28590 AT1G48100 AT1G77410 AT2G40610 AT3G14067 AT3G20820 AT3G47380 AT3G51990 AT4G25140 AT5G50260
CC	GO:0005618	0.03671134	793	7	3.650537634	Cell wall	AT1G02640 AT1G48100 AT1G77410 AT2G40610 AT3G20820 AT5G42630 AT5G50260
CC	GO:0030312	0.03671134	813	7	3.602122016	External encapsulating structure	AT1G02640 AT1G48100 AT1G77410 AT2G40610 AT3G20820 AT5G42630 AT5G50260
CC	GO:0005773	0.002729552	1247	13	3.469050894	Vacuole	AT1G10290 AT1G71980 AT1G77410 AT3G08560 AT3G14067 AT3G45780 AT3G59140 AT4G15920 AT4G17340 AT4G22990 AT4G30190 AT4G32940 AT5G50260

Appendix 4.5 – Cluster 4 ‘UpFlat’ group

TAIR ID	Gene name	Gene annotation	Log2FC SSO/SRC	Log2FC LFO/SSO	Log2FC LFO/SRC
AT5G41370	XPB1	Homolog of xeroderma pigmentosum complementation group B 1	1.421886423	#N/A	#N/A

AT1G31050	AT1G31050	Basic helix-loop-helix (bHLH) DNA-binding superfamily protein	1.333571653	#N/A	#N/A
AT1G76460	AT1G76460	RNA-binding (RRM/RBD/RNP motifs) family protein	1.057357251	#N/A	#N/A
ATCG00040	MATK	Maturase K	1.054953749	#N/A	#N/A
AT2G29630	THIC	Phosphomethylpyrimidine synthase, chloroplastic	1.039098926	#N/A	1.078508786

GO term enrichment for Cluster 4, carried out using ShinyGO (Ge et al. 2020).

Aspect	GO term	Enrichment FDR	nGenes	Pathway Genes	Fold Enrichment	Pathway	Genes
CC	GO:0097550	0.019849143	1	6	839.266667	Transcription preinitiation complex	XPB1
CC	GO:000109	0.019849143	1	5	629.45	Nucleotide-excision repair complex	XPB1
CC	GO:0005675	0.025767011	1	14	251.78	Transcription factor tfiih holo complex	XPB1
CC	GO:0032806	0.025767011	1	19	209.816667	Carboxy-terminal domain protein kinase complex	XPB1
CC	GO:1990391	0.025767011	1	14	193.6769231	DNA repair complex	XPB1
CC	GO:1902554	0.044370569	1	65	78.68125	Serine/threonine protein kinase complex	XPB1
CC	GO:1902911	0.044370569	1	67	74.05294118	Protein kinase complex	XPB1
CC	GO:0090575	0.044370569	1	71	64.55897436	RNA polymerase II transcription regulator complex	XPB1
CC	GO:0032993	0.044370569	1	70	59.94761905	protein-DNA complex	XPB1
CC	GO:0016591	0.044370569	1	60	55.95111111	RNA polymerase II, holoenzyme	XPB1
CC	GO:0005667	0.048371234	1	93	45.77818182	Transcription regulator complex	XPB1
CC	GO:0055029	0.048371234	1	77	42.67457627	Nuclear dna-directed rna polymerase complex	XPB1
MF	GO:0043138	0.047579946	1	12	279.7555556	3-5 DNA helicase activity	XPB1
MF	GO:0001228	0.047579946	1	38	179.8428571	DNA-binding transcription activator activity, RNA polymerase II-specific	AT1G31050
MF	GO:0001216	0.047579946	1	41	157.3625	DNA-binding transcription activator activity	AT1G31050
MF	GO:0005515	0.047579946	3	1997	6.660846561	Protein binding	AT1G31050 THIC XPB1

BP	GO:0033273	0.037683421	1	5	629.45	Response to vitamin	THIC
BP	GO:0007584	0.037683421	1	12	359.6857143	Response to nutrient	THIC
BP	GO:0009228	0.037683421	1	7	359.6857143	Thiamine biosynthetic process	THIC
BP	GO:0033683	0.037683421	1	8	359.6857143	Nucleotide-excision repair, dna incision	XPB1
BP	GO:0042357	0.037683421	1	9	359.6857143	Thiamine diphosphate metabolic process	THIC
BP	GO:0042724	0.037683421	1	7	359.6857143	Thiamine-containing compound biosynthetic process	THIC

Appendix 4.6 – Cluster 7 ‘DownFlat’ group

TAIR ID	Gene name	Gene annotation	Log2FC SSO/SRC	Log2FC LFO/SSO	Log2FC LFO/SRC
AT2G32300	UCC1	Uclacyanin 1	-2.123518034	#N/A	#N/A
AT5G35525	AT5G35525	Protein PLANT CADMIUM RESISTANCE 3	-2.026711572	#N/A	#N/A
AT5G57123	AT5G57123	Uncharacterized protein At5g57123	-1.998459155	#N/A	#N/A
AT4G15610	AT4G15610	Uncharacterised protein family (UPF0497)	-1.968971898	#N/A	#N/A
AT5G67550	AT5G67550	Unknown protein	-1.914154286	#N/A	#N/A
AT5G45870	PYL12	Abscisic acid receptor PYL12	-1.88870438	#N/A	-1.845373077
AT2G21950	SKIP6	F-box/kelch-repeat protein SKIP6	-1.768583686	#N/A	#N/A
AT1G05260	RCI3	Peroxidase superfamily protein	-1.764858564	#N/A	#N/A
AT5G02190	PCS1	Eukaryotic aspartyl protease family protein	-1.671469712	#N/A	-1.619827699
AT1G69930	GSTU11	Glutathione S-transferase TAU 11	-1.585374709	#N/A	#N/A

AT4G37330	CYP81D4	Cytochrome P450, family 81, subfamily D, polypeptide 4	- 1.5171647 59	#N/A	#N/A
AT1G64900	CYP89A2	Cytochrome P450, family 89, subfamily A, polypeptide 2	- 1.4203467 67	#N/A	#N/A
AT5G23270	STP11	Mfs transporter, sp family, sugar:h ⁺ symporter	- 1.4101904 65	#N/A	#N/A
AT1G28370	ERF11	Ethylene-responsive transcription factor 11	- 1.3771220 23	#N/A	#N/A
AT3G55550	AT3G55550	Concanavalin A-like lectin protein kinase family protein	- 1.2266369 62	#N/A	- 1.1690757 39
AT4G21865	AT4G21865	At4g21865	- 1.2207712 68	#N/A	#N/A
AT4G36990	HSF4	Heat stress transcription factor B-1	- 1.2171917 28	#N/A	#N/A
AT5G01740	AT5G01740	Nuclear transport factor 2 (NTF2) family protein	- 1.2015288 66	#N/A	#N/A
AT2G32710	KRP4	Kip-related protein (KRP) gene, encodes CDK (cyclin-dependent kinase) inhibitor (CKI)	- 1.1933360 71	#N/A	#N/A
AT5G12380	ANNAT8	Annexin 8 (ANNAT8)	- 1.1535341 7	#N/A	#N/A
AT3G54700	PHT1;7	Probable inorganic phosphate transporter 1-7	- 1.1451084 53	#N/A	#N/A
AT2G17120	LYM2	LysM domain-containing GPI-anchored protein 2	- 1.0622003 69	#N/A	#N/A
AT3G04530	PPCK2	Phosphoenolpyruvate carboxylase kinase 2	- 1.0558343 33	#N/A	#N/A
AT1G67940	ABCI17	Arabidopsis thaliana non-intrinsic abc protein 3	- 1.0150553 65	#N/A	#N/A
AT5G48930	HCT	Hydroxycinnamoyl-coa shikimate/quinate hydroxycinnamoyl transferase	0.1922999 1	1.2942388 15	1.4956052 5
AT1G32700	AT1G32700	PLATZ transcription factor family protein	0.5670499 72	1.9711820 88	2.5483251 18

GO term enrichment for Cluster 7, carried out using ShinyGO (Ge et al. 2020).

Aspect	GO term	Enrichment FDR	nGenes	Pathway Genes	Fold Enrichment	Pathway	Genes
MF	GO:0005315	0.04448	2	20	64.55897	Inorganic phosphate transmembrane transporter activity	ABC17 PHT1;7

Appendix 4.7 – Cluster 8 ‘DownDown’ group

TAIR ID	Gene name	Gene annotation	Log2FC SSO/SRC	Log2FC LFO/SSO	Log2FC LFO/SRC
AT1G17020	SRG1	Senescence-related gene 1	-3.381859407	#N/A	-3.800144325
AT2G45360	AT2G45360	Protein of unknown function (DUF1442)	-2.697163586	#N/A	#N/A
AT3G13150	AT3G13150	Tetratricopeptide repeat (TPR)-like superfamily protein	-2.246684874	#N/A	#N/A
AT1G10586	AT1G10586	Basic helix-loop-helix (bHLH) DNA-binding superfamily protein	-2.199759191	#N/A	-3.276283645
AT4G30230	AT4G30230	Uncharacterized protein AT4g30230	-2.120468953	#N/A	#N/A
AT3G29635	AT3G29635	HXXXD-type acyl-transferase family protein	-2.103558566	#N/A	#N/A
AT3G04720	PR4	Hevein-like preproprotein	-2.100559033	#N/A	-2.312713424
AT3G49830	AT3G49830	P-loop containing nucleoside triphosphate hydrolases superfamily protein	-2.078622046	#N/A	-2.567701074
AT2G34770	T29F13.2	Dihydroceramide fatty acyl 2-hydroxylase FAH1	-2.023516218	#N/A	-3.67091839
AT5G43350	PHT1;1	Encodes an inorganic phosphate transporter Pht1	-1.967661235	#N/A	-2.324388077
AT5G47220	ERF2	Ethylene responsive element binding factor 2	-1.918381641	#N/A	#N/A

AT1G8084 0	WRKY40	Probable WRKY transcription factor 40	- 1.83460574 1	#N/A	#N/A
AT3G2324 0	ERF1	Ethylene-responsive transcription factor 1B	- 1.79699951 8	#N/A	- 2.00846795 5
AT2G3942 0	AT2G3942 0	alpha/beta-Hydrolases superfamily protein	- 1.71394794 5	#N/A	- 2.97978316 9
AT1G0680 0	F4H5_10	alpha/beta-Hydrolases superfamily protein	- 1.70442982 5	#N/A	#N/A
AT1G7206 0	AT1G7206 0	Serine-type endopeptidase inhibitors	- 1.69266782 5	#N/A	#N/A
AT4G1825 0	AT4G1825 0	Receptor serine/threonine kinase, putative	- 1.68142402 6	#N/A	- 3.06246201 3
AT1G6734 0	AT1G6734 0	HCP-like superfamily protein with MYND-type zinc finger	- 1.67494748 5	#N/A	#N/A
AT2G3014 0	UGT87A2	UDP-Glycosyltransferase superfamily protein	- 1.64323937 3	#N/A	#N/A
AT5G0560 0	AT5G0560 0	2-oxoglutarate (2OG) and Fe(II)-dependent oxygenase superfamily protein	- 1.60224200 1	#N/A	- 2.16578215 1
AT1G6956 0	MYB105	Transcription factor myb, plant	- 1.59977779 9	#N/A	- 2.47299753
AT3G2815 0	TBL22	Protein ALTERED XYLOGLUCAN 4-like	- 1.58512107 2	#N/A	- 1.96879437
AT5G6423 0	AT5G6423 0	1,8-cineole synthase	- 1.57988629 9	#N/A	#N/A
AT5G5655 0	OXS3	Uncharacterized protein At5g56550	- 1.53982201 6	#N/A	#N/A
AT2G4058 0	AT2G4058 0	Protein kinase superfamily protein	- 1.53975552 1	#N/A	- 1.87596265 5
AT5G1077 0	AT5G1077 0	Eukaryotic aspartyl protease family protein	- 1.53396461 4	#N/A	- 1.82044527 2
AT4G1026 5	AT4G1026 5	Wound-responsive family protein	- 1.52891055 2	#N/A	#N/A
AT1G7169 1	AT1G7169 1	GDSL-like Lipase/Acylhydrolase superfamily protein	- 1.52620164 9	#N/A	#N/A

AT5G27420	CNI1	E3 ubiquitin-protein ligase ATL6/9/15/31/42/55	- 1.491860199	#N/A	- 1.908477369
AT1G21326	AT1G21326	VQ motif-containing protein	- 1.482108739	#N/A	#N/A
AT5G11950	LOG8	Cytokinin riboside 5'-monophosphate phosphoribohydrolase LOG8	- 1.467876877	#N/A	- 3.085417955
AT1G73260	KTI1	Arabidopsis thaliana kunitz trypsin inhibitor 1	- 1.467643006	#N/A	#N/A
AT1G02460	AT1G02460	Pectin lyase-like superfamily protein	- 1.460764289	#N/A	- 2.445440334
AT1G61070	LCR66	Low-molecular-weight cysteine-rich 66	- 1.456418951	#N/A	#N/A
AT5G22870	AT5G22870	Late embryogenesis abundant (LEA) hydroxyproline-rich glycoprotein family	- 1.444358232	#N/A	- 2.796744834
AT5G42650	AOS	Allene oxide synthase, chloroplastic	- 1.426896554	#N/A	#N/A
AT1G54700	AT1G54700	Its function is described as molecular_function unknown	- 1.417632866	- 1.563427099	- 2.975415112
AT1G77380	AAP3	Amino acid permease 3	- 1.40827832	#N/A	- 1.601323286
AT1G31670	AT1G31670	Copper amine oxidase family protein	- 1.389592675	#N/A	#N/A
AT1G30270	CIPK23	CBL-interacting serine/threonine-protein kinase 23	- 1.383815116	#N/A	- 2.87127434
At2g47730	GSTF8	Glutathione S-transferase F8, chloroplastic	- 1.381620694	#N/A	- 2.47001152
AT1G29520	AT1G29520	Plasma membrane associated protein, putative	- 1.353192702	#N/A	- 2.76168187
AT1G17860	AT1G17860	Kunitz family trypsin and protease inhibitor protein	- 1.33561807	#N/A	#N/A
AT3G20570	ENODL9	Predicted GPI-anchored protein	- 1.326686156	#N/A	- 2.335011839
AT5G62350	AT5G62350	Plant invertase/pectin methylesterase inhibitor superfamily protein	- 1.320310509	#N/A	- 2.02467588

AT4G35170	AT4G35170	Late embryogenesis abundant (LEA) hydroxyproline-rich glycoprotein family	- 1.278307754	#N/A	- 2.112582069
AT4G30880	AT4G30880	Bifunctional inhibitor/lipid-transfer protein/seed storage 2S albumin superfamily protein	- 1.27317544	#N/A	#N/A
AT5G20510	AL5	PHD finger protein ALFIN-LIKE 5	- 1.265078269	#N/A	#N/A
AT5G59070	AT5G59070	UDP-Glycosyltransferase superfamily protein	- 1.260571385	#N/A	#N/A
AT3G15730	PLDALPHA1	Phospholipase D alpha 1	- 1.254476131	#N/A	- 1.948942864
AT5G15820	AT5G15820	Uncharacterized protein F14F8_200	- 1.237451533	#N/A	#N/A
AT1G26240	AT1G26240	Proline-rich extensin-like family protein	- 1.219535755	#N/A	#N/A
AT3G15080	AT3G15080	Polynucleotidyl transferase, ribonuclease H-like superfamily protein	- 1.212844451	#N/A	- 1.864469487
AT4G15680	AT4G15680	Thioredoxin superfamily protein	- 1.212111986	#N/A	- 1.521410659
AT5G41040	RWP1	Hydroxycinnamoyl-coa:&omega	- 1.198648753	#N/A	- 1.410381309
AT2G46170	AT2G46170	Reticulon-like protein B5	- 1.193463701	#N/A	- 2.981024105
AT1G63310	AT1G63310	Uncharacterized protein At1g63310/F9N12_7	- 1.184996722	#N/A	- 3.274655011
AT1G51400	AT1G51400	Uncharacterized protein F5D21.10	- 1.181260061	#N/A	- 2.698433561
AT1G10010	AAP8	Encodes a high affinity amino acid transporter	- 1.180293456	#N/A	- 1.394447326
AT4G16740	TPS03	Tricyclene synthase, chloroplastic	- 1.17990502	#N/A	#N/A
AT5G41590	AT5G41590	Lurp-one-like protein (duf567)	- 1.176517778	#N/A	#N/A

AT3G15450	AT3G15450	Aluminium induced protein with YGL and LRDR motifs	- 1.165506252	#N/A	#N/A
AT5G25930	AT5G25930	Protein kinase family protein with leucine-rich repeat domain	- 1.140429762	#N/A	- 1.468183971
AT1G07090	LSH6	Light-dependent short hypocotyls-like protein (duf640)	- 1.133176698	#N/A	#N/A
AT1G62770	AT1G62770	Plant invertase/pectin methylesterase inhibitor superfamily protein	- 1.131445592	#N/A	- 1.277094596
AT1G66540	AT1G66540	Cytochrome P450 superfamily protein	- 1.127069939	#N/A	#N/A
AT2G27690	CYP94C1	12-hydroxyjasmonoyl-L-amino acid 12-hydroxylase / fatty acid hydroxylase	- 1.11516194	#N/A	- 1.856799884
AT4G39730	PLAT1	Lipase/lipoxygenase, plat/lh2 family protein	- 1.11234901	#N/A	- 1.29816418
AT5G06860	PGIP1	Encodes a polygalacturonase inhibiting protein involved in defense response	- 1.111248838	#N/A	- 1.397478546
AT5G18850	AT5G18850	Low-density receptor-like protein	- 1.107166745	#N/A	-1.3209134
AT5G59790	AT5G59790	Protein of unknown function DUF966/UCP031043	- 1.102747358	#N/A	- 1.574423219
AT1G68840	RAV2	AP2/ERF and B3 domain-containing transcription repressor RAV2	- 1.100079165	#N/A	#N/A
AT5G51550	EXL3	Exordium like 3	- 1.095235341	#N/A	#N/A
AT1G15000	scpl50	Vitellogenic carboxypeptidase-like protein	- 1.092922464	#N/A	- 1.476134029
AT4G38540	AT4G38540	FAD/NAD(P)-binding oxidoreductase family protein	- 1.091482067	#N/A	#N/A
AT4G06536	AT4G06536	SPLa/Ryanodine receptor (SPRY) domain-containing protein	- 1.081137331	#N/A	- 1.632083308
AT3G52910	GRF4	Growth-regulating factor 4	- 1.078640763	#N/A	- 1.301549717
AT3G01680	SEOR1	Arabidopsis thaliana sieve element occlusion-related 1	- 1.078111209	#N/A	- 2.002927764

AT2G2664 0	KCS11	Encodes KCS11, a member of the 3-ketoacyl-CoA synthase family	- 1.07444687 5	#N/A	- 2.15392110 4
At5g58630	TRM31	TON1 Recruiting Motif 31	- 1.07201297 4	#N/A	- 2.07512894 6
AT3G5704 0	ARR9	Two-component response regulator ARR9	- 1.06721350 1	#N/A	- 2.87433217 1
AT4G1977 0	AT4G1977 0	Glycosyl hydrolase family protein with chitinase insertion domain	- 1.06439936 9	#N/A	#N/A
AT5G1369 0	CYL1	alpha-N-acetylglucosaminidase family / NAGLU family	- 1.06434005 6	#N/A	- 2.04687577 6
AT3G1599 0	SULTR3;4	Probable sulfate transporter 3.4	- 1.06387576 3	#N/A	#N/A
AT1G0997 0	RLK7	Leucine-rich receptor-like protein kinase family protein	- 1.05901607 7	#N/A	-2.0793158
AT5G0534 0	PRX52	Peroxidase superfamily protein	- 1.05361143 5	#N/A	- 1.59867249 8
AT5G2097 0	AT5G2097 0	HSP20-like chaperones superfamily protein	- 1.03894032 1	#N/A	- 2.59858564 1
AT4G0110 0	ADNT1	Solute carrier family 25 (mitochondrial phosphate transporter), member 23/24/25/41	- 1.03869434 3	#N/A	- 1.64376395
AT4G4006 0	HB16	Homeobox-leucine zipper protein ATHB-16	- 1.03033016	#N/A	- 1.13776010 4
AT2G4615 0	AT2G4615 0	Late embryogenesis abundant (LEA) hydroxyproline-rich glycoprotein family	- 1.01960793 1	#N/A	#N/A
AT1G3442 0	AT1G3442 0	Leucine-rich repeat transmembrane protein kinase family protein	- 1.01531667 2	#N/A	#N/A
AT3G4425 0	CYP71B38	Cytochrome P450, family 71, subfamily B, polypeptide 38	- 1.00390117 8	#N/A	#N/A
AT1G3032 0	AT1G3032 0	Uncharacterized protein At1g30320/T4K22_7	- 1.00230153 2	#N/A	- 1.87100371 1
AT1G1206 0	BAG5	BAG family molecular chaperone regulator 5, mitochondrial	- 1.00032409	#N/A	- 1.20496370 8

AT5G18970	AT5G18970	Plasma membrane associated protein-like	- 0.972095022	#N/A	- 2.671914904
AT1G61120	TPS04	(e,e)-geranylinalool synthase	- 0.95123494	#N/A	- 2.677627296
AT3G11600	AT3G11600	Uncharacterized protein At3g11600/T19F11_1	- 0.940751902	#N/A	- 2.179207821
AT2G21660	GRP7	Cold, circadian rhythm, and rna binding 2	- 0.939881559	#N/A	- 1.942111103
AT5G10625	AT5G10625	Flowering-promoting factor 1-like protein 2	- 0.933501094	#N/A	#N/A
AT1G69770	CMT3	DNA (cytosine-5)-methyltransferase CMT3	- 0.908916578	#N/A	#N/A
AT1G60870	MEE9	Uncharacterized protein F23C21.1	- 0.905608905	#N/A	- 2.008282512
AT3G22400	LOX5	PLAT/LH2 domain-containing lipoxygenase family protein	- 0.878247774	#N/A	- 2.324717697
AT5G54270	LHCB3	Light-harvesting complex ii chlorophyll a/b binding protein 3	- 0.848915657	- 1.777773633	- 2.627254284
AT3G59400	GUN4	Tetrapyrrole-binding protein, chloroplastic	- 0.843157815	#N/A	#N/A
AT1G06680	PSBP-1	Oxygen-evolving enhancer protein 2-1, chloroplastic	- 0.834447759	#N/A	- 2.03998268
AT3G26330	CYP71B37	Cytochrome P450, family 71, subfamily B, polypeptide 37	- 0.812137242	#N/A	- 2.401093181
AT1G48130	PER1	1-cysteine peroxiredoxin 1	- 0.806493419	#N/A	- 2.171412851
AT1G08380	PSAO	Photosystem i subunit psao	- 0.776451771	- 1.679243005	- 2.455975808
AT1G30380	PSAK	Photosystem i reaction center subunit psak, chloroplastic	- 0.77379511	#N/A	- 2.409956978
AT3G54890	LHCA1	Light-harvesting complex i chlorophyll a/b binding protein 1	- 0.756378746	#N/A	- 1.930278877
AT4G12800	PSAL	Photosystem i reaction center subunit xi, chloroplastic	- 0.755368668	#N/A	- 2.225971795

AT2G2714 0	AT2G2714 0	HSP20-like chaperones superfamily protein	- 0.74536585 6	#N/A	- 2.30404998 5
AT1G5567 0	PSAG	Photosystem I reaction center subunit V, chloroplastic	- 0.72620921 8	#N/A	#N/A
AT2G3462 0	AT2G3462 0	Mitochondrial transcription termination factor family protein	- 0.71713322	#N/A	#N/A
AT5G1723 0	PSY	Phytoene synthase, chloroplastic	- 0.68223064 2	#N/A	- 1.87298888 7
AT1G6774 0	PSBY	Photosystem II core complex proteins psbY, chloroplastic	- 0.65535867 2	#N/A	- 1.81816868 4
AT3G6147 0	LHCA2	Light-harvesting complex i chlorophyll a/b binding protein 2	- 0.65121344 8	#N/A	- 2.09232923 6
AT4G2470 0	AT4G2470 0	Uncharacterized protein F22K18.100	- 0.63130554 1	#N/A	- 1.66968463 7
AT4G2508 0	CHLM	Magnesium protoporphyrin ix methyltransferase, chloroplastic	- 0.62952405 5	#N/A	- 1.76777092 2
AT5G0153 0	LHCB4.1	Chlorophyll a-b binding protein CP29.1, chloroplastic	- 0.62916814 8	#N/A	- 1.89012079 3
AT5G2063 0	GER3	Germin-like protein subfamily 3 member 3	- 0.60917768 4	#N/A	- 2.09268238 9
AT2G4120 0	AT2G4120 0	Unknown protein	- 0.58865539 9	#N/A	- 2.48153220 2
AT4G1034 0	LHCB5	Chlorophyll a-b binding protein CP26, chloroplastic	- 0.57105364 3	#N/A	- 1.89479629 3
AT1G7604 0	CPK29	Calcium-dependent protein kinase 29	- 0.55705347 4	#N/A	#N/A
AT3G4743 0	PEX11B	Peroxisomal membrane protein 11B	- 0.55680638 5	#N/A	#N/A
AT1G4974 0	AT1G4974 0	PLC-like phosphodiesterases superfamily protein	- 0.54347681 3	- 1.23509404 5	- 1.77373238 7
AT1G0363 0	PORC	Protochlorophyllide reductase c, chloroplastic	- 0.51135983 9	- 1.39421318 4	- 1.90456898 1
AT1G3133 0	PSAF	Photosystem I reaction center subunit III, chloroplastic	- 0.47235845 6	#N/A	- 1.70491261 7

AT1G5537 0	NDF5	Ndh-dependent cyclic electron flow 5	- 0.45011171 3	#N/A	- 1.79843210 7
AT5G6404 0	PSAN	Photosystem I reaction center subunit PSI-N, chloroplast, putative / PSI-N, putative (PSAN)	- 0.43682902	- 1.41877023 5	- 1.85340519 7
AT3G2769 0	LHCB2.3	Light-harvesting complex ii chlorophyll a/b binding protein 2	- 0.42011216 8	#N/A	#N/A
AT1G2150 0	AT1G2150 0	Uncharacterized protein unannotated coding sequence from BAC F24J8	- 0.37766720 4	#N/A	#N/A
AT1G6095 0	FD2	2Fe-2S ferredoxin-like superfamily protein	- 0.36999990 6	#N/A	#N/A
AT4G2825 0	EXPB3	Expansin-B3	- 0.36417217 6	#N/A	#N/A
AT2G4284 0	PDF1	Protodermal factor 1	- 0.35620479 6	- 1.82043270 8	- 2.17164628 1
AT1G5223 0	PSAH2	Photosystem I reaction center subunit VI-2, chloroplastic	- 0.33217702 1	#N/A	#N/A
AT2G3676 0	UGT73C2	UDP-glucosyl transferase 73C2 (UGT73C2)	- 0.32879816 1	#N/A	#N/A
AT1G6152 0	LHCA3	Light-harvesting complex i chlorophyll a/b binding protein 3	- 0.31936708 1	#N/A	- 1.46623636 4
AT1G7902 0	AT1G7902 0	Enhancer of polycomb-like transcription factor protein	- 0.31652899	#N/A	- 2.49778515 5
AT1G7679 0	IGMT5	Hydroxy-3-indolylmethylglucosinolate O-methyltransferase	- 0.29593527 5	#N/A	#N/A
AT3G0243 0	AT3G0243 0	Transmembrane protein, putative (duf679)	- 0.29054307 8	#N/A	- 1.47114647 5
AT5G2394 0	PEL3	HXXXD-type acyl-transferase family protein	- 0.26868857	#N/A	#N/A
AT2G4043 5	AT2G4043 5	Uncharacterized protein At2g40435/T2P4.23	- 0.26833824 4	- 2.01818477 9	- 2.28373069 5
AT3G2674 0	CCL	Ccr-like protein	- 0.24266347 1	#N/A	#N/A
AT3G1308 0	ABCC3	Multidrug resistance-associated protein 3	- 0.23539363 3	#N/A	#N/A

AT3G62040	AT3G62040	Haloacid dehalogenase-like hydrolase (HAD) superfamily protein	- 0.230852968	#N/A	#N/A
AT1G60000	AT1G60000	RNA-binding (RRM/RBD/RNP motifs) family protein	- 0.230602564	- 1.265679189	- 1.49287615
AT5G13630	GUN5	Magnesium-chelatase subunit chlh	- 0.21971899	- 1.349955436	- 1.563836858
AT3G61250	MYB17	Transcription factor myb, plant	- 0.210316201	#N/A	#N/A
AT1G19150	Lhca6	Light-harvesting complex i chlorophyll a/b binding protein 2	- 0.193065043	#N/A	#N/A
AT3G50685	AT3G50685	Uncharacterized protein At3g50685/At3g50680	- 0.189717982	#N/A	#N/A
AT5G61480	PXY	Leucine-rich repeat receptor-like protein kinase TDR	- 0.175946061	#N/A	#N/A
AT3G04290	LTL1	GDSL esterase/lipase LTL1	- 0.159259483	#N/A	#N/A
AT3G48280	CYP71A25	Cytochrome P450, family 71, subfamily A, polypeptide 25	- 0.12276551	#N/A	#N/A

GO term enrichment for Cluster 8 carried out using ShinyGO (Ge et al. 2020).

Aspect	GO term	Enrichment FDR	No. genes	Pathway Genes	Fold Enrichment	Pathway	Genes
BP	GO:0080027	3.58E-05	4	16	54.53247	Response to herbivore	AT1G17860 TPS04 PR4 TPS03
BP	GO:0009769	0.016448	2	4	54.53247	Photosynthesis, light harvesting in photosystem ii	LHCB2.3 LHCB3
BP	GO:0009768	7.71E-12	9	19	49.07922	Photosynthesis, light harvesting in photosystem i	PSAO Lhca6 LHCA3 LHCB2.3 LHCA1 LHCA2 LHCB5 LHCB4.1 LHCB3
BP	GO:0009765	6.19E-09	9	35	26.29244	Photosynthesis, light harvesting	PSAO Lhca6 LHCA3 LHCB2.3 LHCA1 LHCA2 LHCB5 LHCB4.1 LHCB3

BP	GO:0009625	0.009233	3	32	24.53961	Response to insect	AT1G17860 KT11 TPS03
BP	GO:0009645	0.001477	4	18	23.37106	Response to low light intensity stimulus	LHCA3 LHCB2.3 LHCA1 LHCA2
BP	GO:0017003	1.01E-06	8	43	18.69685	Protein-chromophore linkage	Lhca6 LHCA3 LHCB2.3 LHCA1 LHCA2 LHCB5 LHCB4.1 LHCB3
BP	GO:0010218	0.003132	5	53	12.39374	Response to far red light	Lhca6 LHCB2.3 LHCA1 LHCB5 LHCB4.1
BP	GO:0009644	0.000939	6	59	11.68553	Response to high light intensity	LHCA3 PSBY LHCB2.3 LHCA1 LHCA2 LHCB3
BP	GO:0019684	2.68E-08	13	115	10.96271	Photosynthesis, light reaction	PSBP-1 PSAO Lhca6 NDF5 PSAG FD2 LHCA3 LHCB2.3 LHCA1 LHCA2 LHCB5 LHCB4.1 LHCB3
BP	GO:0015995	0.016448	4	38	10.90649	Chlorophyll biosynthetic process	PORC GUN4 CHLM GUN5
BP	GO:0015979	9.21E-13	21	225	10.10455	Photosynthesis	PORC PSBP-1 PSAO Lhca6 PSAK PSAF PSAH2 NDF5 PSAG FD2 LHCA3 PSBY LHCB2.3 LHCA1 LHCA2 LHCB5 PSAL LHCB4.1 GUN5 LHCB3 PSAN
BP	GO:0009637	0.004485	6	92	8.461935	Response to blue light	Lhca6 LHCB2.3 LHCA1 LHCB5 HB16 LHCB4.1
BP	GO:0009642	0.006841	7	134	6.223814	Response to light intensity	FD2 LHCA3 PSBY LHCB2.3 LHCA1 LHCA2 LHCB3
BP	GO:0009611	0.014969	7	182	5.253128	Response to wounding	AT1G17860 TPS04 KT11 WRKY40 CYP94C1 TPS03 AOS
BP	GO:0006091	0.000697	14	409	4.149209	Generation of precursor metabolites and energy	PSBP-1 PSAO Lhca6 NDF5 PSAG FD2 LHCA3 LHCB2.3 LHCA1 LHCA2 LHCB5 AT4G15680 LHCB4.1 LHCB3
BP	GO:0043207	0.019807	16	1226	2.521733	Response to external biotic stimulus	PSBP-1 RLK7 AT1G17860 LCR66 TPS04 KT11 CPK29 WRKY40 GRP7 GSTF8

							PR4 TPS03 AT4G38540 CNI1 AOS ERF2
BP	GO:0009455	0.009233	22	1369	2.304189	Oxidation-reduction process	PORC PSAO SRG1 AT1G31670 PER1 NDF5 PSAG FD2 CYP94C1 T29F13.2 GSTF8 LOX5 CYP71B37 CYP71B38 CYP71A25 AT4G15680 AT4G38540 PLAT1 PRX52 AT5G05600 GER3 AOS
BP	GO:0009628	0.010582	28	1785	2.016165	Response to abiotic stimulus	LSH6 Lhca6 CIPK23 PER1 FD2 LHCA3 PSBY RAV2 KTI1 GRP7 KCS11 AT2G46170 GSTF8 LTL1 AT3G11600 LHCB2.3 LHCA1 LHCA2 LHCB5 PLAT1 HB16 LHCB4.1 AT5G05600 AL5 GER3 CNI1 EXL3 LHCB3
CC	GO:0009503	9.09E-05	3	6	49.07922	Thylakoid light-harvesting complex	LHCB2.3 LHCB5 LHCB3
CC	GO:0009517	9.09E-05	3	6	49.07922	PSII associated light-harvesting complex II	LHCB2.3 LHCB5 LHCB3
CC	GO:0009538	9.09E-05	3	8	49.07922	Photosystem i reaction center	PSAF PSAH2 PSAL
CC	GO:0030076	9.09E-05	3	6	49.07922	Light-harvesting complex	LHCB2.3 LHCB5 LHCB3
CC	GO:0009522	3.09E-20	15	39	43.82073	Photosystem i	PSAO Lhca6 PSAK PSAF PSAH2 PSAG LHCA3 LHCB2.3 LHCA1 LHCA2 LHCB5 PSAL LHCB4.1 LHCB3 PSAN
CC	GO:0098807	7.09E-08	6	17	35.05659	Chloroplast thylakoid membrane	PSAG CCL LHCB2.3 LHCB5 LHCB3 PSAN

						protein complex	
CC	GO:0009521	3.60E-17	17	89	22.07267	Photosystem	PSBP-1 PSAO Lhca6 PSAK PSAF PSAH2 PSAG LHCA3 PSBY LHCB2.3 LHCA1 LHCA2 LHCB5 PSAL LHCB4.1 LHCB3 PSAN
CC	GO:0010287	2.11E-09	11	74	14.28231	Plastoglobule	PSAF PSAH2 LHCA3 LHCB2.3 LHCA1 LHCB5 PSAL PLAT1 LHCB4.1 AOS LHCB3
CC	GO:0009523	9.09E-05	6	64	11.15437	Photosystem ii	PSBP-1 PSBY LHCB2.3 LHCB5 LHCB4.1 LHCB3
CC	GO:0009535	1.57E-11	23	357	6.555297	Chloroplast thylakoid membrane	PORC PSBP-1 PSAO Lhca6 PSAK PSAF PSAH2 NDF5 PSAG LHCA3 PSBY CCL LHCB2.3 LHCA1 LHCA2 LHCB5 PSAL CHLM PLAT1 LHCB4.1 AOS LHCB3 PSAN
CC	GO:0055035	1.57E-11	23	357	6.555297	Plastid thylakoid membrane	PORC PSBP-1 PSAO Lhca6 PSAK PSAF PSAH2 NDF5 PSAG LHCA3 PSBY CCL LHCB2.3 LHCA1 LHCA2 LHCB5 PSAL CHLM PLAT1 LHCB4.1 AOS LHCB3 PSAN
CC	GO:0034357	2.31E-11	23	370	6.313323	Photosynthetic membrane	PORC PSBP-1 PSAO Lhca6 PSAK PSAF PSAH2 NDF5 PSAG LHCA3 PSBY CCL LHCB2.3 LHCA1 LHCA2 LHCB5 PSAL CHLM PLAT1 LHCB4.1 AOS LHCB3 PSAN
CC	GO:0042651	2.31E-11	23	370	6.313323	Thylakoid membrane	PORC PSBP-1 PSAO Lhca6 PSAK PSAF PSAH2 NDF5 PSAG LHCA3 PSBY CCL LHCB2.3 LHCA1 LHCA2 LHCB5 PSAL CHLM PLAT1 LHCB4.1 AOS LHCB3 PSAN

CC	GO:0009579	1.17E-09	24	494	4.871387	Thylakoid	PORC PSBP-1 PSAO Lhca6 PSAK PSAF PSAH2 NDF5 PSAG LHCA3 PSBY GSTF8 CCL LHCB2.3 LHCA1 LHCA2 LHCB5 PSAL CHLM PLAT1 LHCB4.1 AOS LHCB3 PSAN
CC	GO:0098796	1.35E-06	18	495	4.305195	Membrane protein complex	PSBP-1 PSAO Lhca6 PSAK PSAF PSAH2 PSAG LHCA3 PSBY CCL LHCB2.3 LHCA1 LHCA2 LHCB5 PSAL LHCB4.1 LHCB3 PSAN
CC	GO:0031984	1.00E-06	24	765	3.402372	Organelle subcompartment	PORC PSBP-1 PSAO Lhca6 PSAK PSAF PSAH2 NDF5 PSAG LHCA3 PSBY CCL LHCB2.3 CYP71A25 LHCA1 LHCA2 LHCB5 PSAL CHLM PLAT1 LHCB4.1 AOS LHCB3 PSAN
CC	GO:0009941	0.000783	16	591	2.845172	Chloroplast envelope	PORC PSBP-1 PSAF PSAG GSTF8 CCL LHCB2.3 LHCA1 GUN4 PSAL CHLM LHCB4.1 GUN5 PSY AOS LHCB3
CC	GO:0009526	0.000927	16	603	2.790574	Plastid envelope	PORC PSBP-1 PSAF PSAG GSTF8 CCL LHCB2.3 LHCA1 GUN4 PSAL CHLM LHCB4.1 GUN5 PSY AOS LHCB3
MF	GO:0004867	0.026956	2	15	54.53247	Serine-type endopeptidase inhibitor activity	AT1G17860 KT11
MF	GO:0004866	0.039296	2	23	32.71948	Endopeptidase inhibitor activity	AT1G17860 KT11
MF	GO:0030414	0.046412	2	24	27.26623	Peptidase inhibitor activity	AT1G17860 KT11
MF	GO:0061135	0.046412	2	24	27.26623	Endopeptidase regulator activity	AT1G17860 KT11
MF	GO:0016168	3.07E-08	8	30	26.17558	Chlorophyll binding	Lhca6 LHCA3 LHCB2.3 LHCA1

							LHCA2 LHCB5 LHCB4.1 LHCB3
MF	GO:0019904	5.49E-09	10	59	19.9509	Protein domain specific binding	PSBP-1 PSAL LHCA3 LHCA1 LHCA2 LHCB5 PSAL LHCB4.1 LHCB3 PSAN
MF	GO:0046906	4.97E-09	16	297	9.088745	Tetrapyrrole binding	Lhca6 LHCA3 CYP94C1 CYP71B37 LHCB2.3 CYP71B38 CYP71A25 LHCA1 GUN4 LHCA2 LHCB5 PLAT1 LHCB4.1 PRX52 AOS LHCB3
MF	GO:0004497	0.039296	6	207	5.008084	Monooxygenase activity	CYP94C1 CYP71B37 CYP71B38 CYP71A25 AT4G38540 AOS
MF	GO:0020037	0.028026	7	265	4.893939	Heme binding	CYP94C1 CYP71B37 CYP71B38 CYP71A25 PLAT1 PRX52 AOS
MF	GO:0005506	0.046412	6	225	4.461747	Iron ion binding	CYP94C1 T29F13.2 CYP71B37 CYP71B38 CYP71A25 AOS
MF	GO:0016491	0.039296	18	1202	2.207461	Oxidoreductase activity	PORC SRG1 AT1G31670 PER1 FD2 CYP94C1 T29F13.2 GSTF8 LOX5 CYP71B37 CYP71B38 CYP71A25 AT4G15680 AT4G38540 PLAT1 PRX52 AT5G05600 AOS

Appendix 5 – Primer design

Appendix 5.1 – EXPA8

Primer binding sites highlighted in yellow (forward primer) and green (reverse primer) on the read identified as EXPA8 by BLASTx. Sequence data from RNAseq experiment (Chapter 6).

```
>TRINITY_DN3823_c0_g2_i2 len=1017 path=[0:0-218 2:219-836 4:837-1016]
evgclass=main,okay,match:TRINITY_DN3823_c0_g2_i1,pct:100/60/.;
aalen=253,74%,complete;GCCACTCTTTCCTACCGTATTCTTGCAACAGAACCGATTTTCATACTTCTCCTCT
TCCCTCTGCAATGGCAGTTCAGAAAGTGTCTGTTCTATAATGCCATCTTCATCTTCTCTGCTTTCTTCTTAGGTGTC
ATCACAAACATCAATGCTGAGTCCTATGACTGGCAAGGAGGCCACGCCACCTTTTATGGTGGCGGCGATGCCA
CCGGGACTATGGGAGGGGCTTGTGGGTACGGCGGCCTATACAGCCAGGGCTATGGAACCAATACCGCCGCC
CTGAGCACCGCCCTCTCAACAACGGCCTCAGCTGCGGAGCCTGCTACGAAATGCGCTGTGATGATGACCCCA
AATGGTGCCTCCCGGGCTCCATCATCATCACCGCCACCAACTTCTGTCTCCAACTTTGCCAAAGCGAACGAT
GATGGTGGGTGGTGAATCCTCCTCTCCAGCACTTTGACATGGCCGAGCCTGCATTCTCCAGATTGCCAGT
```

ACCGTGCTGGAATCGTCCCGGTTGCTTCCGTAGGGTTTCG **TGCGTGAAGAAAGGAGGGAT** ATGGTTCACCAT
 CAATGGTCACTCCTACTTCAACCTTGTGCTGGTCTCAAACGTTGCTGGAGCCGGAGACGTTTCATGCAGTGTCCA
 TCAAGGGTCCAAGACCGGTTGGCAGGCGATGTCAAGGAACTGGGGCCAGAATTGGCAGAGCAATGGATAC
 CTC AACGGGCAGAGCCTCTCGTTTCAGGTGACTACCAGTGATGGAAGGACCATCACCAGCTACGATGTGGCG
 CCGGCTGGGTGGCAGTTCGGGCAGACCTACCAAGGAGGGTAGCTTTAGTTCTGAAGTTTGTATTAGGGTTTA
 CAATGCAGTTGTATTGGTGGCAGACAGAGTTGGGGTTATGAGAGATTCTGTTTAGTCATTATAGCTTATAGAT
 AGCTTGAATATATAACTCTTATTATAAGTTCACGGACAGGATAGAATGCATCGTCTCGATATTAAATTAT
 TTTGGTTGCAC

Product sequence:

CCTCCTCTCCAGCACTTTGACATGGCCGAGCCTGCATTCTCCAGATTGCCAGTACCGTGCTGGAATCGTCCC
 GGTTGCTTCCGTAGGGTTTCG **TGCGTGAAGAAAGGAGGGAT**

BLASTx results for expected product:

Gene description	Species	Max score	Total score	Query cover	E value	% Identity	Acc. length	Accession
expansin-A8-like isoform X2 [Abrus precatorius]	<i>Abrus precatorius</i>	86.7	86.7	98%	7e-20	100.0%	168	XP_027331520.1

Appendix 5.2 MYB21

Primer binding sites highlighted in yellow (forward primer) and green (reverse primer) on the read identified as unknown R2R3-MYB by BLASTx and later as MYB21 when aligned to *Arabidopsis thaliana* genome. Sequence data from RNAseq experiment (Chapter 6).

>TRINITY_DN2460_c0_g1_i3 len=1090 path=[2:0-428 4:429-558 5:559-560 7:561-1089]
 evgclass=main,okay,match:TRINITY_DN2460_c0_g1_i9,pct:100/74/.;
 aalen=237,65%,complete;ATATATTTGAATTCTCTACTGTTAAGAATACAGAATATTTAGAAAATGCATATAA
 TTTACATGAGTTAGGCCTTGCTTGGACTAAAGATTATGGGTGGCTCAAACGCTCCGATCACTTTGATTGTTAA
 AGCTAGATTAGGGTTTAAGCATATGCTAAGGAATACAAACCACTCATTCTTCTCTATAAAAACTACAACCAC
 CTTCTCCTCACCCACCCTCCAAACATTCTATATCTATCTTTCTCTCATGCTCAAGCCATCACTTCCACGTTGGA
 TGAAGCTAATACCATGGACAAGAGAGTGATCCCTGGTGGAGAAGAAGCGGA **GGTGAGGAAAGGACCATGG**
ACTATGGAGGAAGACCTCATCCTCATGAACTACATAGCCAACCATGGAGAGGGTGTCTGGAACACGCTAGCA
 AAATCCGCAGGACTGA **AGAGGACTGGGAAGAGTTGC**CGGCTCCGTTGGCTGAATTACCTCAGGCCTGATGTC
 CGTCGGGGAAATATAACACCGGAGGAGCAGCTCCTTATCATGGATCTTCACTCCAGATGGGGAAATAGATGG
 TCAAAAATCGCAAGGCAGCTACCAGGGAGGACCGACAATGAAATAAAGA ACTACTGGAGAACACGAATTCA
 GAAGAAAGTCAAGGGTGGAGAATCATCTGAATGCCATAATCCATGCTTTCTGATGAAGCTAGCACGAGCCA
 AGCGAGCGGAGTCGAAGTTATGGGAGCACAACCGAGTTACCTCCGCCGATACTACCAATCCTGAGGCATTT
 GGA ACTCCCTTTCCA ACTGAATCGAACGATAATTTCTGGGCCGACGATGAGTTCTGGGCTATGCAGTCTTTCAA
 TGGAGACTAAGAACTAAGAAATAAACCATCATCTTGCCATTGCCATGATGATGTTGGGGTTGCTTGCTCTAA
 GAATATAAGTGGTGTGCAATTTTATGGTGTACAAATGTCTAGCTATTATTATGCTTATAATGTAATATCATGT
 AATTGAACTTTATTGCTTTTCATGCTTGGTATGGGTATTGAGACGGCCCTAATATATTGTTAGGTCACTGTTTTA
 TTGCAAAAAAAAAA

Gene description	Species	Max score	Total score	Query cover	E value	% Identity	Acc. length	Accession
R2R3-MYB transcription factor [Lilium hybrid cultivar]	<i>Lilium</i> hybrid sp.	401	401	52%	2e-138	100.00	190	AMO43680.1

Appendix 5.3 PSII5

Primer binding sites highlighted in yellow (forward primer) and green (reverse primer) on the read identified as PSII5 by BLASTx. Sequence data from RNAseq experiment (Chapter 6).

```
>TRINITY_DN5555_c0_g1_i1 len=880 path=[0:0-879] evgclass=noclass,okay; aalen=131,45%,partial5-
utrbad;AACACCAAGAAATCAAAAATCAACTCTGGATCAGAGCTGGAGCCCTATCTATCAGTTCACCTCCCTCC
CTGATATACTTCCATGTGGCTTCTTCTGATAGGCTAGAAAGGATAAGGAACTACTGGAACCCTGCGCACTTG
GTCATATGATATCCAAAATCTATTATTTTCATCCATCCCGCTGCCATAGAGCTCCAACCTATTCCGGGCGGAGGA
CATCTTACCATAAGCATGGCATCGTTCACCATGACTGCCCCCTCTTCGTCGGAAGCTCACATCAACCAGAAGC
CTGCCCTAGGCCCGCGGACTCTCATTGTTGCCAAAGCTGCCGGAGTCGAAGGCCAGCAGGACACAGTGAAGG
CTGCCGGCAGTGTGACAAGGGGAGCAACGGGCGTAGGGCTGTGATGTTTGCTGCTGCGGCAGCTGCCATAT
GCACTATTGGGTGCGGTGTTTCAGGAGATGGCGAATGCCGAGGAGCTGAAAAGAGGGTGCCTGGAAGCGAA
GAAGAAGTATGCCCTGTGTGCGTTACCATGCCTACTGCTCGCATCTGTCGTTACTGATGCTGCTTATGTTAAT
TTGTATGCGCCTATATATGTTGTTTCGATATGGTTGGTAATTGTTGTTTGAAGGACATTGTATGTTTTTTCGTG
AATATTCGTTTCTTTTAAAGTATTATTGACTTTGCGGAATGAATAGTTCTAGATTCAACATGTTGGCAGCAGAG
CAGATACTGCTTCGTTGGAAGCATGCGGCTATAATCGCGGCCGTGCTTCCCCCTGTTAAGATGGGAGCAGAA
TTAGGGTTTTCTGGGTGTATTTTTTCCACTCTTGAATACAACATCCAATATATTCGGTAACAAGTACAATAAC
ATAAAG
```

Gene description	Species	Max score	Total score	Query cover	E value	% Identity	Acc. length	Accession
photosystem II 5 kDa protein, chloroplastic -like [Pisum sativum]	<i>Pisum sativum</i>	92.8	92.8	36%	2e-19	56.88%	107	XP_050899925.1

Appendix 5.4 – CWINV4

Sequence data taken from (Shi et al. 2018b).

```
CWINV4(TRINITY_DN251926_c3_g4_i1)
GAACTGGATCAATGATCCGAATGGCCCCATGTACTACAAAGGCATATATCATCTCTTCTATCAATATAACCCTA
AAGGAGCACAATGGGGCAATATAGTATGGGCTCATTCTATCTTTAGATCTCATTAACTGGGTGGCCCTCCA
ACCTGCTATCTACCCATCCAAACCATTTGACAGTAATGGGTGTTGGTTCGGGATCTGCCACCATCCGCCCTGGCA
ACAAACCTGCCATTCTCTACACAGGCATCGACCCCAACAACCGACAAGTTCAAAAACCTGGCCATTCCCAAGAAC
CTGTCAGACCCGTTTCTCCGTGTGTGGCTTAAGCCTGACTACAACCCAGTCATCAATCCGGGACCCGGGATCA
```

ATGCGACCGCCTTCCGTGACCCAACCTACCGCTTGGATGGGATCCGACGGGCATTGGCGGGTGGTGTGGGCA
 GTAGAAAGCCTGGGAAGTTGAGGGGTGAGGCCGTCTGTATAGGAGTCGGGATTTTGTGAAGTGGGTGAAA
 GCTAAGCACCCGTTGCACTCGATGCGGAACAGTGGGATGTGGGAATGTCCGGATTTTTCTGTGGCCGTGA
 CTGGGATGGAAGGGTTGGATACGTTCGGAGAACAGAGAGGGGGTGAAGCATGTGCTTAAGGTAAGCTTGGAT
 CTGAAGAGATTTGATTACTATACGATCGGGACGTACGATGCTAGCGAGGATCGGTATGTGCCTGACAAGAGC
 TCGGTTGATAATAGTACAGGGCTGAGATATGATTATGGTA

Gene description	Species	Max score	Total score	Query cover	E value	% Identity	Acc. length	Accession
cwINV1 [Lilium brownii var. giganteum]	<i>Lilium brownii</i>	494	494	99%	7e-171	92.16%	574	QNQ73363.1

Appendix 5.5 – AMY2

Sequence data from (Shi et al. 2018b).

>TRINITY_DN246719_c0_g2_i1

TGTTGTGAAATCAAATGCGGCACAAAGCCCTCCAGTATTGTCTATCCAGTTAATAATCCTTTGTCTGTGAGTAT
 CTTGATTGTAGTCCAGACGATTACTAGGTGGGCTGTAGCTGCAGTCATCCCAATATTCTCCACAGAGAATATA
 GGTTTCGACGATTCTATATATTCTTCGCAAACCTTGTGCATAACCTTTGCAAATCAAACGGAAATCCTTG
 AATCCAACGCTATTTCTAAGCCATTTCAACCAATTTATTATGTCTTCACGTACAAAGCTTTGTGTATGGTCTACG
 TTGGGAACTCCATCAAATTTGCACCAGTGCCTTTATTTCCAGTCCACCGGTACAAGAGGTTACAGCATGTTT
 ATCCATGGCAAGGGAATCCATCATAGCGATTGTATGCTCCCCATGTCCTTGAGTAGTCCCAACTCGATGGT
 TTATAACTAAGTCAGCCATCGGTCTAACTTTGTGCTGATGCATCTTTCTAGCAAGGTTTTAGTAGGCTTTCTG
 TTCCATAAGAAGAATCAAGGGAGTACAAATTCTGGGGTAGGTAACCTTCGCGAGATAATGAATGAGTTGCAG
 GAGGCAGCCATGCTGACGTAAATCCTGATTTAGCAAGATCTGCGATCTTTTCTCAAGATTCCTCCACCAATCA
 TTTTGTGAGATTCCCAATTGAAAGCCTGGAAAAGAATTTCTCTCCATTTTGGATGACACTACCCGCAGGAGA
 TCTGCTTCTGGGTTGTCATT

Gene description	Species	Max score	Total score	Query cover	E value	% Identity	Acc. length	Accession
probable alpha-amylase 2 isoform X2 [Elaeis guineensis]	<i>Elaeis guineensis</i>	434	434	99%	7e-150	79.76%	407	XP_019705838.1

Appendix 5.6 – SWEET7

Sequence data taken from (Shi et al. 2018b).

SWEET7(TRINITY_DN242720_c0_g2_i4)

CTGCATGCTGTGGGTGATGTACGGCCTCCAATAGTGCACCCCCACAGCACGCTGGTCTCACCATCAACGGC
 TCCGGCCTCATCATCGAGCTCACCTACGTCTTTCTCTTCTTCTACTCAACCGGACGTGCGAGGCTCCGAGTG
 CTCGCATTCTCCTAGCAGAGATCGCTTTGTTGGTGGCGTCTTCATCATCGTCATCGCTTCGGACACACCCAT

GATCGCAGGACTCTCATTGTTGGGATCTTCTGTGTATTCTTCGGGACCATGATGTATGTCGCTCCATTATCAGT
CATGAAATTGGTTCATCCAACTAAGAGTGTGGAATATATGCCACTTTTTCTCTCTGTGGCTTCTTCCCTCAATGG
TGTGGCTGGACGGCCTATGCCCTCATAAAATTCGACCTTTTCATCACGATCCCGAACGGGCTCGGAGTTATGT
TTGCAGTGGTTTCAGTTGATTTGTATGCGGTTTACTACAAATCGACTCAAAGGCAAATCGCAGATCGAAAGAC
GAAGACGGAGATGGGGCTGCCGGAGTGGTGGTGGCGATCGAAGATACCGGGAAGACTAGTAATGCTCCTC
CAAAGTATCTCGAGATGTCTGCAGTATGACCAACAAGTTGGGTTTGCCTGAAGAGGAAATAATTTCTCTCTC
TCTGTTGGGTCTTGTCTGAATGGGAAGTATCCCTCTCTTTCTCTTTGGTCTCAATTACTCAACTGTAGA
AGAGTTCTGTTGGAAAAAATAATAATGAAATTGGGAATGAAATTTCTTTTTCTTGCCTATATAAGGAG
TACTGAGGAAATTAAGAAATTGAGGCATGCATGATTACAATGGAACTTTTTATTACTCCCTGTCTTAAT
TCATTCTAGCCGTAATAAGGAAGCTTTTACCAACATCCAAAACATATGAACAGTTTACGGTTAGCCTCACC
AATTTCTCGAAGACGCCTCTTGCTTAGAGAATTGATGAATAAGTCAAGGATTATCTTTGGACTCTTTGATATC
AACTATTTGATCTTTATTTGATAGGAATATAAGAGAGCTTCGTATTATCCCTCTTGATGTAGATTTTTTAATCT
AATTGATAGAAGTAACATTGTCTTTGTATACCTCTTAATGTAACTTTCGTGGATCTAAATGATAGGAGCAATAT
TGCTTCTCTGTATTATTGTTGTCTAAAACTATTTAAGTATGAACATTTTCTGTGAGGTTTTGTGTCATATA
CC

Gene description	Species	Max score	Total score	Query cover	E value	% Identity	Acc. length	Accession
PREDICTED: bidirectional sugar transporter SWEET4-like [Musa acuminata subsp. malaccensis]	<i>Musa acuminata subsp. malaccensis</i>	265	265	46%	1e-82	71.43%	260	XP_009381769.1

Appendix 5.7 – ARF15

Sequence data from RNAseq experiment (Chapter 6).

>TRINITY_DN686_c1_g1_i2 len=2746 path=[0:0-570 1:571-705 2:706-2227 4:2228-2745]
evgclass=main,okay,match:TRINITY_DN686_c1_g1_i3,pct:100/100/.; aalen=797,87%,complete;

TTTTTTTTAAGATAATATTCGATCAATATCGTCATAAGATAACAGTAATAATGTTTGTGTTGCCTCCTAAGCAG
TGCTCGGTGACAAATCTATCCAGAACTACAAGGGTGCAGCTAGAAAAGTATACACCGATACAACTTTTACAC
GGACTCGGCAGCTGTGTTTAGGCATAATGATTGTGGTCTCCAGCCGCGCAAAAAGAGATCCTACTGAGC
AGAGAAAGCTCACCTCCATCCACCAACTCTGCTGCTACCCGCAGCATTCACTTTACCTCCGACTTGATGGAT
ATCGATCTCAACTGTGGAAGAGGAAGAGGAGGACGAGGGCGGCACTCCTGCCGCCGCTGCCTCTGACCAT
CTCCGCCGCTCGCTGGCCGGCGCCACGGTAGGGCTGGAGCTCTGGCAGGCCTGCGCCGGCCGACGGCGTCT
CTGCCAAAGAACGGCAGCGTCGTCGCTACTTACCGCAGGGGCATCTCGAGCTCCTCGGAGGCGGCGGCGG
GCCTTCCGCCGTGGCAGCCACCTCACGTCTTCTGCCCGTTGTGGCGTTCGAGCTCCACGTAAGTTCGTCGCT
TCCGTTTCTGCCCTTTTGGCGGAACTGCTAAGGGTGCCTCAAGGTCGGGGCAAATTATCTCTGGATGCCGA
GTCGAGAATTTGAATCGGTTTTCTGTGTGTATGACTCGGCGGCTGGTGGCTAATGGGTCCACAGACGAGGTTT
ATGCGCAGCTATCTCATTGCTGATGTTACAGCTGAGGAGGCTGAGAAGCAGTTGAGAGAGGGTGAGGTTG
GAAAAGAGGAGGAATCAGAGGATGTCAATGCTGTTAGCCGGTGCAGTCGATGCCCCACATGTTCTGCAAGA
CCCTCACCGCCTCGGACACAAGCACACATGGGGTTTTCTGTCCCTCGCCGAGCTGCCGAGGATTGCTTCCCC
TCCCTGGACTATAAGCAGCAAAGGCCATCGCAAGAAGTTGTTGCAAAAGATTTGCATGGCACCGAGTGGAGG

TTCAGACATATCTATAGAGGTCAACCACGAAGGCATCTTCTTACTACTGGATGGAGTGCATTTATTAATAAGAA
 AAAACTCGTCTCAGGGGATGCCGTA CTCTTTCTAAGGAGTGATGATGGAGA ACTCAGATTAGGAGTTAGGAG
 AGCAGCTCAAGTAAAGACCGTGATTTCTTATTCAATGATAGGTGGCCATGGCCGAAATCCTGGTACTACTGGCT
 GATGTAGCTGATGCAGTGTCCAAGAAAAGTGTGTTCCACGTCTATTATAACCCAAGGGCAAGCCAGTCAGAA
 TTATAATAACATACTCGAAGTTTTCAAGGAGCTAAGCCGTTGTTTTCCATTGGAATGAGATTCAAATGCAA
 ATTGAAAGTGAGGATGCAGCGGAGAAAAGGCATACAGGTTGGATAACCGGGATTGGCGACATGGATCCTGG
 CAGATGGCCTGGTTCTAAATGGAGATGCCTCTTGGTGAGGTGGGATGATGATTTAGATCCTAGTAGGAAAA
 TAGGGTATCTCCGTGGGAAGTAGAACTGGTTGGTTCCGTTTCCGTTCCGTTCTTAGTCCAAGAGAACCAAA
 ATCTCGCTGCCCTCAGCCGATTCCGATACTCCATTTCAAATGGAAGCGGGTATCCAGACTTCGAGGAATCCG
 AAAGGTTCCACAAGGTCTTGAAGGTCAAGAAATTATGCATTTAGTACCCCTTATGGTGGTATGGATGCAAC
 CAGTTCTCCGGTGTTCGAGACGAGAAATCATCGATGCCTCGAGAGAAGTGGTGTGGGAGTACAGGATTTTC
 GTACAATCGCCTAGGCTTTGGAGAACC GTTGGAGTTCCATAAGGTCTTGAAGGTCAAGAAATTTCCCGTTG
 GGTGTGCCATATCGAGGCACTCCAGTTGATGCTCAGAGCTTTGGTGCGGAAGCAGCTGGGCGCTACCGATC
 CAAGGATACAACGGTCTTATTCAGGCATCTTTACTTCTGCTCCAGTGTGCCTTCGTTCTCTGCTCTTCAACAA
 GTAGCTTCTAGTTTCGATACCCCTCAGTCATCTGGTGCAGGAGGGCTTGCTAAGAATGATTGTCACA ACTCTT
 GGGCCTTCTGATCATGCAAACTGTCTACCAGAAATGAAGCAGCTAGTCATTATCGACCCGATTATATGATGA
 ACACGCCCATCAATGAGAGATTCAAACAAGAAAAGTTGAAAGTGCAGAAAAGCTAGAATTGATCGGTCAGA
 ATACTGGCGAAAACAGTTGCAGACTTTTCGGTTTTCTTTAACTGAGAGAATTCCGATTTGCAACTTGGTTGAT
 GATACTCTGCCAGTGACACCGAAGACTATGGATATGAATTATGCGTCCTCGTCGCATATTCTGAGCTTCAAGA
 GTCAGCTGAACCTTCTGGGGACAGTCGCACTCAAGTGATCGACTTTTATGCTAGGAGTGCTATCAGAGGAGA
 GAATAACGAGCCAGGTTTACGAGCAACATCGTTTGTTCAGTGCTCGATGCGTAAACCTTATGGTGTGGATGG
 AGGTGATTCTAACCGAATTTCTACTTTGGTTCTTATGGATGTA AAAATGAAGGCTAATATTTTCATTTCAATCGA
 ACTTTGGCACAGTGTACTGTTGTGTTGAATTATGATAATTGTATGCTGTTTTCTTCTGGTCTTTTAATAAGTC
 ATGCTTTTTCTTATGATAATTGTACGCTGTTTTCTGCTGG

Gene description	Species	Max score	Total score	Query cover	E value	% Identity	Acc. length	Accession
auxin response factor 15-like isoform X1 [Asparagus officinalis]	<i>Asparagus officinalis</i>	607	607	82%	0.0	49.68%	780	XP_020265250.1

Appendix 5.8 – IAA14

Sequence data from RNAseq experiment (Chapter 6).

```
>TRINITY_DN2664_c0_g1_i3 len=1149 path=[0:0-964 2:965-1025 4:1026-1148]
evgclass=main,okay,match:TRINITY_DN2664_c0_g1_i1,pct:100/99/.; aalen=248,65%,complete;
```

GATCATTTAATTTGATATGACTCGCGTTAATCAGCGATGAGCATGGGTAGCGCTATGGCCCCGCTTTCCACCA
 CCTTCGTCCCCGGCAAACCCGCGGATTGTCCAGCTCATCTCTACAACACGTGTTCCGCCATAATTGGCCAGTG
 GCACAACGAATAACCATTATATCCATCAGCGTTGTCTGTTAGGCCCTCCCCGCATTATTTCTCTCCTCACTTC
 CTTTCAAAGCAAAGAAGAGAGAGACGAAGAGGATAGAGCTGTTCTGATTGAAGA ACTGAGAATTCTTGTGA
 GGGTAAGGTGGATTTCTGTCAATGGCTTGTGTAGTGCGGGCGGACAGGGATGAGCTAGTTCGAGGAGAC
 GGAGCTGAGGTTGGTCTGCCGGTGGTGGTGAGGTA CTGAATAGCAATGGGAAGAGGGGATTCATGGAG
 ACAATTGACTTGAAGCTCAAGCTTAACACTGCAGAGTCCAAGGATGTTGGATTGGAGACGGTGGCCTTCGAC
 AAGCTGAAGTGGCAGGCGAGCCAGAGTATACTCACTTCTAGCAAAAACCTGAGAAGCCA ACTGCTCCGAAG

GCGCAGGTTGTGGGTTGGCCACCCGTTGATCATACCGGAGGAACGTCATGACAGTCCAATCTGAGAAGGTA
AATAAGGACAAGTTAGAGAAGCCCAGCAACAATGCACCACCGACGGCCACATTTGTCAAAGTTAGCATGGAT
GGCGCACCTTATCTTCGTAAGGTGGACCTGAAGATGTATCGGAGCTACCAAGAGCTCTCAATTGCCTTAGAAA
AAATGTTCAAGCTCCCTCAACATGGAGAATTGTGGGTCTCAAGGAATGAATGGGAGGGATTTCATGAACGAGA
GCAAGTCTATGGATCTCTTGAATGGTTCTGAGTTCGTGCCAA^{CGTACGAGGACAAGGATGGA}GATTGGATGC
TGGTCGGAGATGTGCCATGGGAGATGTTCTGCTCATGCAAGCGCTTTCGGATCATGA^{AAGGGTCAGAAG}
^{CCATTGGA}CTAGCACCAAGAGCTATGGAAAAATGCAAGAGCAGAAGCTGAAGGGAGCACCTTGCAGTGTGA
GGAAGAAATGCCGAGCATGATTGTATTTGTGTTCTAATACTATATATATATATATATATATATATATATAT

Gene description	Species	Max score	Total score	Query cover	E value	% Identity	Acc. length	Accession
AUX/IAA protein [Dioscorea alata]	<i>Dioscorea alata</i>	353	353	64%	3e-118	73.49%	242	KAH7675124.1

Appendix 5.9 – MST6

Sequence data taken from (Lombardi et al. 2015).

>Lily_CTTGTA_L001_R1_001_BC19P1ACXX.filt_(paired)_contig_4538

TTTTTGTAAATAATTATGTGTGCTTCGGCATGGACGGAGAGGACGGTTCATCTTGCAATGTAGCATAAGATT
TCCGGTGAGGTCGAATAACCCTAGACTTGGTGGTTGTTCTCGTTGACGAACTGCCCCAGAACCAGTGTGCT
TCCACACGGAAGCCATCTCCTCAATTGGTATATTCTTCGTCTCAGGCAAGAACAAGGCGATGAATACCGTCATC
ACCGCCACCCATGTGCCAAGAAGTAGAAGAGCCCGAACTTCATATGGCACAACATCTGAA^{GGAACACTTGG}
^{GCAATGATGA}AGGTGAAGAACATGTNN
NNNNNNNNNNNNNNNNNNNNNTGAAGGTGAAGAACATGTTGACGGACTGTGATGCTCT^{GGCCAGCAGA}
^{CCTAATTTG}AGCGGGAAAATCTCGCTAGGGACCAACCATCCAAGTGGACCCAGGACCAGGCGAACCCCTGC
CACGTAAATGCAGATGAATGCCACCACATATGCAGCATACTCCTTGACAGGGACCCCTGGCCGGTGGTTCCA
AACTTGATCCCAATTAGCGTTCCTACAACGATCTGGCAGATCAACATCTGGGTCCCGCCTTGTAGGAAGAGNN
NN
NNNNNNNNNNNNNNNNNNNNACTCTTCGGCCAGCGCGTCAACGCTGACGATGGAGACGAAGGTGGCGGCGACATT
GACAACACCACTAATGACGGCGGACATGAGGGCCGCATCGTCGCCAAAGCCGATGGTCTTGAAGAGCACNN
NN
NNNGGA
TGCCATGGTGAAGTGGGGCGGTAAGTGGGCTCGAGGATGTTGACACGGGTGCTCGATCAATTTAGCCT
CCTGGCTGGCGACGACAAGATCGTCGTATTCCAGCTGGATTCATCAGTGCCACGGATCTTCTGAGCATTCC
TTGGCTAGCTCGTCGTGCCGCTCAATAAGGGAGTTGGGGGTGTCAGGCAGGCAGAGGGAGCCGATGGT
GATGATGCCGGCAGGCACGGCTGCAAGCGCCAAGCTTACACGCCACCCCGCCCTCGATCTTTGAGGT
GCCGTAATTGATGAGTTCCCGCGAAAATTCCGATGGTAATCATGAGCTGGAAGCCGATGTNNNNNNNNNN
NN
NN
GTAGAGTGGTACAGACTGGTTGGCAAAGCCTACCCACACCAAGGAGAAGGCGACCAAGAATGAGCATGA
GCACATTCTCGCGGCACCGTTTCAGAGCAGAGCCAACCAGGAAAGTTAGGCCTCCACCGAACATGGACCATT
TGCGACCGAAGACCCTAGTCACATTCGACGCAAAGAATGATGCGACCAAGCCGCGAGATAGAGCGATGAG
GTGAAGAGGGTCAACACGACGCTGTTGAATTTGCAGTATTGGTTGTCGCTCACATTCTTGTGCTTGCTTGA
CACATTCGGGAAGAAGTATTGATTAGAAATGAGTCCATTGATGTCACACCCCTGAAATTCGAATATCGTAACCG

AAGATCAGCCCTCCAGACGAGGGCACCAGGCATGCCATGAAAACGAAAAGGGTCATCTTCCCCGGATAATCT
 CTA CTACTGCTATTAACGACTATCGCGCCTCCCGCCATTGCTACGCACTAGTACTTAGTACTATTATTAGTATTTTAA
 TGATTATTATTATTATTAGAACCGGATGCCGAAGGCCTACCCGCTCCCCCTAGGATGGAACACACTACAGAGC
 GCAGAGGAGGTTGG

Gene description	Species	Max score	Total score	Query cover	E value	% Identity	Acc. length	Accession
sugar transport protein MST6-like [Elaeis guineensis]	<i>Elaeis guineensis</i>	600	719	86%	0.0	63.39%	512	XP_010936607.1

Appendix 5.10 – ORR9

Sequence data taken from (Lombardi et al. 2015).

>Lily_CTTGTA_L001_R1_001_BC19P1ACXX.filt_(paired)_contig_2644

GGAAACAAAGCTCTGGAGTTTCTCGG **GTTGGTAGATGATGGCTGCG** GAACAAATTTAGCTTCTGTCACCTTCTG
 ATCAACATGAAATTGAGGTTAATCTGATAATTACAGACTACTGTATGCCGGCATAACAGGCTA **TGAGCTGCT**
GAAGAGAGTCA AGAAATCTTCATCTCTCCGAGATATTCCGGTTGTCATCATGTCATCCGAGAATGTGCCCTCCA
 GGATCAATAGATGCTTGGAGGAAGGAGCAGAGGAATTTTTACTGAAACCGGTACGATTGTCAGACATGAATA
 AGCTCAGGCCTCGTGTATTGAAAGGGAAATCCAATGAGCAGCGGCAAGAAAGTAGTGTTGTCTTGACCGCAA
 GCAATAAAAGGAAGGCTACAGATGAAGGAATTTCCCATGAGAGGAAGAGGTCAAGATTAGTTACTAATCTGG
 CATT

Gene description	Species	Max score	Total score	Query cover	E value	% Identity	Acc. length	Accession
two-component response regulator ORR9 [Elaeis guineensis]	<i>Elaeis guineensis</i>	196	196	100%	1e-60	64.29%	193	XP_010931988.1

Appendix 5.11 – SAUR75

Sequence data taken from (Shi et al. 2018b).

>TRINITY_DN6323_c0_g1

ATCTCATCCTTAGCCGCTTGGCATCCCTCCAGTCTCCACACCAAAACAATGCTAAGCAGAAAGAGGCTTCTCCA
 GATGGTTAGAAGATGGCATGAATTGGCTTCAATGAGGAGGAGAAGAATCATTCTAGTAGCAAAGAGCTGAA
 ACAATGTAAGTCTGCATCAATTGCGCAGAAAGGTCATCTCTTCAT **GTACACCATCGACGGAAAGC** GTTTCATG
 GTTCCGCTCGAATACCTGACTAGCAATATCTTCAGAGAGCTCTTAAGGTTATC **TGAAGAGGAGTACGGGTTGC**
 CGAGTGGGCCAATTAGGTTGCCTTGTGATGCCGCAAGCATGGTGTACATCATCTCCTTGCCACTGGGAAACAA
 TTGTAGGGACATGGAAATGGCTGTTCTTGCATCCATTGCTAATGGTCACTGTAAGTCTGCTTTGGCTCCAGA

Gene description	Species	Max score	Total score	Query cover	E value	% Identity	Acc. length	Accession
PREDICTED: auxin-responsive protein SAUR64-like [Musa acuminata subsp. malaccensis]	<i>Musa acuminata</i> subsp. malaccensis	139	139	88%	5e-39	57.89%	145	XP_009383463.1

Appendix 5.12 – YUC3

Sequence data taken from RNAseq experiment in Chapter 6.

>TRINITY_DN10715_c0_g1_i2 len=1666 path=[0:0-785 2:786-1156 4:1157-1665]

evgclass=main,okay,match:TRINITY_DN10715_c0_g1_i3,pct:100/96/.; aalen=404,72%,complete;

TCCTCCAATCCTCTCACCTCTCCCTTTCACTGTCACTTTCTCCCTCTTCAAGAACCAACCCCTCTCCTTGTCAAA
 ACACTTCTAGTCACCAACTTAAACCTCTTCTCCCCTTTACCAAGTACTCCTACACTACTCACACAATTCTACCAT
 GGCCCGAACACCACCTCGCTGCGTGTGGGTGAACGGCCCGATAATCGTCGGAGCAGGCCCTTCCGGCCTAGC
 AACTGCTGCCTGCCTGAAGGAGCAGGGTGTCCCTTTCGTGATCGTCGAGCGAGCTGACTGCATTGCCTCCCTT
 TGGCAAAGCGAACCTACGACCGGTGAAGCTCCACCTACCAAGCAGTTCTGCCAGCTCCAAAGCTCCCTT
 TCCCTGAAGACTATCCAGAGTACCCACAAAGCAGCAGTTTCATCGATTACTTGGAGTCATACGCCAAGCAATT
 CGAGATCAGCCCTGACTTCAACAGTCCGTGCAGTCAGCACGGTACGATGAGACTTGGGTTTGTGGCGAGT
 GAGAACTTCTCCATTGATGGCTCTGAGACCGAGTATCTCGACGGTGGCTGGTCGAGCCACCGGGGAGAA
 TGCCGAGAAGGTGATCCCTCATATGGAGGGAATGACTGAGTTTGGTAGCGATGTGACACATGTTTGTGACTA
 CAAGTCTGGCGAGATGTACCGAGGGAAGCGAGTTCTGGTGGTCGGCTGTGGAACTCCGGTATGGAAGTCTC
 CCTCGACCTCTGTGACCACAATGCCTTCCCTTCAATGGTTGTTTCGTGACTCGGTTTCATGTATTGCCTAGAGAGG
 TTTTCGGTAAATCTACATTTAGACCGCGGTGATCCTTTGAAATGGCTACCTCTGTGGCTTGTGGACAAGATT
 ATTCTGGTTCTGGCATGGTTGGTTCTTGGGGACATCAAGAAGTACGGGCTCAGGCGGCCAGAGA **CTGGGCCT**
CTAGAGCTGAAGAACACGCAGGGGAGAACACCGGTTTTGGATATCGGGACTCTGAGCAAGATTAAGTCTGGA
 GAAATCAAGATAGTCCCTGGCGTCAAGAGTTCTCCA **CAGGGAGAGTCGAGCTGATC**GATGGCAGCATACTA
 GACATCGATTCAATCATTCTAGCTACTGGGTACAGGAGCAATCTCCCTTCATGGTTACAGGGAAGTATTCTT
 CTCGAAAGACGGGTACCCAAGAATGGAATCCCAAATGGTTGGAAAGGGGAATCAGGGTTGTATGCAGTTG
 GGTTCACTAAGAGGGGACTCTCTGGTGCATCCTCGGATGCTGTGAGGACCGCTGAGGACATTGGCAAGGTGT
 GGAAGGAGGAAACAAATCAGCCAGAAGTTGATTGCTTGCAATAAAAGATGATTCTCAGAAAAGTGTGAC
 GAAGTCGCTAACCTAGTCCCTCTGATTTTTGATTTTGTCTTTTATTTTGGTAGGACTGATTATACAATTATG
 TGAGTAATCAGAAAAAATAAAATAAAGAAAGGGTGTGAGCGCTCTTCATTAGAGCCCAAGTTTTGAAC
 CAGTAATGGGCCTTGTGTATAGAGGACTGGTGATTATGATGAGGCTTTTCCCTTTAGGGGAACCTTTGTACAT
 GCTTTCTAATCATTACTATATGAATAAAAGTAACATTTTCTGTAAAAA

Gene description	Species	Max score	Total score	Query cover	E value	% Identity	Acc. length	Accession
probable indole-3-pyruvate monooxygen	<i>Phoenix dactylifera</i>	668	668	72%	0.0	79.66%	423	XP_008807966.3

ase YUCCA5 [Phoenix dactylifera]								
--	--	--	--	--	--	--	--	--

Appendix 5.13 – AHP2

Sequence data taken from RNAseq experiment in Chapter 6.

```
>TRINITY_DN688_c0_g1_i2 len=1093 path=[1:0-827 2:828-836 3:837-930 4:931-1037 5:1038-1092]
evgclass=main,okay,match:TRINITY_DN688_c0_g1_i4,pct:100/100/.;
aalen=224,61%,complete;TTTTTTTTTAGGTACGACAAAAGTTGTGTCCTTGGCCCCGTATATTATATTTCTCC
ACCGATAGGGGGCCCTGCCGAAACTTTTGTTCCTCTGTTATACCTCATGTTTATCTTCACCCCAAGCTGGGG
GCTATGAACATTACAATTAGAAGACGACCGCAACATCTTGAAAACATACAAACAGAAATCAAGCTAAACAAAA
TTGTTCCATCACCATTATATAATAAAAGGCCACAACAGTCTAGACACCAAATCCTCATCTCCATCTTGCATTCA
CATAAACACAGTTCACAGCAGTTTGTATATTAATGGTATAAATCTGAATAAGAAACCAGCACCAGTCAAATTC
AGATTCTCCCCATCTTCAACTTTTGTACTACTGAGTTCTACCTTCATAGAATTTGATCCTCTGTTCAGCTGCAAC
ATGGTGTCAAAGTTGCTTCGTATAAGATAGAAGTACTGATTCTTGATAGCATTCAAAGCCATTGGCAGACTTTCTTT
ATTATTCTGCTCACTCAACTGTCGGAAGTGGAAAGCAAGCAATGCTCATGTTACGAACACCCCACTTGCCTGC
TGCTTTTCATCTGATGCACATGAGCATCCACCTTCTCATAATCCACAACAGGCTGCTCCATCAGCGCCATCAGCT
CCTTCAAGATCCGCTCAGCATCATCACAGAACAATCCTATCACCTCCGCCACGAACCCCGGGCAGCTTGAATCC
TGCAGCATCTGGAGCTGCGTGAAGTGTCTCATCCAGCAGCCCCTCCGCGAGCATCGAGTTGATGAGGGCGCTG
TGCTGCTCCTTGAGCGCTGCCACCGCCGCCACCGCCGCCATTGATCGAGGAGAAAGAGAAAGGGAGGCGGG
GAATTGGATGCTGAGGGGGGAGTGGGTGGGGAGGTGGGAATCTGGGGTTTTAAATAATGGAAAGGGGCGG
AGAGATGCAGAGAACAAGTGTGATAACTCCGAGACTGCGAGGTCACGCAGGGTGCCTGTGGCCGTT
GTTGCCCGCGCTTTTCTCGAAGCTGCCTGGAGTTTCACTGGGCATCCGGATGGACTGCAGTTAATTATACTGAC
TTTAGTGACC
```


Appendix 6 – statistical test results

6.1. Negative binomial generalised linear mixed model (GLMM) to identify significant differences between epidermal pavement cell growth between Stages 1-5 in different parts of the tepal in Oriental lilies

Generalized linear mixed model fit by maximum likelihood (Laplace Approximation) [`glmerMod`]
 Family: Negative Binomial(23.5912) (log)
 Formula: Area ~ Number + Tepal + Position + Location + Side + Position:Side + Side:Location + Tepal:Position + Tepal:Number + Number:Position + Number:Side + Number:Location + Location:Tepal + Side:Tepal + Position:Location + (1 | Tepal_ID/Section_ID)
 Data: dat

AIC	BIC	logLik	deviance	df.resid
11789.8	11980.3	-5852.9	11705.8	648

Scaled residuals:

Min	1Q	Median	3Q	Max
-2.3495	-0.6710	-0.0261	0.6286	3.5487

Random effects:

Groups	Name	Variance	Std.Dev.
Section_ID:Tepal_ID	(Intercept)	2.391e-02	0.1546250
Tepal_ID	(Intercept)	1.051e-08	0.0001025

Number of obs: 690, groups: Section_ID:Tepal_ID, 115; Tepal_ID, 5

Fixed effects:

	Estimate	Std. Error	z value	Pr(> z)	
(Intercept)	7.69628	0.12257	62.791	< 2e-16	***
Number2	0.67994	0.14041	4.843	1.28e-06	***
Number3	1.13238	0.13645	8.299	< 2e-16	***
Number4	1.17586	0.13560	8.672	< 2e-16	***
Number5	1.35497	0.13566	9.988	< 2e-16	***
TepalOuter	0.04975	0.10274	0.484	0.62822	.
PositionMid	0.04064	0.11980	0.339	0.73446	.
PositionTop	0.22594	0.11959	1.889	0.05884	.
LocationMidrib	0.27120	0.10293	2.635	0.00842	**
SideAD	-0.47503	0.10233	-4.642	3.45e-06	***
PositionMid:SideAD	-0.05838	0.08164	-0.715	0.47458	.
PositionTop:SideAD	-0.01162	0.08093	-0.144	0.88584	.
LocationMidrib:SideAD	0.01314	0.06619	0.198	0.84266	.
TepalOuter:PositionMid	0.19980	0.08182	2.442	0.01461	*
TepalOuter:PositionTop	-0.08794	0.08098	-1.086	0.27753	.
Number2:TepalOuter	-0.08045	0.10620	-0.758	0.44872	.
Number3:TepalOuter	-0.08638	0.10662	-0.810	0.41785	.
Number4:TepalOuter	-0.43181	0.10328	-4.181	2.90e-05	***
Number5:TepalOuter	-0.53676	0.10326	-5.198	2.02e-07	***
Number2:PositionMid	-0.17906	0.13308	-1.346	0.17844	.
Number3:PositionMid	-0.25394	0.13009	-1.952	0.05093	.
Number4:PositionMid	-0.20438	0.12741	-1.604	0.10867	.
Number5:PositionMid	0.08843	0.12732	0.695	0.48732	.
Number2:PositionTop	-0.10456	0.13012	-0.804	0.42164	.
Number3:PositionTop	-0.22411	0.13025	-1.721	0.08531	.
Number4:PositionTop	-0.14018	0.12741	-1.100	0.27124	.
Number5:PositionTop	-0.20000	0.12734	-1.571	0.11628	.
Number2:SideAD	0.33850	0.10643	3.180	0.00147	**
Number3:SideAD	0.22870	0.10677	2.142	0.03220	*
Number4:SideAD	0.26260	0.10329	2.542	0.01101	*
Number5:SideAD	0.43515	0.10326	4.214	2.51e-05	***
Number2:LocationMidrib	-0.06276	0.10664	-0.589	0.55617	.
Number3:LocationMidrib	-0.19940	0.10677	-1.868	0.06182	.
Number4:LocationMidrib	-0.16824	0.10329	-1.629	0.10334	.
Number5:LocationMidrib	-0.25192	0.10326	-2.440	0.01470	*
TepalOuter:LocationMidrib	0.03253	0.06626	0.491	0.62344	.
TepalOuter:SideAD	0.05187	0.06626	0.783	0.43371	.
PositionMid:LocationMidrib	0.17099	0.08158	2.096	0.03608	*
PositionTop:LocationMidrib	0.14186	0.08096	1.752	0.07975	.

 signif. codes: 0 '***' 0.001 '**' 0.01 '*' 0.05 '.' 0.1 ' ' 1

6.2. Negative binomial generalised linear mixed model (GLMM) to identify significant differences between epidermal pavement cell growth between Stages 1-5 in different parts of the tepal in *L. longiflorum*.

```

Generalized linear mixed model fit by maximum likelihood (Laplace Approxim
ation) ['glmerMod']
Family: Negative Binomial(18.6468) ( log )
Formula: Area ~ Number + Tepal + Position + Location + Side + Tepal:Number
+
  Number:Position + Number:Side + Number:Location + +(1 | Tepal_ID/Secti
on_ID)
Data: dat

```

```

      AIC      BIC   logLik deviance df.resid
11357.8 11512.9 -5644.9 11289.8     674

```

```

Scaled residuals:
  Min       1Q   Median       3Q      Max
-2.4033 -0.6401 -0.0602  0.5530  3.7222

```

```

Random effects:
Groups              Name          Variance Std.Dev.
Section_ID:Tepal_ID (Intercept) 2.955e-02 1.719e-01
Tepal_ID            (Intercept) 7.407e-09 8.606e-05
Number of obs: 708, groups: Section_ID:Tepal_ID, 118; Tepal_ID, 5

```

```

Fixed effects:
              Estimate Std. Error z value Pr(>|z|)
(Intercept)    7.490022   0.098158  76.306 < 2e-16 ***
Number2         0.271355   0.141434   1.919 0.055035 .
Number3         0.581844   0.149888   3.882 0.000104 ***
Number4         0.760485   0.138768   5.480 4.25e-08 ***
Number5         1.217351   0.138948   8.761 < 2e-16 ***
TepalOuter     0.024782   0.080247   0.309 0.757458
PositionMid    -0.281534   0.098265  -2.865 0.004169 **
PositionTop    -0.225144   0.196842  -1.144 0.252715
PositionTop    -0.302199   0.098546  -3.067 0.002165 **
LocationMidrib 0.229332   0.080367   2.854 0.004323 **
SideAD         -0.033953   0.080389  -0.422 0.672766
Number2:TepalOuter -0.207476   0.114988  -1.804 0.071180 .
Number3:TepalOuter 0.198354   0.114989   1.725 0.084532 .
Number4:TepalOuter 0.018520   0.113431   0.163 0.870306
Number5:TepalOuter -0.150799   0.113424  -1.330 0.183677
Number2:PositionMid -0.054666   0.138949  -0.393 0.694006
Number3:PositionMid 0.090660   0.141744   0.640 0.522431
Number4:PositionMid 0.053707   0.138909   0.387 0.699027
Number5:PositionMid -0.004159   0.138883  -0.030 0.976112
Number2:PositionTop -0.135037   0.221794  -0.609 0.542631
Number3:PositionTop -0.464794   0.221795  -2.096 0.036117 *
Number4:PositionTop -0.208110   0.219993  -0.946 0.344157
Number5:PositionTop -0.245009   0.219975  -1.114 0.265362
Number2:SideAD   -0.059882   0.115111  -0.520 0.602916
Number3:SideAD   0.022002   0.115104   0.191 0.848408
Number4:SideAD   -0.041042   0.113531  -0.362 0.717719
Number5:SideAD   0.012895   0.113523   0.114 0.909564
Number2:LocationMidrib 0.027777   0.115119   0.241 0.809331
Number3:LocationMidrib 0.014003   0.115075   0.122 0.903148
Number4:LocationMidrib 0.058391   0.113513   0.514 0.606973
Number5:LocationMidrib -0.139032   0.113492  -1.225 0.220561

```

```

---
Signif. codes:  0 '***' 0.001 '**' 0.01 '*' 0.05 '.' 0.1 ' ' 1

```

The GLMM data shown above in Appendix 6.1 and 6.2 was used to create model prediction lines (Figure 8.2) which show the effect of various factors of interest (region of tepal: inner/outer, top/middle/base, adaxial/abaxial face and midrib/edge) on the change in epidermal pavement cell area over the five stages of development. Significant differences were identified for Oriental lily only, showing significant effects of outer/inner tepal, adaxial/abaxial and edge/midrib on the change in cell area.

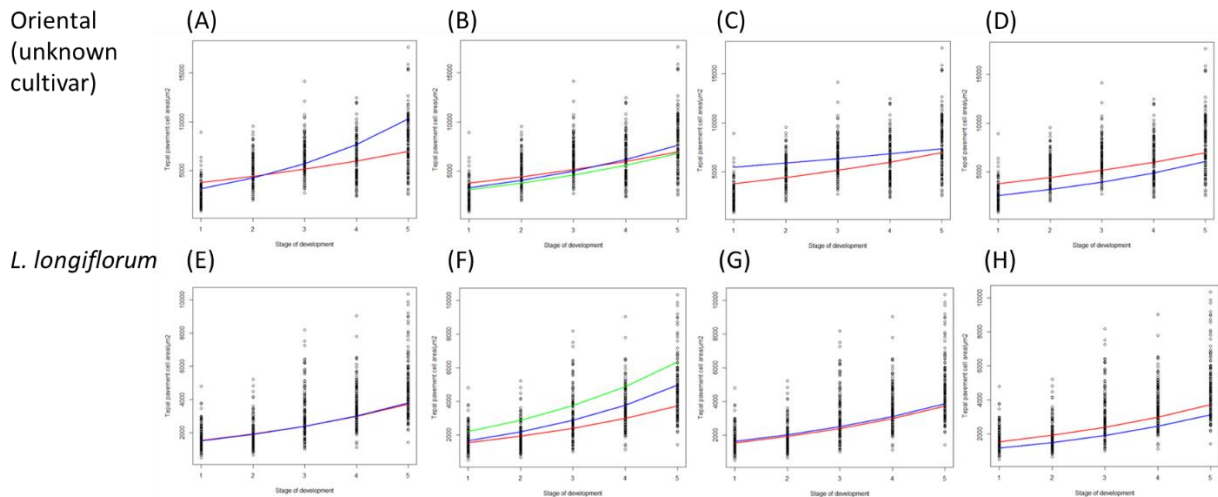


Figure 8.2 – Model prediction lines from negative binomial GLMM looking at effect on tepal pavement cell area change over development of (A, E) outer (red) or inner (blue) tepal, (B, F) position on tepal – top (red), middle (blue), or base (green), (C, G) adaxial (red) or abaxial (blue) side of tepal, and (D, H) midrib (red) or edge (blue). Data shows spread of cell area as individual points at each stage of development. Significant effects are observed where the gradients differ, here only significantly so in 4A, C and D.

6.3. Individual unpaired T-test/Mann-Whitney U test result values comparing OP to CT fold change between Stage 1 and 5 in epidermal pavement cells at different areas on the tepal.

Area on tepal	Test	Degrees of freedom	T-value/W value	P-value
OTM	T-test	13.426	1.1113	>0.05
OTE	T-test	9.4273	2.2977	<0.05
ITM	T-test	13.878	-2.4121	<0.05
ITE	T-test	10.006	0.43707	>0.05
OMM	T-test	8.2149	5.2176	<0.05
OME	T-test	8.2352	5.0426	<0.05
IMM	T-test	9.9761	-0.41633	>0.05
IME	T-test	12.647	-7.2275	<0.05
OBM	Mann-Whitney U	n/a	55	>0.05
OBE	T-test	15.976	-1.1113	>0.05
IBM	T-test	13.932	-0.77	>0.05
IBE	T-test	9.8068	-0.30241	>0.05

6.4. ANOVA to identify differences between the epidermal pavement cell area growth rate according to tepal region and stage of development

Figure	Factor	Degrees of freedom	F value	P value	Post-hoc Tukey test
3.xA - OP	Tepal region	5	11.352	<0.05	IME-IBE: >0.05 ITE-IBE: >0.05

	Stage	2	71.007	<0.05	OBE-IBE: >0.05 OME-IBE: <0.05
	Region:Stage	10	4.706	<0.05	OTE-IBE: >0.05 ITE-IME: >0.05 OBE-IME: >0.05 OME-IME: <0.05 OTE-IME: >0.05 OBE-ITE: >0.05 OME-ITE: <0.05 OTE-ITE: >0.05 OME-OBE: <0.05 OTE-OBE: >0.05 OTE-OME: <0.05
3.xB - CT	Tepal region	5	2.911	<0.05	IME-IBE: >0.05 ITE-IBE: >0.05
	Stage	2	86.505	<0.05	OBE-IBE: >0.05 OME-IBE: >0.05
	Region:Stage	10	1.988	>0.05	OTE-IBE: >0.05 ITE-IME: >0.05 OBE-IME: >0.05 OME-IME: >0.05 OTE-IME: >0.05 OBE-ITE: >0.05 OME-ITE: >0.05 OTE-ITE: >0.05 OME-OBE: >0.05 OTE-OBE: >0.05 OTE-OME: >0.05

6.5. Linear mixed model to identify significant differences between bud opening in 'Tisento' OP vs CT buds, in particular looking at the factors of position on stem or number of buds per inflorescence. ANOVA was used to identify significant p-values in the table below.

Fixed effects:

	Estimate	Std. Error	t value
(Intercept)	4.0704	1.1325	3.594
TreatmentOP	-1.2180	1.9801	-0.615
No.stem	-0.3179	0.3497	-0.909
Position	1.2470	0.1172	10.643
TreatmentOP:Position	0.2530	0.1544	1.638
TreatmentOP:No.stem	-0.2202	0.5869	-0.375

	Chisq	Df	P-value	Significance
Treatment	17.7155	1	2.565e-05	Yes

No. of buds per stem	1.9893	1	0.1584	
Position on stem	333.0781	1	< 2.2e-16	Yes
Treatment:Position	2.6842	1	0.1014	
Treatment: No. buds per stem	0.1408	1	0.7075	

6.6. Linear mixed model to identify significant differences between bud opening in ‘Eyeliner’ OP vs CT buds, in particular looking at the factors of position on stem or number of buds per inflorescence. ANOVA was used to identify significant p-values in the table below.

	Estimate	Std. Error	t value
(Intercept)	1.78101	0.87340	2.039
TreatmentOP	1.30682	1.16064	1.126
No.stem	0.08894	0.21767	0.409
Position	1.07491	0.09492	11.324
TreatmentOP:Position	0.01846	0.14008	0.132
TreatmentOP:No.stem	-0.34137	0.29097	-1.173

	Chisq	Df	P-value	Significance
Treatment	0.0005	1	0.9822	
No. of buds per stem	0.4995	1	0.4797	
Position on stem	240.8676	1	<2e-16	Yes
Treatment:Position	0.0174	1	0.8951	
Treatment: No. buds per stem	1.3764	1	0.2407	

6.7. ANOVA to identify significant differences between flower opening time in Oriental ‘Ascot’ comparing cut stems with no commercial treatment and commercially treated stems to on plant controls (Figure 3.7A, B, C)

Figure	Test	Degrees of freedom	Test statistic (F value/T-value/chi squared)	P value	Post-hoc test padj value if applicable
3.7A	Two way ANOVA				Tukey test
	Treatment	2	26.51	<0.05	CUTONLY-CT: >0.05 OP-CT: <0.05 OP-CUTONLY: <0.05
	Position	4	88.35	<0.05	

	Treatment:Position	6	1.73	>0.05	
3.7B	One way ANOVA	2	17.23	<0.05	Tukey test CUTONLY-CT: >0.05 OP-CT: <0.05 OP-CUTONLY: <0.05
3.7C	One way ANOVA	2	13.44	<0.05	Tukey test CUTONLY-CT: <0.05 OP-CT: >0.05 OP-CUTONLY: <0.05

6.8. Watson U2 test to compare distributions of circadian time of opening in on plant and commercially treated 'Ascot' flowers

	Test statistic	P-value	Significance
Treatment	0.7948	<0.001	Reject null hypothesis

6.9. Binomial general linear model to identify significant differences between groups

Comparison	Estimate	Standard error	T-value	Pr(>)
(Intercept)	-10.5940	4.0132	-2.640	<0.05
Treatment (individual buds vs. on stem)	-4.6664	1.2159	-3.838	<0.05
Bud length /mm	0.3167	0.1036	3.058	<0.05
No. buds per stem (5 buds vs. 4 buds per stem)	-0.6399	0.8196	-0.781	>0.05

Residual standard error: 0.843 on 41 degrees of freedom

Multiple R-squared: 0.01059, Adjusted R-squared: -0.0618

F-statistic: 0.1463 on 3 and 41 DF, p-value: 0.9315

6.10. Statistical tests to analyse tepal starch/sucrose/glucose content comparing Edge/Midrib sections over flower development and opening

Figure	Test	Degrees of freedom	Test statistic (F value/T-value/chi squared)	P value	Post-hoc test padj value if applicable
4.3A Starch	Two way ANOVA Stage	2	12.76	<0.05	Tukey test 3-1: >0.05 5-1: <0.05

	Location	1	10.33	<0.05	5-3: <0.05
4.3B Glucose	Two way ANOVA				Tukey test
	Stage	2	59.188	<0.05	3-1: <0.05 5-1: <0.05 5-3: <0.05
	Location	1	1.567	>0.05	
4.3C Sucrose	Two way ANOVA				Tukey test
	Stage	2	20.792	<0.05	3-1: >0.05 5-1: <0.05 5-3: <0.05
	Location	1	4.987	<0.05	

6.11. Statistical tests to analyse tepal starch content comparing OP and CT flowers over development and opening in different parts of the tepal and position on stem

Figure	Test	Degrees of freedom	Test statistic (F value/T-value/chi squared)	P value	Post-hoc test padj value if applicable
4.6A Position A Edge	Two way ANOVA				Tukey test
	Treatment	1	1.605	>0.05	3-1: >0.05 5-1: >0.05 5-3: <0.05
	Stage	2	10.219	<0.05	
	Treatment:Stage	2	0.877	>0.05	
4.6B Position C Edge	Two way ANOVA				Tukey test
	Treatment	1	1.408	>0.05	3-1: >0.05 5-1: >0.05 5-3: <0.05
	Stage	2	17.890	<0.05	
	Treatment:Stage	2	0.271	>0.05	
4.6C Position A Midrib	Two way ANOVA				Tukey test
	Treatment	1	2.531	>0.05	3-1: <0.05 5-1: >0.05 5-3: <0.05
	Stage	2	13.893	<0.05	
	Treatment:Stage	2	6.745	<0.05	
4.6D Position C Midrib	Two way ANOVA				Tukey test
	Treatment	1	0.48	>0.05	3-1: >0.05 5-1: <0.05 5-3: <0.05
	Stage	2	16.22	<0.05	

	Treatment:Stage	2	0.38	>0.05	
--	-----------------	---	------	-------	--

6.12. Statistical tests to analyse tepal glucose, fructose and sucrose content comparing OP and CT flowers in Edge samples only over development and opening

Figure	Test	Degrees of freedom	Test statistic (F value/T-value/chi squared)	P value	Post-hoc test padj value if applicable
4.7A Glucose isomer 3255	Two way ANOVA				Tukey test OP:1-CT:1 : >0.05 CT:3-CT:1 : >0.05
	Treatment	1	30.71	<0.05	OP:3-CT:1 : <0.05 CT:5-CT:1 : <0.05 OP:5-CT:1 : <0.05
	Stage	2	58.95	<0.05	CT:3-OP:1 : >0.05 OP:3-OP:1 : <0.05 CT:5-OP:1 : <0.05 OP:5-OP:1 : <0.05
	Treatment:Stage	2	4.84	<0.05	OP:3-CT:3 : <0.05 CT:5-CT:3 : <0.05 OP:5-CT:3 : <0.05 CT:5-OP:3 : >0.05 OP:5-OP:3 : <0.05 OP:5-CT:5 : <0.05
4.7B Glucose isomer 1695	Two way ANOVA				Tukey test OP:1-CT:1 : >0.05 CT:3-CT:1 : >0.05
	Treatment	1	18.862	<0.05	OP:3-CT:1 : >0.05 CT:5-CT:1 : >0.05 OP:5-CT:1 : <0.05
	Stage	2	536.271	<0.05	CT:3-OP:1 : >0.05 OP:3-OP:1 : >0.05 CT:5-OP:1 : >0.05 OP:5-OP:1 : <0.05
	Treatment:Stage	2	8.795	<0.05	OP:3-CT:3 : >0.05 CT:5-CT:3 : >0.05 OP:5-CT:3 : <0.05 CT:5-OP:3 : >0.05 OP:5-OP:3 : <0.05 OP:5-CT:5 : <0.05
4.7C Fructose isomer 235	Two way ANOVA				Tukey test OP:1-CT:1 : >0.05 CT:3-CT:1 : >0.05
	Treatment	1	22.728	<0.05	OP:3-CT:1 : <0.05 CT:5-CT:1 : <0.05 OP:5-CT:1 : <0.05
	Stage	2	72.823	<0.05	CT:3-OP:1 : >0.05 OP:3-OP:1 : <0.05 CT:5-OP:1 : <0.05 OP:5-OP:1 : <0.05

	Treatment:Stage	2	6.663	<0.05	OP:3-CT:3 : <0.05 CT:5-CT:3 : <0.05 OP:5-CT:3 : <0.05 CT:5-OP:3 : >0.05 OP:5-OP:3 : <0.05 OP:5-CT:5 : <0.05
4.7D Sucrose	Two way ANOVA				Tukey test
	Treatment	1	29.894	<0.05	OP:1-CT:1 : >0.05 CT:3-CT:1 : >0.05 OP:3-CT:1 : >0.05 CT:5-CT:1 : >0.05 OP:5-CT:1 : <0.05 CT:3-OP:1 : <0.05
	Stage	2	7.936	<0.05	OP:3-OP:1 : >0.05 CT:5-OP:1 : >0.05 OP:5-OP:1 : >0.05 OP:3-CT:3 : >0.05 CT:5-CT:3 : >0.05 OP:5-CT:3 : <0.05 CT:5-OP:3 : >0.05 OP:5-OP:3 : <0.05 OP:5-CT:5 : <0.05
	Treatment:Stage	2	1.566	>0.05	

6.13. Statistical tests to analyse tepal glucose, fructose and sucrose content comparing commercially treated Position A and C flowers in Edge samples only over development and opening

Figure	Test	Degrees of freedom	Test statistic (F value/T-value/chi squared)	P value	Post-hoc test padj value if applicable
4.7E Glucose isomer 3255	Two way ANOVA				Tukey test
	Treatment	2	13.979	<0.05	3-1: >0.05 5-1: <0.05 5-3: <0.05
	Position	1	0.744	>0.05	
4.7F Glucose isomer 1695	Two way ANOVA				Tukey test
	Treatment	2	7.043	<0.05	3-1: >0.05 5-1: <0.05 5-3: <0.05
	Position	1	1.584	>0.05	
4.7G Fructose isomer 235	Two way ANOVA				Tukey test
	Treatment	2	16.076	<0.05	3-1: >0.05 5-1: <0.05 5-3: <0.05
	Position	1	0.848	>0.05	
4.7H Sucrose	Two way ANOVA				Tukey test
	Treatment	2	5.244	<0.05	3-1: >0.05 5-1: >0.05 5-3: <0.05
	Position	1	6.093	<0.05	

6.14. Statistical tests to analyse relative expression of putative flower opening-related genes over flower development and opening

Figure	Test	Degrees of freedom	Test statistic (F value/T-value/chi squared)	P value	Post-hoc test padj value if applicable
4.14A EXPA2	One way ANOVA	4	9.253	<0.05	Tukey test 2-1: >0.05 3-1: >0.05 4-1: >0.05 5-1: >0.05 3-2: >0.05 4-2: <0.05 5-2: <0.05 4-3: <0.05 5-3: <0.05 5-4: >0.05
4.14B XTH2	One way ANOVA	4	2.124	>0.05	Tukey test 2-1: >0.05 3-1: >0.05 4-1: >0.05 5-1: >0.05 3-2: >0.05 4-2: >0.05 5-2: >0.05 4-3: >0.05 5-3: >0.05 5-4: >0.05
4.14C PIP1	One way ANOVA	4	4.669	<0.05	Tukey test 2-1: >0.05 3-1: <0.05 4-1: >0.05 5-1: >0.05 3-2: >0.05 4-2: >0.05 5-2: >0.05 4-3: >0.05 5-3: <0.05 5-4: >0.05
4.14D AMY2	One way ANOVA	4	6.484	<0.05	Tukey test 2-1: >0.05 3-1: >0.05 4-1: >0.05 5-1: <0.05 3-2: >0.05 4-2: >0.05 5-2: <0.05 4-3: >0.05 5-3: <0.05 5-4: >0.05

4.14E SWEET7	One way ANOVA	4	4.311	<0.05	Tukey test 2-1: >0.05 3-1: >0.05 4-1: >0.05 5-1: <0.05 3-2: >0.05 4-2: >0.05 5-2: <0.05 4-3: >0.05 5-3: >0.05 5-4: <0.05
4.14F MST6	Kruskal Wallis	4	11.233	<0.05	Dunn test 2-1: >0.05 3-1: >0.05 4-1: >0.05 5-1: <0.05 3-2: >0.05 4-2: >0.05 5-2: >0.05 4-3: >0.05 5-3: >0.05 5-4: >0.05
4.14G SUT2	One way ANOVA	4	0.848	>0.05	Tukey test 2-1: >0.05 3-1: >0.05 4-1: >0.05 5-1: >0.05 3-2: >0.05 4-2: >0.05 5-2: >0.05 4-3: >0.05 5-3: >0.05 5-4: >0.05
4.14H SUT4	One way ANOVA	4	0.743	>0.05	Tukey test 2-1: >0.05 3-1: >0.05 4-1: >0.05 5-1: >0.05 3-2: >0.05 4-2: >0.05 5-2: >0.05 4-3: >0.05 5-3: >0.05 5-4: >0.05
4.14I CWIN4	One way ANOVA	4	1.45	>0.05	Tukey test 2-1: >0.05 3-1: >0.05 4-1: >0.05 5-1: >0.05 3-2: >0.05 4-2: >0.05

					5-2: >0.05 4-3: >0.05 5-3: >0.05 5-4: >0.05
--	--	--	--	--	--

6.15. Statistical tests to analyse relative expression of putative auxin related genes over flower development and opening

Figure	Test	Degrees of freedom	Test statistic (F value/T-value/chi squared)	P value	Post-hoc test padj value if applicable
6.2A YUC3	One way ANOVA	4	2.48	>0.05	Tukey test 2-1: >0.05 3-1: >0.05 4-1: >0.05 5-1: >0.05 3-2: >0.05 4-2: >0.05 5-2: >0.05 4-3: >0.05 5-3: >0.05 5-4: >0.05
6.2B AUX1	One way ANOVA	4	0.66	>0.05	Tukey test 2-1: >0.05 3-1: >0.05 4-1: >0.05 5-1: >0.05 3-2: >0.05 4-2: >0.05 5-2: >0.05 4-3: >0.05 5-3: >0.05 5-4: >0.05
6.3C IAA14	One way ANOVA	4	9.35	<0.05	Tukey test 2-1: >0.05 3-1: <0.05 4-1: <0.05 5-1: <0.05 3-2: >0.05 4-2: >0.05 5-2: <0.05 4-3: >0.05 5-3: >0.05 5-4: >0.05
6.3D ARF6/8	One way ANOVA	4	4.28	<0.05	Tukey test 2-1: >0.05 3-1: >0.05 4-1: >0.05

					5-1: <0.05 3-2: >0.05 4-2: >0.05 5-2: >0.05 4-3: >0.05 5-3: >0.05 5-4: >0.05
6.3E ARF7/19	Kruskal-Wallis	4	7.97	>0.05	Dunn test 2-1: >0.05 3-1: >0.05 4-1: >0.05 5-1: >0.05 3-2: >0.05 4-2: >0.05 5-2: >0.05 4-3: >0.05 5-3: >0.05 5-4: >0.05
6.3F SAUR75	One way ANOVA	4	7.86	<0.05	Tukey test 2-1: >0.05 3-1: >0.05 4-1: <0.05 5-1: <0.05 3-2: >0.05 4-2: >0.05 5-2: <0.05 4-3: >0.05 5-3: >0.05 5-4: >0.05

6.16. Statistical tests to analyse relative expression of putative cytokinin related genes over flower development and opening

Figure	Test	Degrees of freedom	Test statistic (F value/T-value/chi squared)	P value	Post-hoc test padj value if applicable
6.3A AHP2	One way ANOVA	4	4.386	<0.05	Tukey test 2-1: >0.05 3-1: >0.05 4-1: >0.05 5-1: <0.05 3-2: >0.05 4-2: >0.05 5-2: >0.05 4-3: >0.05 5-3: <0.05 5-4: >0.05
6.3B ORR9	Kruskal-Wallis	4	12.289	<0.05	Tukey test 2-1: >0.05 3-1: >0.05

					4-1: <0.05 5-1: <0.05 3-2: >0.05 4-2: >0.05 5-2: <0.05 4-3: >0.05 5-3: <0.05 5-4: <0.05
--	--	--	--	--	--

6.17. Statistical tests to analyse differences between time of opening of lily flowers with exogenous auxin phytohormone treatments

Figure	Test	Degrees of freedom	Test statistic (F value/T-value/chi squared)	P value	Post-hoc test padj value if applicable
6.4A	One way ANOVA	2	5.598	<0.05	Tukey test NAA10-Control: <0.05 NAA100-Control: >0.05 NAA100-NAA10: <0.05
6.4B	Unpaired T-test	14.733	-2.8496	<0.05	N/a
6.5A	Kruskal-Wallis	2	15.574	<0.05	Dunn test Control-NAA: <0.05 Control-NPA: >0.05 NAA-NPA: <0.05
6.5B	Kruskal-Wallis	2	8.5269	<0.05	Dunn test Control-NAA: >0.05 Control-NPA: <0.05 NAA-NPA: <0.05
6.5C	Kruskal-Wallis	2	3.1468	>0.05	Dunn test Control-NAA: >0.05 Control-NPA: >0.05 NAA-NPA: >0.05
6.6A	Kruskal-Wallis	2	16.683	<0.05	Dunn test CT-NAA: >0.05 CT-OP: <0.05 NAA-OP: <0.05
6.6B	Kruskal-Wallis	2	16.101	<0.05	Dunn test CT-NAA: >0.05 CT-OP: <0.05 NAA-OP: >0.05
6.6C	Kruskal-Wallis	2	8.3338	<0.05	Dunn test CT-NAA: >0.05 CT-OP: <0.05 NAA-OP: <0.05

6.18. Statistical tests to analyse differences in gene expression of putative auxin- and flower opening-related genes between control, NAA and NPA-treated tepal material

Figure	Test	Degrees of freedom	Test statistic (F value/T-value/chi squared)	P value	Post-hoc test padj value if applicable
5.7A IAA14	One way ANOVA	2	0.506	>0.05	Tukey test NAA-Control: >0.05 NPA-Control: >0.05 NAA-NPA: >0.05
5.7B ARF6/8	One way ANOVA	2	0.414	>0.05	Tukey test NAA-Control: >0.05 NPA-Control: >0.05 NAA-NPA: >0.05
5.7C SAUR75	One way ANOVA	2	0.117	>0.05	Tukey test NAA-Control: >0.05 NPA-Control: >0.05 NAA-NPA: >0.05
5.7D PIP1	One way ANOVA	2	0.043	>0.05	Tukey test NAA-Control: >0.05 NPA-Control: >0.05 NAA-NPA: >0.05
5.7E EXPA1	One way ANOVA	2	0.425	>0.05	Tukey test NAA-Control: >0.05 NPA-Control: >0.05 NAA-NPA: >0.05
5.7F XTH1	One way ANOVA	2	0.242	>0.05	Tukey test NAA-Control: >0.05 NPA-Control: >0.05 NAA-NPA: >0.05

6.19. Binomial general linear model to identify significant differences between groups with ANOVA (Figure 5.8)

Comparison	t-value	Pr(> z)	Chisq	Df	Pr(>Chisq)
(Intercept)	-0.011	>0.05			
Treatment (individual buds vs. on stem)	0.009	>0.05	8.553	1	<0.05
Bud length at harvest	0.011	>0.05	38.839	1	<0.05
Treatment:Length	-0.008	>0.05	0.037	1	>0.05

6.20. Statistical tests to analyse relative expression of putative genes used to validate the RNA-seq experiment.

Figure	Test	Degrees of freedom	Test statistic (F value/T-value/chi squared)	P value	Post-hoc test padj value if applicable
--------	------	--------------------	--	---------	--

5.18A MYB21	One way ANOVA	2	0.025	>0.05	Tukey test SRC-SSO: >0.05 SRC-LFO: >0.05 SSO-LFO: >0.05
5.18B EXPA8	One way ANOVA	2	0.381	>0.05	Tukey test SRC-SSO: >0.05 SRC-LFO: >0.05 SSO-LFO: >0.05
5.18C PSII5	One way ANOVA	2	0.095	>0.05	Tukey test SRC-SSO: >0.05 SRC-LFO: >0.05 SSO-LFO: >0.05

6.21. Statistical tests to analyse relative expression of putative genes used to validate the RNA-seq experiment (auxin related).

Figure	Test	Degrees of freedom	Test statistic (F value/T-value/chi squared)	P value	Post-hoc test padj value if applicable
5.22A YUC3	One way ANOVA	2	0.067	>0.05	Tukey test SRC-SSO: >0.05 SRC-LFO: >0.05 SSO-LFO: >0.05
5.22B IAA14	One-way ANOVA	2	0.202	>0.05	Tukey test SRC-SSO: >0.05 SRC-LFO: >0.05 SSO-LFO: >0.05
5.22C ARF15	One way ANOVA	2	0.316	>0.05	Tukey test SRC-SSO: >0.05 SRC-LFO: >0.05 SSO-LFO: >0.05
5.22D SAUR75	One way ANOVA	2	0.138	>0.05	Tukey test SRC-SSO: >0.05 SRC-LFO: >0.05 SSO-LFO: >0.05

6.22 Statistical tests for selected compounds from Random Forest on FIE-HRMS data with regard to treatment

Figure	Test	Degrees of freedom	Test statistic (F value/T-value/chi squared)	P value	Post-hoc test padj value if applicable
--------	------	--------------------	--	---------	--

X1055	Kruskal Wallace	5	53.09	<0.05	Dunn test CT1-CT3: >0.05 CT1-CT5: >0.05 CT3-CT5: >0.05 CT1-OP1: <0.05 CT3-OP1: <0.05 CT5-OP1: <0.05 CT1-OP3: <0.05 CT3-OP3: <0.05 CT5-OP3: <0.05 OP1-OP3: >0.05 CT1-OP5: <0.05 CT3-OP5: <0.05 CT5-OP5: <0.05 OP1-OP5: >0.05 OP3-OP5: >0.05
X4217	Kruskal Wallace	5	54.524	<0.05	Dunn test CT1-CT3: >0.05 CT1-CT5: >0.05 CT3-CT5: >0.05 CT1-OP1: <0.05 CT3-OP1: <0.05 CT5-OP1: <0.05 CT1-OP3: <0.05 CT3-OP3: <0.05 CT5-OP3: <0.05 OP1-OP3: >0.05 CT1-OP5: <0.05 CT3-OP5: <0.05 CT5-OP5: <0.05 OP1-OP5: >0.05 OP3-OP5: >0.05
X4377	Kruskal Wallace	1	54.331	<0.05	Dunn test CT1-CT3: >0.05 CT1-CT5: >0.05 CT3-CT5: >0.05 CT1-OP1: <0.05 CT3-OP1: <0.05 CT5-OP1: <0.05 CT1-OP3: <0.05 CT3-OP3: <0.05 CT5-OP3: <0.05 OP1-OP3: >0.05 CT1-OP5: <0.05 CT3-OP5: <0.05 CT5-OP5: <0.05 OP1-OP5: >0.05 OP3-OP5: >0.05

X3732	Kruskal Wallace	1	55.47	<0.05	Dunn test CT1-CT3: >0.05 CT1-CT5: >0.05 CT3-CT5: >0.05 CT1-OP1: <0.05 CT3-OP1: <0.05 CT5-OP1: <0.05 CT1-OP3: <0.05 CT3-OP3: <0.05 CT5-OP3: <0.05 OP1-OP3: >0.05 CT1-OP5: <0.05 CT3-OP5: <0.05 CT5-OP5: <0.05 OP1-OP5: >0.05 OP3-OP5: >0.05
X4170	Kruskal Wallace	1	54.625	<0.05	Dunn test CT1-CT3: >0.05 CT1-CT5: >0.05 CT3-CT5: >0.05 CT1-OP1: <0.05 CT3-OP1: <0.05 CT5-OP1: <0.05 CT1-OP3: <0.05 CT3-OP3: <0.05 CT5-OP3: <0.05 OP1-OP3: >0.05 CT1-OP5: <0.05 CT3-OP5: <0.05 CT5-OP5: <0.05 OP1-OP5: >0.05 OP3-OP5: >0.05
X2343	Kruskal Wallace	1	56.837	<0.05	Dunn test CT1-CT3: <0.05 CT1-CT5: >0.05 CT3-CT5: >0.05 CT1-OP1: <0.05 CT3-OP1: <0.05 CT5-OP1: <0.05 CT1-OP3: <0.05 CT3-OP3: <0.05 CT5-OP3: <0.05 OP1-OP3: >0.05 CT1-OP5: <0.05 CT3-OP5: <0.05 CT5-OP5: <0.05 OP1-OP5: >0.05 OP3-OP5: >0.05

X4768	Kruskal Wallace	1	53.098	<0.05	Dunn test CT1-CT3: >0.05 CT1-CT5: >0.05 CT3-CT5: >0.05 CT1-OP1: <0.05 CT3-OP1: <0.05 CT5-OP1: <0.05 CT1-OP3: <0.05 CT3-OP3: <0.05 CT5-OP3: <0.05 OP1-OP3: >0.05 CT1-OP5: <0.05 CT3-OP5: <0.05 CT5-OP5: <0.05 OP1-OP5: >0.05 OP3-OP5: >0.05
X4889	Kruskal Wallace	1	57.378	<0.05	Dunn test CT1-CT3: >0.05 CT1-CT5: >0.05 CT3-CT5: >0.05 CT1-OP1: <0.05 CT3-OP1: <0.05 CT5-OP1: >0.05 CT1-OP3: <0.05 CT3-OP3: <0.05 CT5-OP3: <0.05 OP1-OP3: >0.05 CT1-OP5: <0.05 CT3-OP5: <0.05 CT5-OP5: <0.05 OP1-OP5: >0.05 OP3-OP5: >0.05

6.23 ANOVA for selected compounds from Random Forest on FIE-HRMS data with regard to location on tepal

Figure	Test	Degrees of freedom	Test statistic (F value/T-value/chi squared)	P value	Post-hoc test padj value if applicable
X1921	One-way ANOVA	5	68.25	<0.05	Tukey test Edge3-Edge1 <0.05 Edge5-Edge1 >0.05 Midrib1-Edge1 <0.05 Midrib3-Edge1 <0.05 Midrib5-Edge1 <0.05 Edge5-Edge3 >0.05 Midrib1-Edge3 <0.05 Midrib3-Edge3 <0.05 Midrib5-Edge3 <0.05 Midrib1-Edge5 <0.05

					Midrib3:Edge5 <0.05 Midrib5-Edge5 <0.05 Midrib3-Midrib1 >0.05 Midrib5-Midrib1 >0.05 Midrib5-Midrib3 >0.05
X2432	One-way ANOVA	5	73	<0.05	Tukey test Edge3-Edge1 >0.05 Edge5-Edge1 >0.05 Midrib1-Edge1 <0.05 Midrib3-Edge1 <0.05 Midrib5-Edge1 <0.05 Edge5-Edge3 >0.05 Midrib1-Edge3 <0.05 Midrib3-Edge3 <0.05 Midrib5-Edge3 <0.05 Midrib1-Edge5 <0.05 Midrib3:Edge5 <0.05 Midrib5-Edge5 <0.05 Midrib3-Midrib1 >0.05 Midrib5-Midrib1 >0.05 Midrib5-Midrib3 >0.05
X4681	Kruskal Wallace	5	52.545	<0.05	Dunn test Edge3-Edge1 >0.05 Edge5-Edge1 >0.05 Edge5-Edge3 >0.05 Midrib1-Edge1 <0.05 Midrib3-Edge1 <0.05 Midrib5-Edge1 <0.05 Midrib1-Edge3 <0.05 Midrib3-Edge3 <0.05 Midrib5-Edge3 <0.05 Midrib1-Edge5 <0.05 Midrib3:Edge5 <0.05 Midrib5-Edge5 <0.05 Midrib3-Midrib1 >0.05 Midrib5-Midrib1 >0.05 Midrib5-Midrib3 >0.05
X5368	Kruskal Wallace	5	54.23	<0.05	Dunn test Edge3-Edge1 >0.05 Edge5-Edge1 >0.05 Edge5-Edge3 >0.05 Midrib1-Edge1 <0.05 Midrib3-Edge1 <0.05 Midrib5-Edge1 <0.05 Midrib1-Edge3 <0.05 Midrib3-Edge3 <0.05 Midrib5-Edge3 <0.05 Midrib1-Edge5 <0.05 Midrib3:Edge5 <0.05 Midrib5-Edge5 <0.05 Midrib3-Midrib1 >0.05

					Midrib5-Midrib1 >0.05 Midrib5-Midrib3 >0.05
X939	One-way ANOVA	5	42.39	<0.05	Tukey test Edge3-Edge1 >0.05 Edge5-Edge1 >0.05 Midrib1-Edge1 <0.05 Midrib3-Edge1 <0.05 Midrib5-Edge1 <0.05 Edge5-Edge3 >0.05 Midrib1-Edge3 <0.05 Midrib3-Edge3 <0.05 Midrib5-Edge3 <0.05 Midrib1-Edge5 <0.05 Midrib3:Edge5 <0.05 Midrib5-Edge5 <0.05 Midrib3-Midrib1 >0.05 Midrib5-Midrib1 >0.05 Midrib5-Midrib3 >0.05
X1178	Kruskal Wallace	5	52.893	<0.05	Dunn test Edge3-Edge1 >0.05 Edge5-Edge1 >0.05 Edge5-Edge3 >0.05 Midrib1-Edge1 <0.05 Midrib3-Edge1 <0.05 Midrib5-Edge1 <0.05 Midrib1-Edge3 <0.05 Midrib3-Edge3 <0.05 Midrib5-Edge3 <0.05 Midrib1-Edge5 <0.05 Midrib3:Edge5 <0.05 Midrib5-Edge5 <0.05 Midrib3-Midrib1 >0.05 Midrib5-Midrib1 >0.05 Midrib5-Midrib3 >0.05
X5075	One-way ANOVA	5	34.31	<0.05	Tukey test Edge3-Edge1 >0.05 Edge5-Edge1 >0.05 Midrib1-Edge1 <0.05 Midrib3-Edge1 <0.05 Midrib5-Edge1 <0.05 Edge5-Edge3 >0.05 Midrib1-Edge3 <0.05 Midrib3-Edge3 <0.05 Midrib5-Edge3 <0.05 Midrib1-Edge5 <0.05 Midrib3:Edge5 <0.05 Midrib5-Edge5 <0.05 Midrib3-Midrib1 >0.05 Midrib5-Midrib1 >0.05

					Midrib5-Midrib3 >0.05
X5137	Kruskal Wallace	5	51.694	<0.05	Dunn test Edge3-Edge1 >0.05 Edge5-Edge1 >0.05 Edge5-Edge3 >0.05 Midrib1-Edge1 <0.05 Midrib3-Edge1 <0.05 Midrib5-Edge1 <0.05 Midrib1-Edge3 <0.05 Midrib3-Edge3 <0.05 Midrib5-Edge3 <0.05 Midrib1-Edge5 <0.05 Midrib3:Edge5 <0.05 Midrib5-Edge5 <0.05 Midrib3-Midrib1 >0.05 Midrib5-Midrib1 >0.05 Midrib5-Midrib3 >0.05

6.24 ANOVA for selected compounds from Random Forest on FIE-HRMS data with regard to position on stem

Figure	Test	Degrees of freedom	Test statistic (F value/T-value/chi squared)	P value	Post-hoc test padj value if applicable
X2110	One-way ANOVA	5	22.37	<0.05	Tukey test A3-A1 >0.05 A5-A1 >0.05 C1-A1 <0.05 C3-A1 <0.05 C5-A1 <0.05 A5-A3 >0.05 C1-A3 <0.05 C3:A3 <0.05 C5-A3 <0.05 C1-A5 <0.05 C3-A5 <0.05 C5:A5 <0.05 C3-C1 >0.05 C5-C1 >0.05 C5-C3 >0.05
X2102	Kruskal Wallace	5	50.164	<0.05	Dunn test A3-A1 >0.05 A5-A1 >0.05 C1-A1 <0.05 C3-A1 <0.05 C5-A1 <0.05

					A5-A3 >0.05 C1-A3 <0.05 C3:A3 <0.05 C5-A3 <0.05 C1-A5 <0.05 C3-A5 <0.05 C5:A5 <0.05 C3-C1 >0.05 C5-C1 >0.05 C5-C3 >0.05
X2111	Kruskal Wallace	5	52.707	<0.05	Dunn test A3-A1 >0.05 A5-A1 >0.05 C1-A1 <0.05 C3-A1 <0.05 C5-A1 <0.05 A5-A3 >0.05 C1-A3 <0.05 C3:A3 <0.05 C5-A3 <0.05 C1-A5 <0.05 C3-A5 <0.05 C5:A5 <0.05 C3-C1 >0.05 C5-C1 >0.05 C5-C3 >0.05
X2164	One-way ANOVA	5	26.56	<0.05	Tukey test A3-A1 >0.05 A5-A1 <0.05 C1-A1 <0.05 C3-A1 <0.05 C5-A1 <0.05 A5-A3 >0.05 C1-A3 <0.05 C3:A3 <0.05 C5-A3 <0.05 C1-A5 <0.05 C3-A5 <0.05 C5:A5 <0.05 C3-C1 >0.05 C5-C1 >0.05 C5-C3 >0.05
X2172	Kruskal Wallace	5	51.236	<0.05	Dunn test A3-A1 >0.05 A5-A1 >0.05 C1-A1 <0.05 C3-A1 <0.05 C5-A1 <0.05 A5-A3 >0.05 C1-A3 <0.05 C3:A3 <0.05

					C5-A3 <0.05 C1-A5 <0.05 C3-A5 <0.05 C5:A5 <0.05 C3-C1 >0.05 C5-C1 >0.05 C5-C3 >0.05
X2166	One-way ANOVA	5	24.1	<0.05	Tukey test A3-A1 >0.05 A5-A1 <0.05 C1-A1 <0.05 C3-A1 <0.05 C5-A1 <0.05 A5-A3 >0.05 C1-A3 <0.05 C3:A3 <0.05 C5-A3 <0.05 C1-A5 <0.05 C3-A5 <0.05 C5:A5 <0.05 C3-C1 >0.05 C5-C1 >0.05 C5-C3 >0.05
X5498	Kruskal Wallace	5	47.729	<0.05	Dunn test A3-A1 >0.05 A5-A1 >0.05 C1-A1 <0.05 C3-A1 <0.05 C5-A1 <0.05 A5-A3 >0.05 C1-A3 <0.05 C3:A3 <0.05 C5-A3 <0.05 C1-A5 <0.05 C3-A5 <0.05 C5:A5 <0.05 C3-C1 >0.05 C5-C1 >0.05 C5-C3 >0.05
X2176	Kruskal Wallace	5	48.077	<0.05	Dunn test A3-A1 >0.05 A5-A1 >0.05 C1-A1 <0.05 C3-A1 <0.05 C5-A1 >0.05 A5-A3 >0.05 C1-A3 <0.05 C3:A3 <0.05 C5-A3 <0.05 C1-A5 <0.05 C3-A5 >0.05

					C5:A5 >0.05 C3-C1 >0.05 C5-C1 >0.05 C5-C3 >0.05
--	--	--	--	--	--

6.25 ANOVA for selected compounds from Random Forest on FIE-HRMS data with regard to stage of development

Figure	Test	Degrees of freedom	Test statistic (F value/T-value/chi squared)	P value	Post-hoc test padj value if applicable
X5313	One-way ANOVA	2	15.44	<0.05	Tukey test 3-1 >0.05 5-1 <0.05 5-3 <0.05
X1641	Kruskal Wallace	1	55.19	<0.05	Dunn test 3-1 <0.05 5-1 <0.05 5-3 <0.05
X4738	Kruskal Wallace	1	57.551	<0.05	Dunn test 3-1 <0.05 5-1 <0.05 5-3 <0.05
X5450	Kruskal Wallace	1	47.016	<0.05	Dunn test 3-1 <0.05 5-1 <0.05 5-3 <0.05
X4735	Kruskal Wallace	1	58.621	<0.05	Dunn test 3-1 <0.05 5-1 <0.05 5-3 <0.05
X6319	One-way ANOVA	2	63.4	<0.05	Tukey test 3-1 >0.05 5-1 <0.05 5-3 <0.05
X1380	Kruskal Wallace	1	40.782	<0.05	Dunn test 3-1 <0.05 5-1 <0.05 5-3 <0.05
X1969	Kruskal Wallace	1	43.154	<0.05	Dunn test 3-1 >0.05 5-1 <0.05 5-3 <0.05

6.26 ANOVA for selected compounds from Random Forest on FIE-HRMS data with regard to position on stem in a subset of profiles (CT edge samples only).

Figure	Test	Degrees of freedom	Test statistic (F value/T-value/chi squared)	P value	Post-hoc test padj value if applicable
X4899	One-way ANOVA	5	8.843	<0.05	Tukey test A3-A1 >0.05 A5-A1 >0.05 C1-A1 >0.05 C3-A1 <0.05 C5-A1 <0.05 A5-A3 >0.05 C1-A3 <0.05 C3:A3 <0.05 C5-A3 >0.05 C1-A5 >0.05 C3-A5 >0.05 C5:A5 >0.05 C3-C1 >0.05 C5-C1 >0.05 C5-C3 >0.05
X2421	One-way ANOVA	5	13	<0.05	Tukey test A3-A1 >0.05 A5-A1 >0.05 C1-A1 <0.05 C3-A1 <0.05 C5-A1 <0.05 A5-A3 >0.05 C1-A3 <0.05 C3:A3 <0.05 C5-A3 <0.05 C1-A5 >0.05 C3-A5 <0.05 C5:A5 >0.05 C3-C1 >0.05 C5-C1 >0.05 C5-C3 >0.05
X5737	One-way ANOVA	5	8.271	<0.05	Tukey test A3-A1 >0.05 A5-A1 >0.05 C1-A1 >0.05 C3-A1 <0.05 C5-A1 >0.05 A5-A3 >0.05 C1-A3 <0.05 C3:A3 <0.05 C5-A3 >0.05 C1-A5 >0.05 C3-A5 <0.05 C5:A5 >0.05 C3-C1 >0.05 C5-C1 >0.05

					C5-C3 >0.05
X2159	One-way ANOVA	5	27.01	<0.05	Tukey test A3-A1 <0.05 A5-A1 >0.05 C1-A1 <0.05 C3-A1 <0.05 C5-A1 >0.05 A5-A3 <0.05 C1-A3 <0.05 C3:A3 <0.05 C5-A3 <0.05 C1-A5 <0.05 C3-A5 <0.05 C5:A5 >0.05 C3-C1 >0.05 C5-C1 >0.05 C5-C3 >0.05
X1275	One-way ANOVA	5	10.3	<0.05	Tukey test A3-A1 <0.05 A5-A1 >0.05 C1-A1 >0.05 C3-A1 >0.05 C5-A1 >0.05 A5-A3 <0.05 C1-A3 <0.05 C3:A3 <0.05 C5-A3 <0.05 C1-A5 >0.05 C3-A5 >0.05 C5:A5 >0.05 C3-C1 >0.05 C5-C1 >0.05 C5-C3 >0.05
X2102	One-way ANOVA	5	27.47	<0.05	Tukey test A3-A1 <0.05 A5-A1 >0.05 C1-A1 <0.05 C3-A1 <0.05 C5-A1 <0.05 A5-A3 <0.05 C1-A3 <0.05 C3:A3 <0.05 C5-A3 <0.05 C1-A5 >0.05 C3-A5 >0.05 C5:A5 >0.05 C3-C1 >0.05 C5-C1 >0.05

					C5-C3 >0.05
X5515	One-way ANOVA	5	5.384	<0.05	Tukey test A3-A1 >0.05 A5-A1 >0.05 C1-A1 >0.05 C3-A1 <0.05 C5-A1 >0.05 A5-A3 >0.05 C1-A3 >0.05 C3:A3 <0.05 C5-A3 >0.05 C1-A5 >0.05 C3-A5 <0.05 C5:A5 >0.05 C3-C1 >0.05 C5-C1 >0.05 C5-C3 >0.05
X3628	One-way ANOVA	5	5.768	<0.05	Tukey test A3-A1 >0.05 A5-A1 >0.05 C1-A1 >0.05 C3-A1 <0.05 C5-A1 <0.05 A5-A3 >0.05 C1-A3 >0.05 C3:A3 <0.05 C5-A3 <0.05 C1-A5 >0.05 C3-A5 >0.05 C5:A5 >0.05 C3-C1 >0.05 C5-C1 >0.05 C5-C3 >0.05

Appendix 7 – reanalysis of RNAseq data from Oriental lily ‘Siberia’ over development and opening

Transcriptomic data from Shi et al. (2018b) were reanalysed in order to find genes involved in the physical mechanisms and regulation of flower opening.

Transcriptional analysis of lily development and opening of Oriental lily (cv. ‘Siberia’)

Shi et al. (2018b) used outer tepals from Oriental lily cv. ‘Siberia’ at four developmental stages (Early flowering (EF), Semi flowering (SF), Full flowering (FF), and Late flowering (LF)) of lilies grown in greenhouse conditions (18°C) were used to investigate change in gene expression over time (Figure 8.3). Stems were not cold/dark stored but used when the developmental stages indicated were reached, after one day storage in an illuminating incubator (26 26 °C; photoperiod: 12 h, from 08:00 to 20:00). These data points represent two of the developmental stages also investigated in this report (Stage 4=SF, Stage 5=FF), however, EF stage is between Stage 3 and Stage 4, and LF is later in development than the staging used here (See Supplementary 2.1 for staging). Each sample contained three biological replicates. Differentially expressed genes (DEGs) were annotated by BLAST (best hit) using *Arabidopsis thaliana* and *Oryza sativa* gene codes to maximise annotations (Shi et al. 2018b).



Figure 8.3 – Stages of development used by Shi et al. (2018) – (A) Early flowering (EF), (B) Semi flowering (SF), (C) Full flowering (FF), and (D) Late flowering (LF). Figure taken from Shi et al. (2018).

As the Shi et al. (2018b) data provided a useful resource of relevance to the work presented here, the expression (\log_2 fold change of FPKM – referred to as Log2FC) of the Shi et al. (2018b) DEGs was compared timepoint vs. timepoint to look at the change over development. The remainder of the methods outlined here were carried out by me (Rakhee Dhorajiwala). DEGs falling into categories of biological function and genes relating to sucrose or starch metabolism were identified using KOBAS (v3.0) (Xie et al. 2011). MapMan (v3.5.1R2) was used to create heat map diagrams showing an overview of starch and sugar metabolism and types of transcription factor over the stages of development sampled (Thimm et al. 2004).

The clustering and data visualisation program Genesis (Sturn and Quackenbush 2002) was used to create heat maps of DEGs relating to sucrose/starch metabolism and transcription factor activity. It was also used to carry out K-means clustering on the data to separate DEGs into 10 groups (50 maximum iterations, 5 runs) – the full gene list annotated with cluster is available in Supplementary data 3.2.

Genes that fell into groups upregulated at each timepoint comparison were investigated for genes of interest. Clusters were then analysed again using KOBAS (v3.0) (Xie et al. 2011) to identify genes relating to sucrose/starch metabolism and transcription factor activity (Supplementary data 3.3,

3.4). Clusters of interest were analysed for KEGG pathway analysis to identify overrepresented pathways using ShinyGO (Ge et al. 2020) in a background of all expressed *A. thaliana* genes.

Results

Based on the transcriptomic data set for Oriental lily cv. 'Siberia' (Shi et al. 2018b) that compared 4 stages of flower development from EF (Stages 3-4), SF (Stage 4), FF (Stage 5), and LF (beyond Stage 5), there were 22,471 differentially expressed genetic sequences. To be defined as a differentially expressed gene (DEG), the \log^2 fold change (\log^2FC) of a genetic sequence between successive time points during development must show a change of at least $\log^2FC > 1$ at one timepoint comparison at least. When these were compared to the *Arabidopsis thaliana* and *Oryza sativa* genome databases using BLAST, 8901 of these were identified as having a known function and used for further analysis (Shi et al. 2018b).

The remainder of the analysis shown here was carried out by me (Rakhee Dhorajiwala). Figure 8.4 shows the breakdown of upregulated/downregulated DEGs over the developmental timepoints analysed here (Shi et al. 2018b). There were a total of 955 upregulated DEGs (19.8%) and 459 downregulated DEGs (10.3%) shared between all timepoints. There were approximately 9x more unique genes downregulated than upregulated in EF vs. SF stages (2.9% vs. 28.3%), while the comparison between SF/FF stages had 17x more upregulated than downregulated (24.4% vs. 1.6%). There were many upregulated DEGs shared between SF vs. FF and FF vs. LF (28.4%), whilst downregulated genes were for the most part shared between EF vs. SF and FF vs. LF (29.7%). The SF/EF and FF/SF comparisons were identified here as the most important as these were most related both to the stages of development 1-5 used in this thesis (Section 2.2) and also related to the physical opening process.

(A) Upregulated genes

(B) Downregulated genes

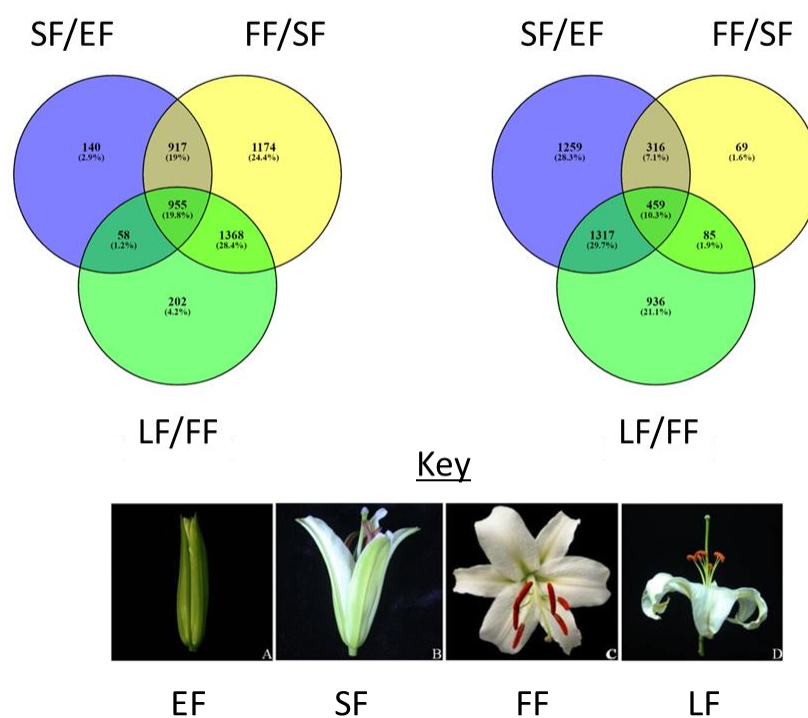
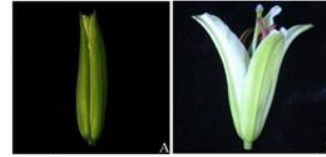
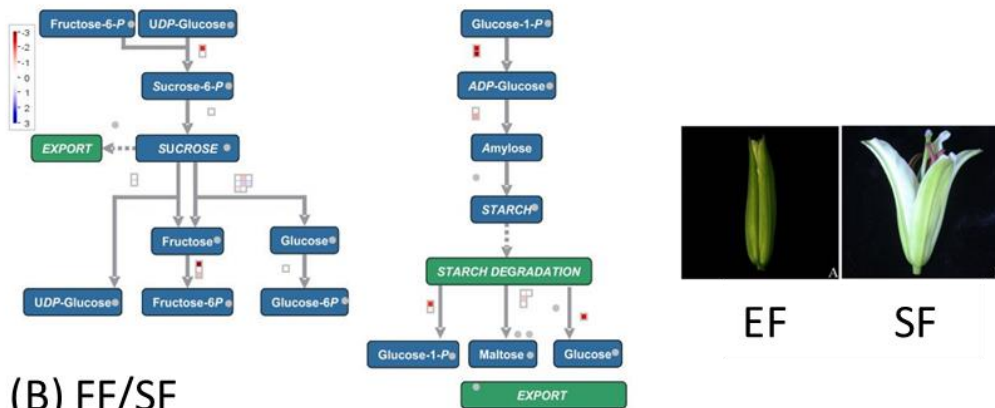


Figure 8.4 – Venn diagram showing the number of (A) upregulated and (B) downregulated genes shared between/unique to each timepoint comparison (comparisons used were only for the timepoints sequentially closest to them). Diagram created using Venny v2.0 software. Images of lilies from Shi et al. (2018b).

Are genes for carbohydrate mobilisation/metabolism expressed differentially during flower opening?

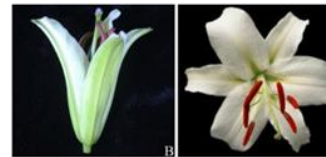
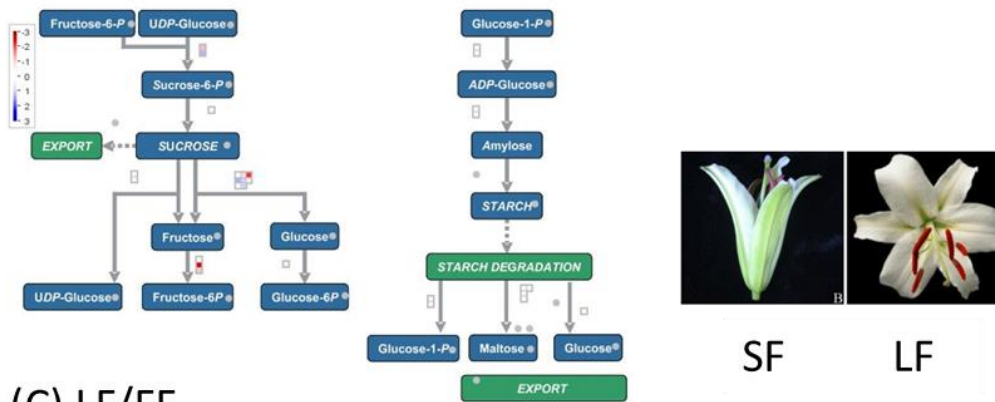
Carbohydrate metabolism and mobilisation genes were identified from the dataset and analysed for patterns in their expression relating to their functions. There is an initial upregulation (shown in red) of sucrose and starch metabolism-related genes early in development (SF/EF) to a general downregulation of sucrose and starch metabolism-related genes later on in development (LF/FF – Figure 8.5). There is an upregulation of some genes involved in sucrose and starch synthesis and degradation in comparisons between EF and SF stages, suggesting there is mobilisation of sucrose occurring throughout the flower. Between SF and FF stages, there was a specific increase in expression of genes involved in sucrose breakdown to fructose and glucose but a slight downregulation of most metabolism, which is continued into also between FF and LF stages, where most of these genes are strongly downregulated.

(A) SF/EF



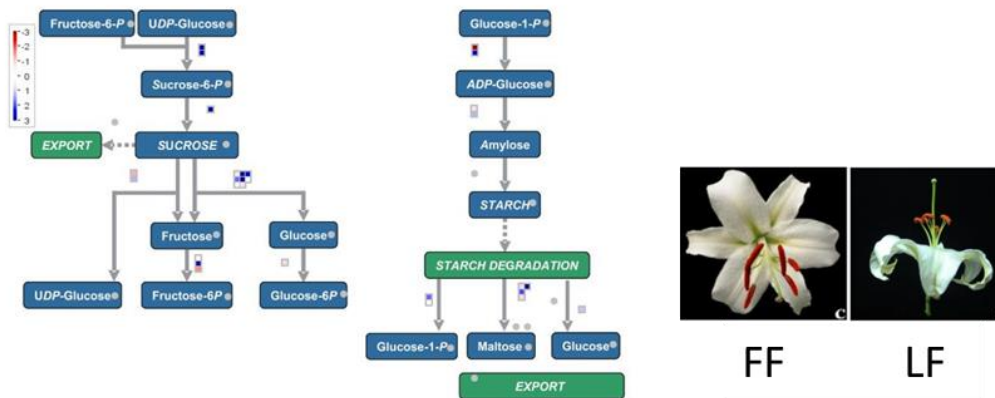
EF SF

(B) FF/SF



SF LF

(C) LF/FF



FF LF

Figure 8.5 – starch and sucrose metabolism-related pathway expression over development and opening – (A) comparisons between EF and SF stages, (B) comparisons between SF and FF stages and (C) between FF and LF stages. Coloured boxes show colour coded log₂FC values for genes coding for enzymes involved in that part of the pathway. Where there are several boxes for the same reaction indicates the number of genes in the *A. thaliana* gene family. Figure created by MapMan (Thimm et al. 2004). Images of lilies from Shi et al. (2018b).

The dataset was analysed for specific sucrose/starch metabolism-related genes to study their expression during flower development (Figure 8.6). Many lily sequences were matched to the same

A. thaliana gene, suggesting either that there are more complex gene families in the *Lilium* genome, or that there was a failure in differentiating between similar genes when not using a database ideal for *Lilium* spp.

A DEG aligning significantly to an *A. thaliana* gene coding for α -amylase (*AMY2*, Figure 8.6F) was only slightly upregulated throughout EF to FF stages. *Starch synthase 2* (*SS2*, Figure 8.6F) was also identified in the dataset and showed a slight increase in late development (increased expression in LF stages compared to FF stage).

Numerous putative sucrose synthases were identified several times in this dataset (*SUS3* and *SUS4*, Figure 8.6A). Seventeen *SUS3-like* genes were identified and showed different expression patterns. Most of them showed an upregulation in FF stage compared to SF and a very strong upregulation in LF stages. Twenty one *SUS4-like* genes were identified and showed very variable patterns, but most showed an increased expression in LF compared to SF and FF stages. Three *SPS* genes (coding for sucrose phosphate synthases) were also putatively identified showing a similar pattern.

Lily genes coding for SWEET transporters expressed here (Figure 8.6E) displayed a varied pattern over development, where some showed upregulation in early stages and some did not. *SWEET11-like* in particular showed a high upregulation during later stages (Upregulated in LF compared to FF stages).

Eight genes coding for cell wall invertases (*CWINV1/4*) and cytoplasmic invertases (*CINV2*) were identified in this dataset and showed a strong trend of upregulation from SF to LF stages (Figure 8.6D), and again were particularly upregulated in later stages (LF compared to FF stage). A *BGLU44-like* gene was identified (coding for a β -glucosidase) and was highly upregulated in SF stage compared to EF, suggesting it is important in the opening process (Figure 8.6C).

GAPC1 is a key glycolytic enzyme catalysing the first step from glucose to glucose-6-phosphate (G6P) and expression of the six lily genes identified here as GAPC1-like also showed a slight upregulation only in the early SF stage compared to EF comparison, but were strongly downregulated after in SF vs FF and FF vs LF comparisons (Figure 8.6B).

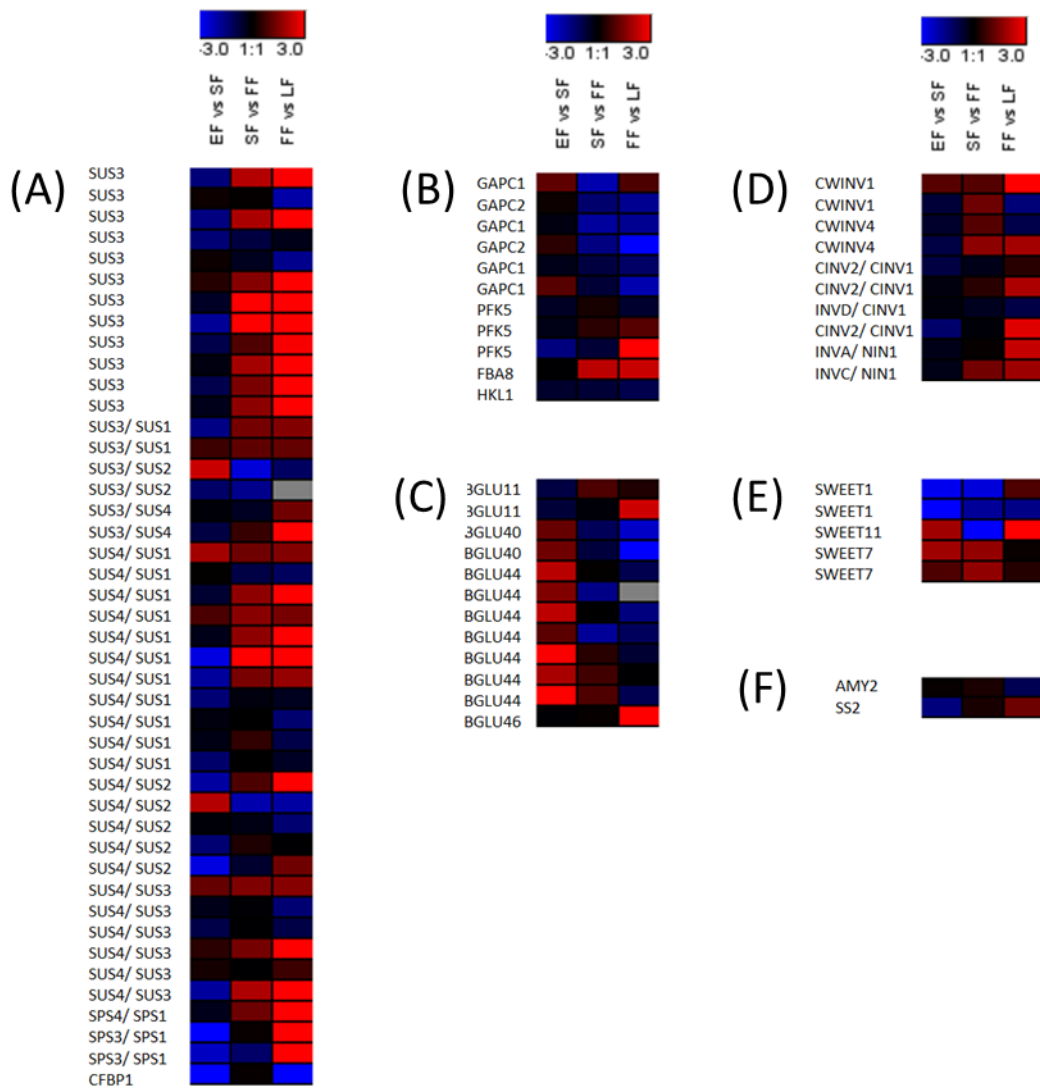


Figure 8.6 – heatmaps showing expression of sucrose mobilisation/sucrose and starch metabolism genes putatively identified using *A. thaliana*/*O. sativa* BLAST databases. Where a single gene has two different identifiers the first was the closest *A. thaliana* homologue and the second was the closest *O. sativa* homologue – if there is only one then the same homologue was identified using both databases. Grouped by (A) sucrose synthases, (B) glycolysis-related genes, (C) cell wall remodelling genes, (D) invertases, (E) sucrose transporters and (F) starch metabolism genes. Gene expression expressed as Log2FC in a timepoint-to-timepoint comparison.

3.5 Which regulatory pathways are enriched over development and opening?

Regulatory genes (defined here as genes with hormonal control, signal transduction, post-translational control and transcriptional control properties) were identified from the dataset and separated into groups showing their regulatory function, showing that those genes involved in regulation of transcription was the largest group (Figure 8.7). Hormonal regulation is also shown as being upregulated even into later stages of flower opening, pointing to interesting patterns that

were looked at in more detail. Finally, pathways related to light regulation were also differentially expressed.

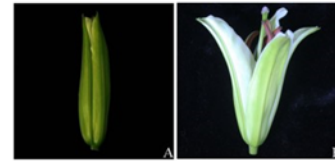
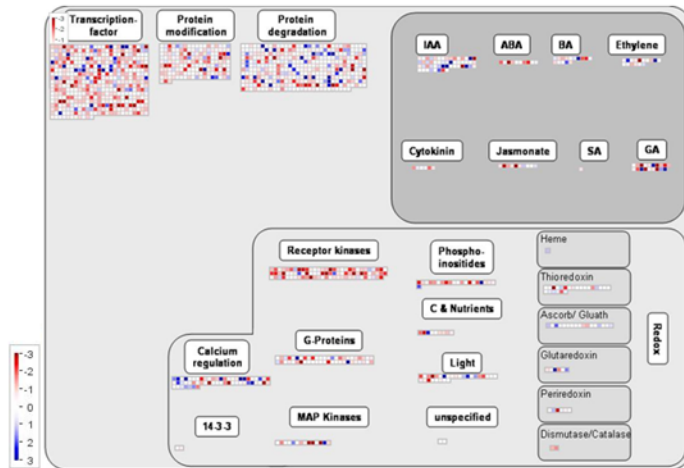
Having observed that there were significant changes to regulatory gene expression, the regulatory gene families which were indicated to perhaps be important in flower opening were analysed individually (Figure 8.8). A wide range of plant TF types were identified by Shi et al (2018) as DEGs, with the most prevalent being in order; bHLH, ERF, NAC, MYB-related, C2H2 and MYB factors (Shi et al. 2018b). The expression of some of these TF families was reanalysed here to compare it to other regulatory genes and sugar/starch metabolism genes

Members of the MAPK pathway generally showed an upregulation in SF vs. FF comparisons and a greater upregulation in FF vs. LF. – this was especially evident for MKK5, MKK9, and MPK20-like genes (Figure 8.8A). This is also correlated with NAC TF genes, which both show a similar pattern (Figure 8.8C) Twelve TOR-like genes were found in this dataset, along with potential homologues of the associated RAPTOR genes. TOR genes were associated with an upregulation in LF compared to FF stages (Figure 8.8B).

Lily ERF and MYB transcription factor genes identified here (Figure 8.8E, G) in a lot of cases showed an upregulation of expression at the early stage comparison (EF vs. SF) and during later stages (FF vs. LF) but not during the comparison of stages during the full flower opening (SF vs. FF).

Some other senescence-related TF genes such as WRKYs (WRKY22-, 33-, 35-, and 65-like) were also strongly expressed during in LF stages compared to FF stages and shows there is expression and activity of TFs well into this stage (Figure 8.8D). However, some WRKY TFs (WRKY35-like) were expressed strongly in EF vs. SF stages too and correlates with the expression of SAG20-like gene (Figure 8.8F).

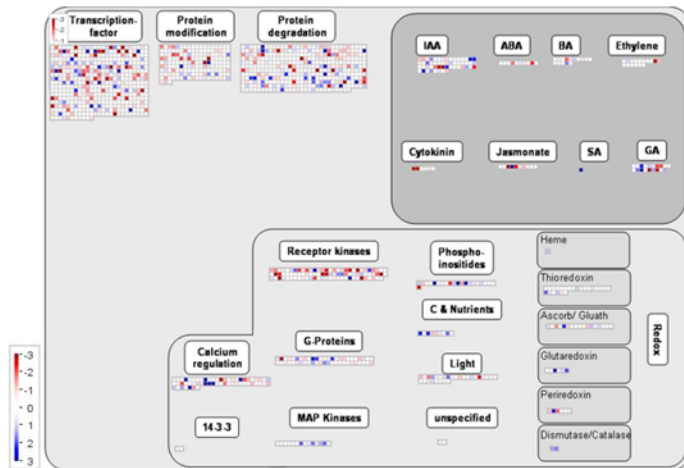
(A) SF/EF



EF

SF

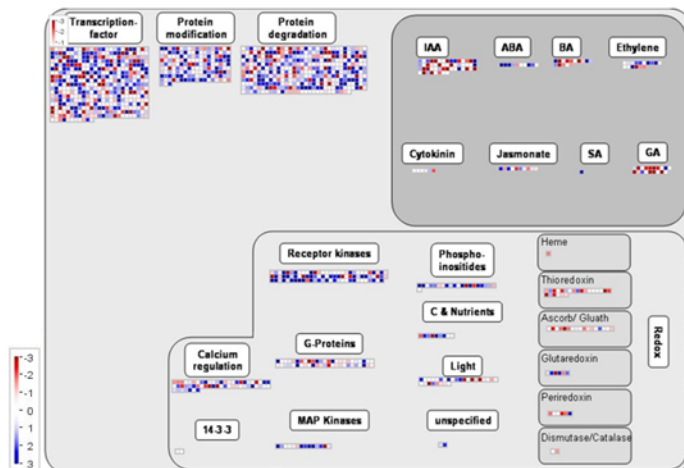
(B) FF/SF



SF

FF

(C) LF/FF



FF

LF

Figure 8.7 – Regulatory genes (separated into groups relating to type) showing differential expression (\log_2FC) between comparisons between (A) EF and SF stages, (B) SF and FF stages and (C)

FF and LF stages. Key shows upregulated genes in red and downregulated genes in blue in each comparison. Images of lilies from Shi et al. (2018b).

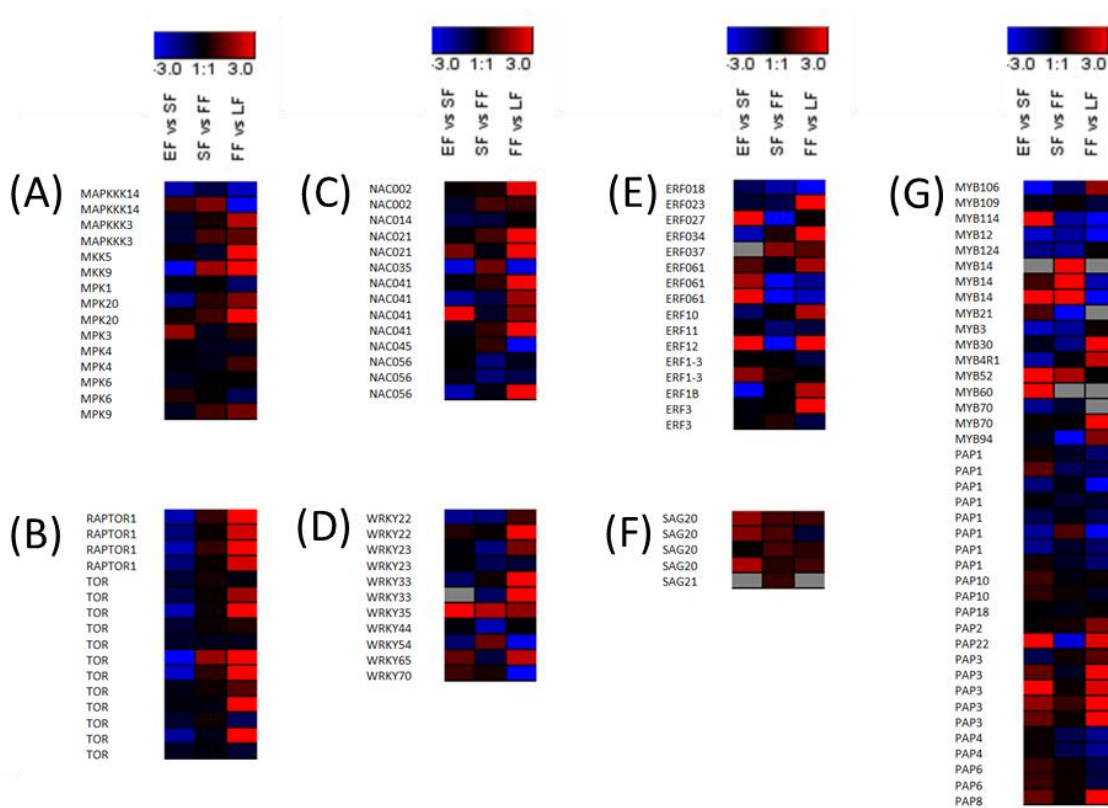


Figure 8.8 – Heatmaps showing expression of DEGs most significantly aligning to *A. thaliana*/*O. sativa* transcription factor genes. Grouped by (A) MAPK, (B) TOR, (C) NAC, (D) WRKY, (E) ERF, (F) SAG and (G) MYB TF families. Gene expression expressed as Log₂FC in a timepoint-to-timepoint comparison.

Auxin was hypothesised to be important in flower opening as it is an important growth driver and regulator in plants. Many auxin-related genes were found in this reanalysis, in particular 18 ARF genes, two AUX genes, seven IAA genes, 15 SAUR genes and 41 TIR genes (Figure 8.9).

Auxin's effect is mediated by the auxin response factor (ARF), which showed a downregulation in SF compared to EF stages and suggested a higher expression in the very earliest stages of flower opening. Many ARFs did not show a strong upregulation again until the LF stage compared to FF stage, particularly for ARF1-like, ARF3-like, ARF6-like and ARF17-like (Figure 8.9A). The IAA protein family is also auxin-regulated. IAA16-like, on the other hand, showed a strong upregulation at SF stage compared to EF. Forty-one TIR1-like genes, coding for a negative auxin regulator, was found many times in the dataset (41 DEGs) upregulated at earlier stages than EF, suggesting they may be more highly expressed prior to opening. Small auxin up-regulated RNA (SAUR) genes play a key role as auxin response genes (Stortenbeker and Bemer 2019) and several were found here mostly during flower opening (SF compared to EF stage), with many of them showing a downregulation in LF stages compared to FF.

Cytokinin signalling-related genes were found to be highly upregulated during and post-flower opening, with the positive regulator ARR17-like upregulated throughout opening, AHK3- and AHK4-like upregulated at the later stage comparison (higher expression in LF compared to EF stage), and ARR15-like upregulated at the two later stage comparisons (SF vs. FF and FF vs. LF). Many of the UDP- glycosyltransferase genes (UGTs), which are cytokinin inhibitors, were found upregulated at various stage comparisons as well. UGT1-like, UGT73C6-like, UGT73C7-like, UGT76F1-like, UGT84A2-like, and UGT85A2-like showed upregulated expression only in LF stage compared to FF, UGT85A5-like, UGT73B5-like, and UGT73C2-like only in SF compared to EF, and UGT73B4-like and UGT85A5-like in both EF vs. SF and SF vs. FF, spanning the full opening process (Figure 8.9B).

Oriental lilies are not ethylene-sensitive but the ethylene-synthesis and -response genes ACC-like and EIL-/ETR-like had an upregulated expression at the later stages of development (higher expression in LF stage compared to FF, Figure 8.9C). Gibberellin signalling is also linked to growth and development. Three GAI-like genes negative gibberellin-response gene, was found 3 times in this dataset. One showed a strong upregulation in LF compared to FF stages while another showed a downregulation (Figure 8.9D).

Some of the circadian control genes identified (Figure 8.9E) were key clock genes (CCA1-like, LHY-like, and TOC1-like) and phytochromes (PHYA/B-like) which for the most part did not show much change in expression over flower development. This is not surprising as all samples were taken at the same time of day (Shi et al. 2018b), and therefore the gene expression of circadian genes should be similar at all stages. However, some genes identified as ELF5A-1 and TOC1-like showed a high upregulation in later stages of development.

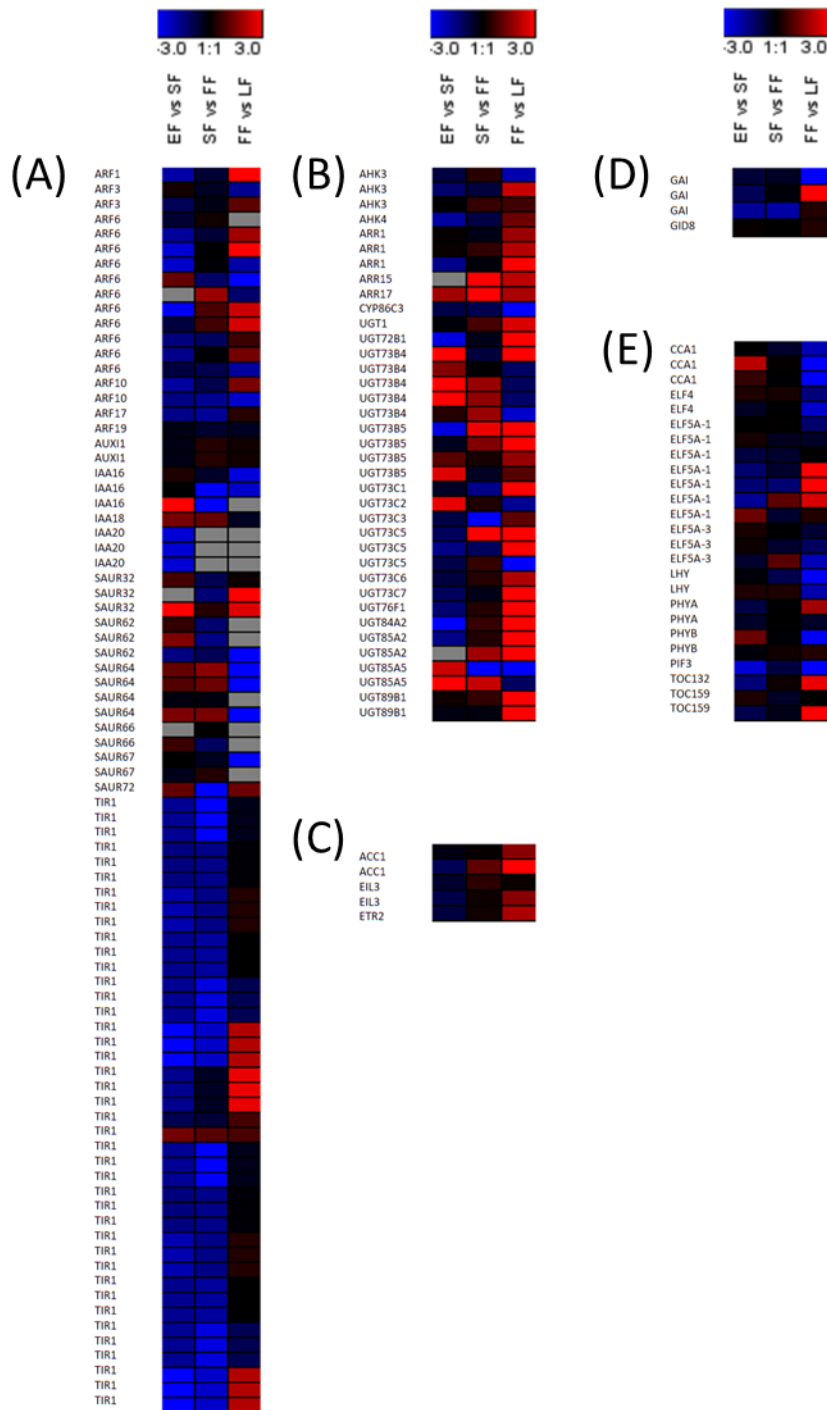


Figure 8.9 – Heatmaps showing expression of DEGs most significantly aligned to *A. thaliana*/*O. sativa* hormone-related genes. Grouped by (A) auxin, (B) cytokinin, (C) ethylene, (D) gibberellin and (E) circadian related genes. Gene expression expressed as Log₂FC in a timepoint-to-timepoint comparison.

How are genes for carbohydrate mobilisation/metabolism regulated?

Clustering of genes expressed in a similar pattern over development (from start of opening EF to the senescing flower LF) grouped DEGs into 10 groups (Figure 8.10 - Full lists in Supplementary data 3.3/3.4).

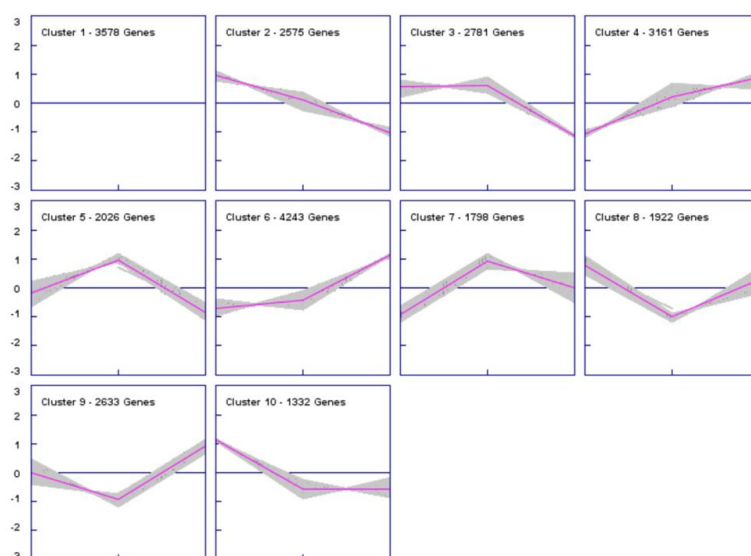


Figure 8.10 – K-means clustering separated DEGs into 10 groups (50 maximum iterations, 5 runs) showing a specific pattern of gene expression over the timepoints investigated (Stages EF-LF). Three timepoint comparison log₂FC values (from SF/EF, FF/SF, LF/FF comparisons) were plotted on each graph.

Clusters 4 and 6 were analysed by KEGG pathway analysis as genes expressed more highly over development and opening. Linoleic and linolenic acid metabolism was indicated to be significantly overrepresented in an *A. thaliana* background, alongside starch and sucrose metabolism and biosynthesis of secondary metabolites (Table 8.2). Genes upregulated throughout these developmental stages were looked at in more detail. Genes in Clusters 4 and 6 correlated with the expression of sucrose metabolism genes *SUS3*, *SUS4*, *SPP3* and the starch breakdown gene *AMY2* and included a range of TFs and hormone-related genes. Some of the most interesting were members of the MAPK family (*MPK1*), auxin related genes (*ARF6*, *TIR1*, *IAA18*), and the gibberellin synthesis *GAI* gene.

Table 8.2 – KEGG pathway analysis of DEGs in Clusters 4 and 6 using ShinyGO (Ge et al. 2020)						
KO pathway	Pathway	Enrichment FDR	nGenes	Pathway Genes	Fold Enrichment	Genes
ko00591	Linoleic acid metabolism	0.017181105	5	9	6.339896278	AT1G55020 AT1G67560 AT1G72520 AT3G22400 AT3G45140
ko04140	Autophagy	0.017181105	11	41	3.061706007	AT1G50030 AT1G54210 AT1G60490 AT2G31260

						AT2G37840 AT2G44140 AT3G08850 AT3G18770 AT3G19190 AT3G49590 AT3G61710
ko00592	Alpha-Linolenic acid metabolism	0.040884599	10	43	2.65391007	AT1G06290 AT1G67560 AT1G72520 AT1G76690 AT2G06050 AT2G33150 AT3G25760 AT3G45140 AT3G51840 AT4G13010
ko03015	MRNA surveillance pathway	0.000275209	27	117	2.633495377	AT1G11400 AT1G13120 AT1G13190 AT1G15200 AT1G16610 AT1G17720 AT1G17760 AT1G17980 AT1G27595 AT1G30460 AT1G61010 AT1G71800 AT2G13540 AT2G36480 AT2G36660 AT2G39260 AT2G39840 AT3G05580 AT3G06560 AT3G07810 AT3G09100 AT3G09880 AT3G20650 AT3G25800 AT3G26020 AT3G52210 AT3G58390
ko03440	Homologous recombination	0.021024034	14	63	2.535958511	AT1G04020 AT1G09815 AT1G50840 AT1G77320 AT1G78650 AT1G80210 AT2G01440

						AT2G06510 AT2G16390 AT2G21450 AT2G22140 AT3G02680 AT3G19210 AT3G20540
ko00562	Inositol phosphate metabolism	0.040884599	15	77	2.223080513	AT1G07230 AT1G14520 AT1G21980 AT1G22620 AT1G34260 AT1G60490 AT1G71010 AT2G14170 AT2G22240 AT3G03530 AT3G07960 AT3G10550 AT3G14205 AT3G14270 AT3G51460
ko03013	Nucleocytoplasmic transport	0.045577337	17	98	1.979600266	AT1G10390 AT1G11400 AT1G13120 AT1G14850 AT1G15200 AT1G16610 AT1G24310 AT1G79280 AT2G13540 AT2G16950 AT2G30050 AT2G31660 AT2G39260 AT2G45000 AT3G06720 AT3G08947 AT3G08960
ko03018	RNA degradation	0.040884599	19	112	1.935932613	AT1G07705 AT1G08370 AT1G48650 AT1G59760 AT1G76630 AT1G79090 AT1G80780 AT2G17510 AT2G22480 AT2G30800 AT2G32070 AT2G35920

						AT2G36660 AT3G03710 AT3G13290 AT3G13300 AT3G22270 AT3G46960 AT3G58560
ko03040	Spliceosome	0.01718110 5	31	187	1.891797927	AT1G03140 AT1G09770 AT1G10580 AT1G14650 AT1G20960 AT1G26370 AT1G27650 AT1G30480 AT1G32490 AT1G44910 AT1G60170 AT1G77180 AT2G13540 AT2G29580 AT2G37340 AT2G40650 AT2G41060 AT2G47250 AT2G47330 AT3G01540 AT3G06480 AT3G09440 AT3G11960 AT3G12580 AT3G13224 AT3G15010 AT3G26560 AT3G50670 AT3G56860 AT4G01020 AT4G03430
ko04144	Endocytosis	0.04088459 9	25	157	1.817167723	AT1G10290 AT1G13980 AT1G15130 AT1G17730 AT1G21630 AT1G21980 AT1G52570 AT1G59610 AT1G73030 AT2G27600 AT2G37550 AT2G43160 AT3G07960

						AT3G09440 AT3G11130 AT3G12400 AT3G12580 AT3G15730 AT3G20290 AT3G46060 AT3G46540 AT3G51310 AT3G53710 AT3G60860 AT4G05000
ko00500	Starch and sucrose metabolism	0.040884599	26	168	1.766113963	AT1G02850 AT1G03310 AT1G04920 AT1G06410 AT1G23870 AT1G27680 AT1G61810 AT1G61820 AT1G68020 AT1G70290 AT2G18700 AT2G35840 AT2G36190 AT2G39930 AT2G40840 AT2G45880 AT3G01180 AT3G13560 AT3G13790 AT3G29320 AT3G43190 AT3G43860 AT3G46970 AT3G47000 AT4G02280 AT4G10120
ko01110	Biosynthesis of secondary metabolites	0.040884599	136	1243	1.248597433	AT1G02500 AT1G02850 AT1G03310 AT1G04920 AT1G06290 AT1G06410 AT1G07230 AT1G08520 AT1G09430 AT1G09830 AT1G11790 AT1G12010 AT1G12550

						AT1G15080 AT1G15110 AT1G16350 AT1G21400 AT1G22340 AT1G22360 AT1G22430 AT1G23870 AT1G27680 AT1G30100 AT1G31690 AT1G36160 AT1G36370 AT1G44180 AT1G44446 AT1G52570 AT1G55920 AT1G58290 AT1G58440 AT1G60550 AT1G61810 AT1G61820 AT1G62810 AT1G63970 AT1G67070 AT1G67560 AT1G68020 AT1G70290 AT1G71695 AT1G72520 AT1G72680 AT1G72880 AT1G74040 AT1G74260 AT1G74910 AT1G75330 AT1G75450 AT1G76490 AT1G76550 AT1G76690 AT1G79550 AT2G05710 AT2G06050 AT2G13360 AT2G17265 AT2G18150 AT2G18700 AT2G20900 AT2G22240 AT2G22250 AT2G22480
--	--	--	--	--	--	---

						AT2G26250
						AT2G26540
						AT2G26640
						AT2G33150
						AT2G34060
						AT2G35040
						AT2G35840
						AT2G36190
						AT2G36230
						AT2G36750
						AT2G36800
						AT2G37500
						AT2G37790
						AT2G38280
						AT2G38700
						AT2G39420
						AT2G39800
						AT2G39930
						AT2G40840
						AT2G41480
						AT2G41540
						AT2G42790
						AT2G43090
						AT2G44520
						AT2G45880
						AT3G01180
						AT3G03530
						AT3G03780
						AT3G06650
						AT3G06810
						AT3G06850
						AT3G07630
						AT3G08860
						AT3G09560
						AT3G10050
						AT3G10230
						AT3G11430
						AT3G13450
						AT3G13790
						AT3G15730
						AT3G16910
						AT3G21560
						AT3G22460
						AT3G22960
						AT3G24200
						AT3G24503
						AT3G25760
						AT3G27380
						AT3G29320
						AT3G43190
						AT3G45140

						AT3G46970 AT3G47000 AT3G47340 AT3G47800 AT3G48560 AT3G49160 AT3G51840 AT3G52930 AT3G53160 AT3G54250 AT3G55410 AT3G59380 AT3G61440 AT3G62860 AT3G63250 AT4G01850 AT4G02280 AT4G05160 AT4G10120 AT4G12290 AT4G13010
--	--	--	--	--	--	---

Genes in the clusters upregulated in EF vs. SF stages only and dropping in expression over development (Cluster 2, Cluster 10) showed enrichment of oxidative phosphorylation pathways and the ribosome and proteasome. Biosynthesis of secondary metabolites and cofactors also was found to be significantly overrepresented in this group. Individual genes consisted of glycolysis-related genes (*GAPC1*, *HKL1*), sucrose related (*SUS3,4*) and cell wall modifying β -glucosidases (*BGLU40,44*). Regulatory genes also upregulated in the same pattern were auxin response genes (*IAA16*, *TIR1*, *ARF6*), MAPK family TFs (*MPK4,6*).

KO pathway	Pathway	Enrichment FDR	nGenes	Pathway Genes	Fold Enrichment	Genes
ko00190	Oxidative phosphorylation	1.02E-07	25	137	4.088894	AT1G15120 AT1G16700 AT1G20260 AT1G22450 AT1G22840 AT1G51650 AT1G78900 AT1G80660 AT2G02050 AT2G21410 AT2G33040 AT2G33220 AT3G01390 AT3G03070 AT3G06310 AT3G08560

						AT3G08610 AT3G12260 AT3G28715 AT3G52300 AT3G58730 AT3G60330 AT3G62790 AT4G10040 AT4G11150
ko03050	Proteasome	0.001973	11	61	4.040631	AT1G13060 AT1G16470 AT1G53750 AT1G56450 AT2G05840 AT2G27020 AT3G05530 AT3G11270 AT3G22630 AT3G26340 AT3G60820
ko03060	Protein export	0.009412	9	53	3.804986	AT1G52600 AT1G53530 AT2G22425 AT2G39960 AT3G08980 AT3G20920 AT3G24590 AT3G49100 AT3G60540
ko04145	Phagosome	0.003267	12	77	3.492021	AT1G11890 AT1G20260 AT1G78900 AT2G21410 AT3G01390 AT3G08560 AT3G28715 AT3G48040 AT3G58730 AT3G60540 AT4G09720 AT4G11150
ko03010	Ribosome	2.29E-09	44	315	3.129886	AT1G02780 AT1G04270 AT1G17560 AT1G57660 AT1G66580 AT1G70190 AT1G70600 AT1G74050 AT1G77940 AT2G09990

						AT2G27720 AT2G32220 AT2G34480 AT2G36160 AT2G36170 AT2G37270 AT2G43030 AT2G43460 AT2G47110 AT3G02080 AT3G04920 AT3G05590 AT3G06680 AT3G06700 AT3G09630 AT3G10610 AT3G13580 AT3G13882 AT3G14600 AT3G16080 AT3G23390 AT3G26360 AT3G27830 AT3G44890 AT3G47370 AT3G49010 AT3G49910 AT3G53740 AT3G55280 AT3G56340 AT3G57490 AT3G60245 AT3G62250 AT3G62870
ko00480	Glutathione metabolism	0.029459	12	103	2.61054	AT1G10360 AT1G10370 AT1G59670 AT1G65820 AT1G65930 AT1G69930 AT2G30870 AT2G31570 AT2G47730 AT3G03190 AT3G62760 AT4G11600
ko01240	Biosynthesis of cofactors	0.029459	22	249	1.979747	AT1G02500 AT1G10070 AT1G22940 AT1G48030 AT1G48320

						AT1G55090 AT1G58290 AT1G64970 AT2G18250 AT2G20690 AT2G22230 AT2G30390 AT2G31955 AT2G37250 AT2G45790 AT2G46760 AT3G07270 AT3G17390 AT3G23820 AT3G48730 AT3G49680 AT4G01850
ko01110	Biosynthesis of secondary metabolites	0.000162	90	1243	1.622399	AT1G02205 AT1G02500 AT1G06520 AT1G07720 AT1G09400 AT1G10070 AT1G10670 AT1G12000 AT1G13440 AT1G13560 AT1G15950 AT1G20050 AT1G22360 AT1G22370 AT1G26560 AT1G30040 AT1G32100 AT1G32780 AT1G48030 AT1G48320 AT1G48850 AT1G50460 AT1G56190 AT1G58290 AT1G58440 AT1G62660 AT1G64970 AT1G65930 AT1G65960 AT1G67730 AT1G68530 AT1G76690 AT1G78440 AT1G79870

						AT1G80600
						AT1G80820
						AT2G02500
						AT2G06925
						AT2G20420
						AT2G20690
						AT2G26640
						AT2G26670
						AT2G30390
						AT2G30490
						AT2G33150
						AT2G35390
						AT2G36750
						AT2G36760
						AT2G36800
						AT2G37040
						AT2G37250
						AT2G41480
						AT2G43420
						AT2G44350
						AT2G45440
						AT2G45790
						AT2G47510
						AT3G02780
						AT3G04120
						AT3G08860
						AT3G10230
						AT3G17070
						AT3G17390
						AT3G18080
						AT3G19450
						AT3G19820
						AT3G20160
						AT3G25530
						AT3G25900
						AT3G43190
						AT3G47520
						AT3G47800
						AT3G48730
						AT3G49680
						AT3G50520
						AT3G52940
						AT3G53130
						AT3G53260
						AT3G55120
						AT3G55360
						AT3G55440
						AT4G00490
						AT4G01320
						AT4G01850
						AT4G02280

						AT4G02780 AT4G11980 AT4G12290 AT4G12430 AT4G13010
--	--	--	--	--	--	---

The genes clustered as upregulated in FF stage compared to the other stages (EF, SF, LF – Cluster 3, Cluster 5, Cluster 7) contained the cell wall invertases *CWINV1,4*, trehalose metabolism genes (*TPS1*, *TPPF*), glycolysis related genes (*FBA1,6*, *PFK5*), and β -glucosidases (*BGLU11*, 46). Their expression was correlated with the regulatory ethylene response gene *EIL3*, cytokinin responsive *ARR15*, *TOR*, and several circadian genes (*PIF3*, *ELF5*).

Clusters 4 and 6 were identified as genes upregulated in later stages of development such as FF and LF. These clusters include putative invertase-coding genes (*CWINVV1,4*, *CINV2*), starch synthase-coding genes (*SS2*) and more trehalose metabolism genes (*TPS8*, 9). This is correlated with starvation response genes *TOR* and *RAPTOR1* and ethylene sensitive *EIL3*. Senescence-associated genes such as *WRKYs* that were hypothesised to have been upregulated at this stage showed an upregulation throughout development.

Discussion

Physical mechanisms of sucrose and starch mobilisation and metabolism in lily tepals during flower opening

Sucrose and starch mobilisation and metabolism is tightly regulated in sink tissues such as flowers in order to ensure there is enough for respiration, cell wall production and for expansion over opening and development. The RNA-seq analysis examined the expression of genes related to sucrose transport and metabolism, and aimed to identify coexpressed regulatory genes in order to make hypotheses on TFs or hormone-related genes important for the expression of genes related to the physical mechanisms of opening.

Sucrose synthases are essential for cellulose and starch biosynthesis, and in particular important in determining sink strength through their effect on phloem loading, as they create a concentration gradient across the cell membrane through conversion of sucrose to UDP-glucose (Baroja-Fernández et al. 2012). Therefore, the strong expression of *SUS3/4* over all stages of development shown here suggests the need for tepals to still produce starch and cellulose into senescence, which conforms with the upregulation of starch synthase (*SS2*) in stages FF vs. LF. This late stage starch production may be important for pollen and ovary development; otherwise starch has not been observed in tepals of fully open flowers. The expression of *CWINVVs* and *CINVs* being upregulated over opening stages (SF-LF) can also be explained by the requirement of several pathways to bring sugars into the cell. The breakdown of sucrose by cell wall invertases (*CWINVs*) in the apoplast at the phloem termini causes uptake of hexose sugars by the cell, and in cut peony increased in expression over time, correlating with a greater accumulation of sugars, and better flower longevity and quality (Xue et al. 2018).

High expression of *CWINVs* and *SWEETs* is also linked to apoplasmic phloem loading, as breakdown of sucrose released directly into the apoplasm is vital for fast hexose uptake by cells (Ruan et al.

2010; Durand et al. 2018), and points to apoplasmic loading being a main strategy used by Oriental lilies. Expression of CWINVs has been linked to cytokinin signalling and a delay in leaf senescence and may also be important in bud competition (Ruan et al. 2010). Cytokinin-related gene expression was found to be very high over development and opening here and therefore may be a good pathway to target for further analysis by qPCR and cytokinin assays.

Glucose taken up by the cell is phosphorylated to stop it from passing the cell membrane again and therefore is an essential regulatory step in respiration. Sugars used up in respiration can no longer help in maintaining osmolarity and therefore it may be expected that tepal cells may preferentially use other pathways to maintain energy levels, as suggested by GAPC1 expression. PFK and FBA are also involved in glycolysis but showed an upregulation in late developmental stages, which contradicts the expression of GAPC1. This may be affected by pollen contamination in flowers which have undergone anthesis already.

Genes relating to starch synthesis and breakdown were not found to be very differentially expressed over development and opening in comparison to the other sucrose metabolism genes. The RNAseq data analysed here shows a slight upregulation of the starch breakdown-related gene coding for an α -amylase (*AMY2*) in FF compared to SF stages. A-amylase has been strongly implicated in increasing turgor pressure in cells to cause expansion and growth through increasing osmotic potential of cells, and experimentally determined that adding specific amylase inhibitors slowed/halted growth of tepal sections (Bieleski et al. 2000a), but this was not observed in its expression in this experiment, which suggests it may not be transcriptionally controlled. The ubiquitous high expression of sucrose synthases (*SUS3/4*) throughout all stages has also been linked to cellulose and starch synthesis (Baroja-fernández et al. 2012). Starch synthase (*SS2*) being upregulated at later stages could point to a similar cycle to the *SUS/SPS* negative feedback loop being used in cells to maintain a constant starch level for respiration.

These data were used to design primers to investigate using qPCR if there are changes in the constant expression of these genes with perturbations to their environment; for example with commercial treatment or position on stem relating to ability of the bud to open.

Regulation of flower opening in Oriental lilies

Many regulatory genes were identified in this dataset and suggest that there is continued regulation of aspects of development throughout flower opening. Previous studies on other species suggest this may be due to the flower opening being regulated to open at a specific time depending on the plant's pollination strategy, and once the flower is opened and preferably pollinated, to conversely recycle the nutrients back into the plant (Van Meeteren et al. 2001).

Specific TFs were found to be expressed at earlier stages of development, such as members of the ERF and MYB family (ERF027, ERF12, MYB1.14, MYB52, MYB60), and this reflects the role of both of these TF families in developmental functions. MYB TFs have been linked to flower opening-related secondary metabolism, for example tepal scent and colour (Deng and Lu 2017; Fatihah et al. 2019) and ERFs have likewise been found involved in these same developmental changes (Liu et al. 2017).

Hormonal regulation is important to coordinate plant functions across organs and tissues. GA-, auxin-, and cytokinin-related genes (*IAA18*, *GAI*, *ARR15*) are even found upregulated into senescence, suggesting there is still a great deal of hormonal regulation at this late stage of development. *GAI* is a repressor of gibberellin and stem elongation (Peng et al. 1997), and could be important in downregulating vegetative growth during a period of reproductive development.

TIR1-like genes were upregulated in EF stages compared to SF, which suggests auxin signalling may be more important in the earlier stages of opening, and perhaps even prior to the stages described here in this experiment. Many other putative auxin related genes such as *ARF6* and *IAA20* show a similar pattern and suggest that the auxin response may be transcriptionally short lived, as has been described in previous studies (Luo et al. 2018).

Cytokinins often have antagonistic roles to auxin, and genes relating to cytokinin showed an increase in expression in later stages of the flower opening process. *AHK*, *AHP* and *ARR* are part of the positive signal transduction pathway, with *ARRs* being the transcriptional regulators, and *UGTs* code for glycosyltransferases which can modify and inhibit cytokinins. This suggests that cytokinin signalling may be involved in late flower opening and senescence. Ethylene-response genes *ACC*-like and *EIL*-/*ETR*-like also had an upregulated expression at the later stages of development (higher expression at LF stage compared to FF stage). This suggests it may be important in controlling the loss in sink strength, nutrient uptake, and flower senescence, which supports its well-known role in ripening and senescence (Eze et al. 1986; Iqbal et al. 2017).

An important consideration of the RNAseq data analysed here was the potential contamination of outer tepal samples by pollen, especially from flowers with dehisced anthers. It has been widely accepted that there is mobilisation of nutrients and signalling molecules particularly to and from the anthers, which contain developing pollen over the same time as the growth of buds in preparation for anther dehiscence and flower opening (Clement et al. 1996). Further work to identify and remove pollen, anther, or ovary-specific genes from the sample, or to repeat this RNA-seq experiment while specifically ensuring there was no contamination of tepal tissue in samples would give more confidence in genes directly related to flower opening.

As the Oriental lily has no full genome sequenced currently, *A. thaliana* gene codes were used to maximise gene annotation. *A. thaliana* may be more comparable to lily than rice (*O. sativa*) or wheat (both monocotyledonous species with good genome annotation), having a similar flowering development. However, there may be more sequence similarity to monocotyledonous species such as oil palm (*E. guineensis*), as found by the initial study (Shi et al. 2018b). Many of the *SUS*/*CWINV* genes did not come up as the same gene comparing sequences significantly aligned by BLAST against an *Arabidopsis thaliana* database compared to against an *Oryza sativa* database, showing similarities between all sequences and varietal differences between monocotyledonous and dicotyledonous species.

Is there evidence that this regulation is linked to the sucrose and starch metabolism and affected by external environmental factors?

Regulatory genes which are known to be linked to the nutritional status of the bud are the *TOR* and related *RAPTOR* genes which have been found differentially expressed over opening in this dataset. *TOR* kinase integrates developmental and environmental information to modulate metabolic pathway regulation, in particular in the starvation response (Shi et al. 2018a), which would suggest starvation-related genes are upregulated when the flowers were weakest as a sink to extend life.

Genes which may play a part in this partitioning of starch and soluble sugar content to different buds were investigated. As discussed in Section 4.1, several sucrose synthases and invertases were found in the RNA-seq dataset. *SUS3* and *SUS4* were expressed highly throughout flower opening stages (EF-FF), and the invertases identified were upregulated in FF compared to SF stages (*CWINV1/4*) and LF compared to FF stages (*CINV2*). This makes sense as plants mobilise energy mostly as sucrose from source organs to sink organs, and both of these enzymes have sucrose catabolising functions; this

means they are vital for regulating carbon partitioning between buds (Barratt et al. 2009). The gene *TPS1* (coding for a trehalose phosphate synthase) has been shown in avocado as a marker for bud competition (Gould et al. 2019). *TPS1* was identified as being upregulated in this dataset in FF compared to SF stages, which could indicate a high sucrose uptake by opening buds.

The experiment carried out did not take position on stem into account and additionally, the flowers were not commercially treated with cold/dark storage, and therefore the effect of bud competition on stem cannot be investigated in great detail. Position on stem has been indicated as a problem in commercially treated stems only; all buds on plant have been reported to open normally under normal commercial greenhouse conditions (personal communication, James Cole, E.M. Cole Farms Ltd.). However, the data shown here has indicated that sucrose mobilisation-related genes are expressed differentially across development and opening and therefore may play a role in changing the sink strength of the particular flower over its developmental age (van Meeteren 2001). Further experiments could be carried out to compare the data collected here to commercially treated flowers, as well as comparing position on stem to indicate if different positions on stem have different expression of sucrose-uptake related genes, for example.

Conclusion

The reanalysis of this dataset kindly shared by Shi et al. (2018b) has provided an overview of gene expression over flower opening in Oriental lilies and identified several groups of genes which are hypothesised to be important in flower opening. Firstly, sucrose and starch metabolism and mobilisation related genes were found to be highly differentially expressed over opening, and in particular *AMY2*, *CWINV* and *SWEET* genes have been indicated to perhaps be involved at earlier stages of development prior to opening. Secondly, several members of the TF classes ERFs, TOR and MYBs have shown upregulation at early stages of flower opening and may indicate important regulatory roles, as well as auxin-related genes *ARF6*, *IAA20* and *TIR1*, all of which may be expressed highly prior to opening. qPCR analysis of earlier stages of development in the gene expression of these indicated genes may elucidate their role in flower opening.

References

- Agehara, S., Finlayson, S. and Leskovar, D. 2013. Abscisic acid inhibits leaf expansion by limiting cell expansion but not cell division in Arabidopsis. In: *ASHS Annual Conference*. Palm Springs, CA, ASHS. Available at:
https://www.researchgate.net/publication/267342555_Abscisic_Acid_Inhibits_Leaf_Expansion_by_Limiting_Cell_Expansion_But_Not_Cell_Division_in_Arabidopsis
- Aghdam, M.S., Jannatizadeh, A., Sheikh-Assadi, M. and Malekzadeh, P. 2016. Alleviation of postharvest chilling injury in anthurium cut flowers by salicylic acid treatment. *Scientia Horticulturae* 202, pp. 70–76. Available at: <https://dx.doi.org/10.1016/j.scienta.2016.02.025>.
- Aloni, R., Aloni, E., Langhans, M. and Ullrich, C.I. 2006. Role of auxin in regulating Arabidopsis flower development. *Planta* 223(2), pp. 315–328. doi: 10.1007/s00425-005-0088-9.
- Altmann, M. et al. 2020. Extensive signal integration by the phytohormone protein network. *Nature* 583(7815), pp. 271–276. doi: 10.1038/s41586-020-2460-0.
- Andersen, C.H., Jensen, C.S. and Petersen, K. 2004. Similar genetic switch systems might integrate the floral inductive pathways in dicots and monocots. *Trends in Plant Science* 9(3), pp. 105–107. Available at: <https://www.sciencedirect.com/science/article/pii/S1360138504000202>.
- Anderson, M.J. and Willis, T.J. 2003. Canonical analysis of principal coordinates: A useful method of constrained ordination for ecology. *Ecology* 84(2), pp. 511–525. doi: 10.1890/0012-9658(2003)084[0511:CAOPCA]2.0.CO;2.
- Anderson, N.O., Berghauer, E., Harris, D., Johnson, K., Lönnroos, J. and Morey, M. 2012. Discovery of novel traits in seed-propagated *Lilium*: Non-vernalization- requiring, day-neutral, reflowering, frost-tolerant, winter-hardy *L. xformolongi*. I. Characterization. *Floriculture and Ornamental Biotechnology* 6(SPEC.ISS.2), pp. 63–72.
- Andrés, F. et al. 2020. The sugar transporter *SWEET10* acts downstream of *FLOWERING LOCUS T* during floral transition of *Arabidopsis thaliana*. *BMC Plant Biology* 20(1), pp. 1–14. doi: 10.1186/s12870-020-2266-0.
- Antonio, A. da S., Oliveira, D.S., Cardoso dos Santos, G.R., Pereira, H.M.G., Wiedemann, L.S.M. and Veiga-Junior, V.F. da 2021. UHPLC-HRMS/MS on untargeted metabolomics: a case study with *Copaifera*(*Fabaceae*). *RSC Advances* 11(40), pp. 25096–25103. doi: 10.1039/d1ra03163e.
- Arana, M.V., Marín-De La Rosa, N., Maloof, J.N., Blázquez, M.A. and Alabadi, D. 2011. Circadian

oscillation of gibberellin signaling in Arabidopsis. *Proceedings of the National Academy of Sciences* 108(22), pp. 9292–9297. doi: 10.1073/pnas.1101050108.

Argüello-astorga, G., Solís-guzm, M.G. and Hidalgo, D. 2017. Gene expression patterns Arabidopsis thaliana sucrose phosphate synthase (SPS) genes are expressed differentially in organs and tissues, and their transcription is regulated by osmotic stress. *Gene Expression Patterns* 25–26, pp. 92–101. doi: 10.1016/j.gep.2017.06.001.

Arrom, L. and Munne-Bosch, S. 2012. Hormonal changes during flower development in floral tissues of Liliium. *Planta* 236(2), pp. 343–354. doi: 10.1007/s00425-012-1615-0.

Arrom, L. and Munné-Bosch, S. 2012. Sucrose accelerates flower opening and delays senescence through a hormonal effect in cut lily flowers. *Plant Science* 41(7), pp. 188–189. doi: 10.1016/j.plantsci.2012.02.012.

Aubert, Y. et al. 2010. RD20, a stress-inducible caleosin, participates in stomatal control, transpiration and drought tolerance in Arabidopsis thaliana. *Plant and Cell Physiology* 51(12), pp. 1975–1987. doi: 10.1093/pcp/pcq155.

Bae, H., Herman, E.M., Bailey, B.A., Bae, H.-J. and Sicher, R.C. 2005. Exogenous trehalose alters Arabidopsis transcripts involved in cell wall modification, abiotic stress, nitrogen metabolism, and plant defense. *Physiologia Plantarum* 125, pp. 114–126.

Bailey, T.L. and Grant, C.E. 2021. SEA: Simple Enrichment Analysis of motifs. *bioRxiv*, p. 2021.08.23.457422. Available at: <https://www.biorxiv.org/content/10.1101/2021.08.23.457422v1> <https://www.biorxiv.org/content/10.1101/2021.08.23.457422v1.abstract>.

Bakshi, M. and Oelmüller, R. 2014. WRKY transcription factors: jack of many trades in plants. *Plant Signaling and Behavior* 9(2), p. e27700. doi: 10.4161/psb.27700.

Balas, J., Gonzalez, P., Teixeira da Silva, J. and Jayatilleke, M. 2006. Supporting postharvest performance of cut flowers using fresh flower refreshments and other vase water additives. Ed. Teixeira da Silva, J. *Floriculture, Ornamental and Plant Biotechnology: Advances and Topical Issues.*, pp. 612–629. Global Science Books, UK.

Bao, F. et al. 2020. Metabolic, enzymatic activity, and transcriptomic analysis reveals the mechanism underlying the lack of characteristic floral scent in Apricot mei varieties. *Frontiers in Plant Science* 11(October), pp. 1–18. doi: 10.3389/fpls.2020.574982.

Baptista, R., Fazakerley, D.M., Beckmann, M., Baillie, L. and Mur, L.A.J. 2018. Untargeted

metabolomics reveals a new mode of action of pretomanid (PA-824). *Scientific Reports* 8(1), pp. 1–7. Available at: <http://dx.doi.org/10.1038/s41598-018-23110-1>.

Baroja-fernández, E., José, F., Li, J., Bahaji, A. and Almagro, G. 2012. Sucrose synthase activity in the *sus1/sus2/sus3/sus4* Arabidopsis mutant is sufficient to support normal cellulose and starch production. *Proceedings of the National Academy of Sciences* 109(1), pp. 321–6. doi: 10.1073/pnas.1117099109.

Barratt, D.H.P. et al. 2009. Normal growth of Arabidopsis requires cytosolic invertase but not sucrose synthase. *Proceedings of the National Academy of Sciences* 106(31), pp. 124–129.

Barsan, C. et al. 2012. Proteomic analysis of chloroplast-to-chromoplast transition in tomato reveals metabolic shifts coupled with disrupted thylakoid biogenesis machinery and elevated energy-production components. *Plant Physiology* 160(2), pp. 708–725. Available at: <https://doi.org/10.1104/pp.112.203679>.

Battle, M., Vegliani, F. and Jones, M.. 2020. Shades of green: untying the knots of green photoperception. *Journal of Experimental Botany* 71(19), pp. 5764–5770. doi: 10.1093/jxb/eraa312.

Beauzamy, L., Nakayama, N. and Boudaoud, A. 2014. Flowers under pressure: Ins and outs of turgor regulation in development. *Annals of Botany* . doi: 10.1093/aob/mcu187.

Beck, E. and Ziegler, P. 1989. Biosynthesis and degradation of starch in higher plants. *Annual Review of Plant Physiology and Plant Molecular Biology* 40(1), pp. 95–117. Available at: <https://doi.org/10.1146/annurev.pp.40.060189.000523>.

Bell, G. 1985. On the function of flowers. *Proceedings of the Royal Society of Biological Sciences* 224, pp. 223–265. doi: doi.org/10.1098/rspb.1985.0031.

Bergquist, S.Å.M., Gertsson, U.E., Nordmark, L.Y.G. and Olsson, M.E. 2007. Effects of shade nettings, sowing time and storage on baby spinach flavonoids. *Journal of the Science of Food and Agriculture* 87(13), pp. 2464–2471. Available at: <https://onlinelibrary.wiley.com/doi/abs/10.1002/jsfa.2956>.

Bích, L.N. and Nhung, N.T.H. 2020. Sucrose pulsing and cold storage on post-storage attributes of cut lily flowers in Dalat, Vietnam. *Dalat University Journal of Science* 10(2), p. 14. doi: 10.37569/dalatuniversity.10.2.575(2020).

Bieleski, R., Elgar, J. and Heyes, J. 2000a. Mechanical aspects of rapid flower opening in Asiatic lily. *Annals of Botany* 86(6), pp. 1175–83. doi: 10.1006/anbo.2000.1291.

Bieleski, R., Elgar, J., Heyes, J. and Woolf, A. 2000b. Flower opening in Asiatic lily is a rapid process

- controlled by dark-light cycling. *Annals of Botany* 86(6), pp. 1169–74. doi: 10.1006/anbo.2000.1289.
- Bieleski, R.L. 1993. Fructan hydrolysis drives petal expansion in the ephemeral daylily flower. *Plant Physiology* 103(1), pp. 213–219. doi: 10.1104/pp.103.1.213.
- Bieleski, R.L. 1995. Onset of phloem export from senescent petals of daylily. *Plant Physiology* 109(2), pp. 557–565. doi: 10.1104/pp.109.2.557.
- Biologists, 2010 American Society of Plant 2010. Introduction to Phytohormones. *The Plant Cell* 22(3), p. 1. Available at: <https://doi.org/10.1105/tpc.110.tt0310>.
- Biswal, B. and Biswal, U.C. 1999. Leaf senescence: Physiology and molecular biology. *Current Science* 77(6), pp. 775–782.
- Bolouri Moghaddam, M.R. and Van den Ende, W. 2013. Sugars, the clock and transition to flowering. *Frontiers in Plant Science* 4(FEB), pp. 1–6. doi: 10.3389/fpls.2013.00022.
- Bose, T.K., Mitra, S.K., Farooqi, A.A. and Sadhu, M.K. 1999. *Tropical Horticulture: Volume I*. First. Kolkata.
- Bozdogan, H. 1987. Model selection and Akaike's Information Criterion (AIC): The general theory and its analytical extensions. *Psychometrika* 52(3), pp. 345–370. doi: 10.1007/BF02294361.
- Brazel, A.J. and Ó'Maoiléidigh, D.S. 2019. Photosynthetic activity of reproductive organs. *Journal of Experimental Botany* 70(6), pp. 1737–1754. Available at: <https://doi.org/10.1093/jxb/erz033>.
- Breiman, L. 2001. Random Forests. *Machine Learning* 45(1), pp. 5–32. Available at: <https://doi.org/10.1023/A:1010933404324>.
- Brioude, F. et al. 2009. Jasmonate controls late development stages of petal growth in *Arabidopsis thaliana*. *Plant Journal* 60(6), pp. 1070–1080. doi: 10.1111/j.1365-3113.2009.04023.x.
- Brodmann, D., Schuller, A., Ludwig-Müller, J., Aeschbacher, R.A., Wiemken, A., Boller, T. and Wingler, A. 2002. Induction of trehalase in *Arabidopsis* plants infected with the trehalose-producing pathogen *Plasmodiophora brassicae*. *Molecular Plant-Microbe Interactions* 15(7), pp. 693–700. doi: 10.1094/MPMI.2002.15.7.693.
- Brown, L. and Pool, K. 2017. *Horticulture Statistics 2016*. Available at: https://assets.publishing.service.gov.uk/government/uploads/system/uploads/attachment_data/file/646536/hort-report-22sep17.pdf.
- Brunet, J. and Charlesworth, D. 1995. Floral sex allocation in sequentially blooming plants. *Evolution*

49(1), pp. 70–79. doi: 10.1111/j.1558-5646.1995.tb05959.x.

Burchi, G., Bianchini, C., Mercuri, A., Foglia, G., Rosellini, D. and Schiva, T. 1999. Analysis of post-harvest flower life in a cross between carnation cultivars with different ethylene responses. *Journal of Genetics and Breeding* 53(4), pp. 301–306.

Burchi, G., Nesi, B., Grassotti, A., Mensuali-Sodi, A. and Ferrante, A. 2005. Longevity and ethylene production during development stages of two cultivars of *Lilium* flowers ageing on plant or in vase. *Acta Horticulturae* 682(June), pp. 813–822. doi: 10.17660/ActaHortic.2005.682.106.

Bustin, S.A. et al. 2009. The MIQE guidelines: Minimum information for publication of quantitative real-time PCR experiments. *Clinical Chemistry* 55(4), pp. 611–622. doi: 10.1373/clinchem.2008.112797.

Cao, Y., Li, K., Li, Y., Zhao, X. and Wang, L. 2020. MYB transcription factors as regulators of secondary metabolism in plants. *Biology* 9(3), pp. 1–16. doi: 10.3390/biology9030061.

Castro, R.I., González-Feliu, A., Muñoz-Vera, M., Valenzuela-Riffo, F., Parra-Palma, C. and Morales-Quintana, L. 2021. Effect of exogenous auxin treatment on cell wall polymers of strawberry fruit. *International Journal of Molecular Sciences* 22(12), pp. 1–14. doi: 10.3390/ijms22126294.

Celikel, F.G. and van Doorn, W.G. 1995. Effects of water stress and gibberellin on flower opening in *Iris x hollandica*. In: *Acta Horticulturae*. International Society for Horticultural Science (ISHS), Leuven, Belgium, pp. 246–252. Available at: <https://doi.org/10.17660/ActaHortic.1995.405.32>.

Chalker-Scott, L. 1999. Environmental significance of anthocyanins in plant stress responses. *Photochemistry and Photobiology* 70(1), pp. 1–9. doi: 10.1111/j.1751-1097.1999.tb01944.x.

Chanasut, U., Rogers, H.J., Leverentz, M.K., Griffiths, G., Thomas, B., Wagstaff, C. and Stead, A.D. 2003. Increasing flower longevity in *Alstroemeria*. *Postharvest Biology and Technology* 29(3), pp. 325–333. Available at: <https://www.sciencedirect.com/science/article/pii/S0925521403000486>.

Chandler, J.W. 2011. The Hormonal regulation of flower development. *Journal of Plant Growth Regulation* 30(2), pp. 242–254. doi: 10.1007/s00344-010-9180-x.

Chapin, L. and Jones, M. 2007. Nutrient remobilization during pollination-induced corolla senescence in petunia. In: *Acta Horticulturae*. International Society for Horticultural Science (ISHS), Leuven, Belgium, pp. 181–190. Available at: <https://doi.org/10.17660/ActaHortic.2007.755.22>.

Chastagner, G.A., van Tuyl, J.M., Verbeek, M., Miller, W.B. and Westerdahl, B.B. 2017. *Diseases of Lily*. doi: 10.1007/978-3-319-32374-9_45-1.

- Chen, C. et al. 2020. An ethylene-inhibited NF-YC transcription factor RhNF-YC9 regulates petal expansion in rose. *Horticultural Plant Journal* 6(6), pp. 419–427. Available at: <https://www.sciencedirect.com/science/article/pii/S2468014120301114>.
- Chen, H., Bullock, D.A., Alonso, J.M. and Stepanova, A.N. 2022a. To fight or to grow: The balancing role of ethylene in plant abiotic stress responses. *Plants* 11(1), p. 33. doi: 10.3390/plants11010033.
- Chen, J. et al. 2022b. Effects of ethephon and low-temperature treatments on blood oranges (*Citrus sinensis* L. Osbeck): Anthocyanin accumulation and volatile profile changes during storage. *Food Chemistry* 393, p. 133381. Available at: <https://www.sciencedirect.com/science/article/pii/S0308814622013437>.
- Chen, Y., Lun, A.T.L. and Smyth, G.K. 2014. Differential expression analysis of complex RNA-seq experiments using edgeR. In: Datta, S. and Nettleton, D. eds. *Statistical Analysis of Next Generation Sequencing Data*. Cham: Springer International Publishing, pp. 51–74. Available at: https://doi.org/10.1007/978-3-319-07212-8_3.
- Cheng, H. et al. 2004. Gibberellin regulates Arabidopsis floral development via suppression of DELLA protein function. *Development* 131(5), pp. 1055–1064. doi: 10.1242/dev.00992.
- Cheng, Y. and Zhao, Y. 2007. A role for auxin in flower development. *Journal of Integrative Plant Biology* 49(1), pp. 99–104. doi: 10.1111/j.1744-7909.2006.00412.x.
- Chomczynski, P. and Sacchi, N. 1987. Single-step method of RNA isolation by acid guanidinium extraction. *Analytical Biochemistry* 162, pp. 156–159.
- Chuang, Y.C. and Chang, Y.C.A. 2013. The role of soluble sugars in vase solutions during the vase life of *Eustoma grandiflorum*. *HortScience* 48(2), pp. 222–226. doi: 10.21273/hortsci.48.2.222.
- Chung, W.C., Wu, R.S., Hsu, C.P., Huang, H.C. and Huang, J.W. 2011. Application of antagonistic rhizobacteria for control of Fusarium seedling blight and basal rot of lily. *Australasian Plant Pathology* 40(3), pp. 269–276. doi: 10.1007/s13313-011-0040-3.
- Clement, C., Burrus, M. and Audran, J.-C. 1996. Floral organ growth and carbohydrate content during pollen development in *Lilium*. *American Journal of Botany* 83(4), pp. 459–469.
- Clément, C., Chavant, L., Burrus, M. and Audran, J.C. 1994. Anther starch variations in *Lilium* during pollen development. *Sexual Plant Reproduction* 7(6), pp. 347–356. doi: 10.1007/BF00230513.
- Colcombet, J. and Hirt, H. 2008. Arabidopsis MAPKs: A complex signalling network involved in multiple biological processes. *Biochemical Journal* 413(2), pp. 217–226. doi: 10.1042/BJ20080625.

- Cosgrove, D.J., Li, L.C., Cho, H.-T., Hoffmann-Benning, S., Moore, R.C. and Blecker, D. 2002. The growing world of expansins. *Plant and Cell Physiology* 43(12), pp. 1436–1444. Available at: <https://doi.org/10.1093/pcp/pcf180>.
- Covington, M.F. and Harmer, S.L. 2007. The circadian clock regulates auxin signaling and responses in Arabidopsis. *PLOS Biology* 5(8), p. e222. doi: 10.1371/journal.pbio.0050222.
- Cristescu, S.M., Mandon, J., Arslanov, D., De Pessemier, J., Hermans, C. and Harren, F.J.M. 2013. Current methods for detecting ethylene in plants. *Annals of Botany* 111(3), pp. 347–360. doi: 10.1093/aob/mcs259.
- Crone, W. and Lord, E.M. 1991. A kinematic analysis of gynoecial growth in *Lilium longiflorum*: Surface growth patterns in all floral organs are triphasic. *Developmental Biology* 143(2), pp. 408–417. doi: 10.1016/0012-1606(91)90091-G.
- Cserhati, M. 2015. Motif content comparison between monocot and dicot species. *Genomics Data* 3, pp. 128–136. Available at: <https://www.sciencedirect.com/science/article/pii/S2213596015000033>.
- van Dam, S., Vösa, U., van der Graaf, A., Franke, L. and de Magalhães, J.P. 2018. Gene co-expression analysis for functional classification and gene-disease predictions. *Briefings in Bioinformatics* 19(4), pp. 575–592. doi: 10.1093/bib/bbw139.
- Darras, A.I. 2020. The chilling injury effect in cut flowers: a brief review. *The Journal of Horticultural Science and Biotechnology* 95(1), pp. 1–7. Available at: <https://doi.org/10.1080/14620316.2019.1629340>.
- Davies, K.M. and Schwinn, K.E. 2003. Transcriptional regulation of secondary metabolism. *Functional Plant Biology* 30(9), pp. 913–925. doi: 10.1071/FP03062.
- Delatte, T.L. et al. 2011. Growth arrest by trehalose-6-phosphate: An astonishing case of primary metabolite control over growth by way of the SnRK1 signaling pathway. *Plant Physiology* 157(1), pp. 160–174. doi: 10.1104/pp.111.180422.
- Deng, Y. and Lu, S. 2017. Biosynthesis and regulation of phenylpropanoids in plants. *Critical Reviews in Plant Sciences* 36(4), pp. 257–290. Available at: <https://doi.org/10.1080/07352689.2017.1402852>.
- Van Dijken, A.J.H., Schluepmann, H. and Smeekens, S.C.M. 2004. Arabidopsis trehalose-6-phosphate synthase 1 is essential for normal vegetative growth and transition to flowering. *Plant Physiology* 135(2), pp. 969–977. doi: 10.1104/pp.104.039743.
- Ding, H. et al. 2016. Jasmonate complements the function of Arabidopsis lipoxygenase3 in salinity

- stress response. *Plant Science* 244, pp. 1–7. doi: 10.1016/j.plantsci.2015.11.009.
- Doorn, W.G. Van 1996. Flower lifespan and disease risk. *Scientific Correspondence, Nature* 379(6568), p. 780. doi: 10.1038/379780a0.
- Van Doorn, W.G. et al. 2003. Gene expression during anthesis and senescence in Iris flowers. *Plant Molecular Biology* 53(6), pp. 845–863. doi: 10.1023/B:PLAN.0000023670.61059.1d.
- Doorn, W.G. Van 2004. Update on senescence: Is petal senescence due to sugar starvation? *Plant Physiology* 134(January), pp. 35–42. doi: 10.1104/pp.103.033084.compounds.
- van Doorn, W.G. and Cruz, P. 2000. Evidence for a wounding-induced xylem occlusion in stems of cut chrysanthemum flowers. *Postharvest Biology and Technology* 19(1), pp. 73–83. Available at: <https://www.sciencedirect.com/science/article/pii/S0925521400000697>.
- van Doorn, W.G., Dole, I., çelikel, F.G. and Harkema, H. 2013. Opening of Iris flowers is regulated by endogenous auxins. *Journal of Plant Physiology* 170(2), pp. 161–164. Available at: <https://www.sciencedirect.com/science/article/pii/S0176161712004993>.
- van Doorn, W.G. and Han, S.S. 2011. Postharvest quality of cut lily flowers. *Postharvest Biology and Technology* 62(1), pp. 1–6. doi: 10.1016/j.postharvbio.2011.04.013.
- van Doorn, W.G. and Kamdee, C. 2014. Flower opening and closure: an update. *Journal of Experimental Botany* 65(20), pp. 5749–5757. doi: 10.1093/jxb/eru327.
- van Doorn, W.G. and Van Meeteren, U. 2003. Flower opening and closure: A review. *Journal of Experimental Botany* 54(389), pp. 1801–1812. doi: 10.1093/jxb/erg213.
- van Doorn, W.G. and de Witte, Y. 1991a. Effect of bacterial suspensions on vascular occlusion in stems of cut rose flowers. *Journal of Applied Bacteriology* 71(2), pp. 119–123.
- van Doorn, W.G. and de Witte, Y. 1991b. Effect of dry storage on bacterial counts in stems of cut rose flowers. *HortScience* 26(12), pp. 1521–1522.
- van Doorn, W.G. and Woltering, E.J. 2008. Physiology and molecular biology of petal senescence. *Journal of Experimental Botany* 59(3), pp. 453–480. doi: 10.1093/jxb/erm356.
- Du, Y.P., Bi, Y., Zhang, M.F., Yang, F.P., Jia, G.X. and Zhang, X.H. 2017. Genome size diversity in *Lilium* (*Liliaceae*) is correlated with karyotype and environmental traits. *Frontiers in Plant Science* 8(July), pp. 1–11. doi: 10.3389/fpls.2017.01303.
- Dubois, M., Van den Broeck, L. and Inzé, D. 2018. The pivotal role of ethylene in plant growth. *Trends*

in *Plant Science* 23(4), pp. 311–323. Available at:

<https://www.sciencedirect.com/science/article/pii/S1360138518300153>.

Durand, M., Mainson, D., Porcheron, B., Maurousset, L. and Lemoine, R. 2018. Carbon source – sink relationship in *Arabidopsis thaliana* : the role of sucrose transporters. *Planta* 247(3), pp. 587–611. doi: 10.1007/s00425-017-2807-4.

Eason, J.R., de Vré, L., Somerfield, S.D. and Heyes, J.A. 1997. Physiological changes associated with *Sandersonia aurantiaca* flower senescence in response to sugar. *Postharvest Biology and Technology* 12, pp. 43–50.

Eklöf, J.M. and Brumer, H. 2010. The XTH gene family: an update on enzyme structure, function, and phylogeny in xyloglucan remodeling. *Plant Physiology* 153(2), pp. 456–466. Available at: <https://doi.org/10.1104/pp.110.156844>.

Elgar, H.J., Woolf, A.B. and Bieleski, R.L. 1999. Ethylene production by three lily species and their response to ethylene exposure. *Postharvest Biology and Technology* 16(3), pp. 257–267. doi: 10.1016/S0925-5214(99)00021-6.

Enot, D.P., Lin, W., Beckmann, M., Parker, D., Overy, D.P. and Draper, J. 2008. Preprocessing, classification modeling and feature selection using flow injection electrospray mass spectrometry metabolite fingerprint data. *Nature Protocols* 3(3), pp. 446–470. doi: 10.1038/nprot.2007.511.

Erpen, L., Devi, H.S., Grosser, J.W. and Dutt, M. 2018. Potential use of the DREB / ERF , MYB , NAC and WRKY transcription factors to improve abiotic and biotic stress in transgenic plants. *Plant Cell, Tissue and Organ Culture* 132(1), pp. 1–25. Available at: <http://dx.doi.org/10.1007/s11240-017-1320-6>.

Erwin, J. 2002. Easter Lily Production. *Minnesota Commercial Flower Growers Bulletin* 1(4). Available at: https://hortscans.ces.ncsu.edu/library/all/doc_id/1428/. [Accessed 30 Sept 2022].

Erwin, J.E. and Heins, R.D. 1990. Temperature effects on lily development rate and morphology from the visible bud stage until anthesis. *Journal of the American Society for Horticultural Science* 115(4), pp. 644–646. doi: 10.21273/jashs.115.4.644.

Eze, J.M.O., Mayak, S., Thompson, J.E. and Dumbroff, E.B. 1986. Senescence in cut carnation flowers: Temporal and physiological relationships among water status, ethylene, abscisic acid and membrane permeability. *Physiologia Plantarum* 68, pp. 323–328.

Fageria, N.K., Filho, M.P.B., Moreira, A. and Guimarães, C.M. 2009. Foliar fertilization of crop plants. *Journal of Plant Nutrition* 32(6), pp. 1044–1064. Available at:

<https://doi.org/10.1080/01904160902872826>.

Fatihah, H.N.N., Moñino López, D., van Arkel, G., Schaart, J.G., Visser, R.G.F. and Krens, F.A. 2019. The ROSEA1 and DELILA transcription factors control anthocyanin biosynthesis in *Nicotiana benthamiana* and *Lilium* flowers. *Scientia Horticulturae* 243, pp. 327–337. Available at: <https://www.sciencedirect.com/science/article/pii/S0304423818305946>.

Feng, K. et al. 2020. Advances in AP2/ERF super-family transcription factors in plant. *Critical reviews in biotechnology* 40(6), pp. 750–776. doi: 10.1080/07388551.2020.1768509.

Filichkin, S.A. et al. 2011. Global profiling of rice and poplar transcriptomes highlights key conserved circadian-controlled pathways and cis-regulatory modules. *PloS one* 6(6), p. e16907. doi: 10.1371/journal.pone.0016907.

Flourat, A.L., Combes, J., Bailly-Maitre-Grand, C., Magnien, K., Haudrechy, A., Renault, J.-H. and Allais, F. 2021. Accessing p-Hydroxycinnamic Acids: Chemical Synthesis, Biomass Recovery, or Engineered Microbial Production? *ChemSusChem* 14(1), pp. 118–129. doi: 10.1002/cssc.202002141.

Fobel, M., Lynch, D. V and Thompson, J.E. 1987. Membrane deterioration in senescing carnation flowers: coordinated effects of phospholipid degradation and the action of membranous lipoxygenase. *Plant Physiology* 85(1), pp. 204–211. Available at: <https://doi.org/10.1104/pp.85.1.204>.

Friedman, W.E., Moore, R.C. and Purugganan, M.D. 2004. The evolution of plant development. *American Journal of Botany* 91(10), pp. 1726–1741. doi: 10.3732/ajb.91.10.1726.

Galati, V.C., Muniz, A.C.C., Guimarães, J.E.R., Mattiuz, C.M.F. and Mattiuz, B.H. 2020. Conservation of alstroemeria cut flowers stored under refrigeration. *Acta Scientiarum - Technology* 43(2014), pp. 1–7. doi: 10.4025/actascitechnol.v43i1.50016.

Galbraith, D.W. and Edwards, J. 2010. Applications of microarrays for crop improvement: here, there, and everywhere. *BioScience* 60(5), pp. 337–348. Available at: <https://doi.org/10.1525/bio.2010.60.5.4>.

Gambino, G., Perrone, I. and Gribaudo, I. 2008. A rapid and effective method for RNA extraction from different tissues of grapevine and other woody plants. *Phytochemical Analysis* 19(6), pp. 520–525. doi: 10.1002/pca.1078.

Gan, S. and Amasino, R.M. 1995. Inhibition of leaf senescence by autoregulated production of cytokinin. *Science* 270(5244), pp. 1986–1988.

- Gan, S. and Amasino, R.M. 1997. Making sense of senescence (molecular genetic regulation and manipulation of leaf senescence). *Plant Physiology* 113(2), p. 313.
- Gan, X., Jing, Y., Shahid, M.Q., He, Y., Baloch, F.S., Lin, S. and Yang, X. 2020. Identification, phylogenetic analysis, and expression patterns of the *SAUR* gene family in loquat (*Eriobotrya japonica*). *Turkish Journal of Agriculture and Forestry* 44(1), pp. 15–23. doi: 10.3906/tar-1810-98.
- García-Pastor, M.E., Serrano, M., Guillén, F., Giménez, M.J., Martínez-Romero, D., Valero, D. and Zapata, P.J. 2020. Preharvest application of methyl jasmonate increases crop yield, fruit quality and bioactive compounds in pomegranate ‘Mollar de Elche’ at harvest and during postharvest storage. *Journal of the Science of Food and Agriculture* 100(1), pp. 145–153. doi: 10.1002/jsfa.10007.
- Garg, A.K., Kim, J.K., Owens, T.G., Ranwala, A.P., Do Choi, Y., Kochian, L. V. and Wu, R.J. 2002. Trehalose accumulation in rice plants confers high tolerance levels to different abiotic stresses. *Proceedings of the National Academy of Sciences* 99(25), pp. 15898–15903. doi: 10.1073/pnas.252637799.
- Ge, S.X., Jung, D., Jung, D. and Yao, R. 2020. ShinyGO: A graphical gene-set enrichment tool for animals and plants. *Bioinformatics* 36(8), pp. 2628–2629. doi: 10.1093/bioinformatics/btz931.
- Gill, S., Dutky, E., Schuster, C. and Wadkins, S. 2006. Production of hybrid lilies as cut flowers. *University of Maryland Extension*. Available at: <https://extension.umd.edu/resource/production-hybrid-lilies-cut-flowers> [Accessed 30 Sept 2022].
- Goldberg, R.B., Beals, T.P. and Sanders, P.M. 1993. Anther development: Basic principles and practical applications. *The Plant Cell* 5(10), pp. 1217–1229. doi: 10.2307/3869775.
- Gould, K.S. and Lord, E.M. 1989. A kinematic analysis of tepal growth in *Lilium longiflorum*. *Planta* 177(1), pp. 66–73. doi: 10.1007/BF00392155.
- Gould, N., Minchin, P.E.H., Bolding, H. and Gould, E.M. 2019. Biochemical and molecular analyses of potential markers for evaluating the competition for resources between mature fruit and open flowers in ‘Hass’ avocado trees. *New Zealand Journal of Crop and Horticultural Science* 47(3), pp. 143–154. doi: 10.1080/01140671.2019.1606020.
- Grassotti, A. and Gimelli, F. 2011. Bulb and cut flower production in the genus *Lilium*: Current status and the future. *Acta Horticulturae* 900(July 2011), pp. 21–36. doi: 10.17660/actahortic.2011.900.1.
- Gu, J., Zeng, Z., Wang, Y. and Lyu, Y. 2020. Transcriptome analysis of carbohydrate metabolism genes and molecular regulation of sucrose transport gene *LoSUT* on the flowering process of developing Oriental hybrid lily ‘Sorbonne’ bulb. *International Journal of Molecular Sciences* 21(9). doi:

10.3390/ijms21093092.

Guo, Y. and Gan, S. 2005. Leaf senescence: signals, execution, and regulation. *Current Topics in Developmental Biology* 71, pp. 83–112.

Haas, B.J. et al. 2013. De novo transcript sequence reconstruction from RNA-seq using the Trinity platform for reference generation and analysis. *Nature Protocols* 8(8), pp. 1494–1512. doi: 10.1038/nprot.2013.084.

Han, S.S. 2001. Benzyladenine and Gibberellins Improve Postharvest Quality of Cut Asiatic and Oriental Lilies. *HortScience* 36(4), pp. 741–745. doi: 10.21273/HORTSCI.36.4.741.

Han, S.S. 2003. Role of sugar in the vase solution on postharvest flower and leaf quality of Oriental lily “Stargazer.” *HortScience* 38(3), pp. 412–416. doi: 10.21273/hortsci.38.3.412.

Han, Y. et al. 2019. Identification of candidate adaxial–abaxial-related genes regulating petal expansion during flower opening in *Rosa chinensis* “Old Blush.” *Frontiers in Plant Science* 10(September), pp. 1–16. doi: 10.3389/fpls.2019.01098.

Hanks, G. 2018. A review of production statistics for the cut flower and foliage sector. (part of AHDB Horticulture funded project PO BOF 002a)." *The National Cut Flower Centre, AHDB Horticulture* 102 (2015).

Harkema, H., Paillart, M., Lukasse, L., Westra, E. and Hogeveen, E. 2017. *Transport and storage of cut roses: endless possibilities?* Available at: <https://edepot.wur.nl/401918>.

Have, A. Ten and Woltering, E.J. 1997. Ethylene biosynthetic genes are differentially expressed during carnation (*Dianthus caryophyllus* L.) flower senescence. *Plant Molecular Biology* 34(1), pp. 89–97. doi: 10.1023/A:1005894703444.

He, G., Hu, F., Ming, J., Liu, C. and Yuan, S. 2017. Pollen viability and stigma receptivity in *Lilium* during anthesis. *Euphytica* 213(10), pp. 1–10. doi: 10.1007/s10681-017-2019-9.

He, S., Joyce, D.C., Irving, D.E. and Faragher, J.D. 2006. Stem end blockage in cut *Grevillea* ‘Crimson Yul-lo’ inflorescences. *Postharvest Biology and Technology* 41(1), pp. 78–84. Available at: <https://www.sciencedirect.com/science/article/pii/S092552140600072X>.

Healy, W.E. and Wilkins, H.F. 1984. Temperature effects on ‘Nellie White’ flower bud development. *HortScience* 19(6), pp. 843–844.

Hedhly, A., Vogler, H., Schmid, M.W., Pazmino, D., Gagliardini, V., Santelia, D. and Grossniklaus, U. 2016. Starch turnover and metabolism during flower and early embryo development. *Plant*

Physiology 172(4), pp. 2388–2402. doi: 10.1104/pp.16.00916.

Heins, R.D., Pemberton, H.B. and Wilkins, H.F. 1982. The influence of light on lily (*Lilium longiflorum* Thunb.): influence of light intensity on plant development. *Journal of the American Society for Horticultural Science* 107(2), pp. 330–335. doi: 10.21273/jashs.107.2.330.

Hentrich, M. et al. 2013. The jasmonic acid signaling pathway is linked to auxin homeostasis through the modulation of *YUCCA8* and *YUCCA9* gene expression. *Plant Journal* 74(4), pp. 626–637. doi: 10.1111/tpj.12152.

Hiratsuka, S., Tezuka, T. and Yamamoto, Y. 1983. Use of longitudinally bisected pistils of *Lilium longiflorum* for studies on self-incompatibility. *Plant and Cell Physiology* 24(4), pp. 765–768. Available at: <https://doi.org/10.1093/oxfordjournals.pcp.a076574>.

Hoekstra, F.A. and van Roekel, T. 1988. Desiccation Tolerance of *Papaver dubium* L. Pollen during Its Development in the Anther. *Plant Physiology* 88(3), pp. 626–632. doi: 10.1104/pp.88.3.626.

Horibe, T., Horie, K., Kawai, M., Kurachi, Y., Watanabe, Y. and Makita, M. 2020. Effect of light environment on flower opening and water balance in cut rose. *Environmental Control in Biology* 58(1), pp. 15–20. doi: 10.2525/ecb.58.15.

Hornett, E.A. and Wheat, C.W. 2012. Quantitative RNA-Seq analysis in non-model species: assessing transcriptome assemblies as a scaffold and the utility of evolutionary divergent genomic reference species. *BMC Genomics* 13(1), p. 361. Available at: <https://doi.org/10.1186/1471-2164-13-361>.

Hu, Z., Tang, Z., Zhang, Y., Niu, L., Yang, F., Zhang, D. and Hu, Y. 2021. Rice SUT and SWEET transporters. *International Journal of Molecular Sciences* 22(20), p. 11198. doi: 10.3390/ijms222011198.

Huang, T. and Irish, V.F. 2015. Temporal control of plant organ growth by TCP transcription factors. *Current Biology* 25(13), pp. 1765–1770. Available at: <https://www.sciencedirect.com/science/article/pii/S0960982215005989>.

Hwang, S.A., Lee, P.O., Lee, H.S., Lee, J.S., Roh, M.S. and Choi, M.P. 2012. Flower bud abscission triggered by the anther in the Asiatic hybrid lily. *Postharvest Biology and Technology* 64(1), pp. 31–39. Available at: <http://dx.doi.org/10.1016/j.postharvbio.2011.09.002>.

Hwang, S.H., Yie, S.W. and Hwang, D.J. 2011. Heterologous expression of *OsWRKY6* gene in *Arabidopsis* activates the expression of defense related genes and enhances resistance to pathogens. *Plant Science* 181(3), pp. 316–323. Available at: <http://dx.doi.org/10.1016/j.plantsci.2011.06.007>.

- iBulb (Royal Anthos). 2022. *Lilies as cut flowers and as pot plants*. Available at: <https://onings.com/wp-content/uploads/Lilium-Forcing-Guide-English.pdf> [Accessed 10 Oct 2022]
- Ichimura, K. 1998. Improvement of postharvest life in several cut flowers by the addition of sucrose. *Japan Agricultural Research Quarterly* 32(4), pp. 275–280.
- Iglesias, A., Andreo, C., Oleary, M. and Oleary, M. 1987. Higher plant phosphoenolpyruvate carboxylase. *FEBS Letters* 213(1), pp. 1–8.
- Iijima, L. et al. 2020. Esterified carotenoids are synthesized in petals of carnation (*Dianthus caryophyllus*) and accumulate in differentiated chromoplasts. *Scientific Reports* 10(1), pp. 1–12. Available at: <https://doi.org/10.1038/s41598-020-72078-4>.
- Dello Iorio, R. et al. 2008. A genetic framework for the control of cell division and differentiation in the root meristem. *Science* 322(5906), pp. 1380–1384. doi: 10.1126/science.1164147.
- Iqbal, N., Khan, N.A., Ferrante, A., Trivellini, A., Francini, A. and Khan, M.I.R. 2017. Ethylene role in plant growth, development and senescence: interaction with other phytohormones. *Frontiers in Plant Science* 8(April), pp. 1–19. doi: 10.3389/fpls.2017.00475.
- Ishiguro, S., Kawai-Oda, A., Ueda, J., Nishida, I. and Okada, K. 2001. The *DEFECTIVE IN ANTHER DEHISCENCE1* gene encodes a novel phospholipase A1 catalyzing the initial step of jasmonic acid biosynthesis, which synchronizes pollen maturation, anther dehiscence, and flower opening in *Arabidopsis*. *The Plant Cell* 13(10), pp. 2191–2209. Available at: <https://doi.org/10.1105/tpc.010192>.
- Izawa, T. 2021. What is going on with the hormonal control of flowering in plants? *The Plant Journal* 105(2), pp. 431–445. Available at: <https://doi.org/10.1111/tpj.15036>.
- Jackman, R.L., Yada, R.Y., Marangoni, A., Parkin, K.L. and Stanley, D.W. 1988. Chilling injury. A review of quality aspects. *Journal of Food Quality* 11(4), pp. 253–278. Available at: <https://doi.org/10.1111/j.1745-4557.1988.tb00887.x>.
- Jain, M., Tyagi, A.K. and Khurana, J.P. 2006. Molecular characterization and differential expression of cytokinin-responsive type-A response regulators in rice (*Oryza sativa*). *BMC Plant Biology* 6(1), pp. 1–11. doi: 10.1186/1471-2229-6-1.
- Jeloudar, N.I., Chamani, E., Shokouhian, A.A. and Zakaria, R.A. 2019. Induction and identification of polyploidy by colchicine treatment in *Lilium regale*. *Cytologia* 84(3), pp. 271–276. doi: 10.1508/cytologia.84.271.
- Jeon, J.-S., Lee, S., Jung, K.-H., Yang, W.-S., Yi, G.-H., Oh, B.-G. and An, G. 2000. Production of

transgenic rice plants showing reduced heading date and plant height by ectopic expression of rice MADS-box genes. *Molecular Breeding* 6(6), pp. 581–592.

Ji, J., Yang, L., Fang, Z., Zhang, Y., Zhuang, M., Lv, H. and Wang, Y. 2022. Plant SWEET family of sugar transporters: structure, evolution and biological functions. *Biomolecules* 12(2), p. 205. doi: 10.3390/biom12020205.

Jiaying, M. et al. 2022. Functions of nitrogen, phosphorus and potassium in energy status and their influences on rice growth and development. *Rice Science* 29(2), pp. 166–178. Available at: <https://www.sciencedirect.com/science/article/pii/S1672630822000075>.

Johansson, M. and Staiger, D. 2015. Time to flower: interplay between photoperiod and the circadian clock. *Journal of Experimental Botany* 66(3), pp. 719–730. doi: 10.1093/jxb/eru441.

Jones, M.L. and Woodson, W.R. 1997. Pollination-induced ethylene in carnation. Role of stylar ethylene in corolla senescence. *Plant Physiology* 115(1), pp. 205–212. doi: 10.1104/pp.115.1.205.

Kader, A.A. 2002. Postharvest Biology and Technology: An Overview. Ed. Kader, A.A. *Postharvest technology of horticultural crops*. University of California Agriculture and Natural Resources.

Kaihara, S. and Takimoto, A. 1983. Effect of plant growth regulators on flower opening of *Pharbitis nil*. *Plant and Cell Physiology* 24(3), pp. 309–316. Available at: <https://doi.org/10.1093/oxfordjournals.pcp.a076519>.

Kanehisa, M. and Goto, S. 2000. KEGG: Kyoto Encyclopedia of Genes and Genomes. *Nucleic Acids Research* 28(1), pp. 27–30. doi: 10.1093/nar/28.1.27.

Kato, M. 2022. Exogenous application of auxin promotes carotenoid accumulation in citrus fruit after harvest. In: *Acta Horticulturae*. International Society for Horticultural Science (ISHS), Leuven, Belgium, pp. 1–8. Available at: <https://doi.org/10.17660/ActaHortic.2022.1336.1>.

Ke, M., Gao, Z., Chen, J., Qiu, Y., Zhang, L. and Chen, X. 2018. Auxin controls circadian flower opening and closure in the waterlily. *BMC Plant Biology* 18(1), pp. 1–21. doi: 10.1186/s12870-018-1357-7.

Kenis, J.D., Silvente, S.T. and Trippi, V.S. 1985. Nitrogen metabolism and senescence-associated changes during growth of carnation flowers. *Physiologia Plantarum* 65, pp. 455–459.

Kleczkowski, K., Schell, J. and Bandur, D.R. 1995. Phytohormone conjugates: Nature and function. *Critical Reviews in Plant Sciences* 14(4), pp. 283–298. Available at: <https://doi.org/10.1080/07352689509382361>.

Knoblauch, M. et al. 2015. Multispectral phloem-mobile probes: properties and applications. *Plant*

Physiology 167(4), pp. 1211–1220. doi: 10.1104/pp.114.255414.

Kou, X., Feng, Y., Yuan, S., Zhao, X., Wu, C., Wang, C. and Xue, Z. 2021. Different regulatory mechanisms of plant hormones in the ripening of climacteric and non-climacteric fruits: a review. *Plant Molecular Biology* 107(6), pp. 477–497. Available at: <https://doi.org/10.1007/s11103-021-01199-9>.

Kovtun, Y., Chiu, W.-L., Zeng, W. and Sheen, J. 1998. Suppression of auxin signal transduction by a MAPK cascade in higher plants. *Nature* 395(6703), pp. 716–720. Available at: <https://doi.org/10.1038/27240>.

Kuhn, A., Harborough, S.R., M. McLaughlin, H., Kepinski, S. and Østergaard, L. 2019. Direct ETTIN-auxin interaction controls chromatin state in gynoecium development. *eLife* 9, p. e51787. Available at: <https://prelights.biologists.com/highlights/direct-ettin-auxin-interaction-controls-chromatin-state-in-gynoecium-development/>. [Accessed 01 Dec 2022].

Kumar, S.V., Lucyshyn, D., Jaeger, K.E., Alós, E., Alvey, E., Harberd, N.P. and Wigge, P.A. 2012. Transcription factor PIF4 controls the thermosensory activation of flowering. *Nature* 484(7393), pp. 242–245. doi: 10.1038/nature10928.

Kumari, S., Kumar, S. and Singh, C.P. 2018. Effect of postharvest treatments on keeping quality and vase life of Asiatic hybrid lily cv. Arcachon. *International Journal of Current Microbiology and Applied Sciences* 7(12), pp. 999–1004. doi: 10.20546/ijcmas.2018.712.124.

Kunst, L., Klenz, J.E., Martinez-Zapater, J. and Haughn, G.W. 1989. AP2 gene determines the identity of perianth organs in flowers of *Arabidopsis thaliana*. *The Plant Cell* 1(12), p. 1195. doi: 10.2307/3868917.

Kuznetsova, I., Lugmayr, A., Siira, S.J., Rackham, O. and Filipovska, A. 2019. CirGO: An alternative circular way of visualising gene ontology terms. *BMC Bioinformatics* 20(1), pp. 1–7. doi: 10.1186/s12859-019-2671-2.

Lastdrager, J., Hanson, J. and Smeeckens, S. 2014. Sugar signals and the control of plant growth and development. *Journal of Experimental Botany* 65(3), pp. 799–807. doi: 10.1093/jxb/ert474.

Lawson, R.H. and Hsu, H.T. 1996. Lily diseases and their control. In: *Acta Horticulturae*. International Society for Horticultural Science (ISHS), Leuven, Belgium, pp. 175–188. Available at: <https://doi.org/10.17660/ActaHortic.1996.414.21>.

Lear, B. 2020. *A physiological, microbial and transcriptomic study of peduncle necking in cut Rosa hybrida*. Royal Holloway University of London.

- Lee, J. and Lee, I. 2010. Regulation and function of SOC1, a flowering pathway integrator. *Journal of Experimental Botany* 61(9), pp. 2247–2254. doi: 10.1093/jxb/erq098.
- Lemoine, R. et al. 2013. Source-to-sink transport of sugar and regulation by environmental factors. *Frontiers in Plant Science* 4(July), pp. 1–21. doi: 10.3389/fpls.2013.00272.
- Li, B. and Dewey, C.N. 2011. RSEM: accurate transcript quantification from RNA-Seq data with or without a reference genome. *BMC Bioinformatics* 12(1), p. 323. Available at: <https://doi.org/10.1186/1471-2105-12-323>.
- Li, Z., Peng, J., Wen, X. and Guo, H. 2013. Ethylene-insensitive3 is a senescence-associated gene that accelerates age-dependent leaf senescence by directly repressing miR164 transcription in *Arabidopsis*. *The Plant Cell* 25(9), pp. 3311–3328.
- Liang, H. and Mahadevan, L. 2011. Growth, geometry, and mechanics of a blooming lily. *Proceedings of the National Academy of Sciences* 108(14), pp. 5516–21. doi: 10.1073/pnas.1007808108.
- Liaw, A. and Wiener, M. 2002. Classification and regression by randomForest. *R News* 2(3), pp. 18–22.
- Licausi, F., Giorgi, F., Zenoni, S., Osti, F., Pezzotti, M. and Perata, P. 2010. Genomic and transcriptomic analysis of the AP2/ERF superfamily in *Vitis vinifera*. *BMC Genomics* 11(1), p. 719. doi: 10.1186/1471-2164-11-719.
- Lim, K.-B., Barba-Gonzalez, R., Shujun, Z., Ramanna, M.S. and Van Tuyl, J.M. 2008. Interspecific hybridization in lily (*Lilium*): Taxonomic and commercial aspects of using species hybrids in breeding. *Floriculture, Ornamental and Plant Biotechnology* 5(June 2014), pp. 146–151.
- Lim, K.B. and van Tuyl, J.M. 2006. Lily: *Lilium* hybrids. In: *Flower Breeding and Genetics: Issues, Challenges and Opportunities for the 21st Century.*, pp. 517–537. doi: 10.1007/978-1-4020-4428-1-19.
- Lim, P.O., Kim, H.J. and Gil Nam, H. 2007. Leaf senescence. *Annual Review of Plant Biology* 58, pp. 115–136.
- Liscum, E. and Reed, J.W. 2002. Genetics of Aux/IAA and ARF action in plant growth and development. *Plant Molecular Biology* 49(3–4), pp. 387–400. doi: 10.1023/A:1015255030047.
- Liu, F., Xiao, Z., Yang, L., Chen, Q., Shao, L., Liu, J. and Yu, Y. 2017. *PhERF6*, interacting with *EOBI*, negatively regulates fragrance biosynthesis in petunia flowers. *New Phytologist* 215(4), pp. 1490–1502. doi: 10.1111/nph.14675.

Liu, J.D., Goodspeed, D., Sheng, Z., Li, B., Yang, Y., Kliebenstein, D.J. and Braam, J. 2015. Keeping the rhythm: Light/dark cycles during postharvest storage preserve the tissue integrity and nutritional content of leafy plants. *BMC Plant Biology* 15(1), pp. 1–9. doi: 10.1186/s12870-015-0474-9.

Liu, Q., Luo, L. and Zheng, L. 2018. Lignins: biosynthesis and biological functions in plants. *International Journal of Molecular Sciences* 19(2), p. 335. doi: 10.3390/ijms19020335.

Greenway Logistics. 2019. Transportation of Flowers. Available at: <https://gwlogistics.biz/en/2019/04/26/перевозка-живых-цветов/>. [Accessed 12 Nov 2022].

Lombardi, L. et al. 2015. Auxin involvement in tepal senescence and abscission in *Lilium*: A tale of two lilies. *Journal of Experimental Botany* 66(3), pp. 945–56. doi: 10.1093/jxb/eru451.

Lucidos, J.G., Ryu, K.B., Younis, A., Kim, C.K., Hwang, Y.J., Son, B.G. and Lim, K.B. 2013. Different day and night temperature responses in *Lilium hansonii* in relation to growth and flower development. *Horticulture Environment and Biotechnology* 54(5), pp. 405–411. doi: 10.1007/s13580-013-1241-1.

Lucidos, J.G., Younis, A. and Lim, K.B. 2017. Determination of flower bud initiation in Oriental hybrid lilies ‘Siberia’ and ‘Sorbonne.’ *Pakistan Journal of Agricultural Sciences* 54(1), pp. 15–20. doi: 10.21162/PAKJAS/17.4439.

Luo, H.L. et al. 2014. Evaluation of candidate reference genes for RT-qPCR in lily (*Lilium brownii*). *Journal of Horticultural Science and Biotechnology* 89(3), pp. 345–351. doi: 10.1080/14620316.2014.11513089.

Luo, J., Li, L. and Kong, L. 2012. Preparative separation of phenylpropanoid glycerides from the bulbs of *Lilium lancifolium* by high-speed counter-current chromatography and evaluation of their antioxidant activities. *Food Chemistry* 131(3), pp. 1056–1062. Available at: <https://www.sciencedirect.com/science/article/pii/S0308814611013896>.

Luo, J., Zhou, J.J. and Zhang, J.Z. 2018. Aux/IAA gene family in plants: Molecular structure, regulation, and function. *International Journal of Molecular Sciences* 19(1), pp. 1–17. doi: 10.3390/ijms19010259.

Lv, B. et al. 2019. Non-canonical AUX / IAA protein IAA 33 competes with canonical AUX / IAA repressor IAA 5 to negatively regulate auxin signaling. *The EMBO Journal* 39(1), pp. 1–14. doi: 10.15252/embj.2019101515.

Ma, N. et al. 2008. *Rh-PIP2;1*, a rose aquaporin gene, is involved in ethylene-regulated petal expansion. *Plant Physiology* 148(2), pp. 894–907. doi: 10.1104/pp.108.120154.

- Macnish, A.J., Leonard, R.T., Borda, A.M. and Nell, T.A. 2010. Genotypic variation in the postharvest performance and ethylene sensitivity of cut rose flowers. *HortScience* 45(5), pp. 790–796. doi: 10.21273/hortsci.45.5.790.
- Madritsch, S., Burg, A. and Sehr, E.M. 2021. Comparing de novo transcriptome assembly tools in di- and autotetraploid non-model plant species. *BMC Bioinformatics* 22(1), pp. 1–17. Available at: <https://doi.org/10.1186/s12859-021-04078-8>.
- Majda, M. and Robert, S. 2018. The role of auxin in cell wall expansion. *International Journal of Molecular Sciences* 19(4), p. 951.
- Mandaokar, A. et al. 2006. Transcriptional regulators of stamen development in Arabidopsis identified by transcriptional profiling. *Plant Journal* 46(6), pp. 984–1008. doi: 10.1111/j.1365-313X.2006.02756.x.
- Mao, J. et al. 2018. Transcriptome analysis revealed glucose application affects plant hormone signal transduction pathway in “Red Globe” grape plantlets. *Plant Growth Regulation* 84(1), pp. 45–56. doi: 10.1007/s10725-017-0320-1.
- Marasek-Ciolakowska, A., Nishikawa, T., Shea, D.J. and Okazaki, K. 2018. Breeding of lilies and tulips—interspecific hybridization and genetic background. *Breeding Science* 68(1), pp. 35–52. doi: 10.1270/jsbbs.17097.
- Marchioni, I., Pistelli, L., Ferri, B., Copetta, A., Ruffoni, B., Pistelli, L. and Najar, B. 2020. Phytonutritional content and aroma profile changes during postharvest storage of edible flowers. *Frontiers in Plant Science* 11(November), pp. 1–16. doi: 10.3389/fpls.2020.590968.
- Marowa, P., Ding, A. and Kong, Y. 2016. Expansins: roles in plant growth and potential applications in crop improvement. *Plant Cell Reports* 35(5), pp. 949–965. doi: 10.1007/s00299-016-1948-4.
- Mason, M.R. 1989. *Investigation into “bud blast” in the Easter lily (Lilium longiflorum Thunb)*. Ann Arbor: The University of Arizona PP - United States -- Arizona. Available at: <http://abc.cardiff.ac.uk/login?url=https://www.proquest.com/dissertations-theses/investigation-into-bud-blast-easter-lily-lilium/docview/303683537/se-2?accountid=9883>. [Accessed 20 Nov 2022]
- Mason, M.R. and Miller, W.B. 1991. Flower bud blast in Easter lily is induced by ethephon and inhibited by silver thiosulfate. *HortScience* 26(9), pp. 1165–1167. doi: 10.21273/hortsci.26.9.1165.
- Matos, M.J., Santana, L., Uriarte, E., Abreu, O.A., Molina, E. and Yordi, E.G. 2015. Coumarins — An Important Class of Phytochemicals. *Phytochemicals - Isolation, Characterisation and Role in Human Health* (September). doi: 10.5772/59982.

- Maximino Leite, V., Antonio Rosolem, C. and Domingos Rodrigues, J. 2003. Gibberellin and cytokinin effects on soybean growth. *Scientia Agricola* 60(3), pp. 537–541. Available at: <http://www.scielo.br/pdf/sa/v60n3/16410.pdf>.
- Maxwell, K. and Johnson, G.N. 2000. Chlorophyll fluorescence--a practical guide. *Journal of Experimental Botany* 51(345), pp. 659–668. doi: 10.1093/jxb/51.345.659.
- Mazzoni-Putman, S.M., Brumos, J., Zhao, C., Alonso, J.M. and Stepanova, A.N. 2021. Auxin interactions with other hormones in plant development. *Cold Spring Harbor Perspectives in Biology* 13(10), p. a039990. doi: 10.1101/cshperspect.a039990.
- McSteen, P. 2010. Auxin and monocot development. *Cold Spring Harbor perspectives in biology* 2(3), p. a001479. doi: 10.1101/cshperspect.a001479.
- Medford, J.I., Horgan, R., El-Sawi, Z. and Klee, H.J. 1989. Alterations of endogenous cytokinins in transgenic plants using a chimeric isopentenyl transferase gene. *The Plant Cell* 1(4), p. 403. doi: 10.2307/3869101.
- van Meeteren, U., Van De Peppel, A. and Van Gelder, A. 2001. Docis: A model to simulate carbohydrate balance and development of inflorescence during vase life. *Acta Horticulturae* 543, pp. 359–365. doi: 10.17660/ActaHortic.2001.543.44.
- Meir, S. et al. 2010. Microarray analysis of the abscission-related transcriptome in the tomato flower abscission zone in response to auxin depletion. *Plant Physiology* 154(4), pp. 1929–1956. Available at: <https://doi.org/10.1104/pp.110.160697>.
- van der Meulen-Muisers, J.J.M. 2000. *Genetic and physiological aspects of postharvest flower longevity in Asiatic hybrid lilies (Lilium L.)*. Wageningen University. Available at: <https://research.wur.nl/en/publications/genetic-and-physiological-aspects-of-postharvest-flower-longevity> [Accessed 27 Aug 2022].
- van der Meulen-Muisers, J.J.M., van Oeveren, J.C., Meijkamp, B.B. and Derks, F.H.M. 1995. Effect of floral bud reduction on individual flower longevity in Asiatic hybrid lilies. In: *Acta Horticulturae*. International Society for Horticultural Science (ISHS), Leuven, Belgium, pp. 46–57. Available at: <https://doi.org/10.17660/ActaHortic.1995.405.5>.
- van der Meulen-Muisers, J.J.M., Van Oeveren, J.C., Van der Plas, L.H.W. and Van Tuyl, J.M. 2001. Postharvest flower development in Asiatic hybrid lilies as related to tepal carbohydrate status. *Postharvest Biology and Technology* . doi: 10.1016/S0925-5214(00)00148-4.
- Miao, Y. and Zentgraf, U. 2007. The antagonist function of Arabidopsis WRKY53 and ESR/ESP in leaf

senescence is modulated by the jasmonic and salicylic acid equilibrium. *The Plant Cell* 19(3), pp. 819–830.

Miceli, A., Vetrano, F., Sabatino, L., D'Anna, F. and Moncada, A. 2019. Influence of preharvest gibberellic acid treatments on postharvest quality of minimally processed leaf lettuce and rocket. *Horticulturae* 5(3), p. 63. doi: 10.3390/horticulturae5030063.

Miller, W.B. 2014. Postharvest of Liliaceae: Experiment to industry adaptation. In: *Acta Horticulturae*. International Society for Horticultural Science (ISHS), Leuven, Belgium, pp. 87–95. Available at: <https://doi.org/10.17660/ActaHortic.2014.1027.9>.

Miller, W.B. and Langhans, R.W. 1989. Reduced irradiance affects dry weight partitioning in Easter lily. *Journal of the American Society for Horticultural Science* 114(2), pp. 306–309. doi: 10.21273/jashs.114.2.306.

Min, J.H., Ju, H.W., Yang, K.Y., Chung, J.S., Cho, B.H. and Kim, C.S. 2014. Heterologous expression of the gourd E3 ubiquitin ligase gene *LsRZF1* compromises the drought stress tolerance in *Arabidopsis thaliana*. *Plant Physiology and Biochemistry* 77, pp. 7–14. Available at: <http://dx.doi.org/10.1016/j.plaphy.2014.01.010>.

Moghe, G.D. and Shiu, S.H. 2014. The causes and molecular consequences of polyploidy in flowering plants. *Annals of the New York Academy of Sciences* 1320(1), pp. 16–34. doi: 10.1111/nyas.12466.

Mohammadi, M., Aelaei, M. and Saidi, M. 2021. Pre-harvest spray of GABA and spermine delays postharvest senescence and alleviates chilling injury of gerbera cut flowers during cold storage. *Scientific Reports* 11(1), pp. 1–14. Available at: <https://doi.org/10.1038/s41598-021-93377-4>.

Morelli, L., Torres-Montilla, S., Glauser, G., Shanmugabalaji, V., Kessler, F. and Rodriguez-Concepcion, M. 2022. Novel insights on the contribution of plastoglobules and reactive oxygen species to chromoplast differentiation. *New Phytologist* (Jan). doi: 10.1111/nph.18585.

Moubayidin, L., Di Mambro, R. and Sabatini, S. 2009. Cytokinin-auxin crosstalk. *Trends in Plant Science* 14(10), pp. 557–562. doi: 10.1016/j.tplants.2009.06.010.

Mroue, S., Simeunovic, A. and Robert, H.S. 2017. Auxin production as an integrator of environmental cues for developmental growth regulation. *Journal of Experimental Botany* 69(2), pp. 201–212. Available at: <https://doi.org/10.1093/jxb/erx259>.

Müller, B. and Sheen, J. 2007. Cytokinin signaling pathway. *Science's STKE* (407), pp. 1–3. doi: 10.1126/stke.4072007cm4.

Müller, C.J., Larsson, E., Spíchal, L. and Sundberg, E. 2017. Cytokinin-auxin crosstalk in the gynoecial primordium ensures correct domain patterning. *Plant Physiology* 175(3), pp. 1144–1157. Available at: <https://doi.org/10.1104/pp.17.00805>.

Müller, G.L., Drincovich, M.F., Andreo, C.S. and Lara, M.V. 2010. Role of photosynthesis and analysis of key enzymes involved in primary metabolism throughout the lifespan of the tobacco flower. *Journal of Experimental Botany* 61(13), pp. 3675–3688. Available at: <https://doi.org/10.1093/jxb/erq187>.

Müller, M. and Munné-Bosch, S. 2015. Ethylene response factors: a key regulatory hub in hormone and stress signaling. *Plant Physiology* 169(1), pp. 32–41. doi: 10.1104/pp.15.00677.

Munné-Bosch, S. and Peñuelas, J. 2003. Photo- and antioxidative protection during summer leaf senescence in *Pistacia lentiscus* L. grown under Mediterranean field conditions. *Annals of Botany* 92(3), pp. 385–391. doi: 10.1093/aob/mcg152.

Muñoz, P., Briones, M. and Munné-Bosch, S. 2018. Photoinhibition and photoprotection during flower opening in lilies. *Plant Science* 272(May), pp. 220–229. Available at: <https://doi.org/10.1016/j.plantsci.2018.04.023>.

Mutasa-Göttgens, E. and Hedden, P. 2009. Gibberellin as a factor in floral regulatory networks. *Journal of Experimental Botany* 60(7), pp. 1979–1989. Available at: <https://doi.org/10.1093/jxb/erp040>.

Nagpal, P. et al. 2005. Auxin response factors ARF6 and ARF8 promote jasmonic acid production and flower maturation. *Development* 132(18), pp. 4107–4118. doi: 10.1242/dev.01955.

Naing, A.H., Ai, T.N., Lim, K.B., Lee, I.J. and Kim, C.K. 2018a. Overexpression of *Rosea1* from snapdragon enhances anthocyanin accumulation and abiotic stress tolerance in transgenic tobacco. *Frontiers in Plant Science* 9(August), pp. 1–14. doi: 10.3389/fpls.2018.01070.

Naing, A.H., Lee, J.H., Park, K. II, Kim, K. ook, Chung, M.Y. and Kim, C.K. 2018b. Transcriptional control of anthocyanin biosynthesis genes and transcription factors associated with flower coloration patterns in *Gerbera hybrida*. *3 Biotech* 8(65), pp. 1–11. Available at: <https://doi.org/10.1007/s13205-018-1099-0>.

Nakano, T., Fujisawa, M., Shima, Y. and Ito, Y. 2014. The AP2/ERF transcription factor *SIERF52* functions in flower pedicel abscission in tomato. *Journal of Experimental Botany* 65(12), pp. 3111–3119. doi: 10.1093/jxb/eru154.

Nakashima, K., Takasaki, H., Mizoi, J., Shinozaki, K. and Yamaguchi-Shinozaki, K. 2012. NAC

transcription factors in plant abiotic stress responses. *Biochimica et Biophysica Acta* 1819(2), pp. 97–103. doi: 10.1016/j.bbagr.2011.10.005.

Nardozza, S. et al. 2020. Carbon starvation reduces carbohydrate and anthocyanin accumulation in red-fleshed fruit via trehalose 6-phosphate and MYB27. *Plant Cell and Environment* 43(4), pp. 819–835. doi: 10.1111/pce.13699.

Naser, V. and Shani, E. 2016. Auxin response under osmotic stress. *Plant Molecular Biology* 91(6), pp. 661–672. doi: 10.1007/s11103-016-0476-5.

Nemati, S.H., Esfandiyari, B., Tehranifar, A., Rezaei, A. and Ashrafi, S.J. 2014. Effect of nano-silver particles on postharvest life of *Lilium orientalis* cv. “Shocking.” *International Journal of Postharvest Technology and Innovation* 4(1), pp. 46–53. doi: 10.1504/IJPTI.2014.064143.

Nemati, S.H., Tehranifar, A., Esfandiari, B. and Rezaei, A. 2018. Improvement of Vase Life and Postharvest Factors of *Lilium orientalis* ‘Bouquet’ by Silver Nano Particles. *Notulae Scientia Biologicae* 5(4), p. 590. doi: 10.15835/nsb549135.

Nepi, M., von Aderkas, P., Pacini, E. 2012. Sugary exudates in Plant Pollination. *Signaling and Communication in Plants* 12, pp. 155–185. doi:10.1007/978-3-642-23047-9_8

Niwa, T., Suzuki, T., Takebayashi, Y., Ishiguro, R., Higashiyama, T., Sakakibara, H. and Ishiguro, S. 2018. Jasmonic acid facilitates flower opening and floral organ development through the upregulated expression of *SIMYB21* transcription factor in tomato. *Bioscience, Biotechnology, and Biochemistry* 82(2), pp. 292–303. doi: 10.1080/09168451.2017.1422107.

Norikoshi, R., Shibata, T. and Ichimura, K. 2016. Cell division and expansion in petals during flower development and opening in *Eustoma grandiflorum*. *The Horticulture Journal* 85(2), pp. 154–160. doi: 10.2503/hortj.MI-071.

Nozue, K., Covington, M.F., Duek, P.D., Lorrain, S., Fankhauser, C., Harmer, S.L. and Maloof, J.N. 2007. Rhythmic growth explained by coincidence between internal and external cues. *Nature* 448(7151), pp. 358–361. doi: 10.1038/nature05946.

Nozue, K., Harmer, S.L. and Maloof, J.N. 2011. Genomic analysis of circadian clock-, light-, and growth-correlated genes reveals PHYTOCHROME-INTERACTING FACTOR5 as a modulator of auxin signaling in Arabidopsis. *Plant Physiology* 156(1), pp. 357–372. doi: 10.1104/pp.111.172684.

O’Donoghue, E.M. 2006. Flower petal cell walls: Changes associated with flower opening and senescence. *New Zealand Journal of Forestry Science* 36(1), pp. 130–144.

- O'Malley, R.C. et al. 2016. Cistrome and episcistrome features shape the regulatory DNA landscape. *Cell* 165(5), pp. 1280–92. doi: 10.1016/j.cell.2016.08.063.
- O'Shea, K.T., Kattupalli, D., Mur, L., Hardy, N., Misra, B.B. and Lu, C. 2018. DIMEdb:: an integrated database and web service for metabolite identification in direct infusion mass spectrometry. *Bioinformatics Preprint* (, p. <https://doi.org/10.1101/291799>.
- Ochiai, M., Matsumoto, S. and Yamada, K. 2013. Methyl jasmonate treatment promotes flower opening of cut *Eustoma* by inducing cell wall loosening proteins in petals. *Postharvest Biology and Technology* 82, pp. 1–5. Available at: <https://www.sciencedirect.com/science/article/pii/S0925521413000628>.
- Ohmiya, A. 2013. Qualitative and quantitative control of carotenoid accumulation in flower petals. *Scientia Horticulturae* 163, pp. 10–19. Available at: <https://www.sciencedirect.com/science/article/pii/S030442381300304X>.
- Ohmiya, A., Hirashima, M., Yagi, M., Tanase, K. and Yamamizo, C. 2014. Identification of genes associated with chlorophyll accumulation in flower petals. *PLoS ONE* 9(12), pp. 1–16. doi: 10.1371/journal.pone.0113738.
- Ohno, H. 1994. Relationship between respiratory change and temperature on flower bud blasting in *Cymbidium*. *J. Japan. Soc. Hort. Sci.* 63(1), pp. 151–157.
- Okamuro, J.K., Caster, B., Villarroel, R., Van Montagu, M. and Jofuku, K.D. 1997. The AP2 domain of APETALA2 defines a large new family of DNA binding proteins in Arabidopsis. *Proceedings of the National Academy of Sciences* 94(13), pp. 7076–7081. doi: 10.1073/pnas.94.13.7076.
- Oksanen, J., Simpson, G.L. and Blanchet, F.G. (2022). vegan: Community Ecology Package. R Package Version 2.3-5. Available at: <https://cran.r-project.org/web/packages/vegan/index.html> [Accessed 10 Aug 2022].
- Okubo, H. and Sochacki, D. 2013. Chapter 4 - Botanical and horticultural aspects of major ornamental geophytes. In: *Ornamental Geophytes: From Basic Science to Sustainable Production*. Global Science Books, UK.
- de Ollas, C. and Dodd, I.C. 2016. Physiological impacts of ABA–JA interactions under water-limitation. *Plant Molecular Biology* 91(6), pp. 641–650. doi: 10.1007/s11103-016-0503-6.
- Oszwald, M., Primavesi, L.F., Griffiths, C.A., Cohn, J., Basu, S.S., Nuccio, M.L. and Paul, M.J. 2018. Trehalose 6-phosphate regulates photosynthesis and assimilate partitioning in reproductive tissue. *Plant Physiology* 176(4), pp. 2623–2638. doi: 10.1104/pp.17.01673.

- Page, D.R. and Grossniklaus, U. 2002. The art and design of genetic screens: *Arabidopsis thaliana*. *Nature Reviews Genetics* 3(2), pp. 124–136. doi: 10.1038/nrg730.
- Pahare, P. and Mishra, S. 2020. Effect of NPK on plant growth and quality of *Lilium* hybrid (Asiatic lily) Tresor under polyhouse and open condition. *International Journal of Current Microbiology and Applied Sciences* 9(6), pp. 1968–1980. doi: 10.20546/ijcmas.2020.906.243.
- Panda, G.P. and Mohanty, C.R. 2016. Effect of scale position on vegetative growth and bulblet formation during scale propagation of *Lilium*. *International Journal of Horticultural & Crop Science Research* 6(1), pp. 9–14.
- Parkin, K.L., Marangoni, A., Jackman, R.L., Yada, R.Y. and Stanley, D.W. 1989. Chilling Injury: a review of possible mechanisms. *Journal of Food Biochemistry* 13(2), pp. 127–153. doi: 10.1111/j.1745-4514.1989.tb00389.x.
- Pattaravayo, R., Ketsa, S. and Doorn, W. 2013. Sucrose feeding of Cut *Dendrobium* inflorescences promotes bud opening, inhibits abscission of open flowers, and delays tepal senescence. *Postharvest Biology and Technology* 77, pp. 7–10. doi: 10.1016/j.postharvbio.2012.09.014.
- Paul, I., Poddar Sarkar, M. and Bhadoria, P.B.S. 2022. Floral secondary metabolites in context of biotic and abiotic stress factors. *Chemoecology* 32(2), pp. 49–68. Available at: <https://doi.org/10.1007/s00049-021-00366-0>.
- Paul, M., Pellny, T. and Goddijn, O. 2001. Enhancing photosynthesis with sugar signals. *Trends in Plant Science* 6(5), pp. 197–200. doi: 10.1016/S1360-1385(01)01920-3.
- Pelkonen, V.P. and Pirttilä, A.M. 2012. Taxonomy and phylogeny of the genus *Lilium*. *Floriculture and Ornamental Biotechnology* 6(SPEC.ISS.2), pp. 1–8.
- Peng, J., Carol, P., Richards, D.E., King, K.E., Cowling, R.J., Murphy, G.P. and Harberd, N.P. 1997. The *Arabidopsis GAI* gene defines a signaling pathway that negatively regulates gibberellin responses. *Genes and Development* 11, pp. 3194–3205.
- Pérez-Alonso, M.-M., Sánchez-Parra, B., Ortiz-García, P., Santamaría, M.E., Díaz, I. and Pollmann, S. 2021. Jasmonic acid-dependent MYC transcription factors bind to a tandem G-Box motif in the *YUCCA8* and *YUCCA9* promoters to regulate biotic stress responses. *International Journal of Molecular Sciences* 22(18). doi: 10.3390/ijms22189768.
- Pernisová, M. et al. 2009. Cytokinins modulate auxin-induced organogenesis in plants via regulation of the auxin efflux. *Proceedings of the National Academy of Sciences* 106(9), pp. 3609–3614. doi: 10.1073/pnas.0811539106.

- Ping, Q. et al. 2019. The heterologous expression in *Arabidopsis thaliana* of a chrysanthemum gene encoding the BBX family transcription factor *CmBBX13* delays flowering. *Plant Physiology and Biochemistry* 144, pp. 480–487. doi: 10.1016/j.plaphy.2019.10.019.
- Rabiza-Świder, J., Skutnik, E., Jędrzejuk, A. and Ratuszek, M. 2015. Effect of postharvest treatments on the longevity of cut inflorescences of 'Rialto' Oriental lily. *Folia Horticulturae* 27(2), pp. 161–168. doi: 10.1515/fhort-2015-0026.
- Ranwala, A.P. and Miller, W.B. 1998. Gibberellin4+7, benzyladenine, and supplemental light improve postharvest leaf and flower quality of cold-stored 'Stargazer' hybrid lilies. *Journal of the American Society of Horticultural Science* 123(4), pp. 563–8.
- Ranwala, A.P. and Miller, W.B. 2005. Effects of cold storage on postharvest leaf and flower quality of potted Oriental-, Asiatic- and LA-hybrid lily cultivars. *Scientia Horticulturae* 105(3), pp. 383–392. doi: 10.1016/j.scienta.2005.01.031.
- Rao, M.S., Van Vleet, T.R., Ciurlionis, R., Buck, W.R., Mittelstadt, S.W., Blomme, E.A.G. and Liguori, M.J. 2019. Comparison of RNA-Seq and microarray gene expression platforms for the toxicogenomic evaluation of liver from short-term rat toxicity studies. *Frontiers in Genetics* 10(JAN), pp. 1–16. doi: 10.3389/fgene.2018.00636.
- Rao, X. and Dixon, R.A. 2019. Co-expression networks for plant biology: why and how. *Acta Biochimica et Biophysica Sinica* 51(10), pp. 981–988. Available at: <https://doi.org/10.1093/abbs/gmz080>.
- Raudvere, U., Kolberg, L., Kuzmin, I., Arak, T., Adler, P., Peterson, H. and Vilo, J. 2019. G:Profiler: A web server for functional enrichment analysis and conversions of gene lists (2019 update). *Nucleic Acids Research* 47(1), pp. 191–198. doi: 10.1093/nar/gkz369.
- Rawat, R. et al. 2009. REVEILLE1, a Myb-like transcription factor, integrates the circadian clock and auxin pathways. *Proceedings of the National Academy of Sciences of the United States of America* 106(39), pp. 16883–16888. doi: 10.1073/pnas.0813035106.
- Redman, P.B., Dole, J.M., Maness, N.O. and Anderson, J.A. 2002. Postharvest handling of nine specialty cut flower species. *Scientia Horticulturae* 92(3–4), pp. 293–303.
- Rees, A.R. 1966. The physiology of ornamental bulbous plants. In: *The Botanical Review.*, pp. 1–23. Available at: <https://doi.org/10.1007/BF02858583>.
- Reid, M.S. 2009. *Handling of Cut Flowers for Export*. Available at: <http://ucanr.edu/datastoreFiles/234-1906.pdf>. [Accessed 20 Sept 2022]

- Reid, M. S., Dodge, L.i.n.d.a. .L., Mor, Y. and Evans, R. .Y. (1989). EFFECTS OF ETHYLENE ON ROSE OPENING. *Acta Horticulturae*. 261, 215-220. DOI: 10.17660/ActaHortic.1989.261.27
- Reid, M.S. and Evans, R.Y. 1985. Control of cut flower opening. In: *III International Symposium on Postharvest Physiology of Ornamentals 181.*, pp. 45–54.
- Reid, M.S. and Jiang, C. 2012. Postharvest biology and technology of cut flowers and potted plants. In: *Horticultural Reviews.*, pp. 3–56.
- Reinhardt, D., Mandel, T. and Kuhlemeier, C. 2000. Auxin regulates the initiation and radial position of plant lateral organs. *The Plant Cell* 12(4), pp. 507–518. doi: 10.1105/tpc.12.4.507.
- Ren, H. and Gray, W.M. 2015. SAUR proteins as effectors of hormonal and environmental signals in plant growth. *Molecular Plant* 8(8), pp. 1153–1164. doi: 10.1016/j.molp.2015.05.003.
- Rennie, E.A. and Turgeon, R. 2009. A comprehensive picture of phloem loading strategies. *Proceedings of the National Academy of Sciences* 106(33), pp. 14162–7.
- Reyes-Olalde, J.I., Zuñiga-Mayo, V.M., Chávez Montes, R.A., Marsch-Martínez, N. and de Folter, S. 2013. Inside the gynoecium: at the carpel margin. *Trends in Plant Science* 18(11), pp. 644–655. Available at: <https://doi.org/10.1016/j.tplants.2013.08.002>.
- RHS 2022a. Cut flowers: cutting and conditioning. Available at: <https://www.rhs.org.uk/plants/for-places/cut-flowers-conditioning> [Accessed 20 Aug 2022].
- RHS 2022b. Lilies: growing in containers. Available at: <https://www.rhs.org.uk/container-gardening/lilies> [Accessed 20 Aug 2022]
- RHS Lily Group 2022. Growing from seed. Available at: <https://rhslilygroup.org/growing-from-seed/>. [Accessed 20 Aug 2022].
- Rodoni, S. et al. 1997. Chlorophyll breakdown in senescent chloroplasts (cleavage of pheophorbide A in two enzymic steps). *Plant Physiology* 115(2), pp. 669–676. Available at: <https://doi.org/10.1104/pp.115.2.669>.
- Rolland, F., Baena-Gonzalez, E. and Sheen, J. 2006. Sugar sensing and signaling in plants: Conserved and novel mechanisms. *Annual Review of Plant Biology* 57, pp. 675–709. doi: 10.1146/annurev.arplant.57.032905.105441.
- Rosen, W.G., Thomas, H.R. 1970. Secretory Cells of Lily Pistils. I. Fine Structure and Function. *American Journal of Botany* 57, pp. 1108-14.

- Ruan, Y.-L. 2014. Sucrose metabolism: gateway to diverse carbon use and sugar signaling. *Annual Review of Plant Biology* 65, pp. 33–67. doi: 10.1146/annurev-arplant-050213-040251.
- Ruan, Y., Jin, Y., Yang, Y., Li, G. and Boyer, J.S. 2010. Sugar input, metabolism, and signaling mediated by invertase: Roles in development, yield potential, and response to drought and heat. *Molecular Plant* 3(6), pp. 942–955. doi: 10.1093/mp/ssq044.
- Rudnicki, R.M., Nowak, J. and Goszczynska, D.M. 1991. Cold storage and transportation conditions for cut flowers, cuttings and pot plants. *Acta Horticulturae* (298), pp. 225–236. Available at: <https://doi.org/10.17660/ActaHortic.1991.298.27>.
- Runkle, E. 2018. Causes of flower bud abortion. *GPN Mag* (March), p. 42. Available at: <https://gpnmag.com/article/causes-of-flower-bud-abortion/> [Accessed 30 Oct 2022].
- Sajid, G.M., Kaukab, M. and Ahmad, Z. 2009. Foliar application of plant growth regulators (PGRs) and nutrients for improvement of lily flowers. *Pakistan Journal of Botany* 41(1), pp. 233–237.
- Sakai, M., Yamagishi, M. and Matsuyama, K. 2019. Repression of anthocyanin biosynthesis by R3-MYB transcription factors in lily (*Lilium spp.*). *Plant Cell Reports* 38(5), pp. 609–622. doi: 10.1007/s00299-019-02391-4.
- Sanderson, C. and Martin, C. 1975. Effects of plant growth regulators on *Lilium longiflorum* Thunb. cv. Georgia. *HortScience* 10(6), pp. 611–613.
- Saxena, I., Srikanth, S. and Chen, Z. 2016. Cross talk between H₂O₂ and interacting signal molecules under plant stress response. *Frontiers in Plant Science* 7(APR2016), pp. 1–16. doi: 10.3389/fpls.2016.00570.
- Sazvar, Z., Sepehri, M. and Baboli, A. 2016. A multi-objective multi-supplier sustainable supply chain with deteriorating products, case of cut flowers. *IFAC* 49(12), pp. 1638–1643. Available at: <http://dx.doi.org/10.1016/j.ifacol.2016.07.815>.
- Scariot, V., Paradiso, R., Rogers, H. and De Pascale, S. 2014. Ethylene control in cut flowers: Classical and innovative approaches. *Postharvest Biology and Technology* 97, pp. 83–92. Available at: <http://dx.doi.org/10.1016/j.postharvbio.2014.06.010>.
- Schaller, G.E., Bishopp, A. and Kieber, J.J. 2015. The yin-yang of hormones: cytokinin and auxin interactions in plant development. *The Plant cell* 27(1), pp. 44–63. doi: 10.1105/tpc.114.133595.
- Schmitzer, V., Veberic, R., Osterc, G. and Stampar, F. 2009. Changes in the phenolic concentration during flower development of rose “KORcrisett.” *Journal of the American Society for Horticultural*

Science 134(5), pp. 491–496. doi: 10.21273/jashs.134.5.491.

Sdiri, S., Navarro, P. and Salvador, A. 2013. Postharvest application of a new growth regulator reduces calyx alterations of citrus fruit induced by degreening treatment. *Postharvest Biology and Technology* 75, pp. 68–74. Available at:
<https://www.sciencedirect.com/science/article/pii/S092552141200186X>.

Seaton, D.D., Toledo-Ortiz, G., Ganpudi, A., Kubota, A., Imaizumi, T. and Halliday, K.J. 2018. Dawn and photoperiod sensing by phytochrome A. *Proceedings of the National Academy of Sciences* 115(41), pp. 10523–10528. doi: 10.1073/pnas.1803398115.

Senapati, A.K., Raj, D., Jain, R. and Patel, N.. 2016. Advances in Packaging and Storage of Flowers. In: N.L. Patel, S.L. Chawla, T. R. A. ed. *Commercial Horticulture*. 1st ed. New Delhi: New India Publishing Agency, pp. 473–88.

Serek, M., Sisler, E.C. and Reid, M.S. 1995. Effects of 1-MCP on the vase life and ethylene response of cut flowers. *Plant Growth Regulation* 16(1), pp. 93–97. doi: 10.1007/BF00040512.

Shen, C. et al. 2010. Functional analysis of the structural domain of ARF proteins in rice (*Oryza sativa* L.). *Journal of Experimental Botany* 61(14), pp. 3971–3981. Available at:
<https://doi.org/10.1093/jxb/erq208>.

Sherson, S.M., Alford, H.L., Forbes, S.M., Wallace, G. and Smith, S.M. 2003. Roles of cell-wall invertases and monosaccharide transporters in the growth and development of Arabidopsis. *Journal of Experimental Botany* 54(382), pp. 525–531. doi: 10.1093/jxb/erg055.

Shi, L., Wu, Y. and Sheen, J. 2018a. TOR signaling in plants : conservation and innovation. *Development* 145(8), pp. 1–13. doi: 10.1242/dev.160887.

Shi, S., Duan, G., Li, D., Wu, J., Liu, X., Hong, B. and Yi, M. 2018b. Two-dimensional analysis provides molecular insight into flower scent of *Lilium* ‘Siberia.’ *Scientific Reports* 8(5352), pp. 1–15. Available at: <http://dx.doi.org/10.1038/s41598-018-23588-9>.

Shibasaki, K., Uemura, M., Tsurumi, S. and Rahman, A. 2009. Auxin response in Arabidopsis under cold stress: underlying molecular mechanisms. *The Plant Cell* 21(12), pp. 3823–3838. doi: 10.1105/tpc.109.069906.

Shim, J.S., Kubota, A. and Imaizumi, T. 2017. Circadian clock and photoperiodic flowering in Arabidopsis: CONSTANS is a hub for signal integration. *Plant Physiology* 173(1), pp. 5–15. doi: 10.1104/pp.16.01327.

- Shimizu-Yumoto, H. and Ichimura, K. 2010. Combination pulse treatment of 1-naphthaleneacetic acid and aminoethoxyvinylglycine greatly improves postharvest life in cut *Eustoma* flowers. *Postharvest Biology and Technology* 56(1), pp. 104–107. Available at: <https://www.sciencedirect.com/science/article/pii/S0925521409002178>.
- Ślesak, I., Libik, M., Karpinska, B., Karpinski, S. and Miszalski, Z. 2007. The role of hydrogen peroxide in regulation of plant metabolism and cellular signalling in response to environmental stresses. *Acta Biochimica Polonica* 54(1), pp. 39–50. doi: 10.18388/abp.2007_3267.
- RHS Society. 2007. *The International Lily Register and Checklist 2007, Fourth Supplement*. RHS, UK.
- Soneson, C. and Delorenzi, M. 2013. A comparison of methods for differential expression analysis of RNA-seq data. *BMC Bioinformatics* 14, p. 91. doi: 10.1186/1471-2105-14-91.
- Song, C. et al. 2020. Genome-wide identification and expression profiling of the *YUCCA* gene family in *Malus domestica*. *Scientific Reports* 10(1), pp. 1–12. doi: 10.1038/s41598-020-66483-y.
- Song, L. and Peng, Y.H. 2004. Effect of cold storage on sensitivity of cut lily to ethylene. *Journal of Horticultural Science and Biotechnology* 79, pp. 723–728. doi: 10.1080/14620316.2004.11511833.
- Spartz, A.K. et al. 2014. SAUR inhibition of PP2C-D phosphatases activates plasma membrane H⁺-ATPases to promote cell expansion in *Arabidopsis*. *The Plant Cell* 26(5), pp. 2129–2142. Available at: <https://doi.org/10.1105/tpc.114.126037>.
- Srivastava, A.K. et al. 2008. Evidence for thiol-induced enhanced in situ translocation of 14C-sucrose from source to sink in *Brassica juncea*. *Environmental and Experimental Botany* 64(3), pp. 250–255. Available at: <https://www.sciencedirect.com/science/article/pii/S0098847208000476>.
- Srivastava, D. et al. 2019. Role of circadian rhythm in plant system: An update from development to stress response. *Environmental and Experimental Botany* 162, pp. 256–271. Available at: <https://www.sciencedirect.com/science/article/pii/S0098847218315661>.
- Stead, A.D. 1992. Pollination-induced flower senescence: a review. *Plant Growth Regulation* 11(1), pp. 13–20. doi: 10.1007/BF00024427.
- Stortenbeker, N. and Bemer, M. 2019. The *SAUR* gene family : the plant's toolbox for adaptation of growth and development. *Journal of Experimental Botany* 70(1), pp. 17–27. doi: 10.1093/jxb/ery332.
- Stracke, R., Werber, M. and Weisshaar, B. 2001. The *R2R3-MYB* gene family in *Arabidopsis thaliana*. *Current Opinion in Plant Biology* 4(5), pp. 447–456. Available at: <https://www.sciencedirect.com/science/article/pii/S1369526600001990>.

- Strickler, S.R., Bombarely, A. and Mueller, L.A. 2012. Designing a transcriptome next-generation sequencing project for a nonmodel plant species. *American Journal of Botany* 99(2), pp. 257–266. Available at: <https://doi.org/10.3732/ajb.1100292>.
- Stuepp, C.A., Wendling, I., Trueman, S.J., Koehler, H.S. and Zuffellato-Ribas, K.C. 2017. The use of auxin quantification for understanding clonal tree propagation. *Forests* 8(1), pp. 14–18. doi: 10.3390/f8010027.
- Stupnikov, A. et al. 2021. Robustness of differential gene expression analysis of RNA-seq. *Computational and Structural Biotechnology Journal* 19, pp. 3470–3481. doi: 10.1016/j.csbj.2021.05.040.
- Sturn, A. and Quackenbush, J. 2002. Genesis: cluster analysis of microarray data. *Bioinformatics* 18(1), pp. 207–208.
- Su, Z., Ma, X., Guo, H., Sukiran, N.L., Guo, B., Assmann, S.M. and Ma, H. 2013. Flower development under drought stress: Morphological and transcriptomic analyses reveal acute responses and long-term acclimation in *Arabidopsis*. *The Plant Cell* 25(10), pp. 3785–3807. Available at: <https://doi.org/10.1105/tpc.113.115428>.
- Sui, J., Jia, W., Xin, Y. and Zhang, Y. 2022. Transcriptomics-based identification of genes related to tapetum degradation and microspore development in lily. *Genes* 13(2), p. 366. Available at: <https://www.mdpi.com/2073-4425/13/2/366>.
- Sun, X. et al. 2021. Molecular understanding of postharvest flower opening and senescence. *Molecular Horticulture* 1(7), pp. 1–12. doi: 10.1186/s43897-021-00015-8.
- Supek, F., Bošnjak, M., Škunca, N. and Šmuc, T. 2011. Revigo summarizes and visualizes long lists of gene ontology terms. *PLoS ONE* 6(7), p. e21800. doi: 10.1371/journal.pone.0021800.
- Szklarczyk, D. et al. 2015. STRING v10: protein-protein interaction networks, integrated over the tree of life. *Nucleic acids research* 43(Database issue), pp. D447-52. doi: 10.1093/nar/gku1003.
- Tabata, R. et al. 2010. Arabidopsis *AUXIN RESPONSE FACTOR6* and 8 regulate jasmonic acid biosynthesis and floral organ development via repression of class 1 KNOX genes. *Plant and Cell Physiology* 51(1), pp. 164–175. doi: 10.1093/pcp/pcp176.
- Takano, M., Inagaki, N., Xie, X., Kiyota, S., Baba-Kasai, A., Tanabata, T. and Shinomura, T. 2009. Phytochromes are the sole photoreceptors for perceiving red/far-red light in rice. *Proceedings of the National Academy of Sciences* 106(34), pp. 14705–14710. doi: 10.1073/pnas.0907378106.

- Tamagnone, L., Merida, A., Parr, A., Mackay, S., Culianez-Macia, F.A., Roberts, K. and Martin, C. 1998. The *AmMYB308* and *AmMYB330* transcription factors from *Antirrhinum* regulate phenylpropanoid and lignin biosynthesis in transgenic tobacco. *The Plant Cell* 10(2), pp. 135–154. Available at: <https://doi.org/10.1105/tpc.10.2.135>.
- Tanaka, O., Wada, H., Yokoyama, T. and Murakami, H. 1987. Environmental factors controlling capitulum opening and closing of dandelion, *Taraxacum albidum*. *Plant and Cell Physiology* 28(4), pp. 727–730. Available at: <https://doi.org/10.1093/oxfordjournals.pcp.a077350>.
- Tardieu, F., Parent, B., Caldeira, C.F. and Welcker, C. 2014. Genetic and physiological controls of growth under water deficit. *Plant Physiology* 164(4), pp. 1628–1635. doi: 10.1104/pp.113.233353.
- Teale, W. and Palme, K. 2018. Naphthylphthalamic acid and the mechanism of polar auxin transport. *Journal of Experimental Botany* 69(2), pp. 303–312. doi: 10.1093/jxb/erx323.
- Tenhaken, R. 2015. Cell wall remodeling under abiotic stress. *Frontiers in Plant Science* 5(January), pp. 1–9. doi: 10.3389/fpls.2014.00771.
- Thakur, J.K., Tyagi, A.K. and Khurana, J.P. 2001. OsIAA1, an Aux/IAA cDNA from rice, and changes in its expression as influenced by auxin and light. *DNA Research* 8(5), pp. 193–203. doi: 10.1093/dnares/8.5.193.
- Thakur, N., Sharma, V. and Kishore, K. 2016. Leaf senescence: an overview. *Indian Journal of Plant Physiology* 21(3), pp. 225–238. Available at: <https://doi.org/10.1007/s40502-016-0234-3>.
- Thimm, O. et al. 2004. MAPMAN : a user-driven tool to display genomics data sets onto diagrams of metabolic pathways and other biological processes. *The Plant Journal* 37, pp. 914–939. doi: 10.1111/j.1365-313X.2004.02016.x.
- Tian, F., Yang, D.C., Meng, Y.Q., Jin, J. and Gao, G. 2020. PlantRegMap: Charting functional regulatory maps in plants. *Nucleic Acids Research* 48(D1), pp. D1104–D1113. doi: 10.1093/nar/gkz1020.
- Tong, Z., Li, Q., Yang, Y., Dai, F., Gao, J. and Hong, B. 2013. Isolation and expression analysis of *LoPIP2*, a lily (*Lilium Oriental Hybrids*) aquaporin gene involved in desiccation-induced anther dehiscence. *Scientia Horticulturae* 164, pp. 316–322. Available at: <http://dx.doi.org/10.1016/j.scienta.2013.09.022>.
- Trapnell, C. et al. 2010. Transcript assembly and quantification by RNA-Seq reveals unannotated transcripts and isoform switching during cell differentiation. *Nature Biotechnology* 28(5), pp. 511–515. Available at: <https://doi.org/10.1038/nbt.1621>.

- Trevaskis, B., Bagnall, D.J., Ellis, M.H., Peacock, W.J. and Dennis, E.S. 2003. MADS box genes control vernalization-induced flowering in cereals. *Proceedings of the National Academy of Sciences* 100(22), pp. 13099–13104. doi: 10.1073/pnas.1635053100.
- Tromas, A. and Perrot-Rechenmann, C. 2010. Recent progress in auxin biology. *Comptes Rendus Biologies* 333(4), pp. 297–306. Available at: <https://www.sciencedirect.com/science/article/pii/S1631069110000065>.
- van Tuyl, J.M. and Arens, P. 2011. *Lilium*: breeding history of the modern cultivar assortment. *Acta Horticulturae* 900, pp. 223–230. doi: 10.17660/ActaHortic.2011.900.27.
- van Tuyl, J.M., Franken, J., Jongerius, R.C., Lock, C.A.M. and Kwakkenbos, T.A.M. 1986. Interspecific hybridization in *Lilium*. In: *Acta Horticulturae*. International Society for Horticultural Science (ISHS), Leuven, Belgium, pp. 591–595. Available at: <https://doi.org/10.17660/ActaHortic.1986.177.98>.
- van Tuyl, J.M. and van Holsteijn, H.C.M. 1996. Lily breeding research in the Netherlands. *Acta Horticulturae* 414(May), pp. 35–45. doi: 10.17660/ActaHortic.1996.414.3.
- Vainstein, A., Lewinsohn, L., Pichersky, E. and Weiss, D. 2001. Floral fragrance. New inroads into an old commodity. *Plant Physiology* 127(4), pp. 1383–1389. doi: 10.1104/pp.010706.
- Vangelisti, A. et al. 2020. Red versus green leaves: transcriptomic comparison of foliar senescence between two *Prunus cerasifera* genotypes. *Scientific Reports* 10(1), pp. 1–11. doi: 10.1038/s41598-020-58878-8.
- Vehniwal, S.S. and Abbey, Lord 2019. Cut flower vase life – influential factors, metabolism and organic formulation. *Horticulture International Journal* 3(6), pp. 275–281. doi: 10.15406/hij.2019.03.00142.
- Vogt, T. 2010. Phenylpropanoid Biosynthesis. *Molecular Plant* 3(1), pp. 2–20. Available at: <https://doi.org/10.1093/mp/ssp106>.
- Vonk, C.R. and Ribôt, S.A. 1982. Assimilate distribution and the role of abscisic acid and zeatin in relation to flower-bud blasting, induced by lack of light, in *Iris* cv. Ideal. *Plant Growth Regulation* 1(2), pp. 93–105. doi: 10.1007/BF00024502.
- Wagstaff, C. et al. 2010. A specific group of genes respond to cold dehydration stress in cut alstroemeria flowers whereas ambient dehydration stress accelerates developmental senescence expression patterns. *Journal of Experimental Botany* 61(11), pp. 2905–2921. doi: 10.1093/jxb/erq113.

- Wahab, A. et al. 2022. Plants' physio-biochemical and phyto-hormonal responses to alleviate the adverse effects of drought stress: A comprehensive review. *Plants* 11(13), p. 1620. doi: 10.3390/plants11131620.
- Wan, J. et al. 2021. MYB70 modulates seed germination and root system development in *Arabidopsis*. *iScience* 24(11), p. 103228. Available at: <https://doi.org/10.1016/j.isci.2021.103228>.
- Wang, C.-S.S., Liao, Y.-E.E., Huang, J.-C.C., Wu, T.-D.D., Su, C.-C.C. and Lin, C.H. 1998. Characterization of a Desiccation-Related Protein in Lily Pollen during Development and Stress. *Plant and Cell Physiology* 39(12), pp. 1307–1314. Available at: <https://doi.org/10.1093/oxfordjournals.pcp.a029335>.
- Wang, P. et al. 2020. Identification and expression analysis of the small auxin-up RNA (SAUR) gene family in apple by inducing of auxin. *Gene* 750, p. 144725. Available at: <https://www.sciencedirect.com/science/article/pii/S0378111920303942>.
- Wang, Y. et al. 2008. Molecular cloning, functional characterization and expression analysis of a novel monosaccharide transporter gene *OsMST6* from rice (*Oryza sativa* L.). *Planta* 228(4), pp. 525–535. doi: 10.1007/s00425-008-0755-8.
- Wang, Y., Chantreau, M., Sibout, R. and Hawkins, S. 2013. Plant cell wall lignification and monolignol metabolism. *Frontiers in Plant Science* 4(JUL), pp. 1–14. doi: 10.3389/fpls.2013.00220.
- Wang, Y., Chen, Y.F. and Wu, W.H. 2021. Potassium and phosphorus transport and signaling in plants. *Journal of Integrative Plant Biology* 63(1), pp. 34–52. doi: 10.1111/jipb.13053.
- Wang, Y.T. 1996. Cytokinin and light intensity regulate flowering of Easter lily. *HortScience* 31(6), pp. 976–977. doi: 10.21273/hortsci.31.6.976.
- Wasternack, C., Forner, S., Strnad, M. and Hause, B. 2013. Jasmonates in flower and seed development. *Biochimie* 95(1), pp. 79–85. Available at: <https://www.sciencedirect.com/science/article/pii/S0300908412002398>.
- Watanabe, Y., Niki, T., Norikoshi, R., Nakano, M. and Ichimura, K. 2022. Soluble carbohydrate concentration and expression of expansin and xyloglucan endotransglucosylase/hydrolase genes in epidermal and parenchyma cells during lily flower opening. *Journal of Plant Physiology* 270(January), p. 153615. Available at: <https://doi.org/10.1016/j.jplph.2022.153615>.
- Watson, L.M., Somerfield, S.D., Brummell, D.A., Hunter, D.A. and O'Donoghue, E.M. 2008. Galactose metabolism in cell walls of opening and senescing petunia petals. *Planta* 229(3), pp. 709–21. doi: 10.1007/s00425-008-0862-6.

- Weber, H., Chételat, A., Reymond, P. and Farmer, E.E. 2004. Selective and powerful stress gene expression in *Arabidopsis* in response to malondialdehyde. *The Plant Journal* 37(6), pp. 877–888. doi: 10.1111/j.1365-3113X.2003.02013.x.
- Wei, F., Wang, J., Huang, S. and Gong, B. 2018. Effect of pre-harvest application of promalin and 1-MCP on preservation of cut lily and its relationship to energy metabolism. *Scientia Horticulturae* 239(3), pp. 1–8. Available at: <https://doi.org/10.1016/j.scienta.2018.04.071>.
- Weijers, D. et al. 2005. Developmental specificity of auxin response by pairs of ARF and Aux/IAA transcriptional regulators. *The EMBO journal* 24(10), pp. 1874–1885. doi: 10.1038/sj.emboj.7600659.
- Werner, S., Bartrina, I., Novák, O., Strnad, M., Werner, T. and Schmülling, T. 2021. The cytokinin status of the epidermis regulates aspects of vegetative and reproductive development in *Arabidopsis thaliana*. *Frontiers in Plant Science* 12(February), pp. 1–16. doi: 10.3389/fpls.2021.613488.
- Williamson, V.G., Parsons, S. and Franz, P. 2002. *Inhibiting the postharvest wounding response in wildflowers*. Available at: <https://docslib.org/doc/1143307/inhibiting-the-postharvest-wounding-response-in-wildflowers> [Accessed 10 Dec 2022].
- Wilson, R.N., Heckman, J.W. and Somerville, C.R. 1992. Gibberellin is required for flowering in *Arabidopsis thaliana* under short days. *Plant Physiology* 100(1), pp. 403–408. doi: 10.1104/pp.100.1.403.
- Wood, W.M.L. 1953. Thermonasty in tulip and crocus flowers. *Journal of Experimental Botany* 4(1), pp. 65–77. Available at: <https://doi.org/10.1093/jxb/4.1.65>.
- Worthen, J.M., Yamburenko, M. V, Lim, J., Nimchuk, Z.L., Kieber, J.J. and Schaller, G.E. 2019. Type-B response regulators of rice play key roles in growth, development and cytokinin signaling. *Development* 146(13), p. 174870. doi: 10.1242/dev.174870.
- Wu, Y. et al. 2021. Change in sucrose cleavage pattern and rapid starch accumulation govern lily shoot-to-bulblet transition in vitro. *Frontiers in Plant Science* 14(11), p. 564713. Available at: <https://www.frontiersin.org/articles/10.3389/fpls.2020.564713>.
- Wu, Z. et al. 2018. Overexpression of lily *HsfA3* s in *Arabidopsis* confers increased thermotolerance and salt sensitivity via alterations in proline catabolism. *Journal of Experimental Botany* 69(8), pp. 2005–2021. doi: 10.1093/jxb/ery035.
- Xiao, Y. et al. 2014. *OsJAR1* is required for JA-regulated floret opening and anther dehiscence in rice. *Plant Molecular Biology* 86(1–2), pp. 19–33. doi: 10.1007/s11103-014-0212-y.

- Xie, C. et al. 2011. KOBAS 2.0 : a web server for annotation and identification of enriched pathways and diseases. *Nucleic Acids Research* 39, pp. 316–322. doi: 10.1093/nar/gkr483.
- Xu, Q., Chen, S., Yunjuan, R., Chen, S. and Liesche, J. 2018. Regulation of sucrose transporters and phloem loading in response to environmental cues. *Plant Physiology* 176(1), pp. 930–945. doi: 10.1104/pp.17.01088.
- Xue, H., Chen, X. and Li, G. 2007. Involvement of phospholipid signaling in plant growth and hormone effects. *Current Opinion in Plant Biology* 10(5), pp. 483–489. doi: 10.1016/j.pbi.2007.07.003.
- Xue, J., Tang, Y., Wang, S., Yang, R., Xue, Y. and Wu, C. 2018. Postharvest biology and technology assessment of vase quality and transcriptional regulation of sucrose transporter and invertase genes in cut peony (*Paeonia lactiflora* ' Yang Fei Chu Yu ') treated by exogenous sucrose. *Postharvest Biology and Technology* 143(May), pp. 92–101. doi: 10.1016/j.postharvbio.2018.04.014.
- Yadav, R., Yadav, N. and Pal, M. 2013. Multiple shoot proliferation , bulblet induction and evaluation of genetic stability in Asiatic hybrid lily (*Lilium* sp.). *Indian Journal of Plant Physiology* 18(December 2013), pp. 354–359. doi: 10.1007/s40502-014-0060-4.
- Yakir, E., Hilman, D., Harir, Y. and Green, R.M. 2007. Regulation of output from the plant circadian clock. *The FEBS Journal* 274(2), pp. 335–345. doi: 10.1111/j.1742-4658.2006.05616.x.
- Yamada, K., Norikoshi, R., Suzuki, K., Nishijima, T., Imanishi, H. and Ichimura, K. 2009a. Cell division and expansion growth during rose petal development. *Journal of the Japanese Society for Horticultural Science* 78(3), pp. 356–362. doi: 10.2503/jjshs1.78.356.
- Yamada, K., Takahashi, R., Fujitani, C., Mishima, K., Yoshida, M., Joyce, D.C. and Yamaki, S. 2009b. Cell wall extensibility and effect of cell-wall-loosening proteins during rose flower opening. *Journal of the Japanese Society for Horticultural Science* 78(2), pp. 242–251. doi: 10.2503/jjshs1.78.242.
- Yamagishi, M., Toda, S. and Tasaki, K. 2014. The novel allele of the *LhMYB12* gene is involved in splatter-type spot formation on the flower tepals of Asiatic hybrid lilies (*Lilium* spp.). *New Phytologist* 201(3), pp. 1009–1020. doi: 10.1111/nph.12572.
- Yamamoto, Y., Kamiya, N., Morinaka, Y., Matsuoka, M. and Sazuka, T. 2007. Auxin biosynthesis by the YUCCA genes in rice. *Plant Physiology* 143(3), pp. 1362–1371. doi: 10.1104/pp.106.091561.
- Yang, C., Xu, Z., Song, J., Conner, K., Barrena, G.V. and Wilson, Z.A. 2007. Arabidopsis *MYB26/MALE STERILE35* regulates secondary thickening in the endothecium and is essential for anther dehiscence. *Plant Cell* 19(2), pp. 534–548. doi: 10.1105/tpc.106.046391.

- Ye, T. et al. 2019. Nitrogen, phosphorus, and potassium fertilization affects the flowering time of rice (*Oryza sativa* L.). *Global Ecology and Conservation* 20, p. e00753. Available at: <https://doi.org/10.1016/j.gecco.2019.e00753>.
- Yoshida, H. and Nagato, Y. 2011. Flower development in rice. *Journal of Experimental Botany* 62(14), pp. 4719–4730. doi: 10.1093/jxb/err272.
- Yourgiftexpert.com 2022. Tesco Flowers. Available at: <https://www.yourgiftexpert.com/tesco-flowers-prices-occasions-order-information/> [Accessed: 20 Sept 2022].
- Yunus, I.S., Cazenave-Gassiot, A., Liu, Y.C., Lin, Y.C., Wenk, M.R. and Nakamura, Y. 2015. Phosphatidic acid is a major phospholipid class in reproductive organs of *Arabidopsis thaliana*. *Plant Signaling and Behavior* 10(8), pp. 3–6. doi: 10.1080/15592324.2015.1049790.
- Zeeman, S.C., Kossmann, J. and Smith, A.M. 2010. Starch: its metabolism, evolution, and biotechnological modification in plants. *Annual Review of Plant Biology* 61, pp. 209–234. doi: 10.1146/annurev-arplant-042809-112301.
- Zhang, C. and Tian, S. 2010. Peach fruit acquired tolerance to low temperature stress by accumulation of linolenic acid and N-acylphosphatidylethanolamine in plasma membrane. *Food Chemistry* 120(3), pp. 864–872. Available at: <http://dx.doi.org/10.1016/j.foodchem.2009.11.029>.
- Zhang, K., Halitschke, R., Yin, C., Liu, C.-J. and Gan, S.-S. 2013. Salicylic acid 3-hydroxylase regulates *Arabidopsis* leaf longevity by mediating salicylic acid catabolism. *Proceedings of the National Academy of Sciences* 110(36), pp. 14807–14812.
- Zhang, M. fang, Jiang, L. min, Zhang, D. mei and Jia, G. xia 2015. *De novo* transcriptome characterization of *Lilium* ‘Sorbonne’ and key enzymes related to the flavonoid biosynthesis. *Molecular Genetics and Genomics* 290(1), pp. 399–412. doi: 10.1007/s00438-014-0919-0.
- Zhang, S., Fang, Z.J., Zhu, J., Gao, J.F. and Yang, Z.N. 2010. *OsMYB103* is required for rice anther development by regulating tapetum development and exine formation. *Chinese Science Bulletin* 55(29), pp. 3288–3297. doi: 10.1007/s11434-010-4087-2.
- Zhang, Y., Zhong, D., Liu, Z. and Gao, J. 2021. Study on the physiological, cellular, and morphological aspects of the postharvest development of cut lily flowers. *Horticultural Plant Journal* 7(2), pp. 149–158. Available at: <https://doi.org/10.1016/j.hpj.2021.02.005>.
- Zhao, X.C., Qu, X., Mathews, D.E. and Schaller, G.E. 2002. Effect of ethylene pathway mutations upon expression of the ethylene receptor ETR1 from *Arabidopsis*. *Plant Physiology* 130(4), pp. 1983–1991. doi: 10.1104/pp.011635.

- Zheng, S., Wu, H., Zhao, Y. and Liu, F. 2010. Crossing *Lilium* Orientals of different ploidy creates Fusarium-resistant hybrid. *Nature Precedings* (doi:10.1038/npre.2010.4830.1), pp. 1–22. doi: 10.1038/npre.2010.4830.1.
- Zhong, R., Richardson, E.A. and Ye, Z.H. 2007. The MYB46 transcription factor is a direct target of SND1 and regulates secondary wall biosynthesis in *Arabidopsis*. *Plant Cell* 19(9), pp. 2776–2792. doi: 10.1105/tpc.107.053678.
- Zhou, J., Lee, C., Zhong, R. and Ye, Z.-H. 2009. MYB58 and MYB63 Are transcriptional activators of the lignin biosynthetic pathway during secondary cell wall formation in *Arabidopsis*. *The Plant Cell* 21(1), pp. 248–266. Available at: <https://doi.org/10.1105/tpc.108.063321>.
- Zhou, S., Barba-Gonzalez, R., Lim, K.B., Ramanna, M.S. and van Tuyl, J.M. 2008. Interspecific hybridization in lily (*Lilium*): Interploidy crosses involving interspecific F1 hybrids and their progenies. In: *Floriculture, Ornamental and Plant Biotechnology.*, pp. 399–409. Available at: http://link.springer.com/10.1007/978-3-642-21102-7%5Cnhttp://www.liliumbreeding.nl/LA_10339_FOPB-311.pdf.
- Zlesak, D. and Anderson, N. 2003. *Inside West Coast Easter Lily Production*.
- Zúñiga-Mayo, V.M., Gómez-Felipe, A., Herrera-Ubaldo, H. and De Folter, S. 2019. Gynoecium development: networks in *Arabidopsis* and beyond. *Journal of Experimental Botany* 70(5), pp. 1447–1460. doi: 10.1093/jxb/erz026.